



University
of Glasgow

Lafferty-Whyte, Kyle (2010) *Senescence signaling, regulation and bypass by telomere maintenance*. PhD thesis.

<http://theses.gla.ac.uk/2212/>

Copyright and moral rights for this thesis are retained by the author

A copy can be downloaded for personal non-commercial research or study, without prior permission or charge

This thesis cannot be reproduced or quoted extensively from without first obtaining permission in writing from the Author

The content must not be changed in any way or sold commercially in any format or medium without the formal permission of the Author

When referring to this work, full bibliographic details including the author, title, awarding institution and date of the thesis must be given

Senescence signaling, regulation and bypass by telomere maintenance

Kyle Lafferty-Whyte BSc (Hons)

Cancer Research UK

Centre for Oncology and Applied Pharmacology

University of Glasgow

A thesis submitted to the University of Glasgow in partial
fulfilment of the requirements for the Degree of Doctor of
Philosophy

April 2010

Abstract

The permanent cell cycle arrest known as cellular senescence is a major block to tumorigenesis. Currently the effects of latent senescence signaling on disease progression, response to therapy and outcome are poorly understood. Furthermore, the role of microRNAs in the regulation of senescence remains to be fully elucidated. For immortalisation to occur replicative senescence must be bypassed usually by activating a telomere maintenance mechanism (TMM). However, the expression differences between TMMs are also poorly understood. To address these questions a combination of gene expression and miRNA microarray profiling, virtual drug and siRNA kinase screening were utilised. These findings highlight the distinct roles of secretory and damage associated senescence pathways in disease progression and in response to therapy. Examination of the differentially expressed genes between TMMs also highlighted a differentially expressed gene expression network surrounding TERT, regulated by c-Myc and TCEAL7 in TMMs. These findings give further insight into the complex regulation network surrounding senescence signaling during tumorigenesis.

Table of Contents

ABSTRACT	II
TABLE OF CONTENTS	III
LIST OF TABLES	VI
LIST OF FIGURES	VII
ABBREVIATIONS	VIII
ACKNOWLEDGEMENTS	IX
AUTHOR'S DECLARATION	X
1 INTRODUCTION	1
1.1 Cellular Senescence	1
1.1.1 Replicative Senescence.....	3
1.1.2 Oncogene induced senescence	8
1.1.3 Stress induced senescence	11
1.2 Senescence pathways	11
1.2.1 Damage associated senescence	12
1.2.2 Secretory senescence	12
1.2.3 Autophagy and senescence	16
1.3 Physiological Senescence: Senescence <i>in vivo</i>	18
1.3.1 Senescence and Aging.....	19
1.3.2 Senescence and Wound Healing	20
1.3.3 Senescence as a block to tumour progression.....	20
1.4 Senescence bypass by telomere maintenance	22
1.4.1 Telomere maintenance by telomerase	22
1.4.2 Telomere maintenance by alternative lengthening of telomeres.....	26
1.5 Aims of this Study	32
2 MATERIALS AND METHODS	33
2.1 Materials	33
2.1.1 Tissue Culture Reagents and Consumables.....	33
2.1.2 Cell Lines	34
2.1.3 Primary Cell Cultures	35
2.1.4 Luciferase Reporter Plasmid Vectors	36
2.1.5 Antibodies.....	36
2.1.6 Kits, Reagents and Enzymes	36
2.1.7 Chemicals.....	38
2.1.8 General laboratory supplies and reagents.....	38
2.1.9 Oligonucleotide Primers for qPCR.....	39
2.1.10 Oligonucleotides for siRNA	40
2.1.11 Equipment	40
2.2 RNA Methods	41
2.2.1 RNA extraction	41
2.2.2 RNA quality assessment.....	42
2.2.3 Gene expression microarray hybridisation, washing and scanning.....	43
2.2.4 miRNA expression microarray hybridisation, washing and scanning	43
2.2.5 cDNA synthesis by reverse transcriptase PCR.....	43
2.2.6 Polymerase Chain reaction.....	44
2.2.7 Quantitative polymerase chain reaction (qPCR)	44
2.2.8 qPCR validation of miRNA expression in mesenchymal tumours.....	46

2.3	DNA techniques.....	46
2.3.1	Transformation of cells with Plasmid DNA	46
2.3.2	Glycerol stocks.....	47
2.3.3	Small scale preparation of plasmid DNA	47
2.3.4	DNA sequencing.....	47
2.3.5	Large scale preparation of plasmid DNA.....	47
2.3.6	Restriction Digests.....	48
2.3.7	UV gel documentation.....	48
2.3.8	Western blotting.....	48
2.3.9	Maintenance and Storage of mammalian cell lines	49
2.3.10	Transient transfection of siRNAs.....	49
2.3.11	Luciferase reporter assay	49
2.3.12	Nuclear extract purification and Trans-AM c-Myc activity assay	50
2.3.13	c-Myc Chromatin ImmunoPrecipitation	50
2.3.14	Telomerase activity assay.....	50
2.4	Bioinformatic Methods	50
2.4.1	Gene expression microarray Data normalisation and quality control.....	50
2.4.2	Deposit of microarray data to GEO.....	51
2.4.3	miRNA expression microarray Data normalisation and quality control	51
2.4.4	Hierarchical clustering	51
2.4.5	Telomere Maintenance Gene expression signature generation Gene selection	51
2.4.6	Mesenchymal tumour miRNA signature generation	52
2.4.7	Survival Analysis	52
2.4.8	Senescence scoring of gene expression data	52
2.4.9	Correlations of senescence signature rankings.....	53
2.4.10	Regression Analysis of Senescence scores and compound GI ₅₀ data.....	53
2.4.11	Predicted compound activity mapping	53
3	SENESCENCE BYPASS BY TELOMERE MAINTENANCE IS A REGULATED BY A GENE EXPRESSION NETWORK WITH A CENTRAL ROLE FOR C-MYC AND TCEAL7 AND HIGHLIGHTS A MESENCHYMAL STEM CELL ORIGIN FOR ALT	54
3.1	Introduction.....	54
3.2	Results	55
3.2.1	Gene expression analysis distinguishes telomerase and ALT cell lines	55
3.2.2	Clustering using the 1305 gene signature is suggestive of a mesenchymal stem cell origin for ALT	58
3.2.3	Refinement of the 1305 gene signature using liposarcoma gene expression improves separation of ALT and telomerase positive liposarcomas and suggests a mesenchymal stem cell origin for ALT in this mesenchymal malignancy.....	60
3.2.4	The refined 297 gene signature is involved in telomerase gene regulation and highlights lower c-MYC activity in ALT	64
3.2.5	Validation of the Gene expression network highlights the highlights protein level differences and lower c-Myc activity in ALT	65
3.2.6	Telomerase positive cells have increased binding of c-Myc at the hTERT promoter but show no change in binding partner expression.	65
3.2.7	c-Myc regulatory factors expression patterns do not explain lower c-Myc activity in ALT ..	65
3.2.8	Differential expression of c-Myc inhibitor TCEAL7 in ALT and telomerase positive cell lines..	68
3.2.9	Perturbation of TCEAL7 expression levels in ALT and telomerase positive cells leads to changes in hTERT expression, c-Myc activity and telomerase activity.	70
3.2.10	Functional Validation of 297 gene expression network using siRNA kinase screen highlights 106 hTERT regulatory kinases in ALT cells	74
3.2.11	Transcriptional Regulation networks of 106 hTERT regulatory kinases highlights c-Myc as top regulator.....	76
3.3	Discussion.....	76
4	MIRNA REGULATION OF SENESCENCE SIGNALING DURING TUMOURIGENESIS.	85

4.1	Introduction	85
4.2	Results	87
4.2.1	Identification of 12 SA-miRNAs and Pathway mapping of their miRNA targets shows cell cytoskeletal, cell cycle and proliferation regulation potential.....	87
4.2.2	Investigation of SA-miRNA regulation of different senescence stimuli.....	96
4.2.3	Unsupervised hierarchical clustering of miRNA expression profiles shows improved separation of mesenchymal tumours over gene expression microarray profiles.....	109
4.2.4	Binary Tree prediction analysis highlights 87 miRNAs that improve separation of mesenchymal tumours in hierarchical clustering.....	111
4.2.5	Tumour type specific miRNAs show prognostic significance and correlation with telomere maintenance mechanism.....	113
4.3	Discussion	120
5	SCORING OF DAMAGE OR SECRETORY ASSOCIATED SENESCENCE PHENOTYPES IN HUMAN TUMOUR GENE EXPRESSION DATASETS AND IDENTIFICATION OF A PRO-INFLAMMATORY SIGNATURE CORRELATING WITH SURVIVAL ADVANTAGE IN PERITONEAL MESOTHELIOMA	120
5.1	Introduction	120
5.2	Results	121
5.2.1	Development of senescence scoring approach.....	121
5.2.2	Validation of the Approach.....	122
5.2.3	Application of Scoring Approach.....	128
5.3	Discussion	135
6	LATENT EXPRESSION OF SENESCENCE PATHWAYS IN NCI60 CELL LINES HIGHLIGHTS PATTERNS OF DRUG RESISTANCE OR SENSITIVITY DIFFERENT FROM THAT OBSERVED WITH APOPTOSIS SCORING	140
6.1	Introduction	140
6.2	Results	141
6.2.1	Senescence scoring of NCI60 cell lines shows no significant correlation between expression of secretory senescence signals and DA senescence signals.....	141
6.2.2	Virtual compound screen identifies differing drug activity resistances linked to damage associated, secretory senescence and apoptosis pathways.....	150
6.2.3	Investigation of predicted activities of significant compounds reveals drug class associations linked with each signaling pathway.....	153
6.3	Discussion	156
7	SUMMARY AND CONCLUSIONS	161
7.1	Transcriptional regulation of senescence bypass	161
7.2	miRNAs as regulators of senescence signaling	162
7.3	Scoring of Latent senescence signaling	164
7.4	The implications of latent senescence signaling in cellular drug response	166
8	REFERENCES	168
	APPENDIX I– GENE-LISTS RESULTING FROM THIS WORK	188
	APPENDIX II– TUMOUR HISTOLOGY AND INFORMATION	227

List of Tables

Table 3.1 -	77
Table 4.1	89
Table 4.2	90
Table 4.3	99
Table 4.4	98
Table 4.5	105
Table 4.6	107
Table 4.7	114
Table 4.8	117
Table 5.1.	123
Table 5.2	131
Table 5.3	134
Table 6.1	144
Table 6.2	148

List of Figures

Figure 1.1	2
Figure 1.2	4
Figure 1.3	29
Figure 3.1	56
Figure 3.2	57
Figure 3.3	59
Figure 3.4	62
Figure 3.5	66
Figure 3.6	67
Figure 3.7.	69
Figure 3.8.	71
Figure 3.9.	73
Figure 3.10	75
Figure 3.11	78
Figure 4.1	93
Figure 4.2	94
Figure 4.3	96
Figure 4.4	97
Figure 4.5	102
Figure 4.6	110
Figure 4.7	112
Figure 4.8	115
Figure 4.9.	119
Figure 5.1	124
Figure 5.2	130
Figure 5.3	133
Figure 6.1	143
Figure 6.2.	145
Figure 6.3	149
Figure 6.4	151
Figure 6.5	152
Figure 6.6.	154

Abbreviations

ALT	Alternative Lengthening of Telomeres
ATP	Adenosine Triphosphate
APB	ALT-associated PML body
ChIP	Chromatin Immunoprecipitation
CSIG	Cellular Senescence Inhibited Gene Protein
DA	Damage Associated
DAS	Damage Associated Senescence
DNA	Deoxyribonucleic Acid
DNase	Deoxyribonuclease
5-FU	5-fluorouracil
hMSC	Human Mesenchymal Stem Cell
hTR	Human Telomerase RNA component
hTERT	Human Telomerase Reverse Transcriptase
Luc	Luciferase
MAPK	Mitogen Activated Protein Kinase
Max	Myc associated factor x
Mad	Max dimerisation protein
mRNA	Messenger Ribonucleic Acid
miRNA	Micro Ribonucleic Acid
mSS	Modified Secretory Senescence signature
PCR	Polymerase Chain Reaction
PKC	Protein Kinase C
PML	promyleocyclic leukaemia
PP2A	Protein Phosphatase 2A
pRB	Retinoblastoma Protein
q-PCR	Quantitative PCR
RNA	Ribonucleic Acid
RNAi	RNA Interference
RT	Reverse Transcriptase
SA-miRNA	Senescence Associated miRNA
SASP	Senescence Associated Secretory Phenotype
SMS	Secretory-Messaging Secretome
siRNA	Small Interfering Ribonucleic Acid
TRAP	Telomere Repeat Amplification Protocol
TRF	TTAGGG Repeat binding factor
UTR	Untranslated Region
WT	Wild Type

Units

°C	Degrees Celsius
bp	Base Pair
g	Gram
hr	Hour
k	Kilo
l	Litre
m	milli
μ	micro
min	minute
n	nano
nt	nucleotide
p	pico
rpm	revolutions per minute
sec	second

Acknowledgements

I would firstly like to thank my supervisor Nicol Keith for the opportunity to do my PhD and his guidance throughout the course of the project.

I would also like to thank everyone in Group O2 for their patience, support and friendship over the past 4 years. Particular thanks go to Claire Cairney for her mentoring and undying patience.

This work would not have been possible without the constant support of my Mum, Kris, and Mother-in-Law, Fiona. Thanks for listening to, supporting and advising me throughout the past 4 years, I owe you many, many drinks!

Finally, I wish to extend great thanks to my partner, Alan. Thank you for putting up with me through the darker moments of this project and helping me celebrate the lighter ones.

Author's declaration

I am the sole author of this thesis. All of the references have been consulted by myself in the preparation of this manuscript. Unless otherwise acknowledged all of the work presented in this thesis was performed personally.

1 Introduction

1.1 Cellular Senescence

To become fully transformed, cancer cells must undergo a process of immortalization after which they are able to grow and divide unrestricted. Immortalization requires the bypass of the permanent cell cycle arrest induced by the activation of the senescence program. Upon induction of the senescence program, cells remain metabolically active but permanently exit the cell cycle, stalling at the G1/S checkpoint (di Fagagna et al. 2003). Senescent cells also become large and flattened in phenotype. Furthermore, senescent cells can be identified *in vitro* through the histological identification of β -galactosidase expression (Dimri 2005). Another marker commonly used in senescence identification, are the formation of senescence associated heterochromatin foci (SAHF). SAHF are unique senescence induced chromatin foci that contain HMGA proteins and are mediated by the heterochromatin chaperone molecules ASF1a and HIRA. Furthermore, SAHF have been associated with the repression of proliferative markers such as the E2F genes and may therefore be directly involved in senescence induction rather than simply associative markers (Narita et al. 2003; Zhang et al. 2005; Narita et al. 2006). Characterisation of the exact mechanisms behind SAHF function and pathways regulating their function continues. Recently, the HIRA associated protein UBN1 was found to be sequestered to SAHF during senescence and was shown to be required for SAHF formation (Banumathy et al. 2009). Furthermore, overexpression of UBN1 was found to reduce cellular proliferation and increased β -galactosidase staining, thus suggesting a direct role for UBN1 and SAHF in the induction of senescence.

Senescence induction occurs in response to multiple stimuli however always results in the same phenotypic endpoint suggesting higher levels of molecular regulation coordinating a preprogrammed cellular response as visualized in Figure 1.1.

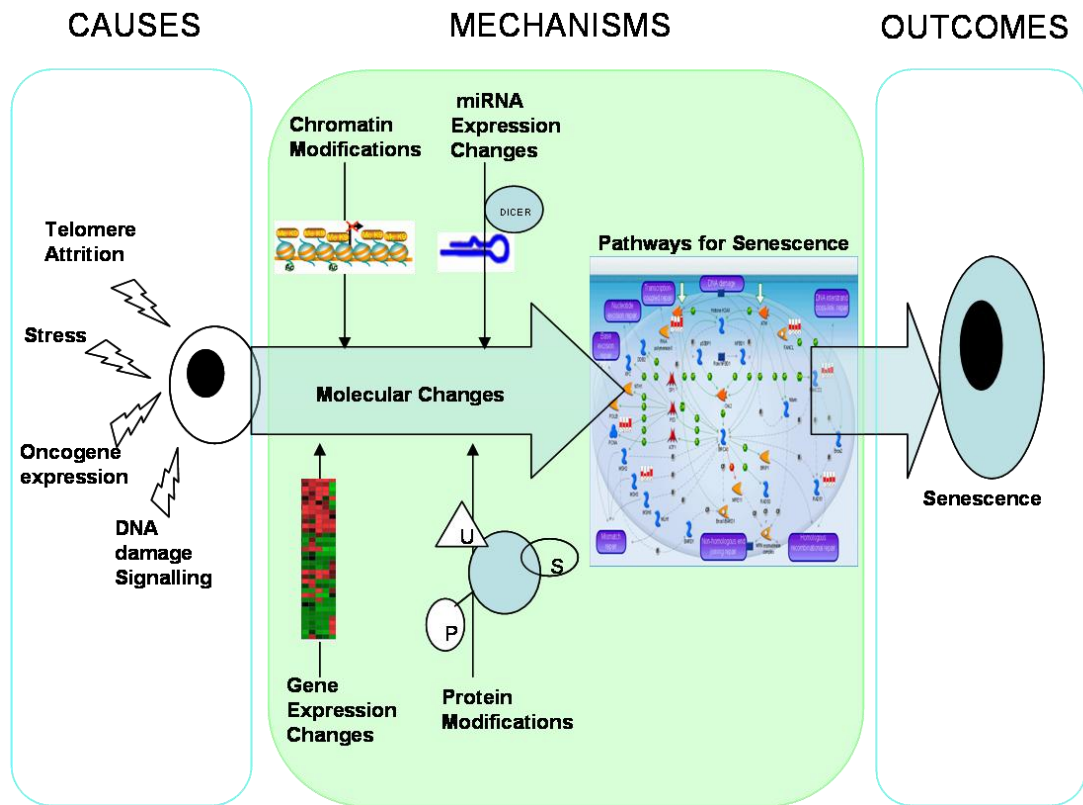


Figure 1.1 - The establishment of a complex cell phenotype, such as senescence, requires the interaction of many regulatory mechanisms leading to changes in individual pathways and processes.

1.1.1 Replicative Senescence

Cellular senescence induced in response to critically short telomeres, known as replicative senescence, represents a key mechanism by which cells prevent unlimited cellular proliferation. Telomeres consist of 1000-2000 tandem DNA hexanucleotide repeats of the sequence, TTAGGG in humans. Telomeres exist at the ends of chromosomes to protect coding DNA from degradation through the end replication problem of the cell cycle (de Lange 2009). To achieve this telomeres form a DNA-protein complex, with 6 protein subunits TRF1, TRF2, POT1, TIN2, Rap1 and TPP1 proteins, known as the shelterin complex (de Lange, 2005) . This complex protects chromosomes from end-to-end fusion events and recognition as DNA double strand breaks by introducing secondary structure to the chromosome end. However, with each successive round of cellular division short sections of the end of the telomeres are lost, circa 50bp per cell doubling, due to the DNA polymerase's inability to copy the last section of a linear chromosome (Levy et al. 1992). Eventually telomeres become critically short, circa 4 kb, and induce a crisis stage, which in turn induces the cellular senescence program. On a molecular level, it is thought that it is the recognition of the critically short telomeres as DNA double strand breaks leading to the induction of a DNA damage response that induces senescence rather than the physical length of the telomeres themselves.

The induction of the senescent phenotype is thought to occur through the complex interactions of multiple signaling cascades (see Figure 1.2). This signaling is thought to primarily occur through the tumour suppressor gene p53 and secondarily through pRB.

Although there is some disagreement in the field as to whether actual p53 protein levels increase (Atadja et al. 1995; Kulju et al. 1995), p53 DNA binding activity has been shown to increase upon the induction of the replicative senescence in diploid fibroblasts. This indicates a primary response of p53 to the DNA damage signaling of telomere erosion (Atadja et al. 1995).The tumour suppressor protein p53 is a transcription factor, encoded by the gene TP53 in humans, commonly expressed at low levels in normal cells and tissues. p53 is a well known mediator of DNA damage responses and the apoptotic pathways and

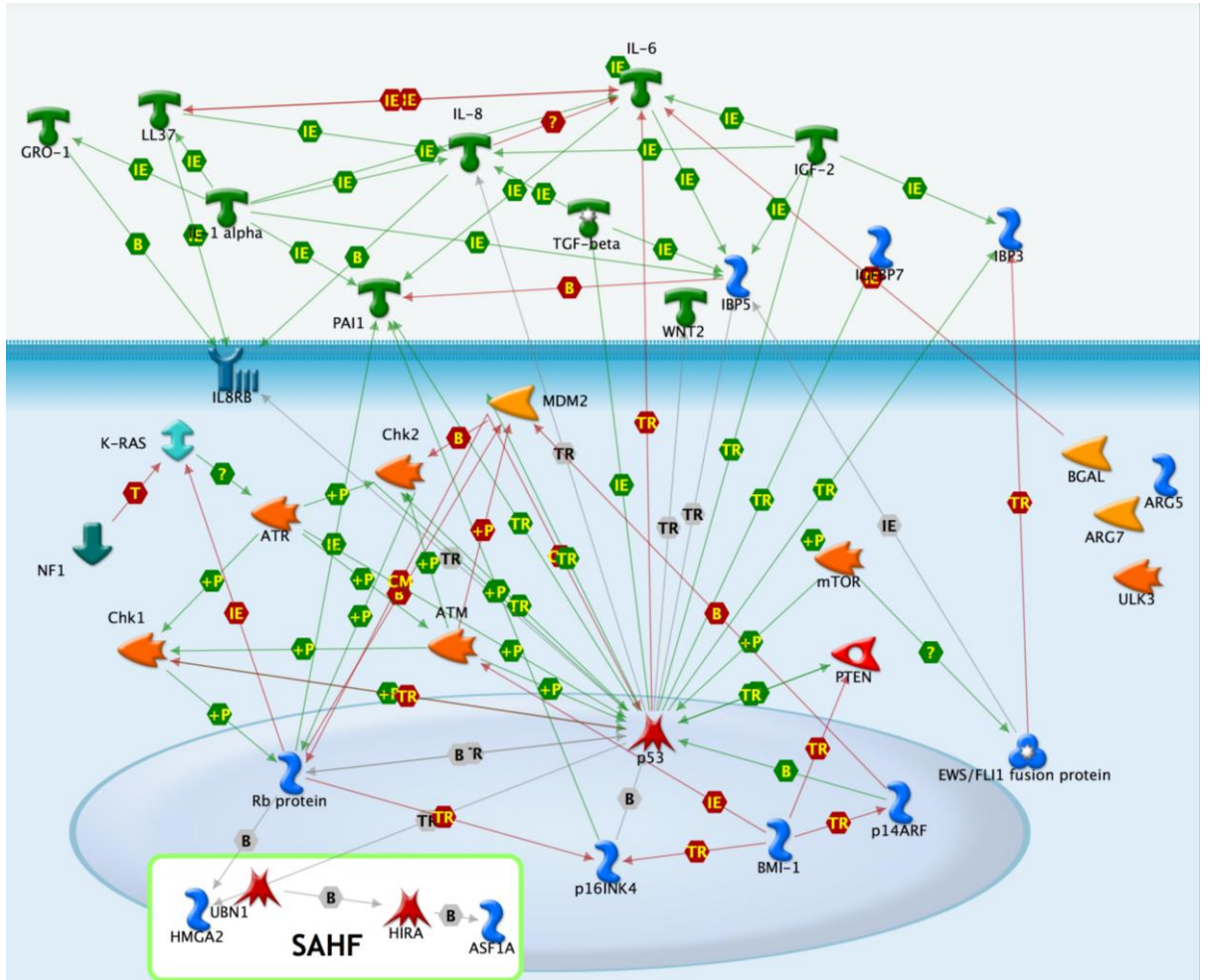


Figure 1.2 - An overview of some of the many genes implicated in senescence signaling. Also shown are the known functional relationships present in the MetaCore interactions database between them. These interactions highlight the multiple feedback loops that exist within the senescence cascades as well as the central nature of p53 and pRB regulation. Red lines indicate negative interactions whereas green indicate positive. P = phosphorylation, TR = transcriptional regulation, IE = influence on expression, CM = covalent modification.

mutations of p53 are found in up to 50% of human tumours (Bitomsky et al. 2009). Furthermore, p53 has been observed to play regulatory roles at the G1 and G2/M cell cycle checkpoints (Agarwal et al. 1995) concurrent with its ability to induce the cell cycle arrest required for the senescent phenotype. As the ability to bypass accumulated DNA damage responses, apoptotic pathways and senescence signaling through the perturbation of a single molecule would be a highly efficient route to tumorigenesis; it is therefore unsurprising that mutation of p53 is commonly observed in cancer. One mechanism thought to influence the activity increase of p53 during replicative senescence is through the neutralisation of p53 inhibitor MDM2 (HDM2 in humans) by p14^{ARF}, commonly known as ARF (Pomerantz et al. 1998). The release of p53 from HDM2 targeted degradation leads to increased p53 stabilisation and activity. Consistent with this concept HDM2 is frequently overexpressed in cancer where such tumours have little or no detectable p53 (Momand et al. 1998). In addition, further inferences to the central nature of p53 in the induction of the senescence program is gained from gain of function p53 mutations in mouse models. Mice with a p53 gain of function mutation in one allele show increased accumulation of senescent cells compared to wild type in response to radiation induced DNA damage (Hinkal et al. 2009).

As a consequence of increased transcriptional activity of p53 in senescing cells, p53 downstream target p21 also shows increased transcription in senescent cells (Roninson 2002). The role of p21 itself in replicative senescence signaling is becoming increasingly investigated. Cyclin-dependent kinase inhibitor 1A, CDKN1a also known as p21, plays a central role in the transduction of DNA damage signals during the cell cycle. Through regulation of cyclin-CDK complexes and PCNA, p21 causes G1/S cell cycle arrest upon the activation of DNA damage signals (Cazzalini et al. 2010). The importance of p21 in mediating p53 signals to bring a successful halt to the cell cycle at the G1/S checkpoint is exemplified by the fact that p21 knockout mice show similar extended proliferative lifespan as those with deficient p53 (Deng et al. 1995). Interestingly, knockout of p21 does not lead to the same tumorigenic potential as the knockout of p53 suggesting that although a key mediator in the prevention of tumorigenesis, p53 may have further effector mechanisms through other downstream targets (Deng et al. 1995). However, increased p21 expression is a well established hallmark of replicative senescence induction and

is therefore likely to be a primary mechanism by which p53 signaling induces a G1/S arrest in response to the DNA damage signals caused by critically short telomeres.

However, the absence of functional p53 signaling alone is not sufficient for complete replicative senescence bypass, although p53 deficient cells do show an increased replicative potential compared to wild type p53 cells (Metcalf et al. 1996; Dulic et al. 2000). p53 independent senescence induction is thought to occur through the actions of the pRB regulator p16^{INK4a}. The nuclear phosphoprotein RB1, or pRB, was the first tumour suppressor gene to be identified. Progression of the cell cycle through the G1/S checkpoint requires inactivation of the pRB protein by phosphorylation. pRB regulates the cell cycle through transcriptional repression of the E2F family of transcription factors (Harbour et al. 2000). The stalling of the cell cycle of senescent cells may therefore be further amplified through deactivation of the proliferative E2F family of transcription factors as hypophosphorylation of pRB is commonly observed (Jarrard et al. 1999). Deactivation of pRB during the cell cycle is caused by phosphorylation by cyclin D-dependent kinases CDK4 and CDK6. During cellular senescence the CDK4/CDK6 inhibitor cyclin dependent kinase 2A, or p16^{INK4a}, shows increased expression (Jarrard et al. 1999) and it is through this mechanism that pRB reactivation is thought to occur during cellular senescence. Consistent with this the INK4a locus, which encodes both ARF and p16^{INK4a}, is frequently deleted in human cancers (Kim et al. 2006). A recent study used a combination of a dominant negative allele of shelterin component TRF2 and siRNA to directly explore the role of p16^{INK4a} in response to telomere damage (Jacobs et al. 2004). Upon transfection with a dominant negative allele of TRF2 and p16^{INK4a} siRNA, some but not complete alleviation of telomere damage induced growth arrest was observed. Although siRNA knockdown of p16 alone was insufficient to alleviate telomere damage induced growth arrest, combination of p16 knockdown with knockdown of p53 lead to near complete bypass of senescence, consistent with previous observations in fibroblasts using SV40 T-antigen (Shay et al. 1991). In addition, perturbation of the pRB-p16^{INK4a} signaling pathway through the expression of polycomb protein BMI1 has been observed to increase the replicative lifespan of human diploid fibroblasts (Itahana et al. 2003) is insufficient for complete senescence bypass. As p16^{INK4a} and ARF are derived from the same locus, BMI1 may therefore be down-

regulating the expression of both p16^{INK4a} and ARF and further enhance the anti-senescence signal by reinstating MDM2 inhibition of p53 in combination with pRB-p16^{INK4a} depletion. This suggests that although not the primary mechanism the pRB-p16^{INK4a} senescence signaling pathway does have a potentially important secondary signaling regulatory role in the induction of the senescent phenotype. Consistent with p16^{INK4a} signaling being a secondary signal, p16^{INK4a} induction has been observed to be a particularly slow event when compared to that of p53 and p21 and has been suggested to be more involved in senescence maintenance than senescence induction per se (te Poele et al. 2002; Jacobs et al. 2005). Furthermore, the observation that p16^{INK4a} is required for the establishment of the senescence associated heterochromatin foci is suggestive that its role in senescence induction may go further than a simple back-up mechanism to p53 signaling (Narita et al. 2006). The induction of replicative senescence signaling appears therefore to be a complex highly regulated process, with multiple opportunities for perturbation to achieve the immortalization required for tumorigenesis.

Additional pathways also have evidence of involvement in response to replicative senescence stimuli. The ATM/ATR kinase pathway is commonly activated in response to damaged telomeres (d'Adda di Fagagna et al. 2003). ATM and ATR are normally activated in response to DNA damage signals, and through inhibitory phosphorylation of cell cycle positive regulator Cdc25 via CHK2 and CHK1 respectively, ATM and ATR regulate cell cycle progression (Reinhardt et al. 2009). Furthermore, ATM and ATR signaling leads to phosphorylation of H2AX (γ H2AX), which then flanks the DNA double strand breaks and attracts further DNA damage machinery to the DNA lesion. Observations of co-localisation of γ H2AX and p53 in senescent cells adds a further mechanism by which ATM and ATR may play an important role in the induction of replicative senescence, by directing the senescence machinery to the critically short telomeres (d'Adda di Fagagna et al. 2003).

Further complexity to the cross-talk between senescence signaling cascades are found when considering reports of the cooperative nature of ARF and ATM/ATR signaling in response to oncogene expression (Pauklin et al. 2005). The complex and often overlapping signaling cascades utilized to induce the senescence phenotype may be reflective not only of the requirement to coordinate multiple

signaling pathways to halt to the cell cycle but also of potential fail-safe mechanisms should one aspect of the senescence machinery be perturbed. Such fail-safe mechanisms may make the successful transformation of damaged cells into neoplasms the rare event it currently is.

1.1.2 Oncogene induced senescence

Replicative senescence although the most studied mechanism for cellular senescence is not the only mechanism by which senescence forms a barrier to tumourigenesis. Senescence induction is also a common event in response to oncogene activation. Upon expression of the oncogene RAS, increased accumulation of p53, p16 and pRB proteins are observed (Serrano et al. 1997). Furthermore, cells undertake a large flat morphology, arrest at the G1/S checkpoint of cell cycle and stain positively for β -galactosidase at pH 6. All of these factors give strong evidence that induction of RAS expression induces a senescence phenotype similar to that induced by telomere erosion in replicative senescence. The human RAS family of oncogenes includes HRAS, NRAS and KRAS all of which under normal circumstances provided proliferative signals following stimulation by growth factor receptors. RAS family activating mutations are common events in human neoplasms. A recent review of RAS mutation rates in different tumour types showed KRAS to be the most frequently activated RAS family member with activation found in up to 90% of pancreatic cancer (Downward 2003). In contrast to the signaling pathway observed in replicative senescence, bypass of oncogene-induced senescence caused by RAS overexpression is achievable by mutation of either p16 or p53 alone (Serrano et al. 1997). This may suggest that the strong proliferative signals given by the oncogene are enough to push the cell forward into the cell cycle and negate the need for bypass of both genes. Further elucidation to the mechanisms behind oncogene induced senescence through RAS overexpression is gained when examining the effects of downstream signaling molecule MEK. Examination of the effects of constitutive MEK overexpression highlighted differential effects on normal mortal fibroblasts and those lacking functional p53 or p16^{INK4a} (Lin et al. 1998). The study showed that in response to a gain-of-function mutant of the dual specificity kinase MEK1, normal fibroblasts were caused to senescence with the characteristic p53, p21 and p16 protein level increases and β -galactosidase staining. Treatment of fibroblasts with a MEK specific inhibitor was sufficient to

bypass RAS induced senescence, suggesting that MEK signaling is a required pathway for oncogene induced senescence by RAS. Consistent with their previous study the group also observed that cells deficient in either p53 or p16 and ARF transfected with the same gain of function mutant in MEK caused senescence bypass. Providing further evidence for a core role in oncogene induced senescence for MEK, the oncogene RAF was also observed to induce cellular senescence that is dependent on MEK function (Zhu et al. 1998). RAF also signals to the proliferative MAP kinases through MEK and therefore MEK dependent senescence appears to form a major barrier to tumour formation by both oncogenes. Furthermore, the senescence inducing potential of the Ras/Raf pathways are further exemplified by the ability of an oncogenic mutant variant of the downstream kinase BRAF, known as BRAF^{E600}, to also induce oncogene induced senescence (Michaloglou et al. 2005). Gain-of-function in the RAS/RAF pathways are not the only mechanism available to tumour cells for senescence bypass. Loss of tumour suppressor genes regulating RAS or RAF would also be sufficient to increase their proliferative signaling. Interestingly however, loss of the tumour suppressive function of the gene NF1 has also been shown to induce oncogene induced senescence (Courtois-Cox et al. 2006) suggesting that activation of this pathway in any form, without the loss of p53 or p16 function, will induce the cellular senescence program. Evidence of RAS induced senescence *in vivo* is given by observations in various benign premalignancies such as adenomas (Collado et al. 2005) and melanocytic nevi (Michaloglou et al. 2005).

Oncogene activation represents only one of the two main mechanisms for neoplastic transformation. The suppression of tumour suppressor genes is also a common event in human cancer. Evidence is beginning to gather for a novel mechanism of senescence induction through the tumour suppressor gene PTEN that is independent of oncogene induced senescence. PTEN deletion/inactivating mutation is a common event in many human cancers, such as prostate cancer (Jiao et al. 2007). The involvement of PTEN loss in the induction of cellular senescence was first highlighted by Chen and colleagues in 2008. The investigation of PTEN and p53 inactivation models in mice showed that PTEN inactivation with a wild-type p53 background induced non-lethal prostate cancers. Furthermore, loss of both p53 and PTEN induced an invasive prostate carcinoma. Examination of mouse embryonic fibroblasts with PTEN loss

highlighted the induction of p53 dependent cellular senescence. Furthermore, recent research by the group confirmed that the induction of PTEN-loss-induced cellular senescence was independent of DNA damage responses and its applicability in humans through its activity in a human xenograft model of prostate cancer (Alimonti et al. 2010). In addition, this study highlighted the requirement of mTOR function for the induction of PTEN-loss induced senescence through the abolishment of the phenotype through the inhibition of mTOR using Rapamycin. However, p53 stabilisation through the application of the MDM2 inhibitor Nutlin-3 was able to overcome mTOR inhibition and restore PTEN-loss induced senescence, further confirming the dependence of the phenotype on p53 activity. Whether PTEN loss causes or represses cellular senescence induction is currently under debate. The identification of CSIG adds confusion to this field. CSIG was identified as a gene whose expression is reduced upon the induction of replicative senescence and CSIG overexpression delayed the onset of replicative senescence (Ma et al. 2008). Characterisation of the function of CSIG showed that it inhibited translation of PTEN conflicting with the reports by Chen and colleagues of PTEN-loss induced senescence induction. Therefore, further investigations into the role of PTEN in cellular senescence is required before therapies targeting this signaling cascade can be utilized.

However, not all oncogenic events trigger a senescence response. Recent evidence has shown that the chromosomal translocation responsible for the Ewing's family of tumours, the EWS/FLI1 fusion, is an inhibitor of senescence. EWS/FLI1 knockdown appears to induce the activation of pRB and down regulation of pRB inhibited targets suggesting that EWS/FLI1 either directly or indirectly represses the activation of the senescence program through the inhibition of pRB (Matsunobu et al. 2006; Hu et al. 2008). Indeed, after knockdown Ewing's cells exhibit the phenotypic characteristics of senescent cells including a large flat morphology and staining for β -galactosidase. The effects of other known oncogenic chromosomal rearrangements on senescence induction pathways is currently unknown, future study in this direct may elucidate new mechanisms of senescence induction and bypass.

1.1.3 Stress induced senescence

A further senescence inducing stimuli is that of non-cytotoxic cellular stress. The induction of oxidative stress through the exposure of multiple cell types to a hyperoxidative environment has been shown to induce the same cellular characteristics as replicative and oncogene induced senescence (Toussaint et al. 2000). Furthermore, treatment of human diploid fibroblasts with an oxygen scavenger extends their replicative potential under oxidative stress. Examination of the mechanisms behind stress induced senescence by H₂O₂ treatment of human diploid fibroblasts highlighted the role TGFβ (Fripiat et al. 2001). Cells that were exposed to sub-cytotoxic doses of H₂O₂ for 2 hours showed senescence induction, measure by β-galactosidase staining, and was thought to be mediated through TGFβ. Consistent with this theory cells stimulated by increasing concentrations of TGFβ showed a dose dependent induction of senescence and antibody mediated knockdown of TGFβ activity significantly decreased the proportion of cells that underwent senescence induction in response to H₂O₂ cellular stress. Furthermore, senescence induced by cellular stress caused by low level UVB exposure show increased levels of TGFβ expression (Debacq-Chainiaux et al. 2005). The exact molecular mechanisms underlying stress induced senescence are currently not fully understood but appear to involve multiple regulatory cascades. For example stress induced senescence caused by treatment with ethanol or tert-butylhydroperoxide is protected against by overexpression of the anti-apoptotic molecule apolipoprotein J (Dumont et al. 2002) and repeated UVB exposure induced an increase of apolipoprotein J expression (Debacq-Chainiaux et al. 2005). This suggests a potential negative feedback loop that could be used to promote cellular survival and prevent senescence induction in high stress environments.

1.2 Senescence pathways

Closer examination of the combined signaling cascades highlights the complex and highly regulated nature of senescence induction and the regulation of key molecules, such as p53 and pRB, by many different mechanisms (Figure 1.1 & 1.2). The roles of individual molecules in the induction of cellular senescence is well studied. However, in today's era of high throughput genomics it is

becoming increasingly necessary to looking beyond individual genes in linear signaling cascades and consider the larger phenotypic implications of signaling pathways and networks. To date, little is clearly understood about the roles and impacts of these larger senescence pathways in human cancer.

1.2.1 Damage associated senescence

The induction of the senescence molecular signaling cascades appears to induce a damage-associated cellular response regardless stimulus. Upon receiving a cellular senescence stimulus cells induce signaling pathways classically associated with DNA damage for example p53, p16^{INK4a}, ARF, ATM and ATR regardless of whether DNA damage is actually involved, for example in the case of oncogene induced senescence. Furthermore, senescence associated heterochromatin foci are suggestive of the recruitment of DNA repair machinery to sites of DNA damage. Again, senescence associated heterochromatin foci are induced in response to oncogene overexpression where no actual DNA damage has occurred. It is therefore possible that the use of the DNA damage machinery is more reflective of the activation of a larger cellular damage pathway that is used to protect against potentially tumorigenic mutations and bypass of cellular replication limits. A recent model of an anti-viral origin for senescence has recently been proposed (Reddel 2010). The induction of this damage associated pathway stalls the cell cycle at the G1/S stage and may therefore help to prevent the successful replication of infecting viral DNA. The induction of cell death by apoptosis after infection by a virus may risk viral particle release into the neighbouring cellular microenvironment and risk infection of nearby cells. The stalling of the cell cycle through the damage associated senescence pathway would therefore protect against such events and allow sufficient opportunity for natural clearance of such cells by the immune system.

1.2.2 Secretory senescence

The clearance of virally infected senescent cells by the immune system would require a mechanism for attracting immune cells to the site of infection. Such opportunity is given by the secretory senescence pathway. The first hints of the importance of the secretory senescence pathway came from a key study into the mechanisms behind oncogene induced senescence (Kuilman et al. 2008). The

authors had observed the requirement for an IL6 regulated pro-inflammatory network for successful oncogene induced senescence induction. The direct observation of a secretory element to senescence signaling led to further investigations and eventually the identification of secretory signatures of senescence. One of the first of these signatures to be published was senescence associated secretory phenotype (SASP). SASP was identified as an independent signaling mechanism from experiments using antibody arrays to assess those factors secreted by cells undergoing senescence (Coppe et al. 2008). The study highlighted the increased secretion of IL6, IL8, IGFBP3 and GRO1 after DNA damage caused senescence induction. Furthermore, SASP induction was observed in a number of different cell types normal epithelial cells, epithelial tumours and normal fibroblasts as well as directly *in vivo* in tumour biopsies from prostate cancer patients after DNA damage inducing chemotherapy. This observation confirmed that the secretory senescence pathway was a novel unexplored aspect of cellular senescence and further similar signatures soon confirmed the importance of secretory senescence signaling, highlighting further elements of the pathway.

Many senescence studies utilise mouse models to investigate the specific role of individual molecules in senescence signaling cascades and recent investigations of the secretory senescence pathway are no exception. However, a recent study of the secretory senescence pathway highlights the need for care when interpreting such results and the false assumption that human senescence signaling will be identical to that in the mouse. Investigations of the presence of SASP in mouse cells under standard culture conditions of ~20% oxygen showed that the fibroblasts showed no signs of SASP unlike they counterpart human fibroblasts (Coppe et al. 2010). Upon culture in lower oxygen levels more similar to those found *in vitro*, ~3% oxygen or senescence induction by radiotherapy the mouse fibroblasts were found to trigger SASP. This may suggest that mouse cells have potentially different pathways for stress induced senescence via oxidative stress that differ from those found in humans, however given the correct environmental conditions these cells can still be utilized to model senescence pathways in humans. This study highlights the need for validation of senescence signaling cascades discovered through the use of mouse cells under standard culture oxygen levels (~20% oxygen) using a more physiological conditions and where possible using human cellular models directly.

Further expansion of the original SASP genes was provided shortly after by Peeper and Kuilman through detailed collation of experimental evidence in the literature for a secretory aspect to senescence, or the secretory-messaging secretome (SMS) (Kuilman et al. 2009). The secretory senescence pathway now included over 13 molecules each with evidence for a role in senescence. IGFBP3 had been previously identified as part of SASP but SMS also included further interferon growth factor bind proteins 5 and 7 as well as IGF1. Both IGFBP3 and IGFBP5 had been found to be associated with the induction of replicative senescence (Kim et al. 2007; Kim et al. 2007) during the study of human umbilical vein endothelial cells whereas IGFBP7 had been similarly shown to be mediate BRAF^{E600} oncogene induced senescence in human fibroblasts and melanocytes (Wajapeyee et al. 2008). The evidence for the involvement of IGF1 was not as direct. IGF1 overexpression was found to extend the replicative lifespan of skeletal muscle cells through the activation of AKT signaling however senescence biomarkers themselves in response to IGF1 have yet to be directly tested (Chakravarthy et al. 2000). Further molecules of particular interest in SMS are WNT2, CXCR2, and PAI1. WNT2 has previously been implicated in the maintenance of cellular proliferation signals. Its potential involvement in senescence is implicated by its pRB and p53 independent repression during both oncogene (RAS) induced and replicative senescence leading to increased SAHF formation (Ye et al. 2007). CXCR2, also known as IL8Rb, is a receptor that transduces multiple cellular signals by molecules previously implicated in the secretory senescence pathway, such as GRO1 and IL8. CXCR2 has been shown to be upregulated during replicative and oncogene induced senescence (Acosta et al. 2008). Furthermore, the same study showed that shRNA mediated knockdown of CXCR2 alleviated replicative and oncogene induced senescence. As a downstream target of p53, the role of the serine protease inhibitor SERPINE1, SERPINE1 in humans, in senescence is unsurprising. RNA interference of SERPINE1 in mouse embryonic fibroblasts and human diploid fibroblasts was, however, found to be sufficient for replicative senescence bypass (Kortlever et al. 2006). This implicates SERPINE1 as a potential key effector of p53 mediated senescence.

Subsequent additions to the secretory senescence pathway provide links between the damage associated pathway and secretory senescence pathways. Study of telomere dysfunctional mesenchymal stem cells, revealed increased

expression of CRAMP, stathmin, EF1 α and chitinase and were detectable in the blood/serum of aging mice and humans (Jiang et al. 2008). As the proteins were induced to be secreted by the damage associated senescence pathway they provide evidence for a functional link between the two pathways. Furthermore, their induction as a post damage event is also suggestive of a higher order to the signaling of the two pathways during senescence induction. Consistent with this concept, a recent study of human diploid fibroblasts with induced DNA damage through high dose radiation exposure highlighted increased IL6 secretion alongside the formation of SAHF in arrested cells (Rodier et al. 2009). Interestingly a low dose of radiation, such that it was only sufficient to induce temporary DNA damage signaling before returning to the cell cycle, did not cause increased IL6 secretion. This suggests that DNA damage signaling alone is not sufficient for secretory senescence activation instead the damage associated pathway and the senescent cell phenotype must instead first be established to trigger the induction of secretory senescence. Through the knockout of key effector molecules of the damage associated senescence pathway the group also showed the secretory senescence signaling was triggered through the ATM signaling cascade and did not require p53 during replicative or oncogene induced senescence. Interplay between the two known senescence pathways is therefore evident and current evidence suggests that the main function of the secretory senescence pathway is to signal the cells' surrounding microenvironment of the induction of cellular senescence.

Unfortunately, such signaling events may have a pro-tumourigenic effect on surround cells due to the increased blood flow from proangiogenic signals and proliferative signals intended to stimulate the immune system. Such antagonistic pleiotropy may have originally been intended to signal cellular distress to surrounding microenvironment due to ongoing tumourigenic events or cause senescence induction in neighbouring cells that may have also been infected with the virus. Regardless of whether senescence was derived from an anti-viral response, the attraction of the immune system through the release of pro-inflammatory and chemotactic signals would also be of benefit to an anti-tumourigenic mechanism and as such may have been retained as the senescence response evolved. Indeed increased local immune infiltration is associated with improved survival in cancer patients (Roxburgh et al. 2009) and activation of the secretory senescence pathway may be intended to evoke this response.

However, as with all biological systems, the exact levels of such signaling must be closely regulated. Over-activation of the secretory senescence pathway may also have a deleterious effect, reflected by the fact that patients showing an increased system-wide immune activation, as opposed to tumour localized immune response, show a poorer prognosis (Roxburgh et al. 2009). Due to the relative infancy of the investigations into the secretory senescence pathway, the exact details and implications upon clinical factors such as outcome of the secretory senescence pathway are still under investigation but may in the future present novel opportunities for adjuvant pro-senescent therapies.

1.2.3 Autophagy and senescence

The latest pathway to be implicated in senescence induction is that of autophagy. Current evidence of the exact mechanisms by which autophagy and senescence interact is underdeveloped but the few studies that do exist have quickly identified what may be a particularly important factor in senescence induction. Autophagy, or self-eating, is the genetically orchestrated process of digesting internal organs and proteins of a cell. As such, it represents a third cell fate upon the receipt of cellular stress signals distinct from that of apoptosis or senescence. More precisely autophagy consists of the formation of double membrane vacuoles, known as autophagosomes, containing the organ or proteins to be digested. The autophagosomes are then fused with lysosomes to provide the digesting enzymes. The most frequently utilized marker of autophagy is LC3, which when bound to the autophagosomes, known as LC3-II, can be identified using immunoblotting techniques (Young et al. 2009). Upon starvation conditions autophagy can be induced to recycle proteins into their amino acid constituents for use in protein synthesis. Furthermore, autophagy activation is frequently observed when a cell needs to change from one metabolic state to another and facilitates the fast turn over of proteins to facilitate this. As senescence involves a major switch from a proliferating cell state to an arrested cell state accompanied by large phenotypic changes it is logical that autophagy may facilitate the large protein turn over required for this.

The most compelling evidence for a link between autophagy and senescence comes from a large and detailed recent study by Young and colleagues (Young et al. 2009). In this study, the authors utilized a combination of the

aforementioned immunoblotting techniques for LC3-II and protein degradation assays on human diploid fibroblasts induced to senescence by RAS or MEK overexpression to investigate whether autophagy became activated upon senescence induction. LC3-II concentration was found to increase upon both RAS and MEK activation implying that upon senescence induction autophagy became activated. Furthermore, LC3-II increases did not occur when the induction of senescence was blocked. The group then went on to model the kinetics of autophagy activation during senescence induction using an inducible RAS activation model. The authors observed that after RAS activation the cells underwent a brief spell of increased cellular proliferation followed by senescence induction 5-6 days after. It was during the 4-5 days between the proliferative burst and induction of senescence that autophagy activation reached its peak. This suggests that autophagy may mediate the conversion of the proliferative cellular state to the senescence phenotype, through increased protein turnover. Some contradictions in the involvement of autophagy do exist however. mTOR has previously been seen to be required to induce the PTEN-loss induced senescence pathway however mTOR has also been observed to be a negative regulator of autophagy (Mathew et al. 2007). As such, senescence induction should repress the autophagic process. Upon investigation of the phosphorylation activity of mTOR, Young and coworkers found that an initial spike in activity following RAS activation then decreased in correlation with the activation of the autophagic transition to senescence. This suggests that continuous mTOR signaling is not required for maintenance of the senescent phenotype, an initial burst of activity is sufficient to activate the signaling cascade and induce senescence completely. This is consistent with the negative feedback loop through NF1 inhibition of downstream RAS pathways previously observed to regulate oncogene induced senescence (Courtois-Cox et al. 2006) Furthermore, NF1 has been shown to directly repress mTOR (Johannessen et al. 2005) and thereby may provide a further direct pro-autophagic signal upon activation of oncogene-induced senescence. Through microarray analysis, Young and colleagues went on to show that overexpression of the gene ULK3 was sufficient to induce both autophagy and senescence and may provide a key signaling molecule for the concurrent activation of both pathways. Although the only study to date that mechanistically links autophagy with senescence induction, Young and colleagues have made a convincing argument for

autophagy as an effector mechanism for the switch from proliferating to senescent phenotype.

Although to date β -galactosidase staining at pH6 has been the most consistent marker for senescence available the exact mechanism behind the association of β -galactosidase expression and senescence still remains a mystery; autophagy may provide a reason behind the marker however. β -galactosidase staining in senescent cells was recently attributed to the activities of the gene GLB1 (Lee et al. 2006). GLB1 encodes lysosomal β -D-galactosidase, which is one of the enzymatic components of autophagosomes. Knockdown of GLB1 with shRNA has been shown to delay β -galactosidase staining but not the induction of the senescent phenotype (Lee et al. 2006). Furthermore, knockdown of autophagy upregulated genes ATG5 and ATG7 has been observed to delay the onset of β -galactosidase activity in senescent cells (Young et al. 2009). If β -galactosidase activity in senescent cells is truly representative of autophagy-mediated senescence then it makes some sense of an observation of lack of β -galactosidase activity in melanocytic nevi *in vivo* (Cotter et al. 2007). If β -galactosidase activity is a product of the autophagic transition phase of senescence and this phase is limited to the transition between proliferative and senescent phenotypes, then the lack of β -galactosidase activity in melanocytic nevi may suggest that these cells have moved passed the transition phase and are fully in the senescent phase. Further investigations of the dynamics of autophagy and senescence *in vivo* are required however, before any firm conclusions as to the relationship between senescence associated β -galactosidase staining and autophagy can be made. It is, however, curious to think that the most recent addition to the senescence story is behind one of the most consistent markers for senescence detection.

1.3 Physiological Senescence: Senescence *in vivo*

With an increased understanding of the molecular mechanisms behind senescence gradually coming to light the physiological roles of senescence become increasingly important. Senescence *in vivo* has so far been seen to play important roles in three major processes; tumour suppression, aging and wound healing.

1.3.1 Senescence and Aging

As senescence is a mechanism of controlling the level of cellular proliferation and, in the case of replicative senescence, halting cell division after a set number of cell cycles it makes logical sense that it should have some links with the larger process of aging. Indeed an increase of cells showing senescent markers in aging tissues and age related diseases such as atherosclerosis, skin ulcers, osteoarthritis and liver cirrhosis has been observed (Herbig et al. 2006, Sedelnikova et al. 2004, Campisi 2005; Price et al. 2002; Wiemann et al. 2002).

The premature aging syndrome dyskeratosis congenita (DKC) adds further weight to the role of senescence in the process of organismal aging. DKC is an autosomal dominant disorder caused by mutations in the genes *diskerin*, *TERT* or *TERC* and results in a failure to maintain telomeres in stem cells and the germ line (Kirwan and Dokal 2009). DKC results in bone marrow stem cell failure as stem cells telomeres are no longer maintained by telomerase and therefore eventually induce replicative senescence. Furthermore, patients with DKC often present with premature aging-like symptoms such as premature hair loss/graying, deafness, osteoporosis and liver disease (de la Fuente and Dokal 2007).

Although observation of the senescence markers in aging tissues and organisms presents a strong case for the role of senescence in the aging process further function studies are required to directly link the two processes. Mechanistic studies in the *BubR1* insufficiency mouse models of premature aging and have shown that p16 inactivation attenuates both cellular senescence and premature aging while ARF inactivation exacerbates both phenotypes (Baker et al. 2008). However, as discussed in the discussion of the secretory senescence pathways (see 1.2.2) the use of mice to model complex phenotypes in humans must be done with caution as results are not always directly comparable. In the case of p16's role in the aging process there is some evidence that this link may not be limited only to mouse models however. Recently p16 has also been suggested as a human molecular marker of ageing due to its increased expression in human tissues and particularly peripheral blood lymphocytes (Liu et al. 2009).

The premature aging of patients with DKC; reduction of tissue function and the induction of age related diseases may be a further example of where senescence, whilst providing a barrier to potentially harmful diseases such as cancer (see 1.3.3) may also cause harm in the longer term.

1.3.2 Senescence and Wound Healing

A recent addition to the repertoire of senescence *in vivo* is its role in the repair of tissue damage known as wound healing. Upon receipt of an injury tissues undergo a program of tissue repair and remodeling that involves the activation of fibrosis to heal the wound and maintain tissue stability (Friedman et al. 2008). Recent evidence highlighted the presence of senescent hepatic stellate cells, the cells initially responsible for the production of the fibrotic extracellular matrix, in the liver in response to injury induced by carbon tetrachloride (Krizhanovsky et al. 2008). These senescent hepatic, like other senescent cells, secrete matrix metalloproteases as part of the secretory senescence pathway and therefore serve to limit the level of fibrosis created during the process of wound healing in the liver. More recently the link between senescence and wound healing was further strengthened by a study by Jun and Lau. In this study the matricellular protein CCN1 was found to induce senescence in fibroblasts through the activation of p53 and pRB pathways (Jun and Lau 2010). These senescent fibroblasts were found to accumulate in cutaneous wounds and CCN1 knockout mice were found to have extra fibrosis in cutaneous wounds, corrected by the application of CCN1 protein solutions directly to the wound. The evidence for the role of senescence as a crucial component of the normal healing process is therefore growing and with further mechanistic studies will continue to aid our understanding of the different physiological roles of senescent cells.

1.3.3 Senescence as a block to tumour progression.

Immortalisation, the ability to proliferate exponentially, is a prerequisite of the transformation of a normal cell into a cancer cell. As senescence has the ability to permanently remove the cell from the cell cycle it forms a major barrier to neoplasia and tumour progression. In fact senescence induction appears to perfectly placed to respond to early tumorigenic events and prevent the

establishment of the tumour through its activation in response to oncogene activation and inhibition of tumour suppressors. Furthermore, the removal of the cells from the cell cycle would also prevent the accumulation of further neoplastic mutations that may overcome other tumour suppressive signaling cascades with continued rounds of cell division.

Detection of cells with the characteristics of senescence have been detected *in vivo* in a number of different tissue types. Through the investigation of senescence markers, β -galactosidase staining and p16 expression, in an inducible KRas mutant mouse model Collado et al highlighted the presence of senescent cells in adenomas of the lung and in premalignant pancreatic lesions (pancreatic intraductal neoplasias (Collado et al. 2005). These senescent cells were seen at much lower levels in adenocarcinomas and pancreatic ductal adenocarcinomas implying that the senescent cells may indeed be early cancer cells prevented from entering full immortality by the senescence program. Similarly, senescent cells have also been observed in benign dermal neurofibromas and melanocytic nevi (Coutois-Cox et al. 2006, Braig et al. 2005. Michaloglou et al. 2005).

As the majority of melanomas rely on activating mutations in BRAF, which has been seen to trigger the senescence response, it makes logical sense that senescence should be activated in the early pre-cancerous cells and establish benign nevi instead. In fact recent clinical trials into the inhibition of BRAF expression in melanoma have been highly successful (Bollag et al. 2010). Unfortunately, many of these studies focus on the oncogenes addiction of these tumours and do not examine senescence markers so it is not always possible to say whether this is through the reversion of cancerous melanoma cells to a senescent state. However, mouse model studies in liver carcinomas and sarcomas, showed that reestablishment of key senescence genes, such as p53, successfully causes tumour regression (Xue et al. 2007; Ventura et al. 2007). Furthermore, senescence has been observed to be induced in response to chemotherapeutic agents *in vivo* (te Poele et al. 2002) and as such senescence therefore presents a strong role as a tumour suppressive mechanism *in vivo* as well as *in vitro*.

A further mechanism by which senescence presents a block to tumorigenesis is through the potential of the secretory senescence pathway to induce a local

immune response and immune clearance of premalignant cells that have entered senescence. As discussed previously (see 1.2.2) the secretory senescence pathway results in the secretion of many proinflammatory and immune activatory proteins and as such may be able to attract the immune system to cells that are undergoing pre-malignant transformations. In support of this concept work in mouse liver carcinomas showed that reactivation of p53 induced cellular senescence and clearance by the innate immune system (Xue et al. 2007). The tumour clearance was seen to be mediated by the NK cells of the immune system which was ablated by the application of NK blocking antibodies or gadolinium chloride. Therefore although the secretory senescence pathway may be pleiotropic in its ability to suppress tumorigenesis there is strong evidence that if utilised correctly it may be an important tool in the induction of tumour regression.

Senescence therefore presents a major block to tumour establishment and progression however as cancer does still exist it is obviously not a fool proof mechanism. In fact even in well established models such as melanocytic nevi it is known that a small number of nevi established for decades still progress to cancerous melanomas (Michaloglou et al. 2005). Therefore although senescence exists as a tumour suppressive mechanism *in vivo*, cancer cells also have adapted a number of senescence bypass mechanisms.

1.4 Senescence bypass by telomere maintenance

The induction of replicative senescence through telomere attrition forms a major barrier to tumour progression. Regardless of a cell's ability to tolerate oncogene overexpression or cellular stress, the gradual telomere shortening caused by repeated cell cycling still requires bypass. In order to become fully tumourigenic cells commonly bypass senescence through the induction of a telomere maintenance mechanism.

1.4.1 Telomere maintenance by telomerase

The enzyme telomerase is a ribonucleoprotein with reverse transcriptase activity capable of lengthening telomeres and is utilised by the majority of cancer cells to overcome crisis and avoid senescence (Ju et al. 2006). The only normal cell

types observed to naturally express active telomerase are germ cells (Kim et al. 1994), stem cell populations, such as haematopoietic stem cells (Vaziri et al. 1994; Counter et al. 1995; Yui et al. 1998) and leukocytes (Counter et al. 1995). Recent evidence from mutations in the hTERT gene suggest that lack of telomerase activity in stem cells may lead to their premature loss (Hills et al. 2009). Furthermore, mutations in the components of the telomerase enzyme have also been observed in cancers such as acute myeloid leukemia (Calado et al. 2009) and may highlight the potential importance of other mechanisms of telomere maintenance in these tumour types.

Telomerase consists of two components, the catalytic component encoded by the hTERT gene and the RNA template component encoded by the hTR gene. Expression of both subunits is required for *in vivo* telomerase activity (Weinrich et al. 1997) and consistent with this, hTERT and hTR, are specifically up regulated in cancer compared to normal tissues and cell lines (Parkinson et al. 1997). Dyskerin, encoded by DKC1, has also recently been shown to be associated with telomerase and is thought to stabilize the RNA/enzyme complex (Cohen et al. 2007). Further evidence for the potential requirement for dyskerin for telomerase activity is provided by the reduced telomerase activity resulting from mutated dyskerin (Mitchell et al. 1999). In addition to this the autosomal dominant disease dyskeratosis congenita is attributed to reduced telomerase activity and, to date, mutations in only DKC1, hTR and hTERT have been seen to cause the phenotype (Mitchell et al. 1999; Vulliamy et al. 2001; Armanios et al. 2005). Previous studies have highlighted the ability of the components of telomerase to dimerise (Wenz et al. 2001) and examination of the molecular weights of hTERT, hTR and dyskerin of purified catalytically active human telomerase suggest that the telomerase construct may exist as 3 dimers of each of these components (Cohen et al. 2007). However, these studies result from *in vitro* reconstitution of recombinant telomerase components or purified telomerase and therefore may not be truly reflective of the *in vivo* active enzyme complex.

Given the tumourigenic properties of telomerase expression, it is not surprising that it is highly regulated on multiple levels. Firstly, both hTERT and hTR transcription are highly regulated processes. Both genes show balance of multiple layers of transcriptional regulation at their promoters. For example,

hTERT expression is repressed by transcription factors such as AP1, p53 and RUNX2 and activated by c-Myc, SP1 and STAT3 (Kanaya et al. 2000; Kyo et al. 2000; Konnikova et al. 2005; Takakura et al. 2005; Isenmann et al. 2007). Of all of these transcriptional regulators probably the most important link with senescence regulation comes from p53 and c-Myc. Given that p53 is a key effector of induction of the senescence pathway it is logical that it should also act as a negative transcriptional regulator of the main mechanism of senescence bypass.

c-Myc's role in senescence and telomere maintenance by telomerase is well studied. Overexpression of c-Myc is common in cancer playing a regulatory role in the cell cycle (Wang et al. 2008), angiogenesis and cell migration (Meyer et al. 2008; Herold et al. 2009). c-Myc therefore presents an attractive target for anti-cancer therapy. A recent study found that the potent anti-cancer drug butein causes a decrease in telomerase expression and inhibits cell proliferation through the suppression of c-Myc expression (Moon et al.). Recent evidence that further chromatin remodelling is required before c-Myc can access the hTERT promoter for activation (Bazarov et al. 2009) suggests chromatin modification may also play a factor in the lack of hTERT expression increases in these cell lines. Aside from hTERT, another down-regulated c-Myc target that may play a role in telomere maintenance is hnRPA3. It was recently shown that hnRPA3 binds the single stranded telomere repeat *in vitro*, protects against nuclease activity and inhibits extension by telomerase (Huang et al. 2008). C-Myc therefore clearly plays an important role in the regulation of telomere maintenance by telomerase. Consistent with this, in melanoma, c-Myc overexpression has been shown to be required for the bypass of oncogene induced senescence (Zhuang et al. 2008). Similarly, c-Myc repression has been shown to induce cellular senescence and tumour regression in osteosarcoma, hepatocellular carcinoma and lymphomas (Wu et al. 2007).

hTERT is further regulated by alternative splicing. Several splice variants of hTERT exist where only the full length variant is active. hTERT has been shown to have at least 6 different splice variants where three main alternative splice forms have been extensively studied to date, known as the α , β and α/β forms. All the splice variants produce truncated inactive forms of the protein, however, there is evidence that the α variant may function as a dominant negative form

(Colgin et al. 2000; Yi et al. 2000). This suggests a further level of post-transcriptional regulation through regulatory feedback loops from alternative splice variants. A more recent study utilized sequential RT-PCR of primer pairs covering the entire full-length hTERT mRNA in a panel of cDNAs from 5 normal and tumour tissues. Upon examination of the resulting fragments the study highlighted a further 6 novel alternative splice forms and therefore the potential for up to 12 alternatively spliced variants of hTERT (Saeboe-Larssen et al. 2006). These observations further highlight the importance of the strict regulation of the telomerase enzyme to prevent senescence bypass and lead to potential tumorigenesis. The importance of this mechanism is further emphasised by their observation in different forms of human cancers. A study of malignant breast tumours and their surrounding tissues showed that expression of full-length hTERT correlated with telomerase activity in breast tumours (Zaffaroni et al. 2002). However, in surrounding normal tissue and benign lesions the study interestingly showed that expression of the full-length splice variant alone was not sufficient for telomerase activity. This suggests that further regulatory mechanisms for the inhibition of telomerase activity are present and active in these cells. Further studies of melanoma cells, typical carcinoids, large cell neuroendocrine carcinomas and small cell lung cancers have highlighted requirement of the full length hTERT splice variant for telomerase activity and the potential importance of alternative splicing as a telomerase regulatory mechanism *in vivo* (Zaffaroni et al. 2005; Lincz et al. 2008). As negative regulators of telomere maintenance by telomerase, the induction of the dominant negative splice variants of telomerase make an attractive target for anti-cancer therapy. The role of splice variants of hTERT in response to therapy has been implicated in recent studies of breast cancer. One study highlighted shifts in splice variants away from negative forms after treatment of breast cancer with tamoxifen, potentially highlighting a primary mechanism of resistance induction in cancer cells surviving treatment (Strati et al. 2009).

A further layer of regulation to senescence bypass by telomerase is given by post-translation protein modification. Phosphorylation of telomerase by AKT and PP2A have been observed to enhance telomerase activity in breast cancer and melanoma cells (Li et al. 1997; Kang et al. 1999). In addition, the recent observation that decreased activity of telomerase in highly differentiated T-cells is due to the decreased activity of AKT further highlights the importance of the

mechanism *in vivo* (Plunkett et al. 2007). Phosphorylation also presents a mechanism by which telomerase activity can be down regulated upon senescence induction as the phosphorylative actions of the tyrosine kinase c-ABL have been found to repress telomerase activity rather than activate it (Kharbanda et al. 2000). As c-ABL is frequently activated in response to DNA damage this represents a further feedback loop by which senescence bypass via telomerase activation could be repressed upon the induction of the damage associated pathway of senescence.

The importance of repressing telomerase activity to prevent senescence bypass is further highlighted by recent evidence of the involvement of the TGF β downstream target SMAD3 in the suppression of telomerase during cancer induction (Li et al. 2007). SMAD3 is a known c-Myc inhibitor and as such its activation would repress the transcription of hTERT. As TGF β is a member of the secretory senescence pathway, it is possible that such secretion acts as a regulatory mechanism to prevent senescence bypass through telomerase telomere maintenance. The repression of telomerase activity after activation of both the damage associated and secretory senescence pathways highlights intrinsic mechanisms by which cells attempt to respond to and prevent the bypass of senescence through telomere maintenance by telomerase.

1.4.2 Telomere maintenance by alternative lengthening of telomeres

There are however, cells that maintain their telomeres without the reactivation of the telomerase enzyme. Such cells are said to use the alternative lengthening of telomeres mechanism or ALT. Currently, the underlying molecular mechanisms of ALT are poorly understood.

Existing assays for ALT rely on phenotypic cellular traits. These include heterogeneous telomere lengths ranging from 3 kb to 50 kb (Henson et al. 2002), small nuclear foci called ALT-associated PML bodies (APBs) (Reddel 2003) and an abundance of extrachromosomal telomeric DNA, known as t-circles (Fajkus et al. 2005). The actual role of these markers in the mechanisms by which these cells maintain their telomeres is yet to be fully understood. The current standard assay for ALT identification is primarily focused on the identification of ALT unique form of the APBs. However, the role of APBs in ALT is still under debate.

These nuclear structures contain the PML protein and SP100 of normal promyelocytic leukaemia bodies (PML bodies) (Yeager et al. 1999) as well as telomeric DNA repeats, telomere binding proteins TRF1 and 2, RAD51, RAD52 and replication factor A. RAD51, RAD52 and Replication factor A have well characterised roles in recombination and DNA synthesis (Benson et al. 1998) and therefore in combination with the TRF1 and 2 highlight a possible role for APBs in telomeric maintenance. Further APB characterization has highlighted that proteins such as NBS1, PML, TRF1, TRF2, TIN2, RAP1, MRE11 and RAD50 are required for APB construction and other molecules, such as BRCA1, hRAP1, SP100 and 53BP1, simply associate with APBs (Wu et al. 2003; W-Q Jiang 2007). These complex and multiple interactions of APBs are indicative of a possible higher order structure in APB construction rather than their production as a byproduct of telomere maintenance by ALT. The association of molecules with various DNA interacting abilities such as the helicases BLM (Stavropoulos et al. 2002) and WRN (Johnson 2001) and DNA damage signaling and repair proteins like MRE11 and RAD50 (in complex with NBS1) gives further weight to their potential for direct involvement in telomere maintenance (Zhu 2000). Evidence for this direct role is, however, still under debate with some evidence ALT telomere maintenance failing in their absence (Jiang et al. 2005) but also evidence of ALT in cells without any APBs (Fasching et al. 2005).

Regardless of the direct involvement of APBs, the most prevalent theory as to the mechanism through which ALT cells maintain their telomeres is by homologous recombination. The use of fluorescently tagged telomeres has demonstrated the copying of telomeres from one chromosome to another (Dunham et al. 2000). In addition, through the introduction of a telomere tag it has also been shown that intra-telomere recombination can also be utilized by ALT cells (Muntoni et al. 2009). Investigation of the telomere recombination rates of ALT cell lines reveals higher rates in ALT in comparison to telomerase positive cells whilst non-telomeric regions show no significant rate differences, adding weight to the concept that this could be the mechanism behind telomere maintenance by ALT (Bechter et al. 2003; Londono-Vallejo et al. 2004). Further suggested models of telomeric recombination that could result in the observed telomere heterogeneity, as shown in Figure 1.3, and add further evidence to the theory (Muntoni et al. 2005).

Certain telomere binding proteins have also been implicated to play roles within the homologous recombination mechanism. This provides opportunities for the recruitment of the homologous recombination machinery to the telomeres. For instance, WRN is a helicase which when mutated causes the premature aging disease Werner Syndrome (Multani et al. 2007). It has been shown to interact with members of the shelterin complex, well known telomere interacting proteins, such as TRF1, TRF2 and POT1 (Smogorzewska et al. 2004) and as such could be seen to potentially have a role in telomere maintenance. However, their role may be more complex than previously thought. Patients with a defect in the WRN gene suffer rapid telomeric shortening. This suggests that the removal of active WRN affects the cell's ability to stabilise the telomeres to their natural gradual degradation rate. WRN has also been successfully used as a tool to investigate spontaneous escape from the cell crisis resulting from short telomere lengths. Laud *et al.* demonstrated that cells deficient in WRN are capable of senescence escape and telomere maintenance through the ALT pathway (Laud et al. 2005). This shows that WRN may not be essential for ALT but that its expression and regulation could still play some role at the telomeres in ALT cells.

Such cross-talk with other telomeric interacting proteins is not the only consideration that the homologous recombination theory has suggested. A study in 2005 examined minisatellite sequences which have known mutations created by homologous recombination. (Jeyapalan et al. 2005) The results showed a much higher level of minisatellite instability of one of these minisatellites, MS32, in ALT cell lines but not in normal or telomerase positive cell lines. This suggests that the increase in homologous recombination in ALT may have far reaching effects in the genome and may not simply affect the pathways involved in this one particular process. The alteration of genomic information in ALT cells could have far reaching effects and possibly allow the involvement of other relevant pathways through alterations in their regulation and expression.

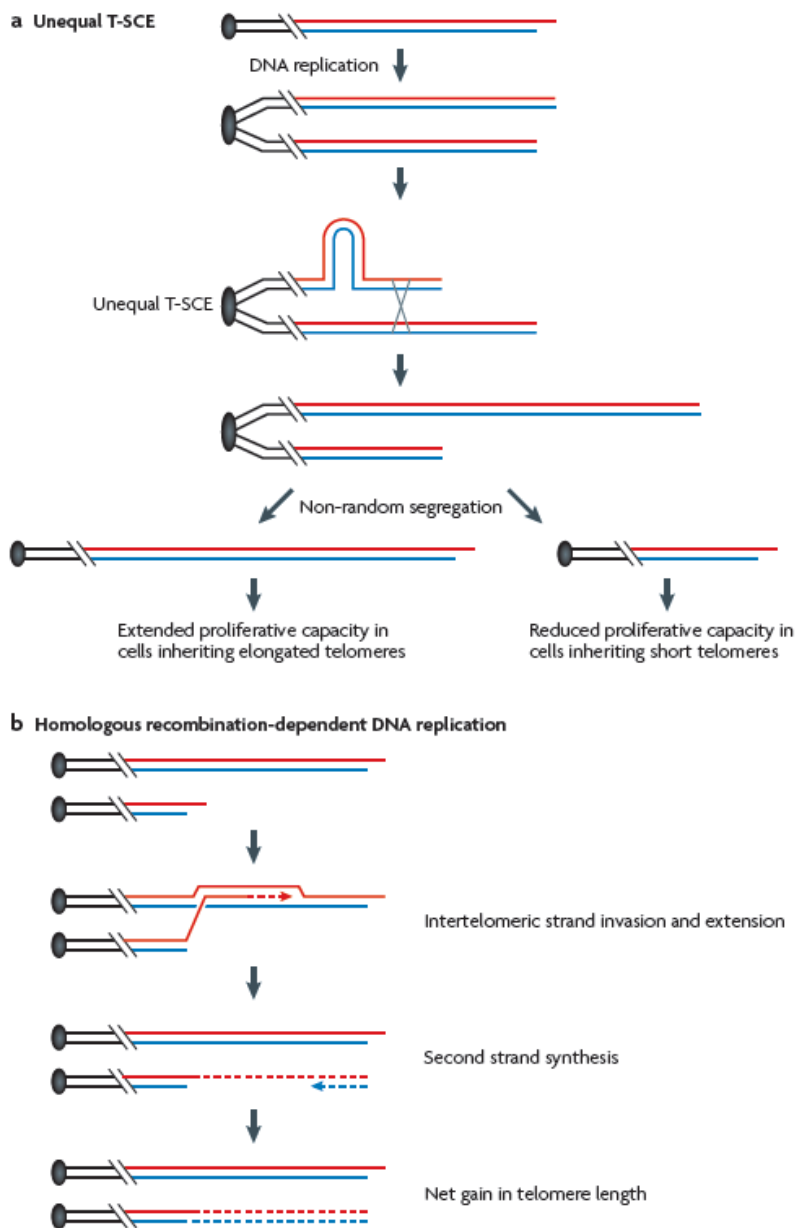


Figure 1.3 - Telomeric heterogeneity achieved through asymmetric telomere recombination and net gain through intertelomeric strand invasion. (A) Model proposed by Cesare and Reddel by which ALT cells would achieve heterogeneity in their telomeric lengths via recombination (B) Secondly a further model is proposed by which telomeres would achieve an overall net gain of telomere length through the utilisation of other telomeres as a template strand for DNA synthesis, Image taken from Cesare and Reddel, 2010. *Nat. Rev. Gen.*, 11(5) 319-330.

Further theories on the mechanisms behind ALT also exist. Evidence is growing for the role of the small telomeric circles, t-circles, in telomere maintenance. Homologous recombination has been found to create a small deletion approximately the size of t-circles (Wang et al. 2004). T-circles are present in high abundance extrachromasomally in ALT cell lines which may suggest a potential “rolling circle” mechanism of telomeric maintenance (Natarajan et al. 2002) or maintenance mechanisms that could involve the integration of t-circle to telomeres or by use of the t-circle as a template (Tomaska et al. 2004). Further evidence is supplied in studies that show that even the smallest of t-circles are active and capable of the rolling circle mechanism of telomeric maintenance (Hartig et al. 2004). This suggests that homologous recombination may not be solely responsible for the maintenance of the telomeres in ALT cell lines. As discussed previously, the interactions of telomere associated and homologous recombination associated proteins with other pathways supplies the opportunity for potential cooperation of mechanisms to a common goal.

The interaction of t-circles as part of other ALT TMMs has become a distinct possibility since a recent study showed that Nbs1 is required for the production of t-circles (Compton et al. 2007). Nbs1 is well characterised as a foundational protein in APBs (Wu et al. 2003) and therefore their requirement for t-circle production suggests that there is a more complex set of interactions required for the full ALT TMM to occur.

The use of ALT for telomere maintenance is predominantly found in cells of mesenchymal origin. However, even within mesenchymal tumour subtypes the frequency of ALT varies greatly, for example 77% of malignant fibrous histiocytomas use ALT whereas only 6% of rhabdomyosarcomas (Henson et al. 2005). ALT has also been shown to correlate with patient outcome and prognosis however the exact correlation of ALT with outcome and prognosis varies depending upon tumour type. Studies of bone and soft tissue sarcomas show an improved survival for patients with ALT or telomerase negative tumours (Terasaki 2004). Osteosarcomas in particular show strongly favourable outcome with ALT (Ulaner et al. 2003; Sanders et al. 2004). Conversely, liposarcomas utilizing ALT have increased linkage to mortality (Costa et al. 2006). Study of metastatic potential of mouse embryonic fibroblasts provides some evidence for

why some ALT tumours may have more favourable outcome than others (Chang et al. 2003). Telomerase reconstitution in subcutaneous ALT tumours led to a high metastatic ability whilst tumours that remained as ALT were unable to undergo metastasis. A lower metastatic potential could be one explanation for the prognostic implications of TMM and why some osteosarcomas, bone and soft tissue sarcomas have a more positive prognosis with ALT. However given the complexity of the ALT phenotype it is likely that other factors are also involved.

Telomere maintenance by either telomerase or ALT is an essential step in the bypass of senescence, however the reason that a cell utilizes one mechanism rather than another is unknown. Examination of the molecular differences between the two mechanisms has shown that chromatin modifications may play a role in the decision. Methylation at the hTR promoter in ALT cell lines has been shown to be responsible for the repression hTR expression in ALT (Hoare et al. 2001) and similarly methylation and hypoacetylation of the hTERT promoter of ALT cells lines is suggestive of epigenetic suppression of hTERT expression in ALT cells (Atkinson et al. 2005). Such active regulation of the promoter of the two components of telomerase in ALT cells is suggestive of a regulatory network initiating and maintaining the choice of TMM during neoplasia. The details of such a regulatory network are currently not explored.

1.5 Aims of this Study

As a major block to tumorigenesis an understanding of the regulatory networks surrounding the process of cellular senescence is required. Although the roles of individual molecules such as p53 and p16 during senescence induction have been well defined, the regulatory mechanisms surrounding the larger processes of senescence are currently poorly understood. The understanding of the regulatory networks involved in senescence bypass through mechanisms such as telomere maintenance may also improve current understanding as to how tumours perturb the process of senescence and achieve immortalization. Furthermore, the degree to which bypassed senescence pathways remain latently expressed in human tumours and their potential impact on clinical factors such as patient outcome is completely unexplored. The investigation of these regulatory networks and latent senescence signaling may therefore facilitate the improved targeting of therapeutics and reveal novel diagnostic and prognostic biomarkers.

It was therefore the specific aim of this study to investigate regulatory networks surrounding senescence signaling and bypass and assess the potential impact upon clinical factors such as outcome.

Through the application of gene expression and miRNA microarray profiling, kinome siRNA and virtual drug screening the following questions were addressed:

- What molecular differences exist between cells utilizing different TMMs for senescence bypass?
- Do miRNAs have a regulatory role in senescence bypass and signaling?
- Does latent senescence signaling exist in human tumours and how can it be measured?
- Can such measures be used to assess the impact of latent signaling on clinical factors such as outcome and response to therapy?

2 Materials and Methods

2.1 Materials

2.1.1 *Tissue Culture Reagents and Consumables*

Minimum Essential Medium (MEM)	Invitrogen
RPMI 1640 growth medium	Invitrogen
Dulbeccos modified Eagles MEM	Invitrogen
L-glutamine (200mM)	Invitrogen
Trypsin (2.5%)	Invitrogen
Foetal calf serum (Batch ID)	Autogen Bioclear
96-well plates	Iwaki
12-well plates	Iwaki
28 cm ² flasks	Nunc
75 cm ² flasks	Iwaki
150 cm ² flasks	Nunc
500 cm ² triple-flasks	Nunc

2.1.2 Cell Lines

Human cell lines used in this study:

Cell Line	Source	Telomere Maintenance Mechanism	Age and Sex of Donor	Known Mutations
SK-LU-1 lung adenocarcinoma	ATCC	ALT	60 years, Female	CDKN2A, CDKN2A(p14), KRAS, TP53
KMST6 immortalised lung fibroblast	CCR	ALT	9 weeks, Female	TP53
Wi38-VA13/2RA (WI38-SV40) immortalised lung fibroblast	CCR	ALT	3 months gestation, Female	SV40 antigen renders TP53 null
SUSM1 carcinogen transformed liver fibroblast	CCR	ALT	Fetal human fibroblasts, unknown	TP53
SAOS-2 osteosarcoma	ATCC	ALT	11 years, Female	RB1, TP53
U2OS osteosarcoma	ATCC	ALT	15 years, Female	CDKN2A
A2780 ovarian carcinoma	ECACC	Telomerase	Unknown, Female	PTEN
HT1080 fibrosarcoma	ATCC	Telomerase	35 years, Male	CDKN2A, CDKN2A(p14), IDH1, NRAS

Cell Line	Source	Telomere Maintenance Mechanism	Age and Sex of Donor	Known Mutations
5637 bladder carcinoma	ATCC	Telomerase	68 years, Male	RB1, TP53
C33a cervical carcinoma	ATCC	Telomerase	66 years, Female	RB1, TP53, PTEN, PIK3CA, MSH2, FBXW7
WI38 lung fibroblast	ECACC	None	3 months gestation, Female	None documented
IMR90 lung fibroblast	ECACC	None	16 weeks, Female	None Documented

2.1.3 Primary Cell Cultures

Primary cells used in this study:

Human mesenchymal stem cells (hMSCs): Primary hMSC aspirates isolated by centrifugation at 700 g for 15 min at 4 °C over a Ficoll-Hypaque gradient (Sigma).

Human Tumour Biopsies

The table in Appendix II details all of the current information on file for the mesenchymal tumours used in this study.

2.1.4 Luciferase Reporter Plasmid Vectors

pGL3 hTERT 24/9: hTERT reporter vector; contains the firefly luciferase gene driven by a 576bp fragment of the hTERT promoter, constructed by Sharon Burns and Rosalind Glasspool.

pSGG MYEOV: MYEOV reporter vector; contains the firefly luciferase gene driven by 1072bp fragment of the MYEOV promoter, constructed by Switchgear Genomics.

2.1.5 Antibodies

KAT2A/GCN5 Rabbit polyclonal	Abcam (ab18381)
E2F1 Rabbit polyclonal	Active Motif (39313)
HDAC5 Rabbit polyclonal	Active Motif (40970)
PKC alpha Rabbit polyclonal	Abcam (ab32376)
Anti-Rabbit IgG HRP-linked Antibody	New England Biolabs (7074)
ERC antibody	Abcam (ab50132)

2.1.6 Kits, Reagents and Enzymes

<u>Kit/Reagent</u>	<u>Supplier</u>
Lipofectamine 2000	Invitrogen
Passive lysis buffer	Promega
Luciferase assay system	Promega
Protein assay reagent	Biorad
Nucleospin II RNA extraction kit	Macheray-Nagel

<u>Kit/Reagent</u>	<u>Supplier</u>
RNeasy lipid tissue RNA extraction kit	Qiagen
RNeasy mini kit	Qiagen
GeneAmp RNA PCR core kit	Roche
Taq PCR core kit	Qiagen
Hotstar Taq DNA polymerase	Qiagen
DyNAmo SYBR Green qPCR kit	Finnzymes
ECL detection reagents for western blotting	Amersham
Restriction endonucleases and buffers	Invitrogen
E.coli Top10 competent cells	Invitrogen
S.O.C. medium	Invitrogen
Plasmid Maxi Prep kit	Qiagen
Qiaquick Spin Miniprep kit	Qiagen
Multimark protein molecular weight marker	Invitrogen
NuPAGE Novex 4-12% BIS-TRIS gels	Invitrogen
NuPAGE MES SDS running buffer	Invitrogen
NuPAGE MOPS SDS running buffer	Invitrogen
NuPAGE antioxidant	Invitrogen
NuPage transfer buffer	Invitrogen
RNaseZap	Ambion
Agilent RNA 6000 Nano reagents & supplies	Agilent Technologies

<u>Kit/Reagent</u>	<u>Supplier</u>
RNA 6000 Nano Chips	Agilent Technologies
Nuclear Extraction Kit	Active Motif
TRANSAM c-Myc	Active Motif
Recombinant c-Myc	Active Motif
Gene expression microarray kits and reagents	Agilent Technologies
MiScript miRNA qPCR kit	Qiagen

2.1.7 Chemicals

2.1.8 General laboratory supplies and reagents

Provided by Beatson Institute Central Services:

LB-Medium (Luria-Bertani Medium)

Sterile Distilled Water

Sterile phosphasphate buffered saline (PBS)

Sterile PBS + EDTA (PE)

10x TBE electrophoresis buffer (Tris Borate/EDTA)

Sterile glassware and measuring pipettes

General:

	<u>Supplier</u>
Ampicillin	Sigma
Kanamycin	Sigma

	<u>Supplier</u>
Falcon Tubes 50 & 15ml	Becton Dickson
Universal containers 5ml, 20ml & 100ml	Bibby Sterilin
Microcentrifuge tubes 1.5ml & 0.5ml	Eppendorf & Abgene
Cell scrapers	Corning
Pipette tips	Gilson & Griener
Plastic stripettes 1ml, 5ml, 10ml, 25ml & 50ml	Corning
X-ray film	Fujifilm
Nitrocellulose membrane	Millipore

2.1.9 Oligonucleotide Primers for qPCR

Oligonucleotide primers given in a 5' to 3' direction.

hTERTF: 5'- CTGCTGCGCACGTGGGAAGC,

hTERTR: 5'- GGACACCTGGCGGAAGGAG,

s15F: 5'-TTCCGCAAGTTCACCTACC,

s15R: 5'-CGGGCCGGCCATGCTTTACG,

MYEOVF: 5'-TGGGAGGACACGCAAGTT,

MYEOVR: 5'-CCAGCAGCCAAAGCAAAG,

WNT5BF: 5'-AGGAGGGAGGTTGTGGTT,

WNT5BR: 5'-GAACCGTGGAGGATGAAG,

DSC54F: 5'-ACCCTTCTACGAAATGGA,

DSC54R: 5'-ACTGTGGCTTATTCCCAT,

NSUN5F: 5'-TGAGACCACACTCAGCAG,

NSUN5R: 5'-GAGAGGACAGGCATCTTC

GAPDHF: 5'ACCACAGTCCATGCCATCAC,

GAPDHR: 5'TCCACCACCCTGTTGCTGTA

TCEAL7F: 5'GAAGGAAGAGCTGGTTGAT

TCEAL7R: 5'GACCCCTTATCTCTTCCAA

ChipTERTF: 5'TCCCCTTCACGTCCGGCATT

ChipTERTR: 5'AGCGGAGAGAGGTCTGAATCG

2.1.10 *Oligonucleotides for siRNA*

<u>Target Gene</u>	<u>Supplier</u>
TCEAL7	Dharmacon

2.1.11 *Equipment*

Medical Air Technologies Bio-MAT class II microbiological safety cabinet

Scharfe Systems Casy-1 cell counter

Forma Scientific CO₂ H₂O jacketed incubator

Olympus CK2 phase contrast microscope

Sigma 4K15/ Beckman GS-6R bench top centrifuges

Bio-Rad sub-cell GT electrophoresis gel tank/model 200 power supply

M.J. Research PTC-200 Peltier thermal cycler

Beckman J6-MC centrifuge

Beckman Microfuge-R refrigerated micro-centrifuge

Turner Biosystems Veritas Luminometer

Molecular Devices 96 well colorometric plate reader

Kodak X-Omat 480 RA film processor

Syngene Gene Genius bioimaging system

SBeckman DU650 spectrophotometer

Atto AE 6450 polyacrylamide gel electrophoresis tank

Atto AE 6675 semi-dry blotting apparatus

Novex XCell SureLock Electrophoresis Cell

Agilent 2100 Bioanalyzer, Agilent Technologies

IKA LabChip vortexer, Agilent Technologies

Nanodrop, Agilent Technologies

Ribolyser, Hybaid

2.2 RNA Methods

2.2.1 RNA extraction

RNase-free filter pipette tips were used throughout RNA extraction and microcentrifuge tubes were pre-treated with Diethyl dicarbonate (DEPC) water. Prior to extraction all surfaces and pipettes were wiped with RNaseZap (Ambion) to remove RNases.

Total RNA was purified from cultured cells using the NucleoSpin RNA II kit as per the manufacturers' instructions. In brief, approximately 1×10^6 cells were lysed by addition of 350 μ l of buffer RA1 and vigorous vortexing. This lysis buffer contains large amounts of chaotropic ions, which inactivate RNases and create appropriate binding conditions which favour adsorption of RNA to the silica membrane. The lysate was homogenised by passing it 10 times through a 20 gauge needle and was then applied to a NucleoSpin filter which contains the silica membrane. Contaminating DNA, which is also bound to the silica membrane, was removed by treatment with DNase-1 solution for 15 minutes at room temperature. Salts, metabolites and macromolecular cellular components

were removed in washing steps and the pure RNA was eluted under low ionic strength conditions with RNase-free water.

Total RNA was extracted from fresh frozen tumour samples using RNeasy lipid tissue RNA purification kit as per manufacturers instructions. In brief, approximately 100 μg of fresh frozen tissue were homogenised in 350 μl of tissue lysis/binding solution using a 20 second pulse at speed setting 5.5 on a Hybaid Ribolyser. This lysis buffer contains the required concentration of chaotropic ions to facilitate bind of nucleic acids to the silica membrane of spin columns in combination with a low concentration of detergent to maximise tissue breakup and cellular disruption. 350 μl of 100% ethanol was then added to create optimal nucleic acid binding conditions. The solution was then applied to a RNAqueous filter cartridge which contains the silica membrane optimised for capturing low RNA concentrations. Contaminating salts, metabolites and macromolecular cellular components were removed in washing steps and the pure RNA was eluted under low ionic strength conditions with RNase-free water.

2.2.2 RNA quality assessment

RNA quality and quantity was analysed using the RNA 6000 Nano Assay reagents, RNA Nano LabChips and Agilent 2100 Bioanalyzer, as per manufacturers instructions. In brief, prefiltered RNA matrix gel combined with RNA dye concentrate in an RNase free microcentrifuge tube, vortexed well and centrifuged for 10 minutes at 13000 g. Gel dye was added to the RNA chip and pressurised to force the gel through the chip's capillaries. 5 μl of RNA 6000 Nano marker was then added to the ladder well and all sample wells on the chip. This low molecular weight RNA complex gives the bioanalyser software a common reference point in all RNA samples for comparison. 1 μl of RNA standards were then added to the ladder well and 1 μl of each RNA sample added to their respective wells. The RNA labChip was then vortexed for 1 minute on the IKA LabChip vortex, Agilent technologies. The Agilent 2100 Bioanalyser electrodes were washed with RNase ZAP followed by DEPC-treated water before insertion of the LabChip for analysis using the 2100 Bioanalyser software. The samples are then filtered through the gel-dye electrophoretically allowing size and quality assessment in relation to the provided standards.

2.2.3 Gene expression microarray hybridisation, washing and scanning

RNA for each tumour sample was amplified and labelled using the Agilent Low RNA Input Linear Amplification Kit PLUS, One-Colour and hybridised to Agilent whole human genome 4 x 44K gene expression arrays as per manufacturers' instructions. Raw data was extracted from scanned images using Agilent Feature Extraction software (Agilent Technologies, Santa Clara, CA).

2.2.4 miRNA expression microarray hybridisation, washing and scanning

miRNA Microarrays were performed by S. Hoare using Agilent's miRNA Microarray System and Human miRNA Rel 12.0 (8 x 15K) arrays as per manufacturers instructions (Agilent Technologies, Santa Clara, CA). 100ng of RNA was dephosphorylated, DMSO added and then denatured. Samples were labelled using T4 ligase and Cyanine 3-pCp, vacuum dried and resuspended in hybridisation buffer mix containing blocking reagent. Samples were denatured and hybridised overnight for 20hrs @ 55°C and 20rpm. Slides were washed then scanned using an Agilent DNA microarray scanner with the miRNA default settings. Data was extracted from scan files using Agilent Feature Extraction software version 10.5.1.1 (Agilent Technologies, Santa Clara, CA).

2.2.5 cDNA synthesis by reverse transcriptase PCR

cDNA was prepared using the GeneAmp RNA PCR core kit (Roche). RNA was quantitated and quality assessed using the Agilent 2100 Bioanayser and adjusted to 1µg in RNase-free dH₂O. Only RNA with an RNA integrity number of 9 or above was used for cDNA synthesis. Reactions were prepared in a PCR workstation (Labcaire) using RNase-free tubes and tips, which were UV crosslinked prior to use. A reaction mix was made up with 4µl of 10x Buffer, 8.8µl MgCl₂, 8 µl dNTPs, 2 µl random hexamers, 0.8µl of RNase inhibitor, 1µl of reverse transcriptase (RT) and 1ug of RNA per sample, made up to 40µl with dH₂O. For

each sample a no RT control mix was also prepared. Samples were then incubated at 25°C for 10 minutes, 48°C for 30 minutes and 95°C for 5 minutes using a Peltier Thermal Cycler (PTC-200) DNA Engine (MJ Research). 1ul of cDNA was used in subsequent PCR reactions. GAPDH specific PCR was performed for RT-PCR reaction products and no RT controls to determine the quality of cDNA produced and to check for DNA contamination of the RNA.

2.2.6 Polymerase Chain reaction

Polymerase Chain Reaction (PCR) master mixes were made using reagents from the Qiagen Taq-core kit. Reaction mixes were prepared in a PCR workstation (Labcaire) and all equipment was UV crosslinked before use. Reactions typically contained 1µl template cDNA along with final concentrations of master-mix components as follows: 1x PCR buffer; 0.5µM each primer; 0.2mM each of dATP, dTTP, dCTP, dGTP; 1 unit Taq polymerase. Reaction volumes were made up to 25µL with sterile distilled H₂O and run on a Peltier Thermal Cycler (PTC-200) DNA Engine (MJ Research) according to the cycling conditions detailed below. PCR products were analysed by agarose gel electrophoresis. Typically 7 µl was loaded onto a 1% agarose gel containing Gel Red (SUPPLIER) for UV visualisation of DNA.

2.2.6.1 Cycling conditions

RT-PCR

1. 25°C for 10 min
2. 48°C for 30 min
3. 95°C for 5 min
4. 4°C forever

GAPDH

1. 94°C for 45 sec
2. 60°C for 45 sec
3. 72°C for 2 min
4. Repeat 29 times from step 2
5. 4°C forever

2.2.7 Quantitative polymerase chain reaction (qPCR)

q-PCR master mixes were made using the Finnzymes DyNAmo SYBR green qPCR kit. The 2x reaction mix provided contained pre-mixed SYBR green dsDNA binding dye, buffer, Taq polymerase and dNTPs. Typical reactions therefore consisted of 1x SYBR green reaction mix, 0.5µM each primer and 1µl DNA made up to a 20µl volume with dH₂O. Reaction mixes were prepared in a PCR

workstation (Labcaire) and all equipment was UV crosslinked before use. All reactions were set up in triplicate alongside a no-DNA control. A known concentration range (100 ng - 10 pg) of 5 genomic DNA standards were also set up in triplicate producing a standard curve to which the PCR product is compared and quantified. Reactions were run on an Opticon 2 DNA Engine from MJ Research according to the cycling conditions detailed below. The average value of the triplicate reactions was taken as the concentration of PCR product.

2.2.7.1 Cycling conditions

DSC54

1. 94°C for 10 min
2. 95°C for 30 sec
3. 60°C for 45 sec
4. 72°C for 30 sec
5. 80°C for 10 sec
6. Plate read
7. Repeat 34 times from step 2

NSUN5

1. 94°C for 10 min
2. 95°C for 30 sec
3. 60°C for 45 sec
4. 72°C for 30 sec
5. 84°C for 10 sec
6. Plate read
7. Repeat 34 times from step 2

TCEAL7

1. 94°C for 10 min
2. 95°C for 30 sec
3. 55.2°C for 45 sec
4. 72°C for 30 sec
5. 82°C for 10 sec
6. Plate read
7. Repeat 34 times from step 2

MYEOV

1. 94°C for 10 min
2. 95°C for 30 sec
3. 58°C for 45 sec
4. 72°C for 30 sec
5. 82°C for 10 sec
6. Plate read
7. Repeat 34 times from step 2

S15

1. 94°C for 10 min
2. 95°C for 30 sec
3. 55°C for 45 sec
4. 72°C for 30 sec
5. 82°C for 10 sec
6. Plate read
7. Repeat 34 times from step 2

WNT5B

1. 94°C for 10 min
2. 95°C for 30 sec
3. 56°C for 45 sec
4. 72°C for 30 sec
5. 82°C for 10 sec
6. Plate read
7. Repeat 34 times from step 2

hTERT

1. 94°C for 15 min
2. 95°C for 30 sec
3. 69°C for 45 sec
4. 72°C for 1 min
5. 87.5°C for 10 sec
6. Plate read
7. Repeat 34 times from step 2

CHIPTERT

1. 94°C for 15 min
2. 95°C for 30 sec
3. 62°C for 45 sec
4. 72°C for 30 sec
5. 88 °C for 10 sec
6. Plate read
7. Repeat 39 times from step 2

2.2.8 qPCR validation of miRNA expression in mesenchymal tumours

miRNA qPCR was performed by S. Hoare according to MiScript protocol (Qiagen, Crawley, West Sussex), in which 250ng-1ug of RNA is transcribed into cDNA by addition of a polyA tail, using oligo dT primers with an additional unique sequence. Quantitative-PCR was then carried out using the universal primer to this sequence and the unique miRNA primer and visualised with SYBR green. Q-PCR was tested for each tumour set with a range of small non-coding miRNA primers (Qiagen). Using the most uniform expression of a control RNA across a tumour type lead to the selection of RNU1A for liposarcomas, MPNST and synovial sarcoma normalisation whereas RNU6B was used for mesothelioma normalisation. A selection of Q-PCR reactions was carried out for the specific miRNA, and these were normalised to the controls. Universal RNA (Stratagene, La Jolla, CA) was used for standards in each case. Q-PCR was carried out on a Chromo4 machine (Bio-RAD Laboratories Ltd., Hemel Hempstead, UK). Average results from at least 2 reactions were plotted as box-plots using Minitab (version 15).

2.3 DNA techniques

2.3.1 Transformation of cells with Plasmid DNA

Transformation of plasmid DNA was performed by adding 1µl of plasmid DNA to 50µl of competent *E. coli* TopTen cells and incubating for 30 minutes on ice. The

bacteria were then heat shocked by placing in a 42°C water bath for 30 seconds and then transferred to ice for 2 minutes. 100µl of S.O.C media was added and the bacteria were incubated on a shaker at 37°C for 1 hour. 800 µl of S.O.C. media was added and 100-300 µl was then spread onto Agar plates containing ampicillin and incubated overnight at 37°C to allow growth of discrete colonies. Individual colonies were then removed from Agar plates using a sterile 10 µl pipette tip and placed in 10 ml LB-media containing ampicillin. Cultures were incubated on a shaker at 37°C overnight.

2.3.2 Glycerol stocks

1 ml glycerol stocks were prepared by combining 500 µl of fresh bacterial culture with 500 µl of 50 % sterile glycerol. Glycerol stocks were stored at -70 °C in 1.5 ml sterile microcentrifuge tubes.

2.3.3 Small scale preparation of plasmid DNA

Mini-preparation of DNA from small volumes of bacterial culture was performed using the QIAprep Spin Miniprep Kit (Qiagen) as per manufacturers' instructions. In brief, 10 ml of overnight culture was pelleted at 2500rpm for 10 minutes and the supernatant discarded. The pellet was subjected to alkaline lysis followed by neutralisation then centrifugation at 13000rpm to remove cell debris. Supernatant was transferred to a spin filter containing a silica-gel membrane to which DNA was specifically adsorbed in the presence of high salt. Following a wash step to remove salts DNA was eluted in 50 µl of distilled water.

2.3.4 DNA sequencing

Sequencing of plasmid DNA was performed by Beatson Molecular Services.

2.3.5 Large scale preparation of plasmid DNA

Maxi-preparation of plasmid DNA was performed using the Qiagen Plasmid Maxiprep kit as per manufacturers' instructions. In brief, 500ml-1L of bacterial culture was harvested by centrifugation at 4000rpm for 10 minutes and alkaline cell lysis performed. Cell lysates were cleared by centrifugation at 4000rpm for 30 minutes at 4°C and then loaded onto an anion exchange column, which

selectively binds plasmid DNA under appropriate low-salt and pH conditions. Following wash steps in medium salt buffer plasmid DNA was eluted in high salt buffer and precipitated by adding 0.7 x volume (10.5ml) of isopropanol and centrifugation at 4000rpm for 30 minutes at 4°C. The DNA pellet was washed with 5ml of 70% ethanol then centrifuged again at 4000rpm for 15 minutes. Finally the pellet was air-dried at 37 °C for 10 to 15 minutes and redissolved in a 200 µl of TE buffer. DNA concentrations were then analysed using a Nanodrop Spectrometer, Agilent Technologies, and adjusted to 1µg/µl.

2.3.6 Restriction Digests

Restriction endonuclease digests using up to 2µg of plasmid DNA were performed in 20µl reactions containing 1µL of each restriction endonuclease (typically 10U/µL) diluted with 1x restriction endonuclease buffer. Reactions were made up to 20 µl with sterile distilled water and incubated at 37°C for a minimum of 1 hour.

2.3.7 UV gel documentation

Analysis and photography of Gel Red (Cambridge bioscience)/ethidium bromide agarose gels visualised under UV was performed using gene genius bioimaging system by syngene.

2.3.8 Western blotting

Fifteen micrograms of protein equivalents were separated on 10% Bis-Tris gels using NuPAGE MES running buffer (Invitrogen, Renfrewshire, UK), and then blotted onto nitrocellulose membrane (Millipore, Watford, UK) and blocked in phosphate buffered saline Tween-20 containing 5% nonfat dried milk. Membranes were probed with the following antibodies: HDAC5 rabbit polyclonal (Active Motif, Rixenstart, Belgium), PKCa rabbit polyclonal and KAT2A/GCN5 rabbit polyclonal (both from Abcam, Cambridge, UK) and secondary anti-rabbit IgG horseradish peroxidase-linked antibody (New England Biolabs UK, Hitchin, UK). After visualization, membranes were stripped of bound primary and secondary antibodies by submerging in 1% SDS and 0.2m glycine (pH 2.5) and shaken for 1 h at room temperature, and rinsed and reblocked before probing with loading

control antibody extracellular signal-regulated kinase 1 rabbit polyclonal (1:3000) (Santa Cruz Biotechnology, Heidelberg, Germany).

2.3.9 Maintenance and Storage of mammalian cell lines

The ALT cell lines used were SKLU (lung adenocarcinoma), SUSM1 (liver fibroblasts), KMST6 (lung fibroblasts), WI38-SV40 (SV40 immortalized lung fibroblasts), SAOS (osteosarcoma) and U2OS (osteosarcoma). Telomerase-positive cells used were C33a (cervical carcinoma), HT1080 (fibrosarcoma), A2780 (ovarian carcinoma) and 5637 (bladder carcinoma). Normal cell strains used were WI38 (normal lung fibroblasts) and IMR90 (normal lung fibroblasts). Bone marrow hMSCs were isolated as described earlier (Serakinci et al., 2006) and cultured using Dulbecco's modified Eagle's medium with low glucose plus Glutamax supplemented with 17% Hyclone fetal bovine serum (Thermo Fisher Scientific, Waltham, MA, USA) at 5% CO₂.

2.3.10 Transient transfection of siRNAs

Whole kinome siRNA library screen from Applied Biosystems (Applied Biosystems Inc, Foster City, CA USA) in SKLU cells. In brief, 50 nM of siRNA or non-coding siRNA control (Applied Biosystems Inc, Foster City, CA USA) were co-transfected with 250ng of hTERT reporter plasmid in 96 well plates (Thermo-Fisher Scientific, Rochester, NY, USA) using lipofectamine 2000 (Invitrogen, Paisley, UK) according to manufacturer's instructions. Cell lysis was achieved using passive lysis buffer (Promega, Madison, WI, USA). TCEAL7 siRNA transfections were performed using Dharmacon Smartpools (Thermo-Fisher Scientific, Rochester, NY, USA) in 75 cm² flasks. TCEAL7 siRNA transfections for c-Myc activity were performed in 125 cm² flasks. pCMV-XL4:TCEAL7 overexpression plasmid was purchased from Origene (Origene Technologies Inc., Rockville, MD, USA) and all transfections were performed in 75 cm² flasks. All transfections were performed in triplicate.

2.3.11 Luciferase reporter assay

Luciferase assay system (Promega, Madison, WI, USA) was used to determine luciferase activities according to manufacturer's instructions.

2.3.12 Nuclear extract purification and Trans-AM c-Myc activity assay

Nuclear extracts of approximately 8×10^8 cells of each of the six ALT cell lines (WI38-SV40, KMST6, SKLU, SUSM1, SAOS and U2OS) and four telomerase-positive cell lines (A2780, C33a, HT1080 and 5637) were extracted in triplicate using an Active motif nuclear extraction kit (Active Motif, Rixenstart, Belgium) as per the manufacturer's instructions. c-MYC DNA-binding ELISAs (Active Motif) were performed on three separate occasions with four technical replicates of each cell line as per the manufacturer's instructions. A standard curve of 5, 2.5, 1.25 and 0.625 ng/well recombinant c-MYC protein (Active Motif) was run on each assay to allow relative quantification. Results of all ALT and telomerase-positive cells were grouped and a t-test was carried out using Minitab (version 14).

2.3.13 c-Myc Chromatin ImmunoPrecipitation

ChIP assays were performed as per manufacturers' instructions (Millipore, Watford, UK) as previously published (Bilsland et al. 2009).

2.3.14 Telomerase activity assay

The TRAPEze XL kit was used for TRAP assay according to the manufacturer's instructions (Millipore, Watford, UK) and was performed by S. Hoare as previously published (Bilsland et al. 2009).

2.4 Bioinformatic Methods

2.4.1 Gene expression microarray Data normalisation and quality control

All array data was then imported into GeneSpring GX (version 7.3.1, Agilent Technologies, Santa Clara, CA) and tumour data was normalised to the 70th percentile and the cell line and hMSC data normalised to the 50th percentile. Further quality control involved filtering based on flag values where only those genes that had non-absent flag values for at least half of the ALT and telomerase

samples were included in downstream analysis. DU145 and HT29 gene expression microarrays were performed by L. Hanley.

2.4.2 Deposit of microarray data to GEO

Fully MIAME compliant gene expression data resulting from this study was deposited with GEO under the following accession numbers: GSE14533 and GSE17118.

2.4.3 miRNA expression microarray Data normalisation and quality control

Raw miRNA microarray data was imported into BRB array tools and the following quality control and normalisation filters were applied: signal intensity threshold of 10, probes labelled as absent excluded, arrays normalised to the median of the entire array using the median array as a reference. Furthermore, genes where less than 20% of the data had a fold change of less than 1.5 from its median expression or where more than 50% of the data was missing were also excluded.

2.4.4 Hierarchical clustering

Gene Expression Hierarchical clustering was performed using Genespring GX (version 7.3.1) using Spearman correlation and average linkage, merging branches with similarity less than 0.01. Hierarchical clustering of NCI60 expression data was performed by importing the median normalized data from BRB-array tools into Partek. miRNA hierarchical clustering was performed within BRB-array tools using Pearson correlation and average linkage.

2.4.5 Telomere Maintenance Gene expression signature generation Gene selection

Within GeneSpring GX, the 1305 gene signature was generated from cell line expression profiles using a WELCH ANOVA with a false discovery rate of 0.05 and the Benjamini and Hochberg multiple testing correction to test for significant differences in gene expression between the two telomere maintenance mechanism groups. A similar analysis in liposarcoma samples generated no

results therefore to generate the refined 297 gene signature a Fishers Exact Test using a p-value of ≤ 0.05 was performed using the liposarcoma expression profiles to test for significant association of gene expression with telomere maintenance mechanism. From this analysis 422 genes were also present within the 1305 signature. Those genes with fold change values in the same direction for both cell line and liposarcoma data (i.e. an increased or decreased expression in ALT compared to telomerase positive) were included in the refined signature.

2.4.6 Mesenchymal tumour miRNA signature generation

The binary tree prediction method (utilising the compound covariate predictor algorithm) in BRB array tools in combination with leave-one-out cross-validation was used to identify miRNAs whose expression patterns had the ability to distinguish between tumour types.

2.4.7 Survival Analysis

Kaplan-Meier plots of survival and Log Rank (Cox Regression) tests adjusting for age and sex were performed using SPSS (v15, SPSS Inc, Chicago, Illinois, USA). miRNAs with significant hazard ratios were highlighted using BRB array tools “find genes correlated with survival” tool which develops an expression based predictor of survival risk group as previously described by Bair and Tibshirani (Bair et al. 2004).

2.4.8 Senescence scoring of gene expression data

Gene expression data was filtered to show only values associated with senescence signature gene lists using BRB array tools. Filtered data was then exported to Excel and normalised to median after which genes were scored as “senescent” or “non-senescent” depending on their gene expression levels relative to the median and their known expression pattern during senescence signaling (see Table 1). For example, expression of the proliferation-associated gene *Kl67* below median would be marked “senescent” but above median expression would not. The overall senescence score was then calculated as a percentage of the genes receiving a “senescent” score over the total number of genes in a particular senescence signature. Median, and maximum and minimum

values plotted using Excel. As such, a senescence score could be summarized by the following formula:

$$\text{Score} = ((\text{number of proscendent genes}) / (\text{Number of genes in pathway})) * 100$$

Senescence scoring of drug treated breast cancer cells was performed by L. Hanley and included for completeness.

2.4.9 Correlations of senescence signature rankings

To assess the correlations of senescence scores given to each individual sample by each signature the scores for each tumour were placed into Minitab (v15, Minitab Inc, Coventry, UK) and rankings for each signature score were used for Pearson correlations.

2.4.10 Regression Analysis of Senescence scores and compound GI₅₀ data

Regression analysis was performed using the stat package of Perl and exporting results to Excel.

2.4.11 Predicted compound activity mapping

This was performed by Cancer Research Technologies UK through the use of graph-theory connectivity indices to build a decision tree model of predicted activities. Compounds showing significant regressions for any of the three scores were then aligned with their predicted activity in Excel.

3 Senescence bypass by telomere maintenance is a regulated by a gene expression network with a central role for c-Myc and TCEAL7 and highlights a mesenchymal stem cell origin for ALT

3.1 Introduction

As previously discussed, for a cell to become fully tumorigenic it must bypass replicative senescence and this is usually achieved through telomere maintenance.

Most cancers utilise the telomere rebuilding activities of the ribonucleoprotein telomerase. Telomerase activity is strictly regulated in normal cells and only occurs in specific normal cell types including germ line cells and activated lymphocytes (Artandi et al. 2006). To obtain telomerase activity cells must express both genetic components hTERT, which encodes the catalytic subunit, and hTR which encodes the RNA template molecule used for reverse transcription of telomeres. The senescence bypass effect of telomerase activity is exemplified by its frequent ectopic expression leading to the creation of immortalised cell lines (Morales et al. 1999; Yang et al. 1999).

However, around 10% of cancers utilise the recombination based mechanism known as the alternative lengthening of telomeres (ALT). ALT is predominantly found in tumours of mesenchymal origin, however even within this group of tumours, the predominance of ALT varies in individual types of tumours from 77% ALT in MFH to 6% in Rhabdomyosarcomas (Ulaner et al. 2004; Henson et al. 2005). Furthermore the prognostic implications of ALT for different tumour types varies from being linked with good prognosis in osteosarcomas (Ulaner et al. 2003) and poor prognosis in liposarcomas (Costa et al. 2006; Cairney et al. 2008). The molecular mechanisms behind telomere maintenance by ALT are currently not well elucidated. Cells utilising the ALT mechanism use both inter and intra telomere recombination to maintain their telomere lengths and have increased rates of telomeric exchange (Dunham et al. 2000; Londono-Vallejo et al. 2004; Muntoni et al. 2009) ALT is currently characterised by a combination of

the presence of ALT associated PML bodies (APBs), lack of detectable telomerase activity, presence of extrachromosomal T-circles and heterogenous telomere lengths.

The telomere maintenance mechanism (TMM) used by a tumour is not usually considered nor investigated during the course of a study and as a result, the molecular details of the decision between telomere maintenance mechanisms is currently poorly understood. To this end gene expression microarrays were utilised to explore the transcriptional differences between TMMs in cell lines and mesenchymal tumour biopsies for which the TMM had been previously established.

3.2 Results

3.2.1 Gene expression analysis distinguishes telomerase and ALT cell lines

To investigate the presence of a telomere maintenance mechanism (TMM) specific gene expression signature expression profiles, 4 ALT (SKLU1, KMST6, WI38-SV40, SUSM1) and 4 telomerase positive cell lines (5637, A2780, C33a, HT1080) were investigated using Agilent whole human genome 1-colour microarrays. A detailed description of the quality control measures and the normalisation options applied can be found in Chapter 2, however boxplots show that the normalised data was equally spread and comparable between the 2 groups (Figure 3.1a) with virtually equal medians of 0.78 and 0.79 for ALT and telomerase positive cell line groups respectively.

A Welch ANOVA was used to find significant differences in gene expression between the 2 groups with aim of exploring the possibility that expression of individual genes within these large profiles was responsible for defining either telomerase positive or ALT cells (Figure 3.1b, left panel). A list of 1307 probes corresponding to 1305 differentially expressed genes with an adjusted p-value ≤ 0.05 was generated (For all gene lists associated with this work see Appendix I). Focusing on the expression values for individual genes within the larger 1305 gene signature it was clear that where expression was high in the ALT cell lines it was low in the telomerase positive cell lines and *vice versa* (Figure 3.2a).

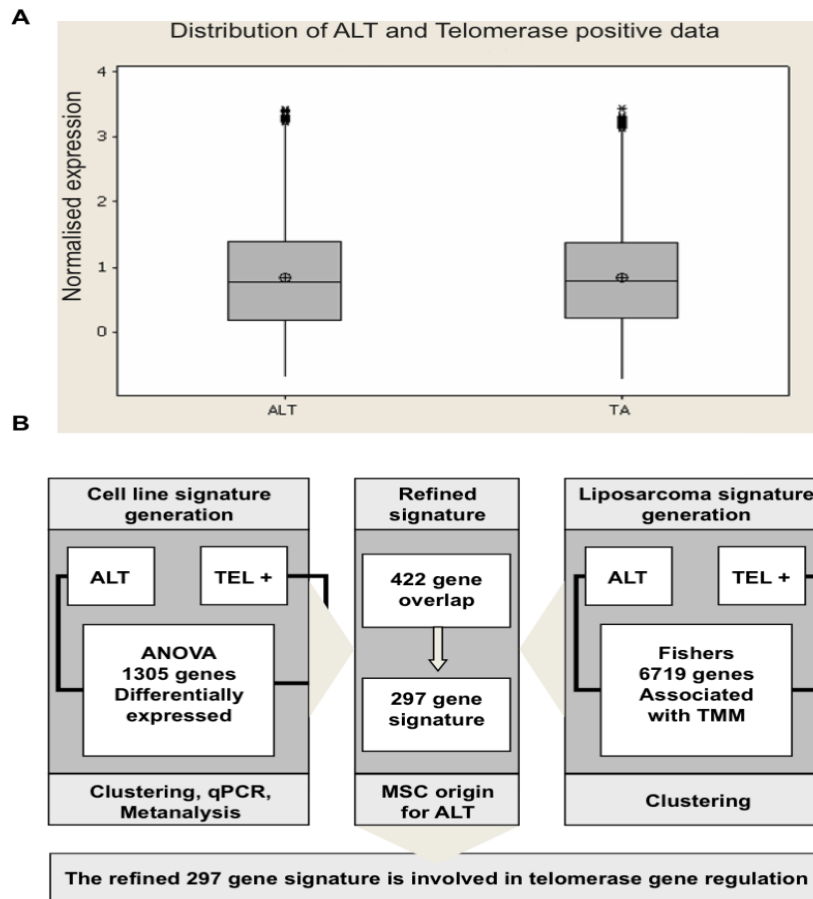


Figure 3.1 - Gene expression analysis of ALT and telomerase positive cell lines. (A) Boxplots show distribution of normalised data in ALT and telomerase positive cell line groups. Grey boxes define 25 and 75% quartiles, while error bars represent the 1st and 99th percentiles of the distribution. Dots represent outliers, black line represents the median, while the cross represents the mean of the distribution. **(B)** Overview of signature generation from cell line and liposarcoma tissue samples. A refined 297 gene signature was generated from a combination of the 1305 gene cell line signature and the 6719 gene liposarcoma signature. This signature shows a potential mesenchymal stem cell origin for ALT and is involved in telomerase gene regulation.

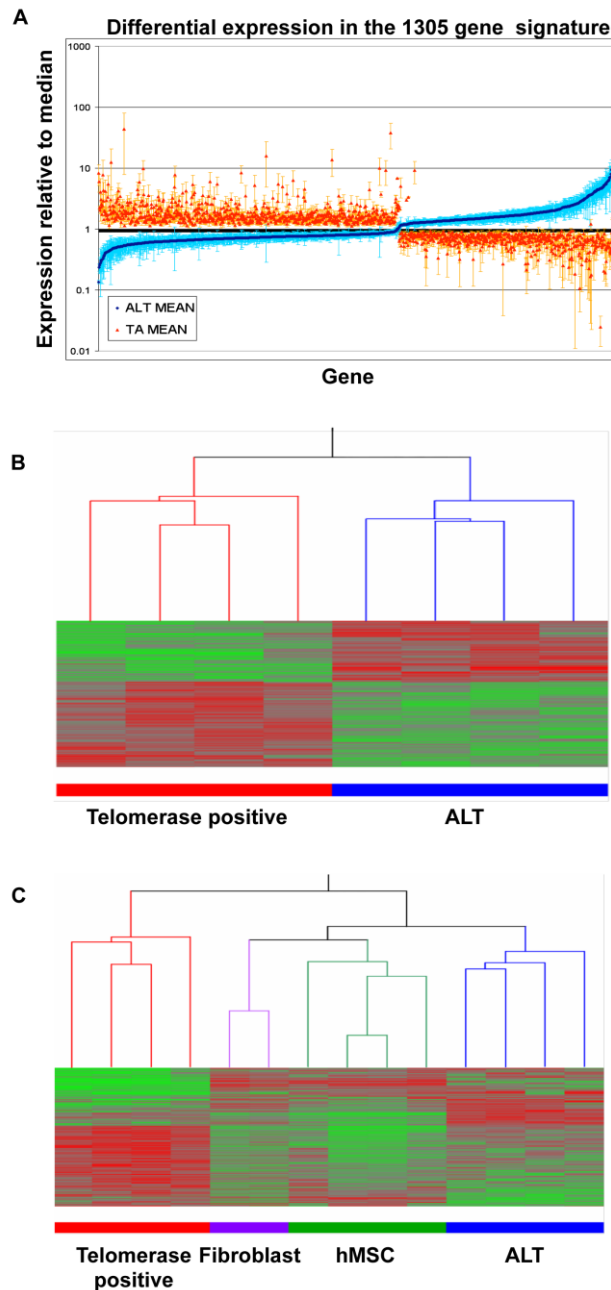


Figure 3.2 - Gene expression profiling distinguishes telomerase positive and ALT cell lines and is suggestive of a mesenchymal stem cell origin for ALT. (A) Scatter plot representing normalised microarray expression values for the 1305 gene signature in ALT (blue) and telomerase positive (red) cell lines relative to overall median expression value. Each dot represents the mean gene expression values for a gene, while error bars represent the standard error. (B) Hierarchical clustering of the cell line data using the 1305 signature accurately separates telomerase positive (red) from ALT (blue) cell lines. (C) Hierarchical clustering cell line, mortal fibroblast and hMSC samples using the 1305 signature whereby hMSC and mortal fibroblasts cluster more closely to ALT than Telomerase positive cell lines. All clustering performed using the Spearman correlation, average linkage and merging branches with a similarity correlation of 0.001 or less.

Furthermore, hierarchical clustering of the cell lines based on this signature accurately separated out ALT and telomerase positive cell lines into 2 separate groups (Figure 3.2b), suggesting that the genes responsible for defining telomerase or ALT or those involved in regulating the decision of which TMM to activate have been present within this signature.

3.2.2 Clustering using the 1305 gene signature is suggestive of a mesenchymal stem cell origin for ALT

The fact that ALT is predominantly found in tumours of mesenchymal origin prompted further investigation into whether ALT was a function of the cell of transformation and if mesenchymal stem cells could be the potential cell of origin for ALT tumours. To this end, supervised hierarchical clustering analysis using the 1305 gene signature was performed to investigate any relationship between telomerase positive, ALT and normal fibroblast cell lines and hMSC (Figure 3.2c). The signature accurately separated out telomerase positive and ALT cell lines, normal fibroblasts and hMSC. However, while the telomerase positive cell lines clustered together on a separate branch the ALT cell lines, normal fibroblasts and hMSC all clustered together. Normal fibroblasts were found to be more directly related to hMSC than ALT, however fibroblasts and hMSC were found to be equally related to the ALT cell lines, suggestive of a mesenchymal stem cell origin for ALT. This may be as predicted, however this was the first time any direct association between mesenchymal stem cells and ALT had been documented.

Analysis of the signature revealed several genes associated with stem cell maintenance and self-renewal processes were differentially expressed between telomerase positive and ALT cell lines. Four of these genes with strong differences in expression were chosen for validation by quantitative PCR (Figure 3.3a). Three of these were significantly up-regulated in ALT cell lines and barely expressed in telomerase positive. DSC54 is a novel mesenchymal stem cell protein for which little information exists; WNT5b is a well-known regulator of stem cell function implicated in oncogenesis and development; MYEOV is overexpressed in myeloma and has a role in promoting invasion and proliferation. The final gene NSUN5 is a proliferation associated nucleolar antigen, deletion of which may contribute to the premature aging effects of the

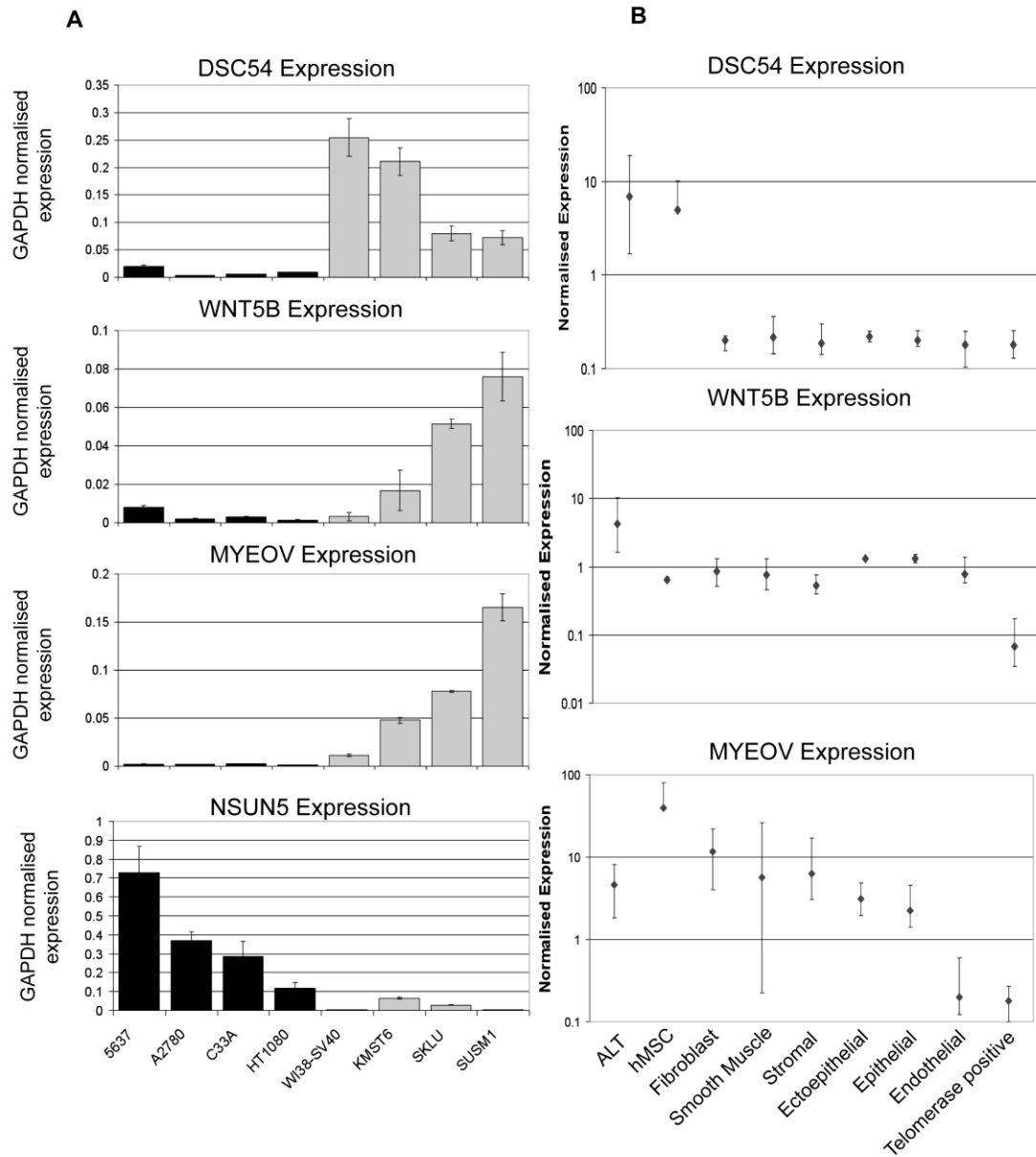


Figure 3.3 - qPCR Validation of the 1305 gene expression signature highlights a stem cell link (A) Expression levels of DSC54, WNT5B, MYEOV and NSUN5 were validated by quantitative PCR in telomerase positive cell lines 5637, A2780, C33a and HT1080 (black bars) and ALT cell lines WI38-SV40, KMST6, SKLU, SUSM1 (grey bars) cell lines. Each bar represents the mean and standard error of triplicate reactions from a representative experiment normalised to GAPDH. (B) Expression values for DSC54, WNT5B and MYEOV in various normal tissues extracted from publicly available microarray expression data (GSE3239), compared to those for ALT and telomerase positive cell lines and hMSC. Dots represent the median while error bars represent the maximum and minimum normalised expression values.

developmental disorder Williams syndrome. NSUN5 was significantly up-regulated in telomerase positive compared to ALT cell lines.

To further explore the link between ALT and mesenchymal stem cells the expression of these genes within a variety of normal tissues of differing embryonic origin and human mesenchymal stem cells (hMSC) was explored. To this end publicly available gene expression profiles from normal fibroblasts, smooth muscle, stromal, ectoepithelial, epithelial and endothelial tissues were downloaded (GSE3239) and expression of DSC54, WNT5b and MYEOV in these tissues was compared to that of hMSC, telomerase positive and ALT cell lines (Figure 3.3b). No comparable data was available for NSUN5 in this dataset and therefore this gene could not be included in the analysis.

Consistent with the Q-PCR validation expression, all 3 genes showed higher expression in ALT than telomerase positive cell lines. When comparing all of the expression patterns, DSC54 was only high in ALT cell lines and hMSC, consistent with a mesenchymal stem cell origin for ALT. WNT5b on the other hand showed varying expression across the different tissue types and cell lines with highest expression in hMSC, ALT and mesenchymally derived tissues and lowest expression in telomerase positive and epithelial tissues. MYEOV distinguished ALT from telomerase positive cell lines, however a similar low level of expression was seen across the various other tissue types.

3.2.3 Refinement of the 1305 gene signature using liposarcoma gene expression improves separation of ALT and telomerase positive liposarcomas and suggests a mesenchymal stem cell origin for ALT in this mesenchymal malignancy

Liposarcomas are tumours of mesenchymal origin in which telomere maintenance mechanism is highly prognostic (Costa et al. 2006). In order to refine the cell line derived signature with data from primary tumours, the power of the 1305 gene expression signature to distinguish telomerase positive and ALT in liposarcomas was investigated. Gene expression profiles were generated for a group of 17 previously characterised liposarcoma samples, of which 9 were ALT

and 8 were telomerase positive. Unsupervised clustering showed some split in the samples depending on their TMM, which was not improved when the 1305 gene signature was applied. Furthermore, hMSC did not cluster with any liposarcoma samples, but clustered together on a separate branch (Figure 3.4 a & b).

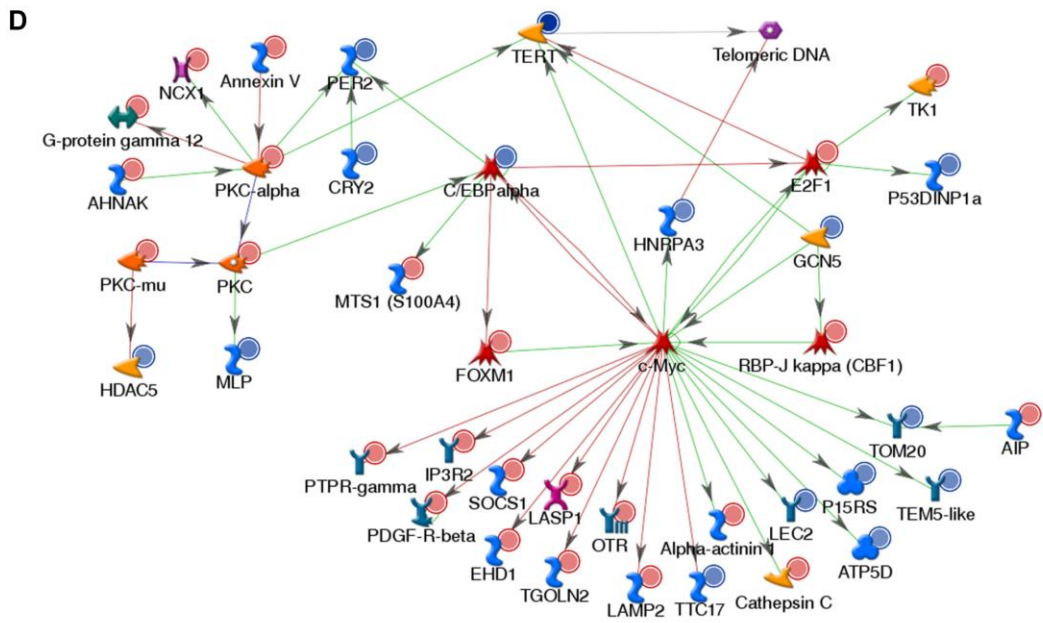
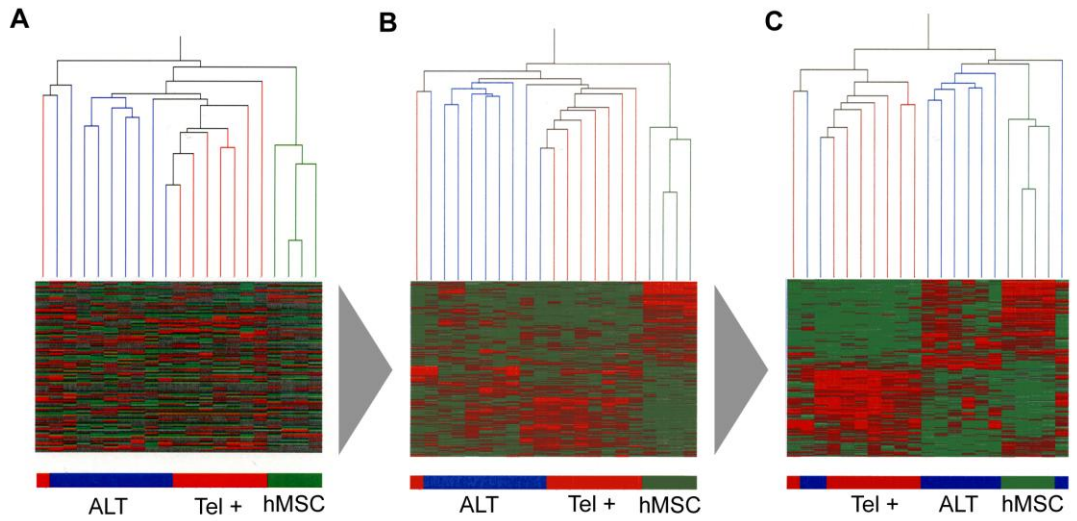
Although the 1305 signature did not improve clustering, the liposarcoma samples, for the most part, clustered together according to their telomere maintenance mechanism. The obvious separation between ALT and telomerase positive tumours in the clustering diagram suggested that differences in gene expression exist between the 2 groups, although no significant differences were found. In order to explore this further a Fisher's exact test was used to test for any association between gene expression level and telomere maintenance mechanism. From this analysis 8227 probes corresponding to 6719 genes were found to be significantly associated with TMM in ALT and telomerase positive liposarcoma samples (Figure 3.1b right-hand panel).

To further refine this large signature the overlap, with the 1305 gene signature determined from the cell lines was examined. Of these 1305 genes 422 genes were also present in the liposarcoma signature and therefore had a significant association with telomere maintenance mechanism in liposarcoma and cell lines. Further refinement of the signature was carried out by examining the direction of gene expression in telomerase positive and ALT tumours in comparison to the cell line data. 297 of the 422 genes had gene expression that was comparable to the cell line data, 152 genes up in ALT, down in telomerase positive and 145 genes down in ALT, up in telomerase positive (Figure 3.1b centre panel).

Hierarchical clustering of ALT and telomerase positive liposarcoma samples using this refined 297 gene signature showed a clear separation between the 2 groups with all but 2 ALT samples clustering on one branch while all telomerase positive samples clustered together on a separate branch (Figure 3.4c). Furthermore, consistent with the hypothesised mesenchymal stem cell origin for ALT seen within the cell line data, hMSC clustered with the ALT liposarcomas using this refined signature rather than as a separate group when the 1305 signature was applied (Figure 4 b & c).

Figure 3.4 - Hierarchical clustering of ALT and telomerase positive liposarcoma sample and hMSC distinguishes telomerase positive from ALT and highlights an hMSC origin for ALT. Liposarcoma samples were previously determined as ALT (blue) or telomerase positive (red) by classical methods. Hierarchical clustering of these samples and hMSC (green) was performed using the Spearman correlation, average linkage and merging branches with a similarity correlation of 0.001 or less using (A) all genes (B) 1305 gene signature or (C) the refined 297 gene signature.

(D) Network analysis of the 297 gene signature shows hTERT regulation. Signaling network of known direct interactions between genes from the 297 gene signature drawn using the analyse network building algorithm within Metacore. Green arrows represent positive, red negative and grey unspecified interactions. Red and blue circles next to network objects represent expression data. Red: up in ALT and down in telomerase positive liposarcoma samples and cell lines; Blue: down in ALT and up in telomerase positive liposarcoma samples and cell lines. The network highlights that a number of molecules activated by c-Myc have reduced expression in ALT cells and those inhibited by c-Myc have increased expression in ALT cells. This is suggestive of lower c-Myc activity in cell using ALT.



Further validation of the refined signature was achieved by applying it back to the cell line data for hierarchical clustering. As predicted it accurately separated out telomerase positive from ALT cell lines (data not shown), further validation that this refined signature held true and no power was lost by reducing gene number.

3.2.4 The refined 297 gene signature is involved in telomerase gene regulation and highlights lower c-MYC activity in ALT

Given the ability of the refined 297 gene signature to separate liposarcomas by TMM it was logical that the genes within the signature may have comprised of functional regulatory networks involved in aspects of TMM. In order to explore this, network modelling using Metacore from GeneGo was performed. Using the direct interactions and transcriptional regulation algorithms within the software, a candidate network indicating possible interactions between genes from the 297 signature, mined from published data, was produced. A regulatory network involving hTERT and telomeric DNA was revealed by this analysis (Figure 3.4d). Expression data from the 297 gene signature was converted to fold change in ALT over telomerase positive, uploaded into Metacore analytical suite and overlaid on the direct interactions network. As can be seen from Figure 3.4d, by combining interactions between known signaling pathways and experimentally defined levels of expression for regulatory genes this approach allowed for predictions relating to hTERT regulation and repression in ALT cells. hTERT expression was reduced in ALT cells and tumours in relation to telomerase positive samples. Consistent with this, expression of E2F1 a known repressor of hTERT, was up-regulated in ALT samples, whereas chromatin modifying enzymes with roles in gene activation such as GCN5 were down-regulated in ALT, in agreement with the known decreased association of acetylated histones and low hTERT expression in ALT cell lines (Atkinson et al. 2005). The analysis also indicated that c-Myc regulation may contribute to the signature. Although c-Myc was not itself differentially expressed, 21 signature genes including hTERT were predicted transcriptional targets of c-Myc.

Interestingly, most signature genes expected to be activated by c-Myc were repressed, while those expected to be inhibited were mainly up-regulated in ALT relative to telomerase positive samples, suggesting that c-Myc activity may be

suppressed in ALT. c-Myc is a known hTERT transcriptional activator (Hao et al. 2008) and therefore decreased activity of c-Myc in ALT cells would serve as a mechanism of down-regulating hTERT transcription.

3.2.5 Validation of the Gene expression network highlights the highlights protein level differences and lower c-Myc activity in ALT

To validate the gene expression differences shown by the network analysis western blotting of three proteins in the network was undertaken, HDAC5, PKC α and GCN5. The results shown in Figure 3.5A demonstrate that the expression differences highlighted in this network were also seen at the protein level.

The network analysis also suggested lower c-Myc activity in ALT cells compared to telomerase positive cells. Additional validation of the network was undertaken through the functional examination of c-Myc activity levels using DNA binding activity ELISAs. The results of the DNA binding ELISAs confirmed that this is indeed the case, as a significantly lower level of c-Myc activity was observed in the ALT cell lines ($p=0.015$) (Figure 3.5B).

3.2.6 Telomerase positive cells have increased binding of c-Myc at the hTERT promoter but show no change in binding partner expression.

To establish the direct regulatory role of c-Myc at the hTERT promoter in these cell lines chromatin immunoprecipitation (ChIP) using a c-Myc antibody and qPCR for the hTERT promoter in the resulting pull-down was performed (Figure 3.6A). Although the levels of c-Myc binding at the hTERT promoter varied between cell lines overall the telomerase positive cell lines had a higher level of c-Myc present at the hTERT promoter than ALT cell lines. This was consistent with the decreased c-Myc activity in ALT cells.

3.2.7 c-Myc regulatory factors expression patterns do not explain lower c-Myc activity in ALT

Relative levels of Myc/Max versus Mad/Max binding have previously been observed to regulate the hTERT promoter chromatin environment, raising the

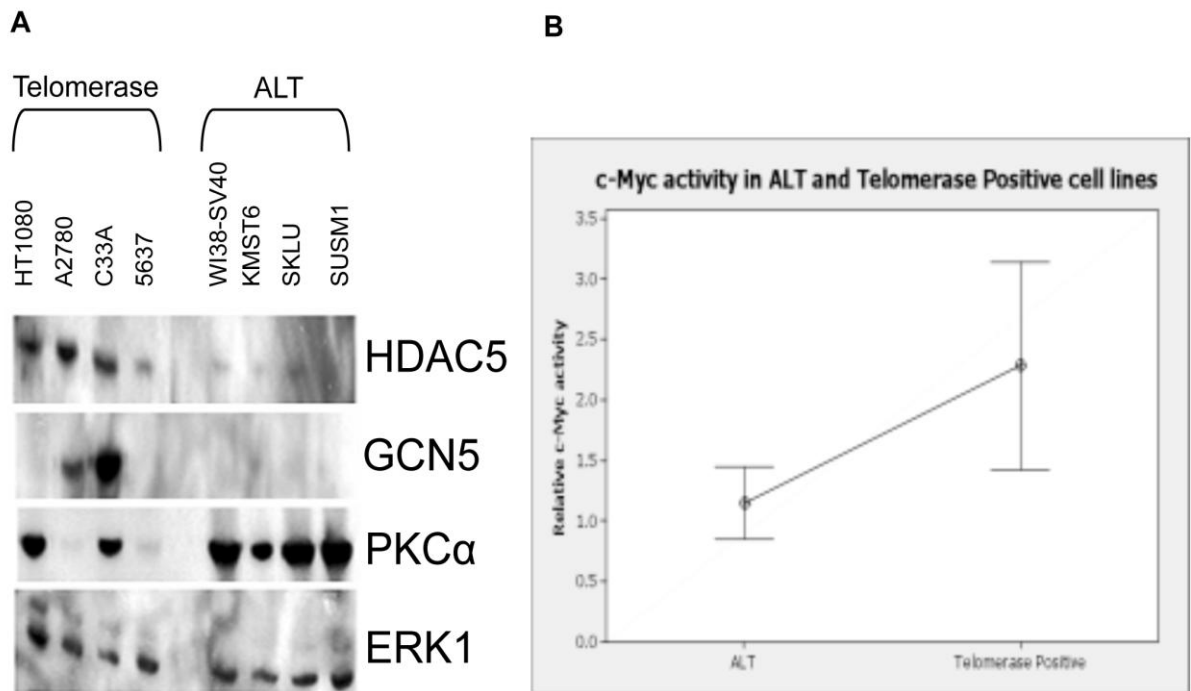


Figure 3.5 - The TERT regulatory network is shown at the protein level and predicted c-Myc activity is confirmed as significantly lower in ALT.

(A) Western blotting shows protein level differences in 3 proteins of the 297 gene network. 15 µg of cell extracts were run on NuPAGE 4-12% Bis-Tris gels, transferred to Millipore nitrocellulose membrane and probed with appropriate antibodies. Blots were then stripped and reprobed with ERK1 loading control. Panels shown are representative panels of 2 separate blots.

(B) c-Myc activity ELISA shows significantly lower activity in ALT cells. Interval plot shows the average of 6 ALT cell lines (WI38-SV40, KMST6, SKLU, SUSM1, SAOS and U2OS) and 4 telomerase cell lines (A2780, C33a, HT1080 and 5637) on 3 separate occasions with 4 replicates of each cell line. Crosshairs show mean expression for each group and error bars show 95% confidence intervals of the mean, p-value = 0.015

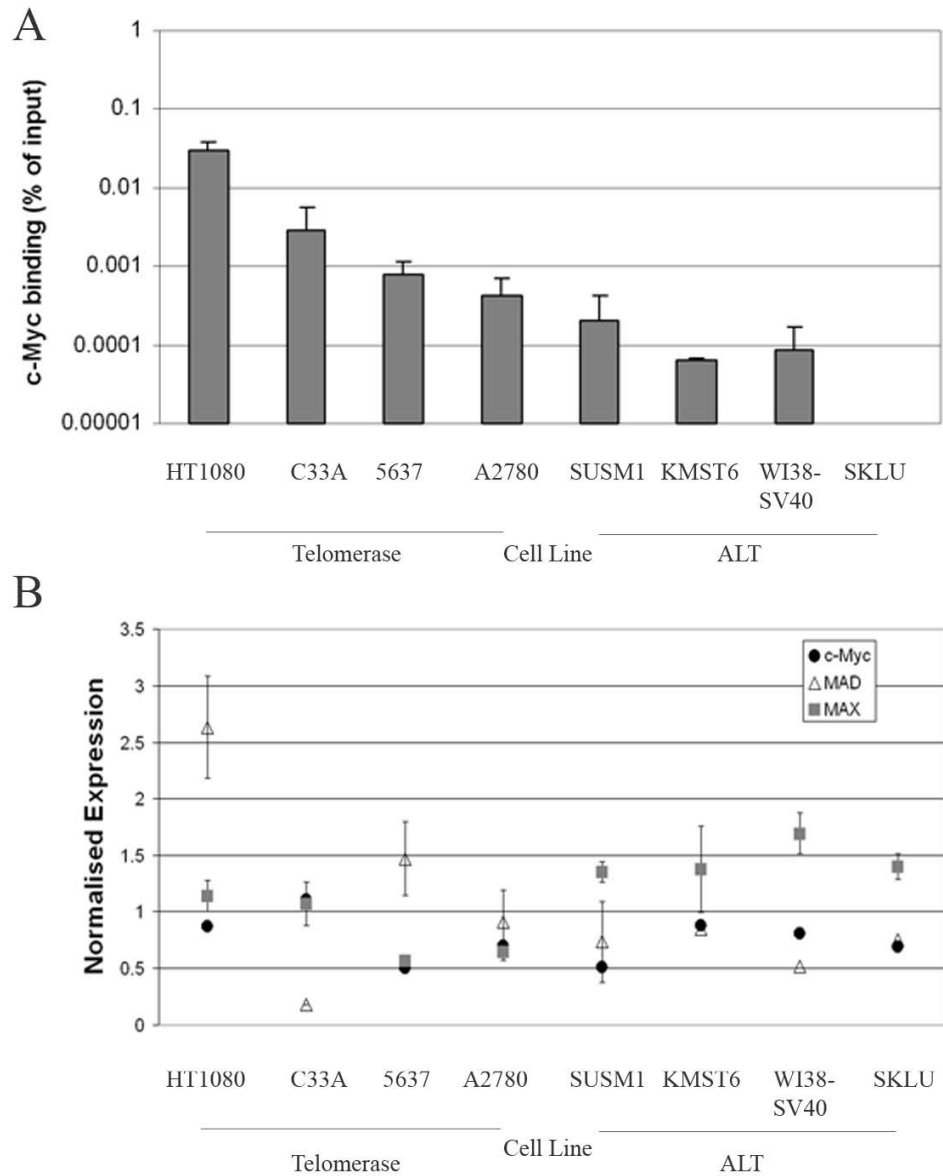


Figure 3.6 - c-Myc shows increased binding at the hTERT promoter in telomerase positive cells while common c-Myc binding partner expression is unaltered between ALT and telomerase positive cells.

(A) ChIP analysis of the hTERT promoter was completed using an antibody against c-Myc performed in duplicate. Each immunoprecipitate was quantified in triplicate by quantitative PCR analysis and related back to an input sample in each experiment to normalize the data. Error bars show standard error.

(B) Gene expression microarray data for the ALT cell lines (SKLU, SUSM1, KMST6, WI38-SV40) and the telomerase positive cell lines (HT1080, C33a, 5637, A2780) shows little expression differences between c-Myc binding partners Mad and Max. Error bars show standard error. c-Myc expression is significantly decreased in ALT ($p = 0.036$) and telomerase cell lines ($p = 0.041$) compare to mortal and MSC cells.

interesting possibility that E-boxes might play a role in establishment of epigenetic silencing of telomerase in ALT. Investigation of whether the difference in c-Myc binding at the hTERT promoter could be accounted for by expression differences in Mad and Max was therefore the logical next step. No significant difference in expression of c-Myc itself or Mad and Max was observed between the ALT and telomerase positive cell lines (Figure 3.6B). Given the lack of differences in expression of c-Myc, Max, or Mad between ALT and telomerase cell lines that could explain the decrease of c-Myc activity observed in ALT, investigation of other possible mechanisms for c-Myc regulation were undertaken.

3.2.8 Differential expression of c-Myc inhibitor TCEAL7 in ALT and telomerase positive cell lines

The transcription elongation factor A (SII)-like protein TCEAL7 had recently been shown to inhibit c-Myc activity through the competitive binding of E-Boxes (Chien et al. 2008). Such competitive inhibition would allow regulation of c-Myc transcriptional activity without the need for a down regulation in expression. TCEAL7 expression was therefore examined to assess whether it could potentially be regulating c-Myc activity in ALT and telomerase positive cells. Figure 3.7A shows RT-qPCR for TCEAL7 in the ALT and telomerase positive cell lines. Three of the four ALT cell lines had high levels of TCEAL7 expression whereas all of the telomerase positive cells had little or no expression of the gene. To investigate whether TCEAL7 and c-Myc could directly interact co-immunoprecipitations for c-Myc and TCEAL7 were performed. Neither pull-down of c-Myc with TCEAL7 antibodies nor TCEAL7 with c-Myc antibodies in any of ALT or telomerase positive cell lines was observed (data not shown). This suggested

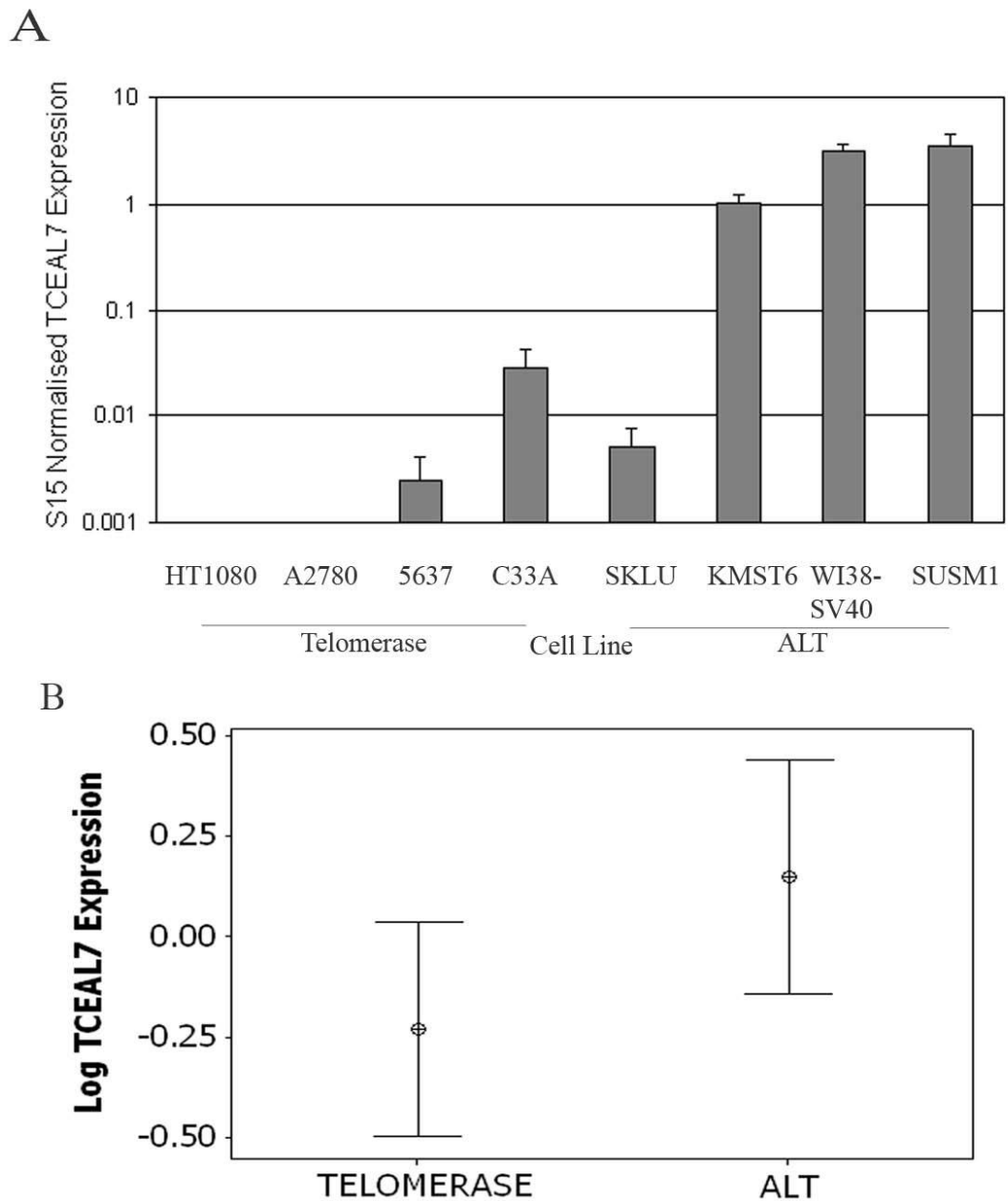


Figure 3.7 - TCEAL7 expression is increased in ALT cell lines and mesenchymal tumours.

(A) S15 normalised qPCR of TCEAL7 of telomerase positive cell lines (HT1080, A2780, 5637, C33A) and ALT cell lines (SKLU, KMST6, WI38-SV40, SUSM1). Error bars show standard error of triplicate experiments.

(B) Interval plot of gene expression microarray data for TCEAL7 of 3 mesenchymal tumour types (liposarcoma, peritoneal mesothelioma and malignant peripheral nerve sheath tumour) previously submitted to GEO under accession number GSE171118. Crosshairs show mean expression and error bars show 95% confidence intervals drawn using Minitab (v.15). P-Value = 0.053

that TCEAL7 and c-Myc do not directly interact and TCEAL7 regulation of c-Myc activity in ALT is through competitive inhibition.

Given that the functional network was generated using a combination of cell line and liposarcoma data and as ALT is predominantly found in tumours of mesenchymal origin *in vivo* (Ulaner et al. 2004; Henson et al. 2005) it was decided to examine the expression levels of TCEAL7 in a larger cohort of mesenchymal tumours. To this end, gene expression microarray data was generated for two further mesenchymal tumour types: peritoneal mesotheliomas and MPNST. Figure 3.7B shows that when combined TCEAL7 expression in the ALT mesenchymal tumours was higher than telomerase positive tumours (p-value = 0.053). This suggested that TCEAL7 could regulate c-Myc activity both *in vitro* and *in vivo*.

3.2.9 Perturbation of TCEAL7 expression levels in ALT and telomerase positive cells leads to changes in hTERT expression, c-Myc activity and telomerase activity.

To investigate the effects of altering TCEAL7 expression levels in ALT cells siRNA knockdowns using a pool of three different siRNAs were performed. Figure 3.8A shows that in all 4 ALT cell lines TCEAL7 expression was significantly reduced in comparison to non-coding siRNA controls. Subsequent examination of the effect of TCEAL7 knockdown on c-Myc activity in ALT cells using transcription factor binding ELISAs was undertaken. Figure 3.8b shows that SKLU and KMST6 showed negligible changes in c-Myc activity. As SKLU and KMST6 were seen to express less TCEAL7 than the other two cell lines it is possible that TCEAL7 is not the main c-Myc regulatory factor in these cells lines. WI38-SV40 and SUSM1 however, showed an increase in c-Myc activity over control transfections of 9 and 2 fold respectively. This suggested that in the ALT cell lines with high levels of TCEAL7 expression c-Myc activity is inhibited by TCEAL7. As lower levels of c-Myc binding at the hTERT promoter in ALT cells had also been observed, investigation of whether TCEAL7 expression knockdown and whether the resulting changes in c-Myc activity were sufficient to alter the expression of hTERT in ALT cells was performed. Although not always reaching significance, RT-qPCR of full length hTERT in ALT cells (Figure 3.8B) showed that in WI38-SV40 and SUSM1 hTERT expression also increased as a result of TCEAL7 knockdown. The decrease in

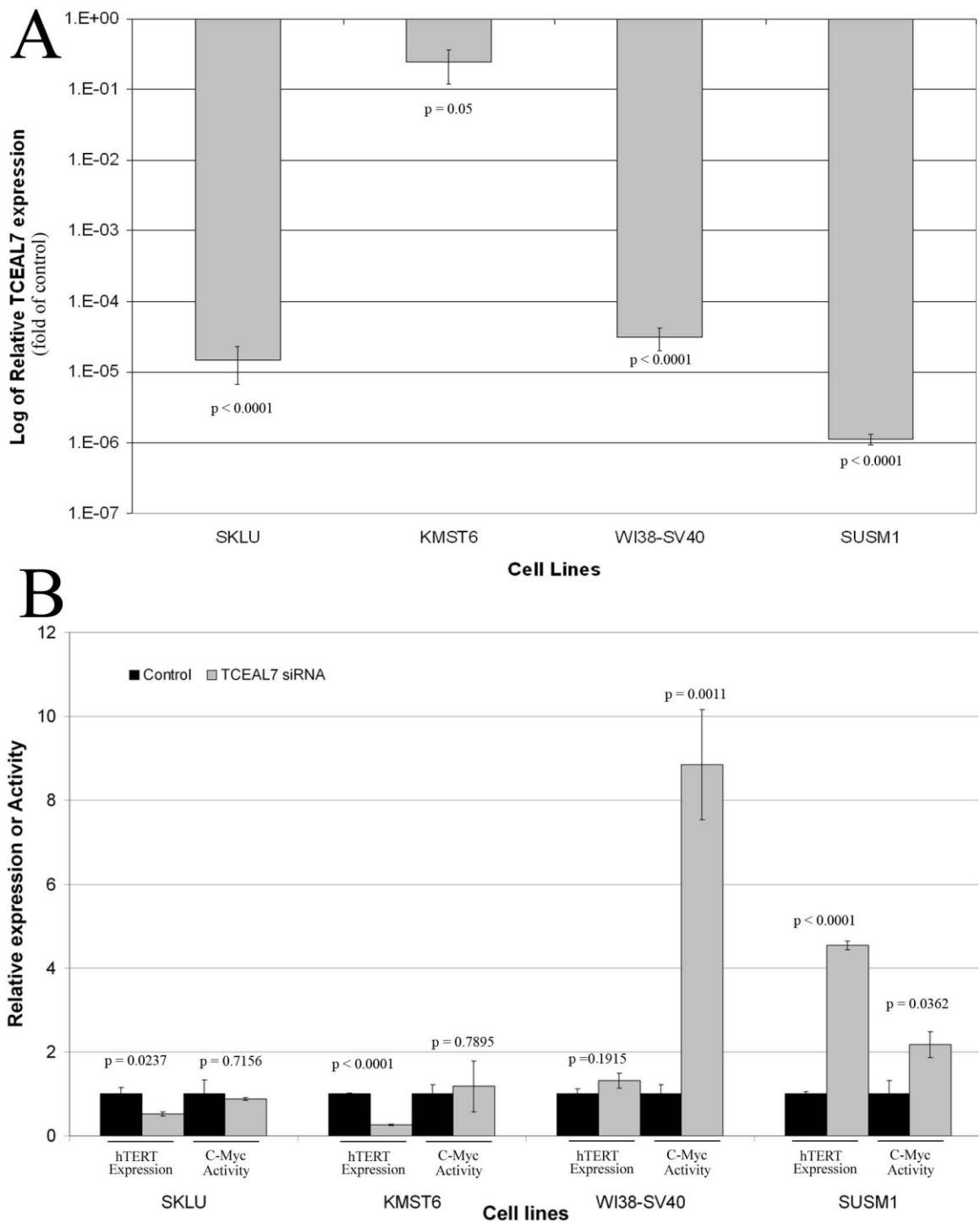


Figure 3.8 - Knockdown of TCEAL7 expression leads to increases in c-Myc activity and increased hTERT expression in ALT cells. TCEAL7 knockdown using a pool of 3 independent TCEAL7 siRNAs (Dharmacon) or non-coding siRNA control were performed in duplicate for each secondary assay in each ALT cell line. (A) qPCR of TCEAL7 expression was normalised to S15 expression before taking fold of control transfections. (B) hTERT expression was normalised to S15 expression before taking fold of control transfections. c-Myc activity was measured using transcription factor ELISA assays (Active Motif) performed in duplicate with at least 6 replicates from two separate transfections. Recombinant c-Myc (Active Motif) was used to create a standard curve for relative quantification. Error bars show standard error of triplicate experiments.

hTERT expression in SKLU and KMST6 also suggested active E-box dependent regulation of telomerase, though c-Myc activity was relatively unaffected. Therefore, additional mechanisms for c-Myc suppression may also be present in these cell lines. One possibility is that TCEAL7 knockdown preferentially relieves Mad rather than c-Myc targeting to E-boxes in these cells resulting in further reduction of hTERT expression.

As telomerase positive cells were seen to express little to no TCEAL7 the effects of TCEAL7 overexpression was investigated in these cells. A cDNA overexpression construct was transfected into the four telomerase positive cell lines and the expression of TCEAL7 was analysed by RT-qPCR compared to an empty vector control. In all four cell lines TCEAL7 expression was significantly increased in comparison to empty vector control (Figure 3.9A). The effect of TCEAL7 overexpression on hTERT expression was then investigated using RT-qPCR (Figure 3.9B). All four cell lines showed decreased hTERT expression after TCEAL7 overexpression. HT1080 showed the smallest decrease in hTERT expression ($p = 0.7993$) and this may be due to the fact that HT1080 showed the highest level of c-Myc binding at the hTERT promoter (Figure 3.6A) and therefore higher levels of TCEAL7 may be required to successfully compete with this. The effect of TCEAL7 overexpression on telomerase activity levels in these cells was then investigated using the TRAP assay (Figure 3.9B). Three of the four telomerase positive cell lines showed decreased telomerase activity over control after TCEAL7 overexpression. Although the cell line 5637 had shown decreased levels of hTERT gene expression, telomerase activity in this cell line increased with TCEAL7 overexpression. 5637 cells have relatively low levels of hTERT transcription and the down regulation of hTERT expression may trigger a regulatory feedback loop to maintain basal telomerase activity through, for example, post-transcriptional mechanisms such as alternative RNA splicing or hTERT phosphorylation. Regardless, taken together the current results clearly indicated that TCEAL7 is a novel regulator of hTERT expression and telomerase activity in both ALT and telomerase positive cell lines.

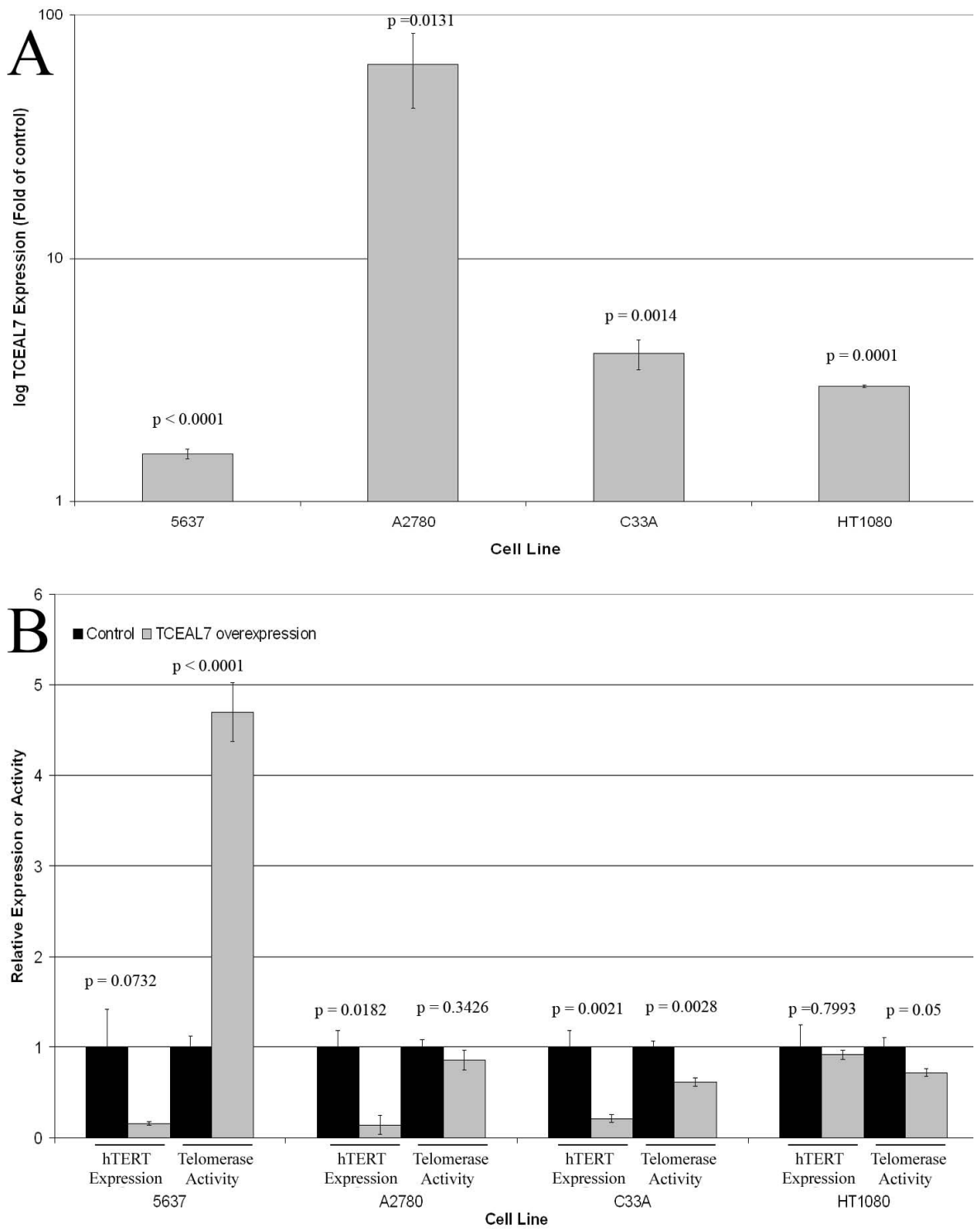


Figure 3.9 - Overexpression of TCEAL7 expression leads to decreases in c-Myc, hTERT expression and telomerase activity in telomerase positive cells. TCEAL7 cDNA overexpression plasmid (Origene) or empty vector control plasmid was transfected into telomerase positive cells in duplicate for each secondary assay. (A) qPCR of TCEAL7 expression was normalised to S15 expression before taking fold of control transfections. (B) hTERT expression was normalised to S15 expression before taking fold of control transfections. Telomerase activity (black) was measured using TRAP assay performed in duplicate for two separate transfections. Error bars shows standard error of triplicate experiments.

3.2.10 Functional Validation of 297 gene expression network using siRNA kinase screen highlights 106 hTERT regulatory kinases in ALT cells

Network analysis of the 297 gene liposarcoma signature identified a number of kinases that contribute to the regulation of hTERT in ALT cells, such as *PKC-alpha* and *TK1* (Figure 3.4). Kinases have previously been observed to regulate hTERT promoter activity in telomerase positive cells (Bilsland et al. 2009). It was therefore hypothesized that the regulation of hTERT in ALT cells may have a further layer of regulation through hTERT regulatory kinases.

To investigate this an siRNA kinase screen was undertaken using an hTERT promoter luciferase reporter construct in the ALT cell line SKLU. 3 separate siRNAs for 719 kinases and kinase-related genes were investigated. The cut-off for hit assessment was a >2 fold change in hTERT promoter activity in at least 2/3 siRNAs. This resulted in 106 kinases that met the criteria (Figure 3.10). Examination of the regulatory effect of these hits showed that 89 were hTERT activators and 17 were hTERT inhibitors. This disproportionate number of telomerase activators may be reflective of the strict regulation of telomerase expression in ALT cells highlighted by the gene expression network. Alteration of one of the multiple regulatory systems preventing telomerase expression in ALT, in this case phosphorylation by kinases, may the majority of the time be insufficient to overcome the larger repressive network effect. This interesting result indicates that SKLU cells retain many active signaling components, which may be required for hTERT expression in telomerase positive cells. In the context of the ALT phenotype, it is likely that their effects on telomerase are muted by additional regulatory systems including epigenetic changes at the hTERT promoter and the altered gene expression networks previously observed in this study. It will be of interest to investigate the potential roles of the inhibitory kinase hits identified here in these processes in future studies.

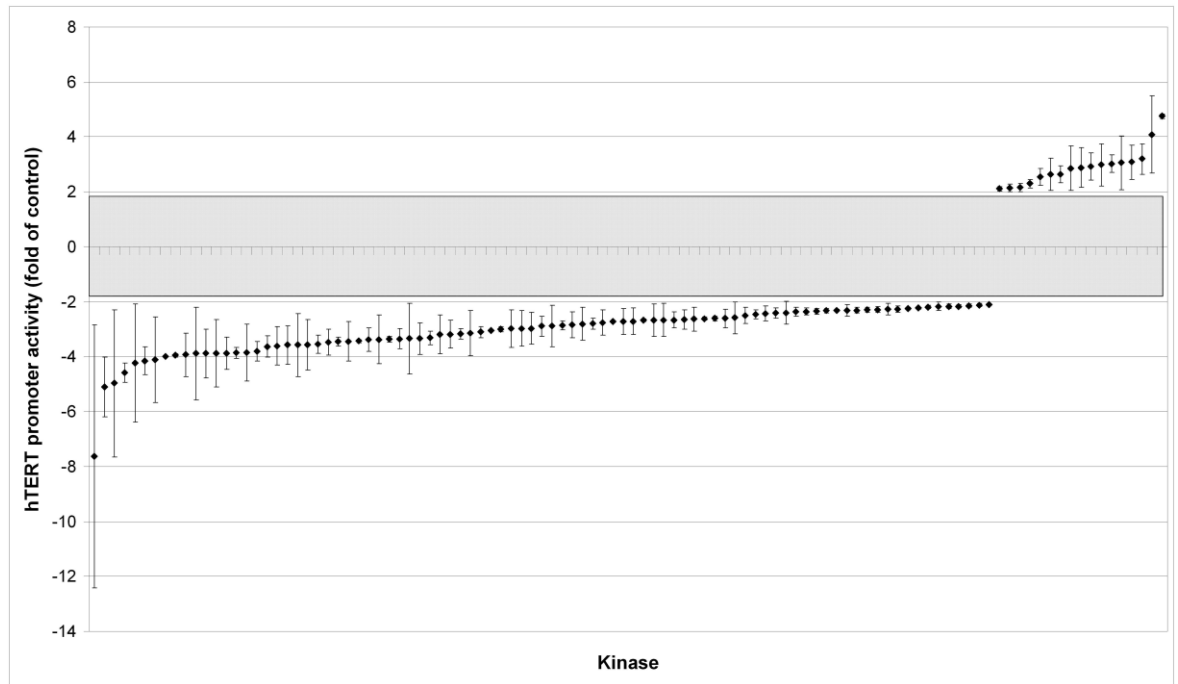


Figure 3.10 - siRNA kinase screen highlights 106 kinases with hTERT regulatory factors. Kinases with two siRNAs that induce a two fold or more change in hTERT promoter activity in the same direction over promoter-less control plasmid. Each point indicates the average change in promoter activity of 2 or more different siRNAs for each kinase assayed in triplicate, error bars show standard error of triplicate repeats.

3.2.11 *Transcriptional Regulation networks of 106 hTERT regulatory kinases highlights c-Myc as top regulator.*

As these kinases have the potential to regulate TERT expression they represent a further level of the TERT regulatory network. Transcriptional regulation of these kinases themselves therefore represents a further potential level of regulation in the TERT regulatory network. To this end the transcriptional regulation network inference algorithm in Metacore was applied. This analysis returned several networks centered on statistically significant transcription factor regulators of the hits, including a number with known hTERT regulatory functions (Table 3.1). Union of the networks surrounding the hTERT transcriptional activators STAT3, SP1 and c-Myc (Figure 3.11A) and repressors p53 and the Androgen receptor (Figure 3.2B) highlighted the interplay between multiple candidate pathways which may influence the expression of hTERT in ALT cells. For example, in Figure 3.11A, the kinase SYK expression was activated by c-Myc which in turn activated the transcription factor STAT3. SYK also negatively regulated SP1 through binding. The negative regulation of an hTERT activating transcription factor may highlight the potential for such complex networks to self-regulate the exact levels of different signaling pathways contained within them.

Interestingly, c-Myc regulated the largest percentage of kinase hits in this study (Table 3.1) showing that not only is c-Myc itself involved with telomerase regulation in ALT but that its downstream kinases themselves are regulators of telomerase expression.

3.3 Discussion

Senescence presents a major block to tumour progression and therefore cells require a mechanism of senescence bypass senescence if they are to become fully tumorigenic. The induction of senescence through telomere attrition, known as replicative senescence, is one mechanism by which cellular proliferation is regulated. To bypass this mechanism most tumours utilize the telomere rebuilding enzyme telomerase. However, a small proportion of tumours utilize an intra- and inter- telomere recombination based mechanism known as the alternative lengthening of telomeres or ALT

No.	Network	% of hits regulated	p-Value
1	c-Myc	17	1.50E-48
2	HNF4-alpha	15	2.42E-40
3	p53	14	1.28E-37
4	SP1	13	6.67E-35
5	STAT3	11	1.73E-29

Table 3.1 - Transcriptional regulation of 106 hTERT regulating kinases shows known hTERT regulating transcription factors and c-Myc as top regulator.

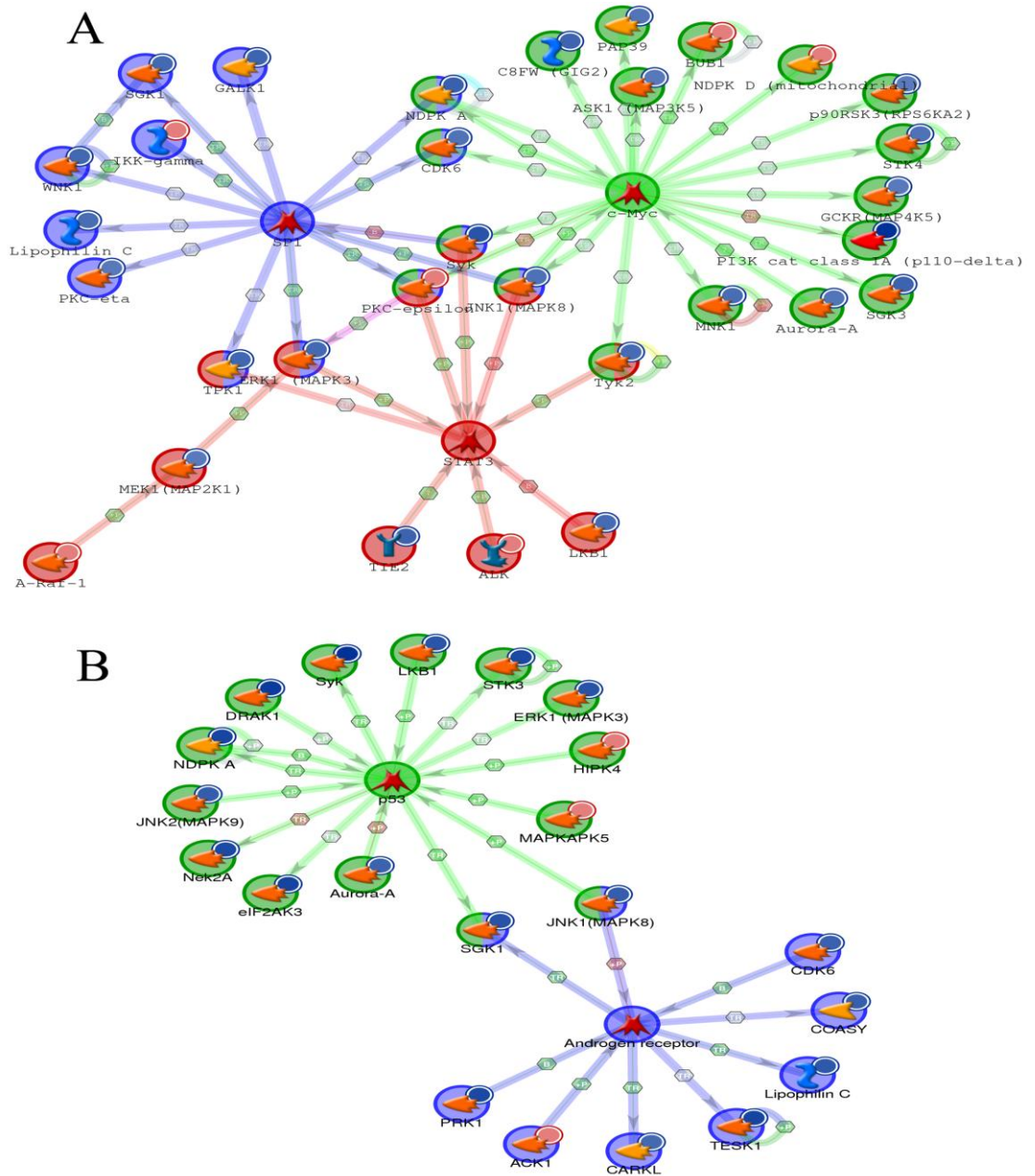


Figure 3.11 - Transcriptional regulation networks highlight synergistic regulation of hTERT regulatory kinases by known hTERT transcriptional regulators. Merged networks of the top 5 transcriptional regulators of 106 siRNA kinase screen hits of known hTERT transcriptional activators (A) and repressors (B). Green lines between objects indicate an activating interaction whereas red lines indicate an inhibitory reaction. Overlaid line colours (red, green or blue) indicate transcriptional networks generated for each transcription factor before network merge. Symbols on the lines indicate the following: TR = transcriptional regulation, +P = phosphorylation, B = binding and ? = unknown mechanism. Blue circles next to kinases indicate an hTERT activating kinase and red circles indicate an hTERT inhibiting kinase

(Dunham et al. 2000; Muntoni et al. 2009). The molecular mechanisms regulating the decision to activate telomerase or ALT during tumourigenesis are currently poorly understood. Lack of expression of the telomerase genes hTR and hTERT is associated with chromatin remodelling at the promoters, suggesting that forced repression of these genes may cause the cells to utilise the ALT mechanism for immortalisation (Atkinson et al. 2005). In this section of the study, gene expression profiling of telomerase and ALT cell lines and liposarcomas was utilised to investigate other signaling pathways and networks that may be operating to control the ALT phenotype and the decision to activate telomerase or ALT for immortalization and senescence bypass.

A gene expression signature was uncovered with the power to distinguish telomerase positive and ALT through hierarchical clustering methods in tumour cell lines (Figures 3.1B, 3.2A & 3.2B). Further refinement of this signature using gene expression profiles from liposarcoma tissue samples revealed a 297 gene signature that had significant association with TMM (Figure 3.1B). By combining clinical samples with cell line profiles some of the underlying biology of ALT *in vivo* and *in vitro* was uncovered. Network analysis of interactions within the refined signature highlighted a signaling network involved in repression of hTERT in ALT liposarcoma samples and cell lines (Figure 3.4D).

Validation of the functional network was undertaken using a number of different approaches. Initially, western blots of 3 of the molecules in the network confirmed that this pattern was also observed at the protein level and qPCR confirmed the differential expression of 4 genes at the mRNA level (Figure 3.5A & 3.3A). The functional network of interactions also highlighted the potential for lower c-Myc activity in cells using the ALT mechanism. Therefore examination of the relative activity levels of c-Myc was undertaken to further validate the patterns observed in the functional gene expression network. Upon direct investigation using c-Myc activity ELISAs, a lower level of c-Myc activity in ALT was confirmed (Figure 3.5B) and through the use of ChIP differential c-Myc binding at the hTERT promoter in ALT and telomerase positive cells was also confirmed (Figure 3.6A).

The role of c-Myc in cell cycle regulation and senescence signaling makes it a key transcriptional regulator during the processes of immortalisation and senescence bypass. c-Myc is well documented as a regulator of telomerase and

therefore its potential as a key regulator of the molecular differences between TMMs is an interesting consideration.

Gene activation by c-Myc binding at DNA E-boxes occurs as a dimer with binding partner Max (Amati et al. 1993). The activities of Max in turn are antagonised by dimerisation with Mad and the resulting binding of Mad/Max to E-boxes within promoter regions leads to gene repression (Ayer et al. 1993). Furthermore, Mad has been found to dimerise with and recruit the histone demethylase RBP2 to E-boxes in the hTERT promoter and repress transcription through chromatin remodelling (Engels et al. 2006). The expression levels of Mad and Max in ALT and telomerase positive cells may therefore have an influence on the activity of c-Myc and telomerase expression. However, investigation of the expression of these factors in the gene expression microarray data (Figure 3.6B) showed no expression difference in c-Myc, MAD or MAX able to explain the decreased c-Myc activity observed in ALT cell lines.

As the expression patterns of c-Myc's regulatory molecules Mad and Max were unable to account for the decreased c-Myc activity, less well characterized c-Myc regulatory mechanisms were investigated. A literature search revealed TCEAL7 as a competitive inhibitor of c-Myc DNA binding. TCEAL7 is a member of the transcription elongation factor A (SII)-like gene family and is relatively poorly studied. The expression of TCEAL7 is epigenetically silenced in epithelial ovarian cancer and forced expression of TCEAL7 in ovarian tumour cell lines induced apoptosis (Chien et al. 2005). Furthermore, TCEAL7 has been observed to have decreased expression in a variety of human tumours (Chien et al. 2008) and recently polymorphisms in the gene have been associated with reduced risk of invasive serous ovarian cancers (Peedicayil et al. 2009). The role of TCEAL7 in cancer risk may be due to its function as a regulator of cyclin D1 expression and c-Myc activity (Chien et al. 2008). TCEAL7 binds to E-boxes of gene promoters and thereby competitively inhibits gene activation by Myc-Max complexes. Such competitive inhibition would effectively decrease c-Myc activity without the need for decreased c-Myc expression and it is for this reason that TCEAL7 was suggested as a potential mechanism for c-Myc activity regulation in ALT. Through RT-qPCR of ALT and telomerase positive cell lines it was found that ALT cells expressed a high level of TCEAL7 whereas telomerase positive cells expressed little or no TCEAL7 (Figure 3.7A). As ALT is predominantly seen in

mesenchymally derived tumours and not just liposarcomas (Ulaner et al. 2004; Henson et al. 2005) the investigation of TCEAL7 expression was expanded to include 2 further mesenchymal tumour types: peritoneal mesotheliomas and malignant peripheral nerve sheath tumours (MPNST). The analysis of the resulting combined mesenchymal tumour cohort showed that TCEAL7 expression was increased in ALT tumours compared to telomerase positive tumours ($p = 0.053$) suggesting that TCEAL7 overexpression may be a c-Myc regulatory mechanism both *in vitro* and *in vivo* (Figure 3.7B). Furthermore, through the use of knockdown and overexpression of TCEAL7 in ALT and telomerase positive cell lines respectively it was shown that TCEAL7 could regulate c-Myc activity, hTERT expression and telomerase activity (Figures 3.8 & 3.9). This was consistent with the fact that c-Myc is a known hTERT transcriptional activator (Zeller et al. 2003; Hao et al. 2008) and may show a further mechanism by which the decision to activate either ALT or telomerase is influenced. As the majority of human tumours utilize telomerase as a telomere maintenance mechanism the decreased expression of TCEAL7 in a wide variety of human tumours (Chien et al. 2008) is consistent with TCEAL7's potential role as an hTERT regulator through c-Myc.

The gene expression network also highlighted PKC α as a known hTERT regulatory molecule (Chang et al. 2006) and kinases have previously been seen to play a role in regulation of telomerase in telomerase positive cells (Bilsland et al. 2009). Through the use of a siRNA kinase hTERT luciferase reporter screen the kinome was probed for hTERT regulatory kinases in ALT cells with the aim of further investigating the role of kinases in ALT. 106 kinases through which hTERT promoter activity was regulated were highlighted (Figure 3.10). A greater proportion of hits which were hTERT activators, such that their knockdown resulted in decreased hTERT expression, were observed which may reflect the strict hTERT regulatory conditions present within ALT cells. This finding would suggest that knockdown of a single molecule would in most cases be insufficient to overcome the effects of the entire network. It is for this reason that decreases in hTERT promoter activity may be easier to achieve than increases.

Through the use of transcriptional regulation network building algorithms it was discovered that the 106 kinases were regulated by known hTERT regulating transcription factors (Table 3.1). Furthermore, merging networks of known

hTERT activating or repressing transcription factors highlighted cooperating interactions between these factors (Figure 3.11). The regulation of the transcription factors themselves by upstream hTERT regulatory kinases highlighted further potential mechanisms by which they could regulate hTERT promoter activity. The data presented here therefore highlights the fact that the complex network of interactions by which the expression of telomerase is regulated in ALT cells further extends to kinase regulation, consistent with previous data in telomerase positive cells (Bilsland et al. 2009). Furthermore, the top transcriptional regulator of the 106 kinase hits was c-Myc. This further emphasized the potential key role that c-Myc may play in the decision between the two telomere maintenance mechanisms through telomerase regulation and its potentially central role in senescence signaling regulation during immortalization and bypass.

The functional validation of the candidate network further highlighted the importance of a global analysis of gene expression. Where significant expression of one gene may be of importance in certain circumstances, it is more likely, as evidenced by the gene expression network and the complex transcriptional networks between the 106 hTERT regulatory kinases, that small changes in a combination of genes in a signaling pathway are responsible for defining a phenotype. By investigating signaling networks on a global scale an increased understanding of the biology underlying the ALT phenotype and its regulation in mesenchymal malignancies has been achieved. Such improved understanding of the mechanisms by which tumours bypass senescence help to further investigations into senescence induction in human tumours.

In addition to the hTERT regulatory network a number of stem cell related genes were also highlighted within the 1305 gene signature. The possibility that the decision to activate either telomerase or ALT is made at the cellular level was an interesting hypothesis to consider. Cancer biology in many ways parallels that of stem cell biology, as pathways regulating the self-renewal phenotype and replicative lifespan of stem cells, such as WNT signaling (Fevr et al. 2007), are commonly deregulated in cancer. With the growing interest in stem cells as the cell of origin for certain tumours, investigating the potential origin for ALT immortality may improve the understanding of the regulation of senescence bypass by telomere maintenance. The preponderance of ALT in mesenchymal

malignancies prompted an investigation of any relationship between human mesenchymal stem cells (hMSC) and ALT or telomerase positive cell lines and liposarcoma tissues. hMSCs are an adult stem cell population with limited replicative lifespan and no detectable telomerase activity (Zimmermann et al. 2003), which is due at least in part to active repression of the telomerase genes at the chromatin level, similar to the situation in ALT cell lines (Serakinci et al. 2006; Cairney et al. 2008). hMSCs do not however display characteristic molecular markers of ALT (Bernardo et al. 2007; Zhao et al. 2008). It is therefore possible that hMSCs upon transformation could become either ALT or telomerase positive tumours. There is however a need for accurate models of the molecular details of the decision between these two mechanisms, such as this, before manipulation of the resulting telomere maintenance mechanism can be achieved.

Hierarchical clustering showed that the expression profile of the signature genes in hMSC was more closely related to ALT than to telomerase positive cell lines with the larger signature and also to ALT liposarcomas when the refined 297 gene signature was utilised, suggesting a mesenchymal stem cell origin for ALT (Figures 3.1C & 3.4C).

Mesenchymal stem cells are known to be potential targets for transformation *in vitro*. Lack of any telomere maintenance mechanism in these cells may be a tumour suppressor mechanism as transduction with hTERT has been shown to extend their lifespan and induce neoplastic characteristics following long term culture *in vitro* and tumour formation *in vivo* (Serakinci et al. 2004). In addition several studies have shown the ability of MSCs to transform spontaneously following long term culture *in vitro* in murine systems (Miura et al. 2006; Zhou et al. 2006), although the situation in human systems remains unclear with conflicting reports suggesting that the capacity for spontaneous transformation may be dependent on the tissue of origin (Rubio et al. 2005; Wang et al. 2005; Miura et al. 2006; Bernardo et al. 2007). More recently several studies have linked hMSC with mesenchymal malignancies including Ewing's sarcoma (Tirode et al. 2007; Riggi et al. 2008) and malignant fibrous histiocytoma (Matushansky et al. 2007). Stem-like tumour initiating cells have also been isolated from various mesenchymal tumours (Gibbs et al. 2005; Wu et al. 2007). Taken

together this data suggests that the stem cell origin for cancer extends to mesenchymal malignancies.

Although the preponderance of ALT in mesenchymal tissues has been documented previously on numerous occasions, this was the first time the link to a mesenchymal stem cell origin for ALT had been made. Furthermore, this was not simply reflective of the mesenchymal origin of ALT cell lines as both the ALT and telomerase positive liposarcoma samples were mesenchymally derived and only the ALT liposarcomas cluster with hMSC. The significance of this association is unknown at present, but certainly warrants further investigation.

The observations of differential c-Myc activity between ALT and telomerase positive cells may potentially be linked to potential cell of transformation, in this case hMSCs and ALT. Exploration of the expression levels of c-Myc and its regulatory factors Mad and Max showed no significant difference in the expression levels of Mad or Max between ALT or telomerase positive cells (Figure 3.6B).

In conclusion, this analysis has highlighted a gene expression signature capable of distinguishing telomerase positive from ALT in cell lines and liposarcoma tissue samples. This signature contained a regulatory signaling network involving hTERT repression in ALT and is indicative of a novel hMSC origin for ALT. A candidate network also highlighted differences in c-Myc activity, further investigation of which highlighted the potentially key role of c-Myc in the decision between ALT and telomerase TMMs during senescence bypass. A better understanding of the regulation of senescence bypass through TMM in the cell of origin will increase knowledge of the biology underlying these tumour types and may highlight novel areas for therapeutic intervention. Furthermore, these investigations show that regulation of senescence bypass by telomere maintenance involves a complex network of interactions involving gene expression differences, transcription factors and kinases, all of which present attractive targets for intervention. To make full use of these gene expression networks further understanding of the regulatory mechanisms behind them, such as chromatin modifications, miRNA regulation and post-translational protein modifications, is required however.

4 miRNA regulation of senescence signaling during tumorigenesis.

4.1 Introduction

Telomere maintenance mechanisms (TMMs) are utilised by tumour cells to bypass telomere induced replicative senescence. Data in the previous chapter highlighted the complex gene expression networks regulating the decision between telomere maintenance mechanisms. Furthermore, the previous chapter also showed that these networks are in part regulated by the actions of kinases, c-Myc and TCEAL7. The coordination of these multiple changes to gene expression and pathway signaling requires regulation at many different molecular levels and in coordination with the regulation of the larger senescence program. For instance multiple chromatin modifications, such as methylation of K9 H3 (Narita et al. 2003), are required to establish the senescence-associated heterochromatin foci during senescence induction (Atkinson et al. 2007; Zhang et al. 2007) and have also been seen to play a role in telomere maintenance mechanisms (Cairney et al. 2008). Of the many ways to regulate gene product expression, miRNAs are relatively poorly understood. These short non-coding molecules ranging in size from 19-22 nucleotides are highly conserved and regulate protein expression through interactions with the 3' untranslated region (UTR) of mRNA (Lee et al. 1993; Wightman et al. 1993). Mammalian miRNAs are produced in two main stages. Initially miRNAs transcripts (known as primary miRNAs) are transcribed by RNA polymerase II and then are then processed in the nucleus by the RNase type III protein Drosha to form precursor miRNA hairpin molecules (Kim et al. 2009). The miRNAs are then exported from the nucleus to the cytoplasm where they are further processed by another RNase type III protein, Dicer, to form the mature 19-22 nucleotide single stranded miRNA. The mature miRNAs are then bound onto Ago proteins to form the final functional RNA induced silencing complex (RISC) (Wahid et al. 2010). miRNA genes have been observed in both coding and non-coding genes in both exonic and intronic regions where the majority of miRNAs are found in intragenic regions (Kim et al. 2009, Lagos-Quinata et al. 2001, Lau et al. 2001).

The binding of a miRNA to the 3'UTR causes inhibition of translation through steric hindrance or degradation of the mRNA, depending on the degree of complementarity between the two sequences (Engels et al. 2006). The ability of miRNAs to regulate a variety of target genes allows them to induce changes in multiple pathways and processes such as development (Harfe 2005), apoptosis, proliferation and differentiation (Bartel 2005). Furthermore, recent observations in breast cancer particularly implicate miRNA expression as having a pivotal role in tumour progression. The expression of some miRNAs, such as the mir-200 family, have been observed to suppress metastasis whereas others, such as mir-373 and mir-520c, are considered pro-metastatic miRNAs (Shi and Guo 2009). As such miRNA expression has the potential to regulate entire pathways in normal developmental processes as well as being potentially hijacked for use in the establishment and progression of cancer.

MiRNAs could therefore facilitate the complex cellular changes required to establish the senescent phenotype. Identification of the mRNA sequences that miRNAs regulate is mainly derived using bioinformatics techniques. The ability of each miRNA to target genes is based on sequence complementarity to 3'UTRs of known mRNAs. Furthermore each miRNA has the potential to regulate on average 1000 gene targets (Griffiths-Jones 2004; Griffiths-Jones et al. 2006; Griffiths-Jones et al. 2008). It is this large number of potential targets across different biological pathways that give miRNAs the power to potentially induce complex cell phenotypes, like senescence.

To investigate whether miRNAs could play a role in the complex regulatory networks of senescence signaling and bypass an initial investigation of 12 miRNAs with known experimental evidence for a role in senescence induction was performed. Using publicly available gene expression data for cells induced to senescence by various stimuli, the potential of these 12 senescence associated miRNAs (SA-miRNAs) to regulate the patterns of differential gene expression was assessed. After establishing the potential of miRNAs to regulate the larger process of senescence, their potential role in senescence bypass by regulation of telomere maintenance mechanisms was investigated. Using miRNA microarray profiling the associations of miRNA expression with telomere maintenance mechanisms and survival in mesenchymal tumours were explored.

4.2 Results

4.2.1 Identification of 12 SA-miRNAs and Pathway mapping of their miRNA targets shows cell cytoskeletal, cell cycle and proliferation regulation potential

Although the gene targets of miRNAs can be identified theoretically by computational algorithms, it is unclear exactly which potential target genes they modulate and to what extent this affects the associated functions of these genes. The identification of miRNAs with the ability to regulate a complex phenotype, like senescence, is therefore not possible using purely bioinformatic techniques. For this reason the literature was searched for miRNAs with experimental evidence of a role in senescence induction. To this end, database searches of the terms “miRNA” and “senescence”, using pubmed and ISI web of knowledge (accessed 18 Nov 2008) were performed. The literature search highlighted 6 studies with direct evidence for regulation of senescence by miRNAs. Two main approaches were used in these studies: microarray based and comprehensive functional genomics; and the investigation of candidate senescence genes and the miRNAs regulating them. The 6 studies highlight a total of 12 senescence-associated miRNAs (SA-miRNAs). Each miRNA has the ability to bind between 953 and 2351 sites on mRNA 3' UTRs (see Table 4.1) and in addition some 3'UTRs potentially have multiple complementary sites for a given miRNA. To add to the complexity, in reality this set of miRNAs may only be a subset of the total number of miRNAs that play a role in senescence regulation.

Before the full impact of miRNAs' role in the regulation of senescence bypass by TMMs could be fully understood, a measure of their ability to regulate the larger process of senescence must be gained. To this end, mapping of the signaling pathways regulated by the SA-miRNAs (shown in Table 4.1) was performed. Furthermore, through this approach it was hypothesised a better understanding of the biological mechanisms by which miRNAs can cooperate to create the complex senescence phenotype would be gained. The free, publicly available Sanger miRNA database contains a registry of computationally calculated gene targets for each known miRNA. The current version of the database (mirBase

targets v5, 25 Aug 2008) was downloaded and queried using Microsoft Access, in order to generate lists of theoretical gene targets for the 12 SA-miRNAs. As the computational method of assigning gene targets to miRNAs cannot assess the level of complementarity required for a biological effect, it was decided to include all theoretical targets in the analysis, as a representation of the maximum regulatory effect these miRNAs could have. The signaling pathways that these gene targets are involved in were explored using the systems biology tool Metacore from Genego (Genego Inc, St Joseph, MI).

The top 5 pathways regulated by the SA-miRNAs are shown in Table 4.2. Two of these maps are involved in cytoskeletal remodelling and are highly saturated with gene targets of the SA-miRNAs (Figure 4.1). Senescent cells are seen to undergo changes in morphology, becoming large and flattened (Berube et al. 1998), which would require significant cytoskeletal remodelling. Such widespread cellular modifications would be associated with the alteration of many different pathways and processes that all contribute to the maintenance of the actin cytoskeleton. Due to their ability to bind a number of different gene targets miRNAs provide a mechanism by which such widespread changes could be induced.

Changes in the processes involved in DNA synthesis in early S-phase are also potentially regulated by the SA-miRNAs (Figure 4.2). Of the objects on this map 59% are potentially regulated by the SA-miRNAs and in particular members of the MCM and ORC complexes. The ORC and MCM complexes are responsible for the initiation of DNA replication by assembly of the pre-replication complexes and ensure that the process only occurs once during the cell cycle (Bell et al. 2002). Recently the ORC complex was reported to be able to interact with the telomere binding protein TRF2 and affect telomere homeostasis (Tatsumi et al. 2008). Replicative senescence relies on the shortening of telomeres to induce a DNA damage checkpoint response that blocks their progression into S-phase (di Fagagna et al. 2003). Since senescence involves irreversible cell cycle arrest, SA-miRNA regulation of cell cycle mechanisms strengthens their possible role in senescence regulation.

Number	Senescence Associated miRNA	Number of predicted complementary sites in the transcriptome	References
1	hsa-let-7f	1018	Wagner <i>et al.</i> , 2008
2	hsa-miR-499	2157	Wagner <i>et al.</i> , 2008
3	hsa-miR-373	1057	Voorhoeve <i>et al.</i> , 2006
4	hsa-miR-372	953	Voorhoeve <i>et al.</i> , 2006
5	hsa-miR-371	2205	Wagner <i>et al.</i> , 2008
6	hsa-miR-369-5P	1107	Wagner <i>et al.</i> , 2008
7	hsa-miR-34c	2351	Kumamoto <i>et al.</i> ,2008
8	hsa-miR-34b	1086	Kumamoto <i>et al.</i> ,2008
9	hsa-miR-34a	1296	Tazawa <i>et al.</i> , 2007, He <i>et al.</i> , 2007, Kumamoto <i>et al.</i> ,2008
A	hsa-miR-29c	1199	Wagner <i>et al.</i> , 2008
B	hsa-miR-217	993	Wagner <i>et al.</i> , 2008
C	hsa-miR-20a	1275	Poliseno <i>et al.</i> , 2008

Table 4.1 - Senescence associated miRNAs from the literature and the number of computationally derived mRNA 3' untranslated regions each can target. (Note some mRNAs may contain multiple binding sites) Numbering denotes the thermometer number representing particular miRNA's targets on Figures 4.2, 4.3 and 4.4.

	Pathway Map	% of objects on the map that are SA-miRNA targets
1	The role of TGF and WNT in Cytoskeletal remodelling	44% (49/111)
2	Cytoskeletal remodelling general process	42% (43/102)
3	Cell Cycle: The start of DNA replication in early S-phase	59%(19/32)
4	Regulation of transcription in the CREB pathway	50% (21/42)
5	Development EGFR signaling via small GTPases	41% (13/32)

Table 4.2 - The top 5 pathways regulated by all 12 SA-miRNAs with the percentage of the map that consists of SA-miRNA gene targets . Gene target lists for each SA-miRNA were input to Metacore and the pathway maps which were commonly regulated were examined. Pathways are ordered by the number of SA-miRNA targets on each map. The presence of 4 regulatory pathways involving different aspects of cellular signaling and only one cell cycle pathway shows that there is more to senescence than just cell cycle regulation. SA-miRNAs therefore present a mechanism by which a variety of the required cellular pathway changes could be regulated.

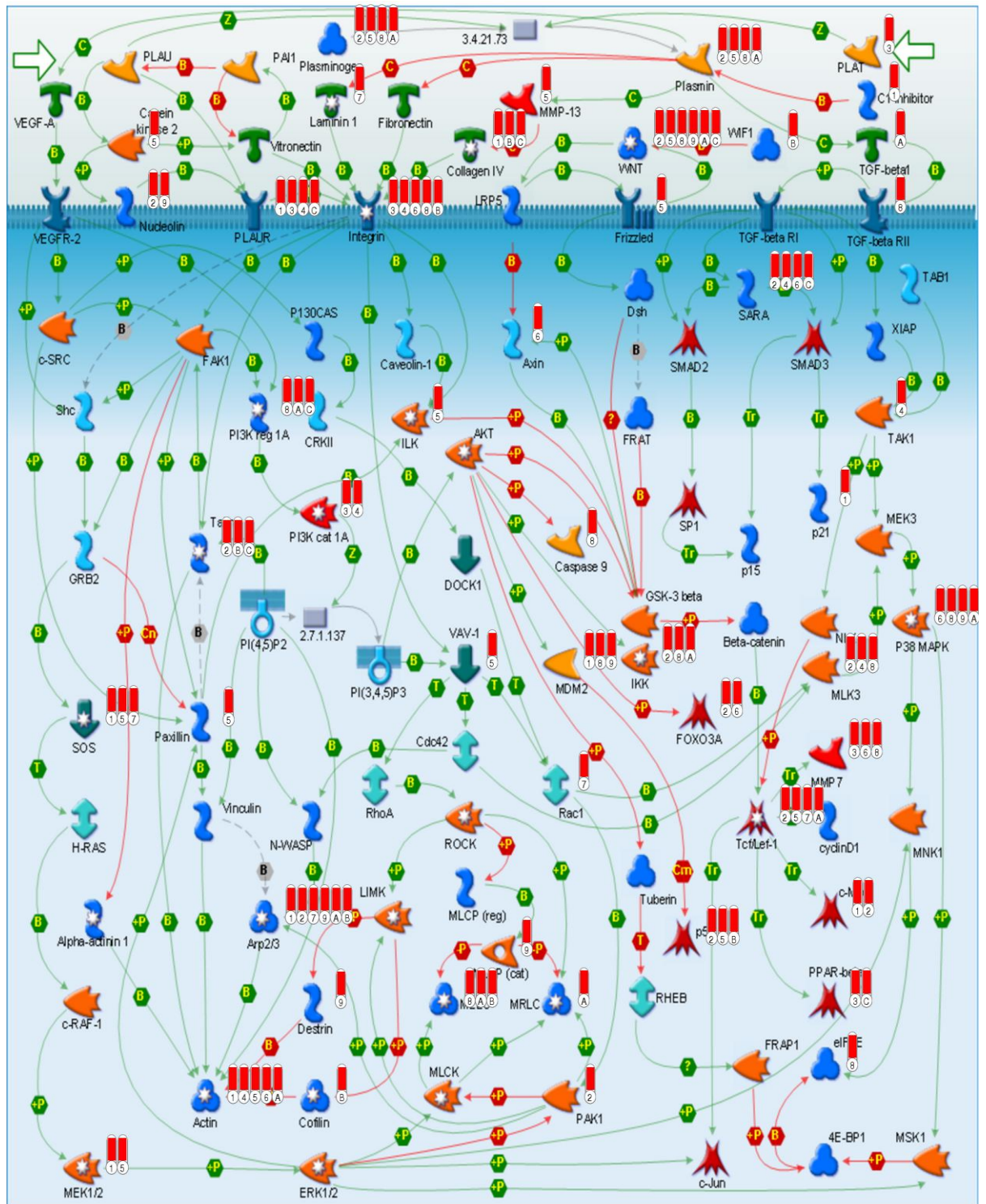


Figure 4.1 - SA-miRNA regulation of the Cytoskeletal remodelling and the role of TGF and WNT biological pathway map. Red thermometers show an object that can be regulated by a SA-miRNA with thermometer numbering corresponding to that seen in Table 2.1. Multiple thermometers denote that the object is a target of multiple SA-miRNAs. Green arrows represent positive, red negative and grey unspecified interactions. Boxes on lines denote the type of regulation where P = phosphorylation; B = binding; Tr = transcriptional regulation, Cm = covalent modification, T = transformation and Z = catalysis.

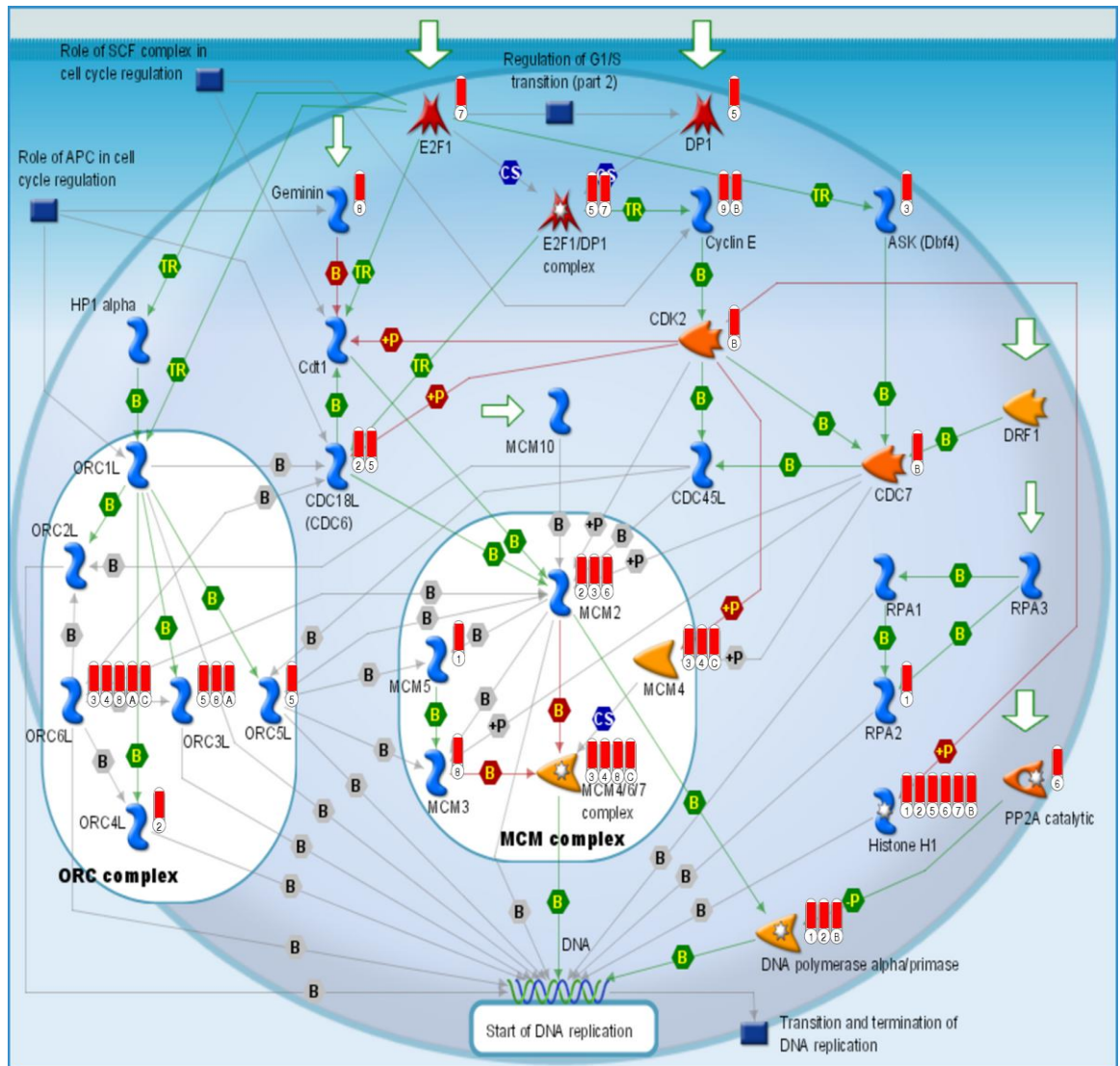


Figure 4.2 -SA-miRNA regulation of Cell cycle and DNA replication in early S phase biological map. Red thermometers show an object that can be regulated by a SA-miRNA with thermometer numbering corresponding to that seen in Table 2.1. Multiple thermometers denote that the object is a target of multiple SA-miRNAs. Green arrows represent positive, red negative and grey unspecified interactions. Boxes on lines denote the type of regulation where P = phosphorylation; B = binding; Tr = transcriptional regulation, Cm = covalent modification, T = transformation and Z = catalysis

The transcription factor CREB is also potentially regulated by SA-miRNAs (Figure 4.3). CREB is a known regulator of cellular growth and proliferation through its transcriptional regulation of genes such as the oncogene *c-fos* (Ahn et al. 1998) and regulators of the cell cycle such as cyclin D1 (Lee et al. 1999) and cyclin A (Desdouets et al. 1995). Alteration of molecules regulating CREB by SA-miRNAs would therefore confer another mechanism to alter the cell growth and proliferation pathways towards a senescent state.

EGFR and its proliferative signaling are not conducive to a senescent cellular environment. Consistent with this, EGFR is repressed at the chromatin level during senescence (Narita et al. 2003) and this analysis showed to be potentially regulated by the 12 SA-miRNAs (Table 4.2). The ability of SA-miRNAs to further repress these signals provides a cell entering senescence another regulatory mechanism by which to ensure their silencing.

The multiple pathway alterations discussed suggest that these SA-miRNAs are potentially regulating many of the necessary steps required to create a fully senescent cell, from changes in the cellular cytoskeleton to alteration of multiple pathways regulating cell cycle and proliferation signals. Senescence can be stimulated by more than one mechanism however, including induction by telomere attrition (replicative senescence), oncogenes, drugs and cellular stress. It remains unclear whether the same pathway alterations and miRNAs are involved in each of the different stimuli or whether each stimulus takes a different route to the same endpoint of a senescent cell, as depicted in Figure 4.4.

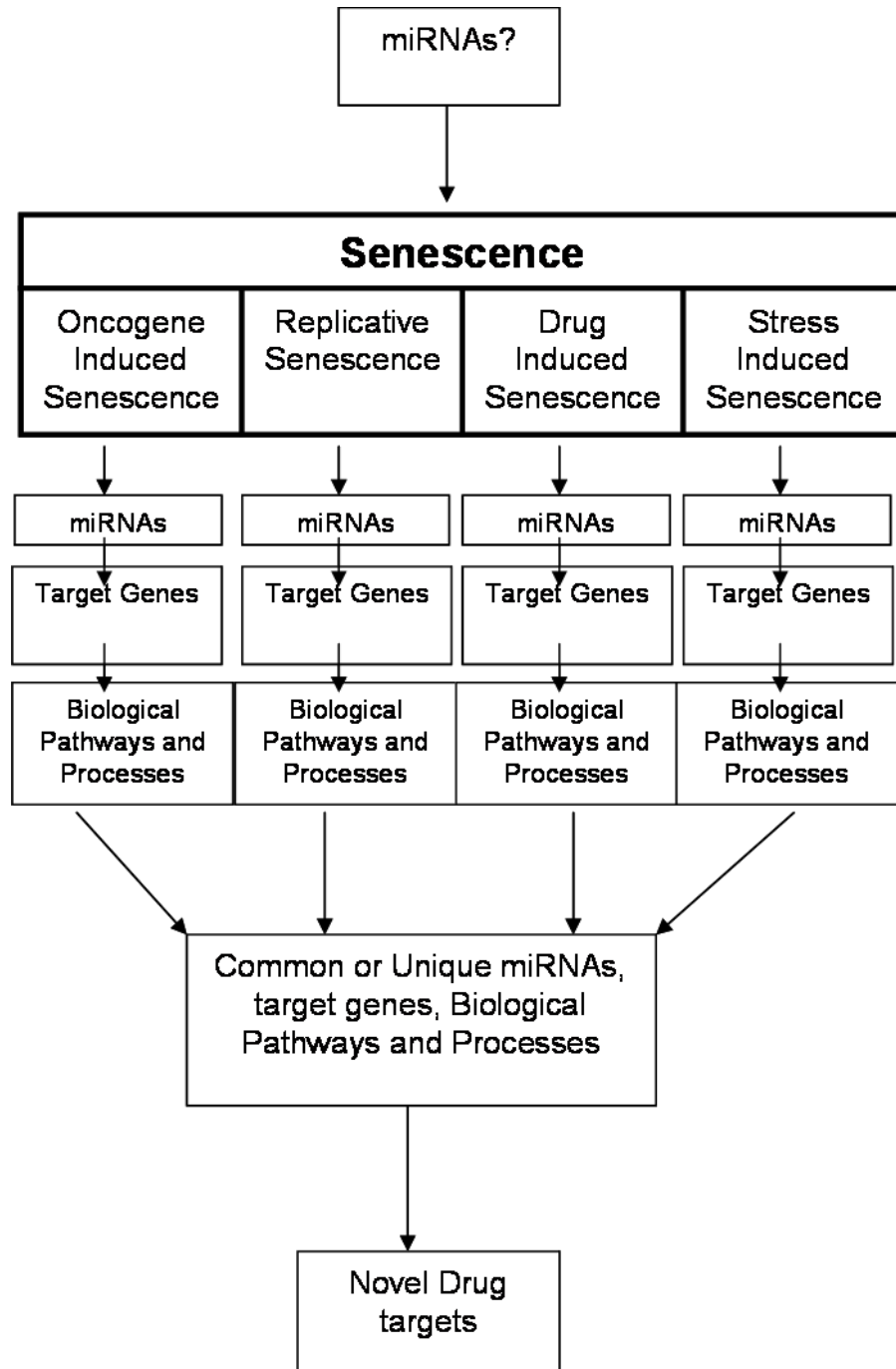


Figure 4.4 — Potential mechanisms of miRNA regulation in Senescence and their potential. A small subset of miRNAs, such as the 12 SA-miRNAs that we have identified, may be acting as master regulators of the senescent phenotype. However it is also possible that individual types of senescence induction may require different miRNAs to create the same cellular changes due to the different stimuli and therefore signaling pathways involved. Overlaps in the biological pathways or miRNAs could therefore be utilised to discover novel drug targets for senescence induction

4.2.2 Investigation of SA-miRNA regulation of different senescence stimuli

In order to investigate the potential of SA-miRNAs to regulate the different senescence stimuli previously published publicly available gene expression data was utilised. This allowed the exploration of the potential roles of miRNAs to regulate the differentially expressed gene lists from replicative senescence in hMSCs (Wagner et al. 2008), drug induced replicative senescence by a telomerase inhibitor (Damm et al. 2001), cellular stress by Ethanol or *tert*-butylhydroperoxide exposure (Pascal et al. 2005) and oncogene induced senescence by BRAF^{E600} (Kuilman et al. 2008).

Each of the datasets queried showed some potential to be regulated by the SA-miRNAs as shown in Table 4.3. Using the results of these 4 analyses, the potential of SA-miRNAs to regulate pathways with gene expression changes for each stimulus was further explored. The differences and similarities in SA-miRNAs and their targeted pathways between stimuli were also investigated.

4.2.2.1 Replicative senescence

By reanalysing the publicly available gene expression data from the study by Wagner and colleagues, it was possible to examine the pathways during replicative senescence that could be regulated by SA-miRNAs (Table 4.4a) (Wagner et al. 2008). Wagner et al measured gene expression changes at different population doublings of hMSCs from early passage into replicative senescence. Gene lists of 2 fold or more changes in expression between early and late passage hMSCs were constructed. Filtering of these lists to only those genes theoretically regulated by the SA-miRNAs led to the construction of 2 lists: 85 gene targets with increased expression and 49 gene targets with expression in late passage compared to early passage hMSCs. The pathways associated with each gene list were then individually explored using Metacore.

Looking initially at the pathways that have gene targets with increased expression in Table 4.4a, it was observed that 3 of the 5 maps on the list were

	Replicative senescence		Drug induced Replicative Senescence		Oncogene Induced Senescence	Stress induced senescence			
	UP 85 target genes	DOWN 49 target genes	UP 76 target genes	DOWN 49 target genes	7 target genes	EtOH UP 10 target genes	EtOH Down 6 target genes	tBHP Up 6 target genes	tBHP Down 6 target genes
SA-miRNA	miRNA	miRNA	miRNA	miRNA	miRNA	miRNA	miRNA	miRNA	miRNA
hsa-let-7f	✓	✓	✓	✓			✓		✓
hsa-mir-20a	✓	✓	✓	✓	✓		✓		✓
hsa-mir-217	✓	✓	✓	✓	✓		✓		✓
hsa-mir-29c	✓	✓	✓	✓	✓	✓		✓	
hsa-mir-34a	✓	✓	✓	✓			✓		✓
hsa-mir-34b	✓	✓	✓	✓	✓	✓	✓		✓
hsa-mir-34c	✓	✓	✓	✓	✓	✓	✓	✓	✓
hsa-mir-369-5P	✓	✓	✓	✓	✓	✓		✓	
hsa-mir-371	✓	✓	✓	✓	✓	✓		✓	
hsa-mir-372	✓	✓	✓	✓					
hsa-mir-373	✓	✓	✓	✓					
hsa-mir-499	✓	✓	✓	✓	✓	✓	✓	✓	✓

Table 4.3 - Regulation of gene expression signatures of different types of senescence induction.

Ticks represent the ability of that SA-miRNA to theoretically regulate one or more genes within the signature. All four senescence induction signatures are regulated by at least 5 SA-miRNAs. These differences in SA-miRNA regulation may represent the differing need for regulation of SA-miRNA target genes by different stimuli. The regulation of all of the senescent signatures studied by microRNAs hsa-mir-499 and hsa-mir-34c may demonstrate their potential as regulators of core senescence genes required by all senescence stimuli.

a

Replicative senescence						
85 Upregulated SA-miRNA gene targets				49 Downregulated SA-miRNA gene targets		
SA-miRNA	Pathway Maps	% Regulated by SA-miRNAs	p-value	Pathway Maps	% Regulated by SA-miRNAs	p-value
1	Apoptosis and survival p53-dependent	9% (2/29)	9.58E-03	Cell Cycle Role of APC in cell cycle regulation	22% (7/32)	5.15E-11
2	Cytoskeletal remodeling Keratin Filaments	6% (2/36)	1.45E-02	Cell Cycle Start of DNA replication in early S-Phase	19% (6/32)	3.79E-09
3	Immune Response IL1 signaling pathway	5% (2/37)	1.53E-02	dCTP/dUTP metabolism	8% (6/75)	7.37E-07
4	Apoptosis and survival FAS signaling cascades	5% (2/43)	2.04E-02	Cell Cycle Role of SCF complex in cell cycle regulation	14% (4/29)	6.82E-06
5	Apoptosis and survival TNFR1 signaling pathway	5% (2/43)	2.04E-02	Cell Cycle Sister chromatid cohesion	14% (3/22)	1.13E-04

b

Drug induced Replicative Senescence						
49 Upregulated SA-miRNA gene targets				76 Downregulated SA-miRNA gene targets		
SA-miRNA	Pathway Maps	% Regulated by SA-miRNAs	p-value	Pathway Maps	% Regulated by SA-miRNAs	p-value
1	Signal Transduction PTEN pathway	11% (5/46)	6.52E-07	Cell Cycle Role of APC in cell cycle regulation	16% (5/32)	1.26E-06
2	Development EGFR signaling via small GTPases	14% (4/28)	3.13E-06	Folic acid metabolism	9% (5/53)	1.63E-05
3	Signal Transduction Activin A signaling regulation	14% (4/28)	3.13E-06	DNA damage ATM/ATR regulation of G1/S checkpoint	13% (4/32)	3.98E-05
4	Transcription role of AP1 in regulation of cellular metabolism	10% (4/42)	1.65E-05	Cell Cycle ESR1 regulation of G1/S transition	12% (4/33)	4.51E-05
5	Development ERBB-family signaling	9% (4/43)	1.81E-05	Cell cycle chromosome condensation in prometaphase	14% (3/21)	2.68E-04

Table 4.4 -Top 5 biological pathway maps that contain SA-miRNA gene targets shown in order of p-value.

(A)Wagner et al microarray data was reanalysed and all genes with a 2 fold or more difference between early passage and late passage hMSCs were selected. These lists were then filtered selecting only gene targets of the 12 SA-miRNAs and biological pathways maps analysed using Metacore from Genego.

(B)Damm et al published differentially expressed gene signatures which were filtered selecting only gene targets of the 12 SA-miRNAs and biological pathways maps analysed using Metacore from Genego

involved with apoptosis and survival through the FAS and TNFR1 signaling pathways or in a p53 dependent manner. In all 3 maps the only molecules that the SA-miRNAs are regulating are BRE and c-FLIP. BRE is known to suppress the apoptotic pathways through binding and inhibition of the FAS receptor (Li et al. 2004) and the TNF-alpha receptor (Gu et al. 1998). C-FLIP is a potent inhibitor of apoptosis through its binding and resulting inhibition of the adaptor protein FADD (Irmeler et al. 1997). Although the SA-miRNAs are only regulating 2 molecules involved in the survival and apoptosis signaling pathways, regulation of the absolute levels of such signals may be one of the mechanisms by which the SA-miRNAs ensure the cells enter senescence rather than apoptosis.

The second most significant pathway with increases in gene expression during replicative senescence is cytoskeletal remodeling centering on the role of intermediary filaments. As discussed previously, changes in the cellular morphology of senescent cells would require significant changes to the cytoskeleton of the cell. Changes in expression of key genes regulating many of these processes would therefore be required. The SA-miRNAs provide one potential mechanism by which these changes could be regulated.

Changes to the immune response and the IL1 signaling pathway during replicative senescence are also potentially regulated by the SA-miRNAs. The concept of the involvement of IL1 and other pro-inflammatory networks in the induction of senescence is concurrent with the current findings (Hardy et al. 2005; Morandi et al. 2008; Sasaki et al. 2008). The regulation of these pro-inflammatory networks by miRNAs may provide a mechanism by which the secretory senescence pathway is regulated.

Table 4.4 also shows that all 12 SA-miRNAs can also target genes with expression 2 fold or more decreased during replicative senescence. Four out of the 5 pathways that contain SA-miRNA gene targets with decreases in expression are involved in various aspects of cell cycle regulation (Table 4.4a). These include DNA replication in early S-phase and the roles of APC, the SCF complex and ESR1. Regulation of key molecules in the multiple processes governing the cell cycle during senescence induction is critical. The SA-miRNAs regulate a subset of molecules (CDK2, EMI1, Cyclin B, SKP2, and CDC18L) that are involved in regulation of these multiple cell cycle pathways. This allows the SA-miRNAs to affect the cell cycle regulatory process as whole rather than at just one

checkpoint or stage. These 12 SA-miRNAs that therefore exemplify the potential of miRNAs to play a regulatory role in this aspect of replicative senescence.

The remaining pathway containing gene targets down-regulated during replicative senescence is involved in dCTP/dUTP metabolism. Since senescent cells are no longer cycling, changes in metabolism will logically follow. SA-miRNAs may only be regulating a small part of cellular metabolism, the metabolism of 2 nucleotide units, however these metabolic changes may have far reaching effects. Furthermore, changes in dATP, ATP and TTP metabolism are seen further down in the list of pathways, 6, 7 and 9 respectively, which are not discussed here. It may therefore be the case that the SA-miRNAs are able to regulate the changes in metabolism required to establish senescence or that only changes to a few molecules or processes are required.

The regulation of cellular survival, pro-inflammatory and cytoskeletal remodeling cellular processes would all logically be required to create the senescent cell phenotype. This analysis shows that these processes can theoretically be regulated by the SA-miRNAs, during replicative senescence, highlighting their potential to regulate the absolute levels and timings of these complex signaling cascades to create a senescent cell.

4.2.2.2 Drug induced replicative senescence

Replicative senescence results from the shortening of telomeres during each round of the cell cycle (Harley et al. 1990). Many cancer cells reactivate the enzyme telomerase, which has the ability to maintain telomeres and therefore overcome this barrier to tumorigenesis (Deng et al. 2008). Application of a drug that inhibits telomerase would, in theory, activate such cells' natural senescence pathways, potentially including the actions of the SA-miRNAs. To explore this hypothesis the differentially expressed genes published by Damm and colleagues were interrogated for potential SA-miRNA regulation (Damm et al. 2001).

Damm and coworkers investigated senescence resulting from treatment of lung carcinoma cells with the telomerase inhibitor BIBR1532. The published genes lists were filtered to include only those genes regulated by the 12 SA-miRNAs. This resulted in a list of 76 down-regulated SA-miRNA gene targets and 49 up-regulated gene targets (Table 4.4b). Pathway analysis was then performed to

investigate the potential effects of SA-miRNA regulation in drug induced replicative senescence.

As seen previously during the analysis of replicative senescence, the pathways associated with gene targets showing increased expression involve a variety of different cellular mechanisms. Two of these pathways are involved in the regulation of cellular signaling by the molecules PTEN and Activin A. The dual specificity phosphatase PTEN is a tumour suppressor gene and regulates cellular proliferation and survival through its ability to bind p53 in the nucleus (Chang et al. 2008). Activin A is a member of the TGF β superfamily and is involved in the regulation of cell growth and apoptosis (Takabe et al. 1999). Both molecules are commonly deregulated in cancers (Jeruss et al. 2003; Jiao et al. 2007) reflecting their importance in regulation of cell proliferation processes. Alterations in these signaling pathways could therefore be beneficial to the establishment of a senescent cell phenotype. The theoretical regulation of these processes by the SA-miRNAs demonstrates further mechanisms by which SA-miRNAs can cause the complex signaling pathway changes required to induce senescence.

Two further pathways associated with gene expression increases in this dataset that show potential regulation by the SA-miRNAs involve EGFR and the ERBB family. As previously discussed, regulating signaling from the ERBB family of tyrosine kinases is an important step in senescence induction due to their role in the regulation of cellular proliferation. The presence of this map demonstrates that SA-miRNAs are a potential regulatory mechanism of these pathways during drug induced replicative senescence as well as natural replicative senescence.

The remaining pathway associated with increased gene target expression is involved with changes in metabolism regulated by the transcription factor AP-1. Closer inspection of the SA-miRNA targets on this map (Figure 4.5) highlights the role of AP-1 in regulation of p21 and the apoptosis molecules *c-fos* and FASR. The involvement of *c-fos* and FASR in pathways regulated by the SA-miRNAs has been highlighted earlier in this study. This demonstrates that regulation of the diverse cellular proliferation and apoptosis signaling pathways affected by these molecules is an important step in senescence establishment, under both natural replicative senescence and when artificially drug induced. SA-miRNA regulation could therefore provide a mechanism by which the absolute levels and timings of these signals can be controlled.

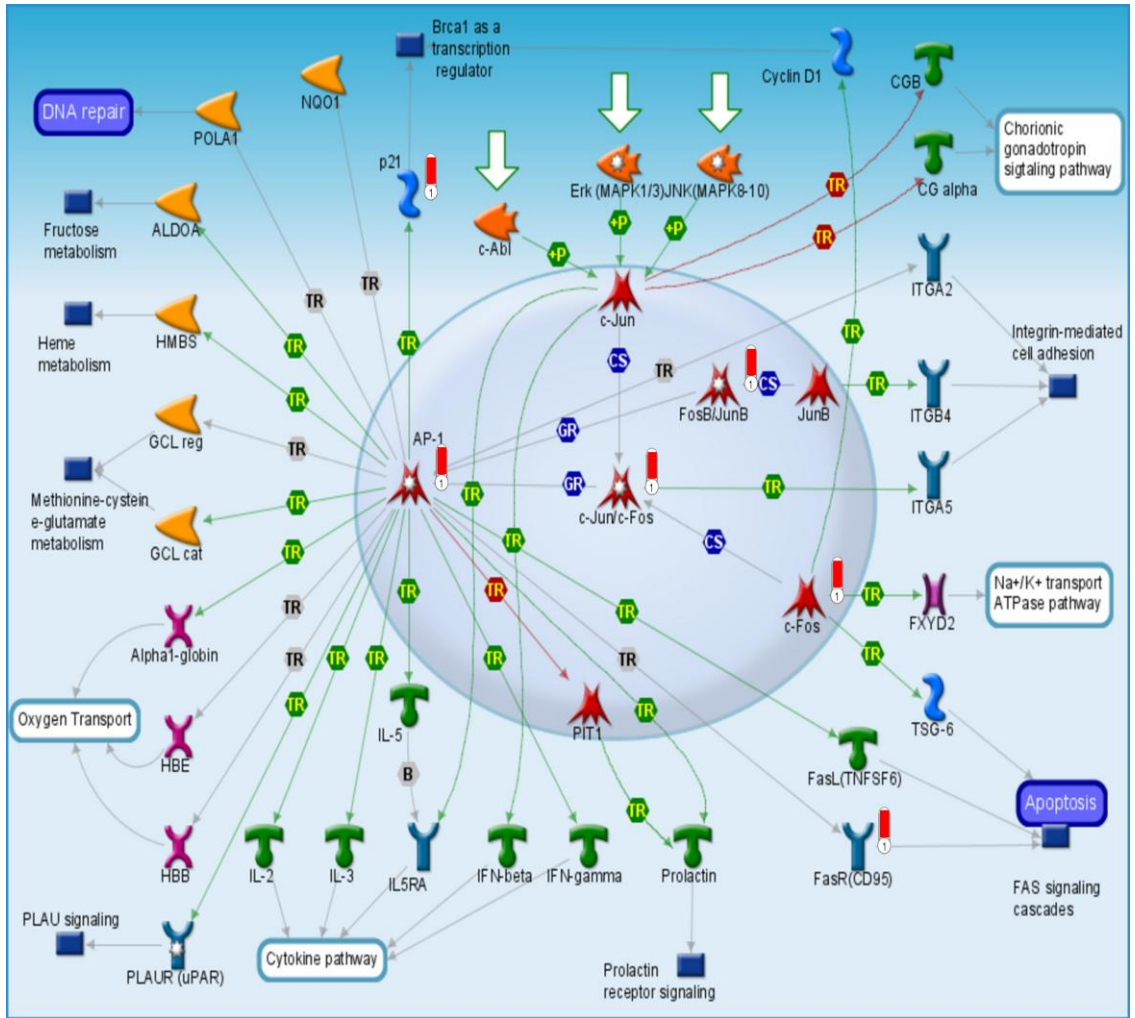


Figure 4.5 - SA-miRNA regulation of transcription and the role of AP1 in regulation of cellular metabolism pathway biological map during drug induced senescence. Red thermometers show an object that can be regulated by a SA-miRNA with thermometer numbering corresponding to that seen in Table 2.1. Multiple thermometers denote that the object is a target of multiple SA-miRNAs. Green arrows represent positive, red negative and grey unspecified interactions. Boxes on lines denote the type of regulation where P = phosphorylation; B = binding; Tr = transcriptional regulation, Cm = covalent modification, T = transformation and Z = catalysis.

The biological pathway map analysis of the decreases in gene expression for telomerase inhibited cells returned results very similar to that of the down-regulated genes in natural replicative senescence. Four of the 5 maps are involved with the regulation of various aspects of the cell cycle including the role of APC, the DNA damage response checkpoint, regulation of ESR1 and chromosome condensation in prometaphase (Table 4.4b). As with the cell cycle pathways seen in replicative senescence, the regulation of cell cycle following telomerase inhibition would be a critical step in senescence induction. Targeting these multiple pathways to cell cycle control gives SA-miRNAs comprehensive regulation of the process.

The remaining map is involved with metabolism of folic acid. As previously discussed, changes in metabolism will be required in cells undergoing senescence. However, this may also reflect metabolic changes involved in the metabolism of BIBR1532, independent of senescence, that the SA-miRNAs are also able to regulate. The ability of SA-miRNAs to target not just the down-regulation cell cycle aspects of senescence but also the metabolic changes demonstrates the flexibility and complexity of their action.

Looking at the pathway analysis of both replicative and drug induced senescence shown in Table 4.4, highlights the fact that the down-regulated pathways in both cases are cell cycle and metabolism related whilst the up-regulated pathways differ between the two stimuli. However, looking at the functions of the up-regulated pathways in both cases reveals a common apoptosis regulatory signal. Cells in replicative senescence appear to be signaling apoptosis survival through FAS and TNFR1 pathways or in a p53 dependant manner whereas the telomerase inhibited cells are using the actions of Activin A and PTEN for this purpose. Thus the SA-miRNAs are potentially using different cellular mechanisms by which to achieve the same goal. The SA-miRNA regulation of the cellular signals behind drug induced and natural replicative senescence are therefore stimuli specific whilst remaining focused towards the common outcome of creating the complex senescent cell phenotype.

4.2.2.3 Oncogene induced senescence (OIS)

Telomere erosion leading to the activation of DNA damage signaling cascades is not the only method of senescence induction. Oncogene induced senescence (OIS) can be caused upon either the loss of tumour suppressor genes like PTEN (Chen et al. 2005) or activation of oncogenes such as MEK, RAS and BRAF^{E600} (Lin et al. 1998; Michaloglou et al. 2005; Courtois-Cox et al. 2006). Recent evidence suggests that senescence induction by these stimuli is dependent upon IL-6 mediated inflammatory responses without which the cells bypass senescence and continue proliferating (Kuilman et al. 2008). The same study also used gene expression microarrays to examine differentially expressed genes between cells that bypass and cells that undergo OIS, revealing a signature of 20 genes shown in Table 4.5. Seven of these genes, including IL-6, can theoretically be regulated by SA-miRNAs.

Due to the small size of the initial signature, and hence the small number of target genes, analysis of the biological pathways underlying the SA-miRNA regulation was not statistically feasible. However, the SA-miRNAs regulate nearly 30% of the OIS signature revealed by Kuilman *et al*, including the key molecule IL-6 (Table 4.5). This may demonstrate the principle that large numbers of gene alterations are not always required for senescence induction, just well targeted ones. The multiple regulation of 3 of the genes in particular (C20orf26, CD55 and IL6) by the SA-miRNAs may show that within this signature these genes require the strictest regulation to ensure the successful induction of senescence, although further validation is required to test this theory.

The analysis of differentially expressed genes during oncogene induced senescence, although limited by the size of gene list, still highlights the potential of SA-miRNAs to regulate key molecules required for this form of senescence induction. Furthermore, the regulation of inflammatory networks shown in this study to be key to senescence induction was also highlighted during the analysis of replicative senescence. This common regulation of pro-inflammatory secretory senescence genes in response to 2 different senescence stimuli by SA-miRNAs is suggestive of its importance in senescence as a whole.

Gene name	Regulating SA-miRNAs
C20ORF26	hsa-mir-369-5P (2), hsa-mir-29c (1), hsa-mir-499 (3), hsa-mir-34b (1), hsa-mir-34c (2)
CD55	hsa-mir-29c (1), hsa-mir-34b (2), hsa-mir-34c (3)
CD9	
CPE	
FAM131A	
FAM43A	hsa-mir-371 (1)
GABRA2	
GEM	
GMFG	hsa-mir-369-5P (1)
IL6	hsa-mir-499 (1), hsa-mir-216 (1), hsa-mir-371 (1)
IQGAP2	
ITGA2	
ITPKA	
NR4A2	
PCNX	
PECAM1	
PTGES	hsa-mir-371 (1)
RPS6KA5	
TESC	hsa-mir-20a (1)
VEGF	

Table 4.5 - 20 Differentially expressed genes upon induction of oncogene induced senescence highlighted by Kuilman *et al.* Also shown are the SA-miRNAs that can theoretically regulate 7 of these genes, brackets show the number of theoretical 3'UTR binding sites that each SA-miRNA has for that gene.

4.2.2.4 Cellular stress induced senescence

Senescence can also be induced by many different types of cellular stress such as UV-B (Debacq-Chainiaux et al. 2005), hydrogen peroxide (Frippiat et al. 2001), *tert*-butylhydroperoxide (*t*-BHP) or ethanol exposure (Dumont et al. 2002). Pascal and colleagues used a combination of differential display RT-PCR and low density DNA arrays to investigate genes involved in senescence induction by ethanol or *t*-BHP (Pascal et al. 2005). They revealed signatures of genes increasing and decreasing in expression for both ethanol and *t*-BHP, many of which overlapped. Table 4.6 highlights the potential of the SA-miRNAs as regulators of stress induced senescence by both treatments. 75% of the genes theoretically regulated by SA-miRNAs overlap between the two treatment types. This may suggest that these target genes are those that are core to senescence induction by SA-miRNA regulation.

Of all the overlapping genes shown in Table 4.6 four have roles in regulation of the actin cytoskeleton, namely ARHGAP24, ARPC2, MACF1 and S100A4 (Belot et al. 2002; Katoh et al. 2004; Daugherty et al. 2008). In the previous analysis of this chapter, cytoskeletal remodelling has always been associated with genes showing increased expression levels. Here however, two of the molecules, ARHGAP24 and ARPC2 show decreased expression. This may therefore represent specific molecules that require negative regulation in the context of stress induced senescence. Alternatively this may represent down-regulation of genes required to create the necessary senescence-associated cytoskeletal alterations. This demonstrates the potential of SA-miRNAs to regulate similar processes through different mechanisms dependant on stimuli.

Cell cycle regulation has in both replicative and drug induced senescence been strongly negatively regulated. Two of the overlapping down-regulated genes, RAD17 and CDC37L1 (Table 4.6), common to both ethanol and *t*-BHP treatments have roles in the cell cycle. RAD17 specifically is involved in cell cycle arrest caused by DNA damage signaling (Dahm et al. 2002). The DNA damage caused by reactive oxygen species in cellular senescence may therefore be activating similar mechanisms of senescence induction as that seen in replicative senescence. These gene targets highlight the fact that the SA-miRNAs are able

Gene	Effect of t-BHP treatment	Effect of ETOH treatment	Regulating SA-miRNAs
ARHGAP24	DOWN	DOWN	hsa-miR-499 (2)
ARPC2	DOWN	DOWN	hsa-miR-217 (2)
RAD17	DOWN	DOWN	hsa-let-7f (3)
CDC37L1	DOWN	DOWN	hsa-miR-20a (2), hsa-miR-34b (1), hsa-miR-499 (2), hsa-miR-34c (1)
EWSR1	DOWN	DOWN	hsa-miR-20a (1)
PHGDH	DOWN	DOWN	hsa-miR-34a (2), hsa-miR-34c (2)
MACF1	UP	UP	hsa-miR-369-5p (2)
RPS12	UP	UP	hsa-miR-369-5p (2)
LOXL2	UP	UP	hsa-miR-29c (1)
S100A4	UP	UP	hsa-miR-499 (2)
SLC35A5	UP	UP	hsa-miR-371 (1)
EEF1A1	UP	UP	hsa-miR-34c (1)
TBRG4	UP		hsa-miR-34c (1)
KPNB1	UP		hsa-miR-29c (1)
TMSB10	UP		hsa-miR-499 (1)
C21orf34	UP		hsa-miR-34b (2), hsa-miR-34c (1)

Table 4.6 - SA-miRNA targets showing alterations in gene expression after stress induced senescence by either *tert*-butylhydroperoxide (t-BHP) or Ethanol (EtOH) and the direction of their alteration, blank cells infer no effect. Also shown is the SA-miRNAs that can theoretically regulate these genes, brackets show the number of theoretical 3'UTR binding sites that each SA-miRNA has for that gene

to induce similar mechanisms Using stimuli specific target genes. The flexibility of the SA-miRNA mechanism of action allows them to remain specific enough for a cell to respond to a particular stimuli whilst general enough to focus pathway changes in those cells to create the senescent cell phenotype.

Two of the overlapping genes, EWSR1 and LOXL2, have previous evidence of senescence association. The EWS fusion protein has recently been reported as a repressor of senescence (Hu et al. 2008) and therefore its down-regulation by SA-miRNAs would provide a mechanism by which to prevent it inhibiting senescence induction. LOXL2 however has been used as a marker of senescent cells due to its increased expression during senescence (Muller et al. 2006). These senescent associated genes can theoretically be regulated by SA-miRNAs and this may therefore present a mechanism by which their roles in senescence induction are controlled.

The remaining overlapping genes may still have roles in senescence. These genes may be involved in senescence induction through previously identified or potentially novel unidentified pathways, which analysis of the individual gene function does not elucidate. Their inclusion into larger data sets of potential senescence associated genes for systems biology analysis may help to elucidate their role.

MiRNA regulation of stress induced senescence can therefore be seen to potentially transcend treatment type and incur changes in core senescence genes. Furthermore, regulation of additional treatment specific genes gives SA-miRNAs the potential to alter diverse cellular pathways required to respond to different stimuli.

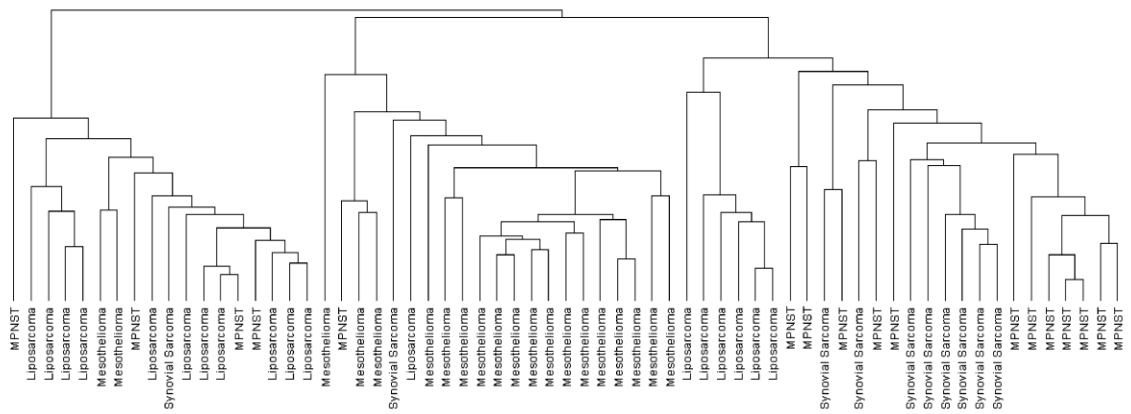
Given the combined evidence of the potential of miRNAs to regulate the induction of senescence presented here; it is possible to hypothesise that perturbation of miRNA expression may play a role in tumorigenesis, senescence bypass mechanisms such as telomere maintenance and hence impact patient survival. To investigate this hypothesis miRNA expression patterns in human mesenchymal tumour biopsies was examined using miRNA microarrays.

4.2.3 Unsupervised hierarchical clustering of miRNA expression profiles shows improved separation of mesenchymal tumours over gene expression microarray profiles

Before examination of the relationships of individual miRNAs with clinical factors, the ability of miRNAs to distinguish between tumour types was compared to that of gene expression data from the previous chapter. After quality control filtering of data from miRNA expression microarrays for 20 peritoneal mesotheliomas, 18 liposarcomas, 17 MPNST and 10 synovial sarcomas, as described in Chapter 2, 325 miRNAs were used for unsupervised hierarchical clustering (Figure 4.6A). Although the majority of peritoneal mesotheliomas clustered together the other tumour types were poorly separated. Comparison of unsupervised hierarchical clustering of gene expression data for peritoneal mesotheliomas, MPNST and liposarcomas from the previous chapter (Figure 4.6B) showed a similar distinct clustering of peritoneal mesotheliomas. The clustering pattern of the miRNA expression profiles highlighted known histological similarities, for example the observation that the MPNST and synovial sarcomas were clustered on the same branch. The spread of the liposarcomas throughout the dendrogram was also consistent with the known heterogeneity of this tumour type. This data suggested that miRNA expression patterns were not only of use for examining the different underlying routes to tumourigenesis between tumour types but were potentially more discriminatory than mRNA profiling.

As unsupervised hierarchical clustering of miRNA expression profiles of the tumour types was suggestive of different miRNA expression profiles for each tumour type but insufficient for complete separation; binary tree prediction analysis was used to investigate whether subgroups of miRNAs were able to improve the separation of these mesenchymal tumour types. These subgroups may be reflective of these individual tumour types route to tumourigenesis and therefore could be utilised to further explore the role of miRNAs in senescence bypass in each tumour type.

A



B

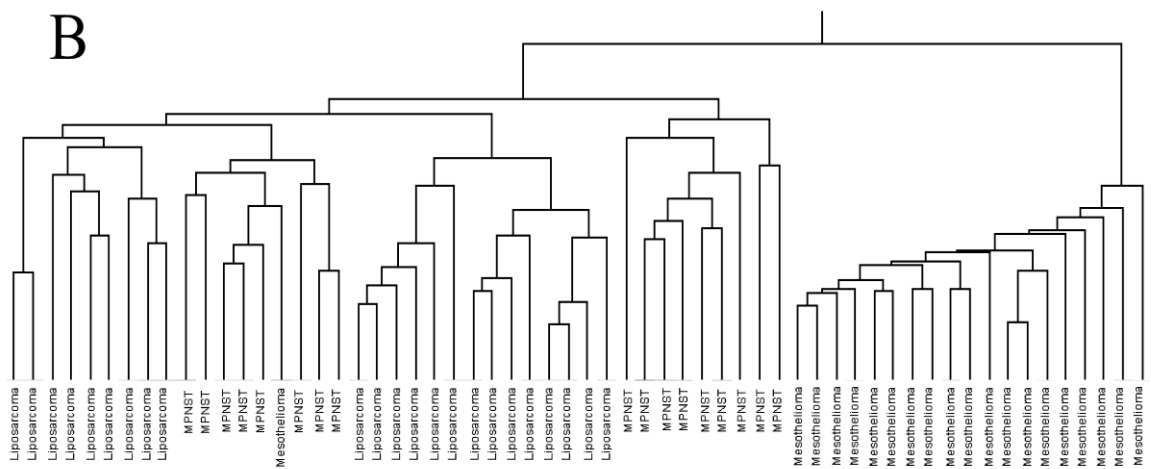


Figure 4.6 - Unsupervised hierarchical clustering of mRNA and miRNA highlights similar tumour biology but is unable to completely distinguish between tumour types. Unsupervised hierarchical clustering of miRNA (A) and gene expression (B) microarray data. Raw data was imported into BRB arraytools normalised and quality control filtered. Clustering was performed using a centred Pearson correlation algorithm and average linkage

4.2.4 Binary Tree prediction analysis highlights 87 miRNAs that improve separation of mesenchymal tumours in hierarchical clustering

To investigate miRNA subgroups whose expression patterns were able to distinguish between tumour types the binary tree prediction method (using the compound covariate predictor algorithm) within BRB array tools was utilised. Through a multi-step process this method builds a hierarchical tree which divides the tumour types by groups of differentially expressed miRNAs. Each node of the tree provides a list of miRNAs whose expression patterns could therefore be used to distinguish between tumour types. This analysis highlighted 3 lists of miRNAs with the ability to distinguish between tumour types (Figure 4.7A) with an average misclassification rate, by “leave-one-out cross-validation” technique, of 14.7%. The resulting binary tree consisted of 3 nodes with the first node being 72 miRNAs able to distinguish between mesotheliomas and the 3 other tumour types. This large number of miRNAs with differential expression patterns in this tumour type was consistent with the high degree of separation observed between mesotheliomas and other tumour types in the hierarchical clustering. Furthermore, 37 miRNAs able to distinguish between liposarcomas and the remaining two tumour types (MPNST and synovial sarcomas) and a further 12 miRNAs able to distinguish between MPNSTs and synovial sarcomas were identified. Closer examination of these lists revealed a number of overlapping miRNAs between nodes. By taking only those miRNAs unique to an individual node the list was reduced to a core set of 87 miRNAs with the ability to distinguish between tumour types (Appendix I). Hierarchical clustering using this 87 miRNA signature showed improved separation of the three tumour types (Figure 4.7B). Synovial sarcomas and MPNSTs showed a similar clustering pattern to that seen in unsupervised clustering (Figure 4.6A), further emphasising the degree of similarity of these tumour types. With the exception of one sample, the previously diverse liposarcomas were now contained within one major cluster suggesting that the miRNAs within the signature may have some biological significance for this tumour type. Furthermore, examination of the liposarcomas by histological subtypes highlighted a branch of 9 myxoid and myxoid-round cell tumour samples (Figure 4.7B*). This 87 miRNA signature was

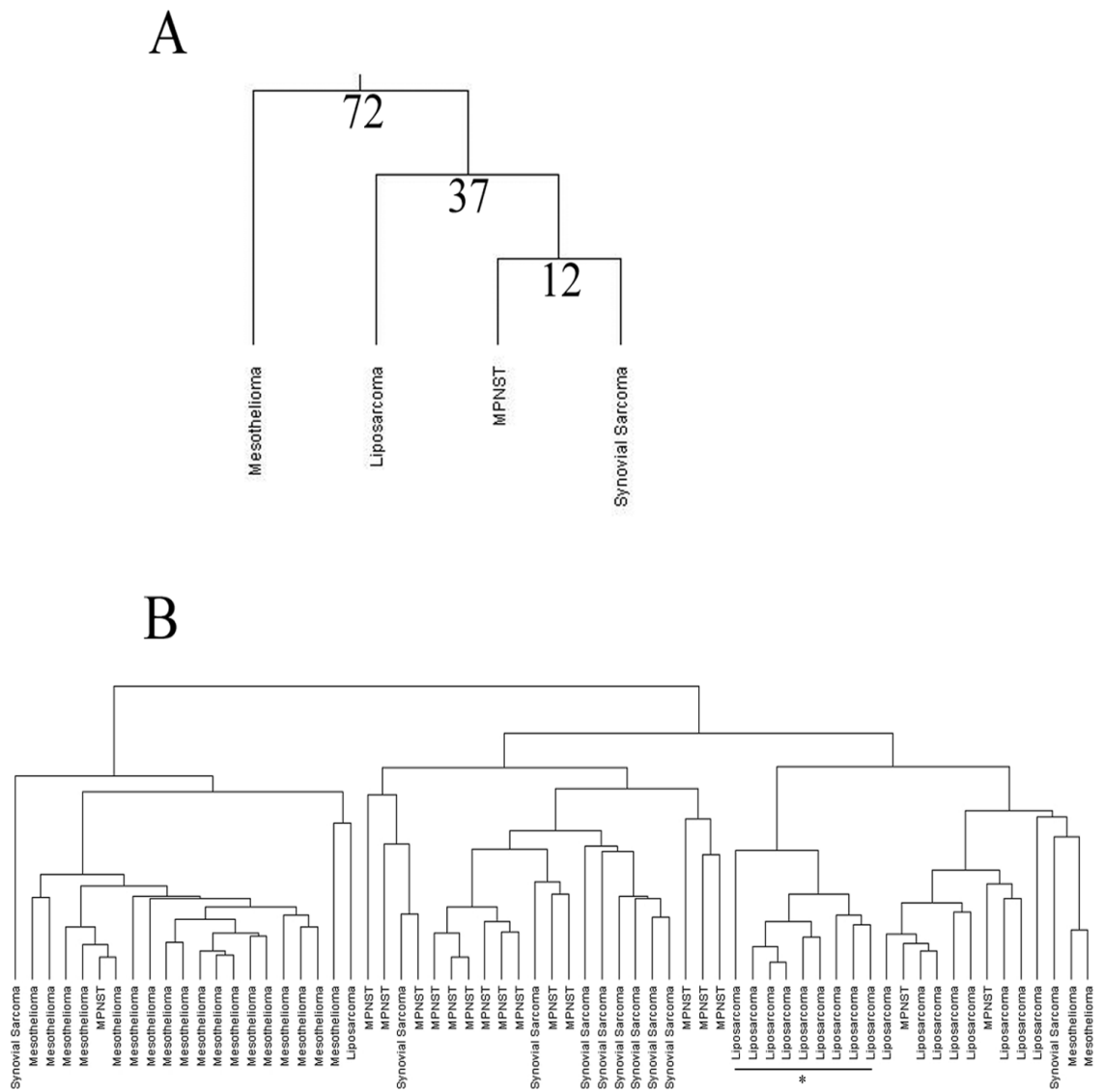


Figure 4.7 – Binary Tree prediction analysis highlights an 87 miRNA signature able to distinguish tumour types. Compound covariate prediction analysis with leave-one-out cross-validation was performed using BRB-Array tools. The resulting three nodes of miRNAs (A) were then examined for overlaps leading to a list of 87 unique miRNAs present at only one node. (B) Supervised hierarchical clustering using the 87 miRNA signature shows improved clustering of tumour groups. * indicates a cluster of myxoid and myxoid round-cell liposarcomas.

therefore not only able to group a previously diverse tumour type but further split that tumour type into histological subtypes.

4.2.5 Tumour type specific miRNAs show prognostic significance and correlation with telomere maintenance mechanism

Given the potential biological significance of these miRNAs the next step of the analysis was to explore whether miRNAs of prognostic significance existed within the 87 miRNA signature. Hazard ratios were calculated for each miRNA using BRB array tools, as detailed in Chapter 2. MiRNAs with a significant hazard ratio ($p \leq 0.05$) were then adjusted for age, sex and grade using Mantel Cox regression in SPSS. The number of miRNAs for each tumour type with a significant hazard ratio varied from 14 in liposarcomas to 5 in synovial sarcomas (Table 4.7) a number of these showed independent prognostic significance when adjusted for grade, age and sex (Table 4.7 & Figure 4.8). Comparison of these prognostic miRNAs and the 87 miRNAs able to distinguish between tumour types showed that 13 of the prognostic miRNAs were also found in the 87 miRNA signature. This data therefore suggested that miRNAs have implications in overall tumour biology as well as prognostic implications in individual tumour types. Furthermore, examination of the lists of prognostic miRNAs showed miR-let7g was prognostic in both MPNST and synovial sarcomas. This commonly prognostic miRNA further highlighted the similarity between these two tumour types previously suggested by the hierarchical clustering (Figure 4.6 and Figure 4.7) potentially extends to miRNA regulatory mechanisms. Additionally, to directly investigate the potential impact of the 12 SA-miRNAs upon survival the list of significant miRNAs for prognosis was examined. 3 of the SA-miRNAs were found to also have prognostic significance in the mesenchymal dataset. miR-20a, 34a and 29c miRNAs in liposarcomas, mesotheliomas and MPNST respectively showed prognostic significance indicating that the regulation of senescence signaling by through SA-miRNAs may be an important factor in patient outcome in these tumour types.

In the previous chapter, complex layers of transcriptional and kinase regulation of the decision between different TMMs (see chapter 3) were highlighted. In addition to this the prognostic implications of TMMs in liposarcomas and peritoneal mesotheliomas have been documented

	Unique id	Hazard ratio p-value	Hazard Ratio	P-value (grade, sex & age adjusted)
Liposarcoma	hsa-miR-212	0.013	13.034	0.085
	hsa-miR-222	0.021	1.674	0.765
	hsa-miR-324-5p	0.026	0.252	0.66
	hsa-miR-494	0.03	1.596	0.023
	hsa-miR-106b	0.031	0.625	0.542
	hsa-miR-92a	0.034	0.484	0.949
	hsa-miR-296-5p	0.036	2.236	0.262
	hsa-miR-21*	0.039	1.569	0.796
	hsa-miR-193a-5p	0.044	0.466	0.531
	hsa-miR-196b	0.045	0.626	0.214
	hsa-miR-20a	0.046	0.677	0.979
	hsa-miR-22	0.047	1.375	0.04
	hsa-miR-125a-3p	0.047	1.708	0.257
	hsa-miR-197	0.048	0.214	0.028
Mesothelioma	hsa-miR-186	0.001	0.049	0.07 *
	hsa-miR-96	0.003	1.971	0.034 *
	hsa-miR-193b	0.005	28.012	0.948 *
	hsa-miR-151-3p	0.015	0.125	0.1 *
	hsa-miR-497	0.016	0.408	0.084 *
	hsa-miR-34a	0.024	0.295	0.928 *
	hsa-miR-30a*	0.026	2.929	0.839 *
hsa-miR-149	0.049	2.233	0.628 *	
MPNST	hsa-miR-142-3p	0.002	0.409	0.007
	hsa-miR-361-3p	0.003	0.152	0.01
	hsa-miR-15a	0.004	0.512	0.002
	hsa-miR-16	0.006	0.554	0.002
	hsa-29b	0.008	0.468	0.182
	hsa-let-7g	0.008	0.575	0.128
	hsa-miR-342-3p	0.008	0.376	0.005
	hsa-miR-29c	0.008	0.433	0.056
hsa-miR-877	0.01	2.245	0.003	
Synovial Sarcoma	hsa-let-7g	0.041	0.125	0.919*
	hsa-let-7d	0.041	0.072	0.997
	hsa-miR-30b	0.046	0.146	0.919*
	hsa-miR-181a2*	0.047	0.090	0.389
	hsa-let-7e	0.05	0.267	0.997

Table 4.7 - miRNAs with significant associations with outcome in mesenchymal tumours. MicroRNAs with significant hazard ratios for liposarcomas, mesotheliomas, MPNST and synovial sarcomas were identified using BRB array tools. Mantel Cox regression was used to adjust for age, sex and grade. * indicates comparisons that could not be adjusted for grade due to missing information.

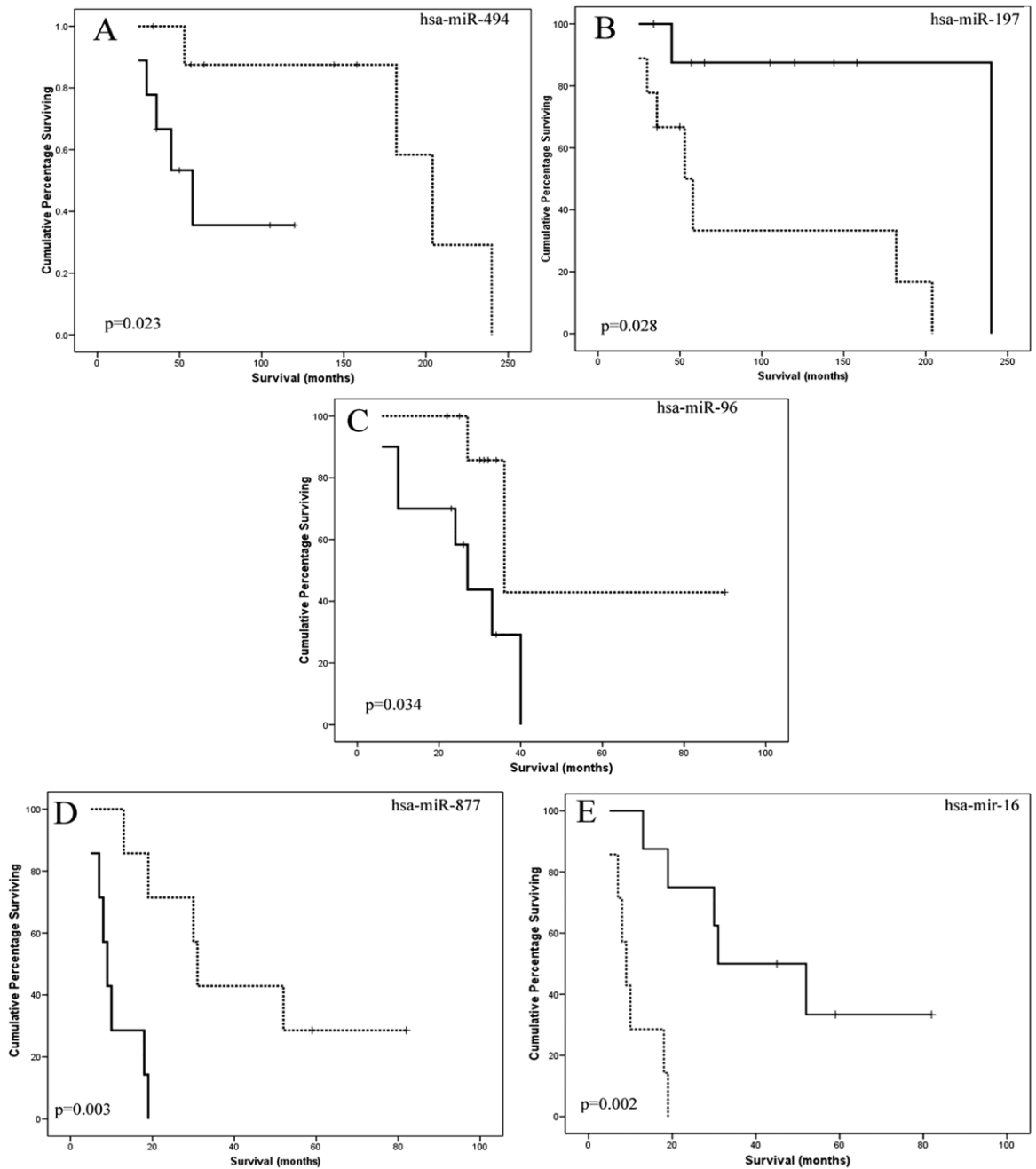


Figure 4.8 - Survival analysis of miRNA expression patterns highlights tumour specific prognostic miRNAs. Kaplan-Meier plots of miRNAs with a significant hazard ratio after adjustment for grade, age and sex from Table 4.7, plotted using SPSS (v.15) (A) and (B) show prognostic miRNAs, in liposarcomas. (C) shows the independent prognostic miRNA in peritoneal mesothelioma. (D) and (E) shows prognostic miRNAsi. Solid lines show high expression whereas dotted lines indicate low expression of respective miRNAs. P values are the result of Mantel-Cox survival analysis after adjusting for grade, age and sex. Mesotheliomas were not adjusted for grade due to missing information.

(Ulaner et al. 2003; Costa et al. 2006; Cairney et al. 2008; Villa et al. 2008). The investigation into the role of miRNAs in the regulation of telomere maintenance in these tumour types may provide a biological explanation for differences in prognosis. Table 4.8 shows 48 miRNAs with significant differences in expression between tumours using either ALT or telomerase as a TMM. Examination of these miRNAs and those that are prognostic for each tumour type revealed overlaps in both liposarcomas and peritoneal mesotheliomas. Furthermore, differential expression of the two arms of miR-193a hairpin (-5p and -3p) that are prognostic or differentially expressed by telomere maintenance groups suggested that both aspects of the miR-193 precursor may be being processed and acting synergistically upon different aspects of cellular signaling to incur the same prognostic endpoint. Common regulation of telomere maintenance mechanisms between tumour types was also suggested by the common differential of expression of 3 miRNAs in these tumours. MicroRNAs miR-181b and miR-39a* were differentially expressed in liposarcomas and MPNSTs and miR-338-3p in liposarcomas and mesotheliomas suggesting that these miRNAs may have key roles in telomere maintenance transcending tumour type.

Further value in some miRNAs that were not found to be independent of age, sex and grade was observed when overlaps between prognostic and TMM associated miRNAs were examined. miR-21* and miR-324-5p show significant hazard ratios but were not independently prognostic. However these miRNAs were also differentially expressed between TMM in liposarcomas (Table 4.7 & 4.8). TMM has previously been associated with poor outcome in liposarcomas (Costa et al. 2006; Cairney et al. 2008) and the expression patterns of these two miRNAs supported their role in both processes. miR-21* had a high hazard ratio, implying that expression of the miRNA was associated with poor outcome and this miRNA was expressed 4 fold higher in ALT liposarcomas. miR-324-5p had a low hazard ratio and ALT liposarcomas had a 4 fold lower expression of this miRNA. These results suggested that the prognostic implications of these miRNAs in liposarcomas could be due to their potential role in the regulation of TMM.

In peritoneal mesothelioma only miR-96 overlapped between the prognostic and TMM miRNAs (Table 4.7 & 4.8). The expression pattern of miR-96, having a high hazard ratio and 5 fold lower expression in ALT tumours, was consistent with the known poorer prognosis of mesotheliomas with higher telomerase activity

	miRNA	p-value	Fold Change in ALT
Liposarcoma	hsa-miR-335	0.004883	-23.199898
	hsa-miR-30c-1*	0.007138	3.7390072
	hsa-miR-30a*	0.009898	-5.8242693
	hsa-miR-486-5p	0.010543	2.8304398
	hsa-miR-193a-3p	0.010899	-12.876934
	hsa-miR-28-3p	0.015438	4.897009
	hsa-miR-21*	0.016361	4.9941235
	hsa-miR-574-5p	0.019532	2.4917157
	hsa-miR-500*	0.025887	3.0363123
	hsa-miR-301a	0.026489	-7.288234
	hsa-miR-484	0.026583	-2.0185635
	hsa-miR-324-5p	0.02697	-4.317892
	hsa-miR-130a	0.03137	-4.395339
	hsa-miR-196a	0.033384	-13.045914
	hsa-miR-30e*	0.03435	-7.026719
	hsa-miR-423-5p	0.035994	2.8050187
	hsa-miR-148b	0.036242	-4.015978
	hsa-miR-30c	0.036682	-6.06015
	hsa-miR-210	0.040692	6.074371
	hsa-miR-224	0.041587	-4.2817516
	hsa-miR-181a	0.042992	-6.0834427
hsa-miR-195*	0.045619	1.9967524	
hsa-miR-338-3p	0.045907	-4.7657657	
hsa-miR-542-3p	0.048172	-3.527204	
hsa-miR-181b	0.048268	-4.576316	
Mesotheliomas	hsa-miR-127-3p	0.016645	3.7975771
	hsa-miR-136	0.001621	4.359817
	hsa-miR-155	0.018422	-3.2325037
	hsa-miR-15b	0.026943	-2.965124
	hsa-miR-194	0.046797	-2.0631874
	hsa-miR-338-3p	0.022587	-2.766093
	hsa-miR-376a	0.004887	3.6602132
	hsa-miR-376c	0.003739	3.8913565
	hsa-miR-377	0.008489	3.1669385
	hsa-miR-381	7.98E-04	3.8659647
	hsa-miR-487b	0.003947	1.8045903
	hsa-miR-532-3p	0.034379	-1.7935005
	hsa-miR-532-5p	0.016508	-2.3147564
hsa-miR-96	0.003053	-5.2199736	
MPNST	hsa-miR-1280	0.02569	2.419457
	hsa-miR-181b	0.040991	-2.3626232
	hsa-miR-30a	0.002819	-2.7609499
	hsa-miR-18b	0.022267	-4.025688
	hsa-miR-30a*	0.004159	-3.7431161
	hsa-miR-22	0.047768	2.3811169
	hsa-miR-125b-2*	0.03621	1.6424195
	hsa-miR-18a	0.023803	-4.9569993
hsa-miR-30d*	0.035203	-2.4478102	

Table 4.8 - miRNAs with significant expression differences between telomere maintenance mechanisms. Significant expression differences were identified using an ANOVA in Genespring GX (version 10)

(Villa et al. 2008). Furthermore, after adjustment for age and sex miR-96 was the most significant prognostic miRNA ($p= 0.034$) coupled with a high level of significance for TMM ($p = 0.003$) suggesting that regulation of TMM by miR-96 may be an important prognostic factor in this tumour type.

No overlaps between the prognostic and significant telomere maintenance miRNAs were observed in MPNST (Table 4.7 & 4.8). Due to the presence of only 1 ALT synovial sarcoma in the cohort examination of miRNAs associated with telomere maintenance mechanism was not statistically feasible in this tumour type.

Interestingly no SA-miRNAs had significance in TMMs. This suggested that SA-miRNAs may play a role in the regulation of senescence signaling but not the decision between TMMs in mesenchymal tumours.

A selection of miRNAs from each tumour type with significant associations with survival or telomere maintenance were selected for validation by qPCR (Figure 4.9). Although not always reaching statistical significance, the expression patterns of each miRNA echoed that seen in the microarray data when comparing high and low expression for survival, or ALT and telomerase for TMM. The confirmation of these expression differences by a second methodology showed that they are not simply an artefact of the microarray and are differentially expressed between these groupings in these tumour types. These validated individual miRNAs associated with telomere maintenance or survival in these tumour types therefore represent attractive targets for future functional studies.

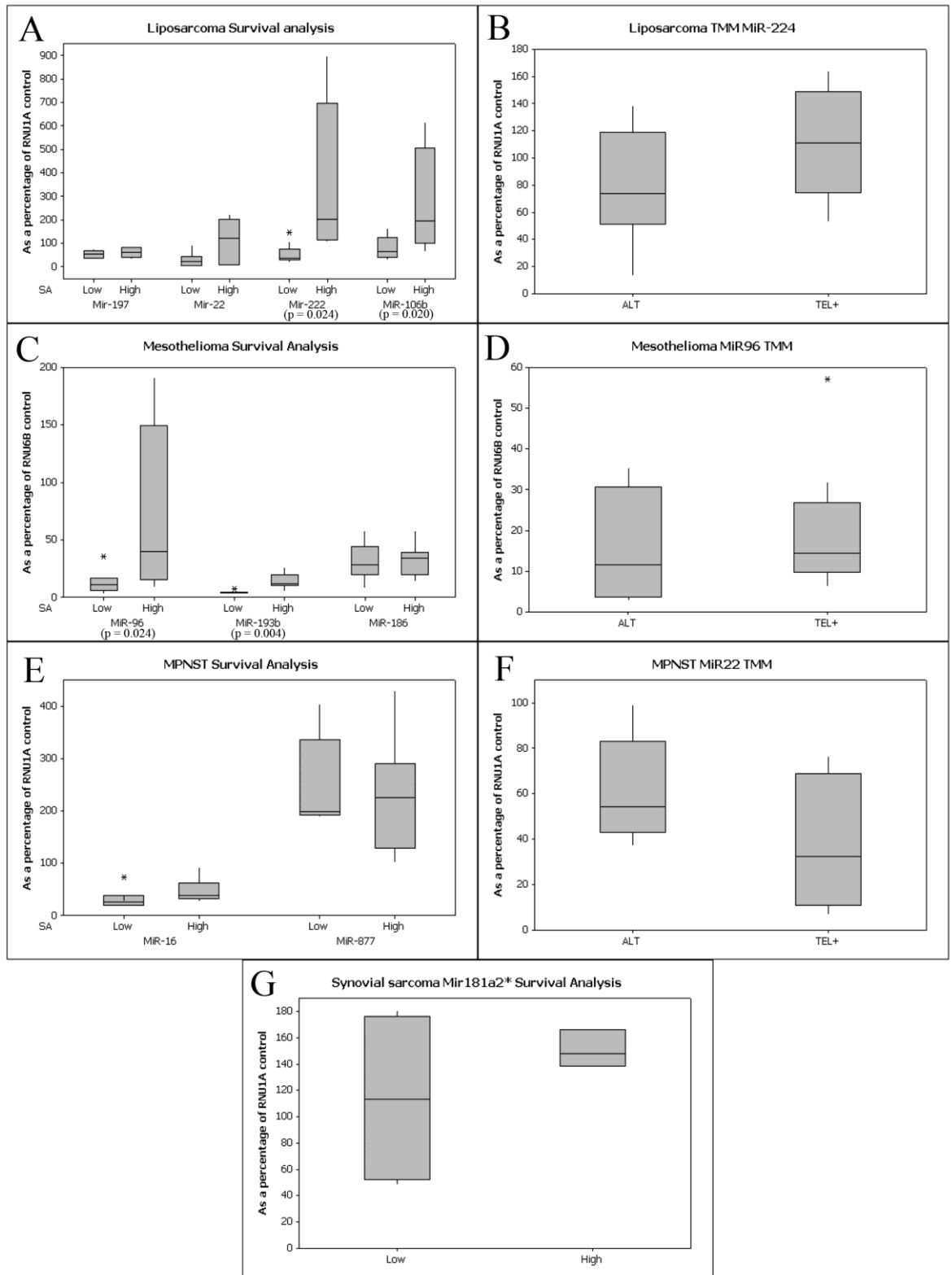


Figure 4.9 - qPCR validation of miRNA expression patterns confirms patterns observed in microarray data. Box plots represent the average of at least 2 Qiagen MiScript qPCR experiments normalised to non-coding small RNAs. Tumours are grouped according to the hazard ratio groupings in the original microarray analysis for miRNAs significantly associated with survival in liposarcomas (A), mesotheliomas (C), MPNST (E) and synovial sarcomas (G). Tumours are grouped by TMM in liposarcomas (B), mesotheliomas (D) and MPNST (F).

4.3 Discussion

As knowledge of the complexities of the signaling pathways involved with senescence induction and bypass grows there is a need for an improved understanding of the regulation of these signaling pathways. miRNAs present a relatively poorly explored mechanism of gene regulation. Due to their ability to simultaneously regulate many different genes on a variety of pathways miRNAs represent a potentially important senescence regulatory mechanism. Through examination of the pathways regulated by 12 miRNAs with previously published evidence of senescence regulation and miRNA microarray data for mesenchymal tumours the potential impact of miRNA regulation of senescence bypass was investigated.

Literature searches revealed a set of 12 miRNAs with experimental evidence for roles in the regulation of senescence induction. When looking at the individual SA-miRNAs some miRNAs have more support for their roles in senescence than others (Table 4.1). The evidence for a regulatory role of the mir-34 family of miRNAs in senescence is growing and has stemmed from the investigation of p53 and its role in senescence. A number of studies have identified the miR-34 family, particularly miR-34a, as downstream effectors of p53 involved in the cell cycle (Bommer et al. 2007). Recent research has found that up-regulation of miR-34a in various cancer cell lines leads to cell cycle arrest, increased expression of β -galactosidase (He et al. 2007) and down-regulation of E2F family target genes (Tazawa et al. 2007). Furthermore, drug treatment of various cancer cell lines with the MDM2 inhibiting drug Nutlin-3, leading to p53 activation, induced up-regulation of primarily miR-34a and later miR-34b and miR-34c (Kumamoto et al. 2008). Reports of a pro-apoptotic effect induced by miR-34a (Chang et al. 2007; Raver-Shapira et al. 2007) may demonstrate that its expression alone is not responsible for senescence.

The potential role of hsa-miR-20a in senescence regulation was discovered through investigation of the candidate senescence associated gene LRF (Poliseno et al. 2008). LRF is a transcriptional repressor of the MDM2 inhibitor p19ARF (Pomerantz et al. 1998; Maeda et al. 2005). The overexpression of miR-20a in mouse embryonic fibroblasts induced senescence by lowering LRF protein levels

and in turn increasing p19ARF levels. The fact that investigation of two different senescence-associated genes, p53 and LRF, yields only two different SA-miRNAs may be a reflection of the range of signaling pathway changes that these molecules contribute to in the induction of the senescent phenotype.

Genome-wide analysis of changes in miRNA expression or investigations of those miRNAs that allow senescence bypass were alternative approaches used in SA-miRNA identification. The use of microarrays identified miRNAs hsa-miR-371, hsa-miR-369-5p, hsa-miR-29c, hsa-miR-499 and hsa-let-7f as significantly up-regulated in senescent human mesenchymal stem cells (hMSCs) when compared to early passage hMSCs (Wagner et al. 2008). miRNA hsa-miR-271 was also seen to be significantly up-regulated by this study but overall had very low expression levels. These varying levels of miRNA expression may suggest different requirements for alterations in their target gene pathways.

MiR-372 and miR-373 were identified as miRNAs whose expression was able to bypass RAS-induced senescence in the presence of wild-type p53 (Voorhoeve et al. 2006). The expression of these miRNAs would therefore not be conducive to senescence and were included in this analysis as examples of miRNAs whose targets may increase in expression during senescence.

These reports in combination with the observation of significant associations of miR-34a, miR-29c and 20a with survival in mesenchymal tumours presented here provide experimental evidence for the molecular mechanisms by which miRNAs may act in the context of senescence and their biological importance. Recent reports of the regulatory effects of miRNAs miR-17-5P and miR-24 on senescence regulators p21 and p16, may offer further miRNAs with a role in senescence (Fontana et al. 2008; Lal et al. 2008). However, lack of β -galactosidase and γ H2AX analysis or the expected alterations to senescence induction prevent whether these miRNAs play a direct role in senescence from being established purely from these initial observations. For this reason they were not included in the SA-miRNA cohort.

The regulation of different senescence induction stimuli by SA-miRNAs was found to vary as shown in Table 4.3. In this study, evidence of the potential SA-miRNAs regulation of core sets of senescence genes regardless of induction mechanism is presented. This analysis highlighted common up-regulation of apoptosis signaling

and pro-inflammatory gene regulation targeted by SA-miRNAs between different senescence stimuli. SA-miRNA targeted down-regulation of cell cycle processes across the induction mechanisms was also observed. This evidence taken in combination with the large degree of overlap between treatment types in stress induced senescence was suggestive of key cellular changes that the SA-miRNAs can facilitate during senescence induction. To date, this is the first report of predicted miRNA regulation of common pathways regardless of senescence stimulus.

2 SA-miRNAs, hsa-miR-499 and hsa-miR-34c, were shown to regulate all of the senescence types examined suggested that these particular SA-miRNAs may act as master regulators for senescence induction. Alterations in different biological signaling pathways by the remaining 10 SA-miRNAs could then tailor the cellular response to suit the alterations required by specific stimuli. This hypothesis requires further laboratory validation, however the fact that both miRNAs already have experimental evidence to show they are senescence regulators adds some weight to the theory. However, no significant associations with survival or TMM were observed in the mesenchymal miRNA microarray data. This suggests that although potential regulators of senescence signaling regardless of stimulus these miRNAs are not utilised by mesenchymal tumours to perturb the senescence programme and become immortalised.

Further exploration of the potential miRNAs as regulators of senescence bypass through TMMs and their impact on survival was undertaken utilizing miRNA expression microarray data for 4 mesenchymal tumour types, liposarcomas, MPNST, synovial sarcomas and peritoneal mesotheliomas. Mesenchymal tumours are a diverse group of tumours with varying median survivals. Senescence associated molecules such as p16, Ki67 and p53 have previously been linked with outcome in many of these tumour types (Kourea et al. 1999; Watanabe et al. 2001; Borczuk et al. 2005; Oda et al. 2005). In addition, the complex regulatory networks presented in the previous chapter and the known prognostic significance of TMMs in mesenchymal tumours further suggests the potential importance of miRNA regulation during tumourigenesis.

Previous analysis of miRNA expression patterns in liposarcomas, MPNSTs and synovial sarcomas has identified a number of differentially expressed miRNAs but failed to correlate the expression levels of any individually with survival (Subramanian et al. 2007; Guled et al. 2009). A recent publication highlighted the expression of 7 miRNAs significantly associated with histological subtype in mesotheliomas, two of which (miR17-5p and miR-30c) also correlated with survival (Busacca et al. 2009). However, for such a large and diverse tumour group relatively few miRNA investigations have been performed for example no known miRNA signatures for liposarcomas, MPNST and synovial sarcomas exist. This may be reflective of the rarity of these tumours and the difficulty in collecting sufficient numbers of tumours for statistically viable studies.

For each tumour type a group of prognostic miRNAs were highlighted. 33% of the prognostic miRNAs overlapped with those in the 87 miRNA signature suggesting unique molecular differences that influence outcome between these tumour types (Table 4.7 & 4.8). These miRNAs therefore present a potential novel target for future clinical trials and mechanistic investigations.

25, 14 and 9 miRNAs were significantly differentially expressed between telomere maintenance mechanisms in liposarcomas, peritoneal mesotheliomas and MPNST respectively were also highlighted (Table 4.7). 2 miRNAs (miR-21* and 324-5p) in liposarcomas and one miRNA (miR-96) in mesotheliomas which also had prognostic significance were also observed (Table 4.7 & 4.8). Agreement of the expression patterns in telomere maintenance mechanism groups and the hazard ratios in each tumour type of these overlapping genes suggested that the prognostic implications of these miRNAs may be due to their role in the regulation of telomere maintenance mechanisms, consistent with the known prognostic implications of telomere maintenance in both tumour types (Costa et al. 2006; Cairney et al. 2008; Villa et al. 2008). For example, miR-21* had a high hazard ratio, implying that expression of the miRNA was associated with poor outcome and this miRNA was expressed 4 fold higher in ALT liposarcomas. To date, there has been no published association between telomere maintenance and patient outcome in MPNSTs and the lack of overlap between prognostic miRNAs and miRNAs involved in telomere maintenance in this miRNA data may therefore reflect the possibility that telomere maintenance mechanism may not have a significant effect on patient outcome. There were

however a number of significantly different miRNAs for telomere maintenance suggesting that although not prognostic, telomere maintenance mechanism regulation may still be an important factor in biology of this tumour type. Although an increased incidence of ALT has previously been seen in synovial sarcomas (Henson et al. 2005) the mesenchymal tumour cohort contained only 1 ALT tumour and examination of the role of miRNAs in telomere maintenance regulation for this tumour type was not possible.

In this chapter, pathway mapping and theoretical gene target identification was used to create a biological framework by which to test the relevance of miRNAs in the regulation of senescence signaling. miRNAs were not only shown to potentially regulate genes previously seen to be involved in senescence but also regulate larger pathway alterations, such as cell cycle and cytoskeletal remodeling, that would logically be required to create the complex phenotype of the senescent cell. Commonly regulated pathways and cellular mechanisms between the senescence stimuli also demonstrated the potential of SA-miRNAs to regulate a core set of pathway modifications regardless of senescence induction mechanism. Furthermore, stimulus specific pathways by which SA-miRNAs can regulate apoptosis survival signals in cells undergoing drug induced or natural replicative senescence were highlighted. Additionally, individual miRNAs that were differentially expressed between telomere maintenance mechanisms and with prognostic significance were identified. In depth examination of these miRNAs highlighted that three of the SA-miRNAs had prognostic significance in specific mesenchymal tumour types suggesting that regulation of senescence signaling by these miRNAs may be an important factor in tumorigenesis and patient outcome and warrants future laboratory investigation. The combination of these findings suggests that miRNAs may present a real senescence signaling regulatory mechanism with potential for targeted therapies. Furthermore, regulation by miRNAs is a post-transcriptional event and therefore would provide a mechanism by which genes could remain transcribed but not translated. This may therefore facilitate the establishment of latent senescence signaling in human tumours; the impact of which is not currently understood.

5 Scoring of damage or secretory associated senescence phenotypes in human tumour gene expression datasets and identification of a pro-inflammatory signature correlating with survival advantage in peritoneal mesothelioma

5.1 Introduction

In the previous chapter significant associations between SA-miRNAs and survival in mesenchymal tumours was observed. Furthermore, previous data within this project highlighted the fact that telomere maintenance mechanisms for senescence bypass are highly regulated processes in these tumours (see chapter 3). This suggests that senescence signaling may have an impact on or be related to a cell's route to tumorigenesis. Although the senescence program must be bypassed for cells to become fully immortalised it is currently unclear as to how much latent senescence signaling remains present in human tumours after this event. Therefore, latent senescence signaling dynamics during disease progression and in response to known senescence induction mechanisms have not been explored. To fully explore the associations between cellular senescence and larger tumourigenic processes it is necessary to look beyond single genes and instead utilise data from larger pathways. To this end, a scoring system that reduces the levels of latent senescence signaling in a human tumour present in gene expression microarray data to one quantifiable number was designed. It must be noted that this is one of the first times such an approach has been taken and as such this represents a pilot study in the field. The list of genes that have been used for the signatures, their assigned directions and even the scoring method itself may require further alterations in future studies. Therefore the results presented here are a first-pass hypothetical study into latent senescence signaling *in vivo* and *in vitro*. After validating the approach in datasets whereby senescence induction would be expected; the scoring system was applied to a mesenchymal data set and the expression pattern of latent secretory senescence signaling and associations with survival was explored.

5.2 Results

5.2.1 *Development of senescence scoring approach*

Bypass of senescence is a requirement for full transformation. However, many cancer cells retain the ability to induce the senescence program in response to genotoxic insults (Braig et al. 2006; Gewirtz et al. 2008). Theoretically, tumours must therefore retain latent senescence pathways, however their impact upon other factors such as patient survival and response to therapy are unclear. To explore these associations it was first necessary to design a method of quantifying the levels of latent expression of senescence signaling pathways in a human tumour. As gene expression changes in a number of well-defined senescence markers during senescence induction are documented, gene expression microarray data was used to gain a measure of the degree to which these markers were still signaling in a senescent manner. To this end, the published literature was mined for gene expression signatures and biomarkers of senescence (Table 5.1) and two sub-signatures were established. DAS biomarkers represent genes with known roles in senescence the damage associated senescence pathway and chromatin responses. Additionally, a modified secretory senescence (mSS) signature was created by combination of elements of the senescence messaging secretome/senescence associated secretory phenotype (SMS/SASP) signatures with a signature of 4 genes representing DNA damage and telomere dysfunction which increase in expression/activity in senescent cells and are detectable in serum of ageing human patients (Coppe et al. 2008; Jiang et al. 2008; Kuilman et al. 2009; Young et al. 2009). Given the reliance of the scoring procedure on the starting gene-lists and directions but also it's inherent adaptability; future studies utilizing this method may choose to alter the content of the gene signatures to reflect current knowledge in the field.

To assign senescence scores, data were imported and normalised to median using BRB array tools. Each gene was then scored as senescent or not depending on whether expression was in a pro-senescence direction (see Table 5.1) with reference to that gene's median expression level. For example, expression of the proliferation-associated gene *Ki67* below median would be marked "senescent" but above median expression would not. The total percentage of genes receiving a "senescent" score was then calculated for each sample to give an overall

senescence score. By this approach, the level of pro-senescence signaling in each pathway can be measured. Although very simple mathematically, taking the percentage of genes still signaling in a senescent manner provides a single continuous senescence measurement in human tumours incorporating the sum contributions of many pathways, something that has not previously been attempted. To attempt to validate the scoring approach in this pilot study, the scoring system was applied to a number of settings in which senescence would be predicted to occur.

5.2.2 Validation of the Approach

5.2.2.1 Senescence signaling pathways induced by radiation therapy

The induction of cellular senescence in response to radiotherapeutic agents has been recently documented. Application of the scoring system in this context would therefore be expected to show increased senescence signaling post radiotherapy. To investigate this, the scoring system was applied to a publicly available dataset (GSE15781) which consisted of tumours and normal tissue of the colon before and after radiotherapy (Figure 5.1). Examination of all biomarkers showed that tumours had a higher level of senescence signaling compared to their respective normal tissues (score 69% and 56%, respectively) (Figure 5.1A). Furthermore, irradiated tumours had higher median levels of pro-senescence signaling than their non-irradiated counterparts (score: 74 % in irradiated tumours compared with 69 % in non-irradiated). These results suggested that the scoring system was potentially able to capture increased senescence signaling resulting from radiotherapy.

As well as measuring overall senescence signaling, the scores of the sub-signatures DAS and mSS were also explored. Irradiation of tumours causes high levels of DNA damage with the aim of causing cell necrosis or apoptosis (Ross 1999). Patterns in the data shown in Figure 5.1B highlighted that irradiated normal tissue have increased median DAS signaling compared to their non-irradiated counterparts, however the overall spread of the data was lower in the irradiated normal tissue (50 % - 87 % in non-irradiated normal compared to 37 % - 75 % in irradiated normal). Median DAS signaling in adenocarcinoma was unchanged by irradiation, although the minimum scores were at a higher level in irradiated tumours than their

Originating Senescence Signatures	Genes	Expression Direction in Senescence
DAS Biomarkers (Campisi et al. 2007; Fridman et al. 2008; Sedivy et al. 2008)	p16	Increase
	HMGA1	Increase
	HMGA2	Increase
	HIRA	Increase
	ASF1a	Increase
	H2AFY	Increase
	H2AFY2	Increase
	PML	Increase
	MMP3	Increase
	53BP1	Increase
	p21	Increase
	Ki67	Decrease
mSS Biomarkers (Coppe et al. 2008; Jiang et al. 2008; Kuilman et al. 2009; Young et al. 2009)	IL6	Increase
	IL8	Increase
	PAI1	Increase
	IGFBP3	Increase
	IGFBP5	Increase
	IGFBP7	Increase
	IL1A	Increase
	CXCR2	Increase
	IGF1	Decrease
	IGF2	Decrease
	WNT2	Decrease
	CAMP	Increase
	STMN1	Increase
	EEF1A1	Increase
	IGF2R	Increase
	TGFB1	Increase

Table 5.1 - Gene expression changes and senescence signatures.

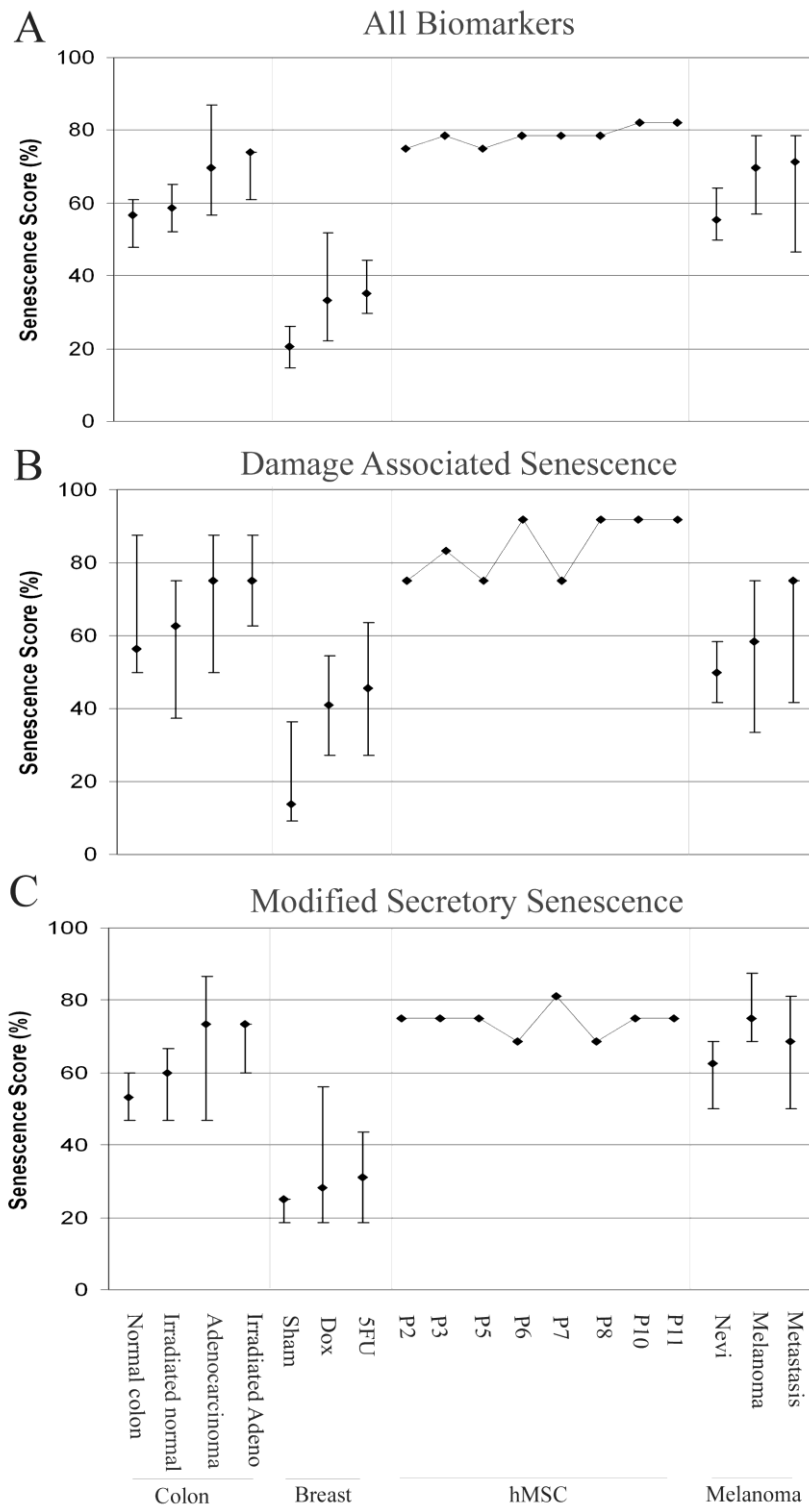


Figure 5.1 - Senescence scoring of public data sets. Datasets tested were: irradiated and non-irradiated colorectal tumour and normal tissue (GSE15781); doxorubicin and 5-FU treated breast cancer cell lines (GSE1647); mesenchymal stem cells cultured to replicative senescence (GSE9593); a melanoma progression set (GSE4587). All sets were scored using (A) All markers from Table 1, (B) DAS markers, (C) mSS markers. Median senescence scores are shown with bars representative of the maximum and minimum values. In the case of the hMSC set, the time-course data are derived from the cells of a single donor without replication and therefore, no bars are shown

non- irradiated counterparts (62 % compared to 50 %) suggesting a trend in favor of higher DAS signaling in irradiated tumours.

Interestingly, irradiation did not increase mSS signaling in tumours (score: 73% pre- and post-irradiation). In contrast, normal tissues showed a median increase of 6.7% (Figure 5.1C). Radiotherapy therefore appeared to specifically activate the DNA damage and chromatin aspects of senescence whilst not altering levels of the secretory senescence signaling pathway in tumours. This finding may present novel opportunities for improved senescence induction through therapeutic activation of secretory pathways in these tumours, however given the preliminary nature of this pilot study further validation of this result in other radiation treatment datasets may be required.

5.2.2.2 Senescence scoring in drug treated breast cancer cells

To assess the performance of the scoring approach in a further situation in which senescence induction would be expected, i.e. drug-induced accelerated senescence, a further the public data set (GSE1647), in which the authors investigated drug-specific toxicity-related expression profiles in a panel of breast cancer cell lines treated with chemotherapy drugs, was explored. Senescence was not directly assessed in this study, though each drug was administered at its IC50 for each cell line (assessed by a mitochondrial dye conversion assay). For statistical robustness, the data for the 3 cancer cell lines ZR-75-1, ME16C, and MCF7 treated for 24 hours (leading to a total of 6 replicates per treatment) with either doxorubicin or 5-FU were pooled, both of which have previously been observed to induce the accelerated senescence phenotype in tissue culture (Bu et al. 2008; Sliwinska et al. 2009).

Across all cell lines, the median basal senescence score was comparatively low (20%). As observed with radiotherapy of colon adenocarcinoma, treatment with either 5-FU or doxorubicin results in induction of the overall senescence score (Figure 5.1A, 5-FU score: 35%; doxorubicin score: 33%). DAS markers had basal expression of 14% in untreated cells. As expected, these genes were strongly induced, resulting in median scores of 45.5% and 41% for 5-FU and doxorubicin, respectively (Figure 5.1B). The mSS component also appeared to be induced by 24 hour drug treatments, though more modestly than the DAS component, rising to 31% and 28% from a basal level of 25%. Thus according to this scoring approach,

both radiotherapy and chemotherapy induced multiple senescence markers as expected, however mSS appeared to have a greater contribution in response to chemotherapeutics.

5.2.2.3 Senescence signaling dynamics during replicative senescence

Having shown that the scoring system highlighted increased senescence signaling after treatment with senescence inducing therapies, the scoring system was next applied to investigate replicative senescence of human mesenchymal stem cells (hMSCs). Passages 2 to 11 in hMSCs from the same patient, (publicly available dataset GSE9593) were scored for latent senescence signaling. This same dataset was also used in the previous chapter to assess miRNAs potential role in senescence. Prior to passage 11, at which time hMSCs were completely senescent, the authors of the study observed continuous changes in the cellular phenotype including gradual increases in cell size and senescence associated β -galactosidase staining (Wagner et al. 2008). These phenotypic changes are consistent with known phenotypic changes during the process of replicative senescence onset.

The analysis of all senescence markers in this data (Figure 5.1A) was consistent with these observations, indicating that senescence gradually increased with passage, albeit to a small degree. A plateau between passages 6 and 8 was evident when all markers were scored (score 79%). Strikingly, however, examination of the DAS and mSS signatures at this time point showed that this plateau was in fact a timed change in signaling type. Secretory senescence signaling remained level at 75% until passage 6 at which point a slight reduction to 69% was observed. At this timepoint there was a corresponding sharp increase in DAS signaling (75 % to 92 %). A subsequent spike in secretory (mSS) expression (score 81%) occurred at passage 7, followed by a return to base levels (Figure 5.1C). Examination of DAS markers at this time point (Figure 5.1B) showed a transient decrease in their expression at passage 7 (score 75% compared with 92% at passage 6) before returning to maximal levels. These changes in latent senescence signaling correspond to a transient change in the global expression profile of these cells observed between passages 6-8 in the original analysis (Wagner et al. 2008).

The dynamics of telomere shortening were not directly explored in the original study. However, passage 7 occurs immediately before the onset of the main plateau phase of growth, suggesting that a significant fraction of cells may have

undergone telomere dysfunction. DAS signaling spiked at P6, prior to the spike in mSS signaling at P7, raising the intriguing possibility that a threshold level of damage signaling triggers cells to communicate cellular stress to the surrounding microenvironment through the mSS pathway (Rodier et al. 2009). Furthermore, the spike in secretory signaling also correlated with a transient increase in expression of glycoprotein GPNMB/osteostatin which was validated by QPCR in the original study (Wagner et al. 2008). GPNMB is an osteoclastic factor also implicated in endothelial cell adhesion and regulation of pro-inflammatory macrophage signaling. The increase of expression of GPNMB at this passage in combination with the observed increase in secretory senescence signaling is therefore consistent with the concept that signaling to the microenvironment is indeed increased at this time point (Sheng et al. 2008; Pahl et al. 2009). This was the first time such a temporal switch in senescence signaling had been documented, however the differential regulation of secretory and other senescence pathways during replicative senescence was also concurrent with other recent findings in human T-cells during senescence bypass (Degerman et al, 2010).

5.2.2.4 Senescence scoring in a Melanoma progression dataset

The above results suggested that the scoring system effectively captured increased activity of senescence pathways during both therapeutically induced and natural replicative senescence. The expression levels of latent senescence pathways are likely to be altered by the processes of transformation and tumour progression and may reflect the route to immortalisation in individual tumour types. To explore this hypothesis the changes in senescence signaling during tumour progression in a melanoma dataset (GSE4587) were explored. Figure 5.1 shows levels of senescence signaling in benign nevi (score 55%, for all markers). Interestingly, an increased senescence score was found in melanoma when compared to benign nevi, regardless of the type of senescence signaling explored (DAS score: 58% versus 50%; mSS score 75% versus 63%). Therefore, although transformation has been achieved in these melanomas some aspects of the senescence program still appeared to be active. Furthermore, the specific identities of induced senescence genes during tumour progression may point to the route of immortalisation for specific tumour types. Given that benign nevi are a well established model of senescence *in vivo* it may also be feasible that the scoring method is not accurately predicting senescence in these cells. Further validation would therefore be required.

Nonetheless, the promising results of the radio- and chemotherapeutic treatment datasets and the replicative senescence data make it possible to hypothesise that the scoring system could potentially be accurate and this could be a new observation in this tumour model. The lower level of scoring in the nevi could be because senescence has been established in the nevi the levels of actual signaling being triggered may be less than that caused by the constant trigger, and bypass, of the senescence signaling cascade caused by abberantly proliferating cells (such as primary tumours and metastasis).

Comparison of primary melanoma and metastasis using all markers showed a slight increase in metastasis (melanoma score: 70%; metastasis score: 71.4%) (Figure 5.1A). However, exploration of DAS and mSS revealed striking differences between the two tumour stages. Primary melanomas had a high contribution from mSS signaling and low levels of expression of the DAS biomarkers (75% and 58% respectively), while metastases had the opposite expression pattern (mSS score 69%; DAS score 75%) (Figure 5.1B & C). These results may reflect the differing selection pressure upon these tumour stages whereby the pro-inflammatory microenvironment produced by the secretory senescence signaling pathway is advantageous to a primary tumour in processes such as angiogenesis but may prevent immune evasion by metastatic tumours. The low DAS senescence scores in primary tumours may be reflective of low levels of signaling shortly after immortalization and senescence bypass. After which, genomic instability may potentially increase during the process of tumour progression leading to higher levels of DAS senescence signaling pathways in metastasis. Furthermore, DAS related signaling pathways may be induced during bypass of anoikis. In summary, these results suggested that DAS signaling increases during tumour progression. However, these increases were clearly insufficient to induce full senescence and cell cycle arrest.

5.2.3 Application of Scoring Approach

5.2.3.1 Differential senescence signaling patterns in mesenchymal tumours

The results above provided preliminary proof of concept that senescence scores obtained using these signatures conformed mostly to expectations, given current

understanding of replicative and accelerated senescence. The scoring system therefore provided an initial tool with which the potential role of latent senescence signaling in human tumours could be explored. To this end, the scoring system was applied to the mesenchymally derived tumour gene expression dataset (Figure 5.2). For this dataset all of the senescence biomarkers had identical median scores across all tumour types (46%) (Figure 5.2A). Dissection of individual senescence signaling pathways showed that DAS signaling was lowest in MPNST (42 %) and mesotheliomas (46 %) and higher in liposarcoma (score: 50%) (Figure 5.2B).

In contrast, mSS expression was higher in mesothelioma (score: 50%) than either MPNST or liposarcomas (44% and 47%, respectively) (Figure 5.2C). This suggests that even small changes in senescence signaling pathways can be detected using this scoring method and therefore allow for hypothesis driven investigations. For example, differences in latent senescence signaling could affect factors such as patient prognosis and response to therapy. In particular, the higher scores for DAS in liposarcoma and mSS in mesothelioma samples were interesting in light of the shorter median survival for patients presenting with peritoneal mesotheliomas (27 months) compared to liposarcoma (99 months). These inverse signaling patterns further reinforce the concept that high levels of signaling of one of the two senescence pathways may be tolerable but both may be sufficient to induce full senescence and block transformation. Furthermore, the lower median survival of mesotheliomas in this example may suggest that the immune activatory signals given by the latent secretory senescence signaling may be advantageous to primary tumour proliferation similar to that observed previously in melanomas (Figure 5.1).

Having observed interesting signaling dynamics in larger tumour types, the scoring system was next utilised to investigate latent senescence scores in individual tumour samples. For each senescence signature the scores for each tumour were ranked within its group to smooth the data. Ranked data was then used to calculate Pearson correlations between senescence signatures for each individual tumour within the group (Table 5.2), allowing investigation of whether the signatures are distinct signaling events or could be co-expressed in individual tumours. In all tumour types both DAS and mSS significantly correlated with All biomarkers (Table 5.2C). Furthermore, DAS and mSS never significantly correlated, suggesting that according to this senescence scoring method these two pathways are distinct signaling events at an individual tumour level. These observations

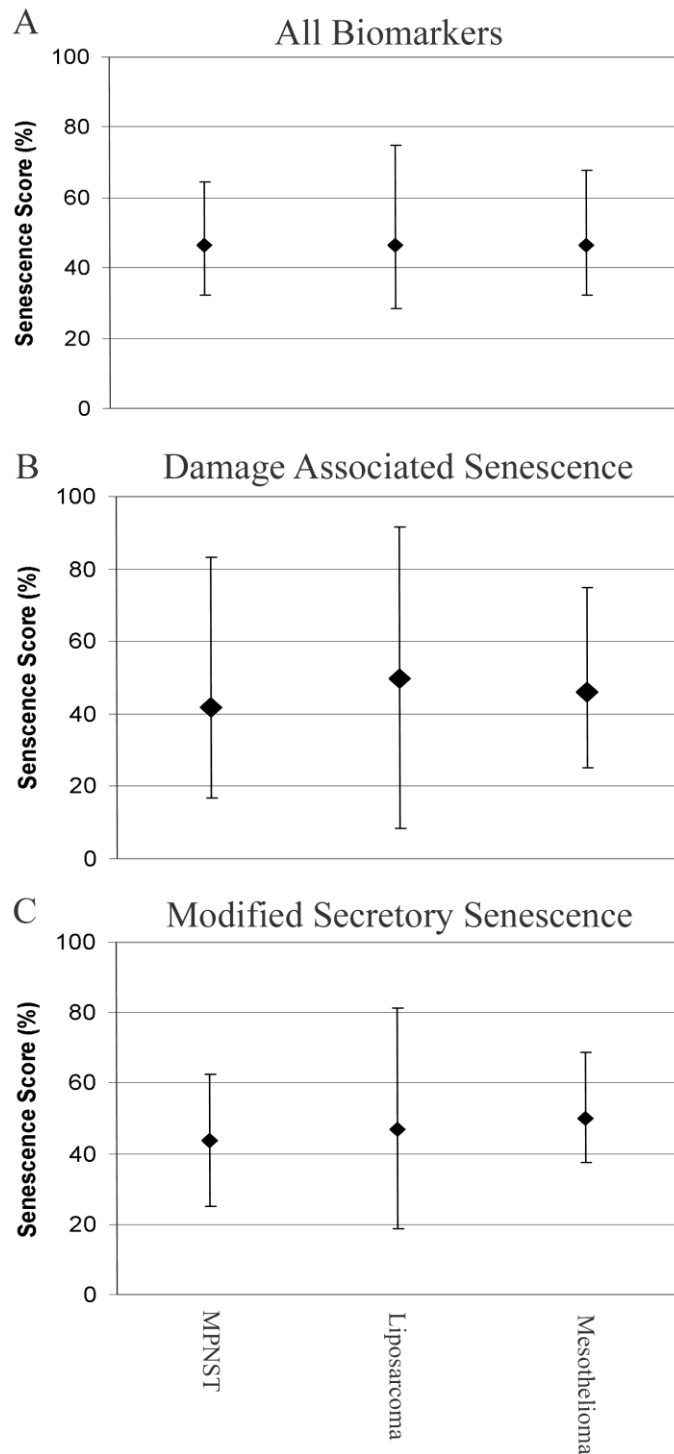


Figure 5.2 - Senescence scoring of mesenchymal tumours. Peritoneal mesothelioma, liposarcoma and MPNST samples were scored using (A) All markers from Table 5.1, (B) DAS markers, (C) mSS markers. Median senescence scores are shown with bars representative of the maximum and minimum values.

A		All	DAS	mSS
MPNST	All	1		
	DAS	0.738 (p = 0.001)	1	
	mSS	0.792 (p = <0.001)	0.245 (p=0.361)	1
B		All	DAS	mSS
Liposarcoma	All	1		
	DAS	0.622 (p = 0.001)	1	
	mSS	0.756 (p = <0.001)	0.007 (p = 0.974)	1
C		All	DAS	mSS
Mesothelioma	All	1		
	DAS	0.858 (p = <0.001)	1	
	mSS	0.627 (p = 0.003)	0.164 (p = 0.489)	1

Table 5.2 - Correlation of senescence score rankings highlights signaling dynamics in individual tumours

confirmed that the results of the group analysis are pertinent at the level of individual tumours, implying that senescence phenotypes may be differentially activated during transformation.

5.2.3.2 Supervised Hierarchical clustering using the mSS signature highlights heterogeneous subgroups within mesenchymal tumours and a prognostic signature in peritoneal mesotheliomas

Given the essential nature of the establishment of a secreted inflammatory network of signaling in senescence induction (Kuilman et al. 2008) and the observations of differential expression patterns of secretory senescence in mesenchymal tumours and hMSCs, it seemed pertinent to utilise the mSS signature to further explore senescence signaling patterns in this pathway in mesenchymal tumours. After normalisation of gene expression array data, the expression patterns of only the mSS signature within each tumour type were examined using supervised hierarchical clustering (Figure 5.3A, and data not shown).

Hierarchical clustering in peritoneal mesotheliomas split these tumours into two distinct groups, A and B (Figure 5.3A), corresponding to differential expression in two gene groups, 1 and 2 (Table 5.3). Specifically, group A tumours had higher expression of group 1 genes and lower expression of group 2 genes than group B tumours. The tumour groups, A and B, did not significantly correlate with any patients' known histological characteristics, such as age or sex. Interestingly, tumours in group A were associated with improved survival compared to those in group B and this remained significant after adjusting for age and sex (Figure 5.3B). This suggested that even though senescence had been bypassed, the latent expression of different subsections of the secretory senescence pathway still affected patient outcome.

To further explore the functions of the differentially expressed gene groups, 1 and 2, enrichment for biological GO processes in each prognostic gene group was investigated. This analysis revealed that group 1 genes have functions in immune activation ($p= 4.1E-10$), chemotaxis ($p= 1.6E-11$), inflammation ($p= 1.2E-8$) and negative regulation of cell proliferation ($p= 3E-16$). This was concurrent with previous findings in other tumour types, that patients with high levels of local inflammation and immune invasion at the tumour site have improved survival

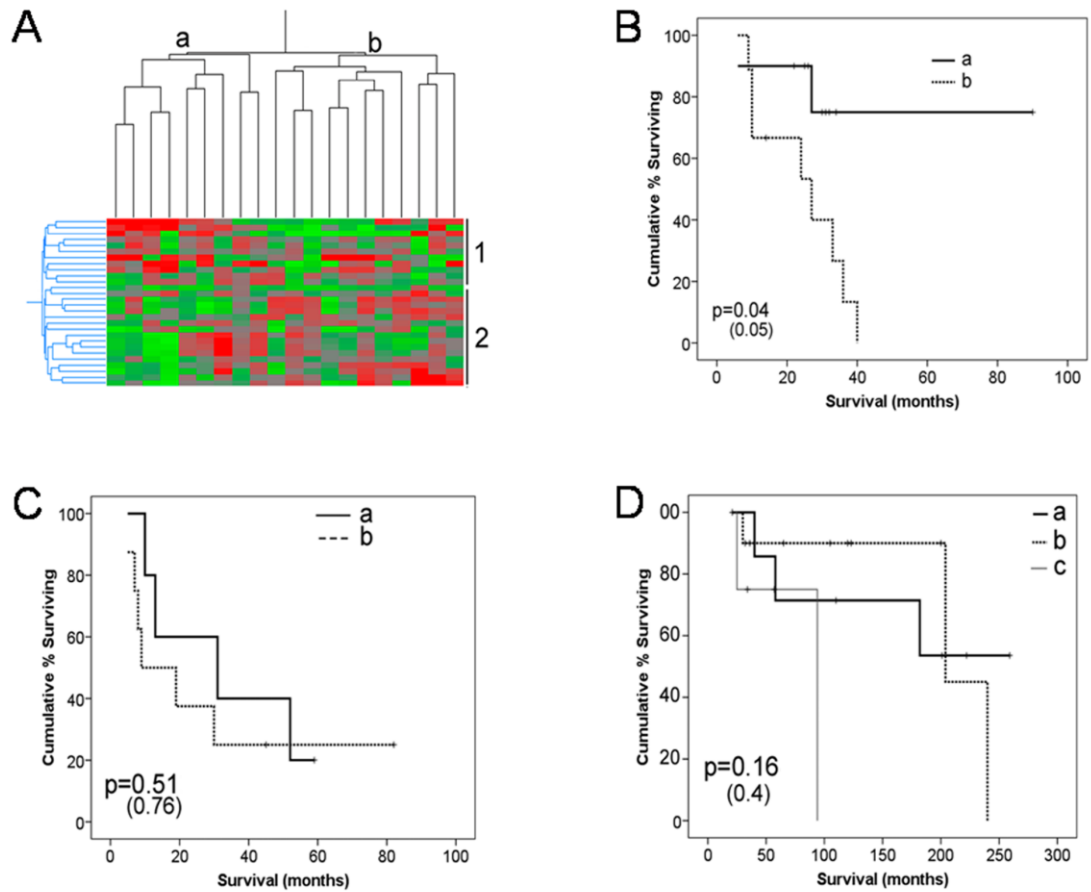


Figure 5.3 – Supervised hierarchical clustering using the mSS signature highlights gene groups correlating with survival in peritoneal mesotheliomas. Clustering of mesothelioma samples is shown in (A). Group A tumours had higher expression of group 1 genes and lower expression of group 2 genes, corresponding to a potential pro-inflammatory phenotype. Gene groups are given in Table 3. (B-D) Kaplan-Meier survival analyses of tumour groups from mSS supervised hierarchical clustering. (B) Peritoneal mesotheliomas, (C) MPNST and (D) Liposarcoma. Note: hierarchical clustering split the liposarcoma cohort into 3 major groups (denoted a, b and c) whereas all other tumours split into two groups (denoted a and b).

Only mesothelioma samples showed a significant association with survival improvement. P values shown in brackets are p-values after adjustment for age and sex. All survival analysis performed in SPSS (version 15).

Gene Group 1	CAMP
	EEF1A1
	IGF2R
	IL1A
	IL6
	IL8
	CXCR2
	WNT2
Gene Group 2	EEF1A1
	IGF1
	IGF2
	IGFBP3
	IGFBP5
	IGFBP7
	CXCR2
	PAI1
	STMN1
TGFB1	

Table 5.3 – Gene groups responsible for clustering in peritoneal mesotheliomas. Probes A_32_P47701, A_32_P44316 and A_32_P15320 for EEF1A1 appeared in group 1 while probe A_24_P763243 featured in group 2.

(Roxburgh et al. 2009). Furthermore, the genes in group 2 were involved with the regulation of cell growth ($p= 3.4E-16$), proliferation ($p= 2E-13$) and cell motion ($p= 1.3E-14$). The increased expression of genes involved in cellular proliferation and cell motion may therefore be indicative of more aggressive tumours leading to decreased survival rate.

The same analysis was also performed on the other two mesenchymal tumour types. Similar gene groups also split MPNST into 2 tumour groupings while liposarcomas were divided into three groups with high group 1 expression (A), low group 1 expression (B) and low expression of both groups (C) (data not shown). However, examination of survival revealed no significant difference between the groups in these tumours (Figures 5.3C & D). Nevertheless, these expression groups may reflect unknown biological factors and may warrant further investigation to improve understanding of the underlying biology and role of senescence in these subgroups.

5.3 Discussion

To improve the understanding of senescence signaling it is becoming increasingly necessary to look beyond the expression of individual genes and at the larger pathways they are involved in. The scoring approach presented here takes a percentage of the known senescence biomarker genes that are signaling in a pro-senescent manner thereby reducing the information given by multiple biomarkers down to one quantifiable number. It is then possible to dissect the levels of particular senescence signaling pathways occurring in a sample at any one time and directly compare the levels of these pathways, giving us an insight into subsystems involved in senescence establishment and maintenance. First, the approach was validated using a number of publicly available datasets corresponding to scenarios where modulation of senescence signaling might be expected. Upon establishment of proof of concept an in-depth study into latent secretory senescence signaling using in-house generated mesenchymally derived tumour datasets was performed. The results of this analysis show that senescence signaling occurs in a context dependent manner. In certain situations, DAS and mSS programs coexist while in others they are distinct signaling events regulated in a time dependent fashion.

It must also be noted however that this exploration of latent senescence signaling using a scoring approach is the first of its kind and therefore future studies may choose to alter the exact combinations of genes in the signatures. Furthermore, additional dimensions to the scoring procedure, such as including an error calculation and/or weighting genes of particular interest, may also be added. However, for this pilot study such further complexities were omitted to allow initial assessment of the core approach.

The induction of DNA damage by radiotherapy in cancer is commonplace in current treatment regimes (Ross 1999). Recent evidence suggests that senescence is frequently induced after radiation exposure (Jones et al. 2005; Quick et al. 2006; Gewirtz et al. 2008). To gain a further understanding of the individual roles of DAS and mSS signaling in this process the examination of colon tumours and normal tissues pre and post radiotherapy from publicly available data, was undertaken. As well as observing a general increase in senescence signaling post radiation exposure concurrent with the literature, this pilot study suggested that secretory senescence signaling is not induced by radiotherapy in colon adenocarcinoma, while there was a trend in favor of an increase in DAS signaling in these samples. This distinction had not previously been made and may present important opportunities for immune activating adjuvant therapies through the activation of secretory senescence signaling in tumours of patients receiving radiotherapy.

The scoring system was next applied to a gene expression dataset comprising doxorubicin or 5-FU treatments of the breast cancer cell lines ZR-75-1, ME16C, and MCF7 (Troester et al. 2004). Here again increased representation of all biomarkers, consistent with the emerging concept of drug-induced accelerated senescence, was observed. The scoring system therefore also reported increased senescence in a second therapeutic intervention scenario. In contrast with the radiotherapeutic context, both DAS and mSS subsystems were induced by drug treatments although induced DAS signaling still predominated. The distinction between the levels of mSS and DAS in response to the two treatment types had not previously been documented.

To determine whether the scoring system identified increased senescence signaling in the normal “physiological” context of replicative senescence, a time-course dataset corresponding to gradual replicative senescence of hMSCs with increasing passage was explored (Wagner et al. 2008). Investigation of all biomarkers showed

a gradual increase with passage with a plateau between passages 6-8. By dissection of DAS and mSS elements the scoring system showed that this plateau corresponded to a point at which DAS signaling sharply increased. This was subsequently followed by an increase in secretory senescence signaling concurrent with a transient decrease in DAS signaling. Such a decrease in DAS signaling may highlight a specific time-point for the secretory senescence pathway to signal cellular distress to surrounding cells, as previously observed in the literature (Rodier et al. 2009) and further highlights the distinct nature of the two signaling pathways. This was the first time such a temporal switch in senescence signaling has been documented.

Previous data on individual senescence genes in melanoma has suggested that senescence is a barrier to tumour progression (Bennett 2008). Application of the scoring approach to a melanoma progression dataset showed that not only did senescence signaling remain active after immortalization but that the levels of senescence signaling of all types in primary tumours were higher than that seen in benign nevi. This suggests that although the senescence program has been bypassed the signaling pathways continue to operate in melanoma. Nevi, however, remain the most established *in vivo* example of senescent cells and therefore this result was somewhat surprising. Given that this was a pilot study of the scoring method this presents two possible scenarios. Firstly, the scoring method may not accurately capture latent senescence levels in this cell type. Alternatively, this experimental approach may have uncovered a novel biological effect not previously seen with other techniques. In the case of this second scenario it is conceivable that as the nevi have progressed to a final senescent phenotype the requirement for repeated latent senescence signaling maybe reduced. However, melanomas and metastatic tumours continue to proliferate and therefore may continue to trigger the senescence signaling cascades leading to high levels of latent signaling despite bypass of the final program.

In addition to the general increase in senescence signaling over nevi, differential expression of secretory and DNA damage/chromatin senescence pathways in primary lesions and metastasis, with secretory elements of senescence showing a trend towards down regulation in metastases, were observed. Down regulation of secretory senescence pathways in metastatic tumours may facilitate immune evasion and disease progression. Despite the down-regulation of secretory senescence the DAS elements of senescence continue to signal. The latent signaling

of senescence in tumours and metastasis may present opportunities for therapies to reinstate the correct endpoint of these pathways and halt further disease progression. The data from this pilot study therefore suggests that therapies targeted to induce secretory senescence in metastatic melanoma may warrant further investigation and together, the results from all public datasets confirmed that this experimental scoring system is potentially able to detect the contribution of individual senescence signaling subsystems in a variety of contexts.

Next, a more in-depth investigation of senescence signaling in individual mesenchymally derived tumours was performed. Initial examination of the correlations between the rankings of individual tumours from three main mesenchymal malignancies, liposarcoma, MPNST and mesothelioma, highlighted similar patterns of senescence signaling in individual tumours of all 3 types. Scores for All biomarkers significantly correlated with those for DAS and mSS in all cases. In contrast, DAS and mSS scores showed no correlation suggesting that these signaling processes are distinct events at an individual tumour level. This is consistent with analysis of the larger tumour groups, where increased mSS scores in mesothelioma and DAS scores in liposarcoma were observed in comparison to other tumour types. As distinct events, it is possible to hypothesise that these signaling processes may influence other clinical factors such as prognosis or response to treatment.

Previous studies have examined individual senescence markers and their prognostic significance in these tumour types (Watanabe et al. 2001; Borczuk et al. 2005; Oda et al. 2005) but not the prognostic significance of entire senescence signaling pathways. Distinctions between the different senescence signaling dynamics in individual tumours gives improved understanding of the cellular context prior to treatment being applied and potentially helps to make the move towards patient tailored targeted therapeutics more realistic. Given the importance of the establishment of a secretory senescence network in the induction of senescence (Kuilman et al. 2008) this may be a pathway that could be perturbed by different mechanisms to effectively prevent senescence induction. To this end, a more in-depth analysis of the patterns of expression of secretory senescence in the three mesenchymal tumour types was undertaken.

Hierarchical clustering of peritoneal mesotheliomas split the tumours into two groups based on distinct expression patterns of subsets of secretory senescence

genes involved either in pro-inflammatory and immune activating processes or in pro-growth and proliferation processes. Interestingly, the groupings showed significant correlation with survival; in particular, those tumours displaying increased expression of pro-inflammatory genes had improved survival compared with the lower expressing group. The functions of these genes are therefore likely to be of importance in the underlying tumour biology of mesotheliomas. Although hierarchical clustering also divided the MPNST and liposarcoma samples into 2 and 3 clusters, respectively, based on similar gene groups, no association with survival was observed. However, improved survival associated with tumours with increased immune infiltration has previously been documented (Roxburgh et al. 2009) and the activation of specific secretory senescence pathways may facilitate this. Given the secretory nature of these molecules, their measurement in patient serum will improve understanding of the role of senescence signaling in patient outcome for these and other tumour types.

The application of senescence scoring is a useful tool for assessing senescence signaling in general, as well as individual senescence pathways, applicable to any gene expression microarray dataset. Application to other tumour types could significantly improve the understanding of senescence signaling in cancer and aid in the development of mechanistic studies of these pathways. This initial pilot study of latent senescence signaling in human tumours provides a first-glimpse of its potential importance in tumour biology.

6 Latent expression of senescence pathways in NCI60 cell lines highlights patterns of drug resistance or sensitivity different from that observed with apoptosis scoring

6.1 Introduction

During the development of an anti-cancer therapeutic drug much time is spent investigating the response of different cell types to drug exposure, with the ideal drug being non-toxic in normal cells and tissues and highly toxic in cancer cells. The efficacy of drugs in different cell types is a highly studied topic and many individual molecules, such as ATP-binding cassette transporters, have been attributed to drug resistance in cancer (Bachmeier et al. 2009). However, the role of larger cellular pathways on cells' responses to drug exposure is still unclear.

The majority of drugs aim to remove the tumour by specifically inducing apoptosis in the cancer cells. This is usually achieved by targeting molecules whose expression is unique and critical to the cellular survival of the tumour. For example, the activation of repressed tumour suppressors such as p53 (Wang et al. 2008), repression of oncogenes' activity such as BRAF (Espinosa et al. 2007) and targeting therapies to genes uniquely expressed in immortalized cells such as hTERT (Shay et al. 2008; Bilslund et al. 2009). However, the induction of cancer cell apoptosis relies upon the ability of this pathway to be successfully activated and implemented. As tumours may have become resistant to pro-apoptotic signaling on their route to neoplasia there exists a subset of tumours that are inherently resistant to pro-apoptotic drugs. In this situation, the permanent removal from the cell cycle through the induction of cellular senescence therefore presents an attractive alternative therapeutic endpoint to apoptosis. (Braig et al. 2006; Majumder et al. 2008; Prieur et al. 2008). Indeed recent published evidence, in combination with the data presented in the previous chapter, suggests that the more traditional cancer therapies of chemo and radiotherapy actually may induce high levels of cellular senescence as well as apoptosis (Jones et al. 2005; Quick et al. 2006; Gewirtz et al. 2008). Knowing when senescence induction will be successful and which drugs to utilize may improve patient outcome. To achieve this

however an improved understanding of the interaction between senescence signaling and drug resistance is needed.

In the previous chapter, the latent expression level of individual senescence signaling pathways, utilizing an experimental scoring technique, was shown to vary between tumour types; during disease progression and in response to chemo- and radiotherapeutics. In the same chapter, the prognostic implications of expression of particular gene subsets of the secretory senescence pathway in peritoneal mesotheliomas were highlighted demonstrating that latent signaling pathways may have an influence on clinical parameters. The effect of latent expression of senescence signaling pathways on drug response in tumours is currently unknown. To this end, publicly available data was utilised to examine associations between expression levels of senescence signaling pathways and drug resistance in the NCI60 cell line panel. Furthermore, through the contrast with apoptosis score associated drug associations; senescence specific drug associations were explored.

6.2 Results

6.2.1 Senescence scoring of NCI60 cell lines shows no significant correlation between expression of secretory senescence signals and DA senescence signals

It was hypothesized that cellular response to individual drug types may be linked to the latent expression of different signaling pathways. However, before examination the relationships of different signaling pathway with response to drugs could occur, an understanding of the relationships between cell types and the signaling pathways themselves in the dataset was required. To this end, a combination of scatter plots, hierarchical clustering and Pearson correlations were generated.

To explore the expression patterns of molecules within the secretory senescence (mSS), damage associated senescence (DAS) and apoptotic signaling pathways between cell types hierarchical clustering was performed. Figure 6.1 shows dendrograms for (A) apoptosis (B) secretory senescence and (C) damage associated senescence. Examination of the clustering of the NCI60 lines by apoptosis scores revealed a potential relationship between cell type and apoptosis score that was not as clearly seen in either of the two senescence scores. Apoptosis score split the

samples into 4 main cluster groups (Figure 6.1A). Enrichment for some of the cell types in the different clusters was observed, for example the first cluster was enriched for melanoma and leukemia cell lines whereas the fourth was enriched for CNS and renal cell lines. This suggested that cell types may have specific expression patterns of particular apoptosis signaling molecules, therefore indicating differing regulation mechanisms for apoptosis signaling between cell types. The dendrograms for secretory senescence (Figure 6.1B) and damage associated senescence (Figure 6.1C) showed less clear clustering by cell type where both are initially split into two large clusters followed by further divisions into smaller clusters. Although some cell type specific clusters were observed, for example small melanoma clusters were seen in both Figure 6.1B and C, in general there was not a strong relationship between the clustering and cell type. This may suggest that underlying the senescence signaling for both of these pathways were expression patterns that are not cell type specific. Regulation mechanisms of secretory or DA senescence respectively may therefore transcend cell type, however further studies using larger cohorts would be required to conclusively prove these hypotheses.

To fully understand the relationship of a larger signaling pathway with other factors, such as drug resistance, it is necessary to look beyond the individual genes and instead use quantitative values of overall pathway signaling. To this end, the latent expression of damage associated (DA) senescence, secretory and apoptotic signaling in the NCI60 cell lines of public data was scored as per chapter 5 of this study. Table 6.1 details apoptosis genes details used for apoptosis scoring. As discussed in the previous chapter this scoring method is relatively experimental and as such may require further alterations (such as the potential addition of methods of measuring error or weighting key genes) in future studies. However, as a first look pilot study into the potential relationship between drug response and latent senescence signaling the method serves as a useful starting point.

Figure 6.2 shows the senescence scores for (A) mSS and (B) DAS and (C) apoptosis in each cell type as a scatter plot. Examination of each individual signaling type revealed that each cell type had an individual range of scores. Comparison of the baseline levels of each signaling pathway revealed similar ranges of both secretory and DA senescence signaling whereas apoptotic signaling was generally much higher in all cell types. This may be reflective of higher tolerance of apoptosis signals in

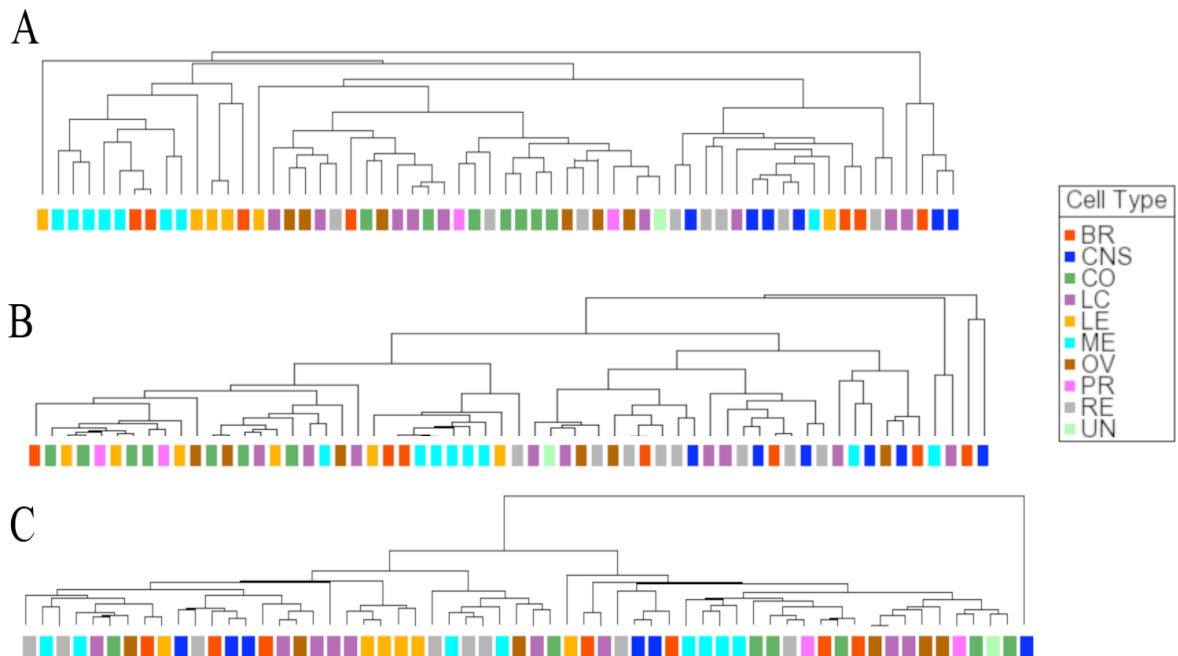


Figure 6.1 – Hierarchical clustering using secretory senescence, damage associated senescence and apoptosis pathways highlights cell type specific regulation of apoptosis. Hierarchical clustering using the genes of (A) the apoptosis pathway (see Table 6.1), (B) mSS and (C) DAS. Branches are labelled by cell type colour according to attached legend. Cell type abbreviations are as follows BR = breast, CNS = central nervous system, CO = colon, LC = lung, LE = leukaemia, ME = melanoma, OV = ovarian, PR = prostate, RE = Renal, UN = Unknown.

Gene Symbol	Direction
ABL1	Increase
APAF1	Increase
BAD	Increase
BARD1	Increase
BAX	Increase
BMF	Increase
BRCA1	Increase
CASP3	Increase
CASP9	Increase
CDC2	Increase
CDKN2A	Increase
DRAM1	Increase
E2F1	Increase
GADD45A	Increase
GADD45B	Increase
JUN	Increase
MAP2K4	Increase
MAP3K4	Increase
MAPK10	Increase
MAPK8	Increase
MAPK9	Increase
POU2F1	Increase
PRKCD	Increase
RAD9A	Increase
RAD9B	Increase
TP53	Increase
TP73	Increase
YWHAQ	Increase
BCL2	Decrease
BCL2L11	Decrease
MDM2	Decrease
SFN	Decrease

Table 6.1 – Genes and their direction of expression used in latent apoptosis scoring.

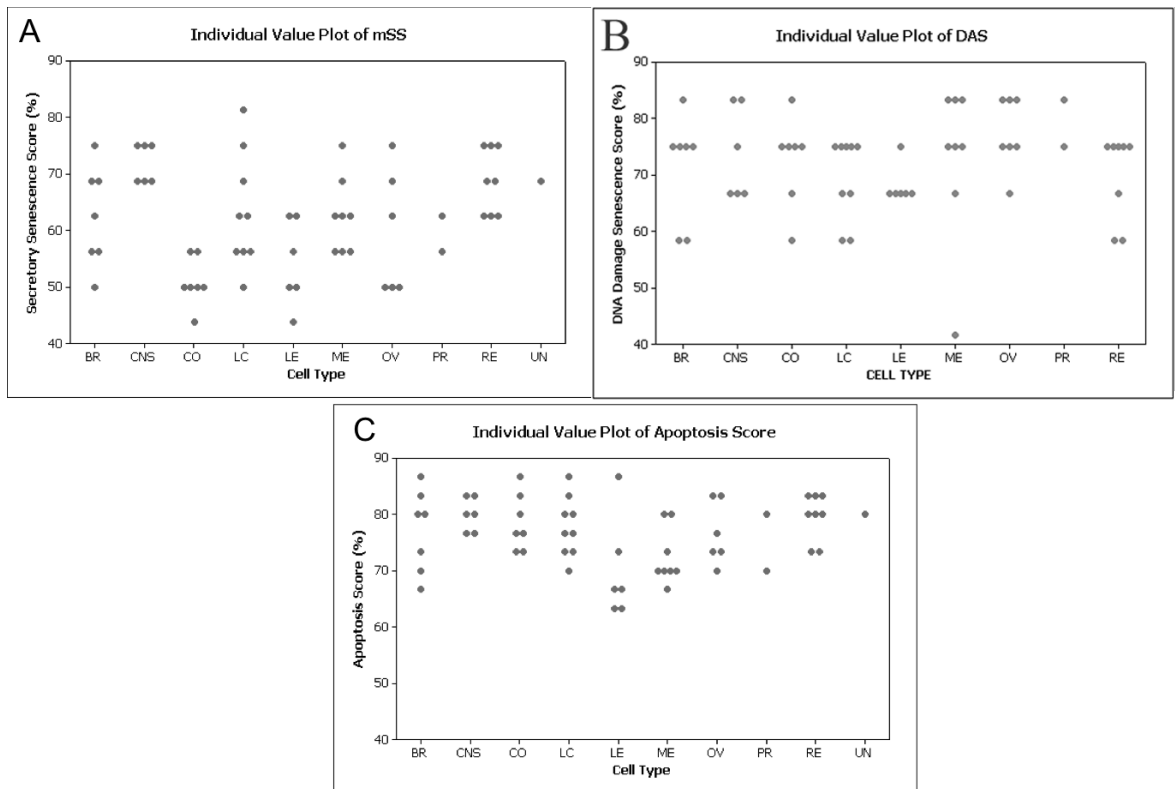


Figure 6.2 - Scatter plot of each signaling pathway highlights cell type specific expression patterns. Scatter plots of (A) mSS, (B) DAS and (C) apoptosis scores grouped by cell type. Cell type abbreviations are as follows BR = breast, CNS = central nervous system, CO = colon, LC = lung, LE = leukaemia, ME = melanoma, OV = ovarian, PR = prostate, RE = Renal, UN = Unknown.

comparison to either of the senescence signaling pathways. Further examination of the relationships between different signaling pathways in individual cell types allowed understanding of the interplay between them. For example, leukemia cell lines had a higher level of DAS signaling (median score 66.7 %) than secretory senescence (median score 53.1 %). Given that apoptosis is also a programmed response to DNA damage signaling, it may therefore be expected that these cells would also have a high level of apoptotic signaling. However, this cell type showed the lowest median levels of apoptosis signaling of 66.7 %. The data generated from this pilot study of latent senescence scoring may therefore suggest that to continue to proliferate, leukemia cells may not be able to tolerate both high levels of DA senescence and apoptosis signaling without triggering one of the two processes. The exact thresholds required to trigger apoptosis or senescence in this manner may vary from tumour to tumour do to different selection pressures induced by their cellular contexts and microenvironments. This may therefore account for the level of variability seen in these relationships.

In addition, cross comparison of the different in individual tumour types using this experimental scoring system highlighted novel signaling patterns in cell types previously unexplored.. For example, observations of higher secretory senescence than DA senescence signaling in central nervous tumour cells (CNS) and the inverse for leukemic cells (LE) had not been previously documented. Such patterns may assist in the understanding of the interaction between cell microenvironment and latent senescence signaling. For example, increased secretion of pro-inflammatory and chemotactic molecules in blood born tumours, such as leukemia, may not be conducive to tumorigenesis due to the potential for fast removal by immune cells. Those cells with high secretory senescence signaling may therefore be selected against in favor of those with low secretory senescence signaling, thus leading to a tumour cell population with low secretory senescence signaling. In contrast, solid tumours of immune privileged sites, such as the central nervous system, may not be under such pressures and expression of secretory senescence molecules may instead assist in processes such angiogenesis.

In this dataset, Melanomas (Me) had generally higher levels of DA senescence than secretory senescence, in contrast with what was observed in the melanoma dataset in chapter 5. However, this pattern of expression is the same as those observed in metastatic melanoma and may therefore suggest that these melanoma cell lines

are more biologically similar to metastatic melanoma than primary melanoma tumours. Alternatively, this may also indicate that the scoring system requires further optimisation to accurately capture latent senescence levels in cell lines as opposed to primary biopsies.

Finally, to gain an understanding of whether the latent expression of any of the combinations of signaling pathways were linked events in individual cell lines, correlations between the signatures were calculated (Table 6.2). As per the previous chapter, the senescence scores were ranked to allow directly comparable in a single cell line. Pearson correlations were then calculated for each combination of scores. No significant correlation between the secretory and DA senescence signaling pathways ($p = 0.119$) was observed, indicating that their expression was not a linked event, consistent with the findings of the previous chapter of this study. This may also suggest that the latent expression of these senescence signaling pathways are under independent selection pressures and/or are regulated differently. Significant correlations between the senescence scores and apoptosis pathways were however observed (mSS $p = < 0.001$, DAS $p = 0.029$). These observations suggest that the latent expression of either senescence pathway may potentially trigger an apoptosis response or vice versa. Alternatively, due to the low strength of the correlations (0.439 for mSS and 0.283 for DAS), this may more reflect the ability of a cell to tolerate both mSS/DAS and apoptotic latent signaling rather than a cause and effect relationship.

The assessment of patterns of latent senescence score in cells grown in culture using this experimental scoring technique may be affected by small variances between experimental conditions when cells are cultured by different groups. To investigate the effect, if any, these variances had on the latent expression patterns of secretory senescence; DA senescence and apoptotic signaling, two of the NCI60 cell lines were assayed in house (DU145 and HT29). The scoring of the gene expression data for GSE5846 showed that both of these cell lines had higher levels of secretory senescence (mSS) than DA senescence and the in house microarray data reflected this pattern (Figure 6.3). In both cases apoptosis signaling was found to be at lower relative levels than that observed in the public data however, these levels remained above those of secretory senescence. These differences may have been due potential experimental factors that differ between this analysis and that of the original dataset, such as age and confluence of cell cultures upon extraction

	mSS	Apoptosis	DAS
mSS	1		
Apoptosis	0.439 (p=< 0.001)	1	
DAS	0.203 (p = 0.119)	0.283 (p = 0.029)	1

Table 6.2 - Correlations between the three latent signaling pathway scores. Correlation is shown with p value beneath in brackets

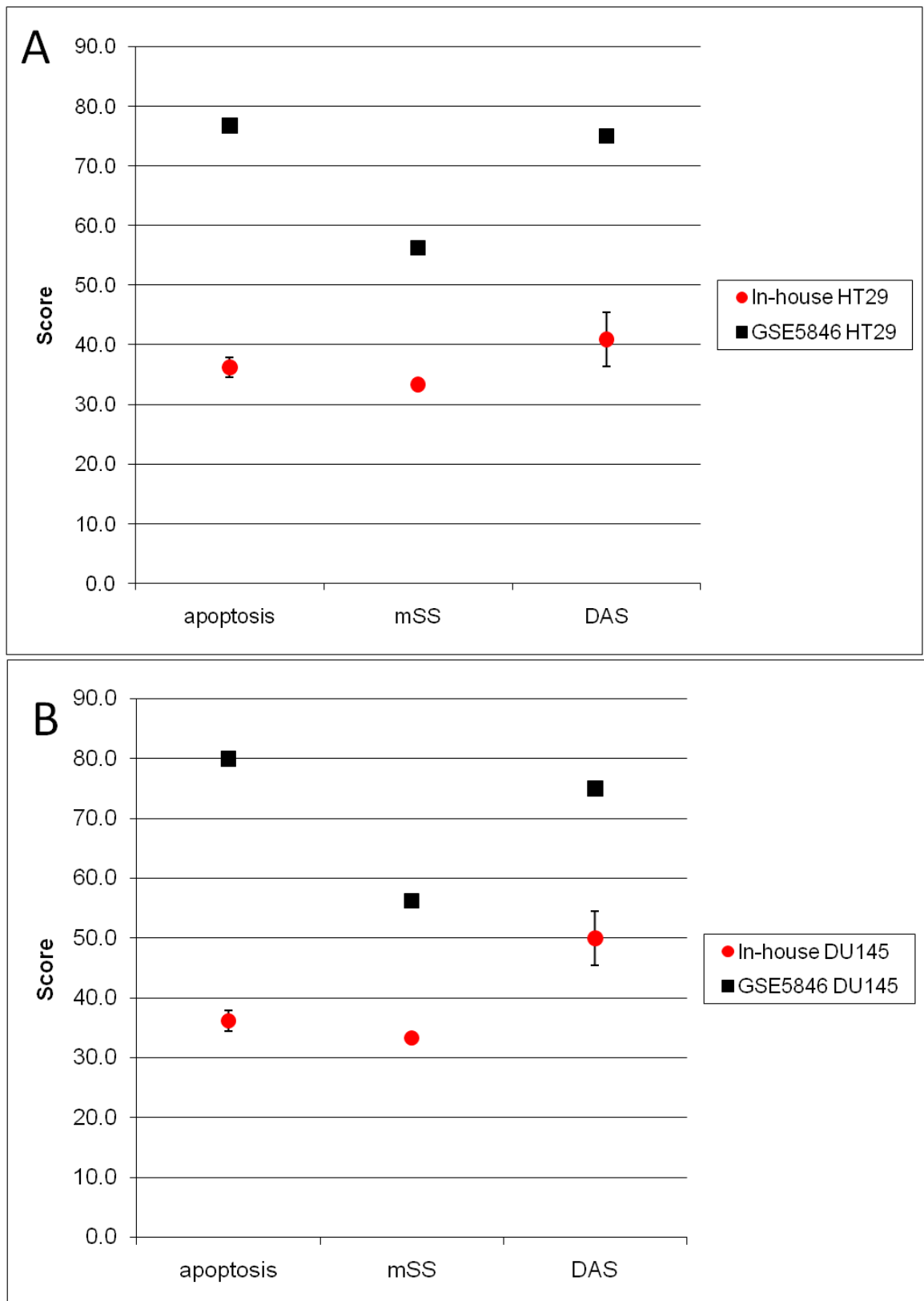


Figure 6.3 - In-house gene expression microarrays and public data of (A) HT29 and (B) DU145 cell lines and latent senescence scoring shows similar patterns of latent expression of senescence pathways. In-house arrays were performed in duplicate and the median value of the two scores is shown with the error bars depicted maximum and minimum values. As GSE5846 data was not performed in duplicate no error bars are available for this data.

or growth medium variations. This data may therefore suggest that to directly compare datasets from different experimental sets some normalization of the actual scores by method such as the ranking may be required. However, as the general patterns of latent senescence signaling remained the same between the two datasets, it was concluded that patterns of latent senescence signaling were not strongly affected by the cell culture variations between sites.

Overall, the combination of the hierarchical clustering and experimental senescence scoring analyses were potentially suggestive of a situation whereby apoptosis signaling was regulated in a cell type specific manner whereas senescence scoring, for either secretory or DA senescence, was reflective of common molecular changes that transcend cell type. Furthermore, the data from this initial study suggested that secretory and DA senescence may be distinct signaling events in the NCI60 cell line panel. However, a combination of a single latent senescence and apoptotic latent signaling may be tolerable by cells and neither is enough to induce full apoptosis nor senescence activation. The dynamic nature of the expression and interplay between these latent signaling pathways suggested that although not fully active these pathways were still regulated. These observations therefore suggested that latent signaling pathways may potentially have an impact on other biological/clinical parameters, such as cellular responses to drugs.

6.2.2 Virtual compound screen identifies differing drug activity resistances linked to damage associated, secretory senescence and apoptosis pathways.

It was therefore hypothesized that the latent signaling levels of secretory senescence, DA senescence and apoptosis pathways may have the ability to affect the efficacy of compounds to induce growth inhibition in tumour cells. Examination of a potential cause-and-effect relationship between secretory senescence, DA senescence, apoptosis scores and the concentration of compounds required to give a 50 % growth inhibition (GI_{50}) through regression analysis was undertaken. 71, 250 and 61 compounds with unique significant relationships (regression $p < 0.05$) between growth inhibition and DA senescence, secretory senescence and apoptosis respectively were identified. A further 3 compounds overlapped between all three

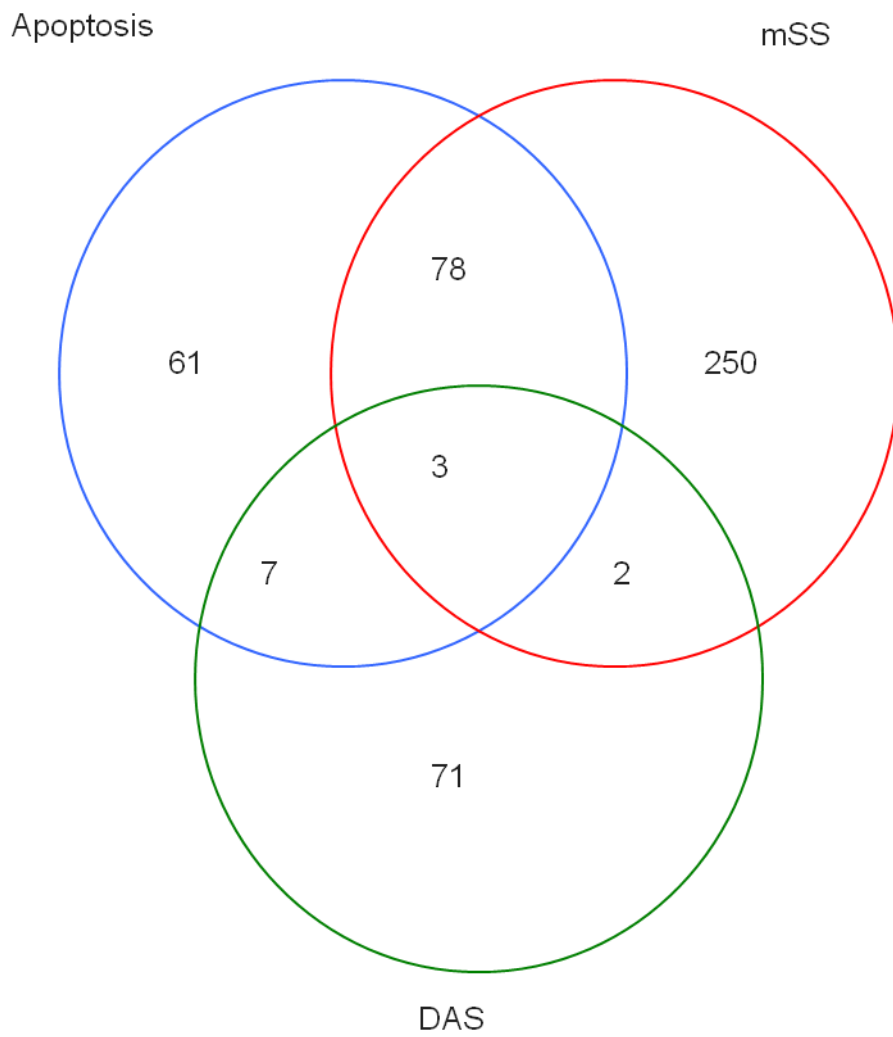


Figure 6.4 - Venn Diagram of compounds with significant regressions for each latent signaling pathway. Compounds with a regression p value of < 0.05 and latent signaling levels of apoptosis (blue), mSS (red) and DAS (green).

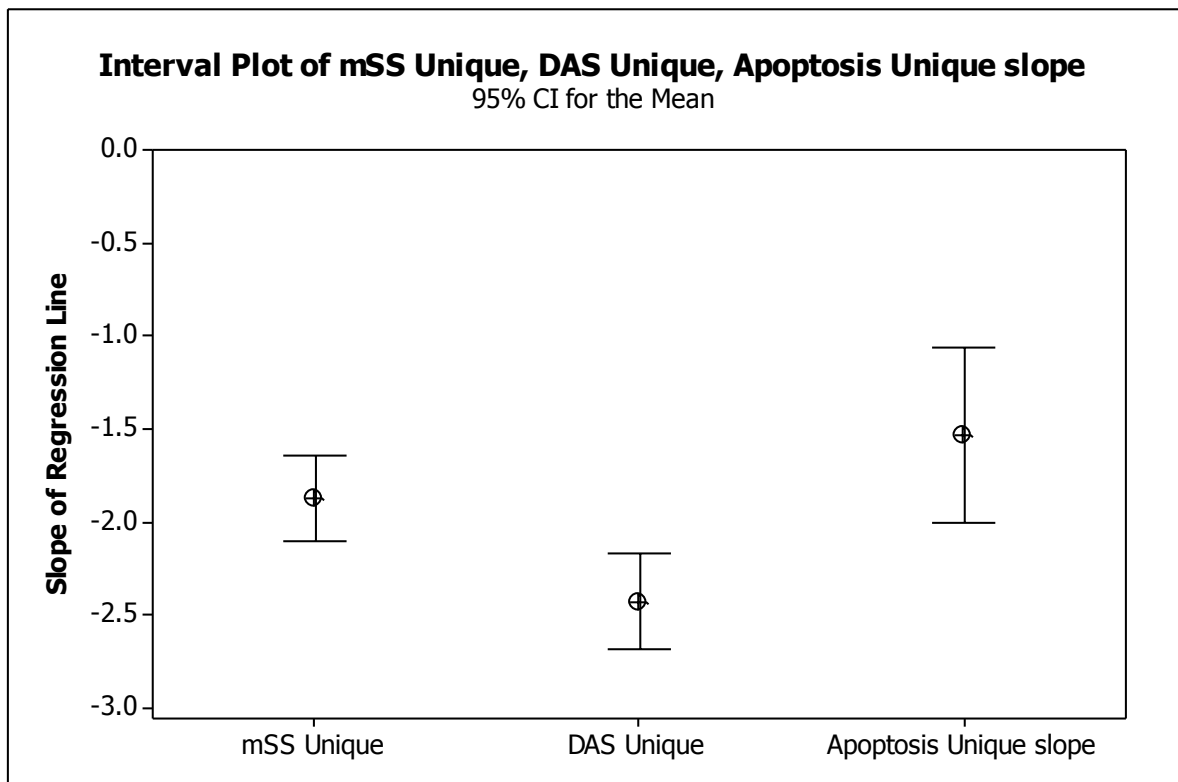


Figure 6.5 - Interval plot of slope of the lines for unique compound regressions. The mean slope of the line for the compounds with unique associations with each pathway is plotted with their 95% confidence intervals. The negative slope of the line for all three scores shows that with increasing score for each of these pathways cell lines become increasingly sensitive to the compounds.

scores (Figure 6.4). To understand whether the different latent signaling pathways were generally causing resistance or sensitivity for different compounds the average direction of the slope of the line was explored (Figure 6.5). This analysis revealed that all three pathways generally identified unique drugs to which cell lines were sensitive shown by the negative values for the slope of the line. This therefore suggests that the latent expression levels of these pathways may potentially have a significant impact on the response to therapy by particular drugs in patients. This analysis is reliant on the experiment scoring procedure presented in chapter 5 and therefore is presented as a proof-of-concept demonstration that the scores of latent signaling pathway can be applied to experimental data to discover potential drugs to which patients may be sensitive. Further laboratory validation of these scores and their relationships with drug sensitivities is required before they could be applied in the clinic. However, as a first exploration of such relationships this virtual screen provides an interesting starting point.

6.2.3 Investigation of predicted activities of significant compounds reveals drug class associations linked with each signaling pathway.

Examination of the predicted molecular targets and activities of the significant compounds for each signaling pathway may improve current understanding of the key molecular types that each latent signaling pathway were targeting uniquely. After further validation, such knowledge may help to tailor the particular drug to use when a particular therapy (such as kinase inhibition) has been suggested. To this end, activity modeling of the original compounds used in the screen using graph-theory connectivity indices to build a decision tree model was performed. The model showed 7 predicted activities of the compounds within the screen GPCR agonist inhibition, GPCR antagonist inhibition, kinase inhibition, protease inhibition, PDE inhibition, ligand-gated ion channel inhibition, nuclear hormone receptor inhibition. The distribution of unique hits to each senescence signaling pathway, as well as those significant for apoptosis, were then graphed as a proportion of the total number of compounds in each list normalized to the total proportion of the original list that each drug class represented. This allowed an analysis of the differential effects of each scoring pathway without the

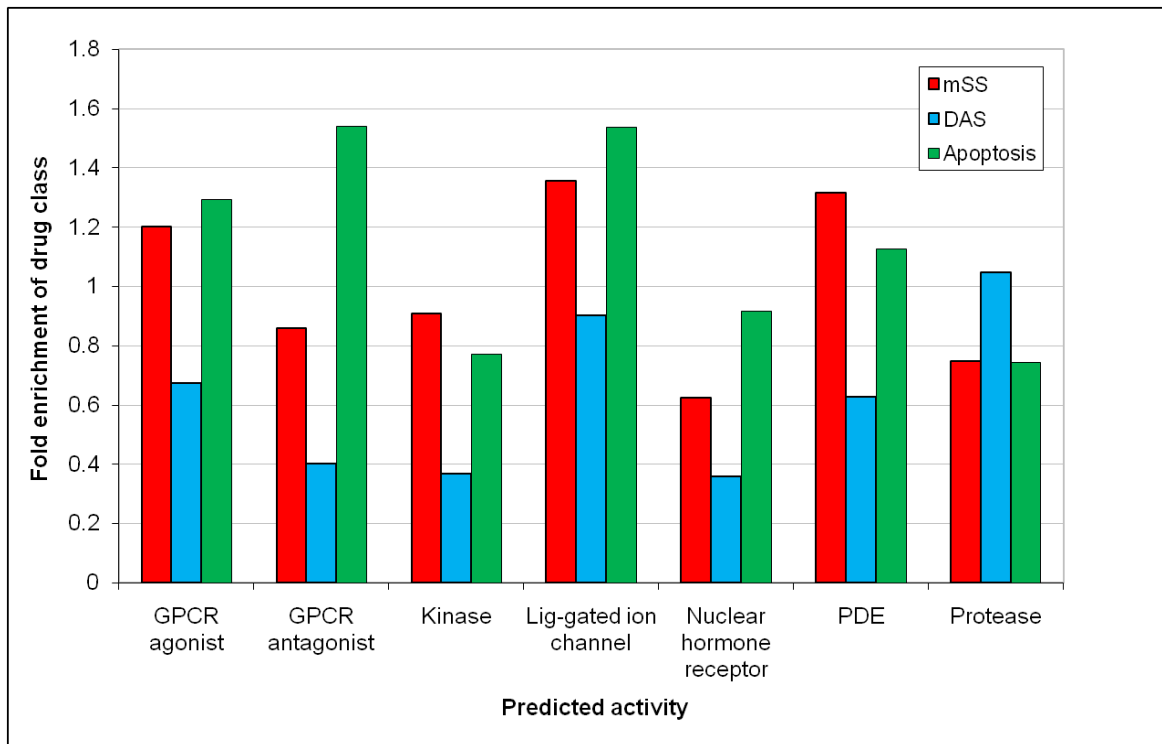


Figure 6.6 - Predicted Activities of compounds significantly associated with latent signaling pathways. Graph-theory connectivity indices were used to create a decision tree model by which compounds were mapped to predicted biological activities. The fold enrichments of predicted activities for the unique compounds for mSS (red), DAS (blue) and apoptosis (green) were normalised to the size of each list and the proportion of drug class present in the entire screen.

confounding of the information with unequal list sizes or proportions of predicted drug activities in the original drug screen for each drug class.

In this plot (Figure 6.6) protease inhibitors were observed to be the only category to have the greatest proportion of significant regressions in DA senescence. Given that the caspase signaling cascade is associated with the activation of apoptosis rather than senescence it is interesting that the latent DA senescence score should identify more protease inhibition sensitivities than apoptosis scoring.

This may be suggestive of a situation whereby cells with a high level of DNA damage signaling (as observed by the high DA senescence scores) have blocked apoptotic effector cascades. The direct inhibition of these pathways may be sufficient to alter the cellular response and trigger the induction of an alternative growth arrest mechanism, such as senescence. Given the experimental nature of the scoring system further validation of such concepts would be required before being able to apply these observations clinically. Further investigation into the exact targets and molecular mechanisms behind this trend are not possible from bioinformatic analysis of this data but may warrant future experimental investigation.

This analysis also revealed that cells with high secretory senescence scoring had a particular enrichment for sensitivity to compounds with predicted activities as kinases and PDE inhibitors. The sensitivity of these cells to PDE inhibition may reflect the requirement for the inhibition of signaling processes mediated by cAMP or cGMP, which PDEs enzymatically degrade, to prevent the full activation of the senescence program.

These relationships between senescence signaling pathways and drug activity in this pilot study therefore suggested that although senescence has been bypassed, expression of latent senescence signaling pathways may still have the potential to cause distinct biological effects.

The cross comparison of senescence signaling and apoptosis signaling data resulted in the observation of a contrast in the predicted drug activity enrichments. For example, cells with high apoptosis score appeared to be particularly enriched for sensitivity to growth inhibition by compounds with predicted activities as ligand-gated ion channel inhibitors, nuclear hormone receptor inhibitors and GPCR antagonist inhibitors, where both senescence signaling pathways show lower

relative levels of association. This suggested that cells showing high apoptosis scores were more sensitive to growth inhibition by these particular mechanisms than cells with high levels of either of the senescence pathways.

6.3 Discussion

Upon treatment with a drug different cell types respond with varying degrees of growth inhibition. The activities of individual molecule types have been previously attributed to drug resistance (Bachmeier et al. 2009) however the impact of larger signaling pathways on drug resistance has not been fully assessed. As the data in the previous chapter highlighted potential differential expression patterns of latent damage associated (DA) and secretory senescence signaling in human tumours, it was decided to examine whether latent senescence signaling could be a factor affecting response to drug treatment, utilizing the experimental latent senescence scoring procedure developed in chapter 5 of this study. Furthermore, the results of these two senescence signaling pathways were then compared with that of apoptosis to try and identify whether these latent signaling pathways could potentially affect response to treatment differently.

Initially the expression levels of secretory senescence, DA senescence and apoptotic signaling pathways themselves and their relationships between cell types were examined. Hierarchical clustering of apoptosis signaling molecules showed some grouping of the cell lines by cell type (Figure 6.1A). This suggested that these expression patterns may be a result of cell type specific regulatory mechanisms. Conversely, hierarchical clustering of both secretory and damage associated senescence signaling molecules showed little clustering by cell type. These observations therefore suggested that the regulatory mechanisms behind latent senescence signaling were potentially common between cell types and not cell type specific. Through the application of the tentative pathway scoring system introduced in chapter 5, the overall levels of latent signaling of each pathway were also examined in each of the 60 cell lines. By examining scatter-plots and correlations between the scores the relationships between the latent signaling pathways were further examined (Figure 6.2 and Table 6.2). Differential expression patterns of secretory and DA senescence utilizing the experimental scoring system in melanomas suggested that these melanoma cell cultures may be more similar in nature to metastatic melanoma than primary melanoma. In addition, further

differential expression patterns not previously observed were also highlighted in this dataset, such as higher levels of damage associated senescence signaling than secretory senescence in leukemia cells. These patterns of differential expression in these signaling pathways may be reflective of differential selection pressures in these cells during tumorigenesis. For example, blood born leukemia cells with high levels of secretory senescence may be selected against due to increased immune activation. A significant correlation between both senescence scores and apoptosis score were observed. As both DA senescence and apoptosis signaling contains an element of DNA damage response it is conceivable that the latent expression of the two pathways could be linked events. Induction of secretory senescence in response to damage associated senescence signaling has also previously been observed (Rodier et al. 2009) and this may account for the correlation of apoptosis and secretory senescence pathways. Alternatively, these observations may also reflect the ability of cells to tolerate different types of latent signaling pathways at the same time. High levels of both senescence pathways and apoptosis signaling may be sufficient to trigger a full apoptotic or senescence response. The additive effects of these pathways may therefore act as a selection mechanism for cells undergoing tumorigenesis. In support of this concept, the cells in which the highest levels of DA senescence were observed, leukemia cells, also had the lowest levels of latent apoptosis signaling. As this scoring technique is the first of its kind to attempt to quantify the latent expression of a pathway in human cells the conclusions drawn from this initial study remain hypothetical and will require further validation.

Next regression analysis was used explore drugs with a cause-and-effect relationship between score and the drug concentration required to induce a 50 % growth inhibition in each cell line. 71, 250 and 61 compounds with significant relationships (regression $p < 0.05$) between growth inhibition and DA senescence, secretory senescence and apoptosis respectively were identified (Figure 6.4). As these compounds showed significance to only one pathway, treatment of tumours could potentially be directed by knowledge of only one pathway score without the requirement for measurement of the other two. However, the fact that these drugs were significant for a particular latent signaling pathway alone would not be sufficient to direct treatment. A measure of drug resistance or sensitivity is required to determine whether a particular drug should be used or avoided. To assess this the slope of the line of regression in each case was examined, whereby

a negative slope would indicate that with increasing latent signaling score, less drug was required to induce 50% growth inhibition i.e. cell lines became increasingly sensitive with increasing latent signaling score. Upon plotting the mean and 95% confidence intervals of the slope of the line for each set of unique significant regressions it was observed that cells with a high score for any of the pathways were generally resistant to their significant compounds (Figure 6.5). These results were validated in part by the unique identification of sensitivity to compounds known to induce apoptosis through the use of apoptosis score, such as bruceantin (CID295929, slope of line = -2.24, $p = 0.0288$) (Cuendet et al. 2004). This pilot study therefore suggested that the virtual drug screening technique may indeed be capable of highlighting drug sensitivity linked with the activities of specific pathways. Such knowledge may aid in the ability to target drugs to induce specific cellular states, such as high latent apoptosis or cellular senescence signaling.

Investigation of the relationship between latent signaling pathways and drug resistance may be of use in targeted drug therapy; however, it does not improve in the understanding of the molecular mechanisms behind drug resistance. To this end, the predicted activities of the significantly associated compounds were explored. Through the use of graph-theory connectivity indices a decision tree model of predicted activities was built. By examining the predicted activities associated with each latent signaling type it was hoped that insights into the potential molecular mechanisms behind the associations could be gained (Figure 6.6). This analysis revealed enrichment for resistance to growth inhibition by proteases in cell lines with high latent DA senescence scores. Given the central role of caspases in initiation of apoptosis (Riedl & Shi, 2004), it was somewhat surprising that it was DA senescence signaling rather than apoptosis signaling that was most enriched in this category. However, this may be indicative of a potential situation whereby direct inhibition of the apoptotic mechanisms under a background of high DNA damage signaling is sufficient to alter the cellular response and trigger senescence. This may therefore suggest that tumours with a high DA senescence score that are resistant to treatment by pro-apoptotic therapies may be better treated through inhibition of proteases directly. As these conclusions are drawn from an experimental and novel technique further laboratory investigation will be required which is unfortunately beyond the scope of this first look bioinformatic study.

Further potential molecular mechanisms were also highlighted through the enrichment of PDE inhibitors in compounds with significant regressions with secretory senescence. PDEs enzymatically degrade cAMP and cGMP (Bender and Beavo 2006). The observation of sensitivity to growth inhibition through the inhibition of PDE inhibitors in cells with high secretory senescence was suggestive of the requirement for deregulation of signaling through these molecules, to prevent the induction of the senescence program. This was consistent with previous reports in melanomas. Melanomas that acquire RAS mutations require deregulated cAMP metabolism, potentially by increased phosphodiesterase activity, for transformation (Dumaz et al. 2006). Furthermore, cAMP is well reported to play a central role in the regulation of the expression of pro-inflammatory and immune responses (Peters-Golden 2009) Given the known pro-inflammatory nature of secretory senescence signaling it is possible to hypothesise that latent secretory senescence signaling and cAMP metabolism disruption in melanoma may be connected. The inhibition of PDEs may therefore alter the regulation of cAMP in these pro-inflammatory pathways leading to reestablishment of the correct cAMP metabolism balance, senescence induction and growth inhibition.

Further contrasting effects of latent signaling pathways were highlighted by the observation that drugs significantly correlated with apoptosis were particularly enriched for predicted activities not enriched in either of the senescence pathways (Figure 6.6 blue bars). For example, sensitivity to growth inhibition via the inhibition of GPCR antagonists was almost highly enriched in latent apoptotic signaling compared to the other latent scores. G-protein coupled receptors (GPCRs) act as central nodes in the transduction of many different extracellular signals and are a highly explored target in drug discovery (Vassilatis et al. 2003). GPCR antagonists therefore block the signal transduction of these extracellular signals. Sensitivity to growth inhibition by inhibition of these molecules may suggest that these cells are utilizing GPCR antagonists to block extracellular signals that may lead to full induction of the apoptotic program. Furthermore, significant correlations between latent apoptosis signaling and latent secretory senescence signaling were observed. These extracellular signals may therefore potentially be in the form of pro-inflammatory signals produced by the cell itself.

In conclusion, this initial examination of relationship between latent senescence and apoptosis signaling to growth inhibition by 1401 different compounds

highlighted the potential impact of these latent signaling patterns on response to drug treatment. This tentative data suggests that cells' route to senescence bypass and the resulting latent expression of senescence signaling pathways may confer sensitivity to induction of growth arrest through particular drug targeting mechanisms. For example, protease inhibition in tumours with high DA senescence scores or dependence on cAMP mediated signals in cells with high secretory senescence scores. Comparison of these findings with the results of the same process using apoptosis signaling showed distinct drug class sensitivities in each class. This therefore suggests that the measurement of latent signaling pathways in patient samples may facilitate improved selection of appropriate compounds to which the tumour would be more sensitive. Furthermore, the impact of latent senescence signaling can be seen to extend to response to specific drug types; thus further highlighting its importance in human cancer.

7 Summary and Conclusions

Before senescence induction can be fully utilised as a realistic anti-cancer therapy there is a requirement for a better understanding of the pathways surrounding senescence signaling. The main aims of this study were to ascertain an improved understanding as to the layers of regulation that surround senescence signaling and bypass and their impact on in human tumours. The results presented here improve the current level of understanding and highlight the importance of senescence signaling and regulation during tumorigenesis. This study has highlighted transcriptional differences in senescence bypass mechanisms, the potential of miRNAs as regulators of senescence and the impact of latent senescence signaling upon patient outcome and response to therapy.

7.1 Transcriptional regulation of senescence bypass

Through the use of gene expression microarrays 1305 genes were found to have differential expression patterns between cells utilizing either ALT or telomerase for bypass of replicative senescence. This study was the first to attempt to characterise the expression differences between the two mechanisms in an attempt to gain a better understanding of the regulation behind choosing and maintaining a particular telomere maintenance mechanism. The observation of similar expression patterns of the 1305 gene signature in ALT cells and human mesenchymal stem cells may explain the preponderance of mesenchymal ALT tumours *in vivo* and points to a potential mesenchymal origin for ALT. This was the first and, to date, only study to have documented a direct link between gene expression patterns in ALT cells and mesenchymal stem cells. To test the applicability of the 1305 gene signature *in vivo*, hierarchical clustering of liposarcoma biopsy gene expression data was utilized and by combining overlapping gene expression profiles found within the 1305 gene signature, a refined 297 sub-signature was generated. Functional investigation of this signature revealed a complex hTERT regulatory network that extended our current knowledge of the strict regulatory mechanisms surrounding telomerase expression in ALT cells. Furthermore, the observation of significant differences in expression of a large number of downstream targets of the transcription factor c-Myc within the 297 gene signature led to further investigation of the

role of c-Myc in senescence bypass by different TMMs. As c-Myc is a well-known transcriptional activator of hTERT, upon direct experimental investigation the findings of lower c-Myc activity and reduced c-Myc binding at the hTERT promoter in ALT cell lines was unsurprising. However, upon further investigation as to the mechanism behind the decreased expression of c-Myc in ALT cells this project highlighted that c-Myc regulation difference in ALT were not primarily caused by differences in expression of c-Myc itself nor either of its DNA binding partners MAX and MAD. Instead, the competitive binding of the DNA E-boxes by the relatively understudied gene TCEAL7 was highlighted as one of the potential mechanisms by which ALT cells regulate c-Myc activity. Furthermore, probing of the kinome through siRNA screening revealed 106 hTERT regulatory kinases in ALT cells, of which the top transcriptional regulator was c-Myc.

The data presented in Chapter 3 therefore extends current knowledge of the molecular differences between senescence bypass mechanisms. In addition, further functional investigations of these regulatory networks highlighted a central role for c-Myc in the regulation of both telomerase expression and the larger regulatory network surrounding telomerase regulation. It is unlikely that perturbation of a single molecule within this complex regulatory network would be sufficient to induce senescence. However, detailed knowledge of such regulatory networks may improve the ability to develop adjuvant therapeutics to further reinforce therapeutic approaches targeted at cells utilizing telomerase.

7.2 miRNAs as regulators of senescence signaling

Chapter 3 highlighted the complex gene expression and kinase regulatory networks surrounding the decision between telomere maintenance mechanisms. The establishment of such large complex networks during the bypass of senescence would require multiple levels of regulation and miRNAs represent a relatively simple mechanism by which this could be achieved. Given the knowledge that each miRNA has many targets, each with on average 1000 target genes, it would be possible to establish such networks through the actions of a relatively small number of miRNAs. The role of miRNAs in the regulation of senescence signaling is currently poorly understood. Therefore, before their potential for perturbation during the process senescence bypass could be established their overall potential in senescence signaling regulation was

assessed. To this end, a literature search revealed 12 miRNAs with experimental evidence of involvement in senescence regulation. The potential of these senescence associated miRNAs (SA-miRNAs) to regulate the multiple pathway changes required to create the senescent cell phenotype was then assessed through functional enrichment analysis on their theoretical target genes. The analysis showed significant enrichment for pathways involving cytoskeletal remodeling, cell-cycle and proliferation, thus demonstrating the potential of the SA-miRNAs to not only regulate the cell-cycle arrest but also the morphological changes in cell size and shape required for the formation of the senescent phenotype. Furthermore, the SA-miRNAs were shown to be able to regulate significant pathways for senescence regardless of the senescence stimulus through regulation of apoptosis signaling, pro-inflammatory and cell cycle processes. The observation of potential apoptosis signaling and pro-inflammatory signaling regulation potential highlights the potential of miRNAs to operate at the pathway level, regulating both the damage associated and secretory senescence pathways regardless of the type of senescence stimulation received. Having demonstrated the potential for miRNAs to regulate senescence signaling pathways, miRNA microarrays on mesenchymal tumours were then utilised to examine their potential in regulating the decision between telomere maintenance mechanisms during senescence bypass. 25, 14 and 9 miRNAs which were significantly differentially expressed between telomere maintenance mechanisms in liposarcomas, peritoneal mesotheliomas and MPNST respectively. Furthermore, examination of miRNA expression in relation to patient outcome also revealed groups of miRNAs with prognostic significance in each tumour type. Overlaps between the prognostic and TMM associated miRNAs further highlighted the potential prognostic significance and implications of TMM in these tumour types consistent with the current literature (Costa et al. 2006; Cairney et al. 2008).

When combined, the data presented in Chapter 4 therefore demonstrate the importance of miRNAs as potential regulators of senescence induction as well as their potential implications during tumorigenesis. Furthermore, as miRNA regulation is a post-transcriptional process, senescence pathways may remain latently expressed after transformation, thus removing the requirement to transcriptionally regulate every gene involved in the senescence individually during senescence bypass.

7.3 Scoring of Latent senescence signaling

The data showing the potential regulation of senescence by miRNAs in the previous chapter presented the possibility of latent expression of genes involved in senescence signaling pathways after senescence bypass. Such expression has been observed in animal models, however, has not been previously explored in human tumours. Furthermore, the impact of such latent expression upon clinical factors, such as disease progression and patient outcome, has not previously been established.

However, before this could be ascertained there was a requirement to develop a method by which the latent expression levels of these pathways could be measured quantitatively. To this end, an experimental scoring approach was developed which reduced the latent expression levels of the senescence signaling to a single percentage. Furthermore, the method also allowed the dissection of the latent expression levels of individual senescence pathways in any gene expression dataset. After development, the method was first applied to a number of publicly available datasets whereby senescence induction would be expected to occur. The scoring system confirmed increased senescence scoring in response to both chemo- and radiotherapeutics in human tumours. Furthermore, dissection of the secretory and damage associated pathways highlighted induction of both senescence signaling pathways to varying degrees after both treatments. The experimental scoring system also highlighted dynamic expression patterns of the two signaling pathways during disease progression in melanoma. High levels of damage associated senescence signaling appears to be more associated with metastatic tumours whereas increased secretory senescence signaling was observed in primary lesions. This suggests that although unable to induce the senescence program these pathways are still actively regulated and may potentially have an impact on tumour progression. Finally, the scoring system was applied to human mesenchymal stem cells undergoing replicative senescence through repeated passage. As well as a general increase in overall senescence score with increasing passage, a transient spike in damage associated senescence was observed at passage 6, immediately followed by a spike in secretory senescence signaling at passage 7. Such timed

differential expression patterns are consistent with concept that secretory senescence is induced upon prolonged damage associated signaling (Rodier et al. 2009) and therefore potentially demonstrate the ability of the scoring method to correctly characterize signaling dynamics during senescence induction. It must be noted however that as this is an initial pilot study and the first method of its kind to quantify the latent activities of an entire pathway further validation of the results are required. The method itself is inherently flexible and future studies may choose to alter the gene content and direction of expression required for the signatures or introduce further statistical tests of error or weighting.

Having validated the scoring approach in multiple cell types the method was utilised to explore latent senescence signaling in the mesenchymal tumour dataset. Dynamic latent expression patterns of the secretory and damage associated senescence pathways were observed in the mesenchymal tumours consistent with their potentially different routes to tumour progression. Examination of correlations between these scores in individual tumours however highlighted that the two pathways are potentially distinct events in all three tumour types. Further examination of the secretory senescence pathway in these tumours was undertaken using hierarchical clustering. The resulting dendrograms highlighted subgroups of peritoneal mesotheliomas with distinct patterns of latent expression of 2 gene groups of the secretory senescence pathway. Furthermore, these groups showed significant correlation with survival. Upon investigation as to the functional differences in the responsible gene groups it was discovered that tumours expressing the pro-inflammatory, chemotactic and anti-proliferative aspects of the secretory senescence pathway showed improved survival, consistent with similar observations in the literature (Roxburgh et al. 2009).

The results presented in this chapter firstly highlight the potential of the developed senescence scoring method to explore latent signaling in any gene expression dataset. To date, this is the first method presented to quantitatively estimate latent senescence signaling in human tumours and as such, after further validation may facilitate further investigations in other tumour and tissue types. Application of the method highlighted the potential prognostic implications of latent senescence signaling and therefore suggests that further

investigation is warranted. The data presented in this chapter suggests that although the senescence program has been bypassed during the process of tumorigenesis the latent expression of its signaling pathways may still have the potential to influence cellular responses.

7.4 The implications of latent senescence signaling in cellular drug response

A first look at the potential biological effects of latent senescence signaling in human tumours had been explored in the previous chapter. Different cell types respond to drug treatments in different ways. Whether latent senescence signaling levels play a role in these differential responses had not been previously explored. Through the combined exploration of publicly available gene expression data and GI_{50} data for 1401 drugs in the NCI60 cell lines, a virtual drug screen was performed exploring the relationship between these experimental latent senescence score and response to particular drugs. Furthermore, application of the same novel scoring methodology using an apoptosis signature allowed exploration of the relationships between the latent expression of the two pathways as well as their common and distinct drug associations.

Initial exploration of the relationships between the cell types and latent expression of the senescence and apoptosis signaling pathways using hierarchical clustering highlighted potentially tissue type specific mechanisms of latent apoptosis regulation not observed in latent senescence signaling. Furthermore, exploration of signaling dynamics of these pathways within cell types confirmed similar signaling dynamics in melanoma cell lines as those observed in the metastatic melanoma biopsies in the previous chapter. The significant correlation of the apoptosis score with both the senescence signaling pathways at the individual cell line level was also observed. This may reflect the linkage of the two latent signaling pathways to apoptosis signaling. However, given that the correlation was relatively weak it is more likely that this in fact represents an ability to tolerate both signal types simultaneously rather than direct linkage. However, the lack of significant correlations between the senescence pathways

in this dataset supports the observations of the previous chapter that these are unlinked distinct signaling events.

To examine the relationships between latent expression of senescence pathways and apoptosis, linear regression was used to find drugs with significant cause-and-effect relationships with individual drugs. 71, 250 and 61 compounds with unique significant relationships (regression $p < 0.05$) between growth inhibition and DA senescence, secretory senescence and apoptosis respectively were identified. Furthermore, examination of the direction of the regressions showed that associated scores generally identified drugs to which cell lines were sensitive rather than resistant. The identification of these individual drugs uniquely with their respective latent signaling scores further highlights the potential differing biological effects of the two senescence pathways, even after senescence bypass. Analysis of the predicted activities of the significant compounds also highlighted differences between the impacts of each latent signaling pathway. Cells with a high damage associated senescence score show particular sensitivity to protease inhibitors whereas cells with high secretory senescence are particularly sensitive to PDE inhibitors. The ability to distinguish particular drugs to which tumours are sensitive from a single experiment would be invaluable to the clinical community. As with the previous chapter the results and conclusions built on this experimental scoring technique would require further validation before they could be applied clinically. However, the data presented in chapter 6 suggests that even after bypass, senescence signaling may remain an important factor in cancer cell biology.

8 References

- Acosta, J. C., A. O'Loughlen, A. Banito, M. V. Guijarro, A. Augert, S. Raguz, M. Fumagalli, M. Da Costa, C. Brown, N. Popov, Y. Takatsu, J. Melamed, F. d'Adda di Fagagna, D. Bernard, E. Hernando and J. Gil (2008). "Chemokine signaling via the CXCR2 receptor reinforces senescence." Cell **133**(6): 1006-18.
- Agarwal, M. L., A. Agarwal, W. R. Taylor and G. R. Stark (1995). "p53 controls both the G2/M and the G1 cell cycle checkpoints and mediates reversible growth arrest in human fibroblasts." Proc Natl Acad Sci U S A **92**(18): 8493-7.
- Ahn, S., M. Olive, S. Aggarwal, D. Krylov, D. D. Ginty and C. Vinson (1998). "A dominant-negative inhibitor of CREB reveals that it is a general mediator of stimulus-dependent transcription of c-fos." Molecular and Cellular Biology **18**(2): 967-977.
- Alimonti, A., C. Nardella, Z. Chen, J. G. Clohessy, A. Carracedo, L. C. Trotman, K. Cheng, S. Varmeh, S. C. Kozma, G. Thomas, E. Rosivatz, R. Woscholski, F. Cognetti, H. I. Scher and P. P. Pandolfi (2010). "A novel type of cellular senescence that can be enhanced in mouse models and human tumor xenografts to suppress prostate tumorigenesis." J Clin Invest **120**(3): 681-93.
- Amati, B., M. W. Brooks, N. Levy, T. D. Littlewood, G. I. Evan and H. Land (1993). "Oncogenic activity of the c-Myc protein requires dimerization with Max." Cell **72**(2): 233-45.
- Armanios, M., J. L. Chen, Y. P. Chang, R. A. Brodsky, A. Hawkins, C. A. Griffin, J. R. Eshleman, A. R. Cohen, A. Chakravarti, A. Hamosh and C. W. Greider (2005). "Haploinsufficiency of telomerase reverse transcriptase leads to anticipation in autosomal dominant dyskeratosis congenita." Proc Natl Acad Sci U S A **102**(44): 15960-4.
- Artandi, S. E. and R. A. DePinho (2006). "Telomeres and telomerase in cancer." Carcinogenesis **31**(1): 9-18.
- Atadja, P., H. Wong, I. Garkavtsev, C. Veillette and K. Riabowol (1995). "Increased activity of p53 in senescing fibroblasts." Proc Natl Acad Sci U S A **92**(18): 8348-52.
- Atkinson, S. P., S. F. Hoare, R. M. Glasspool and W. N. Keith (2005). "Lack of telomerase gene expression in alternative lengthening of telomere cells is associated with chromatin remodeling of the hTR and hTERT gene promoters." Cancer Research **65**(17): 7585-7590.
- Atkinson, S. P., S. F. Hoare, R. M. Glasspool and W. N. Keith (2005). "Lack of telomerase gene expression in alternative lengthening of telomere cells is associated with chromatin remodeling of the hTR and hTERT gene promoters." Cancer Res **65**(17): 7585-90.
- Atkinson, S. P. and W. N. Keith (2007). "Epigenetic control of cellular senescence in disease: opportunities for therapeutic intervention." Expert Rev Mol Med **9**(7): 1-26.
- Ayer, D. E., L. Kretzner and R. N. Eisenman (1993). "Mad: a heterodimeric partner for Max that antagonizes Myc transcriptional activity." Cell **72**(2): 211-22.
- Bachmeier, B. E., C. M. Iancu, P. H. Killian, E. Kronschi, V. Mirisola, G. Angelini, M. Jochum, A. G. Nerlich and U. Pfeffer (2009). "Overexpression of the

- ATP binding cassette gene ABCA1 determines resistance to Curcumin in M14 melanoma cells." Mol Cancer **8**: 129.
- Bair, E. and R. Tibshirani (2004). "Semi-Supervised Methods to Predict Patient Survival from Gene Expression Data." PLoS Biol **2**(4): e108.
- Baker, D.J., C. Perez-Terzic, F. Jin, K. Pitel, N.J. Niederlander K. Jeganathan, S. Yamada, S. Reyes, L. Rowe, H.J. Hiddinga, N.L. Eberhardt, A. Terzic and J.M. van Deursen. (2008) "Opposing roles for p16Ink4a and p19Arf in senescence and ageing caused by BubR1 insufficiency." Nat Cell Biol. **10**(7):825-36.
- Banumathy, G., N. Somaiah, R. Zhang, Y. Tang, J. Hoffmann, M. Andrade, H. Ceulemans, D. Schultz, R. Marmorstein and P. D. Adams (2009). "Human UBN1 is an ortholog of yeast Hpc2p and has an essential role in the HIRA/ASF1a chromatin-remodeling pathway in senescent cells." Mol Cell Biol **29**(3): 758-70.
- Bartel, D. P. (2005). "MicroRNAs and their regulatory roles in plants and animals." Developmental Biology **283**(2): 575-575.
- Bazarov, A. V., W. C. Hines, R. Mukhopadhyay, A. Beliveau, S. Melodyev, Y. Zaslavsky and P. Yaswen (2009). "Telomerase activation by c-Myc in human mammary epithelial cells requires additional genomic changes." Cell Cycle **8**(20).
- Bechter, O. E., Y. Zou, J. W. Shay and W. E. Wright (2003). "Homologous recombination in human telomerase-positive and ALT cells occurs with the same frequency." Embo Reports **4**(12): 1138-1143.
- Bell, S. P. and A. Dutta (2002). "DNA replication in eukaryotic cells." Annual Review of Biochemistry **71**: 333-374.
- Belot, N., R. Pochet, C. W. Heizmann, R. Kiss and C. Decaestecker (2002). "Extracellular S100A4 stimulates the migration rate of astrocytic tumor cells by modifying the organization of their actin cytoskeleton." Biochimica Et Biophysica Acta-Proteins and Proteomics **1600**(1-2): 74-83.
- Bennett, D. C. (2008). "How to make a melanoma: what do we know of the primary clonal events?" Pigment Cell Melanoma Res **21**(1): 27-38.
- Benson, F. E., P. Baumann and S. C. West (1998). "Synergistic actions of Rad51 and Rad52 in recombination and DNA repair." Nature **391**(6665): 401-404.
- Bernardo, M. E., N. Zaffaroni, F. Novara, A. M. Cometa, M. A. Avanzini, A. Moretta, D. Montagna, R. Maccario, R. Villa, M. G. Daidone, O. Zuffardi and F. Locatelli (2007). "Human bone marrow derived mesenchymal stem cells do not undergo transformation after long-term in vitro culture and do not exhibit telomere maintenance mechanisms." Cancer Res **67**(19): 9142-9.
- Berube, N. G., J. R. Smith and O. M. Pereira-Smith (1998). "The genetics of cellular senescence." American Journal of Human Genetics **62**(5): 1015-1019.
- Bilsland, A. E., S. Hoare, K. Stevenson, J. Plumb, N. Gomez-Roman, C. Cairney, S. Burns, K. Lafferty-Whyte, J. Roffey, T. Hammonds and W. N. Keith (2009). "Dynamic telomerase gene suppression via network effects of GSK3 inhibition." PLoS One **4**(7): e6459.
- Bitomsky, N. and T. G. Hofmann (2009). "Apoptosis and autophagy: Regulation of apoptosis by DNA damage signaling - roles of p53, p73 and HIPK2." FEBS J **276**(21): 6074-83.
- Bollag G., P. Hirth, J. Tsai, J. Zhang, P. N. Ibrahim, H. Cho, W. Spevak, C. Zhang, Y. Zhang, G. Habets, E.A. Burton, B. Wong, G. Tsang, B. L. West, B. Powell, R. Shellooe, A. Marimuthu, H. Nguyen, K.Y.J. Zhang, D. R. Artis,

- J. Schlessinger, F. Su, B. Higgins, R. Lyer, K. D'Andrea, A. Koehler, M. Stumm, P.S. Lin, R. J. Lee, J. Grippo, I. Puzanov, K. B. Kim, A. Ribas, G. A. McArthur, J.A. Sosman, P.B. Chapman, K.T. Flaherty, X. Xu, K.L. Nathanson and K. Nolop. (2010) "Clinical efficacy of a RAFinhibitor needs broad target." Nature 467: 596-599.
- blockade in BRAF-mutant melanoma"
- Bommer, G. T., I. Gerin, Y. Feng, A. J. Kaczorowski, R. Kuick, R. E. Love, Y. Zhai, T. J. Giordano, Z. S. Qin, B. B. Moore, O. A. MacDougald, K. R. Cho and E. R. Fearon (2007). "p53-mediated activation of miRNA34 candidate tumor-suppressor genes." Current Biology 17(15): 1298-1307.
- Borcuk, A. C., R. N. Taub, M. Hesdorffer, H. Hibshoosh, J. A. Chabot, M. L. Keohan, R. Alsberry, D. Alexis and C. A. Powell (2005). "P16 loss and mitotic activity predict poor survival in patients with peritoneal malignant mesothelioma." Clin Cancer Res 11(9): 3303-8.
- Braig, M. and C. A. Schmitt (2006). "Oncogene-induced senescence: putting the brakes on tumor development." Cancer Res 66(6): 2881-4.
- Bu, X., C. Le, F. Jia, X. Guo, L. Zhang, B. Zhang, M. Wu and L. Wei (2008). "Synergistic effect of mTOR inhibitor rapamycin and fluorouracil in inducing apoptosis and cell senescence in hepatocarcinoma cells." Cancer Biol Ther 7(3): 392-6.
- Busacca, S., S. Germano, L. De Cecco, M. Rinaldi, F. Comoglio, F. Favero, B. Murer, L. Mutti, M. Pierotti and G. Gaudino (2009). "MicroRNA Signature of Malignant Mesothelioma with Potential Diagnostic and Prognostic Implications." Am J Respir Cell Mol Biol.
- Cairney, C. J., S. F. Hoare, M. G. Daidone, N. Zaffaroni and W. N. Keith (2008). "High level of telomerase RNA gene expression is associated with chromatin modification, the ALT phenotype and poor prognosis in liposarcoma." Br J Cancer 98(8): 1467-74.
- Cairney, C. J. and W. N. Keith (2008). "Telomerase redefined: integrated regulation of hTR and hTERT for telomere maintenance and telomerase activity." Biochimie 90(1): 13-23.
- Calado, R. T., J. A. Regal, M. Hills, W. T. Yewdell, L. F. Dalmazzo, M. A. Zago, P. M. Lansdorp, D. Hogge, S. J. Chanock, E. H. Estey, R. P. Falcao and N. S. Young (2009). "Constitutional hypomorphic telomerase mutations in patients with acute myeloid leukemia." Proc Natl Acad Sci U S A 106(4): 1187-92.
- Campisi, J. (2005) "Senescent Cells, Tumor Suppression, and organismal aging: Good citizens, bad Neighbors." Cell, 120: 513-522.
- Campisi, J. and F. d'Adda di Fagagna (2007). "Cellular senescence: when bad things happen to good cells." Nat Rev Mol Cell Biol 8(9): 729-40.
- Cazzalini, O., A. I. Scovassi, M. Savio, L. A. Stivala and E. Prosperi (2010). "Multiple roles of the cell cycle inhibitor p21(CDKN1A) in the DNA damage response." Mutat Res Epub In Press.
- Cesare A.J.,and R.R. Reddel (2010). "Alternative lengthening of telomere: models, mechanisms and implications." Nat. Rev. Gen., 11(5) 319-330
- Chakravarthy, M. V., T. W. Abraha, R. J. Schwartz, M. L. Fiorotto and F. W. Booth (2000). "Insulin-like growth factor-I extends in vitro replicative life span of skeletal muscle satellite cells by enhancing G1/S cell cycle progression via the activation of phosphatidylinositol 3'-kinase/Akt signaling pathway." J Biol Chem 275(46): 35942-52.
- Chang, C. J., D. J. Mulholland, B. Valamehr, S. Mosessian, W. R. Sellers and H. Wu (2008). "PTEN nuclear localization is regulated by oxidative stress and mediates p53-dependent tumor suppression." Mol Cell Biol 28(10): 3281-9.

- Chang, J. T., Y. C. Lu, Y. J. Chen, C. P. Tseng, Y. L. Chen, C. W. Fang and A. J. Cheng (2006). "hTERT phosphorylation by PKC is essential for telomerase holoprotein integrity and enzyme activity in head neck cancer cells." Br J Cancer **94**(6): 870-8.
- Chang, S., C. M. Khoo, M. L. Naylor, R. S. Maser and R. A. DePinho (2003). "Telomere-based crisis: functional differences between telomerase activation and ALT in tumor progression." Genes & Development **17**(1): 88-100.
- Chang, T. C., E. A. Wentzel, O. A. Kent, K. Ramachandran, M. Mullendore, K. H. Lee, G. Feldmann, M. Yamakuchi, M. Ferlito, C. J. Lowenstein, D. E. Arking, M. A. Beer, A. Maitra and J. T. Mendell (2007). "Transactivation of miR-34a by p53 broadly influences gene expression and promotes apoptosis." Molecular Cell **26**(5): 745-752.
- Chen, Z., L. C. Trotman, D. Shaffer, H. K. Lin, Z. A. Dotan, M. Niki, J. A. Koutcher, H. I. Scher, T. Ludwig, W. Gerald, C. Cordon-Cardo and P. P. Pandolfi (2005). "Crucial role of p53-dependent cellular senescence in suppression of Pten-deficient tumorigenesis." Nature **436**(7051): 725-30.
- Chien, J., K. Narita, R. Rattan, S. Giri, R. Shridhar, J. Staub, D. Belefrod, J. Lai, L. R. Roberts, J. Molina, S. H. Kaufmann, G. C. Prendergast and V. Shridhar (2008). "A role for candidate tumor-suppressor gene TCEAL7 in the regulation of c-Myc activity, cyclin D1 levels and cellular transformation." Oncogene **27**(58): 7223-34.
- Chien, J., J. Staub, R. Avula, H. Zhang, W. Liu, L. C. Hartmann, S. H. Kaufmann, D. I. Smith and V. Shridhar (2005). "Epigenetic silencing of TCEAL7 (Bex4) in ovarian cancer." Oncogene **24**(32): 5089-100.
- Cohen, S. B., M. E. Graham, G. O. Lovrecz, N. Bache, P. J. Robinson and R. R. Reddel (2007). "Protein composition of catalytically active human telomerase from immortal cells." Science **315**(5820): 1850-3.
- Colgin, L. M., C. Wilkinson, A. Englezou, A. Kilian, M. O. Robinson and R. R. Reddel (2000). "The hTERTalpha splice variant is a dominant negative inhibitor of telomerase activity." Neoplasia **2**(5): 426-32.
- Collado, M., J. Gil, A. Efeyan, C. Guerra, A. J. Schuhmacher, M. Barradas, A. Benguria, A. Zaballos, J. M. Flores, M. Barbacid, D. Beach and M. Serrano (2005). "Tumour biology: senescence in premalignant tumours." Nature **436**(7051): 642.
- Compton, S. A., J. H. Choi, A. J. Cesare, S. Ozgur and J. D. Griffith (2007). "Xrcc3 and Nbs1 are required for the production of extrachromosomal telomeric circles in human alternative lengthening of telomere cells." Cancer Research **67**(4): 1513-1519.
- Coppe, J. P., C. K. Patil, F. Rodier, A. Krtolica, C. M. Beausejour, S. Parrinello, J. G. Hodgson, K. Chin, P. Y. Desprez and J. Campisi (2010). "A human-like senescence-associated secretory phenotype is conserved in mouse cells dependent on physiological oxygen." PLoS One **5**(2): e9188.
- Coppe, J. P., C. K. Patil, F. Rodier, Y. Sun, D. P. Munoz, J. Goldstein, P. S. Nelson, P. Y. Desprez and J. Campisi (2008). "Senescence-associated secretory phenotypes reveal cell-nonautonomous functions of oncogenic RAS and the p53 tumor suppressor." PLoS Biol **6**(12): 2853-68.
- Costa, A., M. G. Daidone, L. Daprai, R. Villa, S. Cantu, S. Pilotti, L. Mariani, A. Gronchi, J. D. Henson, R. R. Reddel and N. Zaffaroni (2006). "Telomere maintenance mechanisms in liposarcomas: Association with histologic subtypes and disease progression." Cancer Research **66**(17): 8918-8924.
- Costa, A., M. G. Daidone, L. Daprai, R. Villa, S. Cantu, S. Pilotti, L. Mariani, A. Gronchi, J. D. Henson, R. R. Reddel and N. Zaffaroni (2006). "Telomere

- maintenance mechanisms in liposarcomas: association with histologic subtypes and disease progression." Cancer Res **66**(17): 8918-24.
- Cotter, M. A., S. R. Florell, S. A. Leachman and D. Grossman (2007). "Absence of senescence-associated beta-galactosidase activity in human melanocytic nevi in vivo." J Invest Dermatol **127**(10): 2469-71.
- Counter, C. M., J. Gupta, C. B. Harley, B. Leber and S. Bacchetti (1995). "Telomerase activity in normal leukocytes and in hematologic malignancies." Blood **85**(9): 2315-20.
- Courtois-Cox, S., S. M. Genter Williams, E. E. Reczek, B. W. Johnson, L. T. McGillicuddy, C. M. Johannessen, P. E. Hollstein, M. MacCollin and K. Cichowski (2006). "A negative feedback signaling network underlies oncogene-induced senescence." Cancer Cell **10**(6): 459-72.
- Cuendet, M., K. Christov, D. D. Lantvit, Y. Deng, S. Hedayat, L. Helson, J. D. McChesney and J. M. Pezzuto (2004). "Multiple myeloma regression mediated by bruceantin." Clin Cancer Res **10**(3): 1170-9.
- d'Adda di Fagagna, F., P. M. Reaper, L. Clay-Farrace, H. Fiegler, P. Carr, T. Von Zglinicki, G. Saretzki, N. P. Carter and S. P. Jackson (2003). "A DNA damage checkpoint response in telomere-initiated senescence." Nature **426**(6963): 194-8.
- Dahm, K. and U. Hubscher (2002). "Colocalization of human Rad17 and PCNA in late S phase of the cell cycle upon replication block." Oncogene **21**(50): 7710-9.
- Damm, K., U. Hemmann, P. Garin-Chesa, N. Hael, I. Kauffmann, H. Priepke, C. Niestroj, C. Daiber, B. Enenkel, B. Guilliard, I. Lauritsch, E. Muller, E. Pascolo, G. Sauter, M. Pantic, U. M. Martens, C. Wenz, J. Lingner, N. Kraut, W. J. Rettig and A. Schnapp (2001). "A highly selective telomerase inhibitor limiting human cancer cell proliferation." Embo J **20**(24): 6958-68.
- Daugherty, K. M. and B. L. Goode (2008). "Functional surfaces on the p35/ARPC2 subunit of Arp2/3 complex required for cell growth, actin nucleation, and endocytosis." Journal of Biological Chemistry **283**(24): 16950-16959.
- Degerman S., J.K. Siwicki, P. Osterman, K. Lafferty-Whyte, W.N. Keith and G.Roos. (2010) "Telomerase upregulation is a postcrisis event during senescence bypass and immortalization of two Nijmegen breakage syndrome T cell cultures." Aging Cell **9**(2):220-35.
- de la Fuente, J. and I. Dokal (2007) "Dyskeratosis congenita: Advances in the understanding of the telomerase defect and the role of stem cell transplantation." Pediatr Transplantation **11**:584-594.
- de Lange, T. (2005). "Shelterin: the protein complex that shapes and safeguards human telomeres." Genes Dev **19**(18): 2100-10
- de Lange, T. (2009). "How telomeres solve the end-protection problem." Science **326**(5955): 948-52.
- Debacq-Chainiaux, F., C. Borlon, T. Pascal, V. Royer, F. Eliaers, N. Ninane, G. Carrard, B. Friguet, F. de Longueville, S. Boffe, J. Remacle and O. Toussaint (2005). "Repeated exposure of human skin fibroblasts to UVB at subcytotoxic level triggers premature senescence through the TGF-beta1 signaling pathway." J Cell Sci **118**(Pt 4): 743-58.
- Deng, C., P. Zhang, J. W. Harper, S. J. Elledge and P. Leder (1995). "Mice lacking p21CIP1/WAF1 undergo normal development, but are defective in G1 checkpoint control." Cell **82**(4): 675-84.
- Deng, Y. B., S. S. Chan and S. Chang (2008). "Telomere dysfunction and tumour suppression: the senescence connection." Nature Reviews Cancer **8**(6): 450-458.

- Desdouets, C., G. Matesic, C. A. Molina, N. S. Foulkes, P. Sassonecorsi, C. Brechot and J. Sobczakthepot (1995). "Cell-Cycle Regulation of Cyclin-a Gene-Expression by the Cyclic Amp-Responsive Transcription Factors Creb and Crem." Molecular and Cellular Biology **15**(6): 3301-3309.
- di Fagagna, F. D., P. M. Reaper, L. Clay-Farrace, H. Fiegler, P. Carr, T. von Zglinicki, G. Saretzki, N. P. Carter and S. P. Jackson (2003). "A DNA damage checkpoint response in telomere-initiated senescence." Nature **426**(6963): 194-198.
- Dimri, G. P. (2005). "What has senescence got to do with cancer?" Cancer Cell **7**(6): 505-12.
- Downward, J. (2003). "Targeting RAS signaling pathways in cancer therapy." Nat Rev Cancer **3**(1): 11-22.
- Dulic, V., G. E. Beney, G. Frebourg, L. F. Drullinger and G. H. Stein (2000). "Uncoupling between phenotypic senescence and cell cycle arrest in aging p21-deficient fibroblasts." Mol Cell Biol **20**(18): 6741-54.
- Dumaz, N., R. Hayward, J. Martin, L. Ogilvie, D. Hedley, J. A. Curtin, B. C. Bastian, C. Springer and R. Marais (2006). "In melanoma, RAS mutations are accompanied by switching signaling from BRAF to CRAF and disrupted cyclic AMP signaling." Cancer Res **66**(19): 9483-91.
- Dumont, P., F. Chainiaux, F. Eliaers, C. Petropoulou, J. Remacle, C. Koch-Brandt, E. S. Gonos and O. Toussaint (2002). "Overexpression of apolipoprotein J in human fibroblasts protects against cytotoxicity and premature senescence induced by ethanol and tert-butylhydroperoxide." Cell Stress Chaperones **7**(1): 23-35.
- Dunham, M. A., A. A. Neumann, C. L. Fasching and R. R. Reddel (2000). "Telomere maintenance by recombination in human cells." Nature Genetics **26**(4): 447-450.
- Dunham, M. A., A. A. Neumann, C. L. Fasching and R. R. Reddel (2000). "Telomere maintenance by recombination in human cells." Nat Genet **26**(4): 447-50.
- Engels, B. M. and G. Hutvagner (2006). "Principles and effects of microRNA-mediated post-transcriptional gene regulation." Oncogene **25**(46): 6163-6169.
- Espinosa, A. V., L. Porchia and M. D. Ringel (2007). "Targeting BRAF in thyroid cancer." Br J Cancer **96**(1): 16-20.
- Fajkus, J. Ā., E. SĀ½korovĀ; and A. R. Leitch (2005). "Telomeres in evolution and evolution of telomeres." Chromosome Research **13**(5): 469-479.
- Fasching, C. L., K. Bower and R. R. Reddel (2005). "Telomerase-Independent Telomere Length Maintenance in the Absence of Alternative Lengthening of Telomeres-Associated Promyelocytic Leukemia Bodies 10.1158/0008-5472.CAN-04-2881." Cancer Res **65**(7): 2722-2729.
- Fevr, T., S. Robine, D. Louvard and J. Huelsken (2007). "Wnt/beta-catenin is essential for intestinal homeostasis and maintenance of intestinal stem cells." Mol Cell Biol **27**(21): 7551-9.
- Fontana, L., M. E. Fiori, S. Albini, L. Cifaldi, S. Giovinnazzi, M. Forloni, R. Boldrini, A. Donfrancesco, V. Federici, P. Giacomini, C. Peschle and D. Fruci (2008). "Antagomir-17-5p abolishes the growth of therapy-resistant neuroblastoma through p21 and BIM." PLoS ONE **3**(5): e2236.
- Fridman, A. L. and M. A. Tainsky (2008). "Critical pathways in cellular senescence and immortalization revealed by gene expression profiling." Oncogene **27**(46): 5975-87.
- Friedman, S.L. (2008). "Mechanisms of Hepatic Fibrogenesis." Gastroenterology. **134**(6): 1655-1669.

- Frippiat, C., Q. M. Chen, S. Zdanov, J. P. Magalhaes, J. Remacle and O. Toussaint (2001). "Subcytotoxic H₂O₂ stress triggers a release of transforming growth factor-beta 1, which induces biomarkers of cellular senescence of human diploid fibroblasts." J Biol Chem **276**(4): 2531-7.
- Frippiat, C., Q. M. Chen, S. Zdanov, J. P. Magalhaes, J. Remacle and O. Toussaint (2001). "Subcytotoxic H₂O₂ stress triggers a release of transforming growth factor-beta 1, which induces biomarkers of cellular senescence of human diploid fibroblasts." Journal of Biological Chemistry **276**(4): 2531-7.
- Gewirtz, D. A., S. E. Holt and L. W. Elmore (2008). "Accelerated senescence: an emerging role in tumor cell response to chemotherapy and radiation." Biochem Pharmacol **76**(8): 947-57.
- Gibbs, C. P., V. G. Kukekov, J. D. Reith, O. Tchigrinova, O. N. Suslov, E. W. Scott, S. C. Ghivizzani, T. N. Ignatova and D. A. Steindler (2005). "Stem-like cells in bone sarcomas: implications for tumorigenesis." Neoplasia **7**(11): 967-76.
- Griffiths-Jones, S. (2004). "The microRNA Registry." Nucleic Acids Res **32**(Database issue): D109-11.
- Griffiths-Jones, S., R. J. Grocock, S. van Dongen, A. Bateman and A. J. Enright (2006). "miRBase: microRNA sequences, targets and gene nomenclature." Nucleic Acids Res **34**(Database issue): D140-4.
- Griffiths-Jones, S., H. K. Saini, S. van Dongen and A. J. Enright (2008). "miRBase: tools for microRNA genomics." Nucleic Acids Res **36**(Database issue): D154-8.
- Gu, C., A. Castellino, J. Y. Chan and M. V. Chao (1998). "BRE: a modulator of TNF-alpha action." Faseb J **12**(12): 1101-8.
- Guled, M., L. Lahti, P. M. Lindholm, K. Salmenkivi, I. Bagwan, A. G. Nicholson and S. Knuutila (2009). "CDKN2A, NF2, and JUN are dysregulated among other genes by miRNAs in malignant mesothelioma - A miRNA microarray analysis." Genes, Chromosomes and Cancer **48**(7): 615-623.
- Hao, H., Y. Nancai, F. Lei, W. Xiong, S. Wen, H. Guofu, W. Yanxia, H. Hanju, L. Qian and X. Hong (2008). "siRNA directed against c-Myc inhibits proliferation and downregulates human telomerase reverse transcriptase in human colon cancer Colo 320 cells." J Exp Clin Cancer Res **27**: 27.
- Harbour, J. W. and D. C. Dean (2000). "Rb function in cell-cycle regulation and apoptosis." Nat Cell Biol **2**(4): E65-7.
- Hardy, K., L. Mansfield, A. Mackay, S. Benvenuti, S. Ismail, P. Arora, M. J. O'Hare and P. S. Jat (2005). "Transcriptional networks and cellular senescence in human mammary fibroblasts." Mol Biol Cell **16**(2): 943-53.
- Harfe, B. D. (2005). "MicroRNAs in vertebrate development." Current Opinion in Genetics & Development **15**(4): 410-415.
- Harley, C. B., A. B. Futcher and C. W. Greider (1990). "Telomeres Shorten during Aging of Human Fibroblasts." Nature **345**(6274): 458-460.
- Hartig, J. S. and E. T. Kool (2004). "Small circular DNAs for synthesis of the human telomere repeat: varied sizes, structures and telomere-encoding activities
10.1093/nar/gnh149." Nucl. Acids Res. **32**(19): e152-.
- He, L., X. Y. He, L. P. Lim, E. De Stanchina, Z. Y. Xuan, Y. Liang, W. Xue, L. Zender, J. Magnus, D. Ridzon, A. L. Jackson, P. S. Linsley, C. F. Chen, S. W. Lowe, M. A. Cleary and G. J. Hannon (2007). "A microRNA component of the p53 tumour suppressor network." Nature **447**(7148): 1130-U16.
- Henson, J. D., J. A. Hannay, S. W. McCarthy, J. A. Royds, T. R. Yeager, R. A. Robinson, S. B. Wharton, D. A. Jellinek, S. M. Arbuckle, J. Yoo, B. G.

- Robinson, D. L. Learoyd, P. D. Stalley, S. F. Bonar, D. Yu, R. E. Pollock and R. R. Reddel (2005). "A robust assay for alternative lengthening of telomeres in tumors shows the significance of alternative lengthening of telomeres in sarcomas and astrocytomas." Clin Cancer Res **11**(1): 217-25.
- Henson, J. D., J. A. Hannay, S. W. McCarthy, J. A. Royds, T. R. Yeager, R. A. Robinson, S. B. Wharton, D. A. Jellinek, S. M. Arbuckle, J. Y. Yoo, B. G. Robinson, D. L. Learoyd, P. D. Stalley, S. F. Bonar, D. H. Yu, R. E. Pollock and R. R. Reddel (2005). "A robust assay for alternative lengthening of telomeres in tumors shows the significance of alternative lengthening of telomeres in sarcomas and astrocytomas." Clinical Cancer Research **11**(1): 217-225.
- Henson, J. D., A. A. Neumann, T. R. Yeager and R. R. Reddel (2002). "Alternative lengthening of telomeres in mammalian cells." Oncogene **21**(4): 598-610.
- Herbig, U., M. Ferreira, L. Condell, D. Carey, and J.M. Sedivy (2006). "Cellular senescence in aging primates. *Science* **311**: 1257
- Herold, S., B. Herkert and M. Eilers (2009). "Facilitating replication under stress: an oncogenic function of MYC?" Nat Rev Cancer **9**(6): 441-4.
- Hills, M. and P. M. Lansdorp (2009). "Short telomeres resulting from heritable mutations in the telomerase reverse transcriptase gene predispose for a variety of malignancies." Ann N Y Acad Sci **1176**: 178-90.
- Hinkal, G. W., C. E. Gatz, N. Parikh and L. A. Donehower (2009). "Altered senescence, apoptosis, and DNA damage response in a mutant p53 model of accelerated aging." Mech Ageing Dev **130**(4): 262-71.
- Hoare, S. F., L. A. Bryce, G. B. A. Wisman, S. Burns, J. J. Goings, A. G. J. van der Zee and W. N. Keith (2001). "Lack of Telomerase RNA Gene hTERT Expression in Alternative Lengthening of Telomeres Cells Is Associated with Methylation of the hTERT Promoter." Cancer Res **61**(1): 27-32.
- Hong, E. H., S. J. Lee, J. S. Kim, K. H. Lee, H. D. Um, J. H. Kim, S. J. Kim, J. I. Kim and S. G. Hwang (2009). "Ionizing radiation induces cellular senescence of articular chondrocytes via negative regulation of SIRT1 by p38 kinase." J Biol Chem **285**(2): 1283-95.
- Hu, H. M., A. Zielinska-Kwiatkowska, K. Munro, J. Wilcox, D. Y. Wu, L. Yang and H. A. Chansky (2008). "EWS/FLI1 suppresses retinoblastoma protein function and senescence in Ewing's sarcoma cells." J Orthop Res **26**(6): 886-93.
- Huang, P. R., S. T. Tsai, K. H. Hsieh and T. C. Wang (2008). "Heterogeneous nuclear ribonucleoprotein A3 binds single-stranded telomeric DNA and inhibits telomerase extension in vitro." Biochim Biophys Acta **1783**(2): 193-202.
- Irmeler, M., M. Thome, M. Hahne, P. Schneider, K. Hofmann, V. Steiner, J. L. Bodmer, M. Schroter, K. Burns, C. Mattmann, D. Rimoldi, L. E. French and J. Tschopp (1997). "Inhibition of death receptor signals by cellular FLIP." Nature **388**(6638): 190-5.
- Ishenmann, S., D. Cakouros, A. Zannettino, S. Shi and S. Gronthos (2007). "hTERT transcription is repressed by Cbfa1 in human mesenchymal stem cell populations." J Bone Miner Res **22**(6): 897-906.
- Itahana, K., Y. Zou, Y. Itahana, J. L. Martinez, C. Beausejour, J. J. Jacobs, M. Van Lohuizen, V. Band, J. Campisi and G. P. Dimri (2003). "Control of the replicative life span of human fibroblasts by p16 and the polycomb protein Bmi-1." Mol Cell Biol **23**(1): 389-401.
- Jacobs, J. J. and T. de Lange (2004). "Significant role for p16INK4a in p53-independent telomere-directed senescence." Curr Biol **14**(24): 2302-8.

- Jacobs, J. J. and T. de Lange (2005). "p16INK4a as a second effector of the telomere damage pathway." Cell Cycle 4(10): 1364-8.
- Jarrard, D. F., S. Sarkar, Y. Shi, T. R. Yeager, G. Magrane, H. Kinoshita, N. Nassif, L. Meisner, M. A. Newton, F. M. Waldman and C. A. Reznikoff (1999). "p16/pRb pathway alterations are required for bypassing senescence in human prostate epithelial cells." Cancer Res 59(12): 2957-64.
- Jeruss, J. S., C. D. Sturgis, A. W. Rademaker and T. K. Woodruff (2003). "Down-regulation of activin, activin receptors, and Smads in high-grade breast cancer." Cancer Research 63(13): 3783-3790.
- Jeyapalan, J. N., H. Varley, J. L. Foxon, R. E. Pollock, A. J. Jeffreys, J. D. Henson, R. R. Reddel and N. J. Royle (2005). "Activation of the ALT pathway for telomere maintenance can affect other sequences in the human genome." Human Molecular Genetics 14(13): 1785-1794.
- Jiang, H., E. Schiffer, Z. Song, J. Wang, P. Zurbig, K. Thedieck, S. Moes, H. Bantel, N. Saal, J. Jantos, M. Brecht, P. Jenö, M. N. Hall, K. Hager, M. P. Manns, H. Hecker, A. Ganser, K. Dohner, A. Bartke, C. Meissner, H. Mischak, Z. Ju and K. L. Rudolph (2008). "Proteins induced by telomere dysfunction and DNA damage represent biomarkers of human aging and disease." Proc Natl Acad Sci U S A 105(32): 11299-304.
- Jiang, W.-Q., Z.-H. Zhong, J. D. Henson, A. A. Neumann, A. C.-M. Chang and R. R. Reddel (2005). "Suppression of Alternative Lengthening of Telomeres by Sp100-Mediated Sequestration of the MRE11/RAD50/NBS1 Complex 10.1128/MCB.25.7.2708-2721.2005." Mol. Cell. Biol. 25(7): 2708-2721.
- Jiao, J., S. Wang, R. Qiao, I. Vivanco, P. A. Watson, C. L. Sawyers and H. Wu (2007). "Murine Cell Lines Derived from Pten Null Prostate Cancer Show the Critical Role of PTEN in Hormone Refractory Prostate Cancer Development." Cancer Research 67(13): 6083-6091.
- Jiao, J., S. Wang, R. Qiao, I. Vivanco, P. A. Watson, C. L. Sawyers and H. Wu (2007). "Murine Cell Lines Derived from Pten Null Prostate Cancer Show the Critical Role of PTEN in Hormone Refractory Prostate Cancer Development." Cancer Res 67(13): 6083-6091.
- Johannessen, C. M., E. E. Reczek, M. F. James, H. Brems, E. Legius and K. Cichowski (2005). "The NF1 tumor suppressor critically regulates TSC2 and mTOR." Proc Natl Acad Sci U S A 102(24): 8573-8.
- Johnson, F. B., Marciniak, R.A., McVey, M., Stewart, S.A., Hahn, W.C. and Guarente, L. (2001). "The *Saccharomyces cerevisiae* WRN homolog Sgs1p participates in telomere maintenance in cells lacking telomerase." The EMBO Journal 20(4): 905-913.
- Jones, K. R., L. W. Elmore, C. Jackson-Cook, G. Demasters, L. F. Povirk, S. E. Holt and D. A. Gewirtz (2005). "p53-Dependent accelerated senescence induced by ionizing radiation in breast tumour cells." Int J Radiat Biol 81(6): 445-58.
- Ju, Z. and K. L. Rudolph (2006). "Telomeres and telomerase in cancer stem cells." European Journal of Cancer 42(9): 1197-1203.
- Jun, J. and L.F. Lau. "The matricellular protein CCN1 induces fibroblast senescence and restricts fibrosis in cutaneous wound healing." Nat Cell Biol. 12(7):676-685.
- Kanaya, T., S. Kyo, K. Hamada, M. Takakura, Y. Kitagawa, H. Harada and M. Inoue (2000). "Adenoviral expression of p53 represses telomerase activity through down-regulation of human telomerase reverse transcriptase transcription." Clin Cancer Res 6(4): 1239-47.

- Kang, S. S., T. Kwon, D. Y. Kwon and S. I. Do (1999). "Akt protein kinase enhances human telomerase activity through phosphorylation of telomerase reverse transcriptase subunit." J Biol Chem **274**(19): 13085-90.
- Katoh, M. and M. Katoh (2004). "Identification and characterization of ARHGAP24 and ARHGAP25 genes in silico." International Journal of Molecular Medicine **14**(2): 333-338.
- Kharbanda, S., V. Kumar, S. Dhar, P. Pandey, C. Chen, P. Majumder, Z. M. Yuan, Y. Whang, W. Strauss, T. K. Pandita, D. Weaver and D. Kufe (2000). "Regulation of the hTERT telomerase catalytic subunit by the c-Abl tyrosine kinase." Curr Biol **10**(10): 568-75.
- Kim, K. S., M. S. Kim, Y. B. Seu, H. Y. Chung, J. H. Kim and J. R. Kim (2007). "Regulation of replicative senescence by insulin-like growth factor-binding protein 3 in human umbilical vein endothelial cells." Aging Cell **6**(4): 535-45.
- Kim, K. S., Y. B. Seu, S. H. Baek, M. J. Kim, K. J. Kim, J. H. Kim and J. R. Kim (2007). "Induction of cellular senescence by insulin-like growth factor binding protein-5 through a p53-dependent mechanism." Mol Biol Cell **18**(11): 4543-52.
- Kim, N.V. , J. Han, M.K. Siomi (2009) "Biogenesis of small RNAs in animals." Nat Cell Rev Mol Cell Biol **126**(10):126-139.
- Kim, N. W., M. A. Piatyszek, K. R. Prowse, C. B. Harley, M. D. West, P. L. Ho, G. M. Coviello, W. E. Wright, S. L. Weinrich and J. W. Shay (1994). "Specific association of human telomerase activity with immortal cells and cancer." Science **266**(5193): 2011-5.
- Kim, W. Y. and N. E. Sharpless (2006). "The regulation of INK4/ARF in cancer and aging." Cell **127**(2): 265-75.
- Kirwal, M. and I. Dokal (2009). " Dyskeratosis congenita, stem cells and telomeres" Biochim Biophys Acta. **1792**(4): 371-379
- Konnikova, L., M. C. Simeone, M. M. Kruger, M. Kotecki and B. H. Cochran (2005). "Signal transducer and activator of transcription 3 (STAT3) regulates human telomerase reverse transcriptase (hTERT) expression in human cancer and primary cells." Cancer Res **65**(15): 6516-20.
- Kortlever, R. M., P. J. Higgins and R. Bernards (2006). "Plasminogen activator inhibitor-1 is a critical downstream target of p53 in the induction of replicative senescence." Nat Cell Biol **8**(8): 877-84.
- Kourea, H. P., I. Orlow, B. W. Scheithauer, C. Cordon-Cardo and J. M. Woodruff (1999). "Deletions of the INK4A gene occur in malignant peripheral nerve sheath tumors but not in neurofibromas." Am J Pathol **155**(6): 1855-60.
- Krizhanovsky, V., M. Yon, R.A. Dickins, S. Hearn, J. Simon, C. Miething, H. Yee, L. Zender and S.W. Lowe (2008) " Senescence of activated stellate cells limits liver fibrosis. Cell **134**: 657-667.
- Kuilman, T., C. Michaloglou, L. C. Vredeveld, S. Douma, R. van Doorn, C. J. Desmet, L. A. Aarden, W. J. Mooi and D. S. Peeper (2008). "Oncogene-induced senescence relayed by an interleukin-dependent inflammatory network." Cell **133**(6): 1019-31.
- Kuilman, T., C. Michaloglou, L. C. W. Vredeveld, S. Douma, R. van Doorn, C. J. Desmet, L. A. Aarden, W. J. Mooi and D. S. Peeper (2008). "Oncogene-induced senescence relayed by an interleukin-dependent inflammatory network." Cell **133**(6): 1019-1031.
- Kuilman, T. and D. S. Peeper (2009). "Senescence-messaging secretome: SMS-ing cellular stress." Nat Rev Cancer **9**(2): 81-94.
- Kulju, K. S. and J. M. Lehman (1995). "Increased p53 protein associated with aging in human diploid fibroblasts." Exp Cell Res **217**(2): 336-45.

- Kumamoto, K., E. A. Spillare, K. Fujita, I. Horikawa, T. Yamashita, E. Appella, M. Nagashima, S. Takenoshita, J. Yokota and C. C. Harris (2008). "Nutlin-3a activates p53 to both down-regulate inhibitor of growth 2 and up-regulate mir-34a, mir-34b, and mir-34c expression, and induce senescence." Cancer Research **68**(9): 3193-3203.
- Kyo, S., M. Takakura, T. Taira, T. Kanaya, H. Itoh, M. Yutsudo, H. Ariga and M. Inoue (2000). "Sp1 cooperates with c-Myc to activate transcription of the human telomerase reverse transcriptase gene (hTERT)." Nucleic Acids Res **28**(3): 669-77.
- Lagos-Quinana, M., R. Rauhut, W. Lendeckel and T. Tuschul (2001) "Identification of novel genes encoding small expressed RNAs." Science **294**(5543): 853.
- Lal, A., H. H. Kim, K. Abdelmohsen, Y. Kuwano, R. Pullmann, Jr., S. Srikantan, R. Subrahmanyam, J. L. Martindale, X. Yang, F. Ahmed, F. Navarro, D. Dykxhoorn, J. Lieberman and M. Gorospe (2008). "p16(INK4a) translation suppressed by miR-24." PLoS ONE **3**(3): e1864.
- Lau, N.C., L.P. Lim, E.G. Weinstein and D.P. Bartel. (2001) "An abundant class of tiny RNAs with probably regulatory roles in *Caenorhabditis elegans*." Science **294**(5543): 858.
- Laud PR, A.S. Multani, S.M. Bailey, L.Wu, J. Ma, C. Kingsley, M. Lebel, S. Pathak, R.A. DePinho, S. Chang. (2005) "Elevated telomere-telomere recombination in WRN-deficient, telomere dysfunctional cells promotes escape from senescence and engagement of the ALT pathway." Genes Dev **19**(21): 2560-70
- Lee, B. Y., J. A. Han, J. S. Im, A. Morrone, K. Johung, E. C. Goodwin, W. J. Kleijer, D. DiMaio and E. S. Hwang (2006). "Senescence-associated beta-galactosidase is lysosomal beta-galactosidase." Aging Cell **5**(2): 187-95.
- Lee, R. C., R. L. Feinbaum and V. Ambros (1993). "The C-Elegans Heterochronic Gene Lin-4 Encodes Small Rnas with Antisense Complementarity to Lin-14." Cell **75**(5): 843-854.
- Lee, R. J., C. Albanese, R. J. Stenger, G. Watanabe, G. Inghirami, G. K. Haines, M. Webster, W. J. Muller, J. S. Brugge, R. J. Davis and R. G. Pestell (1999). "pp60(v-src) induction of cyclin D1 requires collaborative interactions between the extracellular signal-regulated kinase, p38, and Jun kinase pathways - A role for cAMP response element-binding protein and activating transcription factor-2 in pp60(v-src) signaling in breast cancer cells." Journal of Biological Chemistry **274**(11): 7341-7350.
- Levy, M. Z., R. C. Allsopp, A. B. Futcher, C. W. Greider and C. B. Harley (1992). "Telomere end-replication problem and cell aging." J Mol Biol **225**(4): 951-60.
- Li, H. and J. P. Liu (2007). "Mechanisms of action of TGF-beta in cancer: evidence for Smad3 as a repressor of the hTERT gene." Ann N Y Acad Sci **1114**: 56-68.
- Li, H., L. L. Zhao, J. W. Funder and J. P. Liu (1997). "Protein phosphatase 2A inhibits nuclear telomerase activity in human breast cancer cells." J Biol Chem **272**(27): 16729-32.
- Li, Q., A. K. Ching, B. C. Chan, S. K. Chow, P. L. Lim, T. C. Ho, W. K. Ip, C. K. Wong, C. W. Lam, K. K. Lee, J. Y. Chan and Y. L. Chui (2004). "A death receptor-associated anti-apoptotic protein, BRE, inhibits mitochondrial apoptotic pathway." J Biol Chem **279**(50): 52106-16.
- Lin, A. W., M. Barradas, J. C. Stone, L. van Aelst, M. Serrano and S. W. Lowe (1998). "Premature senescence involving p53 and p16 is activated in response to constitutive MEK/MAPK mitogenic signaling." Genes Dev **12**(19): 3008-19.

- Lincz, L. F., L. M. Mudge, F. E. Scorgie, J. A. Sakoff, C. S. Hamilton and M. Seldon (2008). "Quantification of hTERT splice variants in melanoma by SYBR green real-time polymerase chain reaction indicates a negative regulatory role for the beta deletion variant." *Neoplasia* **10**(10): 1131-7.
- Liu Y., H.K. Sanoff, H. Cho, C.E. Burd, C. Torrice, J.G. Ibrahim, N.E. Thomas and N.E. Sharpless. (2009) Expression of p16(INK4a) in peripheral blood T-cells is a biomarker of human aging. *Aging Cell*. **8**(4):439-48
- Londono-Vallejo, J. A., H. Der-Sarkissian, L. Cazes, S. Bacchetti and R. R. Reddel (2004). "Alternative lengthening of telomeres is characterized by high rates of telomeric exchange." *Cancer Research* **64**(7): 2324-2327.
- Londono-Vallejo, J. A., H. Der-Sarkissian, L. Cazes, S. Bacchetti and R. R. Reddel (2004). "Alternative lengthening of telomeres is characterized by high rates of telomeric exchange." *Cancer Res* **64**(7): 2324-7.
- Ma, L., N. Chang, S. Guo, Q. Li, Z. Zhang, W. Wang and T. Tong (2008). "CSIG inhibits PTEN translation in replicative senescence." *Mol Cell Biol* **28**(20): 6290-301.
- Maeda, T., R. M. Hobbs, T. Merghoub, I. Guernah, A. Zelent, C. Cordon-Cardo, J. Teruya-Feldstein and P. P. Pandolfi (2005). "Role of the proto-oncogene Pokemon in cellular transformation and ARF repression." *Nature* **433**(7023): 278-85.
- Majumder, P. K., C. Grisanzio, F. O'Connell, M. Barry, J. M. Brito, Q. Xu, I. Guney, R. Berger, P. Herman, R. Bikoff, G. Fedele, W. K. Baek, S. Wang, K. Ellwood-Yen, H. Wu, C. L. Sawyers, S. Signoretti, W. C. Hahn, M. Loda and W. R. Sellers (2008). "A prostatic intraepithelial neoplasia-dependent p27 Kip1 checkpoint induces senescence and inhibits cell proliferation and cancer progression." *Cancer Cell* **14**(2): 146-55.
- Mathew, R., V. Karantza-Wadsworth and E. White (2007). "Role of autophagy in cancer." *Nat Rev Cancer* **7**(12): 961-7.
- Matsunobu, T., K. Tanaka, T. Nakamura, F. Nakatani, R. Sakimura, M. Hanada, X. Li, T. Okada, Y. Oda, M. Tsuneyoshi and Y. Iwamoto (2006). "The possible role of EWS-Fli1 in evasion of senescence in Ewing family tumors." *Cancer Res* **66**(2): 803-11.
- Matushansky, I., E. Hernando, N. D. Socci, J. E. Mills, T. A. Matos, M. A. Edgar, S. Singer, R. G. Maki and C. Cordon-Cardo (2007). "Derivation of sarcomas from mesenchymal stem cells via inactivation of the Wnt pathway." *J Clin Invest* **117**(11): 3248-57.
- Medcalf, A. S., A. J. Klein-Szanto and V. J. Cristofalo (1996). "Expression of p21 is not required for senescence of human fibroblasts." *Cancer Res* **56**(20): 4582-5.
- Meyer, N. and L. Z. Penn (2008). "Reflecting on 25 years with MYC." *Nat Rev Cancer* **8**(12): 976-90.
- Michaloglou, C., L. C. W. Vredeveld, M. S. Soengas, C. Denoyelle, T. Kuilman, C. van der Horst, D. M. Majoor, J. W. Shay, W. J. Mooi and D. S. Peeper (2005). "BRAF(E600)-associated senescence-like cell cycle arrest of human naevi." *Nature* **436**(7051): 720-724.
- Mitchell, J. R., E. Wood and K. Collins (1999). "A telomerase component is defective in the human disease dyskeratosis congenita." *Nature* **402**(6761): 551-5.
- Miura, M., Y. Miura, H. M. Padilla-Nash, A. A. Molinolo, B. Fu, V. Patel, B. M. Seo, W. Sonoyama, J. J. Zheng, C. C. Baker, W. Chen, T. Ried and S. Shi (2006). "Accumulated chromosomal instability in murine bone marrow mesenchymal stem cells leads to malignant transformation." *Stem Cells* **24**(4): 1095-103.

- Momand, J., D. Jung, S. Wilczynski and J. Niland (1998). "The MDM2 gene amplification database." Nucleic Acids Res **26**(15): 3453-9.
- Moon, D.-O., M.-O. Kim, J.-D. Lee, Y. H. Choi and G.-Y. Kim "Butein suppresses c-Myc-dependent transcription and Akt-dependent phosphorylation of hTERT in human leukemia cells." Cancer Letters In Press, Corrected Proof.
- Morales, C. P., S. E. Holt, M. Ouellette, K. J. Kaur, Y. Yan, K. S. Wilson, M. A. White, W. E. Wright and J. W. Shay (1999). "Absence of cancer-associated changes in human fibroblasts immortalized with telomerase." Nat Genet **21**(1): 115-8.
- Morandi, E., C. Severini, D. Quercioli, G. D'Ario, S. Perdichizzi, M. Capri, G. Farruggia, M. G. Mascolo, W. Horn, M. Vaccari, R. Serra, A. Colacci and P. Silingardi (2008). "Gene expression time-series analysis of camptothecin effects in U87-MG and DBTRG-05 glioblastoma cell lines." Mol Cancer **7**: 66.
- Muller, K. C., L. Welker, K. Paasch, B. Feindt, V. J. Erpenbeck, J. M. Hohlfeld, N. Krug, M. Nakashima, D. Branscheid, H. Magnussen, R. A. Jorres and O. Holz (2006). "Lung fibroblasts from patients with emphysema show markers of senescence in vitro." Respir Res **7**: 32.
- Multani, A. S. and S. Chang (2007). "WRN at telomeres: implications for aging and cancer10.1242/jcs.03397." J Cell Sci **120**(5): 713-721.
- Muntoni, A., A. A. Neumann, M. Hills and R. R. Reddel (2009). "Telomere elongation involves intra-molecular DNA replication in cells utilizing alternative lengthening of telomeres." Hum Mol Genet **18**(6): 1017-27.
- Muntoni, A. and R. R. Reddel (2005). "The first molecular details of ALT in human tumor cells." Human Molecular Genetics **14**: R191-R196.
- Narita, M., V. Krizhanovsky, S. Nunez, A. Chicas, S. A. Hearn, M. P. Myers and S. W. Lowe (2006). "A novel role for high-mobility group a proteins in cellular senescence and heterochromatin formation." Cell **126**(3): 503-14.
- Narita, M., S. Nunez, E. Heard, M. Narita, A. W. Lin, S. A. Hearn, D. L. Spector, G. J. Hannon and S. W. Lowe (2003). "Rb-mediated heterochromatin formation and silencing of E2F target genes during cellular senescence." Cell **113**(6): 703-716.
- Natarajan, S. and M. J. McEachern (2002). "Recombinational Telomere Elongation Promoted by DNA Circles." Mol. Cell. Biol. **22**(13): 4512-4521.
- Oda, Y., H. Yamamoto, T. Takahira, C. Kobayashi, K. Kawaguchi, N. Tateishi, Y. Nozuka, S. Tamiya, K. Tanaka, S. Matsuda, R. Yokoyama, Y. Iwamoto and M. Tsuneyoshi (2005). "Frequent alteration of p16(INK4a)/p14(ARF) and p53 pathways in the round cell component of myxoid/round cell liposarcoma: p53 gene alterations and reduced p14(ARF) expression both correlate with poor prognosis." J Pathol **207**(4): 410-21.
- Pahl, M. V., N. D. Vaziri, J. Yuan and S. G. Adler (2009). "Upregulation of Monocyte/Macrophage HGFIN (Gpnmb/Osteoactivin) Expression in End-Stage Renal Disease." Clin J Am Soc Nephrol.
- Parkinson, E. K., R. F. Newbold and W. N. Keith (1997). "The genetic basis of human keratinocyte immortalisation in squamous cell carcinoma development: The role of telomerase reactivation." European Journal of Cancer Telomeres and Telomerase in Cancer **33**(5): 727-734.
- Pascal, T., F. Debacq-Chainlaux, A. Chretien, C. Bastin, A. F. Dabee, V. Bertholet, J. Remacle and O. Toussaint (2005). "Comparison of replicative senescence and stress-induced premature senescence combining differential display and low-density DNA arrays." Febs Letters **579**(17): 3651-3659.

- Pauklin, S., A. Kristjuhan, T. Maimets and V. Jaks (2005). "ARF and ATM/ATR cooperate in p53-mediated apoptosis upon oncogenic stress." Biochem Biophys Res Commun **334**(2): 386-94.
- Peedicayil, A., R. A. Vierkant, V. Shridhar, J. M. Schildkraut, S. Armasu, L. C. Hartmann, B. L. Fridley, J. M. Cunningham, C. M. Phelan, T. A. Sellers and E. L. Goode (2009). "Polymorphisms in TCEAL7 and risk of epithelial ovarian cancer." Gynecologic Oncology **114**(2): 260-264.
- Peters-Golden, M. (2009). "Putting on the brakes: cyclic AMP as a multipronged controller of macrophage function." Sci Signal **2**(75): pe37.
- Plunkett, F. J., O. Franzese, H. M. Finney, J. M. Fletcher, L. L. Belaramani, M. Salmon, I. Dokal, D. Webster, A. D. Lawson and A. N. Akbar (2007). "The loss of telomerase activity in highly differentiated CD8+CD28-CD27- T cells is associated with decreased Akt (Ser473) phosphorylation." J Immunol **178**(12): 7710-9.
- Poliseno, L., L. Pitto, M. Simili, L. Mariani, L. Riccardi, A. Ciucci, M. Rizzo, M. Evangelista, A. Mercatanti, P. P. Pandolfi and G. Rainaldi (2008). "The proto-oncogene LRF is under post-transcriptional control of MiR-20a: implications for senescence." PLoS ONE **3**(7): e2542.
- Pomerantz, J., N. Schreiber-Agus, N. J. Liegeois, A. Silverman, L. Alland, L. Chin, J. Potes, K. Chen, I. Orlow, H. W. Lee, C. Cordon-Cardo and R. A. DePinho (1998). "The Ink4a tumor suppressor gene product, p19Arf, interacts with MDM2 and neutralizes MDM2's inhibition of p53." Cell **92**(6): 713-23.
- Price, J.S., J.G. Waters, C. Darrah, C. Pennington, D.R. Edwards, S.T. Donnell and I.M. Clark (2002) "The role of chondrocyte senescence in osteoarthritis." Aging Cell **1**: 57-65.
- Prieur, A. and D. S. Peeper (2008). "Cellular senescence in vivo: a barrier to tumorigenesis." Curr Opin Cell Biol **20**(2): 150-5.
- Quick, Q. A. and D. A. Gewirtz (2006). "An accelerated senescence response to radiation in wild-type p53 glioblastoma multiforme cells." J Neurosurg **105**(1): 111-8.
- Raver-Shapira, N., E. Marciano, E. Meiri, Y. Spector, N. Rosenfeld, N. Moskovits, Z. Bentwich and M. Oren (2007). "Transcriptional activation of miR-34a contributes to p53-mediated apoptosis." Molecular Cell **26**(5): 731-743.
- Reddel, R. R. (2003). "Alternative lengthening of telomeres, telomerase, and cancer." Cancer Letters **194**(2): 155-162.
- Reddel, R. R. (2010). "Senescence: an antiviral defense that is tumor suppressive?" Carcinogenesis **31**(1): 19-26.
- Reinhardt, H. C. and M. B. Yaffe (2009). "Kinases that control the cell cycle in response to DNA damage: Chk1, Chk2, and MK2." Curr Opin Cell Biol **21**(2): 245-55.
- Riggi, N., M. L. Suva, D. Suva, L. Cironi, P. Provero, S. Tercier, J. M. Joseph, J. C. Stehle, K. Baumer, V. Kindler and I. Stamenkovic (2008). "EWS-FLI-1 expression triggers a Ewing's sarcoma initiation program in primary human mesenchymal stem cells." Cancer Res **68**(7): 2176-85.
- Rodier, F., J. P. Coppe, C. K. Patil, W. A. Hoeijmakers, D. P. Munoz, S. R. Raza, A. Freund, E. Campeau, A. R. Davalos and J. Campisi (2009). "Persistent DNA damage signaling triggers senescence-associated inflammatory cytokine secretion." Nat Cell Biol **11**(8): 973-9.
- Roninson, I. B. (2002). "Oncogenic functions of tumour suppressor p21(Waf1/Cip1/Sdi1): association with cell senescence and tumour-promoting activities of stromal fibroblasts." Cancer Lett **179**(1): 1-14.

- Ross, G. M. (1999). "Induction of cell death by radiotherapy." Endocr Relat Cancer **6**(1): 41-4.
- Roxburgh, C. S. D., J. M. Salmond, P. G. Horgan, K. A. Oien and D. C. McMillan (2009). "Tumour inflammatory infiltrate predicts survival following curative resection for node-negative colorectal cancer." European Journal of Cancer [Epub ahead of print].
- Rubio, D., J. Garcia-Castro, M. C. Martin, R. de la Fuente, J. C. Cigudosa, A. C. Lloyd and A. Bernad (2005). "Spontaneous human adult stem cell transformation." Cancer Res **65**(8): 3035-9.
- Saeboe-Larssen, S., E. Fossberg and G. Gaudernack (2006). "Characterization of novel alternative splicing sites in human telomerase reverse transcriptase (hTERT): analysis of expression and mutual correlation in mRNA isoforms from normal and tumour tissues." BMC Mol Biol **7**: 26.
- Sanders, R. P., R. Drissi, C. A. Billups, N. C. Daw, M. B. Valentine and J. S. Dome (2004). "Telomerase Expression Predicts Unfavorable Outcome in Osteosarcoma 10.1200/JCO.2004.03.043." J Clin Oncol **22**(18): 3790-3797.
- Sasaki, M., H. Ikeda, Y. Sato and Y. Nakanuma (2008). "Proinflammatory cytokine-induced cellular senescence of biliary epithelial cells is mediated via oxidative stress and activation of ATM pathway: a culture study." Free Radic Res **42**(7): 625-32.
- Sedelnikovka, O.A., I. Horikawa, D.B. Zimonjic, N.C. Popescu, W.M. Bonner and J.C. Barrett (2004). Senescing human cells and ageing mice accumulate DNA lesions with unreparable double-strand breaks. Nat Cell Biol **6**: 168-170.
- Sedivy, J. M., G. Banumathy and P. D. Adams (2008). "Aging by epigenetics--a consequence of chromatin damage?" Exp Cell Res **314**(9): 1909-17.
- Serakinci, N., P. Guldborg, J. S. Burns, B. Abdallah, H. Schrodder, T. Jensen and M. Kassem (2004). "Adult human mesenchymal stem cell as a target for neoplastic transformation." Oncogene **23**(29): 5095-8.
- Serakinci, N., S. F. Hoare, M. Kassem, S. P. Atkinson and W. N. Keith (2006). "Telomerase promoter reprogramming and interaction with general transcription factors in the human mesenchymal stem cell." Regen Med **1**(1): 125-31.
- Serrano, M., A. W. Lin, M. E. McCurrach, D. Beach and S. W. Lowe (1997). "Oncogenic ras provokes premature cell senescence associated with accumulation of p53 and p16INK4a." Cell **88**(5): 593-602.
- Shay, J. W. and W. N. Keith (2008). "Targeting telomerase for cancer therapeutics." Br J Cancer **98**(4): 677-83.
- Shay, J. W., O. M. Pereira-Smith and W. E. Wright (1991). "A role for both RB and p53 in the regulation of human cellular senescence." Exp Cell Res **196**(1): 33-9.
- Sheng, M. H., J. E. Wergedal, S. Mohan and K. H. Lau (2008). "Osteoactivin is a novel osteoclastic protein and plays a key role in osteoclast differentiation and activity." FEBS Lett **582**(10): 1451-8.
- Shi, M. and N Guo. (2009) "MicroRNA expression and its implications for the diagnosis and therapeutic strategies of breast cancer." Cancer Treatment Rev **35**: 328-334.
- Sliwinska, M. A., G. Mosieniak, K. Wolanin, A. Babik, K. Piwocka, A. Magalska, J. Szczepanowska, J. Fronk and E. Sikora (2009). "Induction of senescence with doxorubicin leads to increased genomic instability of HCT116 cells." Mech Ageing Dev **130**(1-2): 24-32.

- Smogorzewska, A. and T. de Lange (2004). "REGULATION OF TELOMERASE BY TELOMERIC PROTEINS doi:10.1146/annurev.biochem.73.071403.160049." Annual Review of Biochemistry **73**: 177-208.
- Stavropoulos, D. J., P. S. Bradshaw, X. Li, I. Pasic, K. Truong, M. Ikura, M. Ungrin and M. S. Meyn (2002). "The Bloom syndrome helicase BLM interacts with TRF2 in ALT cells and promotes telomeric DNA synthesis 10.1093/hmg/11.25.3135." Hum. Mol. Genet. **11**(25): 3135-3144.
- Strati, A., Z. Papoutsis, E. Lianidou and P. Moutsatsou (2009). "Effect of ellagic acid on the expression of human telomerase reverse transcriptase (hTERT) alpha+beta+ transcript in estrogen receptor-positive MCF-7 breast cancer cells." Clin Biochem **42**(13-14): 1358-62.
- Subramanian, S., W. O. Lui, C. H. Lee, I. Espinosa, T. O. Nielsen, M. C. Heinrich, C. L. Corless, A. Z. Fire and M. van de Rijn (2007). "MicroRNA expression signature of human sarcomas." Oncogene **27**(14): 2015-2026.
- Takabe, K., J. J. Lebrun, Y. Nagashima, Y. Ichikawa, M. Mitsushashi, N. Momiyama, T. Ishikawa, H. Shimada and W. W. Vale (1999). "Interruption of activin A autocrine regulation by antisense oligodeoxynucleotides accelerates liver tumor cell proliferation." Endocrinology **140**(7): 3125-3132.
- Takakura, M., S. Kyo, M. Inoue, W. E. Wright and J. W. Shay (2005). "Function of AP-1 in transcription of the telomerase reverse transcriptase gene (TERT) in human and mouse cells." Mol Cell Biol **25**(18): 8037-43.
- Tatsumi, Y., K. Ezura, K. Yoshida, T. Yugawa, M. Narisawa-Saito, T. Kiyono, S. Ohta, C. Obuse and M. Fujita (2008). "Involvement of human ORC and TRF2 in pre-replication complex assembly at telomeres." Genes to Cells **13**(10): 1045-1059.
- Tazawa, H., N. Tsuchiya, M. Izumiya and H. Nakagama (2007). "Tumor-suppressive miR-34a induces senescence-like growth arrest through modulation of the E2F pathway in human colon cancer cells." Proceedings of the National Academy of Sciences of the United States of America **104**(39): 15472-15477.
- te Poele, R. H., A. L. Okorokov, L. Jardine, J. Cummings and S. P. Joel (2002). "DNA damage is able to induce senescence in tumor cells in vitro and in vivo." Cancer Res **62**(6): 1876-83.
- Terasaki, T., Kyo, S., Takakura, M., Maida, Y., Tsuchiya, H., Tomita, K. and Inoue, M. (2004). "Analysis of telomerase activity and telomere length in bone and soft tissue tumors." Oncology Reports **11**(6): 1307-1312.
- Tirode, F., K. Laud-Duval, A. Priour, B. Delorme, P. Charbord and O. Delattre (2007). "Mesenchymal stem cell features of Ewing tumors." Cancer Cell **11**(5): 421-9.
- Tomaska, L., M. J. McEachern and J. Nosek (2004). "Alternatives to telomerase: keeping linear chromosomes via telomeric circles." FEBS Letters Warsaw Special Issue **567**(1): 142-146.
- Toussaint, O., E. E. Medrano and T. von Zglinicki (2000). "Cellular and molecular mechanisms of stress-induced premature senescence (SIPS) of human diploid fibroblasts and melanocytes." Exp Gerontol **35**(8): 927-45.
- Troester, M. A., K. A. Hoadley, J. S. Parker and C. M. Perou (2004). "Prediction of toxicant-specific gene expression signatures after chemotherapeutic treatment of breast cell lines." Environ Health Perspect **112**(16): 1607-13.
- Ulaner, G. A., A. R. Hoffman, J. Otero, H. Y. Huang, Z. Zhao, M. Mazumdar, R. Gorlick, P. Meyers, J. H. Healey and M. Ladanyi (2004). "Divergent patterns of telomere maintenance mechanisms among human sarcomas:

- sharply contrasting prevalence of the alternative lengthening of telomeres mechanism in Ewing's sarcomas and osteosarcomas." Genes Chromosomes Cancer **41**(2): 155-62.
- Ulaner, G. A., H.-Y. Huang, J. Otero, Z. Zhao, L. Ben-Porat, J. M. Satagopan, R. Gorlick, P. Meyers, J. H. Healey, A. G. Huvos, A. R. Hoffman and M. Ladanyi (2003). "Absence of a Telomere Maintenance Mechanism as a Favorable Prognostic Factor in Patients with Osteosarcoma." Cancer Res **63**(8): 1759-1763.
- Ulaner, G. A., H. Y. Huang, J. Otero, Z. Zhao, L. Ben-Porat, J. M. Satagopan, R. Gorlick, P. Meyers, J. H. Healey, A. G. Huvos, A. R. Hoffman and M. Ladanyi (2003). "Absence of a telomere maintenance mechanism as a favorable prognostic factor in patients with osteosarcoma." Cancer Res **63**(8): 1759-63.
- Vassilatis, D. K., J. G. Hohmann, H. Zeng, F. Li, J. E. Ranchalis, M. T. Mortrud, A. Brown, S. S. Rodriguez, J. R. Weller, A. C. Wright, J. E. Bergmann and G. A. Gaitanaris (2003). "The G protein-coupled receptor repertoires of human and mouse." Proc Natl Acad Sci U S A **100**(8): 4903-8.
- Vaziri, H., W. Dragowska, R. C. Allsopp, T. E. Thomas, C. B. Harley and P. M. Lansdorp (1994). "Evidence for a mitotic clock in human hematopoietic stem cells: loss of telomeric DNA with age." Proc Natl Acad Sci U S A **91**(21): 9857-60.
- Ventura, A., D.G. Krisch, M.E. McLaughlin, D.A. Tuveson, J. Grimm, L. Lintault, J. Newman, E.E. Reczek, R. Weissleder and T. Jacks. (2007) "Restoration of p53 function leads to tumour regression in vivo." Nature. 455: 661-665.
- Villa, R., M. G. Daidone, R. Motta, L. Venturini, C. De Marco, A. Vannelli, S. Kusamura, D. Baratti, M. Deraco, A. Costa, R. R. Reddel and N. Zaffaroni (2008). "Multiple mechanisms of telomere maintenance exist and differentially affect clinical outcome in diffuse malignant peritoneal mesothelioma." Clin Cancer Res **14**(13): 4134-40.
- Voorhoeve, P. M., C. le Sage, M. Schrier, A. J. Gillis, H. Stoop, R. Nagel, Y. P. Liu, J. van Duijse, J. Drost, A. Griekspoor, E. Zlotorynski, N. Yabuta, G. De Vita, H. Nojima, L. H. Looijenga and R. Agami (2006). "A genetic screen implicates miRNA-372 and miRNA-373 as oncogenes in testicular germ cell tumors." Cell **124**(6): 1169-81.
- Vulliamy, T., A. Marrone, F. Goldman, A. Dearlove, M. Bessler, P. J. Mason and I. Dokal (2001). "The RNA component of telomerase is mutated in autosomal dominant dyskeratosis congenita." Nature **413**(6854): 432-5.
- W-Q Jiang, Z.-H. Z., J D Henson and R R Reddel (2007). "Identification of candidate alternative lengthening of telomeres genes by methionine restriction and RNA interference." Oncogene advanced online publication **5 February**.
- Wagner, W., P. Horn, M. Castoldi, A. Diehlmann, S. Bork, R. Saffrich, V. Benes, J. Blake, S. Pfister, V. Eckstein and A. D. Ho (2008). "Replicative senescence of mesenchymal stem cells: a continuous and organized process." PLoS One **3**(5): e2213.
- Wajapeyee, N., R. W. Serra, X. Zhu, M. Mahalingam and M. R. Green (2008). "Oncogenic BRAF Induces Senescence and Apoptosis through Pathways Mediated by the Secreted Protein IGFBP7." Cell **132**(3): 363-374.
- Wang, H., S. Mannava, V. Grachtchouk, D. Zhuang, M. S. Soengas, A. V. Gudkov, E. V. Prochownik and M. A. Nikiforov (2008). "c-Myc depletion inhibits proliferation of human tumor cells at various stages of the cell cycle." Oncogene **27**(13): 1905-15.

- Wang, R. C., A. Smogorzewska and T. de Lange (2004). "Homologous Recombination Generates T-Loop-Sized Deletions at Human Telomeres." Cell **119**(3): 355-368.
- Wang, W. and W. S. El-Deiry (2008). "Restoration of p53 to limit tumor growth." Curr Opin Oncol **20**(1): 90-6.
- Wang, Y., D. L. Huso, J. Harrington, J. Kellner, D. K. Jeong, J. Turney and I. K. McNiece (2005). "Outgrowth of a transformed cell population derived from normal human BM mesenchymal stem cell culture." Cytotherapy **7**(6): 509-19.
- Watanabe, T., Y. Oda, S. Tamiya, N. Kinukawa, K. Masuda and M. Tsuneyoshi (2001). "Malignant peripheral nerve sheath tumours: high Ki67 labelling index is the significant prognostic indicator." Histopathology **39**(2): 187-97.
- Weinrich, S. L., R. Pruzan, L. Ma, M. Ouellette, V. M. Tesmer, S. E. Holt, A. G. Bodnar, S. Lichtsteiner, N. W. Kim, J. B. Trager, R. D. Taylor, R. Carlos, W. H. Andrews, W. E. Wright, J. W. Shay, C. B. Harley and G. B. Morin (1997). "Reconstitution of human telomerase with the template RNA component hTR and the catalytic protein subunit hTRT." Nat Genet **17**(4): 498-502.
- Wenz, C., B. Enenkel, M. Amacker, C. Kelleher, K. Damm and J. Lingner (2001). "Human telomerase contains two cooperating telomerase RNA molecules." EMBO J **20**(13): 3526-34.
- Wiemann, S.U., A. Satyanarayana, M. Tsahuridu, H.L. Tillmann, L. Zender, J. Klempnauer, P. Flemming, S. Franco, M.A. Blasco, M.P. Manns and K.L. Rudolph (2002). "Hepatocyte telomere shortening and senescence are general markers of human liver cirrhosis. FASEB J. **16**: 935-942.
- Wightman, B., I. Ha and G. Ruvkun (1993). "Posttranscriptional Regulation of the Heterochronic Gene Lin-14 by Lin-4 Mediates Temporal Pattern-Formation in C-Elegans." Cell **75**(5): 855-862.
- Wu, C., Q. Wei, V. Utomo, P. Nadesan, H. Whetstone, R. Kandel, J. S. Wunder and B. A. Alman (2007). "Side population cells isolated from mesenchymal neoplasms have tumor initiating potential." Cancer Res **67**(17): 8216-22.
- Wu, C.-H., J. van Riggelen, A. Yetil, A. C. Fan, P. Bachireddy and D. W. Felsher (2007). "Cellular senescence is an important mechanism of tumor regression upon c-Myc inactivation." Proceedings of the National Academy of Sciences **104**(32): 13028-13033.
- Wu, G. K., X. Z. Jiang, W. H. Lee and P. L. Chen (2003). "Assembly of functional ALT-associated promyelocytic leukemia bodies requires Nijmegen breakage syndrome 1." Cancer Research **63**(10): 2589-2595.
- Xue, W., L. Zender, C. Miething, R.A. Dickins, E. Hernandez, V. Krizhanovsky, C. Cordon-Cardo and S.W. Lowe. (2007) "Senescence and tumour clearance is triggered by p53 restoration in murine liver carcinomas. Nature **445**: 66-660.
- Yang, J., E. Chang, A. M. Cherry, C. D. Bangs, Y. Oei, A. Bodnar, A. Bronstein, C. P. Chiu and G. S. Herron (1999). "Human endothelial cell life extension by telomerase expression." J Biol Chem **274**(37): 26141-8.
- Ye, X., B. Zerlanko, A. Kennedy, G. Banumathy, R. Zhang and P. D. Adams (2007). "Downregulation of Wnt signaling is a trigger for formation of facultative heterochromatin and onset of cell senescence in primary human cells." Mol Cell **27**(2): 183-96.
- Yeager, T. R., A. A. Neumann, A. Englezou, L. I. Huschtscha, J. R. Noble and R. R. Reddel (1999). "Telomerase-negative Immortalized Human Cells

- Contain a Novel Type of Promyelocytic Leukemia (PML) Body." Cancer Res **59**(17): 4175-4179.
- Yi, X., D. M. White, D. L. Aisner, J. A. Baur, W. E. Wright and J. W. Shay (2000). "An alternate splicing variant of the human telomerase catalytic subunit inhibits telomerase activity." Neoplasia **2**(5): 433-40.
- Young, A. R. and M. Narita (2009). "SASP reflects senescence." EMBO Rep **10**(3): 228-30.
- Young, A. R., M. Narita, M. Ferreira, K. Kirschner, M. Sadaie, J. F. Darot, S. Tavares, S. Arakawa, S. Shimizu and F. M. Watt (2009). "Autophagy mediates the mitotic senescence transition." Genes Dev **23**(7): 798-803.
- Yui, J., C. P. Chiu and P. M. Lansdorp (1998). "Telomerase activity in candidate stem cells from fetal liver and adult bone marrow." Blood **91**(9): 3255-62.
- Zaffaroni, N., C. Della Porta, R. Villa, C. Botti, S. Buglioni, M. Mottolise and M. Grazia Daidone (2002). "Transcription and alternative splicing of telomerase reverse transcriptase in benign and malignant breast tumours and in adjacent mammary glandular tissues: implications for telomerase activity." J Pathol **198**(1): 37-46.
- Zaffaroni, N., R. Villa, U. Pastorino, R. Cirincione, M. Incarbone, M. Alloisio, M. Curto, S. Pilotti and M. G. Daidone (2005). "Lack of telomerase activity in lung carcinoids is dependent on human telomerase reverse transcriptase transcription and alternative splicing and is associated with long telomeres." Clin Cancer Res **11**(8): 2832-9.
- Zeller, K. I., A. G. Jegga, B. J. Aronow, K. A. O'Donnell and C. V. Dang (2003). "An integrated database of genes responsive to the Myc oncogenic transcription factor: identification of direct genomic targets." Genome biology.
- Zhang, R. and P. D. Adams (2007). "Heterochromatin and its relationship to cell senescence and cancer therapy." Cell Cycle **6**(7): 784-9.
- Zhang, R., M. V. Poustovoitov, X. Ye, H. A. Santos, W. Chen, S. M. Daganzo, J. P. Erzberger, I. G. Serebriiskii, A. A. Canutescu, R. L. Dunbrack, J. R. Pehrson, J. M. Berger, P. D. Kaufman and P. D. Adams (2005). "Formation of MacroH2A-containing senescence-associated heterochromatin foci and senescence driven by ASF1a and HIRA." Dev Cell **8**(1): 19-30.
- Zhang, Y., J. Zhou, X. Cao, Q. Zhang, C. U. Lim, R. L. Ullrich, S. M. Bailey and H. L. Liber (2007). "Partial deficiency of DNA-PKcs increases ionizing radiation-induced mutagenesis and telomere instability in human cells." Cancer Lett **250**(1): 63-73.
- Zhao, Y. M., J. Y. Li, J. P. Lan, X. Y. Lai, Y. Luo, J. Sun, J. Yu, Y. Y. Zhu, F. F. Zeng, Q. Zhou and H. Huang (2008). "Cell cycle dependent telomere regulation by telomerase in human bone marrow mesenchymal stem cells." Biochem Biophys Res Commun **369**(4): 1114-9.
- Zhou, Y. F., M. Bosch-Marce, H. Okuyama, B. Krishnamachary, H. Kimura, L. Zhang, D. L. Huso and G. L. Semenza (2006). "Spontaneous transformation of cultured mouse bone marrow-derived stromal cells." Cancer Res **66**(22): 10849-54.
- Zhu, J., D. Woods, M. McMahon and J. M. Bishop (1998). "Senescence of human fibroblasts induced by oncogenic Raf." Genes Dev **12**(19): 2997-3007.
- Zhu, X.-D., Küster, B., Mann, M., Petrini J.H.J and de Lange, T. (2000). "Cell-cycle-regulated association of RAD50/MRE11/NBS1 with TRF2 and human telomeres." Nature Genetics **25**(3): 347-352.
- Zhuang, D., S. Mannava, V. Grachtchouk, W. H. Tang, S. Patil, J. A. Wawrzyniak, A. E. Berman, T. J. Giordano, E. V. Prochownik, M. S. Soengas and M. A. Nikiforov (2008). "C-MYC overexpression is required for continuous

suppression of oncogene-induced senescence in melanoma cells." Oncogene **27**(52): 6623-34.

Zimmermann, S., M. Voss, S. Kaiser, U. Kapp, C. F. Waller and U. M. Martens (2003). "Lack of telomerase activity in human mesenchymal stem cells." Leukemia **17**(6): 1146-9.

Appendix I– Gene-lists resulting from this work

Table 3 - 1305 genes Differentially Expressed between ALT and Telomerase Cell lines.

Genename	Genbank	Fold Change in ALT
TERT	NM_198253	-46.32
C10orf35	NM_145306	-29.45
ST6GAL1	NM_173216	-28.83
CHD7	NM_017780	-22.15
EEF1A2	NM_001958	-21.87
DUSP2	NM_004418	-21.86
K03200	K03200	-21.74
SLC39A4	NM_130849	-18.24
FAM83H	NM_198488	-17.30
CHD7	NM_017780	-16.78
PRKCZ	NM_002744	-16.58
B3GNT5	NM_032047	-14.16
ARHGAP4	NM_001666	-13.92
RAB11FIP4	NM_032932	-13.66
LOC112703	NM_138411	-11.78
ZDHHC23	NM_173570	-11.15
BM802662	BM802662	-10.70
ENST00000361080	AW136529	-10.50
DIAPH2	NM_007309	-10.43
AK123704	AK123704	-10.17
PNPLA4	NM_004650	-10.00
C9orf58	NM_001002260	-9.72
MDFI	NM_005586	-9.23
SLC6A8	NM_005629	-8.78
ADAM11	NM_002390	-8.75
CEBPA	NM_004364	-8.74
LAMA5	NM_005560	-8.34
ENST00000330947	BC035081	-8.18
ZFP64	NM_199427	-8.17
LOC649542	XM_938617	-8.07
SLC6A10P	NR_003083	-8.03
HOMER2	NM_199330	-7.90
FAM59A	NM_022751	-7.55
TP53TG3	NM_016212	-7.44
CEBPA	NM_004364	-6.93
BOLA1	NM_016074	-6.92
LOC254057	AK024653	-6.89
BG741106	BG741106	-6.81
RHOF	NM_019034	-6.70
RHOF	NM_019034	-6.63
LLGL2	NM_004524	-6.60
AK025613	AK025613	-6.49

Genename	Genbank	Fold Change in ALT
RAB11FIP1	NM_001002233	-6.40
LRRC8B	NM_015350	-6.34
MAPK11	NM_002751	-6.28
STAU2	AK002152	-6.20
FOXO1A	NM_002015	-6.00
KIAA0485	AB007954	-5.93
HCP1	AL832613	-5.86
BTG2	NM_006763	-5.83
ENST00000220507	CR618466	-5.75
GP1BB	NM_000407	-5.60
ARID3B	NM_006465	-5.50
LPHN1	NM_001008701	-5.41
GPRC5C	NM_022036	-5.14
AFG3L1	NM_001132	-5.05
TCF15	NM_004609	-5.05
THC2337923	THC2337923	-4.94
BCAN	BC005081	-4.93
LRP4	NM_002334	-4.93
SMAD9	NM_005905	-4.93
LOC92312	XM_044166	-4.89
AFG3L1	NM_001132	-4.83
ORF1-FL49	NM_032412	-4.79
ASB13	NM_024701	-4.76
ELL3	NM_025165	-4.73
A_32_P26721	A_32_P26721	-4.72
AF086442	AF086442	-4.70
THC2290002	THC2290002	-4.66
ACOT11	NM_147161	-4.63
LONRF1	NM_152271	-4.57
RHOF	NM_019034	-4.49
PRKX	NM_005044	-4.47
ARHGAP27	NM_199282	-4.42
P15RS	NM_018170	-4.41
AP1S3	BC021898	-4.40
ELL3	NM_025165	-4.38
CR607745	CR607745	-4.34
DRG2	NM_001388	-4.32
CDC42SE1	NM_020239	-4.29
CR603803	CR603803	-4.28
RNF44	NM_014901	-4.28
CBS	NM_000071	-4.22
AP1S3	NM_001039569	-4.14
FLJ35740	NM_147195	-4.14
PIGZ	NM_025163	-4.13
SULT4A1	NM_014351	-4.11
EPB41L4B	NM_018424	-4.11
C9orf16	NM_024112	-4.05

Genename	Genbank	Fold Change in ALT
BAIAP2	NM_017451	-4.02
C10orf77	NM_024789	-4.01
LOC155060	NM_001004302	-4.01
ACCN2	NM_020039	-4.00
THC2350463	THC2350463	-3.98
HES4	NM_021170	-3.97
TMCC1	NM_001017395	-3.97
ABHD14B	NM_032750	-3.97
KLHL24	NM_017644	-3.91
RICS	NM_014715	-3.90
MSTP9	NR_002729	-3.88
TMEM80	NM_174940	-3.85
C20orf45	NM_016045	-3.85
KIAA1984	AB075864	-3.85
NSUN5	NM_148956	-3.84
SLC6A8	NM_005629	-3.80
AK094629	AK094629	-3.79
TMCC1	NM_001017395	-3.78
LONRF1	NM_152271	-3.78
RICS	NM_014715	-3.72
TRIM72	NM_001008274	-3.68
CBS	NM_000071	-3.67
LASS6	NM_203463	-3.65
AA554330	AA554330	-3.64
THC2455149	THC2455149	-3.63
BQ072652	BQ072652	-3.60
CENTA1	NM_006869	-3.59
REEP6	NM_138393	-3.56
ASB13	NM_024701	-3.54
PIK3C2B	NM_002646	-3.53
KGFLP1	NM_174950	-3.52
ANKRD13B	NM_152345	-3.51
GOLGA8E	NM_001012423	-3.50
ME2	NM_002396	-3.49
RBM38	NM_017495	-3.49
ENST00000372821	ENST00000372821	-3.49
C10orf57	NM_025125	-3.48
TADA3L	NM_006354	-3.46
PLS1	NM_002670	-3.46
BC039151	BC039151	-3.45
BC030211	BC030211	-3.41
BC038512	BC038512	-3.40
RP11-138L21.1	AK024257	-3.39
TMEM80	NM_174940	-3.38
LOC137886	AK126300	-3.37
THC2411839	THC2411839	-3.35
FLJ22795	NM_025084	-3.33

Genename	Genbank	Fold Change in ALT
SLC16A9	NM_194298	-3.32
DUSP22	NM_020185	-3.32
THC2408033	THC2408033	-3.26
AK123627	AK123627	-3.25
C3orf17	NM_015412	-3.24
ATP6V1E2	NM_080653	-3.24
DPM3	NM_018973	-3.21
STRBP	NM_018387	-3.21
DPM3	NM_018973	-3.21
CRIPAK	NM_175918	-3.20
NUDT14	NM_177533	-3.19
FLJ22795	AF316855	-3.18
SLC44A1	NM_022109	-3.18
GLI4	NM_138465	-3.18
ZNF692	NM_017865	-3.18
AK023328	AK023328	-3.15
MLLT10	NM_004641	-3.13
VWA1	NM_022834	-3.13
POU5F1	NM_002701	-3.13
PAPOLG	AB209304	-3.12
LASS6	NM_203463	-3.10
LYPLA2	NM_007260	-3.09
BC015977	BC015977	-3.09
DECR2	NM_020664	-3.09
RHBDD1	NM_032276	-3.09
RABGAP1L	AB007940	-3.08
SR140	AB002330	-3.08
AATK	AK131529	-3.07
COMTD1	NM_144589	-3.04
AK026811	AK026811	-3.04
P15RS	NM_018170	-3.03
SEPN1	NM_020451	-3.03
RRM2B	NM_015713	-3.03
A_32_P163472	A_32_P163472	-3.03
SLC22A18AS	NM_007105	-3.02
HNRPA3	NM_194247	-3.02
C8orf73	AF289596	-3.00
TTLL3	NM_015644	-2.99
SNCB	NM_001001502	-2.98
ANKRD57	NM_023016	-2.97
NSUN5B	NM_145645	-2.96
C9orf9	NM_018956	-2.96
AP2A2	NM_012305	-2.94
FLJ22795	AF316855	-2.93
NHLRC2	AK126751	-2.91
SSBP4	NM_032627	-2.90
C16orf14	NM_138418	-2.90

Genename	Genbank	Fold Change in ALT
ABCA2	NM_001606	-2.89
TMTC4	NM_032813	-2.88
C19orf25	NM_152482	-2.88
TPM1	NM_001018008	-2.88
OR5L2	NM_001004739	-2.88
AK023412	AK023412	-2.86
TNFRSF10B	NM_003842	-2.85
PER2	NM_022817	-2.83
TMUB1	NM_031434	-2.82
MARCKSL1	NM_023009	-2.81
NFE2L2	AF323119	-2.79
BC065260	BC065260	-2.78
ENST00000357529	AB033064	-2.78
C3orf64	NM_173654	-2.78
NARS	NM_004539	-2.78
UBE2Q1	NM_017582	-2.77
MMP15	NM_002428	-2.76
NUDT12	NM_031438	-2.76
FDXR	NM_024417	-2.75
THC2281304	THC2281304	-2.74
TRABD	NM_025204	-2.74
RASA2	NM_006506	-2.72
ENST00000377492	ENST00000377492	-2.71
SEPW1	NM_003009	-2.71
AK024035	AK024035	-2.70
BM984383	BM984383	-2.70
ENST00000368426	AK127884	-2.70
LOC132241	AK096589	-2.69
C18orf17	NM_153211	-2.69
THC2303284	AA988138	-2.69
USPL1	NM_005800	-2.69
THC2371272	THC2371272	-2.69
BQ017638	BQ017638	-2.68
BIVM	NM_017693	-2.67
BC064492	BC064492	-2.66
CR620599	CR620599	-2.66
FUK	NM_145059	-2.66
MGC4172	NM_024308	-2.64
ABCA1	NM_005502	-2.64
BCORL1	NM_021946	-2.63
NUDT14	NM_177533	-2.63
PRKY	NM_002760	-2.63
BCL7A	NM_020993	-2.62
A_23_P20793	A_23_P20793	-2.62
AK057710	AK057710	-2.59
UGT2B17	NM_001077	-2.59
MLSTD2	NM_032228	-2.59

Genename	Genbank	Fold Change in ALT
LOC389634	BC037255	-2.59
A_24_P410256	A_24_P410256	-2.59
C1orf63	NM_020317	-2.59
THC2428713	THC2428713	-2.58
CXorf15	NM_018360	-2.57
A_32_P98854	A_32_P98854	-2.57
LOC90835	NM_001014979	-2.57
FAM72A	NM_207418	-2.56
A_32_P225768	A_32_P225768	-2.56
ENST00000251847	AB046810	-2.55
FAM27E2	NM_001013404	-2.55
TLOC1	NM_003262	-2.55
ASAH1	NM_004315	-2.55
LOC653801	XM_934188	-2.55
THC2271717	THC2271717	-2.54
ZNF508	NM_014913	-2.52
SECISBP2	NM_024077	-2.52
CR625561	CR625561	-2.52
THC2280003	THC2280003	-2.51
NSUN5C	NM_148936	-2.50
KIAA1893	NM_052899	-2.50
C1orf63	AK027318	-2.50
ZNF658	NM_033160	-2.50
GALNT1	NM_020474	-2.50
C6orf115	BC014953	-2.50
CDC42SE1	NM_020239	-2.49
FAM120C	BC016138	-2.49
PICK1	NM_012407	-2.48
BC000228	BC000228	-2.48
ENST00000377492	ENST00000377492	-2.48
C9orf9	NM_018956	-2.48
DCPS	NM_014026	-2.48
C21orf119	NM_032910	-2.47
SERGEF	AJ243950	-2.47
ATP5D	NM_001001975	-2.47
TADA3L	NM_006354	-2.46
JAM3	NM_032801	-2.46
THC2437177	THC2437177	-2.46
THC2438117	THC2438117	-2.45
STAU2	NM_014393	-2.45
HDHD2	NM_032124	-2.45
BX093417	BX093417	-2.45
MRPS21	NM_031901	-2.45
C13orf8	NM_032436	-2.45
BM461836	BM461836	-2.45
PTP4A3	NM_032611	-2.44
A_24_P455100	A_24_P455100	-2.43

Genename	Genbank	Fold Change in ALT
AK054852	AK054852	-2.42
BC000845	BC000845	-2.41
C21orf59	NM_021254	-2.41
GSR	NM_000637	-2.40
PSME3	NM_176863	-2.40
LOC90835	NM_001014979	-2.40
DSCR3	NM_006052	-2.40
ZNF444	NM_018337	-2.40
LOC653639	XM_934787	-2.39
LOC285813	AK094269	-2.39
TP53INP1	NM_033285	-2.39
C17orf58	NM_181655	-2.39
Magmas	NM_016069	-2.39
DA234975	DA234975	-2.38
ADAM11	NM_002390	-2.38
AGPAT4	NM_020133	-2.37
ENST00000377492	BC032035	-2.37
ZMYM2	NM_003453	-2.36
MRPL23	NM_021134	-2.36
INTS10	NM_018142	-2.36
ATPAF1	NM_022745	-2.35
MRPS21	NM_031901	-2.35
CR610205	CR610205	-2.34
A_24_P204334	A_24_P204334	-2.34
ENST00000295628	BC013757	-2.33
YOD1	NM_018566	-2.33
INTS3	NM_023015	-2.33
ZDHHC13	NM_019028	-2.32
LYPLA1	NM_006330	-2.32
AK131288	AK131288	-2.31
AK057071	AK057071	-2.31
LOC440295	NM_198181	-2.31
RABL2A	NM_013412	-2.30
RNASSET2	NM_003730	-2.30
ZCCHC14	NM_015144	-2.30
THC2373624	THC2373624	-2.30
ZNF195	NM_007152	-2.29
THC2435127	THC2435127	-2.29
AK022936	AK022936	-2.28
ENST00000358583	AK090778	-2.28
A_24_P651129	A_24_P651129	-2.28
CR600908	CR600908	-2.28
EHMT1	NM_024757	-2.27
PIK3C2A	NM_002645	-2.27
TMEM67	NM_153704	-2.27
SERGEF	NM_012139	-2.26
PRKCBP1	AL137703	-2.26

Genename	Genbank	Fold Change in ALT
ENST00000361227	AY423734	-2.25
MBD5	BC014534	-2.25
PRKCBP1	NM_012408	-2.25
THC2363557	THC2363557	-2.24
GUK1	NM_000858	-2.24
CMTM7	NM_138410	-2.24
C1orf121	BC020640	-2.24
SNAPC4	NM_003086	-2.24
THC2263651	THC2263651	-2.24
ZNF658	NM_033160	-2.24
SELI	NM_033505	-2.22
WDR42A	NM_015726	-2.22
QSER1	NM_024774	-2.22
SESN2	NM_031459	-2.22
WDR4	NM_033661	-2.22
LRDD	NM_018494	-2.22
BE388027	BE388027	-2.22
PDIA5	NM_006810	-2.22
SLC4A2	NM_003040	-2.21
IVNS1ABP	NM_016389	-2.21
ENST00000366847	ENST00000366847	-2.21
TM6SF1	AK055438	-2.21
DNMT3A	NM_175630	-2.20
PCGF1	NM_032673	-2.20
BG259069	BG259069	-2.20
HEATR2	NM_017802	-2.20
THC2373625	THC2373625	-2.20
HNRPA3	NM_194247	-2.19
TAF5L	NM_001025247	-2.19
THC2312785	THC2312785	-2.19
SBF2	NM_030962	-2.19
C6orf70	NM_018341	-2.19
ENST00000361453	AK026903	-2.19
LENG8	NM_052925	-2.18
SCYL3	NM_020423	-2.18
BTBD3	NM_014962	-2.18
AF085351	AF085351	-2.18
FLYWCH1	NM_020912	-2.18
PVRL1	NM_203286	-2.17
DAB2IP	NM_032552	-2.17
RHPN1	BC025767	-2.17
CR590163	CR590163	-2.17
SETDB1	NM_012432	-2.17
CLK2	NM_001291	-2.16
LOC643837	CR601056	-2.16
tcag7.1017	NM_001004351	-2.16
UBE2D1	NM_003338	-2.16

Genename	Genbank	Fold Change in ALT
A_24_P169903	A_24_P169903	-2.15
A_24_P384239	A_24_P384239	-2.15
ENST00000382957	AK124953	-2.15
ENST00000380985	ENST00000380985	-2.14
ULK3	AL117482	-2.14
ZNF33B	NM_006955	-2.14
PRKAR1B	NM_002735	-2.14
AF038199	AF038199	-2.14
A_24_P101601	A_24_P101601	-2.14
G6PC3	NM_138387	-2.13
GPIAP1	NM_005898	-2.13
KIAA1545	AB046765	-2.13
CREM	NM_001881	-2.13
IGF2R	NM_000876	-2.13
BE612504	BE612504	-2.13
ENST00000369239	AL080186	-2.13
C17orf85	BC011733	-2.13
CSK	NM_004383	-2.13
THC2450500	THC2450500	-2.12
CR601496	CR601496	-2.12
HSD17B1	BC033110	-2.11
RHBDD1	BC062636	-2.11
POU2F1	NM_002697	-2.11
AV645774	AV645774	-2.11
WDR8	NM_017818	-2.11
DDB2	NM_000107	-2.11
FAM3C	NM_014888	-2.10
APOA1BP	NM_144772	-2.10
USP21	NM_012475	-2.10
CLK2	NM_003993	-2.10
AGTPBP1	NM_015239	-2.10
A_32_P73580	A_32_P73580	-2.10
CREG1	NM_003851	-2.10
PLEKHA8	NM_032639	-2.09
KIAA1008	NM_014953	-2.09
RGS14	NM_006480	-2.09
CRYZL1	AK057604	-2.09
ZDHHC13	NM_019028	-2.09
SLC37A3	NM_032295	-2.09
TXNL4A	NM_006701	-2.08
CAMSAP1	AL834528	-2.08
ENST00000339986	AF242519	-2.08
LYPLA1	NM_006330	-2.08
AK097322	AK097322	-2.08
COX17	NM_005694	-2.07
B4GALT3	NM_003779	-2.07
ATP5D	NM_001001975	-2.07

Genename	Genbank	Fold Change in ALT
TMCO3	NM_017905	-2.07
BX393727	BX393727	-2.06
TTC13	NM_024525	-2.06
ZBTB39	NM_014830	-2.06
PYCR2	NM_013328	-2.06
EHMT1	NM_024757	-2.06
MAN1B1	NM_016219	-2.06
ENST00000299756	XM_939387	-2.05
APOM	NM_019101	-2.05
GMCL1	NM_178439	-2.05
BC092421	BC092421	-2.05
ALDH5A1	NM_170740	-2.05
ZFP64	NM_018197	-2.04
TFB2M	NM_022366	-2.04
ZNF124	NM_003431	-2.04
KLHL11	NM_018143	-2.04
IARS	NM_013417	-2.03
POLG2	NM_007215	-2.03
A_32_P32923	A_32_P32923	-2.03
SETDB1	NM_012432	-2.03
POGK	NM_017542	-2.02
MBOAT1	AK131269	-2.02
KRTAP4-7	BX648343	-2.02
BC002811	BC002811	-2.02
BX107836	BX107836	-2.01
C9orf86	NM_024718	-2.01
ENST00000367590	AK023131	-2.01
BC065520	BC065520	-2.01
THC2338854	THC2338854	-2.01
DUSP22	AK000383	-2.01
TMEM68	NM_152417	-2.01
ISG20L2	NM_030980	-2.01
A_24_P681563	A_24_P681563	-2.01
ELMO3	NM_024712	-2.01
A_24_P552987	A_24_P552987	-2.00
SFRS7	NM_001031684	-2.00
AF143879	AF143879	-2.00
USPL1	NM_005800	-2.00
SATB1	NM_002971	-2.00
DMTF1	NM_021145	-2.00
ZNF337	NM_015655	-2.00
BX648950	BX648950	-2.00
TFB1M	NM_016020	-1.99
MAPBPIP	NM_014017	-1.99
RFX5	NM_000449	-1.98
THC2374442	THC2374442	-1.98
LOC168850	NM_176814	-1.98

Genename	Genbank	Fold Change in ALT
WHSC1	NM_133334	-1.98
PLEKHG2	NM_022835	-1.98
ENST00000378954	CR617774	-1.98
YY1AP1	NM_139118	-1.98
CR608275	CR608275	-1.98
THC2320516	THC2320516	-1.98
BF576096	BF576096	-1.97
PLEKHJ1	NM_018049	-1.97
THC2309459	THC2309459	-1.97
THC2437122	THC2437122	-1.97
NENF	NM_013349	-1.97
PERLD1	NM_033419	-1.97
SIRT5	NM_012241	-1.97
CNDP2	NM_018235	-1.97
C16orf35	NM_001039476	-1.97
LRSAM1	NM_138361	-1.97
A_24_P920664	A_24_P920664	-1.96
TXNDC4	NM_015051	-1.96
ATP6V1F	NM_004231	-1.96
PCGF3	NM_006315	-1.96
BC019667	BC019667	-1.96
FAS	NM_000043	-1.96
ENST00000361789	M28016	-1.96
RP11-125A7.3	NM_015058	-1.96
ITIH5	NM_030569	-1.96
ENST00000361227	AB017116	-1.96
PYGO2	NM_138300	-1.96
LOC653056	XM_930744	-1.95
THC2300907	THC2300907	-1.95
PEX7	NM_000288	-1.95
CUGBP1	AB210019	-1.94
CR611122	CR611122	-1.94
HSD17B1	BC033110	-1.94
RALGDS	NM_006266	-1.94
DBR1	NM_016216	-1.94
CR608907	CR608907	-1.94
GTF3C3	NM_012086	-1.94
REPIN1	NM_014374	-1.93
ACAD11	NM_032169	-1.93
KIAA0907	NM_014949	-1.93
TCF12	NM_207038	-1.93
MDS032	AK074683	-1.93
THC2336404	THC2336404	-1.93
TMTC4	NM_032813	-1.92
ECT2	NM_018098	-1.92
GCN5L2	NM_021078	-1.92
C1orf26	NM_017673	-1.92

Genename	Genbank	Fold Change in ALT
PPCDC	NM_021823	-1.92
AA714039	AA714039	-1.91
HAX1	NM_006118	-1.91
TOMM20	NM_014765	-1.91
C9orf37	NM_032937	-1.91
A_23_P2032	A_23_P2032	-1.91
ZNF499	NM_032792	-1.91
AARS	NM_001605	-1.90
CTAGE3	AF338231	-1.89
ANKS6	NM_173551	-1.89
ENST00000270201	AF231919	-1.89
GMCL1	NM_178439	-1.89
C14orf124	NM_020195	-1.89
AI090937	AI090937	-1.89
NT5C	NM_014595	-1.89
MAPBPIP	NM_014017	-1.89
C7orf28A	NM_015622	-1.88
KIAA0368	BC021127	-1.88
UEVLD	NM_018314	-1.88
THC2309459	THC2309459	-1.88
PIK3R4	NM_014602	-1.88
AF144054	AF144054	-1.88
TUBGCP3	NM_006322	-1.88
NFE2L2	NM_006164	-1.87
THUMPD3	NM_015453	-1.87
TBC1D16	AK091923	-1.87
CREB3L4	NM_130898	-1.87
GYLTL1B	NM_152312	-1.87
ZBTB41	NM_194314	-1.87
ARRDC2	NM_015683	-1.87
NFX1	NM_002504	-1.87
ZCSL3	NM_181706	-1.87
CCBL1	NM_004059	-1.87
ARL6IP2	NM_022374	-1.86
MRPS26	NM_030811	-1.86
BX537520	BX537520	-1.86
RYK	NM_001005861	-1.86
A_24_P912871	A_24_P912871	-1.86
IRF2BP1	NM_015649	-1.86
HGS	AK097197	-1.85
SNRPA	NM_004596	-1.85
ENST00000301042	AL713659	-1.85
A_24_P290134	A_24_P290134	-1.85
A_32_P85880	A_32_P85880	-1.84
PFAAP5	NM_014887	-1.84
NIT1	NM_005600	-1.84
PCGF3	NM_006315	-1.84

Genename	Genbank	Fold Change in ALT
PIGV	NM_017837	-1.84
TOR2A	NM_130459	-1.84
THRAP6	NM_080651	-1.83
THC2409451	THC2409451	-1.83
ENST00000367620	ENST00000367620	-1.83
GNA13	NM_006572	-1.83
RAP2B	NM_002886	-1.82
C15orf39	BC011905	-1.82
RAI16	NM_022749	-1.82
ZNF385	NM_015481	-1.82
SENP8	NM_145204	-1.82
NSUN5C	NM_032158	-1.82
MAN1B1	NM_016219	-1.82
GPR125	NM_145290	-1.82
CLK2	NM_001291	-1.82
CYFIP1	NM_014608	-1.81
ATP2A2	NM_001681	-1.81
A_24_P834646	A_24_P834646	-1.81
SPTY2D1	NM_194285	-1.81
ATP9B	NM_198531	-1.81
CCDC24	NM_152499	-1.81
THC2371517	THC2371517	-1.81
STX6	NM_005819	-1.81
GNPTAB	NM_024312	-1.80
WDR68	NM_005828	-1.80
PDDC1	NM_182612	-1.80
CD518214	CD518214	-1.79
NCKAP1	NM_205842	-1.78
KIAA1468	NM_020854	-1.78
ENST00000361204	CR614040	-1.78
ZNF687	NM_020832	-1.78
STARD3	NM_006804	-1.77
ENST00000252509	ENST00000252509	-1.77
A_24_P341731	A_24_P341731	-1.77
TTC17	BC041893	-1.76
A_24_P213284	A_24_P213284	-1.76
A_24_P608790	A_24_P608790	-1.76
DDX46	NM_014829	-1.76
THC2304728	THC2304728	-1.76
DYNC2H1	AF288405	-1.76
CACNB1	NM_000723	-1.76
ACSL3	NM_004457	-1.76
BC033528	BC033528	-1.75
DKFZp667M2411	AL713754	-1.75
SARS2	NM_017827	-1.75
AGPAT4	NM_001012733	-1.75
CCNL1	NM_020307	-1.75

Genename	Genbank	Fold Change in ALT
BX116163	BX116163	-1.75
THC2365025	AA385540	-1.75
ENST00000222396	AB017004	-1.74
ZNF524	NM_153219	-1.74
PLEKHJ1	NM_018049	-1.74
RBAK	NM_021163	-1.74
TFDP2	NM_006286	-1.74
C11orf17	NM_020642	-1.74
COQ7	NM_016138	-1.74
ENST00000319822	BC111692	-1.73
NDUFA1	NM_004541	-1.73
METT5D1	NM_152636	-1.73
FRAT2	NM_012083	-1.73
LOC653319	NM_001040715	-1.73
GIPC1	NM_005716	-1.73
TOP1MT	NM_052963	-1.73
C9orf142	NM_183241	-1.72
SNX4	NM_003794	-1.72
ENST00000366862	AB007952	-1.72
BX648855	BX648855	-1.71
MAG	NM_080600	-1.71
AK058000	AK058000	-1.71
NOM1	NM_138400	-1.71
THC2437430	THC2437430	-1.71
BTBD12	NM_032444	-1.71
PMS2L1	BC044214	-1.70
A_24_P212764	A_24_P212764	-1.70
RABL2A	BC111008	-1.70
WDR85	NM_138778	-1.70
THC2355570	THC2355570	-1.70
AK026497	AK026497	-1.69
FLJ12700	NM_024910	-1.69
AF289615	AF289615	-1.69
FAM108A1	NM_031213	-1.68
AA807805	AA807805	-1.68
CRTC2	NM_181715	-1.68
ENST00000373816	CA438977	-1.68
MCL1	NM_021960	-1.67
BM054818	BM054818	-1.67
CBLL1	NM_024814	-1.67
RAB14	NM_016322	-1.67
SETD4	NM_001007260	-1.67
LPGAT1	NM_014873	-1.67
MRPS2	NM_016034	-1.67
AK129652	AK129652	-1.66
TADA1L	NM_053053	-1.66
CUTL1	NM_181552	-1.66

Genename	Genbank	Fold Change in ALT
PRSS15	NM_004793	-1.66
ZBED5	NM_021211	-1.66
ARMC4	NM_018076	-1.65
PRKD3	NM_005813	-1.65
LOC653256	XM_926634	-1.65
GNB1	NM_002074	-1.65
LOC389607	NM_001013651	-1.64
SUZ12	NM_015355	-1.64
IFT122	NM_018262	-1.64
THC2407545	THC2407545	-1.64
ZNF7	NM_003416	-1.64
SYMPK	NM_004819	-1.64
HMG20B	NM_006339	-1.64
PMS2L5	NM_174930	-1.62
USP48	NM_032236	-1.62
BC031316	BC031316	-1.62
THC2274016	THC2274016	-1.61
C7orf28B	NM_198097	-1.61
SMEK2	NM_020463	-1.61
AGGF1	NM_018046	-1.60
ATXN2L	NM_145714	-1.60
THC2312955	THC2312955	-1.59
RFWD2	NM_022457	-1.59
ARRDC2	NM_015683	-1.59
ADH5	NM_000671	-1.59
CRTC2	NM_181715	-1.59
ENST00000275546	ENST00000275546	-1.59
THC2406595	THC2406595	-1.59
FAM108A1	NM_031213	-1.58
HDAC5	NM_001015053	-1.58
THC2388093	THC2388093	-1.58
76P	NM_014444	-1.57
RP4-691N24.1	NM_025176	-1.57
KIAA1370	NM_019600	-1.57
MAPK6	NM_002748	-1.57
CRY2	NM_021117	-1.57
HDAC1	NM_004964	-1.56
YOD1	NM_018566	-1.56
ENST00000321795	AK096609	-1.56
GCS1	NM_006302	-1.56
BANP	NM_017869	-1.56
A_24_P67268	A_24_P67268	-1.54
THC2366654	THC2366654	-1.54
CDK5RAP2	NM_018249	-1.53
GTF3C2	NM_001521	-1.53
KIAA1333	NM_017769	-1.53
ITPA	NM_033453	-1.53

Genename	Genbank	Fold Change in ALT
DHX8	NM_004941	-1.53
DBF4B	NM_145663	-1.52
ENST00000244249	XM_497963	-1.52
ANKHD1	NM_017747	-1.52
LOC285749	AK026691	-1.52
A_24_P761386	A_24_P761386	-1.51
THC2267302	THC2267302	-1.51
A_24_P913961	A_24_P913961	-1.51
CN431194	CN431194	-1.50
DKFZP434A0131	NM_018991	-1.50
ZFAND5	NM_006007	-1.49
ING1	NM_198219	-1.48
APRIN	NM_015032	-1.48
IGF2BP3	NM_006547	-1.48
CDK10	NM_052987	-1.48
TASP1	NM_017714	-1.46
C17orf37	NM_032339	-1.46
SLC25A36	AL049246	-1.46
A_24_P50666	A_24_P50666	-1.45
MYOHD1	NM_025109	-1.45
KIAA1542	NM_020901	-1.44
SMG5	NM_015327	-1.44
ATXN7L3	BC037418	-1.43
CDC42SE2	NM_020240	-1.42
VBP1	NM_003372	-1.42
ENST00000374865	BC015133	-1.40
GRB2	NM_002086	-1.40
RFWD2	NM_022457	-1.40
C7orf38	NM_145111	-1.40
COG2	AL832190	-1.39
NEK8	NM_178170	-1.37
A_32_P80587	A_32_P80587	-1.37
CDC2L1	NM_033489	-1.36
UBADC1	NM_016172	-1.36
SNAPC4	NM_003086	-1.31
ENST00000295907	CR593252	-1.26
C21orf96	AK024509	-1.25
TMEM41B	NM_015012	-1.23
A_32_P112531	A_32_P112531	-1.18
A_24_P477102	A_24_P477102	-1.18
THC2280383	THC2280383	-1.14
ZNF638	NM_014497	-1.13
APOBEC3C	NM_014508	-1.01
MUTYH	NM_012222	1.03
AF086548	AF086548	1.03
ENST00000217537	BC108287	1.05
FAM3C	NM_014888	1.05

Genename	Genbank	Fold Change in ALT
ENST00000375816	BM458572	1.06
CDC2L1	BC062579	1.07
ZNF414	AK074191	1.16
ENST00000375664	ENST00000375664	1.27
COX5A	NM_004255	1.30
THC2280867	THC2280867	1.32
EEF1D	NM_032378	1.37
EIF2C3	NM_024852	1.38
AF086335	AF086335	1.41
HERC5	NM_016323	1.42
ENST00000266712	CR749309	1.44
FRYL	BC021803	1.46
DA292134	DA292134	1.47
GSG1	NM_031289	1.47
MMP19	NM_002429	1.48
CCIN	NM_005893	1.49
LOC51035	NM_015853	1.49
SPCS2	NM_014752	1.50
C11orf2	NM_013265	1.50
ENST00000298129	AK056666	1.51
BTBD11	NM_152322	1.52
TM9SF4	NM_014742	1.54
TSR2	NM_058163	1.55
A_32_P48066	A_32_P48066	1.56
LOC51035	NM_015853	1.57
PTP4A2	NM_080392	1.57
POLD3	NM_006591	1.57
USP33	NM_201626	1.57
KLHDC2	NM_014315	1.58
PCBD2	NM_032151	1.59
KRTAP2-4	NM_033184	1.59
ATP5S	NM_001003803	1.59
C14orf166	NM_016039	1.60
LEMD2	NM_181336	1.60
HTRA2	NM_145074	1.60
SNX8	NM_013321	1.60
FN3KRP	NM_024619	1.62
XRCC1	NM_006297	1.62
ECOP	NM_030796	1.62
TJP1	NM_003257	1.63
KITLG	NM_000899	1.63
GOSR2	NM_054022	1.63
CRSP8	NM_004269	1.63
IL13RA1	NM_001560	1.64
IL1RAP	NM_002182	1.65
CYB5R1	NM_016243	1.65
TIMP3	NM_000362	1.65

Genename	Genbank	Fold Change in ALT
DRAP1	NM_006442	1.66
ROCK2	NM_004850	1.66
THC2275767	THC2275767	1.66
A_24_P75408	A_24_P75408	1.66
TMTC3	NM_181783	1.66
A_32_P174385	A_32_P174385	1.67
AK098307	AK098307	1.68
MGAT1	NM_002406	1.69
CR611332	CR611332	1.69
ZFP91	NM_053023	1.70
A_24_P943429	A_24_P943429	1.70
MRPL30	NM_145212	1.71
PPM1A	NM_177951	1.71
HIPK1	NM_152696	1.71
TK1	NM_003258	1.71
TEX261	NM_144582	1.71
TPX2	NM_012112	1.72
TGOLN2	NM_006464	1.72
ACTR10	NM_018477	1.72
EDARADD	NM_080738	1.73
C2orf18	NM_017877	1.73
ARHGAP10	NM_024605	1.74
C20orf172	NM_024918	1.74
CR594732	CR594732	1.74
ZNF197	NM_006991	1.75
ZNF136	NM_003437	1.75
PGK1	NM_000291	1.75
TYW1	NM_018264	1.75
C15orf24	NM_020154	1.75
AK2	NM_001625	1.76
C20orf24	NM_018840	1.76
SAP30L	NM_024632	1.76
ENO1	NM_001428	1.76
M6PRBP1	NM_005817	1.77
THRA	NM_003250	1.77
TANC2	AJ278120	1.77
RAP1A	NM_001010935	1.77
PRKRIP1	NM_024653	1.78
TBC1D19	NM_018317	1.78
GPATC1	NM_018025	1.78
RABAC1	NM_006423	1.78
THC2406192	THC2406192	1.78
NAGK	NM_017567	1.79
RBL1	NM_002895	1.79
TMEM97	NM_014573	1.80
ZFYVE26	NM_015346	1.81
SRD5A1	NM_001047	1.81

Genename	Genbank	Fold Change in ALT
MTCH1	NM_014341	1.81
ERBB2IP	NM_018695	1.82
C14orf100	NM_016475	1.82
FBXO33	NM_203301	1.82
FADS1	NM_013402	1.84
CDADC1	NM_030911	1.85
SNAI2	U97060	1.86
MAX	NM_145113	1.86
CUL4B	BX647096	1.87
MYO18A	NM_078471	1.87
ENST00000238571	L40403	1.87
ENST00000297145	AF274937	1.88
LOC51255	NM_016494	1.88
FAM50A	NM_004699	1.90
FLJ10099	NM_017994	1.90
C14orf106	NM_018353	1.90
RBPSUH	NM_203284	1.90
MTHFD1	NM_005956	1.91
NRM	NM_007243	1.91
CREB3	NM_006368	1.91
BRMS1	NM_015399	1.91
ACOT8	NM_005469	1.92
TIMM9	NM_012460	1.92
THC2275804	CB133932	1.92
MSH2	NM_000251	1.93
GGCX	NM_000821	1.94
ATP6V0E	NM_003945	1.94
AK022110	AK022110	1.94
STX5	NM_003164	1.94
PTTG2	NM_006607	1.94
THC2346166	THC2346166	1.94
KIAA1458	BC031691	1.95
ENST00000332935	BC053534	1.95
TRAPPC6B	BC030604	1.95
BX101252	BX101252	1.95
ZNF43	NM_003423	1.96
U69195	U69195	1.96
COMMD9	NM_014186	1.96
C14orf10	NM_017917	1.97
ACTR10	NM_018477	1.97
AIP	NM_003977	1.97
COMMD1	NM_152516	1.97
ENST00000355691	L06133	1.97
TMEM127	NM_017849	1.98
FAM14B	NM_206949	1.98
PTRF	NM_012232	1.98
MGC10433	NM_024321	1.98

Genename	Genbank	Fold Change in ALT
AIP	NM_003977	1.98
FANCM	NM_020937	1.98
FZD1	NM_003505	1.99
WDHD1	NM_007086	1.99
AK092888	AK092888	1.99
ETNK1	NM_018638	2.01
VTI1B	NM_006370	2.02
PTTG3	NR_002734	2.02
SBDS	NM_016038	2.03
GOLT1B	NM_016072	2.04
AI933337	AI933337	2.04
COTL1	NM_021149	2.04
C14orf112	NM_016468	2.05
SLC4A7	NM_003615	2.05
CGRRF1	NM_006568	2.06
TEGT	NM_003217	2.07
NLN	NM_020726	2.07
SBDS	NM_016038	2.08
SNX15	NM_013306	2.08
TMEM127	NM_017849	2.08
ACTR1A	NM_005736	2.08
ERGIC2	NM_016570	2.09
AHCYL1	NM_006621	2.09
A_23_P136857	A_23_P136857	2.10
ANLN	NM_018685	2.10
BG284526	BG284526	2.10
SPATA7	NM_018418	2.11
ZNF138	NM_006524	2.11
NAT12	NM_001011713	2.11
RCP9	NM_014478	2.12
VEGFB	NM_003377	2.12
BI771091	BI771091	2.12
ZDHHC7	NM_017740	2.13
DYNC1H1	NM_001376	2.13
CALU	NM_001219	2.13
CTTN	NM_005231	2.14
CEP57	BC039711	2.14
CR601835	CR601835	2.15
AK3L1	NM_001005353	2.15
MYL6	NM_079423	2.15
SSH1	NM_018984	2.16
MLH1	NM_000249	2.17
A_32_P4608	A_32_P4608	2.17
ZC3H14	NM_207660	2.17
AK092468	AK092468	2.17
A_24_P340886	A_24_P340886	2.17
CR602702	CR602702	2.18

Genename	Genbank	Fold Change in ALT
BC090057	BC090057	2.18
ENST00000310218	ENST00000310218	2.18
FOXM1	NM_202002	2.19
WDR22	NM_003861	2.19
ZFP41	AK024438	2.19
MAP4K5	NM_198794	2.19
ARF4	NM_001660	2.19
CD63	NM_001780	2.19
KIAA1641	NM_020970	2.20
RELA	BC014095	2.20
A_32_P64894	A_32_P64894	2.20
C14orf159	NM_024952	2.20
STAT2	NM_005419	2.20
VTI1B	NM_006370	2.21
STK38	NM_007271	2.22
SCYL1	NM_020680	2.22
FGFR1OP2	NM_015633	2.22
C6orf106	NM_024294	2.22
FBXW8	NM_153348	2.22
BC024198	BC024198	2.22
TP53INP2	NM_021202	2.22
GALNTL4	NM_198516	2.22
DRAP1	NM_006442	2.24
KDEL2	NM_006854	2.25
A_24_P835388	A_24_P835388	2.25
POLA2	NM_002689	2.26
C12orf43	NM_022895	2.26
UBL3	NM_007106	2.26
AK022059	AK022059	2.26
THC2406182	THC2406182	2.27
DA422275	DA422275	2.27
A_24_P341058	A_24_P341058	2.28
POP4	NM_006627	2.29
SMPD3	NM_018667	2.29
VEGFB	NM_003377	2.30
THC2334619	THC2334619	2.30
MXRA7	NM_001008528	2.30
SAR1B	NM_016103	2.30
SEC61G	NM_014302	2.30
ENST00000252134	AB020626	2.31
A_24_P144556	A_24_P144556	2.31
THC2268341	AA701118	2.31
KDEL2	NM_006854	2.31
WDR20	NM_181302	2.33
PTPRG	NM_002841	2.33
MTCH1	NM_014341	2.33
C14orf151	NM_032714	2.34

Genename	Genbank	Fold Change in ALT
DB328061	DB328061	2.34
A_24_P101493	A_24_P101493	2.34
THC2308298	THC2308298	2.34
DDEF1	NM_018482	2.34
ZC3H14	NM_024824	2.35
CD63	NM_001780	2.35
MGAT2	NM_002408	2.36
SLC6A6	NM_003043	2.36
KIAA1666	BC035246	2.38
SEC24D	NM_014822	2.39
AK124956	AK124956	2.40
C12orf23	NM_152261	2.41
LRRFIP2	NM_006309	2.41
LASP1	NM_006148	2.41
AYP1	NM_032193	2.42
ZNF313	NM_018683	2.42
THC2364429	THC2364429	2.43
AHCYL1	NM_006621	2.44
AF118081	AF118081	2.44
C6orf148	NM_030568	2.44
GNG12	NM_018841	2.45
A_24_P32735	A_24_P32735	2.45
A_32_P63886	A_32_P63886	2.45
MGC24039	BC020855	2.46
RBPSUH	NM_203284	2.46
RCP9	NM_014478	2.46
DNAJB4	NM_007034	2.46
LMAN2L	NM_030805	2.47
ZHX3	NM_015035	2.47
C6orf148	NM_030568	2.48
MMP19	NM_002429	2.48
KDELR3	NM_016657	2.49
SLC44A2	NM_020428	2.49
ALG14	NM_144988	2.50
THC2431726	THC2431726	2.50
CYP2U1	NM_183075	2.51
MPP5	NM_022474	2.51
MPP5	NM_022474	2.53
CA420826	CA420826	2.54
CXorf43	NM_144657	2.54
STK38	NM_007271	2.54
C20orf111	NM_016470	2.54
MGC14376	NM_032895	2.54
GRPR	U57365	2.55
KIAA0831	NM_014924	2.55
ATP6V1D	NM_015994	2.55
DNAJB4	NM_007034	2.56

Genename	Genbank	Fold Change in ALT
FIBCD1	NM_032843	2.57
PARVA	NM_018222	2.57
ABHD4	NM_022060	2.58
REXO2	NM_015523	2.58
LOC253981	AK025431	2.59
ENST00000381942	AK126071	2.59
AP4S1	NM_007077	2.60
WDR25	NM_024515	2.60
PTPN21	NM_007039	2.60
ARHGEF17	NM_014786	2.60
PCDHB13	NM_018933	2.62
SEC14L1	NM_003003	2.64
SLC39A7	NM_006979	2.64
C12orf4	NM_020374	2.64
E2F1	NM_005225	2.65
THC2267829	CN429806	2.66
NDST1	BC012888	2.67
MEIS3P1	NR_002211	2.67
OXSR1	NM_005109	2.68
LPP	NM_005578	2.68
COMMD10	NM_016144	2.71
B2M	NM_004048	2.71
SGCB	NM_000232	2.72
FLJ40330	BC031698	2.72
DOPEY2	NM_005128	2.73
ENST00000334564	ENST00000334564	2.75
CXXC5	NM_016463	2.76
AK098360	AK098360	2.76
PUS7L	NM_031292	2.77
NUBPL	NM_025152	2.77
C9orf39	NM_017738	2.78
KIAA1666	BC035246	2.78
MICB	NM_005931	2.79
CDKN3	NM_005192	2.81
PML	NM_002675	2.84
UCP3	NM_003356	2.85
PXK	AK131385	2.85
STOM	NM_198194	2.85
WDR21A	NM_181340	2.85
ATP10D	NM_020453	2.86
DKFZP564J0863	NM_015459	2.86
CCDC6	S72869	2.86
PTEN	NM_000314	2.87
BMP2K	NM_017593	2.88
LOC286016	NR_002187	2.88
MYL6	NM_079423	2.88
ERCC2	NM_000400	2.89

Genename	Genbank	Fold Change in ALT
CXXC5	NM_016463	2.90
SOCS5	NM_144949	2.93
LOC221362	AK095359	2.93
ITPR2	NM_002223	2.93
CENPQ	NM_018132	2.95
CFL2	NM_021914	2.95
FLJ40330	BX648045	2.96
KLHDC1	NM_172193	2.97
C14orf28	NM_001017923	2.99
A_24_P753760	A_24_P753760	2.99
BG009439	BG009439	3.00
ICK	NM_016513	3.02
ENST00000375180	AK125664	3.03
AVEN	NM_020371	3.04
WDR21A	NM_181340	3.04
BF217859	BF217859	3.05
FTL	NM_000146	3.07
PARVA	NM_018222	3.08
CDH24	AK057922	3.08
A_24_P101352	A_24_P101352	3.09
IL6ST	NM_002184	3.11
C11orf60	NM_020153	3.15
SLC30A7	NM_133496	3.16
FLJ31715	AK056277	3.17
BE825944	BE825944	3.17
ANKRD13A	NM_033121	3.18
ANXA5	NM_001154	3.19
SELPLG	NM_003006	3.20
TSPAN9	NM_006675	3.20
TRAM2	NM_012288	3.20
MET	NM_000245	3.26
CHST7	NM_019886	3.26
GULP1	NM_016315	3.26
DNAJB5	NM_012266	3.31
COL18A1	NM_030582	3.34
BX101288	BX101288	3.34
LOC387882	NM_207376	3.39
STOM	NM_198194	3.42
ENST00000367545	AK023675	3.42
FZD2	NM_001466	3.43
CREB3L1	NM_052854	3.44
TACC1	NM_006283	3.51
AK3L2	NM_001002921	3.54
TRIM62	NM_018207	3.55
GPRASP2	NM_001004051	3.57
CSDE1	NM_001007553	3.57
GALNT10	NM_198321	3.58

Genename	Genbank	Fold Change in ALT
C14orf132	NM_020215	3.60
RBPSUH	D14041	3.63
C6orf128	NM_145316	3.68
PIGK	NM_005482	3.68
MYH9	NM_002473	3.72
ENST00000308604	BC070200	3.74
A_32_P93792	A_32_P93792	3.75
DKFZp667G2110	NM_153605	3.77
CHES1	NM_005197	3.82
STK17B	NM_004226	3.84
TRIM16	NM_006470	3.85
MGC4677	NM_052871	3.88
MET	NM_000245	3.88
CD109	NM_133493	3.88
SLC16A2	NM_006517	3.88
ENST00000372072	AK000180	3.92
BHLHB9	NM_030639	3.93
PCDHB7	NM_018940	3.93
HPSE	NM_006665	3.93
TMEM25	NM_032780	3.95
CD40	NM_001250	3.96
ARID5B	NM_032199	3.99
TACC1	NM_006283	3.99
EHD1	NM_006795	4.01
LMCD1	NM_014583	4.02
C14orf46	BC009539	4.03
A_24_P917668	A_24_P917668	4.03
ABHD9	NM_024794	4.05
APLN	NM_017413	4.11
LONRF3	NM_024778	4.11
LOC92689	NM_138389	4.24
FZD7	NM_003507	4.24
SEL1L	NM_005065	4.27
STC2	NM_003714	4.29
FTL	NM_000146	4.33
LAMP2	NM_002294	4.38
BIN1	NM_139346	4.38
ENO2	NM_001975	4.40
ADC	NM_052998	4.40
AF075027	AF075027	4.41
PRKCA	NM_002737	4.43
UPP1	NM_181597	4.44
RAB8B	NM_016530	4.48
THC2267053	THC2267053	4.51
CUZD1	NM_022034	4.54
BE816002	BE816002	4.61
SOCS1	NM_003745	4.64

Genename	Genbank	Fold Change in ALT
C14orf139	BC008299	4.66
SCD5	NM_001037582	4.67
APOLD1	NM_030817	4.71
TEAD3	NM_003214	4.74
HLA-E	NM_005516	4.76
APLN	NM_017413	4.77
A_24_P938006	A_24_P938006	4.82
BU684362	BU684362	4.83
TPM1	NM_001018004	4.83
CAMK2D	NM_172127	4.84
BE795374	BE795374	4.85
FTL	NM_000146	4.86
TCHP	NM_032300	4.91
BIN1	NM_139346	4.94
A_24_P281683	A_24_P281683	4.95
PXK	NM_017771	4.96
ACTN1	NM_001102	4.97
HLA-C	BC002463	5.00
AK127258	AK127258	5.02
HLA-E	NM_005516	5.03
CHES1	NM_005197	5.03
CACNA1C	NM_000719	5.14
HLA-A	NM_002116	5.17
SCGB3A2	NM_054023	5.22
PRKCA	NM_002737	5.26
CAMK2D	NM_001221	5.29
THC2346243	THC2346243	5.35
NRN1	NM_016588	5.54
N48043	N48043	5.57
C10orf25	NM_001039380	5.57
TMEM45A	NM_018004	5.64
GLYATL2	NM_145016	5.70
HLA-G	NM_002127	5.71
A_24_P32715	A_24_P32715	5.71
SH3BP4	NM_014521	5.72
AHNAK	NM_001620	5.73
ZNF501	NM_145044	5.75
TRAM2	NM_012288	5.78
ENST00000376802	AF287958	5.79
BF217859	BF217859	5.95
EHD1	AF099011	5.98
ALDH6A1	NM_005589	5.98
EPS8	NM_004447	6.03
C6orf65	NM_152731	6.21
ADAMTSL1	NM_139238	6.21
ACTN1	NM_001102	6.22
BNC2	NM_017637	6.35

Genename	Genbank	Fold Change in ALT
RSNL2	NM_024692	6.42
RP1-32F7.2	NM_173698	6.49
SAMD4A	AB028976	6.52
TPM1	NM_000366	6.53
HLA-C	CR598918	6.60
ENST00000380195	BC001304	6.90
C16orf45	NM_033201	6.92
TPM1	NM_001018004	6.97
HLA-H	NR_001434	7.45
TPM1	NM_001018004	7.47
PRKCDBP	NM_145040	7.48
FAM46B	NM_052943	7.62
HLA-E	NM_005516	7.63
PRKD1	NM_002742	7.63
AK094175	AK094175	7.65
FLNC	NM_001458	7.71
A_24_P237896	A_24_P237896	7.76
CR608347	CR608347	7.79
EDG2	NM_057159	7.84
C1orf118	NM_001039463	8.18
STC2	NM_003714	8.22
ENST00000383518	M64259	8.31
MATN2	NM_030583	8.33
S100A4	NM_002961	8.36
A_24_P101771	A_24_P101771	8.47
HLA-F	NM_018950	8.54
HLA-C	BC008457	8.64
MGC16121	BC007360	8.71
FGF2	NM_002006	8.75
TFPI	NM_001032281	8.92
RGNEF	AK025816	8.98
DKFZP686A01247	NM_014988	9.05
PAPSS2	NM_001015880	9.14
ENST00000376793	ENST00000376793	9.24
ENST00000373886	AK130049	9.28
HLA-B	NM_005514	9.33
MN1	NM_002430	9.45
FLJ45422	NM_001004349	9.60
RBMS3	NM_014483	9.94
PCDHB9	NM_019119	10.08
FBLN5	NM_006329	10.15
A_23_P125109	A_23_P125109	10.54
HLA-C	NM_002117	10.88
NEXN	NM_144573	11.08
HLA-F	NM_018950	11.10
AHNAK	NM_024060	11.11
PPP1R3C	NM_005398	11.38

Genename	Genbank	Fold Change in ALT
COL6A1	NM_001848	11.55
BC035647	BC035647	11.61
NEXN	NM_144573	11.76
SLC8A1	NM_021097	11.97
SYNC1	NM_030786	12.83
PPAP2B	NM_003713	12.97
AK092921	AK092921	13.22
BC089454	BC089454	13.23
PAX8	NM_003466	13.38
GPR39	AK122643	13.64
EMR1	NM_001974	13.72
DKFZP686A01247	NM_014988	13.86
ADAMTS5	NM_007038	14.00
GYPC	NM_002101	14.76
HLA-B	NM_005514	14.95
OXTR	NM_000916	15.22
C1R	NM_001733	16.11
KCNIP3	NM_013434	16.72
ITGA1	NM_181501	16.73
TFPI	NM_006287	17.31
FGF13	NM_004114	18.82
AHRR	AB033060	20.14
DOC1	NM_182909	20.94
FLJ36748	NM_152406	22.36
SLC8A1	BX648299	22.73
SYTL2	NM_206927	22.78
CTSC	NM_148170	23.35
JAM2	NM_021219	25.15
WNT5B	NM_030775	26.41
WNT5A	NM_003392	28.99
DPF3	NM_012074	29.49
FBLN5	NM_006329	30.74
PDGFRB	NM_002609	30.77
SFRP1	NM_003012	37.96
MYEOV	NM_138768	38.48
COL16A1	NM_001856	47.62
LOC51334	NM_016644	49.61
SFRP1	NM_003012	50.92
PTN	NM_002825	54.79
PTN	NM_002825	66.78
COL1A2	NM_000089	84.24
PRKCDBP	NM_145040	107.13
COL1A1	Z74615	298.49

Table 4 : 297 Genes differentially expressed between ALT and telomerase positive cells in both liposarcomas and cell lines.

Gene Name	Genbank	Fold Change in ALT Liposarcomas	Fold Change in ALT Cell Lines
TERT	NM_198253	-10.33	-46.32
SLC6A10P	NR_003083	-9.98	-8.03
MDFI	NM_005586	-5.35	-9.23
LOC92312	XM_044166	-5.31	-4.89
TP53TG3	NM_016212	-5.08	-7.44
LOC649542	XM_938617	-4.30	-8.07
ITIH5	NM_030569	-4.28	-1.96
LOC112703	NM_138411	-4.08	-11.78
ALDH5A1	NM_170740	-3.31	-2.05
SLC6A8	NM_005629	-3.27	-8.78
KIAA1370	NM_019600	-3.13	-1.57
PER2	NM_022817	-3.05	-2.83
CEBPA	NM_004364	-2.96	-8.74
MSTP9	NR_002729	-2.93	-3.88
CR625561	CR625561	-2.89	-2.52
CEBPA	NM_004364	-2.89	-6.93
MARCKSL1	NM_023009	-2.88	-2.81
SLC6A8	NM_005629	-2.85	-3.80
C10orf35	NM_145306	-2.85	-29.45
ENST00000361453	AK026903	-2.82	-2.19
LRRC8B	NM_015350	-2.81	-6.34
FLJ22795	AF316855	-2.77	-3.18
ENST00000330947	BC035081	-2.73	-8.18
AK097322	AK097322	-2.64	-2.08
MMP15	NM_002428	-2.50	-2.76
ENST00000361227	AY423734	-2.49	-2.25
FLJ22795	NM_025084	-2.48	-3.33
BF576096	BF576096	-2.47	-1.97
BC065260	BC065260	-2.42	-2.78
TP53INP1	NM_033285	-2.40	-2.39
KLHL24	NM_017644	-2.38	-3.91
LYPLA1	NM_006330	-2.35	-2.32
ENST00000301042	AL713659	-2.34	-1.85
ENST00000361227	AB017116	-2.27	-1.96
ST6GAL1	NM_173216	-2.25	-28.83
GPRC5C	NM_022036	-2.22	-5.14
DUSP22	AK000383	-2.22	-2.01
AK057071	AK057071	-2.22	-2.31
BC019667	BC019667	-2.20	-1.96
ASB13	NM_024701	-2.19	-3.54
LYPLA1	NM_006330	-2.17	-2.08
CR601496	CR601496	-2.16	-2.12

Gene Name	Genbank	Fold Change in ALT Liposarcomas	Fold Change in ALT Cell Lines
RNF44	NM_014901	-2.16	-4.28
SLC39A4	NM_130849	-2.16	-18.24
RP11-138L21.1	AK024257	-2.11	-3.39
FLJ35740	NM_147195	-2.11	-4.14
A_24_P204334	A_24_P204334	-2.08	-2.34
AK131288	AK131288	-2.07	-2.31
ORF1-FL49	NM_032412	-2.06	-4.79
ZNF195	NM_007152	-2.05	-2.29
PLEKHG2	NM_022835	-2.04	-1.98
A_24_P384239	A_24_P384239	-2.04	-2.15
RP11-125A7.3	NM_015058	-2.04	-1.96
PIK3C2B	NM_002646	-2.02	-3.53
TFDP2	NM_006286	-2.01	-1.74
AK023328	AK023328	-2.01	-3.15
BX093417	BX093417	-2.01	-2.45
DUSP22	NM_020185	-2.00	-3.32
SULT4A1	NM_014351	-1.98	-4.11
ENST00000252509	ENST00000252509	-1.97	-1.77
CHD7	NM_017780	-1.96	-22.15
THC2428713	THC2428713	-1.95	-2.58
LPHN1	NM_001008701	-1.93	-5.41
GCN5L2	NM_021078	-1.93	-1.92
ENST00000372821	ENST00000372821	-1.90	-3.49
CHD7	NM_017780	-1.90	-16.78
ADAM11	NM_002390	-1.89	-8.75
TBC1D16	AK091923	-1.89	-1.87
CRY2	NM_021117	-1.89	-1.57
TOP1MT	NM_052963	-1.88	-1.73
ZNF692	NM_017865	-1.85	-3.18
KIAA1545	AB046765	-1.84	-2.13
ANKRD13B	NM_152345	-1.83	-3.51
FLJ22795	AF316855	-1.82	-2.93
TTC17	BC041893	-1.82	-1.76
76P	NM_014444	-1.82	-1.57
CCNL1	NM_020307	-1.79	-1.75
A_24_P608790	A_24_P608790	-1.79	-1.76
ENST00000220507	CR618466	-1.78	-5.75
THC2437122	THC2437122	-1.78	-1.97
ENST00000369239	AL080186	-1.77	-2.13
LOC653801	XM_934188	-1.77	-2.55
KIAA0485	AB007954	-1.76	-5.93
BCL7A	NM_020993	-1.75	-2.62
PCGF3	NM_006315	-1.73	-1.84
MGC4172	NM_024308	-1.73	-2.64
PMS2L1	BC044214	-1.73	-1.70
ENST00000275546	ENST00000275546	-1.70	-1.59

Gene Name	Genbank	Fold Change in ALT Liposarcomas	Fold Change in ALT Cell Lines
AA554330	AA554330	-1.69	-3.64
DECR2	NM_020664	-1.69	-3.09
LOC440295	NM_198181	-1.69	-2.31
GOLGA8E	NM_001012423	-1.69	-3.50
A_32_P80587	A_32_P80587	-1.67	-1.37
THC2411839	THC2411839	-1.67	-3.35
ASB13	NM_024701	-1.66	-4.76
TOMM20	NM_014765	-1.63	-1.91
tcag7.1017	NM_001004351	-1.63	-2.16
P15RS	NM_018170	-1.63	-3.03
NUDT14	NM_177533	-1.61	-3.19
FAM59A	NM_022751	-1.60	-7.55
LOC653639	XM_934787	-1.59	-2.39
ASAH1	NM_004315	-1.59	-2.55
B3GNT5	NM_032047	-1.59	-14.16
REPIN1	NM_014374	-1.57	-1.93
SLC16A9	NM_194298	-1.56	-3.32
ENST00000270201	AF231919	-1.55	-1.89
GLI4	NM_138465	-1.55	-3.18
ADH5	NM_000671	-1.54	-1.59
LONRF1	NM_152271	-1.54	-4.57
ENST00000319822	BC111692	-1.53	-1.73
HNRPA3	NM_194247	-1.53	-2.19
BIVM	NM_017693	-1.52	-2.67
PMS2L5	NM_174930	-1.52	-1.62
STAU2	AK002152	-1.51	-6.20
LOC389607	NM_001013651	-1.51	-1.64
A_24_P341731	A_24_P341731	-1.51	-1.77
GP1BB	NM_000407	-1.49	-5.60
HNRPA3	NM_194247	-1.48	-3.02
GPR125	NM_145290	-1.47	-1.82
SIRT5	NM_012241	-1.47	-1.97
CLK2	NM_003993	-1.47	-2.10
APOM	NM_019101	-1.46	-2.05
AFG3L1	NM_001132	-1.46	-5.05
TMEM80	NM_174940	-1.42	-3.38
BX537520	BX537520	-1.41	-1.86
ZMYM2	NM_003453	-1.37	-2.36
ZFP64	NM_018197	-1.36	-2.04
BC064492	BC064492	-1.34	-2.66
PEX7	NM_000288	-1.33	-1.95
DRG2	NM_001388	-1.32	-4.32
ZFAND5	NM_006007	-1.32	-1.49
PERLD1	NM_033419	-1.31	-1.97
NSUN5B	NM_145645	-1.29	-2.96
GMCL1	NM_178439	-1.29	-1.89

Gene Name	Genbank	Fold Change in ALT Liposarcomas	Fold Change in ALT Cell Lines
HDAC5	NM_001015053	-1.29	-1.58
TFB2M	NM_022366	-1.29	-2.04
NSUN5C	NM_148936	-1.27	-2.50
MAPK11	NM_002751	-1.26	-6.28
NSUN5C	NM_032158	-1.24	-1.82
THC2455149	THC2455149	-1.23	-3.63
ENST00000378954	CR617774	-1.22	-1.98
NIT1	NM_005600	-1.20	-1.84
AF086442	AF086442	-1.18	-4.70
ATP5D	NM_001001975	-1.15	-2.07
HEATR2	NM_017802	-1.10	-2.20
TM9SF4	NM_014742	1.10	1.54
ZFP91	NM_053023	1.13	1.70
A_32_P64894	A_32_P64894	1.14	2.20
SBDS	NM_016038	1.15	2.08
CCIN	NM_005893	1.15	1.49
MGC24039	BC020855	1.16	2.46
AIP	NM_003977	1.18	1.97
AIP	NM_003977	1.21	1.98
CR602702	CR602702	1.24	2.18
SPCS2	NM_014752	1.24	1.50
MYL6	NM_079423	1.29	2.15
LEMD2	NM_181336	1.29	1.60
FBXO33	NM_203301	1.31	1.82
STX5	NM_003164	1.32	1.94
TMEM127	NM_017849	1.34	1.98
APOLD1	NM_030817	1.36	4.71
ATP6V1D	NM_015994	1.36	2.55
C20orf24	NM_018840	1.37	1.76
DYNC1H1	NM_001376	1.37	2.13
WDHD1	NM_007086	1.38	1.99
PTP4A2	NM_080392	1.39	1.57
KIAA1458	BC031691	1.39	1.95
UBL3	NM_007106	1.39	2.26
NAT12	NM_001011713	1.40	2.11
MGC10433	NM_024321	1.41	1.98
POLA2	NM_002689	1.41	2.26
ATP10D	NM_020453	1.42	2.86
MGAT1	NM_002406	1.43	1.69
C12orf23	NM_152261	1.44	2.41
U69195	U69195	1.44	1.96
MTCH1	NM_014341	1.45	1.81
BC024198	BC024198	1.45	2.22
SYNC1	NM_030786	1.47	12.83
C2orf18	NM_017877	1.49	1.73
MGC16121	BC007360	1.49	8.71

Gene Name	Genbank	Fold Change in ALT Liposarcomas	Fold Change in ALT Cell Lines
TEAD3	NM_003214	1.50	4.74
A_32_P93792	A_32_P93792	1.52	3.75
FZD2	NM_001466	1.53	3.43
APLN	NM_017413	1.54	4.77
AF086335	AF086335	1.55	1.41
BRMS1	NM_015399	1.55	1.91
ACOT8	NM_005469	1.55	1.92
ZNF414	AK074191	1.55	1.16
RBPSUH	NM_203284	1.56	1.90
POLD3	NM_006591	1.57	1.57
SEC61G	NM_014302	1.57	2.30
ENST00000266712	CR749309	1.58	1.44
LOC51255	NM_016494	1.61	1.88
TPX2	NM_012112	1.62	1.72
FAM50A	NM_004699	1.63	1.90
PTPN21	NM_007039	1.64	2.60
ARF4	NM_001660	1.64	2.19
THC2406182	THC2406182	1.65	2.27
STK38	NM_007271	1.66	2.54
CR601835	CR601835	1.66	2.15
IL1RAP	NM_002182	1.66	1.65
C9orf39	NM_017738	1.67	2.78
C15orf24	NM_020154	1.68	1.75
CREB3	NM_006368	1.70	1.91
PDGFRB	NM_002609	1.70	30.77
SLC4A7	NM_003615	1.71	2.05
MICB	NM_005931	1.72	2.79
SAP30L	NM_024632	1.72	1.76
ECOP	NM_030796	1.73	1.62
PTPRG	NM_002841	1.73	2.33
ACTN1	NM_001102	1.73	4.97
ACTN1	NM_001102	1.76	6.22
AHNAK	NM_024060	1.77	11.11
AK022110	AK022110	1.78	1.94
RAB8B	NM_016530	1.78	4.48
LASP1	NM_006148	1.79	2.41
A_24_P835388	A_24_P835388	1.84	2.25
ATP6V0E	NM_003945	1.84	1.94
ANXA5	NM_001154	1.85	3.19
TGOLN2	NM_006464	1.88	1.72
KDEL2	NM_006854	1.88	2.31
FAM14B	NM_206949	1.89	1.98
SYTL2	NM_206927	1.89	22.78
C20orf172	NM_024918	1.91	1.74
ENST00000381942	AK126071	1.91	2.59
FGF2	NM_002006	1.92	8.75

Gene Name	Genbank	Fold Change in ALT Liposarcomas	Fold Change in ALT Cell Lines
STK17B	NM_004226	1.92	3.84
PXK	AK131385	1.93	2.85
AK098360	AK098360	1.94	2.76
CXXC5	NM_016463	1.94	2.76
CYP2U1	NM_183075	1.95	2.51
GNG12	NM_018841	1.99	2.45
COTL1	NM_021149	2.00	2.04
FLJ45422	NM_001004349	2.05	9.60
NRM	NM_007243	2.05	1.91
RABAC1	NM_006423	2.07	1.78
ITPR2	NM_002223	2.08	2.93
A_24_P281683	A_24_P281683	2.09	4.95
SNX8	NM_013321	2.13	1.60
EHD1	NM_006795	2.14	4.01
FTL	NM_000146	2.14	3.07
MXRA7	NM_001008528	2.14	2.30
FTL	NM_000146	2.16	4.86
TPM1	NM_001018004	2.17	4.83
E2F1	NM_005225	2.18	2.65
FTL	NM_000146	2.19	4.33
LAMP2	NM_002294	2.19	4.38
A_24_P32715	A_24_P32715	2.20	5.71
SLC8A1	BX648299	2.25	22.73
TK1	NM_003258	2.25	1.71
KDEL3	NM_016657	2.27	2.49
FOXM1	NM_202002	2.28	2.19
TPM1	NM_001018004	2.30	6.97
NEXN	NM_144573	2.30	11.08
TPM1	NM_001018004	2.31	7.47
ZHX3	NM_015035	2.32	2.47
ENST00000376802	AF287958	2.32	5.79
DKFZP564J0863	NM_015459	2.33	2.86
SELPLG	NM_003006	2.34	3.20
SOCS1	NM_003745	2.37	4.64
SLC8A1	NM_021097	2.42	11.97
HLA-F	NM_018950	2.44	11.10
PXK	NM_017771	2.54	4.96
LOC253981	AK025431	2.56	2.59
FADS1	NM_013402	2.63	1.84
AK022059	AK022059	2.67	2.26
NEXN	NM_144573	2.68	11.76
PRKD1	NM_002742	2.69	7.63
LOC92689	NM_138389	2.70	4.24
CALU	NM_001219	2.73	2.13
SEC24D	NM_014822	2.80	2.39
PTTG2	NM_006607	2.86	1.94

Gene Name	Genbank	Fold Change in ALT Liposarcomas	Fold Change in ALT Cell Lines
AK094175	AK094175	2.86	7.65
ENST00000308604	BC070200	3.02	3.74
CTSC	NM_148170	3.05	23.35
TACC1	NM_006283	3.07	3.99
CDKN3	NM_005192	3.10	2.81
MGC4677	NM_052871	3.13	3.88
SAMD4A	AB028976	3.17	6.52
ADAMTS5	NM_007038	3.26	14.00
ABHD4	NM_022060	3.30	2.58
KCNIP3	NM_013434	3.33	16.72
TACC1	NM_006283	3.35	3.51
HERC5	NM_016323	3.40	1.42
PRKCDBP	NM_145040	3.41	107.13
KIAA1666	BC035246	3.68	2.38
A_24_P753760	A_24_P753760	3.74	2.99
TRAM2	NM_012288	3.78	5.78
COL16A1	NM_001856	4.31	47.62
ANLN	NM_018685	4.64	2.10
S100A4	NM_002961	4.89	8.36
BNC2	NM_017637	5.38	6.35
OXTR	NM_000916	5.52	15.22
ENO2	NM_001975	5.54	4.40
PRKCA	NM_002737	5.84	5.26
TMEM45A	NM_018004	6.09	5.64
C1R	NM_001733	6.26	16.11
FZD1	NM_003505	6.35	1.99
COL1A1	Z74615	10.18	298.49
COL1A2	NM_000089	14.53	84.24

Table 5: 106 hTERT regulatory kinases

Gene Name	Average Fold Change of Hits	SE
Q19PIK3CD	-7.63	4.80
SYK	-5.1	1.08
ERK8	-4.97	2.68
STK17A	-4.58	0.35
EIF2AK3	-4.23	2.14
TESK1	-4.15	0.51
NME1	-4.11	1.56
STK3	-3.98	0.01
SGK2	-3.95	0.06
NEK2	-3.93	0.79
TEK	-3.88	1.68
STK38L	-3.88	0.88
T3JAM	-3.87	1.22

Gene Name	Average Fold Change of Hits	SE
TESK2	-3.87	0.59
GALK1	-3.85	0.20
STK22D	-3.85	1.04
TRIB1	-3.81	0.35
TPK1	-3.63	0.40
STK10	-3.61	0.70
EEF2K	-3.58	0.70
PRKWNK1	-3.57	1.15
PTK7	-3.56	0.92
STK32C	-3.54	0.33
SGK	-3.47	0.47
STK17B	-3.46	0.17
MAPK3	-3.44	0.71
STK35	-3.43	0.06
TXNDC3	-3.37	0.42
SNRK	-3.37	0.89
LOC390975	-3.37	0.12
TYK2	-3.34	0.36
STK11	-3.34	1.30
TTBK1	-3.33	0.58
STK22C	-3.30	0.25
STK32A	-3.19	0.71
SCGB2A1	-3.19	0.51
MKNK1	-3.16	0.19
STK24	-3.14	0.83
TAO1	-3.1	0.20
STK19	-3.05	0.01
DKFZp434B1231	-3.00	0.09
MAPK9	-2.98	0.69
SBK1	-2.97	0.65
PKMYT1	-2.97	0.58
SH3BP4	-2.89	0.37
MAPK8	-2.89	0.75
STK4	-2.87	0.17
COASY	-2.84	0.48
SSTK	-2.81	0.60
SIK2	-2.80	0.20
NEK9	-2.76	0.46
NEK8	-2.72	0.02
CDK6	-2.72	0.47
NEK7	-2.71	0.48
SPHK2	-2.67	0.05
PIP5K2C	-2.66	0.58
CRIM1	-2.66	0.60
PGK2	-2.66	0.29
DGUOK	-2.65	0.35
PRPSAP1	-2.63	0.45

Gene Name	Average Fold Change of Hits	SE
CAMK1	-2.62	0.06
PRKCN	-2.61	0.08
TXNDC6	-2.60	0.35
STK6	-2.59	0.58
PRKWINK2	-2.50	0.30
STK16	-2.45	0.17
KIAA1361	-2.42	0.28
PTK9L	-2.41	0.19
SMG1	-2.40	0.41
HRI	-2.36	0.16
PIK3CB	-2.35	0.13
TEX14	-2.34	0.10
YES1	-2.32	0.08
EPHB4	-2.31	0.03
MAP3K5	-2.31	0.21
PRKCH	-2.31	0.11
CARKL	-2.29	0.09
IHPK2	-2.28	0.10
MAP4K5	-2.27	0.21
MAP2K1	-2.27	0.11
LOC390877	-2.24	0.05
NEK3	-2.23	0.04
PSKH2	-2.20	0.06
MAP3K6	-2.17	0.15
RPS6KA2	-2.17	0.08
MAP3K14	-2.16	0.06
RIPK5	-2.15	0.05
TRIB2	-2.12	0.07
PCTK2	-2.10	0.02
CCRK	2.12	0.08
MAP2K6	2.15	0.14
NME4	2.17	0.16
PRKCE	2.31	0.16
CHKB	2.54	0.31
IKBKE	2.64	0.59
LOC91807	2.64	0.31
AKAP2	2.86	0.82
HIPK4	2.89	0.72
BUB1	2.93	0.49
ALK	2.99	0.77
FLJ22955	3.03	0.32
KIAA1811	3.06	0.98
ARAF1	3.08	0.63
IKBKG	3.20	0.56
ACK1	4.09	1.39
MAPKAPK5	4.76	0.09

Table 6: 87 Unique miRNAs able to distinguish between mesenchymal tumour types.

miRNA
hsa-let-7a*
hsa-let-7e
hsa-miR-100
hsa-miR-103
hsa-miR-125a-5p
hsa-miR-127-3p
hsa-miR-128
hsa-miR-1299
hsa-miR-130b
hsa-miR-135b
hsa-miR-142-3p
hsa-miR-142-5p
hsa-miR-144
hsa-miR-146a
hsa-miR-146b-5p
hsa-miR-148a
hsa-miR-150
hsa-miR-152
hsa-miR-1539
hsa-miR-15a
hsa-miR-15b
hsa-miR-16
hsa-miR-181a
hsa-miR-181b
hsa-miR-192
hsa-miR-193a-5p
hsa-miR-195*
hsa-miR-196a
hsa-miR-196b
hsa-miR-21
hsa-miR-21*
hsa-miR-210
hsa-miR-214
hsa-miR-215
hsa-miR-218
hsa-miR-22
hsa-miR-22*
hsa-miR-223
hsa-miR-24-1*
hsa-miR-27a
hsa-miR-27b
hsa-miR-28-3p
hsa-miR-28-5p
hsa-miR-29a
hsa-miR-29a*
hsa-miR-29b
hsa-miR-29b-1*
hsa-miR-29c
hsa-miR-29c*
hsa-miR-301a
hsa-miR-30a*
hsa-miR-30e
hsa-miR-30e*
hsa-miR-32

miRNA
hsa-miR-320c
hsa-miR-320d
hsa-miR-331-3p
hsa-miR-337-5p
hsa-miR-337-5p
hsa-miR-338-3p
hsa-miR-34a
hsa-miR-34b*
hsa-miR-361-3p
hsa-miR-377
hsa-miR-379
hsa-miR-381
hsa-miR-409-5p
hsa-miR-410
hsa-miR-454
hsa-miR-455-3p
hsa-miR-455-5p
hsa-miR-487b
hsa-miR-493
hsa-miR-493*
hsa-miR-500
hsa-miR-500*
hsa-miR-501-3p
hsa-miR-513b
hsa-miR-513c
hsa-miR-532-5p
hsa-miR-551b
hsa-miR-566
hsa-miR-574-5p
hsa-miR-590-5p
hsa-miR-660
hsa-miR-874
hsa-miR-95
hsa-miR-99b

Appendix II– Tumour Histology and information.

The following Table details all known Histological, telomere maintenance and survival information on record for tumour samples used in this study. The following abbreviations are used in the table: Tel = Telomerase positive, ALT = Alternative Lengthening of Telomeres, F = Female, M = Male, M.R.C = myxoid round cell, Retroperit. = Retroperitoneum. N/A indicates points where data was unavailable.

ID	Tumour Type	TMM	Grade	Histology	Location	Survival Status	Survival (month)	Age	Sex
S1038R	Liposarcoma	TEL	2	M.R.C.	N/A	0	57	48	F
S1111	Liposarcoma	TEL	2	M.R.C. (20-30%)	Lower Extremity	N/A	N/A	43	M
S1138R	Liposarcoma	ALT	2	WD, Lipoma-Like	N/A	0	50	N/A	N/A
S1364	Liposarcoma	TEL	3	Dedifferentiated	N/A	1	45	53	F
S1423	Liposarcoma	ALT	2	M.R.C.	N/A	0	158	N/A	N/A
S272	Liposarcoma	ALT	1	Myxoid	Retroperit.	N/A	N/A	76	M
S281	Liposarcoma	ALT	3	Pleomorphic, Myxoid Areas	Upper Extremity	N/A	N/A	84	M
S344	Liposarcoma	ALT	1	Dedifferentiated	Retroperit.	1	182	66	M
S384	Liposarcoma	ALT	2	M.R.C. (50%)	Lower Extremity	N/A	N/A	54	F
S498R	Liposarcoma	TEL	N/A	M.R.C. (70%)	Lower Extremity	N/A	N/A	64	F
S498R	Liposarcoma	TEL	N/A	M.R.C.	N/A	1	240	64	F
S670R	Liposarcoma	TEL	2	M.R.C.	Lower Extremity	N/A	N/A	48	F
S694R	Liposarcoma	ALT	2	M.R.C.	N/A	1	53	71	M
S711R	Liposarcoma	TEL	1	Myxoid	Lower Extremity	N/A	N/A	55	F
S717R1	Liposarcoma	ALT	3	Pleomorphic	Thorax	N/A	N/A	51	F
S750R	Liposarcoma	TEL	2	M.R.C. (>25%)	Lower Extremity	N/A	N/A	56	M
S787	Liposarcoma	TEL	2	M.R.C. (>25%)	Lower Extremity	0	65	47	M
S850	Liposarcoma	ALT	2	Dedifferentiated	Retroperit.	1	25	74	M
S860	Liposarcoma	TEL	2	M.R.C.	Lower Extremity	1	204	73	F
S861R	Liposarcoma	TEL	2	M.R.C. (>25%)	Retroperit.	N/A	N/A	42	F
S861R	Liposarcoma	TEL	2	M.R.C.	N/A	1	30	42	F
S867R	Liposarcoma	ALT	2	Pleomorphic	Lower Extremity	0	34	66	F

ID	Tumour Type	TMM	Grade	Histology	Location	Survival Status	Survival (month)	Age	Sex
S904R	Liposarcoma	ALT	2	Pleomorphic	Lower Extremity	N/A	N/A	N/A	F
S909	Liposarcoma	ALT	1	Dedifferentiated	Trunk	0	105	54	M
3	Mesothelioma	TEL	3	Biphasic	N/A	1	33	63	M
4	Mesothelioma	TEL	2	Epithelial Solid	N/A	0	30	29	M
10	Mesothelioma	TEL	3	Epithelial Solid	N/A	0	26	66	F
14	Mesothelioma	ALT	2	Epithelial Solid	N/A	0	25	37	F
18	Mesothelioma	TEL	3	Epithelial Solid	N/A	1	40	66	M
19	Mesothelioma	TEL	3	Epithelial Solid	N/A	1	6	42	F
20	Mesothelioma	TEL	3	Epithelial Solid	N/A	1	36	55	M
22	Mesothelioma	TEL	3	Epithelial Solid	N/A	1	27	73	F
25	Mesothelioma	TEL	N/A	Epithelial	N/A	N/A	N/A	62	M
28	Mesothelioma	TEL	N/A	Biphasic	N/A	1	10	65	F
29	Mesothelioma	ALT	N/A	Epithelial	N/A	0	34	62	F
31	Mesothelioma	ALT	N/A	Epithelial	N/A	0	32	22	M
32	Mesothelioma	ALT	N/A	Epithelial	N/A	N/A	N/A	54	M
33	Mesothelioma	ALT	N/A	Epithelial	N/A	0	31	58	M
43	Mesothelioma	TEL	3	Epithelial Tubulopapillary	N/A	0	90	47	M
7A	Mesothelioma	TEL	3	Epithelial Tubulopapillary	N/A	0	34	52	F
8B	Mesothelioma	TEL	2	Epithelial Tubulopapillary	N/A	1	27	54	F
S1223	MPNST	ALT	2	Malignant (MPNST)	N/A	0	59	64	F
S1313	MPNST	TEL	3	Malignant (MPNST)	N/A	1	7	26	F
S1451	MPNST	ALT	3	Malignant (MPNST)	N/A	1	8	51	M
S1856	MPNST	ALT	2	Malignant (MPNST)	N/A	0	45	54	F
S37	MPNST	ALT	3	Malignant (MPNST)	N/A	1	9	20	M

ID	Tumour Type	TMM	Grade	Histology	Location	Survival Status	Survival (month)	Age	Sex
S579M	MPNST	ALT	2	Malignant (MPNST)	N/A	1	5	28	M
S737	MPNST	ALT	3	Malignant (MPNST)	N/A	1	52	59	M
S738M	MPNST	TEL	N/A	Malignant (MPNST)	N/A	1	30	59	F
S758	MPNST	TEL	3	Malignant (MPNST)	N/A	1	10	33	F
S767M	MPNST	TEL	3	Malignant (MPNST)	N/A	1	19	42	M
S802R	MPNST	TEL	3	Malignant (MPNST)	N/A	0	82	24	F
S900R	MPNST	TEL	2	Malignant (MPNST)	N/A	1	31	28	F
S966R	MPNST	ALT	N/A	Malignant (MPNST)	N/A	1	31	28	F
S327R	Synovial Sarcoma	TEL	2	Monophasic, Spindle Cells, G2	N/A	1	60	53	F
S554M	Synovial Sarcoma	TEL	N/A	N/A	N/A	N/A	N/A	N/A	N/A
S678M	Synovial Sarcoma	TEL	N/A	Lung Metastasis	N/A	1	98	49	M
S695	Synovial Sarcoma	TEL	3	Biphasic G3	N/A	1	41	27	F
S865M	Synovial Sarcoma	TEL	N/A	Metastasis (Lung)	N/A	1	60	56	F
S989	Synovial Sarcoma	ALT	3	G3 PNET-Like	N/A	1	16	38	F



ELSEVIER

Contents lists available at ScienceDirect

Biochimica et Biophysica Acta

journal homepage: www.elsevier.com/locate/bbadis

Review

Pathway analysis of senescence-associated miRNA targets reveals common processes to different senescence induction mechanisms

Kyle Lafferty-Whyte, Claire J. Cairney, Nigel B. Jamieson, Karin A. Oien, W. Nicol Keith*

Centre for Oncology and Applied Pharmacology, University of Glasgow, Cancer Research UK Watson Laboratories, Garraube Estate, Switchback Road, Bearsden, Glasgow G61 1BQ, UK

ARTICLE INFO

Article history:

Received 18 December 2008

Received in revised form 2 February 2009

Accepted 3 February 2009

Available online 12 February 2009

Keywords:

Senescence

miRNA

Pathway

Regulation

mirBase

ABSTRACT

Multiple mechanisms of senescence induction exist including telomere attrition, oxidative stress, oncogene expression and DNA damage signalling. The regulation of the cellular changes required to respond to these stimuli and create the complex senescent cell phenotype has many different mechanisms. miRNAs present one mechanism by which genes with diverse functions on multiple pathways can be simultaneously regulated. In this study we investigated 12 miRNAs previously identified as senescence regulators. Using pathway analysis of their target genes we tested the relevance of miRNA regulation in the induction of senescence. Our analysis highlighted the potential of these senescence-associated miRNAs (SA-miRNAs) to regulate the cell cycle, cytoskeletal remodelling and proliferation signalling logically required to create a senescent cell. The reanalysis of publicly available gene expression data from studies exploring different senescence stimuli also revealed their potential to regulate core senescence processes, regardless of stimuli. We also identified stimulus specific apoptosis survival pathways theoretically regulated by the SA-miRNAs. Furthermore the observation that miR-499 and miR-34c had the potential to regulate all 4 of the senescence induction types we studied highlights their future potential as novel drug targets for senescence induction.

© 2009 Elsevier B.V. All rights reserved.

1. Cellular senescence

The irreversible cell-cycle arrest known as senescence can be induced by a number of factors including: telomere attrition, known as replicative senescence [1]; oxidative stress [2]; oncogene expression [3] and DNA damage signalling [4]. Senescence is involved in the regulation of cellular aging and tissue maintenance and acts as a barrier to immortality and tumorigenesis. Individual regulatory mechanisms promoting the establishment of senescence have been characterised, including for example gene expression changes in p16, p53 and p21 [5]; chromatin silencing of E2F target genes [6] and protein phosphorylation by DNA damage checkpoint kinases [7]. All of these molecular changes occur in the larger cellular context and result in changes to pathways regulating different cellular processes, as summarised in Fig. 1.

Complex cell phenotypes such as senescence are unlikely to result simply from a change in a single pathway but instead from cooperative changes in multiple systems. The complete network of underlying pathways resulting in cellular senescence is currently unclear. Investigations of mechanisms by which senescence is regulated continue to present novel pathways and regulatory

molecules involved in the process. MicroRNAs (miRNAs) present a mechanism by which genes involved in a variety of different signalling pathways can be regulated simultaneously. They therefore present a further level of molecular interactions by which senescence may be induced.

1.1. miRNAs as potential regulators of cellular senescence

Of the many ways to regulate gene product expression, miRNAs are relatively poorly understood. These short non-coding molecules ranging in size from 19 to 22 nucleotides are highly conserved and regulate protein expression through interactions with the 3' untranslated region (UTR) of mRNA [8,9]. The binding of a miRNA to the 3'UTR causes inhibition of translation through steric hindrance or degradation of the mRNA, depending on the degree of complementarity between the two sequences [10]. The ability of miRNAs to regulate a variety of target genes allows them to induce changes in multiple pathways and processes such as development [11], apoptosis, proliferation and differentiation [12]. miRNAs could therefore facilitate the complex cellular changes required to establish the senescent phenotype. Identification of the mRNA sequences that miRNAs regulate is mainly derived using bioinformatics techniques. The ability of each miRNA to target genes is based on sequence complementarity to 3'UTRs of known mRNAs. The miRBase sequence database is the main repository for miRNA sequence and target information and (as of

* Corresponding author.

E-mail address: n.keith@beatson.gla.ac.uk (W.N. Keith).

the 18 Nov 2008) contains 695 human miRNA sequences, each with the potential to regulate on average 1000 gene targets [13–15]. It is this large number of potential targets across different biological pathways that give miRNAs the power to potentially induce complex cell phenotypes, like senescence.

2. Twelve senescence associated miRNAs with experimental evidence for regulation of senescence

Although the gene targets of miRNAs can be identified theoretically by computational algorithms, it is unclear exactly which potential target genes they modulate and to what extent this affects the associated functions of these genes. The identification of miRNAs with the ability to regulate a complex phenotype, like senescence, is therefore not possible using purely bioinformatic techniques. For this reason we performed database searches of the terms miRNA and senescence, using pubmed and ISI web of knowledge (accessed 18 Nov 2008), to identify miRNAs with experimental evidence of involvement in senescence. The literature search highlighted 6 studies with direct evidence for regulation of senescence by miRNAs. Two main approaches were used in these studies; microarray based and comprehensive functional genomics; and the investigation of candidate senescence genes and the miRNAs regulating them. The 6 studies highlight a total of 12

senescence-associated miRNAs (SA-miRNAs). Each miRNA has the ability to bind between 953 and 2351 sites on mRNA 3' UTRs (see Table 1) and in addition some 3'UTRs potentially have multiple complementary sites for a given miRNA. To add to the complexity, in reality this set of miRNAs may be a subset of the total number of miRNAs that play a role in senescence.

Looking at the individual SA-miRNAs we can see that some miRNAs have more support for their roles in senescence than others (Table 1). The evidence for a regulatory role of the miR-34 family of miRNAs in senescence is growing and has stemmed from the investigation of p53 and its role in senescence. A number of studies have identified the miR-34 family, particularly miR-34a, as downstream effectors of p53 involved in the cell cycle [16]. Recent research has found that up-regulation of miR-34a in various cancer cell lines leads to cell cycle arrest, increased expression of β -galactosidase [17] and down-regulation of E2F family target genes [18]. Furthermore, drug treatment of various cancer cell lines with the MDM2 inhibiting drug Nutlin-3, leading to p53 activation, induced up-regulation of primarily miR-34a and later miR-34b and miR-34c [19]. Reports of a pro-apoptotic effect induced by miR-34a [20,21] may demonstrate that its expression alone is not responsible for senescence.

The potential role of hsa-miR-20a in senescence regulation was discovered through investigation of the candidate senescence

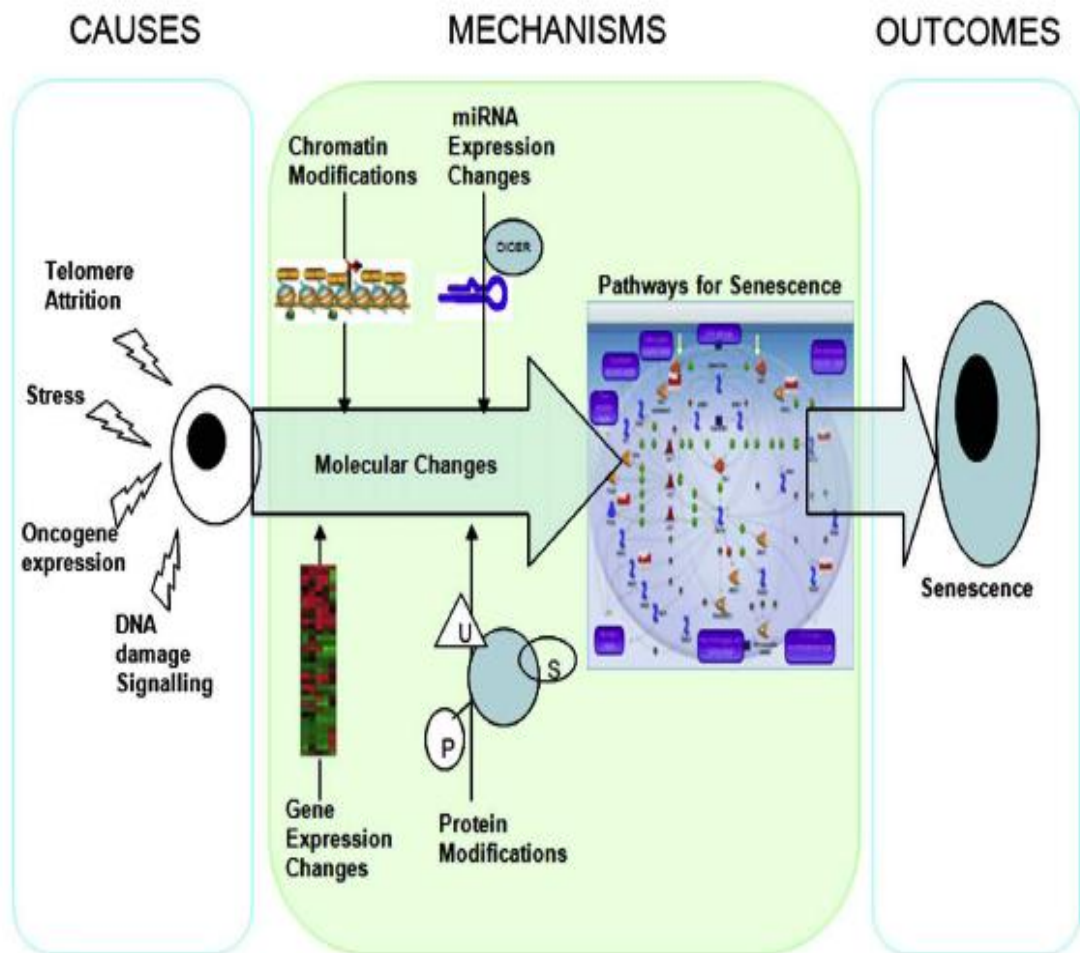


Fig. 1. The establishment of a complex cell phenotype, such as senescence, requires the interaction of many regulatory mechanisms leading to changes in individual pathways and processes.

Table 1
Senescence associated miRNAs from the literature and the number of computationally derived mRNA 3' untranslated regions each can target

Number	Senescence Associated miRNA	Number of predicted complementary sites in the transcriptome	References
1	hsa-let-7f	1038	[25]Wagner et al., 2008
2	hsa-miR-499	2157	[25]Wagner et al., 2008
3	hsa-miR-373	3057	[26]Voorhoeve et al., 2006
4	hsa-miR-372	953	[26]Voorhoeve et al., 2006
5	hsa-miR-371	2205	[25]Wagner et al., 2008
6	hsa-miR-369-5P	1107	[25]Wagner et al., 2008
7	hsa-miR-34c	2351	[19]Kumamoto et al., 2008
8	hsa-miR-34b	3086	[19]Kumamoto et al., 2008
9	hsa-miR-34a	1296	[17–19]Tazawa et al., 2007, He et al., 2007, Kumamoto et al., 2008
A	hsa-miR-29c	1899	[25]Wagner et al., 2008
B	hsa-miR-217	993	[25]Wagner et al., 2008
C	hsa-miR-20a	1275	[22]Poliseno et al., 2008

(Note some miRNAs may contain multiple binding sites.) Numbering denotes the thermometer number representing particular miRNA's targets on Figs. 2–4.

associated gene LRF [22]. LRF is a transcriptional repressor of the MDM2 inhibitor p19ARF [23,24]. The overexpression of miR-20a in mouse embryonic fibroblasts induced senescence by lowering LRF protein levels and in turn increasing p19ARF levels. The fact that investigation of two different senescence-associated genes, p53 and LRF, yields different SA-miRNAs may be a reflection of the range of signalling pathway changes that these molecules contribute to the induction of the senescent phenotype.

Genome-wide analysis of changes in miRNA expression or investigations of those miRNAs that allow senescence bypass are alternative approaches that have been used in SA-miRNA identification. The use of microarrays identified miRNAs hsa-miR-371, hsa-miR-369-5p, hsa-miR-29c, hsa-miR-499 and hsa-let-7f as significantly up-regulated in senescent human mesenchymal stem cells (hMSCs) when compared to early passage hMSCs [25]. miRNA hsa-miR-271 was also seen to be significantly up-regulated by this study but overall had very low expression levels. These varying levels of miRNA expression may suggest different requirements for alterations in their target gene pathways.

miR-372 and miR-373 were identified as miRNAs whose expression was able to bypass RAS-induced senescence in the presence of wild-type p53 [26]. The expression of these miRNAs would therefore not be conducive to senescence and we include them in our analysis as examples of miRNAs whose targets may increase in expression during senescence.

These reports provide experimental evidence for the molecular mechanisms by which miRNAs may act in the context of senescence. Recent reports of the regulatory effects of miRNAs miR-17-5P and miR-24 on senescence regulators p21 and p16, may offer further miRNAs with a role in senescence [27,28]. However, lack of β -galactosidase and γ H2AX analysis or the expected alterations to senescence induction prevent us from being completely clear whether these miRNAs play a direct role in senescence. For this reason we did not include miR-17-5P or miR-24 in our SA-miRNA cohort. By examining the biological pathways that the 12 SA-miRNAs named in Table 1 can theoretically regulate, we aim to gain a greater understanding of the biological changes that these miRNAs could create that potentially lead a cell into senescence.

2.1. Pathway mapping of senescence associated miRNA targets shows cell cytoskeletal, cell cycle and proliferation regulation potential

By mapping the signalling pathways regulated by the SA-miRNAs we aimed to better understand the biological mechanisms by which

they can cooperate to create the complex senescence phenotype. The free, publicly available Sanger miRNA database contains a registry of computationally calculated gene targets for each known miRNA. We downloaded (25 Aug 2008) and queried the current version of the database (miRBase targets v5) using Microsoft Access, in order to generate lists of theoretical gene targets for the 12 SA-miRNAs. As the computational method of assigning gene targets to miRNAs cannot assess the level of complementarity required for a biological effect, we decided to include all theoretical targets in our analysis.

The signalling pathways and processes that these gene targets are involved in were explored using the systems biology tool Metacore from Genego (Genego Inc, St Joseph, MI). This database of known molecular interactions, pathways and processes manually curated from published data allows the user to visualise known biological systems within their data. Input of the SA-miRNA target gene lists into the Metacore database allowed us to explore the potential biological implications of their regulation during the induction of senescence.

The top 5 pathways regulated by the SA-miRNAs are shown in Table 2. Two of these maps are involved in cytoskeletal remodelling and are highly saturated with gene targets of the SA-miRNAs (Fig. 2). Senescent cells are seen to undergo changes in morphology, becoming large and flattened [29], which would require significant cytoskeletal remodelling. Such widespread cellular modifications would be associated with the alteration of many different pathways and processes that all contribute to the maintenance of the actin cytoskeleton. Due to their ability to bind a number of different gene targets miRNAs provide a mechanism by which such widespread changes could be induced.

Changes in the processes involved in DNA synthesis in early S-phase are also potentially regulated by the SA-miRNAs (Fig. 3). Of the objects on this map 59% are potentially regulated by the SA-miRNAs and in particular members of the MCM and ORC complexes. The ORC and MCM complexes are responsible for the initiation of DNA replication by assembly of the pre-replication complexes and ensure that the process only occurs once during the cell cycle [30]. Recently the ORC complex was reported to be able to interact with the telomere binding protein TRF2 and affect telomere homeostasis [31]. Replicative senescence relies on the shortening of telomeres to induce a DNA damage checkpoint response that blocks their progression into S-phase [7]. Since senescence involves irreversible cell cycle arrest, SA-miRNA regulation of cell cycle mechanisms strengthens their possible role in senescence regulation.

Table 2
The top 5 pathways regulated by all 12 SA-miRNAs with the percentage of the map that consists of SA-miRNA gene targets

Pathway map	% of objects on the map regulated by SA-miRNAs
1 The role of TGF and WNT in cytoskeletal remodelling	44% (49/111)
2 Cytoskeletal remodelling general process	42% (43/102)
3 Cell cycle: the start of DNA replication in early S-phase	59% (19/32)
4 Regulation of transcription in the CREB pathway	50% (21/42)
5 Development EGFR signalling via small GTPases	41% (13/32)

Gene target lists for each SA-miRNA were input to Metacore and the pathway maps which were commonly regulated were examined. Pathways are ordered by the number of SA-miRNA targets on each map. The presence of 4 regulatory pathways involving different aspects of cellular signalling and only one cell cycle pathway shows that there is more to senescence than just cell cycle regulation. SA-miRNAs therefore present a mechanism by which a variety of the required cellular pathway changes could be regulated.

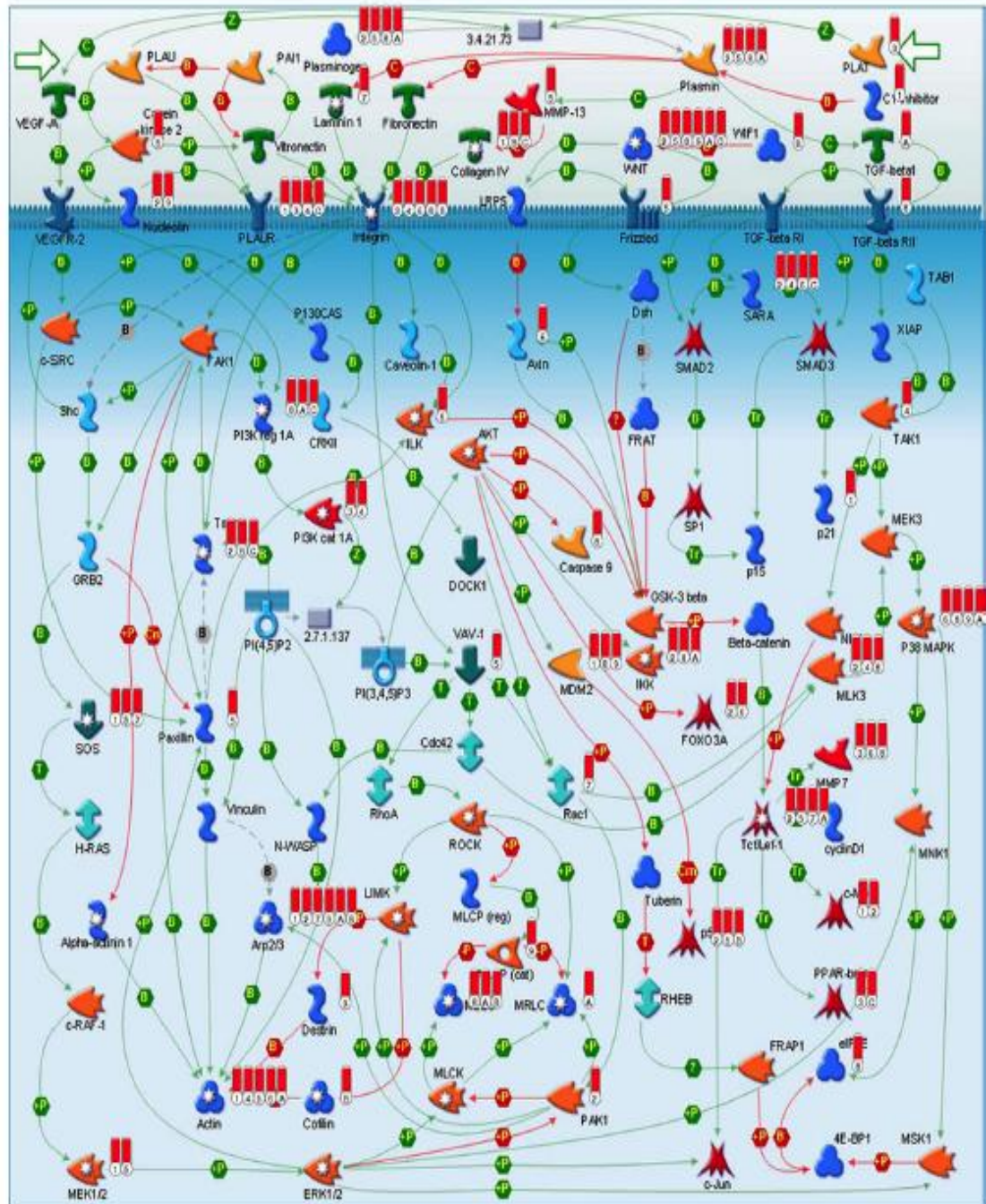


Fig. 2. SA-miRNA regulation of the cytoskeletal remodelling and the role of TGF and WNT biological pathway map. Red thermometers show an object that can be regulated by a SA-miRNA with thermometer numbering corresponding to that seen in Table 1. Multiple thermometers denote that the object is a target of multiple SA-miRNAs. Green arrows represent positive, red negative and grey unspecified interactions. Boxes on lines denote the type of regulation where P—phosphorylation; B—binding; Tr—transcriptional regulation, Cm—covalent modification, T—translocation and Z—catalysis.

The transcription factor CREB is also potentially regulated by SA-miRNAs (Fig. 4). CREB is a known regulator of cellular growth and proliferation through its transcriptional regulation of genes such as the oncogene *c-fos* [32] and regulators of the cell cycle such as cyclin D1 [33] and cyclin A [34]. Alteration of molecules regulating CREB by SA-miRNAs would therefore confer another mechanism to alter the cell growth and proliferation pathways towards a senescent state.

The regulation of EGFR and its proliferative signalling is not conducive to a senescent cellular environment. Consistent with this, EGFR is repressed at the chromatin level during senescence [6] and is shown to be potentially regulated by the 12 SA-miRNAs (Table 2). The ability of SA-miRNAs to further repress these signals provides a cell entering senescence another regulatory mechanism by which to ensure their silencing.

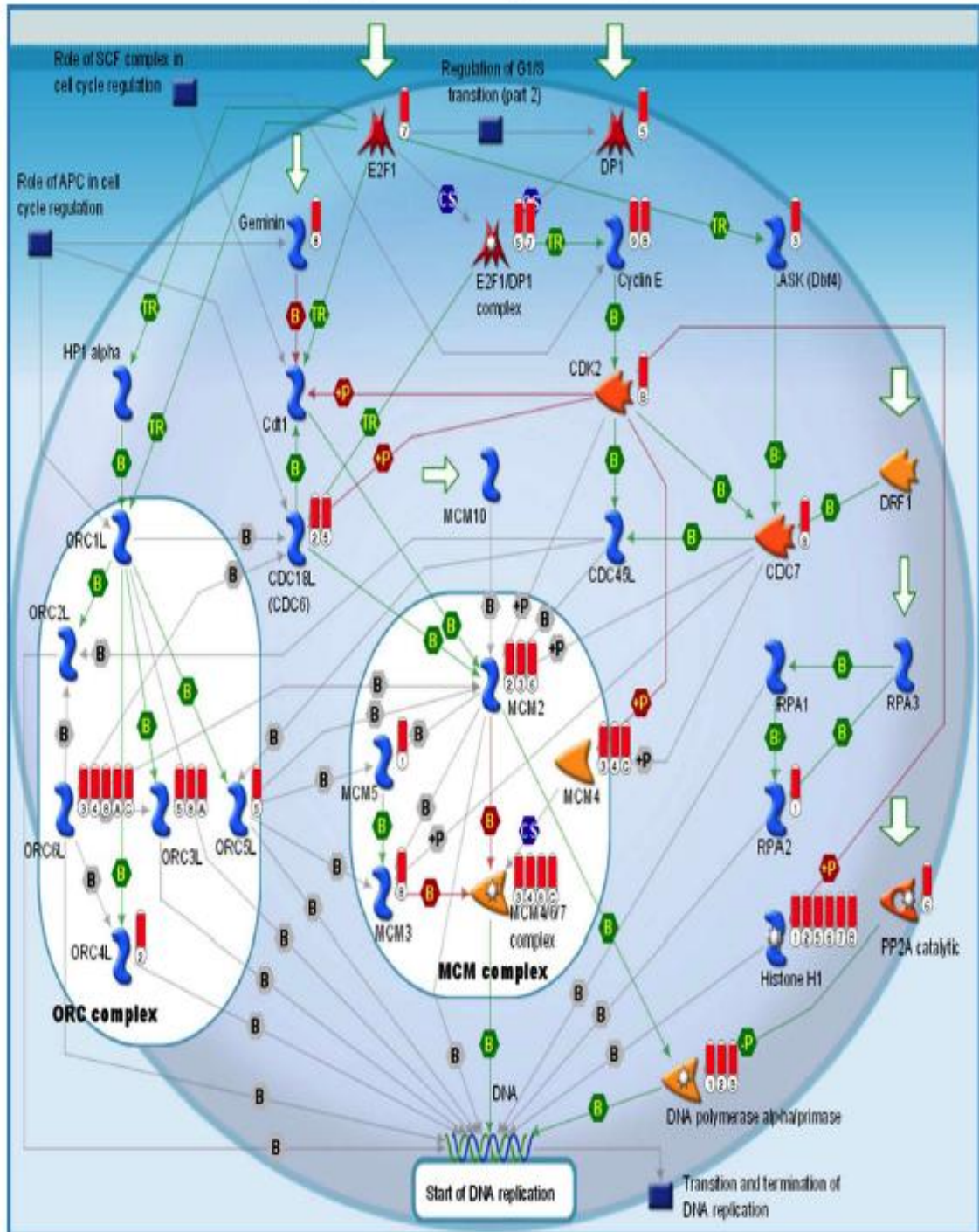


Fig. 3. SA-miRNA regulation of Cell cycle and DNA replication in early S phase biological map. Red thermometers show an object that can be regulated by a SA-miRNA with thermometer numbering corresponding to that seen in Table 1. Multiple thermometers denote that the object is a target of multiple SA-miRNAs. Green arrows represent positive, red negative and grey unspecified interactions. Boxes on lines denote the type of regulation where P = phosphorylation; B = binding; Tr = transcriptional regulation; Cm = covalent modification and Z = catalysis.

The multiple pathway alterations discussed suggest that these SA-miRNAs are potentially regulating many of the necessary steps required to create a fully senescent cell, from changes in the cellular cytoskeleton to alteration of multiple pathways regulating cell cycle and proliferation signals. Their potential to act as master regulators of

senescence could be a prospective source of novel drug targets and biomarkers. Senescence can be stimulated by more than one mechanism however, including induction by telomere attrition (replicative senescence), oncogenes, drugs and cellular stress. It remains unclear whether the same pathway alterations and miRNAs

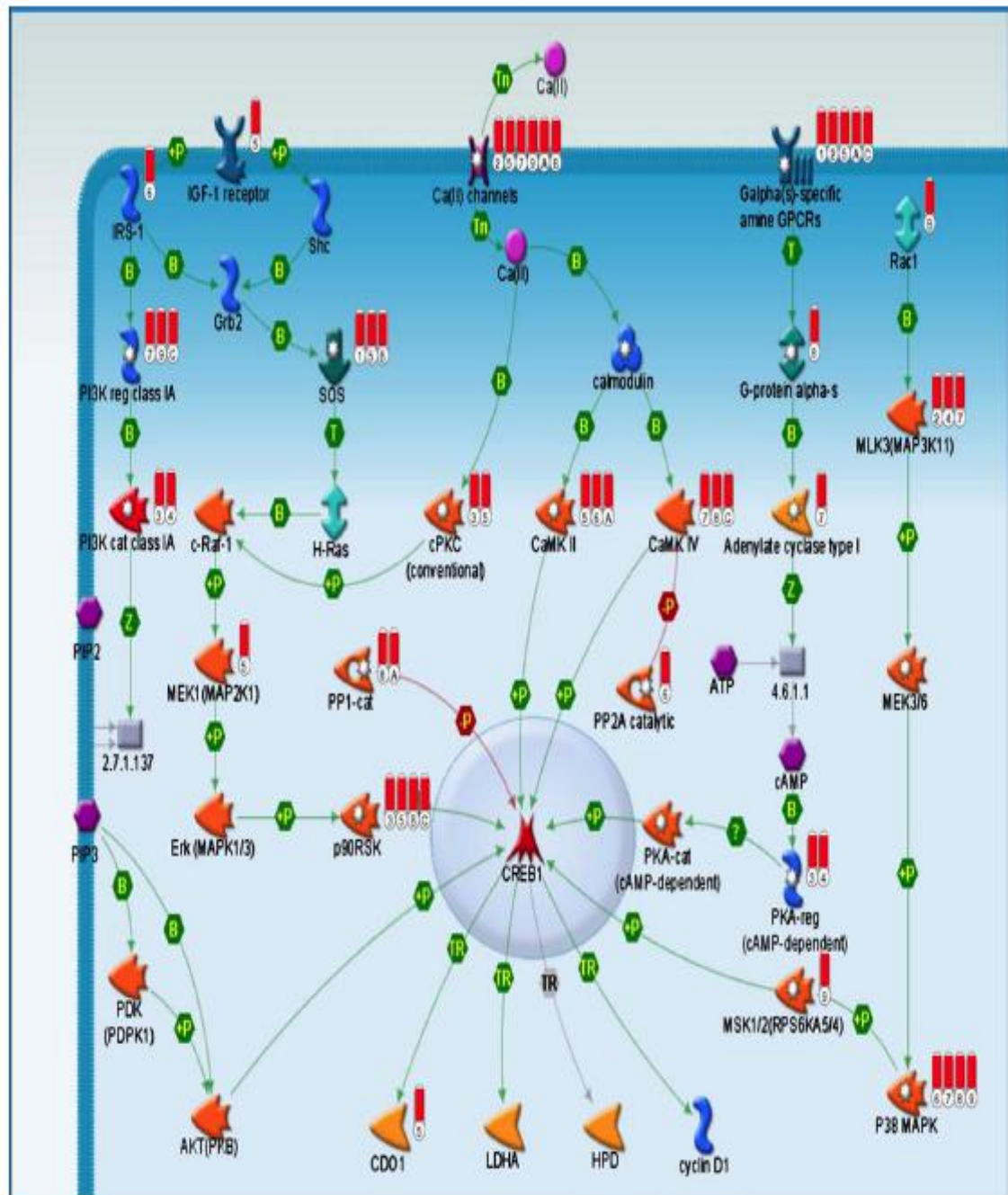


Fig. 4. SA-miRNA regulation of transcription and the CREB pathway biological map. Red thermometers show an object that can be regulated by a SA-miRNA with thermometer numbering corresponding to that seen in Table 1. Multiple thermometers denote that the object is a target of multiple SA-miRNAs. Green arrows represent positive, red negative and grey unspecified interactions. Boxes on lines denote the type of regulation where P = phosphorylation; B = binding; Tr = transcriptional regulation, Cm = covalent modification, T = transformation and Z = catalysis.

are involved in each of the different stimuli or whether each stimulus takes a different route to the same endpoint of a senescent cell, as depicted in Fig. 5.

3. Investigation of SA-miRNA regulation of different senescence stimuli

In order to investigate the potential of SA-miRNAs to regulate the different senescence stimuli we returned to the literature. Using

previously published data we queried differentially expressed gene lists from replicative senescence in hMSCs [25], drug induced replicative senescence by a telomerase inhibitor [35], cellular stress by Ethanol or tert-butylhydroperoxide exposure [2] and oncogene induced senescence by BRAF^{H600} [3].

Each of the datasets queried showed some potential to be regulated by the SA-miRNAs as shown in Table 3. Using the results of these 4 analyses, we explored the potential of SA-miRNAs to regulate pathways with gene expression changes for each stimulus.

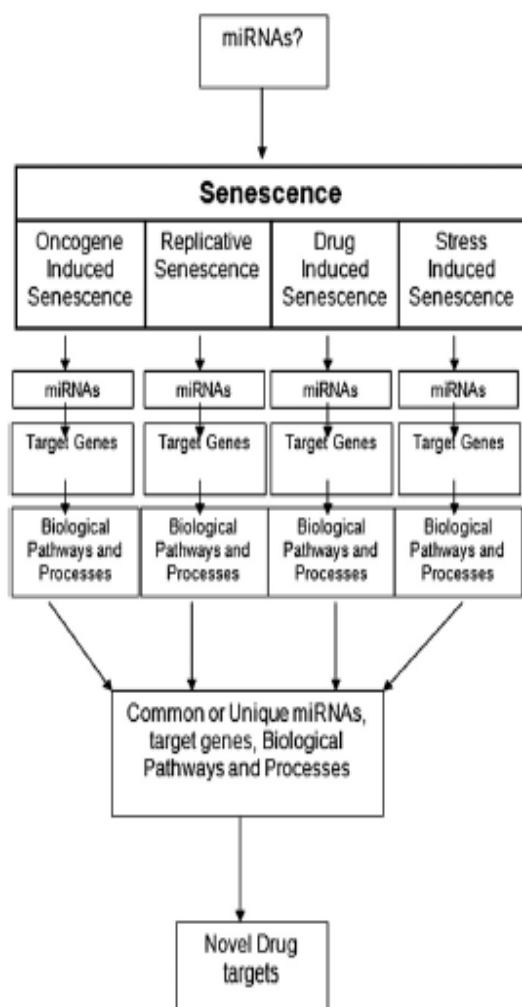


Fig. 5. Potential mechanisms of miRNA regulation in senescence and their potential. A small subset of miRNAs, such as the 12 SA-miRNAs that we have identified, may be acting as master regulators of the senescent phenotype. However it is also possible that individual types of senescence induction may require different miRNAs to create the same cellular changes due to the different stimuli and therefore signalling pathways involved. Overlaps in the biological pathways or miRNAs could therefore be utilised to discover novel drug targets for senescence induction.

The differences and similarities in SA-miRNAs and their targeted pathways between stimuli were also investigated.

3.1. Pathways regulated by SA-miRNAs during replicative senescence show increased cell survival and decreased cell cycle signalling

By reanalysing the publicly available gene expression data from the study by Wagner et al., we examined the pathways during replicative senescence that could be regulated by SA-miRNAs (Table 4A) [25]. Gene lists of 2 fold or more changes in expression between early and late passage hMSCs were constructed. Filtering of these lists to only those genes theoretically regulated by the SA-miRNAs led to the construction of 2 lists: 85 gene targets with increased expression and 49 gene targets with decreased expression in late passage compared to early passage hMSCs. The pathways associated with each gene list were then individually explored using Metacore.

Looking initially at the pathways that have gene targets with increased expression in Table 4A, we see that 3 of the 5 maps on the list are involved with apoptosis and survival through the FAS and TNFR1 signalling pathways or in a p53 dependent manner. In all 3

maps the only molecules that the SA-miRNAs are regulating are BRE and c-FLIP. BRE is known to suppress the apoptotic pathways through binding and inhibition of the FAS receptor [36] and the TNF-alpha receptor [37]. C-FLIP is a potent inhibitor of apoptosis through its binding and resulting inhibition of the adaptor protein FADD [38]. Although the SA-miRNAs are only regulating 2 molecules involved in the survival and apoptosis signalling pathways, regulation of the absolute levels and timing of such signals may be one of the mechanisms by which the SA-miRNAs ensure the cells enter senescence rather than apoptosis.

The second most significant pathway with increases in gene expression during replicative senescence is cytoskeletal remodelling centering on the role of intermediary filaments. As discussed previously, changes in the cellular morphology of senescent cells would require significant changes to the cytoskeleton of the cell. Increases in expression of key genes regulating many of these processes would therefore be required. The SA-miRNAs provide one potential mechanism by which these changes could be regulated.

Changes to the immune response and the IL1 signalling pathway during replicative senescence are also potentially regulated by the SA-miRNAs. The concept of the involvement of IL1 and other pro-inflammatory networks in the induction of senescence is concurrent with current findings [39–41]. Therefore the ability of SA-miRNAs to regulate this pathway demonstrates a further mechanism by which they could induce senescence.

The regulation of cellular survival, pro-inflammatory and cytoskeletal remodelling cellular processes would all logically be required to create the senescent cell phenotype. These processes can theoretically be regulated by the SA-miRNAs, during replicative senescence, showing that they have the potential to regulate the absolute levels and timings of these complex signalling cascades to create a senescent cell.

However, these are not the only pathways that the SA-miRNAs can regulate during this process. Four out of the 5 pathways that contain SA-miRNA gene targets with decreases in expression are involved in various aspects of cell cycle regulation (Table 4A). These include DNA replication in early S-phase and the roles of APC, the SCF complex and ESR1. Regulation of key molecules in the multiple processes governing the cell cycle during senescence induction is critical. The SA-miRNAs regulate a subset of molecules (CDK2, EMI1, Cyclin B, SKP2, and CDC18L) that are involved in regulation of these multiple cell cycle pathways. This allows the SA-miRNAs to affect the cell cycle regulatory process as whole rather than at just one checkpoint or stage. The 12 SA-miRNAs that we have highlighted therefore exemplify the potential of miRNAs to play a regulatory role in this aspect of replicative senescence.

The remaining pathway containing gene targets down-regulated during replicative senescence is involved in dCTP/dUTP metabolism. Since senescent cells are no longer cycling, changes in metabolism will follow. SA-miRNAs may only be regulating a small part of cellular metabolism, the metabolism of 2 nucleotide units, however these metabolic changes may have far reaching effects. Furthermore, changes in dATP, ATP and TTP metabolism are seen further down in the list of pathways, 6, 7 and 9 respectively, which are not discussed here. It may therefore be the case that the SA-miRNAs are able to regulate the changes in metabolism required to establish senescence or that only changes to a few molecules or processes are required.

Changes in gene expression during the establishment of replicative senescence in hMSCs are potentially being regulated by the SA-miRNAs. We have observed that the SA-miRNAs targeted down-regulation of cell cycle pathways and increased signalling by pathways involved in cytoskeletal remodelling and apoptosis survival. The ability of a relatively small number of SA-miRNAs to differentially regulate such diverse changes demonstrates their potential in the induction of complex cellular phenotypes.

Table 3
Regulation of gene expression signatures of different types of senescence induction

SA-miRNA	Replicative senescence		Drug induced replicative senescence		Oncogene induced senescence	Stress induced senescence			
	Up 85 target genes	Down 49 target genes	Up 76 target genes	Down 49 target genes	7 target genes	ETOH up 10 target genes	BOH down 6 target genes	tBHP up 6 target genes	tBHP down 6 target genes
	miRNA	miRNA	miRNA	miRNA	miRNA	miRNA	miRNA	miRNA	miRNA
hsa-let-7f	✓	✓	✓	✓			✓		✓
hsa-miR-20a	✓	✓	✓	✓	✓		✓		✓
hsa-miR-217	✓	✓	✓	✓	✓		✓		✓
hsa-miR-29c	✓	✓	✓	✓	✓		✓	✓	✓
hsa-miR-34a	✓	✓	✓	✓	✓		✓		✓
hsa-miR-34b	✓	✓	✓	✓	✓		✓		✓
hsa-miR-34c	✓	✓	✓	✓	✓		✓	✓	✓
hsa-miR-369-5P	✓	✓	✓	✓	✓		✓	✓	✓
hsa-miR-371	✓	✓	✓	✓	✓		✓	✓	✓
hsa-miR-372	✓	✓	✓	✓	✓		✓	✓	✓
hsa-miR-373	✓	✓	✓	✓	✓		✓	✓	✓
hsa-miR-499	✓	✓	✓	✓	✓	✓	✓	✓	✓

Ticks represent the ability of that SA-miRNA to theoretically regulate one or more genes within the signature. All four senescence induction signatures are regulated by at least 5 SA-miRNAs. These differences in SA-miRNA regulation may represent the differing need for regulation of SA-miRNA target genes by different stimuli. The regulation of all of the senescent signatures studied by microRNAs hsa-miR-499 and hsa-miR-34c may demonstrate their potential as regulators of core senescence genes required by all senescence stimuli.

3.2. Regulation of drug induced senescence by SA-miRNAs also highlights increased cell survival and decreased cell cycle signalling

Replicative senescence results from the shortening of telomeres during each round of the cell cycle [1]. Many cancer cells reactivate the enzyme telomerase, which has the ability to maintain telomeres and therefore overcome this barrier to tumorigenesis [42]. Application of a drug that inhibits telomerase would, in theory, activate the cells' natural senescence pathways, potentially including the actions of the SA-miRNAs. To explore this hypothesis we interrogated the differentially expressed genes published by Damm et al. for potential SA-miRNA regulation [35].

Damm et al. investigated senescence resulting from treatment of lung carcinoma cells with the telomerase inhibitor BIBR1532. We

filtered the published genes lists to include only those genes regulated by the 12 SA-miRNAs. This resulted in a list of 76 down-regulated SA-miRNA gene targets and 49 up-regulated gene targets (Table 4B). Pathway analysis was then performed to investigate the potential effects of SA-miRNA regulation in drug induced replicative senescence.

As seen previously during the analysis of replicative senescence, the pathways associated with gene targets showing increased expression involve a variety of different cellular mechanisms. Two of these pathways are involved in the regulation of cellular signalling by the molecules PTEN and Activin A. The dual specificity phosphatase PTEN is a tumour suppressor gene and regulates cellular proliferation and survival through its ability to bind p53 in the nucleus [43]. Activin A is a member of the TGF β superfamily and is involved in the

Table 4
Top 5 biological pathway maps that contain SA-miRNA gene targets shown in order of p-value

A						
Replicative senescence						
85 upregulated SA-miRNA gene targets						
SA-miRNA	Pathway maps	% Regulated by SA-miRNAs	p-value	49 downregulated SA-miRNA gene targets	% Regulated by SA-miRNAs	p-value
1	Apoptosis and survival p53-dependent	9% (2/29)	9.58E-08	Cell cycle role of APC in cell cycle regulation	22% (7/32)	5.15E-11
2	Cytoskeletal remodelling keratin filaments	6% (2/36)	1.45E-02	Cell cycle start of DNA replication in early S-phase	19% (6/32)	3.79E-09
3	Immune response IL1 signalling pathway	5% (2/37)	1.53E-02	dCTP/dUTP metabolism	8% (6/75)	7.37E-07
4	Apoptosis and survival FAS signalling cascades	5% (2/43)	2.04E-02	Cell cycle role of SCF complex in cell cycle regulation	14% (4/29)	6.82E-06
5	Apoptosis and survival TNFR1 signalling pathway	5% (2/43)	2.04E-02	Cell cycle sister chromatid cohesion	14% (3/22)	1.13E-04
B						
Drug induced replicative senescence						
Replicative Senescence						
49 Upregulated SA-miRNA gene targets						
SA-miRNA	Pathway maps	% Regulated by SA-miRNAs	p-value	76 Downregulated SA-miRNA gene targets	% Regulated by SA-miRNAs	p-value
1	Signal transduction PTEN pathway	11% (5/46)	6.52E-07	Cell cycle role of APC in cell cycle regulation	16% (5/32)	1.26E-06
2	Development EGF/R signalling via small GTPases	14% (4/28)	3.13E-06	Folic acid metabolism	9% (5/53)	1.63E-05
3	Signal Transduction Activin A signalling regulation	14% (4/28)	3.13E-06	DNA damage ATM/ATR regulation of G1/S checkpoint	13% (4/32)	3.98E-05
4	Transcription role of AP1 in regulation of cellular metabolism	10% (4/42)	1.65E-05	Cell cycle ESR1 regulation of G1/S transition	12% (4/33)	4.51E-05
5	Development ERBB-family signalling	9% (4/43)	1.81E-05	Cell cycle chromosome condensation in prometaphase	14% (3/21)	2.68E-04

Wagner et al. microarray data were reanalysed and all genes with a 2 fold or more difference between early passage and late passage hMSCs were selected. These lists were then filtered selecting only gene targets of the 12 SA-miRNAs and biological pathways maps analysed using Metacore from Geneo. Damm et al. published differentially expressed gene signatures which were filtered selecting only gene targets of the 12 SA-miRNAs and biological pathways maps analysed using Metacore from Geneo.

regulation of cell growth and apoptosis [44]. Both molecules are commonly deregulated in cancers [45,46] reflecting their importance in regulation of cell proliferation processes. Alterations in these signalling pathways could therefore be beneficial to the establishment of a senescent cell phenotype. The theoretical regulation of these processes by the SA-miRNAs demonstrates further mechanisms by which SA-miRNAs can cause the complex signalling pathway changes required to induce senescence.

Two further pathways associated with gene expression increases that could be regulated by the SA-miRNAs involve EGFR and the ERBB family. As previously discussed, regulating signalling from the ERBB family of tyrosine kinases is an important step in senescence induction due to their role in the regulation of cellular prolifera-

tion. The presence of this map demonstrates that SA-miRNAs are a potential regulatory mechanism of these pathways during drug induced replicative senescence as well as natural replicative senescence.

The remaining pathway associated with increased gene target expression is involved with changes in metabolism regulated by the transcription factor AP-1. Closer inspection of the SA-miRNA targets on this map (Fig. 6) highlights the role of AP-1 in regulation of p21 and the apoptosis molecules *c-fos* and *FASR*. The involvement of *c-fos* and *FASR* in pathways regulated by the SA-miRNAs has been highlighted earlier in this study. This demonstrates that regulation of the diverse cellular proliferation and apoptosis signalling pathways affected by these molecules is an important step in senescence establishment,

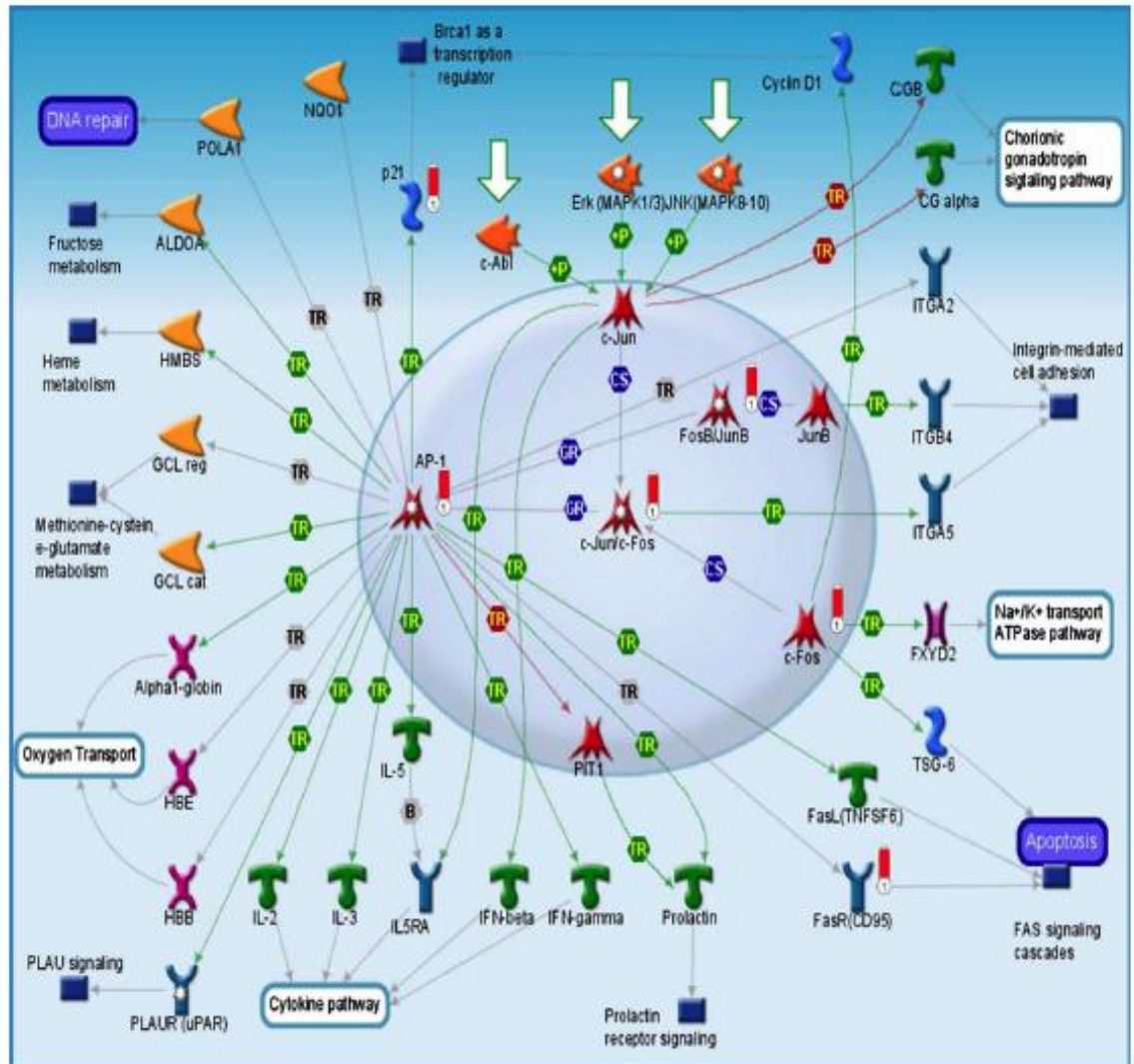


Fig. 6 SA-miRNA regulation of transcription and the role of AP1 in regulation of cellular metabolism pathway biological map during drug induced senescence. Red thermometers show an object that can be regulated by a SA-miRNA with thermometer numbering corresponding to that seen in Table 1. Multiple thermometers denote that the object is a target of multiple SA-miRNAs. Green arrows represent positive, red negative and grey unspecified interactions. Boxes on lines denote the type of regulation where P—phosphorylation; B—binding; TR—transcriptional regulation, C—covalent modification, T—transformation and Z—catalysis.

under both natural replicative senescence and when artificially drug induced, SA-miRNA regulation could therefore provide a mechanism by which the absolute levels and timings of these signals can be controlled.

The biological pathway map analysis of the decreases in gene expression for telomerase inhibited cells returned results very similar to that of the down-regulated genes in natural replicative senescence. Four of the 5 maps are involved with the regulation of various aspects of the cell cycle including the role of APC, the DNA damage response checkpoint, regulation of ESR1 and chromosome condensation in prometaphase (Table 4B). As with the cell cycle pathways seen in replicative senescence, the regulation of cell cycle following telomerase inhibition would be a critical step in senescence induction. Targeting these multiple pathways to cell cycle control gives SA-miRNAs comprehensive regulation of the process.

The remaining map is involved with metabolism of folic acid. As previously discussed, changes in metabolism will be required in cells undergoing senescence. However, this may also reflect metabolic changes involved in the metabolism of BIBR 1532, independent of senescence, that the SA-miRNAs are also able to regulate. The ability of SA-miRNAs to target not just the down-regulation cell cycle aspects of senescence but also the metabolic changes demonstrates the flexibility and complexity of their action.

Looking at the pathway analysis of both replicative and drug induced senescence shown in Table 4, highlights the fact that the down-regulated pathways in both cases are cell cycle and metabolism related whilst the up-regulated pathways differ between the two stimuli. However, looking at the functions of the up-regulated pathways in both cases reveals a common apoptosis regulatory signal. Cells in replicative senescence appear to be signalling apoptosis survival through FAS and TNFR1 pathways or in a p53 dependant manner whereas the telomerase inhibited cells are using the actions of Activin A and PTEN for this purpose. Thus the SA-miRNAs are potentially using different cellular mechanisms by which to achieve the same goal. The SA-miRNA regulation of the cellular signals behind drug induced and natural replicative senescence are therefore stimuli specific whilst remaining focused towards the common outcome of creating the complex senescent cell phenotype.

3.3. SA-miRNA regulation of oncogene induced senescence emphasises the importance of inflammatory signals in senescence

Telomere erosion leading to the activation of DNA damage signalling cascades is not the only method of senescence induction. Oncogene induced senescence (OIS) can be caused upon either the loss of tumour suppressor genes like PTEN [47] or activation of oncogenes such as MEK, RAS and BRAF^{V600E} [48–50]. Recent evidence suggests that senescence induction by these stimuli is dependent upon IL-6 mediated inflammatory responses without which the cells bypass senescence and continue proliferating [3]. The same study also used gene expression microarrays to examine differentially expressed genes between cells that bypass and cells that undergo OIS, revealing a signature of 20 genes shown in Table 5. Seven of these genes, including IL-6, can theoretically be regulated by SA-miRNAs.

Due to the small size of the initial signature, and hence the small number of target genes, analysis of the biological pathways underlying the SA-miRNA regulation was not statistically feasible. However, the SA-miRNAs regulate nearly 30% of the OIS signature revealed by Kulman et al., including the key molecule IL-6 (Table 5). This may demonstrate the principle that large numbers of gene alterations are not always required for senescence induction, just well targeted ones. The multiple regulation of 3 of the genes in particular (C20orf26, CD55 and IL6) by the SA-miRNAs may show that within this signature these genes require the strictest regulation to ensure the successful induction of senescence, although further validation is required to test this theory.

Table 5

20 Differentially expressed genes upon induction of oncogene induced senescence highlighted by Kulman et al.

Gene name	Regulating SA-miRNAs
C20orf26	hsa-miR-369-5P (2), hsa-miR-29c (1), hsa-miR-499 (3), hsa-miR-34b (1), hsa-miR-34c (2)
CD55	hsa-miR-29c (1), hsa-miR-34b (2), hsa-miR-34c (3)
CD9	
CPE	
FAM131A	
FAM43A	hsa-miR-371 (1)
GABRA2	
GEM	
GMFC	hsa-miR-369-5P (1)
IL6	hsa-miR-499 (1), hsa-miR-236 (1), hsa-miR-371 (1)
IQGAP2	
ITGA2	
ITPKA	
NR4A2	
PCNX	
PECAM1	
PTGES	hsa-miR-371 (1)
RPS8KA5	
TESC	hsa-miR-20a (1)
VGF	

Also shown are the SA-miRNAs that can theoretically regulate 7 of these genes, brackets show the number of theoretical 3'UTR binding sites that each SA-miRNA has for that gene.

Our analysis of differentially expressed genes during oncogene induced senescence, although limited by the size of gene list, still highlights the potential of SA-miRNAs to regulate key molecules required for this form of senescence induction. Furthermore the regulation of inflammatory networks shown in this study to be key to senescence induction was also highlighted during our analysis of replicative senescence. This common regulation of pro-inflammatory genes in response to 2 different senescence stimuli by SA-miRNAs is suggestive of its importance in senescence as a whole.

3.4. Regulation of stress induced senescence by SA-miRNAs transcends treatment type to control core senescence processes

Senescence can also be induced by many different types of cellular stress such as UV-B [51], hydrogen peroxide [52], *tert*-butylhydroperoxide (*t*-BHP) or ethanol exposure [53]. Pascal et al. used a combination of differential display RT-PCR and low density DNA arrays to investigate genes involved in senescence induction by ethanol or *t*-BHP [2]. They revealed signatures of genes increasing and decreasing in expression for both ethanol and *t*-BHP, many of which overlapped. Table 6 highlights the potential of the SA-miRNAs as regulators of stress induced senescence by both treatments, 75% of the genes theoretically regulated by SA-miRNAs overlap between the two treatment types. This may suggest that these target genes are those that are core to senescence induction by SA-miRNA regulation.

Of all the overlapping genes shown in Table 6 four have roles in regulation of the actin cytoskeleton, namely ARHGAP24, ARPC2, MACF1 and S100A4 [54,55,56]. In our previous analysis cytoskeletal remodelling has always been associated with genes showing increased expression levels. Here however two of the molecules, ARHGAP24 and ARPC2 show decreased expression. This may therefore represent specific molecules that require negative regulation in the context of stress induced senescence. Alternatively this may represent down-regulation of genes required to create the necessary senescence-associated cytoskeletal alterations. This demonstrates the potential of SA-miRNAs to regulate similar processes through different mechanisms dependant on stimuli.

Cell cycle regulation has in both replicative and drug induced senescence been strongly negatively regulated. Two of the overlapping down-regulated genes, RAD17 and CDC37L1 (Table 6),

Table 6

SA-miRNA targets showing alterations in gene expression after stress induced senescence by either *tert*-butylhydroperoxide (t-BHP) or Ethanol (EtOH) and the direction of their alteration, blank cells infer no effect

Gene	Effect of t-BHP treatment	Effect of EtOH treatment	Regulating SA-miRNAs
ARHGAP24	Down	Down	hsa-miR-499 (2)
ARPC2	Down	Down	hsa-miR-217 (2)
RAD17	Down	Down	hsa-let-7f (3)
CDC37L1	Down	Down	hsa-miR-20a (2), hsa-miR-34b (1), hsa-miR-499 (2), hsa-miR-34c (1)
EWSR1	Down	Down	hsa-miR-20a (1)
PHGDH	Down	Down	hsa-miR-34a (2), hsa-miR-34c (2)
MACF1	Up	Up	hsa-miR-369-5p (2)
RPS12	Up	Up	hsa-miR-369-5p (2)
LOXL2	Up	Up	hsa-miR-29c (1)
S100A4	Up	Up	hsa-miR-499 (2)
SILCSA5	Up	Up	hsa-miR-371 (1)
EEF1A1	Up	Up	hsa-miR-34c (1)
TBRG4	Up	Up	hsa-miR-34c (1)
KPNB1	Up	Up	hsa-miR-29c (1)
TMSB10	Up	Up	hsa-miR-499 (1)
C21orf54	Up	Up	hsa-miR-34b (2), hsa-miR-34c (1)

Also shown is the SA-miRNAs that can theoretically regulate these genes, brackets show the number of theoretical 3'UTR binding sites that each SA-miRNA has for that gene.

common to both ethanol and t-BHP treatments have roles in the cell cycle. RAD17 specifically is involved in cell cycle arrest caused by DNA damage signalling [57]. The DNA damage caused by reactive oxygen species in cellular senescence may therefore be activating similar mechanisms of senescence induction as that seen in replicative senescence. These gene targets highlight the fact that the SA-miRNAs are able to induce similar mechanisms through the use of stimuli specific target genes. The flexibility of the SA-miRNA mechanism of action allows them to remain specific enough for a cell to respond to a particular stimuli whilst general enough to focus pathway changes in those cells to create the senescent cell phenotype.

Two of the overlapping genes, EWSR1 and LOXL2, have previous evidence of senescence association. The EWS fusion protein has recently been reported as a repressor of senescence [58] and therefore its down-regulation by SA-miRNAs would provide a mechanism by which to prevent it inhibiting senescence induction. LOXL2 however has been used as a marker of senescent cells due to its increased expression during senescence [59]. These senescent associated genes can theoretically be regulated by SA-miRNAs and this may therefore present a mechanism by which their roles in senescence induction are controlled.

The remaining overlapping genes may still have roles in senescence. These genes may be involved in senescence induction through previously identified or potentially novel unidentified pathways, which analysis of the individual gene function does not elucidate. Their inclusion into larger data sets of potential senescence associated genes for systems biology analysis may help to elucidate their role.

MiRNA regulation of stress induced senescence can therefore be seen to potentially transcend treatment type and incur changes in core senescence genes. Furthermore regulation of additional treatment specific genes gives SA-miRNAs the potential to alter diverse cellular pathways required to respond to different stimuli.

4. SA-miRNAs regulate common cellular mechanisms regardless of stimuli

The regulation of different senescence induction stimuli by miRNAs varies as shown in Table 3. In this study we have seen evidence of the potential SA-miRNAs regulation of core sets of senescence genes regardless of induction mechanism. Our analysis has highlighted common up-regulation of apoptosis signalling and pro-inflammatory gene regulation targeted by SA-miRNAs between

different senescence stimuli. We have also seen SA-miRNA targeted down-regulation of cell cycle processes across the induction mechanisms. This evidence taken in combination with the large degree of overlap between treatment types in stress induced senescence is suggestive of key cellular changes that the SA-miRNAs can facilitate during senescence induction. To our knowledge, this is the first report of predicted miRNA regulation of common pathways regardless of senescence stimulus.

The fact that 2 SA-miRNAs, hsa-miR-499 and hsa-miR-34c, can regulate all of the senescence types we have examined takes this concept one step further and may suggest that these particular SA-miRNAs act as master regulators for senescence induction. Alterations in different biological signalling pathways by the remaining 10 SA-miRNAs could then tailor the cellular response to suit the alterations required by specific stimuli. This hypothesis requires further laboratory validation, however the fact that both miRNAs already have experimental evidence to show they are senescence regulators adds some weight to the theory.

5. Conclusions

In this study we have used pathway mapping and theoretical gene target identification to create a biological framework by which to test the relevance of miRNAs in senescence induction. We have shown not only that miRNAs can potentially regulate genes previously seen to be involved in senescence but also regulate larger pathway alterations, such as cell cycle and cytoskeletal remodelling, that would logically be required to create the complex phenotype of the senescent cell. Commonly regulated pathways and cellular mechanisms between the senescence stimuli also demonstrate the potential of SA-miRNAs to regulate a core set of pathway modifications regardless of senescence induction mechanism. Furthermore, we have identified stimulus specific pathways by which SA-miRNAs can regulate apoptosis survival signals in cells undergoing drug induced or natural replicative senescence. The identification of miR-499 and miR-34c as common regulators of all senescence stimuli we have studied may highlight their potential as future drug targets for senescence induction and further investigation of their role in regulation of the senescence phenotype certainly warrants further investigation.

Acknowledgements

Work in the authors laboratory is supported by Cancer Research UK, European Community grants LSHC-CT-2004-502943; Health-F2-2007-200950 and Glasgow University.

References

- [1] C.B. Harley, A.B. Futcher, C.W. Greider, Telomeres shorten during aging of human fibroblasts, *Nature* 345 (1990) 458–460.
- [2] T. Pascal, F. Dehaq-Chainiaux, A. Chretien, C. Bastin, A.F. Dabec, V. Bertholet, J. Remacle, O. Toussaint, Comparison of replicative senescence and stress-induced premature senescence combining differential display and low-density DNA arrays, *FEBS Lett.* 579 (2005) 3651–3659.
- [3] T. Kullman, C. Michaloglou, L.C.W. Vredevelde, S. Douma, R. van Doorn, C.J. Desmet, L.A. Aarden, W.J. Mooi, D.S. Peepec, Oncogene-induced senescence relayed by an interleukin-dependent inflammatory network, *Cell* 133 (2008) 1019–1031.
- [4] S. Parinello, Oxygen sensitivity severely limits the replicative lifespan of murine fibroblasts (Vol 5, Pg 740, 2003), *Nat. Cell Biol.* 5 (2003) 839.
- [5] A.L. Fridman, M.A. Tainsky, Critical pathways in cellular senescence and immortalization revealed by gene expression profiling, *Oncogene* 27 (2008) 5975–5987.
- [6] M. Narita, S. Nunez, E. Heard, M. Narita, A.W. Lin, S.A. Hearn, D.L. Specter, G.J. Hannon, S.W. Lowe, Rb-mediated heterochromatin formation and silencing of EZF target genes during cellular senescence, *Cell* 113 (2003) 703–716.
- [7] F.J. di Fagagna, P.M. Reaper, I. Clay-Farrace, H. Fiegler, P. Carr, T. von Zglinnick, G. Saretzki, N.P. Carter, S.P. Jackson, A DNA damage checkpoint response in telomere-initiated senescence, *Nature* 426 (2003) 194–198.
- [8] R.C. Lee, R.L. Feinbaum, V. Ambros, The *C. elegans* heterochronic gene *lin-4* encodes small mas with antisense complementarity to *lin-14*, *Cell* 75 (1993) 843–854.

- [9] B. Wightman, I. Ha, G. Ravliko, Posttranscriptional regulation of the heterochronic gene *lin-14* by *lin-4* mediates temporal pattern formation in *C. elegans*, *Cell* 75 (1993) 855–862.
- [10] B.M. Engels, G. Hutvagner, Principles and effects of microRNA-mediated posttranscriptional gene regulation, *Oncogene* 25 (2006) 6163–6169.
- [11] B.D. Hafler, MicroRNAs in vertebrate development, *Curr. Opin. Genet. Dev.* 15 (2005) 410–415.
- [12] D.P. Bartel, MicroRNAs and their regulatory roles in plants and animals, *Dev. Biol.* 283 (2005) 575.
- [13] S. Griffiths-Jones, The microRNA registry, *Nucleic Acids Res.* 32 (2004) D109–D111.
- [14] S. Griffiths-Jones, R.J. Crocock, S. van Dongen, A. Bateman, A.J. Enright, Mirbase: microRNA sequences, targets and gene nomenclature, *Nucleic Acids Res.* 34 (2006) D140–D144.
- [15] S. Griffiths-Jones, H.K. Salim, S. van Dongen, A.J. Enright, Mirbase: tools for microRNA genomics, *Nucleic Acids Res.* 36 (2008) D154–D158.
- [16] G.T. Bommer, I. Gerin, Y. Feng, A.J. Kaczorowski, R. Kuick, R.E. Love, Y. Zhai, T.J. Gordon, Z.S. Qin, B.B. Moore, Q.A. MacDougald, K.R. Cho, E.R. Fearon, P53-mediated activation of *Mirna34* candidate tumor-suppressor genes, *Curr. Biol.* 17 (2007) 1298–1307.
- [17] L. He, X.Y. He, L.P. Lim, E. De Stanchina, Z.Y. Xuan, Y. Liang, W. Xue, L. Zender, J. Magnus, D. Ridzon, A.L. Jackson, P.S. Linsley, C.F. Chen, S.W. Lowe, M.A. Cleary, G.J. Hannon, A microRNA component of the P53 tumour suppressor network, *Nature* 447 (2007) 1130–1136.
- [18] H. Tazawa, N. Tsuchiya, M. Izumiya, H. Nakagawa, Tumor-suppressive *Mir-34a* induces senescence-like growth arrest through modulation of the E2f pathway in human colon cancer cells, *Proc. Natl. Acad. Sci. U.S.A.* 104 (2007) 15472–15477.
- [19] K. Kumamoto, E.A. Spillare, K. Fujita, I. Horikawa, T. Yamashita, E. Appella, M. Nagashima, S. Takenoshita, J. Yokota, C.C. Harris, Nutlin-3a activates P53 to both down-regulate inhibitor of growth 2 and up-regulate *Mir-34a*, *Mir-34b*, and *Mir-34c* expression, and induce senescence, *Cancer Res.* 68 (2008) 3193–3203.
- [20] N. Raver-Shapira, E. Marciano, E. Meiri, Y. Spector, N. Rosenfeld, N. Moskovits, Z. Bentwich, M. Oren, Transcriptional activation of *Mir-34a* contributes to P53-mediated apoptosis, *Mol. Cell* 26 (2007) 731–743.
- [21] T.C. Chang, E.A. Wenthe, O.A. Kent, K. Ramchandran, M. Mullendore, K.H. Lee, G. Feldman, M. Yamakuchi, M. Fedirko, C.J. Lowenstein, D.E. Adkins, M.A. Beer, A. Maltra, J.T. Mendell, Transcriptional activation of *Mir-34a* by P53 broadly influences gene expression and promotes apoptosis, *Mol. Cell* 26 (2007) 745–752.
- [22] L. Poliseno, L. Hrist, M. Simili, L. Mariani, L. Riccardi, A. Ciucci, M. Rizzo, M. Evangelista, A. Mercatanti, P.P. Pandolfi, G. Rainaldi, The proto-oncogene *lrf1* is under post-transcriptional control of *Mir-20a*: implications for senescence, *PLoS ONE* 3 (2008) e2542.
- [23] T. Maeda, R.M. Hobbs, T. Merghouh, L. Guernah, A. Zelen, C. Cordon-Cardo, J. Teuya-Feldstein, P.P. Pandolfi, Role of the proto-oncogene *pokemon* in cellular transformation and *Aif1* expression, *Nature* 433 (2005) 278–285.
- [24] J. Pomerantz, N. Schreiber-Agus, N.J. Liegeois, A. Silverman, L. Alland, L. Chin, J. Pates, K. Chen, L. Orlov, H.W. Lee, C. Cordon-Cardo, R.A. DeHnck, The *Ink4a* tumor suppressor gene product, *P19^{INK4}*, interacts with *Mdm2* and neutralizes *Mdm2*'s inhibition of P53, *Cell* 92 (1998) 713–723.
- [25] W. Wagner, P. Horn, M. Castoldi, A. Diehlmann, S. Bork, R. Saffrich, V. Benes, J. Blake, S. Pfister, V. Eckstein, A.D. Ho, Replicative senescence of mesenchymal stem cells: a continuous and organized process, *PLoS ONE* 3 (2008) e2213.
- [26] P.M. Voohtoeve, C. le Sage, M. Schrier, A.J. Gillis, H. Stoop, R. Nagel, Y.P. Liu, J. van Duijse, J. Drost, A. Griekspoor, E. Zlotorynski, N. Yabuta, G. De Vito, H. Nijima, L.H. Looyenga, R. Agami, A genetic screen implicates *Mirna-372* and *Mirna-373* as oncogenes in testicular germ cell tumors, *Cell* 124 (2006) 1169–1181.
- [27] L. Fontana, M.E. Fiori, S. Albin, L. Cifaldi, S. Giovannazzi, M. Forloni, R. Boldrini, A. Donfrancesco, V. Federci, P. Giacomini, C. Peschle, D. Fruci, Antagomir-T7-5p abolishes the growth of therapy-resistant neuroblastoma through P21 and *Bim*, *PLoS ONE* 3 (2008) e2236.
- [28] A. Lal, H.H. Kim, K. Abdelmohsen, Y. Kuwano, R. Pullmann Jr., S. Srikanan, R. Subrahmanyam, J.L. Martindale, X. Yang, F. Ahmed, F. Navarro, D. Dykxhoorn, J. Lieberman, M. Gorospe, P19(*Ink4a*) translation suppressed by *Mir-24*, *PLoS ONE* 3 (2008) e1864.
- [29] N.G. Benabe, J.R. Smith, O.M. Pereira-Smith, The genetics of cellular senescence, *Am. J. Hum. Genet.* 62 (1998) 1015–1019.
- [30] S.P. Bell, A. Dutta, DNA replication in eukaryotic cells, *Ann. Rev. Biochem.* 71 (2002) 333–374.
- [31] Y. Tsumami, K. Brura, K. Yoshida, T. Yagawa, M. Narisawa-Saito, T. Kiyono, S. Ohta, C. Ohue, M. Fujita, Involvement of human *Orc* and *Trf2* in pre-replication complex assembly at telomeres, *Genes Cells* 13 (2008) 3045–3059.
- [32] S. Ahn, M. Olive, S. Aggarwal, D. Krylov, D.D. Ginty, C. Vinson, Adominant-negative inhibitor of *Creb* reveals that it is a general mediator of stimulus-dependent transcription of *C-Fos*, *Mol. Cell Biol.* 18 (1998) 967–977.
- [33] R.J. Lee, C. Albanese, R.J. Stenger, G. Watanabe, G. Inghirami, G.K. Haines, M. Webster, W.J. Muller, J.S. Brugge, R.J. Davis, R.G. Pestell, Pp60(V-Src) induction of cyclin D1 requires collaborative interactions between the extracellular signal-regulated kinase, F38, and Jun kinase pathways – a role for camp response element-binding protein and activating transcription factor-2 in Pp60(V-Src) signaling in breast cancer cells, *J. Biol. Chem.* 274 (1999) 7341–7350.
- [34] C. Desdouets, G. Matesic, C.A. Molina, N.S. Poulkes, P. Sassonecorsi, C. Brechet, J. Sobczakhepot, Cell-cycle regulation of cyclin-a gene-expression by the cyclic Amp-responsive transcription factors *Creb* and *Crem*, *Mol. Cell Biol.* 15 (1995) 3301–3309.
- [35] K. Damm, U. Hemmann, P. Gadin-Chesa, N. Huel, I. Kauffmann, H. Pfeleke, C. Nistroj, C. Dalber, B. Enkel, B. Guillard, I. Lauritsch, E. Muller, E. Pascolo, G. Sauter, M. Pantic, U.M. Martens, C. Wenz, J. Lingner, N. Kraut, W.J. Rettig, A. Schnapp, A highly selective telomerase inhibitor limiting human cancer cell proliferation, *EMBO J.* 20 (2001) 6958–6968.
- [36] Q. Li, A.K. Ching, B.C. Chan, S.K. Chow, P.L. Lim, T.C. Ho, W.K. Ip, C.K. Wong, C.W. Lam, K.K. Lee, J.Y. Chan, Y.L. Chui, A death receptor-associated anti-apoptotic protein, *Bre*, inhibits mitochondrial apoptotic pathway, *J. Biol. Chem.* 279 (2004) 52306–52316.
- [37] C. Gu, A. Castellino, J.Y. Chan, M.V. Chao, *Bre*: a modulator of *Tnf-alpha* action, *FASEB J.* 12 (1998) 1101–1108.
- [38] M. Irmir, M. Thome, M. Hahne, P. Schneider, K. Hofmann, V. Steiner, J.L. Bodmer, M. Schroter, K. Burns, C. Mattmann, D. Rimoldi, L.E. French, J. Tschopp, Inhibition of death receptor signals by cellular *flp*, *Nature* 388 (1997) 190–195.
- [39] E. Morandi, C. Severini, D. Quercioli, G. D'Ario, S. Perdicchi, W. Capri, G. Farruggia, M.G. Mascolo, W. Horn, M. Vaccaro, R. Serra, A. Colacci, P. Sillingardi, Gene expression time-series analysis of camptothecin effects in U87-Mg and Dbrg-05 glioblastoma cell lines, *Mol. Cancer* 7 (2008) 66.
- [40] M. Sasaki, H. Ikeda, Y. Sato, Y. Nakanuma, Proinflammatory cytokine-induced cellular senescence of biliary epithelial cells is mediated via oxidative stress and activation of *Atm* pathway: a culture study, *Free Radic. Res.* 42 (2008) 625–632.
- [41] K. Hardy, L. Mansfield, A. Mackay, S. Benvenuti, S. Ismail, P. Arora, M.J. O'Hare, P.S. Jai, Transcriptional networks and cellular senescence in human mammary fibroblasts, *Mol. Biol. Cell* 16 (2005) 943–953.
- [42] Y.B. Deng, S.S. Chan, S. Chang, Telomere dysfunction and tumour suppression: the senescence connection, *Nat. Rev. Cancer* 8 (2008) 460–468.
- [43] C.J. Chang, D.J. Mullholland, B. Valameh, S. Mossessian, W. Selles, H. Wu, Pten nuclear localization is regulated by oxidative stress and mediates P53-dependent tumor suppression, *Mol. Cell Biol.* 28 (2008) 3281–3289.
- [44] K. Takabe, J.J. Lebrun, Y. Nagashima, Y. Ichikawa, M. Mitsuhashi, N. Momiya, T. Ishikawa, H. Shimada, W.W. Vale, Interruption of *activin* a autocrine regulation by antisense oligodeoxynucleotides accelerates liver tumor cell proliferation, *Endocrinology* 140 (1999) 3125–3132.
- [45] J. Jiao, S. Wang, R. Qiao, L. Vranco, P.A. Watson, C.L. Sawyers, H. Wu, Murine cell lines derived from *Pten* null prostate cancer show the critical role of *Pten* in hormone refractory prostate cancer development, *Cancer Res.* 67 (2007) 6083–6091.
- [46] J.S. Jeruss, C.D. Sturgis, A.W. Rademaker, T.K. Woodruff, Down-regulation of *activin*, *activin* receptors, and *smads* in high-grade breast cancer, *Cancer Res.* 63 (2003) 3783–3790.
- [47] Z. Chen, L.C. Trotman, D. Shaffer, H.K. Lin, Z.A. Dotan, M. Niki, J.A. Koutcher, H.L. Scher, T. Ludwig, W. Gerald, C. Cordon-Cardo, P.P. Pandolfi, Crucial role of P53-dependent cellular senescence in suppression of *Pten*-deficient tumorigenesis, *Nature* 436 (2005) 725–730.
- [48] A.W. Lin, M. Barndas, J.C. Stone, L. van Aelst, M. Setraro, S.W. Lowe, Premature senescence involving P53 and P16 is activated in response to constitutive *Mek1*/Mapk mitogenic signalling, *Genes Dev.* 12 (1998) 3008–3019.
- [49] S. Courtillot-Cox, S.M. Genth Williams, E.E. Reszek, B.W. Johnson, L.T. McGillivuddy, C.M. Johannessen, P.E. Hollstein, M. MacCollin, K. Cichowski, A negative feedback signaling network underlies oncogene-induced senescence, *Cancer Cell* 10 (2006) 459–472.
- [50] C. Michaloglou, L.C.W. Vredevel, M.S. Sengas, C. Denoyelle, T. Kallman, C. van der Hout, D.M. Majum, J.W. Shay, W.J. Modi, D.S. Peepker, *Braf*(E600)-associated senescence-like cell cycle arrest of human *Nasvi*, *Nature* 436 (2005) 720–724.
- [51] F. Debacqz-Chainiaux, C. Borion, T. Pascal, V. Royer, F. Eliaes, N. Ninane, G. Garrard, B. Friguet, F. de Longueville, S. Boffe, J. Remacle, O. Toussaint, Repeated exposure of human skin fibroblasts to *Uvb* at subcytotoxic level triggers premature senescence through the *Tgf-Beta1* signaling pathway, *J. Cell Sci.* 118 (2005) 743–758.
- [52] C. Frippliat, Q.M. Chen, S. Zhanov, J.P. Magalhaes, J. Remacle, O. Toussaint, Subcytotoxic H2O2 stress triggers a release of transforming growth factor-Beta 1, which induces biomarkers of cellular senescence of human diploid fibroblasts, *J. Biol. Chem.* 276 (2001) 2531–2537.
- [53] P. Dumont, F. Chainiaux, F. Eliaes, C. Petropoulou, J. Remacle, C. Koch-Brandt, E.S. Gonos, O. Toussaint, Overexpression of apolipoprotein J in human fibroblasts protects against cytotoxicity and premature senescence induced by ethanol and tert-butylhydroperoxide, *Cell Stress Chaperones* 7 (2002) 23–35.
- [54] M. Katoh, M. Katoh, Identification and characterization of *Ahm*gp24 and *Arhg*gp25 genes in silico, *Int. J. Mol. Med.* 14 (2004) 333–338.
- [55] K.M. Daugherty, R.L. Goode, Functional surfaces on the *P35/Arp2* subunit of *Arp2/3* complex required for cell growth, actin nucleation, and endocytosis, *J. Biol. Chem.* 283 (2008) 16930–16939.
- [56] N. Belot, R. Pocher, C.W. Heizmann, R. Kiss, C. Decaestecker, Extracellular S100a4 stimulates the migration rate of astrocytic tumor cells by modifying the organization of their actin cytoskeleton, *Biochimica et Biophysica Acta-Proteins and Proteomics* 1600 (2002) 74–83.
- [57] K. Dahm, U. Hubscher, Colocalization of human *Rad17* and *Pcna* in late S phase of the cell cycle upon replication block, *Oncogene* 21 (2002) 7710–7719.
- [58] H.M. Hu, A. Zielinska-Kwiatkowska, K. Munro, J. Wilcox, D.Y. Wu, L. Yang, H.A. Chansky, *Ews/Flil1* suppresses retinoblastoma protein function and senescence in Ewing's sarcoma cells, *J. Orthop. Res.* 26 (2008) 886–893.
- [59] K.C. Muller, L. Welker, K. Faasch, B. Reindt, V.J. Erpenbeck, J.M. Hohlheid, N. Krug, M. Nakashima, D. Branschedl, H. Magnusson, R.A. Jones, O. Holz, Lung fibroblasts from patients with emphysema show markers of senescence in vitro, *Respir. Res.* 7 (2006) 32.

Dynamic Telomerase Gene Suppression via Network Effects of GSK3 Inhibition

Alan E. Bilsland¹, Stacey Hoare¹, Katrina Stevenson¹, Jane Plumb¹, Natividad Gomez-Roman¹, Claire Cairney¹, Sharon Burns¹, Kyle Lafferty-Whyte¹, Jon Roffey², Tim Hammonds², W. Nicol Keith^{1*}

1 Centre for Oncology and Applied Pharmacology, University of Glasgow, Cancer Research UK Beatson Laboratories, Garscube Estate, Bearsden, Glasgow, United Kingdom, **2** Cancer Research Technology Ltd., Wolfson Institute for Biomedical Research, The Cruciform Building, London, United Kingdom

Abstract

Background: Telomerase controls telomere homeostasis and cell immortality and is a promising anti-cancer target, but few small molecule telomerase inhibitors have been developed. Reactivated transcription of the catalytic subunit *hTERT* in cancer cells controls telomerase expression. Better understanding of upstream pathways is critical for effective anti-telomerase therapeutics and may reveal new targets to inhibit *hTERT* expression.

Methodology/Principal Findings: In a focused promoter screen, several GSK3 inhibitors suppressed *hTERT* reporter activity. GSK3 inhibition using 6-bromoindirubin-3'-oxime suppressed *hTERT* expression, telomerase activity and telomere length in several cancer cell lines and growth and *hTERT* expression in ovarian cancer xenografts. Microarray analysis, network modelling and oligonucleotide binding assays suggested that multiple transcription factors were affected. Extensive remodelling involving Sp1, STAT3, c-Myc, NFκB, and p53 occurred at the endogenous *hTERT* promoter. RNAi screening of the *hTERT* promoter revealed multiple kinase genes which affect the *hTERT* promoter, potentially acting through these factors. Prolonged inhibitor treatments caused dynamic expression both of *hTERT* and of c-Jun, p53, STAT3, AR and c-Myc.

Conclusions/Significance: Our results indicate that GSK3 activates *hTERT* expression in cancer cells and contributes to telomere length homeostasis. GSK3 inhibition is a clinical strategy for several chronic diseases. These results imply that it may also be useful in cancer therapy. However, the complex network effects we show here have implications for either setting.

Citation: Bilsland AE, Hoare S, Stevenson K, Plumb J, Gomez-Roman N, et al. (2009) Dynamic Telomerase Gene Suppression via Network Effects of GSK3 Inhibition. PLoS ONE 4(7): e6459. doi:10.1371/journal.pone.006459

Editor: Edithara Abraham, University of Arkansas for Medical Sciences, United States of America

Received: April 15, 2009; **Accepted:** June 30, 2009; **Published:** July 31, 2009

Copyright: © 2009 Bilsland et al. This is an open-access article distributed under the terms of the Creative Commons Attribution License, which permits unrestricted use, distribution, and reproduction in any medium, provided the original author and source are credited.

Funding: This work was supported by Cancer Research UK (www.cancerresearchuk.org), European Community grant Health-F2-2007-200950 (http://cordis.europa.eu/home_en.html) and Glasgow University (www.gla.ac.uk). The funders had no role in study design, data collection and analysis, decision to publish, or preparation of the manuscript.

Competing Interests: The authors have declared that no competing interests exist.

* E-mail: nk101@beatson.gla.ac.uk

Introduction

Telomerase is a ribonucleoprotein reverse transcriptase which counteracts telomere attrition in dividing cells by synthesising telomere DNA [1]. Telomerase activity requires the catalytic subunit *hTERT* and the RNA subunit *hTERC*, which contains the template sequence for reverse transcription. Both gene products are over-expressed in cancer cells relative to somatic cells and in most human cancers. Telomere homeostasis is essential for cell immortalisation and telomerase is an attractive anti-cancer target [2].

Telomerase expression in cancer cells is dependent on aberrant *hTERC* and *hTERT* transcription, resulting from multiple events including altered signalling and changes in the promoter chromatin environments relative to normal cells [3]. However, the cloned promoters also have cancer cell specific activity, leading many groups to develop telomerase-specific gene therapy models [4]. Several transcription factors affecting each gene promoter are known. The *hTERT* promoter, for example, is regulated by multiple factors including Myc, Mad, Sp1, STAT3, E2F and p53, among others [5].

Current clinical trials of telomerase therapeutics include several immunotherapeutics, an oncolytic adenovirus, and GRN163L, a modified oligonucleotide telomerase inhibitor [2,5,6]. Targeting telomerase transcription using signal transduction inhibitors may also hold value [2,7]. However, signalling events upstream of the telomerase genes remain poorly understood and in most studies in which signal transduction inhibitors have been found to affect expression of telomerase genes, long term treatments to examine effects on telomere length and telomere dependent senescence have not been performed. In this study, we tested whether focused cell-based screening using well-defined kinase inhibitors could provide a platform to identify new telomerase regulatory pathways and candidate targets for pharmacological intervention.

We show that glycogen synthase kinase 3 (GSK3) activates *hTERT* transcription and characterise the pathway upstream of *hTERT*. GSK3 inhibition reduced *hTERT* promoter activity, expression, telomerase activity and telomere lengths in several cell lines and suppressed tumour growth and *hTERT* expression in a xenograft model. Therefore, GSK3 inhibition may be an appropriate anti-cancer strategy. Prolonged GSK3 inhibition in A2780 cells profoundly reduced telomere lengths; interestingly

however, *hTERT* expression was not stably suppressed but showed dynamic oscillation.

GSK3 α and β isoforms, which are both targets of GSK3 inhibitors, variously regulate diverse cellular processes including survival and apoptosis, energy metabolism, cell fate specification and stem cell self renewal through phosphorylation of multiple substrates in several distinct pathways including Wnt and insulin signalling [8,9]. We present a network model of *hTERT* activation and show that GSK3 inhibition affects multiple transcription factors converging on *hTERT*. Interestingly, expression levels of several transcription factors were also dynamically regulated under prolonged GSK3 inhibitor treatments, suggesting that GSK3 may control steady state behaviour of the network. A whole-kinome RNAi screen of the *hTERT* promoter is interpreted using this model to predict rational combinatorial targets to enhance anti-telomerase effects of GSK3 inhibitors.

Results

GSK3 activates the *hTERT* promoter

In a focused screen of 79 well characterised kinase inhibitors, A2780 cells were transfected with *hTERT* reporter construct and 32 h post transfection were exposed to 10 μ M each inhibitor for 16 h. Six compounds suppressed promoter activity by at least 2-fold (figure 1A). Compounds 38 (Ro-31-8220, bis indole maleimide family; 4.6-fold), 69 (indirubin-3'-monoxime, indirubin core; 2.2-fold) and 79 (kenpaullone, indolo benzazepinone core; 11.1-fold) are all reported to inhibit GSK3 [10]. The other hit compounds were: 26, typhostin AG 1295 (inhibitor of PDGFR [11]); 50, 5-iodotubercidin (inhibitor of adenosine kinase [12]); and 55, SU4312 (inhibitor of PDGFR and FGFR [13]).

To extend the observation that diverse GSK3 inhibitors suppress *hTERT* promoter activity, we performed *hTERT* reporter assays and parallel MTT assays, titrating the selective inhibitors AR-A014418 (benzyl-thiazolyl urea substructure), TWS119 (pyrrolopyrimidine core), and 6-bromoindirubin-3'-oxime (BIO, indirubin core) alongside the GSK3-inactive BIO derivative 1-methyl-BIO (MeBIO) [10]. Structures of all GSK3 inhibitors used in this study are available in supporting figure S1. All supporting figure and file legends are given in supporting file S4. Active inhibitors of different chemotypes, but not MeBIO, suppressed *hTERT* promoter activity at sub-toxic concentrations (figure 1B). At optimal doses of 10 μ M (AR-A01448) and 5 μ M (TWS119 and BIO) promoter activities were 62%, 67% and 55% of control. BIO and MeBIO were also titrated against the *hTERT* reporter in 5637, C33A, A549 and HCT116 cells (figure 1C). BIO, but not MeBIO, suppressed the *hTERT* promoter in all cells with IC₅₀s in the range 5.4 μ M–8.2 μ M. Similarly, BIO, but not MeBIO activated Topflash reporter activity in all cells, indicative of specific GSK3 β inhibition (supporting figure S2).

To further characterise the effect of GSK3 on the *hTERT* reporter we over-expressed mWnt3, mWnt5A or human DVL2 in each cell line, which all inhibit GSK3 β in Wnt signalling. Additionally, we examined the effect of β -catenin over-expression. Both Wnts and DVL2 reduced *hTERT* promoter activity in 5637, HCT116 and A549. Wnt3 had the strongest effect and DVL2 the weakest (figure 2A). Only mWnt3 had a significant effect in A2780 and the effect of mWnt5A was not significant in C33A. Promoter repression was not correlated with basal β -catenin expression (figure 2B). For example, despite low expression in A549 and constitutively stable expression in HCT116, each construct had similar effects, reducing promoter activity to 32% of control (mWnt3), 8% (mWnt5A) and 14% (DVL2) in HCT116 and 33%, 8%, and 15%, respectively, in A549. Interestingly, wild type β -

catenin induced promoter activity in HCT116, A549 and C33A. Supporting figure S3 shows the effect of each construct on Topflash reporter activity in each cell line. β -catenin and DVL2 generally resulted in the strongest increase of Topflash activity, whereas mWnt5A had a weaker effect. Interestingly, mWnt3 mildly decreased Topflash activity in some cells. The effect of each transfection on canonical Wnt signalling presumably depends on the specific status of the pathway in each cell type.

To confirm that GSK3 β regulates the *hTERT* promoter, we co-transfected each cell line with reporter and with 50 nM GSK3 β -specific siRNA (two GSK3 β -specific siRNA were tested—siRNA-203 and siRNA-42839). Both siRNAs tested reduced promoter activity in all cells relative to non-specific control (Figure 2C). All effects were significant except siRNA-42839 in 5637 cells. Promoter activities ranged between 38%–75% of control for siRNA-203 and 34%–83% for siRNA-42839 at 48 h post-transfection. Both specific siRNAs produced a GSK3 β knockdown in A2780 at 50 nM (figure 2D). SiRNA-42839 produced a greater knockdown than siRNA-203 and, interestingly, also resulted in some knockdown of GSK3 α . The GSK3 α transcript is highly homologous with that of GSK3 β in the 42839 target site, sharing 16/19 nucleotides. It is possible that GSK3 α knockdown might result from target sequence homology. However, given the high nucleotide specificity of the RNAi mechanism, it is perhaps more plausible that GSK3 β affects GSK3 α expression. Together these data confirm that GSK3 activates the cloned *hTERT* promoter in multiple cell lines.

Functional specificity of BIO

Specificity of the GSK3 inhibitor BIO was assessed by phospho-specific multiplex western blotting. A2780 were treated with DMSO, 5 μ M BIO, or 10 μ M roscovitine to control for inhibition of possible off-target kinases CDK 1, 2, and 5 [10]. Protein samples from treated cells were separated by SDS-PAGE using single-well 10% Bis-Tris minigels and blotted onto PVDF filters. 28 individual lanes were isolated on the filters using a miniblotted dual apparatus. To provide a detailed view of effects on GSK3 signalling, each lane was probed with an individual antibody or antibody cocktail to quantify expression (figure 3A) and phosphorylation (figure 3B) of multiple proteins involved in GSK3 signalling and other pathways. Intensity change of quantifiable bands relative to control was assessed by densitometry. Note the log scale in figure 3A.

BIO treatment strongly induced β -catenin (30.9-fold), cyclin D1 (8.2-fold) and glycogen synthase (GS) (6.3-fold), which are all destabilised by GSK3 [14–16]. Expression of cyclins B1 and E2, p90-RSK, STAT3, c-Jun and I κ B were also increased by around 2–3 fold each. It has previously been reported that c-Jun and I κ B stability are also regulated by GSK3 [17,18]. Roscovitine also mildly induced cyclin D1 (2.7-fold) but, in contrast with BIO, decreased β -catenin (49% of control) and cyclin E2 (34%). As previously reported, roscovitine induced MAPK phosphorylation [19], while BIO blocked phosphorylation on AKT S473 (29% of control), p90-RSK S380 (12%), STAT3 S727 (26%), and GS (56%) and induced PP1 α T320 phosphorylation (4.9-fold). Thus, the effects of BIO are consistent with GSK3 inhibition and largely non-overlapping with those of a pan-CDK inhibitor.

BIO inhibits endogenous telomerase

To determine whether GSK3 inhibition suppresses endogenous telomerase, 5637, HCT116 and A2780 cells were cultured continuously in log phase with BIO or DMSO given twice-weekly for five weeks. Drug was not removed between treatments. Cells were counted weekly and at each time point individual cell pellets

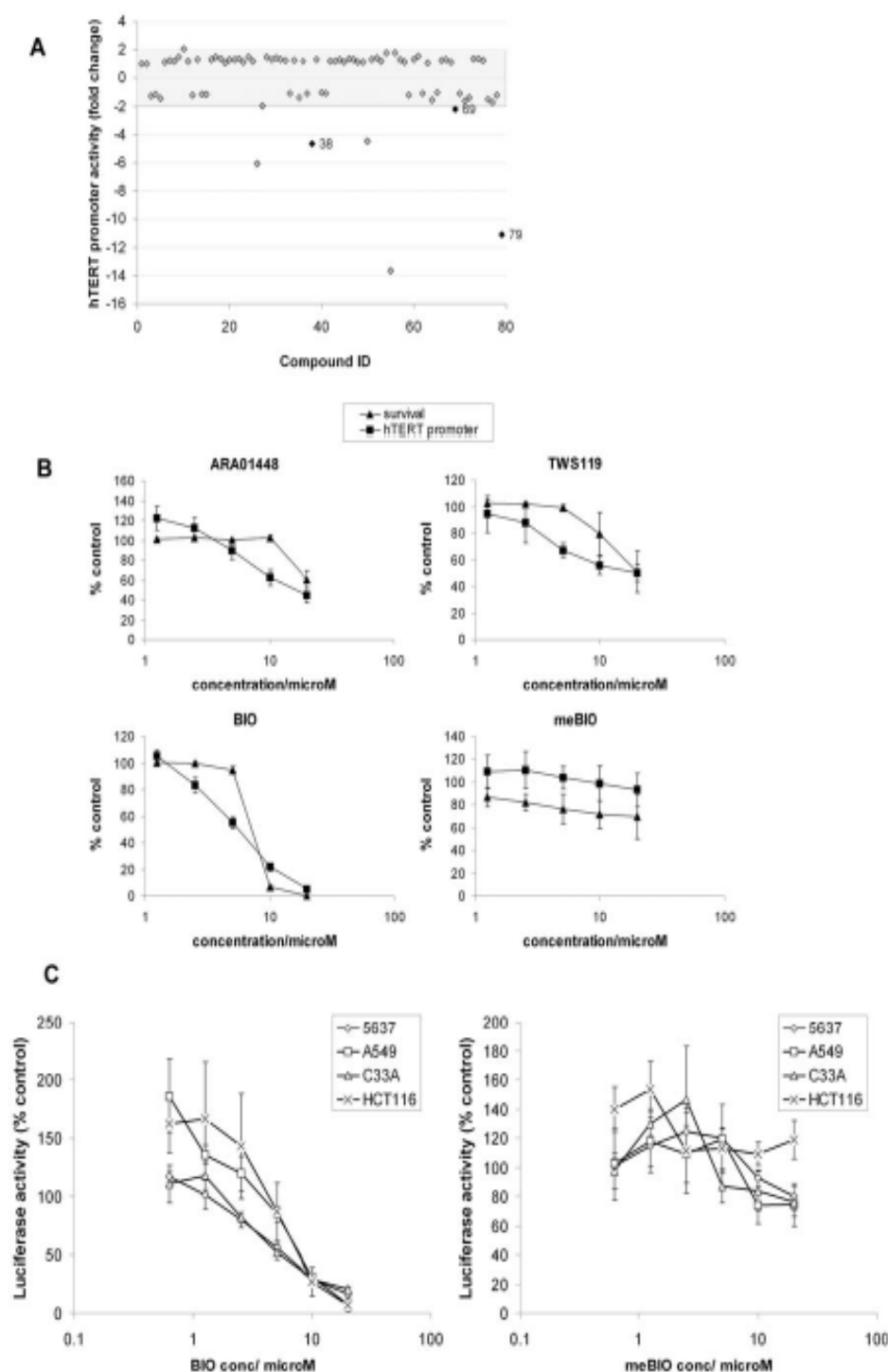


Figure 1. GSK3 inhibitors suppress the *hTERT* promoter. (A) Kinase inhibitor screen: A2780 cells were transfected with *hTERT*-luciferase reporter. 32 h later cells were treated for 16 h with DMSO or 10 μ M kinase inhibitors prior to luciferase assay. Hits are shown outside the shaded area. 38: Ro-31-8220; 69: indirubin-3'-monoxime; 79: lenpaulone. Mean \pm SEM of 3 experiments. (B) *hTERT* promoter inhibition and toxicity of GSK3 inhibitors. A2780 cells were transfected with *hTERT*-luciferase reporter. 32 h later cells were treated for 16 h with compounds at 20 μ M, 10 μ M, 5 μ M, 2.5 μ M and 1.25 μ M or DMSO for 16 h prior to luciferase assay. Parallel MTT assays of compound toxicity were performed. Mean \pm SEM of 3 experiments. (C) BIO suppresses the *hTERT* promoter in multiple cell lines. Cells were transfected with *hTERT*-luciferase reporter. 32 h later cells were treated for 16 h with inhibitor titrations as in (B) prior to luciferase assay. Mean \pm SEM of 3 experiments. doi:10.1371/journal.pone.0006459.g001

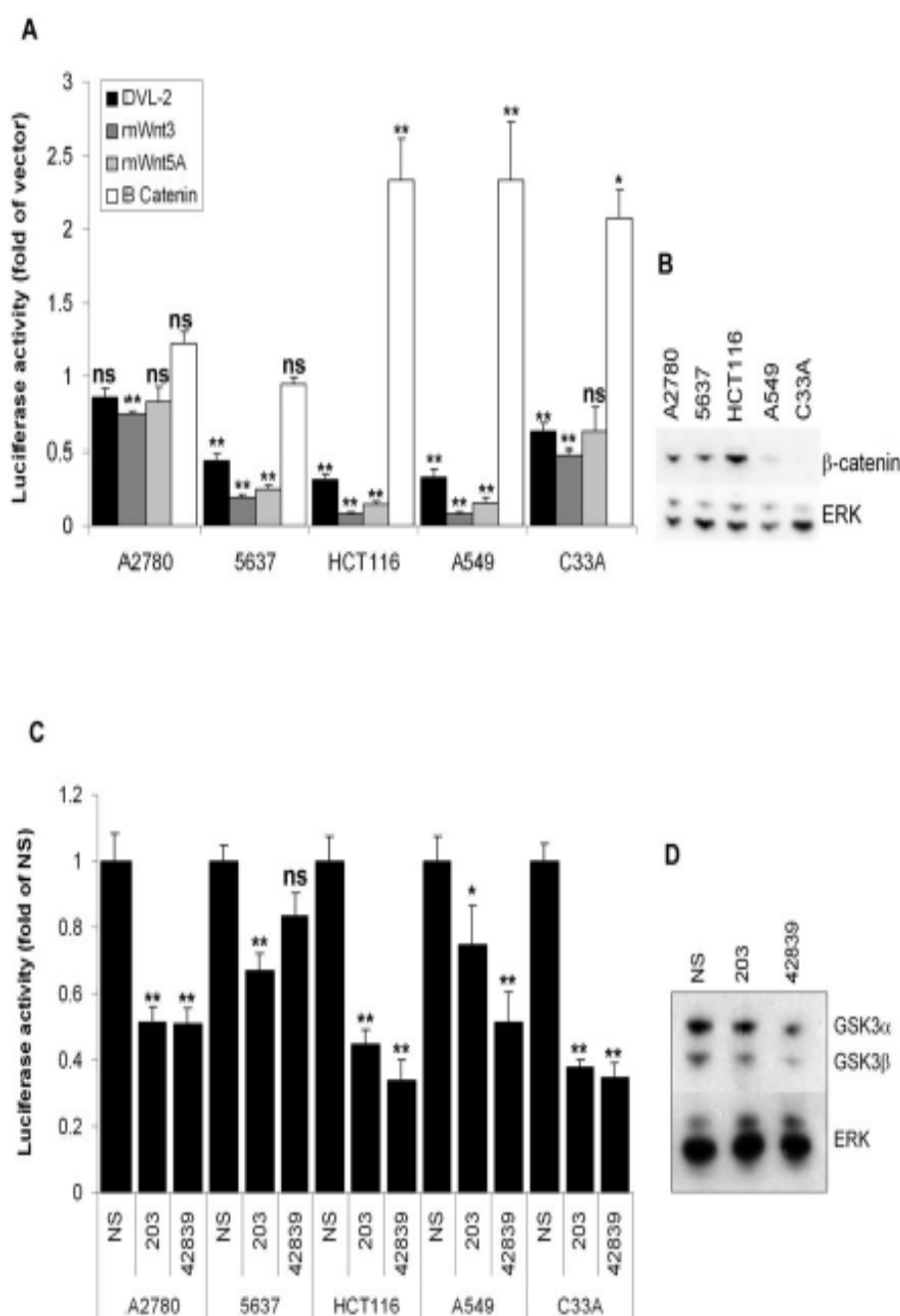


Figure 2. GSK3 β activates the *hTERT* promoter. (A) Wnt signalling inhibits the *hTERT* promoter. A2780 cells were transfected with *hTERT*-luciferase and the CMV expression vectors shown. 48 h later reporter activities were determined relative to empty vector. Mean \pm SEM of 3 experiments (ns: not significant; *: $p < 0.5$; **: $p < 0.01$). (B) Basal β -catenin expression in 20 μ g protein samples was analysed by western blotting. The experiment was performed twice. Representative blots are shown. (C) GSK3 β RNAi inhibits the *hTERT* promoter. A2780 cells were transfected with *hTERT*-luciferase and 50 nM non-specific (NS) siRNA or GSK3 β specific siRNAs 203 or 42839. 48 h later reporter activities were determined. Mean \pm SEM of 3 experiments (ns: not significant; *: $p < 0.5$; **: $p < 0.01$). (D) Knockdown of GSK3 β by siRNA-203 and -42839. A2780 were transfected with 50 nM siRNA and harvested after 48 h. 20 μ g protein samples were analysed by western blotting. The experiment was performed twice. Representative blots are shown. doi:10.1371/journal.pone.0006459.g002

were taken from both control and treated cells for telomere length analysis, *hTERT* expression analysis by RT-QPCR, microarray analysis, western blotting of GSK3 inhibition markers, and for TRAP analysis of telomerase activity (figure 3C). At the time of sampling, drug had not been replenished for 3 days. BIO concentrations used in these experiments were 2.5 μ M (A2780), 1 μ M (HCT116) and 500 nM (5637).

Western blotting was performed to detect levels of β -catenin, GSK3 and expression and phosphorylation of GS and PPI α at

each sampling time point (figure 3D). β -catenin is constitutively stable in HCT116 but was also unaffected in the other cell lines, presumably indicating rapid return to basal levels as the effects of BIO diminish between treatment and sampling. However, GS S641 phosphorylation decreased progressively in all BIO treated cells and its expression was also increased throughout in A2780. Therefore, GSK3 was inhibited in all cell lines. Additionally, increased PPI α T320 phosphorylation and reduced GSK3 α and β expression were detected at all times in A2780 and HCT116.

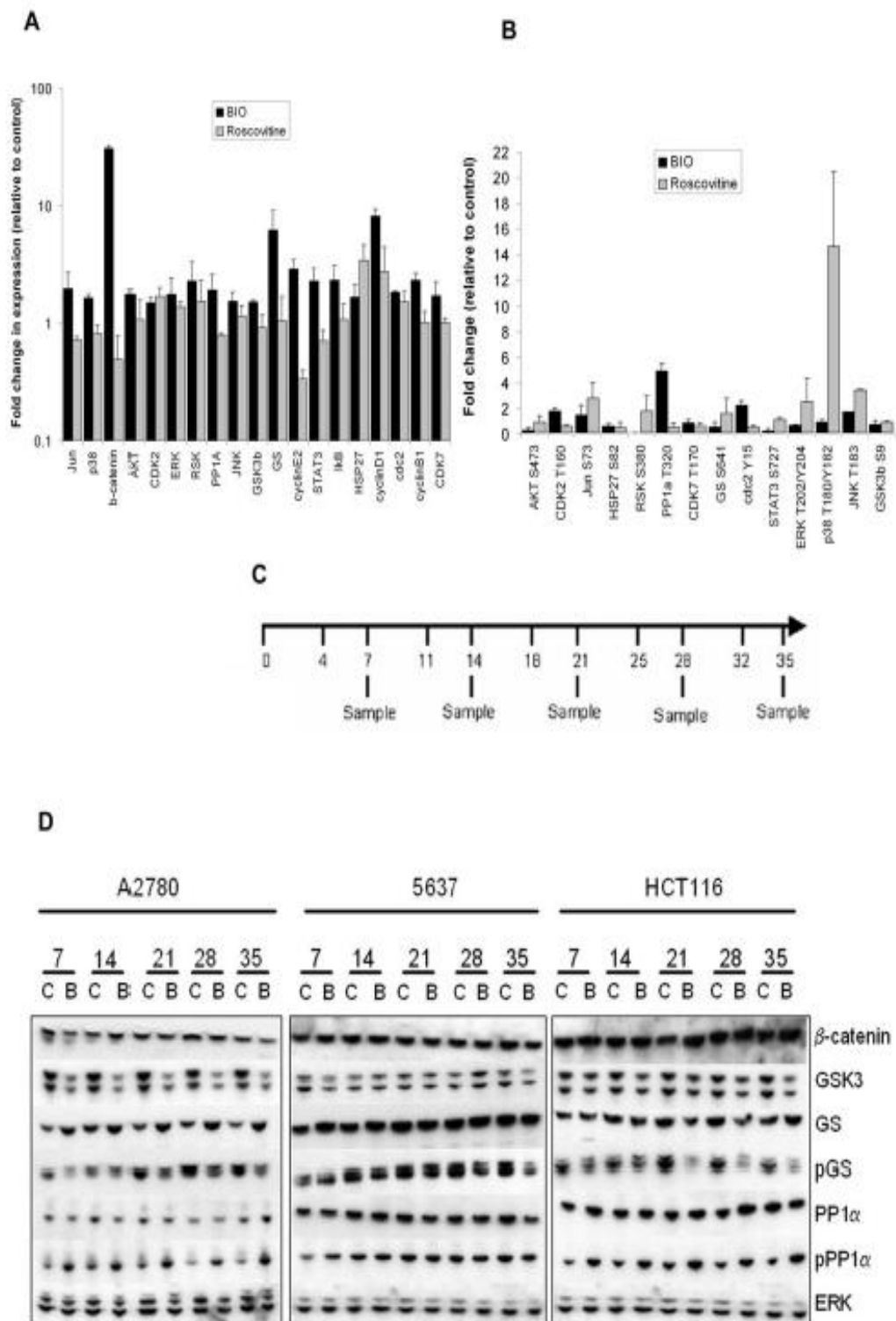


Figure 3. Specificity of BIO. A2780 cells were treated for 16 h with 5 μ M BIO, 10 μ M roscovitine, or DMSO. 1 mg protein samples were analysed by multiplex western blotting to detect (A) expression and (B) phosphorylation of indicated proteins. Band intensity changes were assessed by densitometry relative to DMSO. Phosphospecific bands are normalised with expression. Mean \pm SEM of 2 experiments. (C) BIO schedule in 5 week treatments. Cells were treated twice weekly on days 1 and 4 with DMSO or BIO (A2780, 2.5 μ M; HCT116, 1 μ M; 5637, 500 nM). BIO was not removed between treatments. Counting and harvesting was on treatment day 1 of each week. (D) GSK3 inhibition over 5 week BIO treatment. 20 μ g protein samples from each time point were analysed by western blotting (C, Control; B, BIO). Two independent treatments were analysed. Representative blots are shown.

doi:10.1371/journal.pone.0006459.g003

Prolonged telomerase inhibition is predicted to result in growth plateau by analysis of cumulative population doublings (PD), but this was not observed over five week BIO treatment, though treated cells grew more slowly than controls (Figure 4A). Average growth rates were around 7 PD/week (control) and 6 PD/week (BIO) for 5637 and 8 PD/week (control) and 7 PD/week (BIO) for HCT116. However, A2780 growth rates decreased under BIO treatment. Controls grew steadily at approximately 8.5 PD/week, whereas BIO treated cells had an initial rate of 8 PD/week, slowing to <7 PD by day 35.

RT-QPCR analysis confirmed that BIO suppressed *hTERT* expression in all three cell lines (figure 4B). In A2780, *hTERT* expression under BIO treatment was reduced to 25% of control on day 28. Expression in treated HCT116 was 7% of control on day 28 and in 5637 was 24% of control on day 21. Analysis of *hTERT* splice variants in A2780 cells revealed selective repression of the full length transcript (supporting figure S4). We observed that *hTERT* expression in BIO treated 5637 returned to control levels on day 35. This observation is expanded below.

We next performed QPCR-TRAP analysis using the TRAPeze XL kit to determine telomerase activity in control and treated samples. Cell pellets from each time point were lysed in CHAPS buffer and protein samples incubated with reaction mix containing TS and RP primers in addition to the control K2 primer. Each assay included no-telomerase, no-Taq, and heat-treated controls. QPCR detection of fluorescein labelled RP product confirmed that telomerase activity was reduced by BIO (figure 4C). TRAP activity was reduced in all BIO treated cells by day 7 (A2780, 74% of control; HCT116, 59%; 5637, 67%) and generally diminished over the treatment, reaching 44% of control in A2780 on day 28, then increasing slightly to 57% on day 35. In 5637, TRAP activity rose on days 14 and 21, approaching control activity before recommencing a downward trend to reach 71% by day 35, though this reduction relative to control was not statistically significant. HCT116 TRAP activity decreased continuously to 33% of control levels by day 35.

Telomere lengths were reduced by BIO in all cell lines as determined by telomere restriction fragment (TRF) analysis (figure 4D). Genomic DNA was extracted from control and treated cell pellets and digested with *HinfI/RsaI*. Digestion products were separated by electrophoresis and analysed by Southern blotting using a DIG-labelled telomere sequence probe to determine telomere length range. The decreases were small and were most evident at later time points, consistent with the short treatment period. In HCT116 we also observed reduction of the overall signal in treated samples. Therefore, GSK3 inhibition suppresses *hTERT* expression, telomerase activity and decreases telomere lengths in several cancer cell lines.

Network model of *hTERT* regulation

To characterise the mechanism of *hTERT* repression, we performed microarray expression analysis using cDNA from day 21 control or BIO treated A2780. Three independent treatments were analysed in duplicate. Mean intensity of 1048 differentially expressed transcript IDs changed by >5-fold, $p < 0.01$ between control and treated cells across all repeats. Raw Agilent ID list with fold intensity changes of the differentially expressed genes used for modelling are available in supporting file S2. The full MIAME compliant array data have been deposited for public access in the Gene Expression Omnibus. The profile included multiple transcriptional targets of Wnt signalling, such as *uPAR*, *EphB*, *Rumx2*, *stromelysin*, *Irx3*, *Pitx2*, *Isl1*, *Tcf1*, *LEF1*, *dickkopf-4*, *axin-2*, *Wnt5B* and *Wnt11*, consistent with ongoing inhibition of GSK3 on treatment day 21.

Network modelling was performed on the profile using MetaCore from Genego Inc [20]. 622 unique database objects were recognised (note that several tags may correspond to a single gene). We first identified networks centred on individual high-degree transcription factor neighbours of differentially expressed genes using the transcription-regulation algorithm (supporting figure S5). All 144 unique genes from the ten highest scoring networks were combined in an enriched list and a best-fit transcriptional network was generated using the auto-expand algorithm. Network size was optimised to include all differentially expressed genes from the enriched list (23.2% of all input genes) (supporting figure S6).

The analysis returned a network involving NF κ B, ESR1, STAT1, CREB1, c-Myc, p53 and AP-1 (figure 5A; blue and red circles adjacent to network object icons represent fold intensity change with values given in supporting file S3). Thus, altered activity of these transcription factors may significantly contribute to the observed BIO treatment profile. We therefore determined shortest paths between GSK3 and these high-degree nodes using the analyse-network algorithm (figure 5B). Interestingly, *hTERT* is returned by this analysis as a high probability component of the final network, defining a candidate network linking GSK3 and telomerase. For clarity, only network objects downstream of GSK3 or upstream of *hTERT* are shown. The analysis suggests that multiple transcription factors may participate in regulation of *hTERT* by GSK3, including some or all of Sp1, E2F1, SMAD3, STAT3, HIF-1 α , Androgen Receptor (AR), p53, c-Myc, ESR1, AP-1 and NF κ B. All are reported to regulate *hTERT* or its cloned promoter [5]. GSK3 inhibition may affect their activities both directly and through several effectors.

Network validation

To validate the model, we first performed a multiplex consensus oligonucleotide binding assay using the protein/DNA array I kit from Panomics. 56 biotin-labelled double stranded consensus transcription factor binding site probes were mixed with nuclear extracts of A2780 treated for 16 h with DMSO or 5 μ M BIO. DNA-Protein complexes were bound to spin columns and unbound probe washed off. Bound probes were then eluted and hybridised to an unlabelled membrane array containing spots of each consensus sequence. Hybridisation of labelled probes to the membrane, indicative of binding to the nuclear extract, was detected with streptavidin-HRP. Figure 5C shows densitometry of quantifiable spots showing >1.5-fold intensity change in BIO treated cells.

Signals for c-Myc, and Smad3/4 binding sequences were reduced by 2.1-fold and 1.9-fold, respectively. Increased signal was detected for NF κ B (1.5-fold), p53 (2-fold), Sp1 (3.9-fold) and STAT3 (3.9-fold) consensus sequences. HIF-1 α was not represented on the array and we did not detect altered binding to sequences for ESR1, AR, AP-1, or E2F1. However, longer treatments may also affect these factors. Several other consensus sequences also showed altered binding activity and their cognate transcription factors may also participate in the overall effect of GSK3 inhibition.

To validate the model with respect to *hTERT*, we performed chromatin immunoprecipitation (ChIP) of Sp1, STAT3, p53, c-Myc, and NF κ B p65 in 16 h BIO or DMSO treated A2780. QPCR detection of the *hTERT* promoter in precipitates revealed widespread promoter remodelling, affecting both activators and repressors (Figure 5D). Detectable immunoreactive epitopes of c-Myc, p65 and p53 were reduced 2.9-fold, 4-fold and 2-fold respectively, while that of STAT3 was increased 4.5-fold, confirming that GSK3 inhibition rapidly affects the *hTERT*

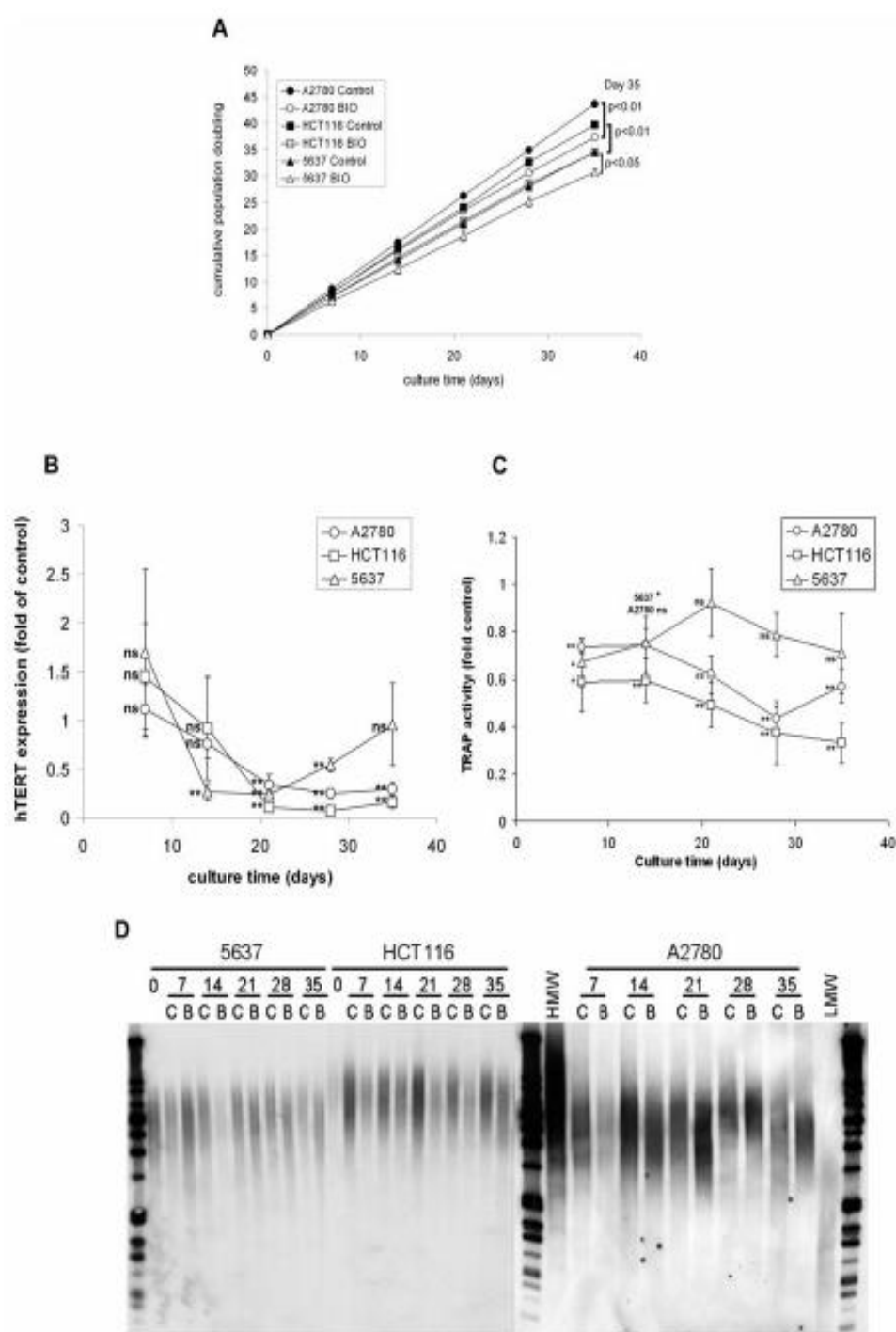


Figure 4. BIO inhibits telomerase. (A) 5 week cell growth curves under BIO treatment. Cells were counted weekly to determine cumulative population doublings (PD). Mean \pm SEM of three experiments. (B) BIO represses *hTERT* expression. Control and treated samples from each time point were analysed by Q-RT-PCR for *hTERT* expression normalised to *RPS15*. Mean \pm SEM of *hTERT* expression in BIO treated cells relative to control from three experiments (ns: not significant; **; $p < 0.01$). (C) BIO represses telomerase activity. Telomerase activity was determined by Q-PCR TRAP analysis in control or BIO treated cells. Mean \pm SEM of treated cells relative to controls from three experiments (ns: not significant; *; $p < 0.05$; **; $p < 0.01$). (D) BIO shortens telomeres. 1 μ g genomic DNA from control or treated cells was digested with *Hinf*/*Rsa*I and southern blotted with DIG-labelled telomere detection probe (C, Control; B, BIO; HMW and LMW, high and low molecular weight markers). Two independent treatments were analysed. Representative blots are shown.
doi:10.1371/journal.pone.006459.g004

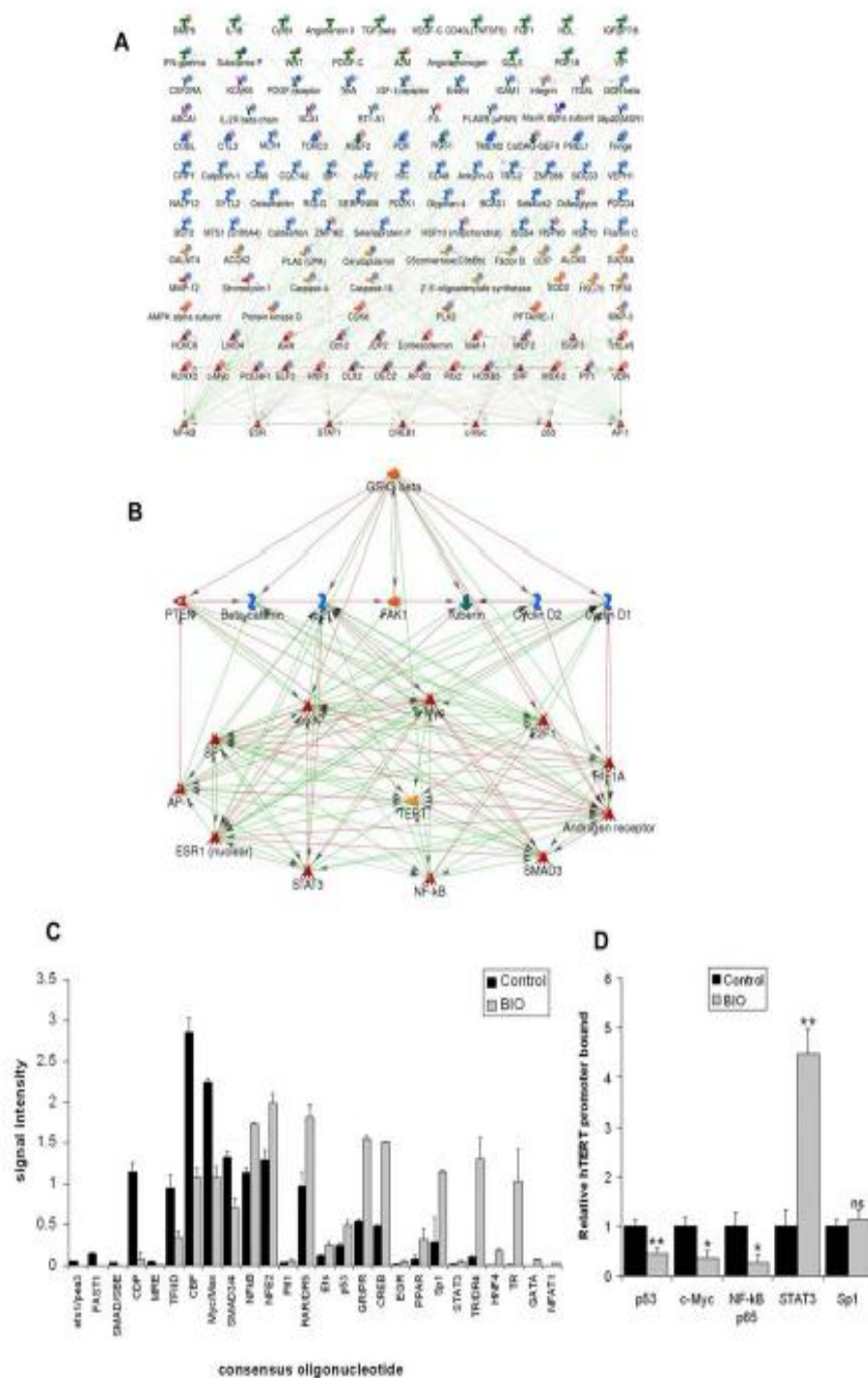


Figure 5. Network modelling and validation. (A) Transcriptional network of GSK3 inhibition. Differentially expressed genes from day 21 BIO treated cells were identified using Agilent whole genome expression arrays ($n = 3$; mean fold change > 5 ; $p < 0.01$). High degree transcription factor neighbours of differentially expressed genes were identified by network analysis in MetaCore. Blue circles: down-regulated in BIO treated cells; red circles: up-regulated. Shading intensity indicates fold change (minimum 5-fold). Green arrows: activation; red: inhibition (reaction mechanisms not shown). (B) Candidate network linking GSK3 to *hTERT*. Shortest paths linking transcription factors from (A) and GSK3 were identified in MetaCore. Green arrows: activation; red: inhibition; reaction mechanisms not shown. (C) Multiplex consensus oligonucleotide binding in A2780 nuclear extracts. 16 h DMSO or BIO treated cell nuclear extracts were incubated with labelled consensus oligonucleotide probe mix prior to column purification and hybridisation of eluted bound probes to oligonucleotide array. Mean \pm SEM of duplicate spots. (D) *hTERT* promoter remodeling. A2780 were treated for 16 h with DMSO or 5 μ M BIO prior to Chromatin IP (ChIP) with antibodies shown and QPCR detection of the *hTERT* promoter. Mean \pm SEM of three experiments (ns: not significant; *: $p < 0.05$; **: $p < 0.01$). doi:10.1371/journal.pone.0066459.g005

promoter environment involving direct regulation by at least four factors suggested by network analysis. Sp1 binding to the *hTERT* promoter was unaffected by 16 h BIO treatment. Interestingly, *hTERT* expression in 16 h BIO treated A2780 was not significantly repressed and was even slightly increased, suggesting that promoter remodelling may proceed dynamically in longer treatments (supporting figure S7).

BIO inhibits *hTERT* expression and tumour growth in xenografts

To determine whether GSK3 inhibition suppresses *hTERT* expression in a tumour model, we inoculated A2780 into athymic mice. BIO (2 mg/kg every second day or 6 mg/kg twice weekly) or vehicle treatment was initiated via the intraperitoneal route when mean tumour diameters reached ~0.5 cm. Tumours in control animals took 7.8 days to increase five-fold in volume, whereas the time taken was 13.1 days in the 2 mg/kg BIO group and 16.9 days in the 6 mg/kg BIO group (figure 6A). No overt toxicity was observed in treated groups. Therefore, BIO suppressed growth of established A2780 xenografts.

Animals were sacrificed after 3 weeks treatment at 2 mg/kg or 4 weeks treatment at 6 mg/kg. Tumours were harvested for QPCR analysis of *hTERT* expression (figure 6B). Median *hTERT* expression of the control group is fixed at 100% (range 71.82%–138.74%). BIO treatment suppressed *hTERT* expression to similar levels in both treatment groups. Median expression in the 2 mg/kg group was 58.62% that of the control group (range 39.85%–95.55%) and 55.01% in the 6 mg/kg group (40.5%–95.33%). The relative decrease in each treated group was statistically significant as determined by the Mann-Whitney test ($p = 0.026$). Therefore, GSK3 inhibition suppresses *hTERT* expression in established A2780 xenografts.

Dynamic regulation of *hTERT* expression

To determine whether persistent inhibition of GSK3 results in telomere dependent growth arrest in cancer cells, A2780 were cultured in the presence of DMSO or 2.5 μ M BIO for 25 weeks with twice weekly dosing as in the schedule in figure 3. Cells were counted weekly and analysis samples taken every four weeks. We again examined markers of GSK3 inhibition by western blotting (figure 6C). Because of decreasing growth rates, insufficient protein was obtained in day 28 BIO treated cells. However, in earlier experiments GSK3 was inhibited at this time point (figure 3D). As previously observed, GS phosphorylation was suppressed, its expression was increased and PP1 α phosphorylation was also elevated until day 140. However, on day 168, little differential was observed between control and treated cells for GS expression or PP1 α phosphorylation.

To extend this observation we assessed levels of cyclin E2 which increased after a single BIO dose (figure 3A). Cyclin E2 was increased in treated cells on days 56, 84 and 140, but not days 112 or 168. Thus, cyclin E2 apparently oscillated in treated cells. In contrast, GSK3 expression was reduced in treated cells at all time points as in the earlier time course. Therefore, persistent exposure to BIO had differential dynamic effects on downstream pathways.

To determine whether *hTERT* expression was suppressed throughout the time course, we performed RT-QPCR (figure 6D). Consistent with previous results, *hTERT* expression was strongly repressed on day 28 in BIO treated cells (29% of control). However, at subsequent time points until day 112, *hTERT* suppression was less efficient. On day 112, coinciding with the first loss of cyclin E2 induction, *hTERT* expression in treated cells was not significantly different from controls, as observed for 5637 cells on treatment day 35. Thereafter, expression decreased

to a new low value on day 140 (10% of control) and remained at 12% of control on day 168. Thus, *hTERT* also appeared to oscillate in treated cells.

TRF analysis showed that a substantial lag phase preceded profound telomere shortening between days 112 and 140 in treated A2780. Densitometric estimates of average length on day 140 were ~2 kb in treated cells, compared with ~5 kb in control cells (Figure 6E). Therefore, persistent GSK3 inhibition significantly reduced telomere length of ovarian cancer cells. However, the blots also suggested that some extension occurred at days 112 and 168, which may be explained by the oscillation in *hTERT* expression and/or other effects on telomerase mediated by dynamic regulation of GSK3 effectors.

In these experiments, A2780 proliferation rapidly declined in the first weeks of treatment, though full culture crisis was not observed. While control cells grew steadily over the entire time course at ~8.6 PD/week, growth of BIO treated cells decreased from 8.2 PD/week at day 7 to 3.5 PD/week at day 35, causing a partial growth plateau (figure 6F). Treated cells then grew at 3.5 PD/week until day 56, at which time growth accelerated, reaching a rate of ~7 PD/week at day 126 which persisted for the rest of the time course.

Network topology and dynamic behaviour

Although network modelling can successfully identify many of the players in a pathway, predicting the outcome of manipulating individual highly connected components of complex networks such as figure 5B is a challenge. However, genetic networks are mainly composed of recurring “wiring patterns” (network motifs) which can be modelled or even synthetically constructed to investigate relationships between motif topology and function [21]. Thus, identification of a network’s constituent motifs may help to predict its behaviour. To better understand *hTERT* regulation by GSK3, we searched for several previously described motif types in the network model using MetaCore [21–23].

We identified multiple potential reciprocal repression (toggle switch) and feedback oscillator motifs as in the examples in figure 7A, which may provide substantial scope for dynamic network behaviour. We also identified several types of coherent feed forward motifs. In particular, three distinct sub-networks form candidate activation and repression “modules”. The activation module links all positive regulators of *hTERT* via densely overlapping coherent type 1 motifs, while the repression module comprises several coherent type 2 motifs organised by p53 and AR which inhibit *hTERT* and its activators. Both motif types are reported to reduce noise in gene expression networks [21].

To further investigate the network structure, we determined the presence of the *MYC*, *RELA*, and *ESR1* gene promoters in the p53 ChIP experiments from figure 5D in which p53 binding to the *hTERT* promoter was decreased. We found that 16 h BIO treatment also reduced immunoreactive p53 at the *MYC* promoter by 2.2-fold, by 3.6-fold at *RELA* and 5-fold at *ESR1* (Figure 7B). Therefore, the early outcome of BIO treatment with respect to p53 includes co-ordinate regulation of the *hTERT* promoter and the promoters of at least three of its activators also present in the putative repression module sub-network.

Based on the proposed network topology, we hypothesised that prolonged GSK3 inhibition might affect dynamic behaviour of some transcription factors. Re-analysis of the 25 week time course revealed complex, fluctuating expression patterns for c-Jun, p53, c-Myc, AR and STAT3 expression, but not Sp1 or p65 in BIO treated samples (figures 7C and D). AR, STAT3 and c-Jun each showed a clear oscillation, particularly striking in the case of c-Jun, with a trough occurring on day 112 for AR and STAT3 and on

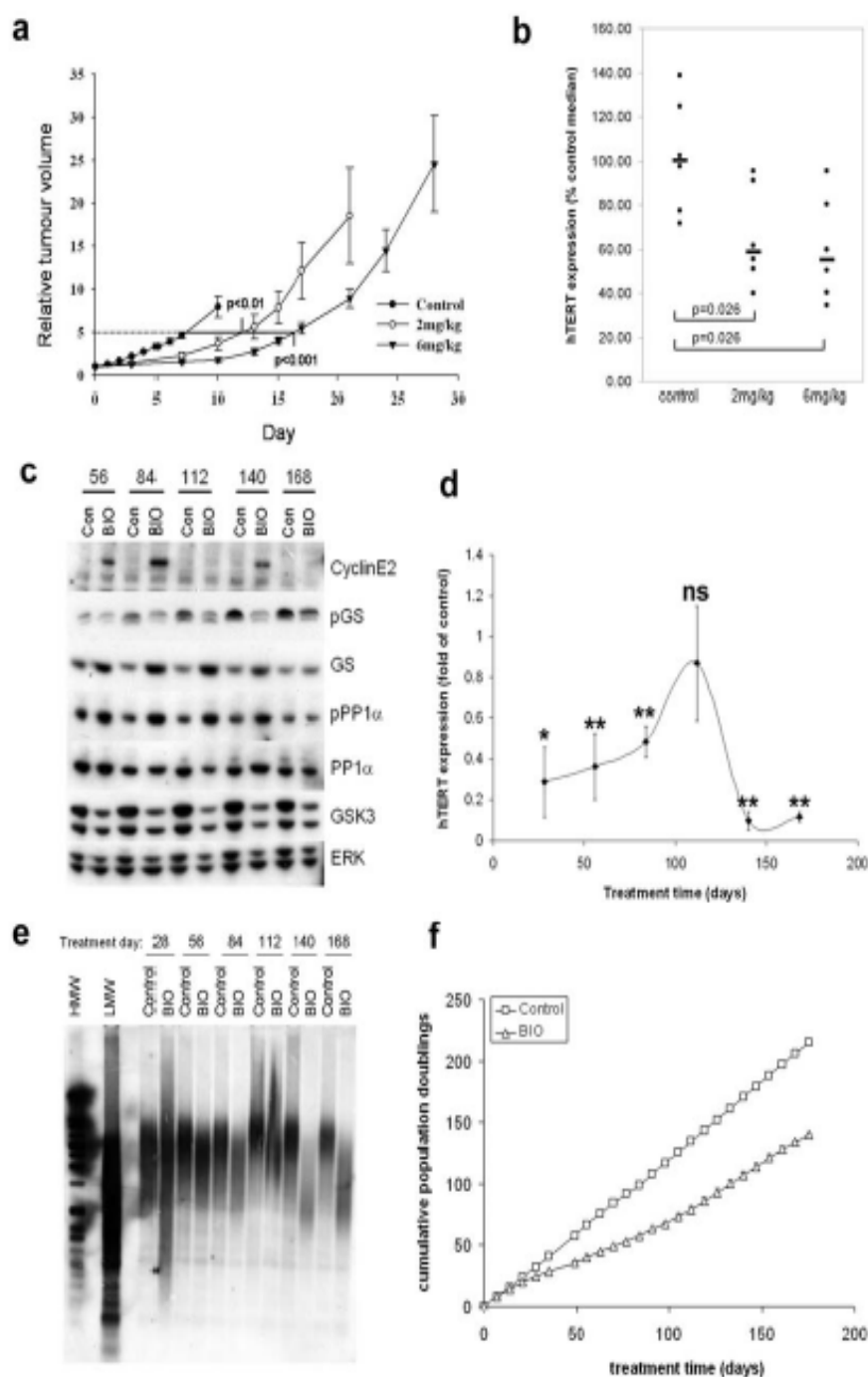


Figure 6. Therapeutic assessment of GSK inhibition. (A) Growth delay of A2780 xenografts. Athymic mice ($n = 6/\text{group}$) with established A2780 xenografts were treated intraperitoneally with BIO (2 mg/kg every two days, or 6 mg/kg twice weekly on days 1 and 4). Mean \pm SEM of calliper estimated tumour volumes relative to treatment day 0. (B) *hTERT* expression in A2780 xenografts. Tumours from vehicle or treated animals were excised and Q-RT-PCR was performed. *hTERT* expression normalised to *RPS15* in each tumour is shown. Bars show median expression (control = 100%). (C) GSK3 inhibition during prolonged BIO treatment. A2780 cells were treated twice weekly on days 1 and 4 with 2.5 μM BIO or DMSO for 25 weeks. Analysis samples were taken every 4 weeks on treatment day 1. 20 μg protein samples were analysed by western blotting. Two experiments were analysed. Representative blots are shown. (D) Dynamic oscillation of *hTERT* expression. Control and treated samples from each time point were analysed by Q-RT-PCR for *hTERT* expression normalised to *RPS15*. Mean \pm SEM of *hTERT* expression relative to control from two experiments (ns: not significant; *; $p < 0.5$; **; $p < 0.01$). (E) Prolonged BIO treatment shortens telomeres. 1 μg genomic DNA from control or treated cells was digested with *HinfI*/*RsaI* and southern blotted with DIG-labelled telomere sequence probe. Two independent treatments were assessed. Representative blots are shown. (F) Growth of A2780 cells during prolonged BIO treatment. Cells were counted weekly to determine cumulative population doublings (PD). Mean \pm SEM of two experiments.

doi:10.1371/journal.pone.0006459.g006

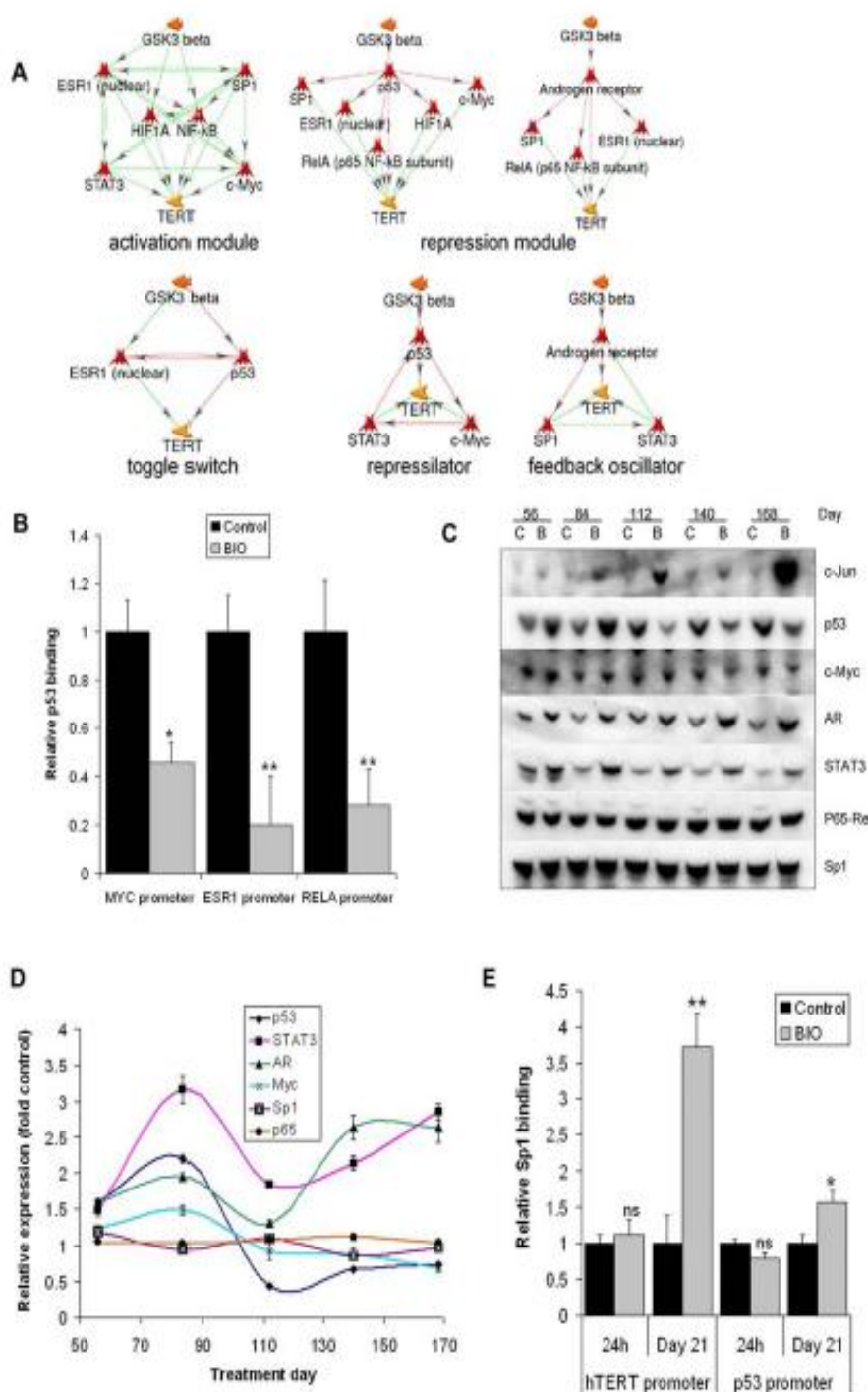


Figure 7. Network topology and dynamic behaviour. (A) Network motif analysis. Motifs in figure 5(B) were identified in MetaCore. Representative examples are shown. Green arrows: positive regulation; red arrows: negative regulation (reaction mechanisms not shown). (B) BIO regulates the repression module. A2780 were treated for 16 h with DMSO or 5 μ M BIO prior to ChIP with p53 antibody and QPCR detection of indicated promoters. Mean \pm SEM of three experiments (*: $p < 0.05$; **: $p < 0.01$). (C) Dynamic regulation of network transcription factor expression levels under long term BIO treatment. Expression of network transcription factors in 20 μ g protein samples from each time point of the 25 week time course were analysed by western blotting (C, Control; B, BIO treatment). Two independent treatments were analysed. Representative blots are shown. (D) Densitometry of (C): expression relative to control (c-Jun not shown due to scale). Mean \pm SEM of three measurements of each band. (E) Dynamic regulation of *hTERT* and *TP53* promoters by Sp1. A2780 were treated for 16 h with 5 μ M BIO or 21 days with 2.5 μ M prior to ChIP with Sp1 antibody and QPCR detection of the *hTERT* and *TP53* promoters. Mean \pm SEM of three experiments (ns: not significant; *: $p < 0.5$; **: $p < 0.01$). doi:10.1371/journal.pone.0006459.g007

day 140 for c-Jun. Levels of p53 were induced by BIO on days 56 and 84 but were lower than control at all other times. A similar, though less pronounced result was observed for c-Myc. Therefore, at least 5 transcription factors known to affect *hTERT* are subject to dynamic regulation under persistent GSK3 inhibition.

Since Sp1 levels were unaffected, we assessed whether its activity might be dynamically affected under prolonged GSK3 inhibition by ChIP in A2780 after 21 day 2.5 μ M BIO treatments. Recovery of both *hTERT* and *TP53* promoters were analysed and compared with recovery after 16 h treatments. In contrast with the results after 16 h, immunoreactive Sp1 levels at the *hTERT* promoter were increased by 3.7-fold after 21 days treatment. Furthermore, Sp1 epitope at the *TP53* promoter was also increased by 1.6-fold at day 21. These data confirm that Sp1 is also dynamically regulated and participates in ongoing remodelling of both *hTERT* and *TP53* promoters under persistent GSK3 inhibition.

Whole kinome siRNA screen of the *hTERT* promoter

Finally, to enable rational prediction of *hTERT* regulatory pathways overlapping with GSK3, we performed a whole kinome siRNA screen using the *hTERT* reporter in A2780. 3 independent siRNA against each of 719 kinase and kinase-related genes were assessed. Hit criterion was >2-fold change in promoter activity by at least 2/3 siRNA. A complex network of kinases controls activity of the transfected *hTERT* promoter, with 235/719 target genes in total scoring as hits. 232 were activators of the promoter (repression by siRNA) and only 3 were repressors.

We searched MetaCore for direct phosphorylation interactions between hits and network transcription factors (figure 8A; blue circles represent mean fold promoter repression with *hTERT* promoter activity values for each network target given in figure 8B). At least 54 hit kinases participate in upstream pathways and 38 hits directly phosphorylate one or more of the transcription factors. Critical divergence hubs with respect to the network transcription factors are GSK3 itself, p90-RSK, several PKC isoforms, PKA, JNK and p38. These hubs are predicted to be important modifiers of *hTERT* suppression with GSK3 inhibitors and preferred targets for combinatorial inhibition.

Discussion

In this study we show that GSK3 activates *hTERT* gene expression and regulates telomere length homeostasis. We identified GSK3 as a potential pharmacological target to inhibit *hTERT* expression in a promoter screen of well defined kinase inhibitors. The result was confirmed using independent selective inhibitors of different chemotypes. BIO, GSK3 β -specific siRNA, and genetic agonists of Wnt signalling all suppressed *hTERT* promoter activity in five cancer cell lines. Interestingly, over-expression of β -catenin increased promoter activity, suggesting a possible dual effect of Wnts on the *hTERT* promoter mediated by both canonical and non-canonical pathways. Regulation of endogenous *hTERT* by Wnts was not assessed in this study, though Wnt5A was previously shown to suppress telomerase in renal carcinoma cells [24]. Telomerase suppression by GSK3 inhibitors may partly involve Wnt pathways, but presumably also involves other GSK3 activities.

Multiplex phospho-specific western analysis in BIO treated A2780 revealed a complex functional signature involving altered expression of β -catenin, cyclins D1, B1 and E2, GS, as well as p90-RSK, STAT3 and I κ B. Additionally, altered phosphorylation of AKT, p90-RSK, PP1 α , cdc2 and STAT3 were observed. Observation of several markers over five weeks continuous treatment confirmed that GSK3 could be inhibited over prolonged periods.

Most importantly, BIO suppressed *hTERT* expression and telomerase activity with resultant telomere shortening over five weeks treatment in three cancer cell lines, indicating that a promoter screening approach can identify *bona fide* telomerase inhibitors. Microarray and network analysis of GSK3 inhibited A2780 suggested that the activities of multiple transcription factors could be altered. We defined a candidate network linking GSK3 and *hTERT* via some or all of Sp1, E2F1, STAT3, SMAD3, ESR1, AR, HIF-1 α , NF κ B, AP-1, p53 and c-Myc.

In support of the network model, 16 h BIO treatment altered binding affinity of A2780 nuclear extracts to multiple consensus oligonucleotides, including sites for c-Myc, NF κ B, SMAD3, p53, Sp1 and STAT3. Critically, ChIP analysis indicated that immunoreactive c-Myc, p53 and NF κ B p65 were reduced at the endogenous *hTERT* promoter by 16 h BIO treatment while STAT3 was increased. It should be noted that ChIP results may reflect changes either in DNA binding or in epitope masking. In either case, GSK3 inhibition causes rapid and widespread remodelling of the *hTERT* promoter involving at least these factors and possibly others suggested by the network and oligo binding analyses. Both activators and repressors of *hTERT* were affected, underscoring the difficulty of interpreting the transcriptional effect in terms of single factors.

GSK3 regulates several transcription factors directly and effectors PTEN, β -catenin, p21, FAK1, Tuberin, cyclin D1 and cyclin D2 may also play a role. We have not directly addressed their roles in this study, though FAK1 siRNA suppressed the *hTERT* promoter in A2780 and β -catenin over-expression up-regulated the promoter in several cell lines. Furthermore, BIO increased expression of β -catenin and cyclin D1 in A2780 cells and reduced AKT phosphorylation which may occur downstream of PTEN [25]. Previous studies have shown regulation of *hTERT* and/or telomerase in various experimental settings by several of these factors [26,27].

Consequently, GSK3 may control *hTERT* expression in a broad range of cells, including those with mutation or disruption in one or more branches of the network as in 5637 (mutant p53) or HCT116 (mutant β -catenin). Thus, GSK3 could be an attractive pharmacological target for broad spectrum suppression of telomerase in cancer cells. In support of a therapeutic application, BIO caused tumour growth delay and inhibited endogenous *hTERT* expression in established A2780 xenografts without overt toxicity. Unexpectedly, however, prolonged inhibition of GSK3 in cultured A2780 did not lead to stable *hTERT* suppression, although telomere lengths were profoundly reduced. Rather, dynamic oscillation of *hTERT* was observed.

Complex inter-transcription factor interactions are expected from the model. Upstream of *hTERT* are multiple densely overlapping coherent type 1 feed-forward motifs mainly organised by ESR1 and Sp1 (activation module). A series of coherent type 2 motifs emanates from AR and p53 (repression module). Both motif architectures may reduce the impact of transient noise in genetic networks and may therefore govern stable activation or repression of *hTERT* [21]. Although direct validation of individual motifs is beyond the scope of this study, BIO reduced p53 binding at *hTERT*, *MYC*, *RELA*, and *ESR1* promoters in ChIP experiments, suggesting coordinated functional regulation of transcriptional interactions consistent with the proposed topology of the repression module. The network also contains multiple potential switch and feedback oscillator motifs, suggesting there is substantial scope for dynamic network behaviour [21–23].

Indeed, several network components, including p53 and NF κ B are known to exhibit dynamic oscillations under certain conditions [28,29]. Inter-transcription factor interactions may provide

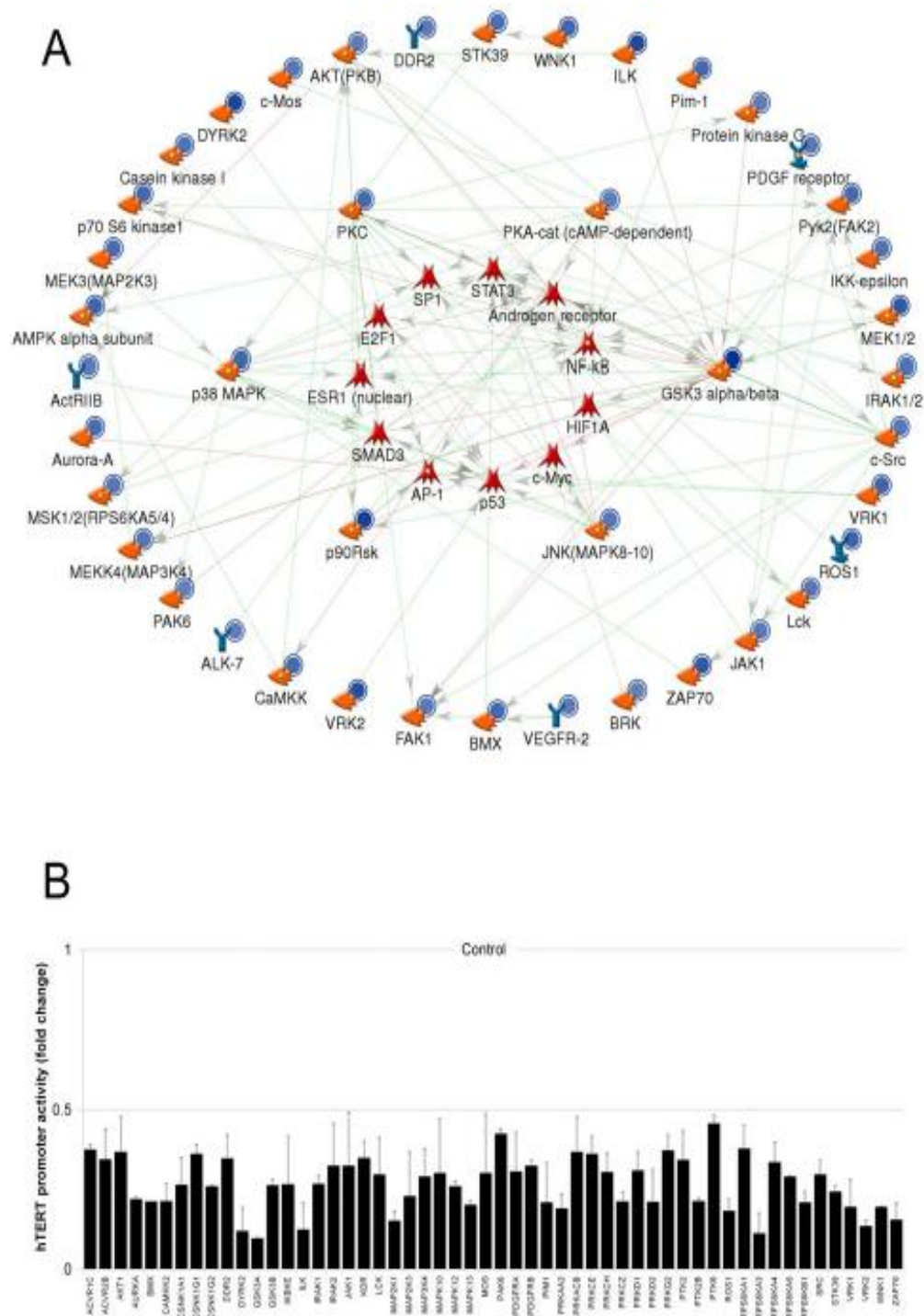


Figure 8. Whole-kinome RNAi screen of the *hTERT* promoter in A2780. (A) *hTERT*-luciferase was cotransfected with 50 nM siRNA in triplicate. 48 h post-transfection, luciferase assays were performed. 3 independent siRNA per target were assessed. Hit criterion was >2-fold change in promoter activity by at least 2/3 siRNA. 235 hit IDs were analysed in MetaCore using the "direct interactions" algorithm limited to phosphorylation interactions. Green arrows: positive regulation; red: negative regulation. Blue circles: siRNA repressed the *hTERT* promoter. Circle shading intensity indicates fold change (minimum 2-fold). Average derived from all independent hit siRNA is shown. (B) Relative repression of the *hTERT* promoter by siRNA against targets in the network model. Luciferase activities were calculated relative to control (non-specific) for each siRNA. Figure shows mean \pm SEM derived from all independent hit siRNA for each target. doi:10.1371/journal.pone.0006459.g008

another mechanism for dynamic behaviour. Notably, GSK3 directly controls stability of several transcription factors [30]. An interesting possibility is that GSK3 exerts a “compressor” effect which fine-tunes the overall network steady state. Consistent with this interpretation, expression of several transcription factors varied dynamically over long term GSK3 inhibition.

Currently, the frequency of these fluctuations is unknown and may even involve stochastic events. Therefore, other apparently unaffected factors may also be regulated at different time points, or their activities may be subject to dynamic changes independently of expression, as would appear to be the case with Sp1. Overnight BIO treatment had no effect on Sp1 levels at the *hTERT* promoter and its expression was unaffected in the time course. However, 3 week treatments did increase Sp1 epitope at both the *hTERT* and *TP53* promoters, confirming that it participates in dynamic regulation of *hTERT* and other network components.

Knowledge of other druggable target pathways affecting the network may provide strategies to complement and/or stabilise telomerase inhibition. To discover other candidate kinase targets potentially affecting *hTERT*, we performed a whole kinome siRNA screen using the *hTERT* reporter, revealing 235 kinase genes that regulate promoter activity in A2780, of which at least 54 phosphorylate components of the network model. Key hubs were GSK3 itself, p90-RSK, several PKC isoforms, PKA, and the JNK and p38 MAP kinases. Future studies will determine their functional involvement in regulation of telomerase by GSK3.

In summary, our results suggest computational and screening approaches combined with appropriate focused validation efforts may lead to a more nuanced understanding of telomerase gene regulation. Our data lend support to the emerging prospect of GSK3 inhibitor therapy of cancer, both from the standpoint of telomerase inhibition and because of the rapid xenograft growth reduction effect observed which may also involve additional effects of GSK3 inhibition [31]. However, prolonged GSK3 inhibition has complex network effects, at least in cancer cells. Therefore, combinatorial regimens may be most appropriate. This finding may also have implications for the use of single agent GSK3 inhibitors in the settings of bipolar disorder, Alzheimer’s disease and diabetes in which long term treatment schedules are also required. We have identified several markers of dynamic network behaviour. Their examination in suitable model systems for these disorders may also be advisable. Finally, GSK3 inhibition has been proposed as a method to expand stem and progenitor cell pools. Protocols involving telomerase positive progenitors should also address telomere status.

Materials and Methods

Cell lines, plasmids, siRNA and inhibitors

Cells used were: 5637 bladder carcinoma, C33A cervical carcinoma, A549 lung adenocarcinoma, and HCT116 colon carcinoma cells, obtained from ATCC, and A2780 ovarian adenocarcinoma cells, originally obtained from Dr RF Ozols [32]. Reporter pGL3-*hTERT* contains the *hTERT* promoter region -585/-9, relative to the translational start site. Plasmids pCMV-mWnt3 and pCMV-mWnt5a were kindly provided by Dr. Mejlinda Lako (Institute for Ageing and Health, Newcastle University, UK). Human DVL2 and β -catenin expression vectors were obtained from Origene (Rockville, MD). The whole kinome siRNA library, non-specific siRNA and GSK3 β -specific siRNA (siRNA 42839: sense sequence 5'-GGACAAGAGAUUUAA-GAAUtt; siRNA 203: sense sequence 5'-GGUGACAACAGUG-GUGGCAtt) were obtained from Applied Biosystems (Warrington, UK). The kinase inhibitor library was obtained from Biomol

International Ltd (UK). BIO, AR-A014418, TWS119, Roscovitine, and 1-MeBIO were obtained from EMD Biosciences (Nottingham, UK).

Transfections and luciferase assay

All transfections were performed in quadruplicate using lipofectamine according to the manufacturer’s instructions using a 2:1 ratio reagent:DNA (Invitrogen, Paisley, UK). Under these conditions, transfection efficiencies were found by pSV40- β Gal assay to be: HCT116, 51%; A549, 39%; A2780, 27%; 5637, 29%; C33A, 28%. 250 ng *hTERT* reporter plasmid per well was transfected in 96-well luminometer plates (Fisher Scientific UK, Leicestershire, UK). 32 h post-transfection cells were exposed to inhibitors for 16 h. In cotransfections, 250 ng expression vectors or 50 nM siRNAs were included. 30 ng pSV40-Renilla luciferase expression plasmid (Promega Ltd, Madison, WI) was included in each well for normalisation. 48 h post-transfection, luciferase activities were determined using dual luciferase assay reagents according to the manufacturer’s instructions (Promega Ltd, Madison, WI). All experiments were repeated at least 3 times.

MTT assay

Cells were seeded in quadruplicate wells and triplicate 96-well plates 2 days prior to addition of inhibitor titrations. Cells were exposed to inhibitors for 16 h then incubated for an additional 3–4 days prior to MTT assay (MTT supplied by Sigma (Dorset, UK)). MTT reduction assays were performed using Softmax Pro 4.6 software (Molecular Devices Ltd, Wokingham, UK). All experiments were repeated at least 3 times.

Western blotting

Protein extracts were prepared in passive lysis buffer (Promega Ltd, Madison, WI). Protein concentrations were estimated at OD595 using the BioRad protein assay (BioRad Laboratories Ltd, Hemel Hempstead, UK). 20 μ g protein for singleplex experiments, or 1 mg protein for multiplex analysis, were separated by SDS-PAGE, blotted onto PVDF filter (Millipore, Watford, UK) and blocked overnight in PBS-T containing 5% non-fat dried milk. All antibodies are listed in supporting file S1. For multiplex analysis, membrane was separated into lanes using Immunetics’ miniblotter 20 dual apparatus (Web Scientific, UK). Primary antibodies were detected with HRP-conjugated secondary. HRP was detected using ECL HRP detection reagents (Amersham Pharmacia, Buckinghamshire, U.K.). All experiments were performed at least twice.

ChIP assays

DMSO or BIO treated cells were harvested at 70%–80% confluence. ChIP assays were performed following instructions of the kit supplier (Millipore, Watford, UK). Cell layers were fixed in formaldehyde and lysed in SDS buffer with protease inhibitors. Chromatin fragments of 500 bp–1 kb were generated by sonication using a Branson S250D sonifier (Branson Ultrasonics Corp., Danbury, CT). All antibodies are listed in supporting file S1. Each assay included a no antibody control. Each promoter was detected by Q-PCR in triplicate using Genefic Research Instrumentation Option monitor equipment and software (Essex, UK) and sybrgreen fluorophore. Promoter-specific primers used were *hTERT*, 5'-CATTCGTGGTGCCCGGAGC and 5'-GCC-CAGCGGAGAGAGGTCG or 5'-GCGACCTGTAACTCTA-AGTATT and 5'-GGGTTGCTCAAGTTTGGATCTAA for p53 binding analysis; *TP53*, 5'-GCACCAGGTCGGCAGGAATCTG and 5'-CGTGGAAAGCAGCTCCAGCC; *ESR1*, 5'-CCAA-TGTCAGGGCAAGGCAA and 5'-GGAGCCTGCGGGTCC-

GGTGAA; *RELA*, 5'-AGTTCAACCACCGGCCTCT and 5'-GAGGGTGGGTCGCGGATTA; *MYC*, 5'-GCTGCCCGGCTGAGTCTGCTCC and 5'-CCTCCACCTTCGCCACGCTC. Optical read temperatures were optimised to exclude primer dimers. All ChIP experiments were performed at least 3 times. Q-PCR was repeated twice for each experiment.

TRAP assay

The TRAPeze XL kit was used for TRAP assay according to the manufacturer's instructions (Millipore, Watford, UK). Cell pellets were lysed in CHAPS lysis buffer and protein concentrations estimated by Bio-Rad assay (BioRad Laboratories Ltd, Hemel Hempstead, UK). 0.5 µg protein was mixed with TRAPeze reaction mix containing TS primer, fluorescein labelled RP primer, control template and sulforhodamine labelled control K2 primer. Each assay included no-telomerase, no-Taq, and heat-treated controls. Extension products were generated at 30°C followed by Q-PCR detection in triplicate using Chromo4 equipment and software (BioRad Laboratories Ltd, Hemel Hempstead, UK). Total product generated was measured against TRB standards and normalised to the ROX internal control. All experiments were performed three times and the TRAP assay was repeated twice for each experiment.

TRF analysis

Telomere length assays were performed using the teloTAGGG kit according to the manufacturer's instructions (Roche Diagnostics Ltd, West Sussex, UK). 1 µg genomic DNA from cell pellets was digested with *HinfI/RsaI*. Digestion products were separated by gel electrophoresis alongside DIG-labelled molecular weight markers and blotted onto positively charged nylon membrane (Roche Diagnostics Ltd, West Sussex, UK). Membranes were UV cross-linked, baked at 120°C and washed in 2×SSC solution. Hybridisation of the DIG-labelled telomeric probe was performed using buffers and probe provided. Finally, membranes were washed, probed with alkaline phosphatase conjugated anti-DIG and exposed to the CDP-star substrate. All experiments were performed at least twice.

Quantitative RT PCR

Q-PCR was performed in triplicate using Genetic Research Instrumentation (Essex, UK) Opticon monitor equipment and software. Sybr green was used as fluorophore. The primers used were *RPS15*, 5'-TTCCGCAAGTTACCTACC and 5'-CGGGCCGGCCATGCTTTACG; *ATERT* 5'-CTGCTGCGCACGTGGGAAGC and 5'-GGACACCTGGCGGAAGGAG. Optical read temperatures were optimised to exclude primer dimers. All treatments were repeated three times and Q-PCR was performed twice for each assay. Splice variant PCR was performed with primers 5'-GCCTGAGCTGTACTTTGTCAA and 5'-GCCAAACAGCTTGTTCCTCATGTC and analysed using an Agilent Bioanalyser 2100 and DNA-1000 assay chips (Agilent Technologies, Santa Clara, CA).

Microarray processing

RNA from 3 independent treatments was labelled and amplified using the two-colour microarray gene expression analysis protocol (Agilent Technologies, Santa Clara, CA). Control cell RNA was labelled with cyanine 3-CTP and BIO treated cell RNA labelled with cyanine 5-CTP. 750 ng of cy-3 and cy-5 labelled, amplified cRNA were mixed and hybridised in duplicate to 44 k Agilent whole human genome microarrays, according to the manufacturer's instructions and incubated for 17 hrs at 60°C in a rotating hybridisation oven. Arrays were washed on a magnetic stirrer

using Agilent wash buffers. Slides were scanned on an Agilent DNA microarray scanner at 5 µm resolution, PMT at 100% and 10%. The extended dynamic range setting corrected for saturation.

Microarray data analysis

Microarray data was processed in line with the Microarray Gene Expression Data Society (<http://www.mged.org/>) to standardize the presentation of microarray data. MIAME compliant data have been deposited for public access in the Gene Expression Omnibus (GEO) at <http://www.ncbi.nlm.nih.gov/geo/> with the accession number GSE14532. Data was extracted using Agilent Feature Extraction software version 8.1 (Agilent Technologies). Background-subtracted data for separated red and green channels was imported into GeneSpring GX 7.3.1 (Agilent Technologies, Santa Clara, CA) for normalisation and statistical analysis. Intra-array normalisation was carried out using the 50th percentile for each microarray. Significant differences in expression between DMSO control and BIO treated cells were determined using Welch analysis of variance (ANOVA) assuming normality, but not equal variances and Benjamini and Hochberg false discovery rate multiple testing correction of 5%. IDs with >5-fold intensity change, $p < 0.01$ were selected for further analysis.

MetaCore network analysis

Differentially expressed genes from supporting file S2 were analysed using the "transcription regulation" algorithm in MetaCore from GeneGo Inc. (filters: positive and negative interaction types; all mechanisms). All genes from the 10 most significant returned networks were merged to an enriched list and analysed using the "auto expand" algorithm (filters: positive and negative interaction types; all mechanisms). A best fit transcriptional network was identified by varying the network size. Edges linking high-degree transcription factors with GSK3 were identified using the "analyse network" algorithm (filters: positive and negative interaction types, all mechanisms). For kinome-wide RNAi analysis, edges linking hits with high-degree transcription factors from the candidate pathway were identified using the "direct interactions" algorithm (filters: positive and negative phosphorylation interaction types only, kinase and transcription factor object-types only). Algorithms are described in [20]. All interactions in MetaCore are manually compiled from full text articles. All references are available on request.

Multiplex oligonucleotide binding assay

Consensus oligonucleotide binding assay was performed using the protein/DNA array I kit from Panomics (Freemont, CA) according to the manufacturer's instructions. 10 µg nuclear extracts prepared with Panomics nuclear extraction kit were incubated with biotin labelled consensus oligonucleotide probe mix. Bound probes were isolated on spin columns, denatured and hybridised to nylon membrane containing a consensus transcription factor binding sequence array. Membranes were washed in hybridisation wash I and wash II then blocked using blocking buffer supplied. Finally, membranes were incubated with streptavidin-HRP, washed, and labelled probes were detected with chemiluminescent detection reagents supplied.

Xenograft experiments

Animal studies were carried out under an appropriate United Kingdom Home Office Project Licence and all work conformed to UKCCCR Guidelines for welfare of animals in experimental neoplasia. 10⁷ A2780 cells in PBS were injected subcutaneously

into the right flank of CD1 *nu/nu* mice (Charles River). After 7 to 10 days when mean tumour diameter was ~0.5 cm (day 0), animals were randomized in groups of 6. A stock solution of 2 mg/ml BIO was prepared and diluted into PBS immediately before injection. Mice were treated intraperitoneally with BIO at a dose of 2 mg/kg on alternate days or at a dose of 6 mg/kg twice weekly on days 1 and 4. Tumour volumes were estimated by calliper measurements assuming spherical geometry (volume = $d^3 \times \pi/6$).

Densitometry

Densitometry was performed on telomere length experiments, western blots and multiplex oligonucleotide binding experiments using a BioRad GS-800 densitometer (BioRad Laboratories Ltd, Hemel Hempstead, UK) and Quantity One software.

Statistical analysis

Statistical analysis of all experiments was performed by one way ANOVA except *hTERT* expression in xenografts, which was analysed by Mann-Whitney U test.

Supporting Information

Figure S1 Chemical structures of GSK3 inhibitors reported in the study.
Found at: doi:10.1371/journal.pone.0006459.s001 (0.14 MB TIF)

Figure S2 BIO, but not MeBIO, activates β -catenin signalling.
Found at: doi:10.1371/journal.pone.0006459.s002 (0.07 MB TIF)

Figure S3 Regulation of Topflash reporter activity by over-expression of Wnt pathway components.
Found at: doi:10.1371/journal.pone.0006459.s003 (0.15 MB TIF)

Figure S4 BIO selectively represses expression of the full length *hTERT* transcript in A2780.
Found at: doi:10.1371/journal.pone.0006459.s004 (0.94 MB TIF)

References

- Palm W, de Lange T (2008) How shelterin protects mammalian telomeres. *Annu Rev Genet* 42: 301–334.
- Keith WN, Birkland AE (2008) Targeting telomerase: Therapeutic options for cancer treatment. *Telomeres and Telomerase in Aging, Disease, and Cancer*. Berlin: Springer-Verlag, pp 247–283.
- Adkinson SP, Hoare SF, Glasgow RM, Keith WN (2005) Lack of telomerase gene expression in alternative lengthening of telomere cells is associated with chromatin remodeling of the *hTR* and *hTERT* gene promoters. *Cancer Res* 65: 7580–7590.
- Keith WN, Birkland A, Handic M, Evans TR (2004) Drug insight: Cancer cell immortality-telomerase as a target for novel cancer gene therapies. *Nat Clin Pract Oncol* 1: 88–96.
- Kyo S, Takakura M, Fujiwara T, Inoue M (2008) Understanding and exploiting *hTERT* promoter regulation for diagnosis and treatment of human cancers. *Cancer Sci* 99: 1328–1338.
- Hadley CB (2008) Telomerase and cancer therapeutics. *Nat Rev Cancer* 8: 167–179.
- Helder MN, Wiseman GB, van der Zee GJ (2002) Telomerase and telomeres from basic biology to cancer treatment. *Cancer Invest* 20: 82–101.
- Jope RS, Yuskivits CJ, Beaulieu E (2007) Glycogen synthase kinase-3 (GSK3): inflammation, disease, and therapeutics. *Neurochem Res* 32: 577–595.
- Beaulieu E, Jope RS (2006) The paradoxical pro- and anti-apoptotic actions of GSK3 in the intrinsic and extrinsic apoptosis signaling pathways. *Prog Neurobiol* 79: 173–189.
- Meijer L, Flajolet M, Greengard P (2004) Pharmacological inhibitors of glycogen synthase kinase-3. *Trends Pharmacol Sci* 25: 471–480.
- Kovalenko M, Casati A, Bekker A, Rozman C, Rosenstrand L, et al. (1994) Selective platelet-derived growth factor receptor kinase blockers reverse cis-transformation. *Cancer Res* 54: 6106–6114.
- Cottam HB, Watson DB, Shih HC, Raychaudhuri A, Di Pasquale G, et al. (1993) New adenosine kinase inhibition with oral anti-inflammatory activity: synthesis and biological evaluation. *J Med Chem* 36: 3424–3430.
- Zaman CJ, Vink PM, van den Drielen AA, Vermeulen GH, Theunissen HJ (1999) Tyrosine kinase activity of purified recombinant cytoplasmic domain of platelet-derived growth factor beta-receptor (beta-PDGFR) and discovery

Figure S5 Representative results of MetaCore “transcriptional-regulation” algorithm analysis.
Found at: doi:10.1371/journal.pone.0006459.s005 (3.60 MB TIF)

Figure S6 Optimisation of the best-fit transcriptional network.
Found at: doi:10.1371/journal.pone.0006459.s006 (1.23 MB TIF)

Figure S7 Expression of *hTERT* after 16 h treatment with 5 μ M BIO
Found at: doi:10.1371/journal.pone.0006459.s007 (1.92 MB TIF)

Supporting File S1 Antibodies used in the study.
Found at: doi:10.1371/journal.pone.0006459.s008 (0.02 MB XLS)

Supporting File S2 Differentially expressed Agilent IDs and fold intensity change.
Found at: doi:10.1371/journal.pone.0006459.s009 (0.09 MB XLS)

Supporting File S3 Best fit transcriptional network statistics.
Found at: doi:10.1371/journal.pone.0006459.s010 (0.21 MB XLS)

Supporting File S4 Legends to supporting figures and files
Found at: doi:10.1371/journal.pone.0006459.s011 (0.03 MB DOC)

Acknowledgments

We thank Dr. Mejlinda Iako (Institute for Ageing and Health, Newcastle University, UK) for the kind gift of plasmids pCMV-mWnt3 and pCMV-mWnt5A.

Author Contributions

Conceived and designed the experiments: AEB WNK. Performed the experiments: AEB SH KS JP NGR CC SB KLW. Analyzed the data: AEB SH KS JP NGR CC SB KLW WNK. Contributed reagents/materials/analysis tools: JR TH. Wrote the paper: AEB JR WNK.

- of a novel inhibitor of receptor tyrosine kinases. *Biochem Pharmacol* 57: 57–64.
- Alarid H, Bazer A, Stappert J, Kipert A, Kemler R (1997) β -catenin is a target for the ubiquitin-proteasome pathway. *EMBO J* 16: 3797–3804.
- Dohl JA, Cheng M, Russell MF, Sherr CJ (1998) Glycogen synthase kinase-3 β regulates cyclin D1 proteolysis and subcellular localization. *Genes Dev* 12: 3499–3511.
- MacAulay K, Blair AS, Hajkovich E, Tomihata T, Baba O, et al. (2005) Constitutive activation of GSK3 down-regulates glycogen synthase abundance and glycogen deposition in rat skeletal muscle cells. *J Biol Chem* 280: 9509–9518.
- Gotschlich F, Kern C, Lang S, Sporna T, Markmann C, et al. (2008) Inhibition of GSK3 differentially modulates NF- κ B, CREB, AP-1 and β -catenin signaling in hepatocytes, but fails to promote TNF- α -induced apoptosis. *Exp Cell Res* 314: 1351–1366.
- Wei W, Jin J, Schläpfer S, Harper JW, Kaelin WG Jr (2005) The v-jun point mutation allows c-Jun to escape GSK3-dependent recognition and destruction by the Fbw7 ubiquitin ligase. *Cancer Cell* 8: 25–33.
- Whittaker SR, Walton MI, Garrett MD, Workman P (2004) The Cyclin-dependent kinase inhibitor CYC202 (R-roscovitine) inhibits retinoblastoma protein phosphorylation, causes loss of Cyclin D1, and activates the mitogen-activated protein kinase pathway. *Cancer Res* 64: 262–272.
- Ekim S, Bugrin A, Brovold I, Kirillov E, Nikolov Y, et al. (2006) Algorithms for network analysis in systems-ADME/Tox using the MetaCore and MetaDrug platforms. *Xenobiotica* 36: 877–901.
- Mangan S, Alon U (2003) Structure and function of the feed-forward loop network motif. *Proc Natl Acad Sci U S A* 100: 11980–11985.
- Judd EM, Lash MT, McAdams HH (2000) Toggles and oscillators: new genetic circuit designs. *Bioessays* 22: 507–509.
- Tyson JJ, Chen KC, Novak B (2003) Sniffers, buzzers, toggles and blinkers: dynamics of regulatory and signaling pathways in the cell. *Curr Opin Cell Biol* 15: 221–231.
- Okon DJ, Ohshima M, Ose AP, Kumar R (1998) Ectopic expression of wnt-5a in human renal cell carcinoma cells suppresses in vitro growth and telomerase activity. *Tumour Biol* 19: 244–252.

25. Maccario H, Petrus NM, Davison I, Downes CP, Leslie NR (2007) PTEN is destabilized by phosphorylation on Thr366. *Biochem J* 405: 439–444.
26. Hamada K, Kurisu K, Sadamoto T, Tahara H, Tahara E, et al. (2000) Growth inhibition of human glioma cells by transfection-induced P21 and its effects on telomerase activity. *J Neurooncol* 47: 39–46.
27. Zhou C, Bao-Junp VI, Whang YE, Gelrig PA, Boggess JF (2006) The PTEN tumor suppressor inhibits telomerase activity in endometrial cancer cells by decreasing hTERT mRNA levels. *Gynecol Oncol* 101: 305–310.
28. Monk NA (2003) Oscillatory expression of Hes1, p53, and NF-kappaB driven by transcriptional time delays. *Cell Biol* 13: 1409–1413.
29. Nelson DE, See V, Nelson G, White MR (2004) Oscillations in transcription factor dynamics: a new way to control gene expression. *Biochem Soc Trans* 32: 1090–1092.
30. Frame S, Cohen P (2001) GSK3 takes center stage more than 20 years after its discovery. *Biochem J* 359: 1–16.
31. Patel S, Woodgett J (2008) Glycogen synthase kinase-3 and cancer: good cop, bad cop? *Cancer Cell* 14: 351–353.
32. Louis KG, Behrens BC, Kinoshita TJ, Hamilton TC, Gotsinger KR, et al. (1985) Radiation survival parameters of antineoplastic drug-sensitive and -resistant human ovarian cancer cell lines and their modification by bothiazine sulfonamide. *Cancer Res* 45: 2110–2115.

ORIGINAL ARTICLE

A gene expression signature classifying telomerase and ALT immortalization reveals an hTERT regulatory network and suggests a mesenchymal stem cell origin for ALT

K Lafferty-Whyte¹, CJ Cairney¹, MB Will¹, N Serakinci², M-G Daidone³, N Zaffaroni³, A Bilsland¹ and WN Keith¹

¹Centre for Oncology and Applied Pharmacology, University of Glasgow, Cancer Research UK Beatson Laboratories, Bearsden, Glasgow, UK; ²Institute of Regional Health Services (IRS), Telomere and Aging Group, Southern Denmark University, Vejle, Denmark and ³Unit 10, Department of Experimental Oncology and Laboratories, Fondazione IRCCS Istituto Nazionale dei Tumori, Milan, Italy

Telomere length is maintained by two known mechanisms, the activation of telomerase or alternative lengthening of telomeres (ALT). The molecular mechanisms regulating the ALT phenotype are poorly understood and it is unknown how the decision of which pathway to activate is made at the cellular level. We have shown earlier that active repression of telomerase gene expression by chromatin remodelling of the promoters is one mechanism of regulation; however, other genes and signalling networks are likely to be required to regulate telomerase and maintain the ALT phenotype. Using gene expression profiling, we have uncovered a signature of 1305 genes to distinguish telomerase-positive and ALT cell lines. By combining this with the gene expression profiles of liposarcoma tissue samples, we refined this signature to 297 genes. A network analysis of known interactions between genes within this signature revealed a regulatory signalling network consistent with a model of human telomerase reverse transcriptase (hTERT) repression in ALT cell lines and liposarcomas. This network expands on our existing knowledge of hTERT regulation and provides a platform to understand differential regulation of hTERT in different tumour types and normal tissues. We also show evidence to suggest a novel mesenchymal stem cell origin for ALT immortalization in cell lines and mesenchymal tissues.

Oncogene (2009) 28, 3765–3774; doi:10.1038/onc.2009.238; published online 17 August 2009

Keywords: telomerase; ALT; mesenchymal; microarray; signalling; c-Myc

Introduction

A central hallmark of cancer cells is their capacity for unlimited proliferation, made possible partly by

telomere length maintenance. Most human tumours maintain telomeres by activating telomerase; however, in a smaller subset of tumours, maintenance occurs in the absence of telomerase through a recombination-based mechanism termed alternative lengthening of telomeres (ALT). The ALT is characterized phenotypically by long, heterogeneous telomeres and the presence of ALT-associated promyelocytic leukaemia bodies, which contain telomeric DNA, telomere-binding proteins such as telomere repeat binding factors 1 and 2 and proteins implicated in DNA recombination and replication, including Mre11-Rad50-Nbs1 complex proteins MRE11, RAD51 and NBS (Yeager *et al.*, 1999; Henson *et al.*, 2002). Association of these proteins with the ALT phenotype make them attractive as potential markers or regulators of ALT (Jiang *et al.*, 2007); indeed, the MRN complex is required for ALT-associated promyelocytic leukaemia body formation and telomere maintenance in ALT cells (Zhong *et al.*, 2007).

Although the overall prevalence of ALT in tumours is relatively low, it is observed at high frequency in tumours of mesenchymal origin. However, the prevalence of ALT varies even within this group. About 77% of malignant fibrous histiocytomas (Henson *et al.*, 2005) and 47–66% of osteosarcomas (Ulaner *et al.*, 2003; Henson *et al.*, 2005) were shown to be ALT positive, whereas 25% of glioblastoma multiforme (Hakin-Smith *et al.*, 2003) and liposarcomas (Johnson *et al.*, 2005; Costa *et al.*, 2006) and no Ewing's sarcomas (Ulaner *et al.*, 2004) showed evidence of ALT. Since the prognostic significance of ALT varies, signifying a good prognosis for patients with glioblastoma multiforme but a poor prognosis for those with liposarcoma (Costa *et al.*, 2006; Cairney *et al.*, 2008), and understanding the molecular details regulating ALT immortalization and the cell of origin may impact future diagnosis or treatment of these malignancies.

A possible explanation for the prevalence of ALT in mesenchymal malignancies is that the telomerase genes are more tightly repressed in mesenchymal tissues over those of epithelial origin (Henson *et al.*, 2002). We have earlier reported that both human telomerase RNA and human telomerase reverse transcriptase (hTERT) are

Correspondence: Professor WN Keith, Centre for Oncology and Applied Pharmacology, University of Glasgow, Cancer Research UK Beatson Laboratories, Alexander Stone Building, Garscube Estate, Switchback Road, Bearsden, Glasgow G61 1BD, UK.
E-mail: n.keith@beatson.gla.ac.uk

Received 1 March 2009; revised 8 June 2009; accepted 13 July 2009; published online 17 August 2009

actively repressed at the chromatin level in ALT cell lines (Atkinson *et al.*, 2005), suggesting forced repression of telomerase as one potential molecular mechanism promoting immortalization by ALT. However, other genes and signalling networks also regulate telomerase and may contribute to the decision of selecting ALT versus telomerase. In this study we investigate the gene expression profiles of telomerase-positive and ALT cell lines and liposarcoma tissue samples to better understand the molecular mechanisms regulating the decision to activate telomerase or ALT. In addition, we show a link between mesenchymal tumours and human mesenchymal stem cells (hMSCs) as the target cell for transformation in ALT immortalization.

Results

Gene expression analysis distinguishes telomerase and ALT cell lines

We initially investigated the presence of a telomere maintenance mechanism (TMM)-specific gene expression signature by generating expression profiles for four ALT and four telomerase-positive cell lines using Agilent whole human genome 1-colour microarrays (Agilent Technologies, Santa Clara, CA, USA). A detailed description of the quality control measures and the normalization options applied can be found in the section Materials and methods; however, boxplots show that the normalized data are equally spread and comparable between the two groups (Figure 1a), with virtually equal medians of 0.78 and 0.79 for ALT and telomerase-positive cell line groups, respectively.

To explore the possibility that expression of individual genes within these large profiles is responsible for defining either telomerase-positive or ALT cells, we performed Welch's analysis of variance test to look for significant differences in gene expression between the two groups (Figure 1b, left panel). A list of 1307 probes corresponding to 1305 differentially expressed genes with a *P*-value of ≤ 0.05 was generated. By focussing on the expression values for individual genes within the larger 1305 gene signature, it was clear that whereas expression was high in the ALT cell lines it was low in the telomerase-positive cell lines and *vice versa* (Figure 2a). Furthermore, hierarchical clustering of the cell lines on the basis of this signature helped to accurately bifurcate ALT and telomerase-positive cell lines into two separate groups (Figure 2b), suggesting that the genes responsible for defining telomerase or ALT or those involved in regulating the decision of which TMM to activate may lie within this signature.

Clustering by using the 1305 gene signature is suggestive of a mesenchymal stem cell origin for ALT

The fact that ALT is predominantly found in tumours of mesenchymal origin prompted us to investigate whether ALT is a function of the cell of transformation and whether mesenchymal stem cells could be the potential

cell of origin for ALT tumours. We performed a hierarchical clustering analysis by using the 1305 gene signature to investigate any relationship between telomerase-positive, ALT and normal fibroblast cell lines, and hMSCs (Figure 2c). The signature helped to accurately separate telomerase-positive and ALT cell lines, normal fibroblasts, and hMSCs. However, whereas the telomerase-positive cell lines clustered together on a separate branch, the ALT cell lines, normal fibroblasts and hMSCs all clustered together. Normal fibroblasts are more directly related to hMSCs than ALT; however, fibroblasts and hMSCs are equally related to the ALT cell lines, suggesting a mesenchymal stem cell origin for ALT. This might be as predicted; however, to our knowledge, this is the first time any association between mesenchymal stem cells and ALT has been shown.

Analysis of the signature revealed several genes associated with stem cell maintenance, and self-renewal processes were differentially expressed between telomerase-positive and ALT cell lines. Four of these genes with strong differences in expression were chosen for validation by quantitative PCR (Q-PCR) (Figure 3a). Three of these genes were significantly upregulated in ALT cell lines and barely expressed in telomerase-positive cell lines. DSC54 is a novel mesenchymal stem cell protein for which little information exists; WNT5b is a well-known regulator of stem cell function implicated in oncogenesis and development; MYEOV is overexpressed in myeloma and has a role in promoting invasion and proliferation; and the final gene, NSUN5, is a proliferation-associated nucleolar antigen, the deletion of which may contribute to the premature ageing effects of the developmental disorder William's syndrome. NSUN5 is significantly upregulated in telomerase-positive compared with ALT cell lines.

To further explore the link between ALT and mesenchymal stem cells, we examined the expression of these genes within a variety of normal tissues of differing embryonic origin and hMSCs. The publicly available gene expression profiles from normal fibroblasts, smooth muscle, stromal, ectoepithelial, epithelial and endothelial tissues were downloaded from the National Centre for Biotechnology Information Gene Expression Omnibus database and expression of DSC54, WNT5b and MYEOV in these tissues was compared with that of hMSC, telomerase-positive and ALT cell lines (Figure 3b). No comparable data were available for NSUN5, and therefore this gene could not be included in the analysis.

Consistent with the Q-PCR validation, the expression of all three genes is higher in ALT than in telomerase-positive cell lines. When comparing all the expression patterns, DSC54 is only high in ALT cell lines and hMSCs, consistent with a mesenchymal stem cell origin for ALT. In contrast, WNT5b shows varying expression across the different tissue types and cell lines, with highest expression in hMSC, ALT and mesenchymally derived tissues and lowest expression in telomerase-positive and epithelial tissues. MYEOV distinguishes ALT from telomerase-positive cell lines; however, a

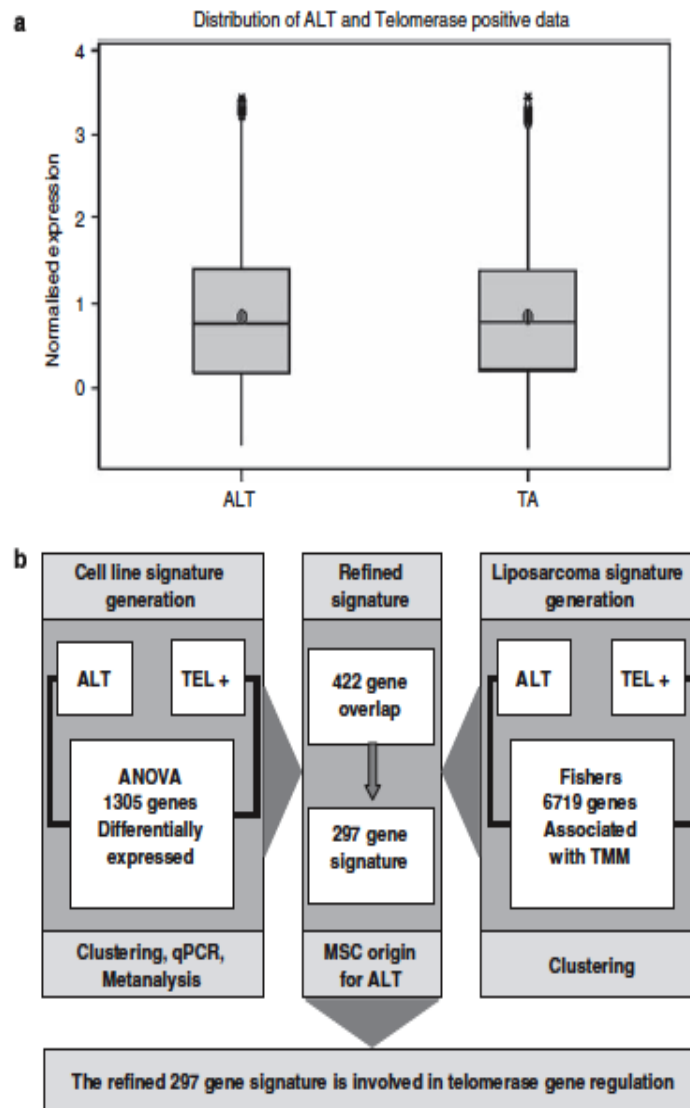


Figure 1 Gene expression analysis of alternative lengthening of telomeres (ALT) and telomerase-positive cell lines. (a) The boxplots show distribution of normalized data in ALT and telomerase-positive cell line groups. Grey boxes define 25 and 75% quartiles, whereas error bars represent the 1st and 99th percentiles of the distribution. Dots represent outliers, black line represents the median, and the cross represents the mean of the distribution. (b) Overview of signature generation from cell line and liposarcoma tissue samples. A refined 297 gene signature was generated from a combination of the 1305 gene cell line signature and the 6719 gene liposarcoma signature. This signature shows a potential mesenchymal stem cell origin for ALT and is involved in telomerase gene regulation. Gene expression data were submitted to the National Center for Biotechnology Information Gene Expression Omnibus (<http://www.ncbi.nlm.nih.gov/geo/>) under accession number GSE14533.

similar low level of expression is seen across the various other tissue types.

Refinement of the 1305 gene signature using liposarcoma gene expression improves separation of ALT and telomerase-positive liposarcomas and suggests a mesenchymal stem cell origin for ALT in this mesenchymal malignancy

Liposarcomas are tumours of mesenchymal origin. In order to refine the cell line-derived signature with data from primary tumours, we analysed the power of the 1305 gene expression signature to distinguish between telomerase positive and ALT in liposarcomas. Gene

expression profiles were generated for a group of 17 previously characterized liposarcoma samples, of which 9 were ALT and 8 were telomerase positive. Unsupervised clustering showed some split in the samples depending on their TMM, which was not improved when the 1305 gene signature was applied. Furthermore, hMSCs did not cluster with any liposarcoma samples, but clustered together on a separate branch (Figure 4, compare a and b).

Although the 1305 signature does not improve clustering, the liposarcoma samples, for the most part, cluster together according to their TMM. The obvious separation between ALT and telomerase-positive tumours in the clustering diagram led us to believe that

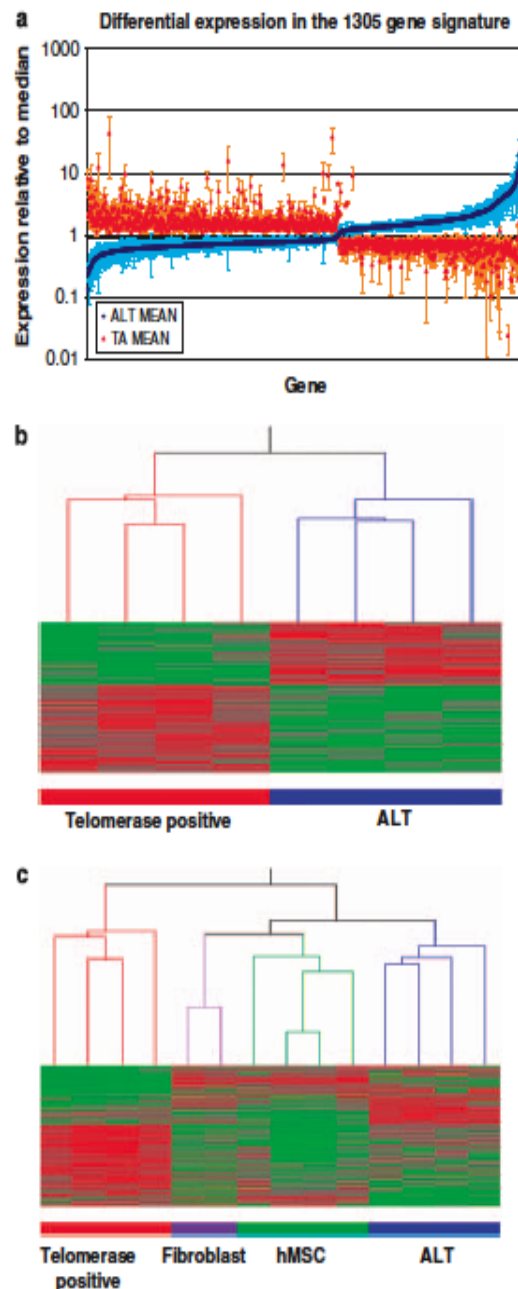


Figure 2 Gene expression profiling distinguishes telomerase-positive and alternative lengthening of telomeres (ALT) cell lines and is suggestive of a mesenchymal stem cell origin for ALT. (a) Scatter plot representing normalized microarray expression values for the 1305 gene signature in ALT (blue) and telomerase-positive (red) cell lines relative to overall median expression value. Each dot represents the mean gene expression values for a gene, and error bars represent the standard error. (b) Hierarchical clustering of the cell line data performed using the Spearman's correlation, average linkage and merging branches with a similarity correlation of 0.001 or less with the 1305 signature accurately separates telomerase positive (red) from ALT (blue) cell lines. (c) Hierarchical clustering of telomerase-positive (red) and ALT (blue) cell lines, normal fibroblasts (purple) and human mesenchymal stem cells (hMSCs; green) performed using the Spearman's correlation, average linkage and merging branches with a similarity correlation of 0.001 or less with the 1305 gene signature.

differences in gene expression exist between the two groups, although no significant differences were found. To explore this further, we used Fisher's exact test to test for any association between gene expression level and TMM. From this analysis, 8227 probes corresponding to 6719 genes were found to be significantly associated with TMM in ALT and telomerase-positive liposarcoma samples (Figure 1b, right-hand panel).

To further refine this large signature, we looked for any overlap with the 1305 gene signature determined from the cell lines previously. Of these 1305 genes, 422 genes are also present in the liposarcoma signature and therefore have a significant association with TMM in liposarcoma and cell lines. Further refinement of the signature was carried out by looking at the direction of gene expression in telomerase-positive and ALT tumours in comparison with the cell line data. In total, 297 of the 422 genes had gene expression that was comparable with the cell line data, 152 genes up in ALT and down in telomerase-positive, and 145 genes down in ALT and up in telomerase-positive (Figure 1b, centre panel).

The hierarchical clustering of ALT and telomerase-positive liposarcoma samples using this refined 297 gene signature showed a clear separation between the two groups, with all except two ALT samples clustering on one branch and all telomerase-positive samples clustering together on a separate branch (Figure 4c). Furthermore, consistent with the hypothesized mesenchymal stem cell origin for ALT seen within the cell line data, hMSCs clustered with the ALT liposarcomas using this refined signature rather than as a separate group when the 1305 signature was applied (Figure 4, compare b and c).

To further verify the refined signature, we applied it back to the cell line data for hierarchical clustering. As predicted, it accurately separated telomerase-positive from ALT cell lines (data not shown), further validating that this refined signature holds true and no power is lost by reducing gene number.

The refined 297 gene signature is involved in telomerase gene regulation and highlights lower c-MYC activity in ALT

Given the ability of the refined 297 gene signature to separate liposarcomas by TMM, we hypothesized that the genes within the signature may comprise functional regulatory networks involved in aspects of TMM. To explore this, we performed network modelling using Metacore from Genego (St Joseph, MI, USA), allowing us to build a candidate network indicating possible interactions between genes from the 297 signature mined from published data. A regulatory network involving hTERT and telomeric DNA was revealed by this analysis (Figure 4d). Expression data from the 297 gene signature were converted to fold change in ALT over telomerase positive, uploaded into Metacore analytical suite and overlaid on the direct interactions network. As can be seen from Figure 4d, by combining interactions between known signalling pathways and

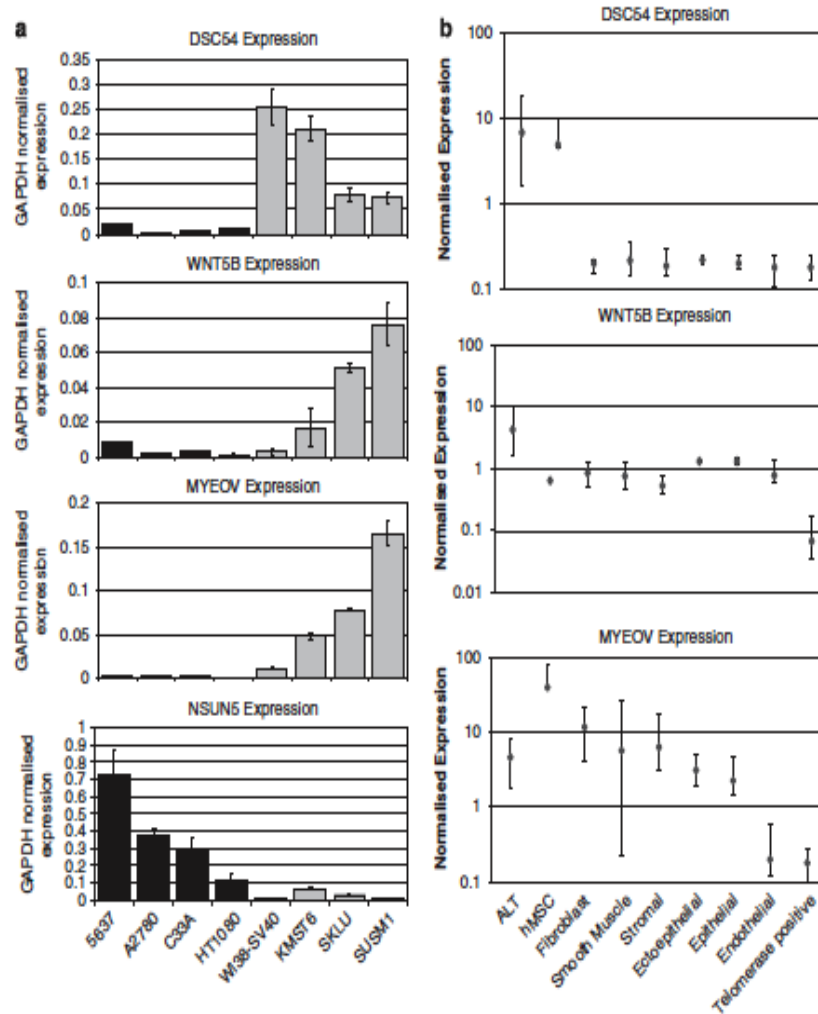


Figure 3 Validation of the 1305 gene expression signature highlights a stem cell link. (a) Expression levels of DSC54, WNT5B, MYEOV and NSUN5 were validated by quantitative PCR in telomerase-positive cell lines 5637, A2780, C33a and HT1080 (black bars) and alternative lengthening of telomeres (ALT) cell lines WI38-SV40, KMST6, SKLU, SUSM1 (grey bars) cell lines. Each bar represents the mean and standard error of triplicate reactions from a representative experiment normalized to glyceraldehyde 3-phosphate dehydrogenase. (b) Expression values for DSC54, WNT5B and MYEOV in various normal tissues extracted from publicly available microarray expression data, compared with those for ALT and telomerase-positive cell lines and human mesenchymal stem cells (hMSCs). Dots represent the median and the error bars represent the maximum and minimum normalized expression values.

experimentally defined levels of expression for regulatory genes, this approach allows for predictions relating to hTERT regulation and repression in ALT cells. The hTERT expression is reduced in ALT cells and tumours in relation to telomerase-positive samples. Consistent with this, expression of E2F1, a known repressor of hTERT, is upregulated in ALT samples, whereas the expression of chromatin-modifying enzymes with roles in gene activation, such as GCN5, are downregulated in ALT, which is in agreement with the decreased association of acetylated histones and low hTERT expression in ALT cell lines as we have previously shown. Western blotting of HDAC5, PKC α and GCN5 (Figure 5a) shows that the expression differences highlighted in this network are also seen at the protein level.

The analysis also indicates that c-Myc regulation may contribute to the signature. Although c-Myc was not

itself differentially expressed, 21 signature genes including hTERT are predicted transcriptional targets of c-Myc. Interestingly, most signature genes expected to be activated by c-Myc are repressed whereas those expected to be inhibited are mainly upregulated in ALT, relative to telomerase-positive samples, suggesting that c-Myc activity may be suppressed in ALT. Functional examination of c-Myc activity levels using DNA-binding activity enzyme-linked immunosorbent assays (ELISAs) confirms that this is indeed the case, as a significantly lower level of c-Myc activity is seen in the ALT cell lines ($P=0.015$; see Figure 5b). Apart from hTERT, another downregulated c-Myc target that may have a role in telomere maintenance is heterogeneous nuclear ribonucleoprotein A3. It was recently shown that this gene binds the single-stranded telomere repeat *in vitro*, protects against nuclease activity and inhibits extension by telomerase (Huang *et al.*, 2008).

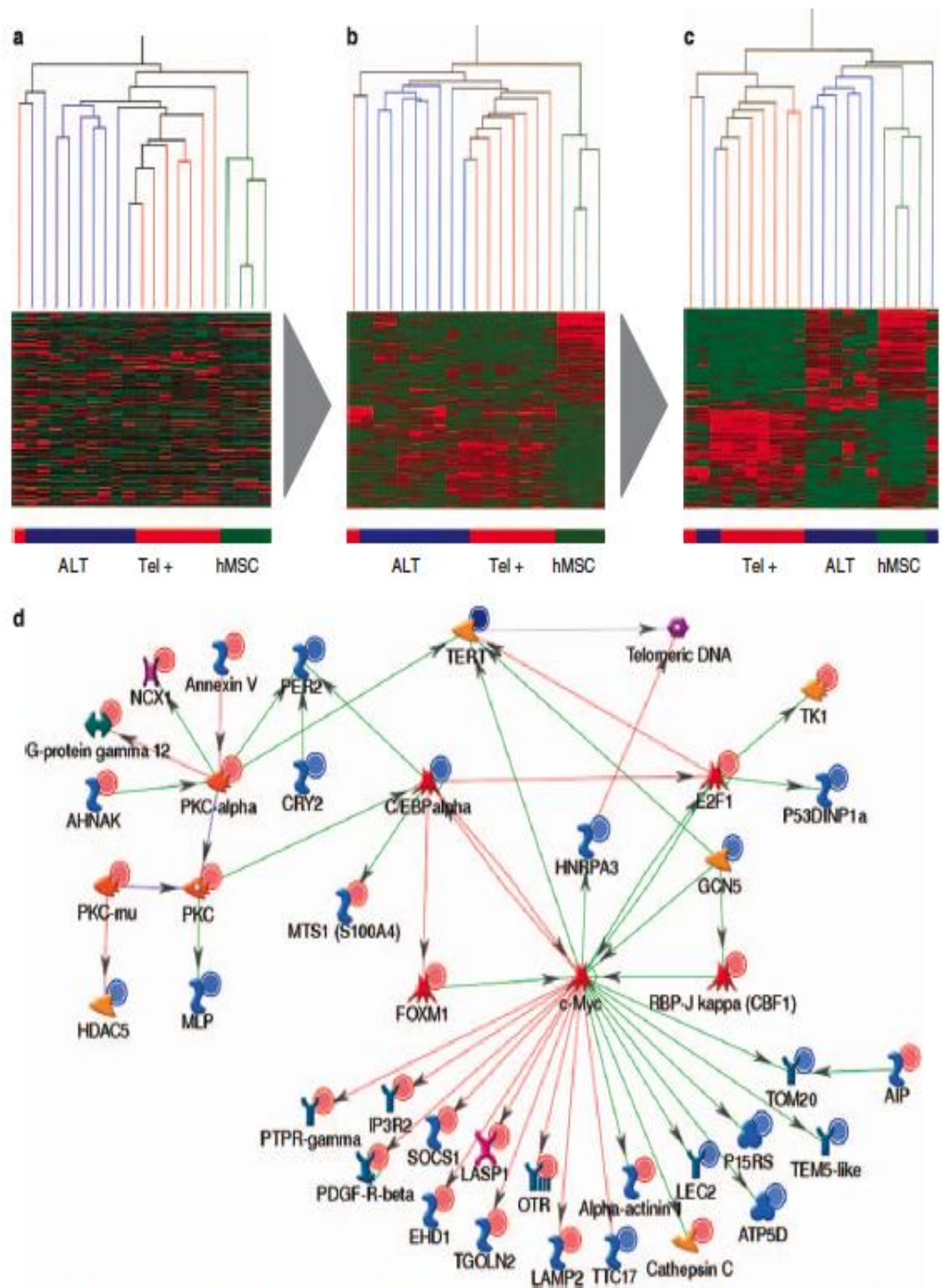


Figure 4 Hierarchical clustering of alternative lengthening of telomeres (ALT) and telomerase-positive liposarcoma samples and human mesenchymal stem cells (hMSCs) distinguishes telomerase-positive from ALT and highlights an hMSC origin for ALT. Liposarcoma samples were previously determined as ALT (blue) or telomerase-positive (red) by classical methods. Hierarchical clustering of these samples and hMSC (green) was performed using the Spearman's correlation, average linkage and merging branches with a similarity correlation of 0.001 or less, using (a) all genes (b) 1305 gene signature or (c) the refined 297 gene signature. (d) Network analysis of the 297 gene signature shows hTERT regulation. Signalling network of known direct interactions between genes from the 297 gene signature drawn using the analyse network-building algorithm within Metacore. Green arrows represent positive, red negative and grey unspecified interactions. Red and blue circles next to the network objects represent expression data. Red: up in ALT and down in telomerase-positive liposarcoma samples and cell lines; Blue: down in ALT and up in telomerase-positive liposarcoma samples and cell lines. The network highlights that a number of molecules activated by c-Myc have reduced expression in ALT cells and those inhibited by c-Myc have increased expression in ALT cells. This is suggestive of lower c-Myc activity in cells using ALT.

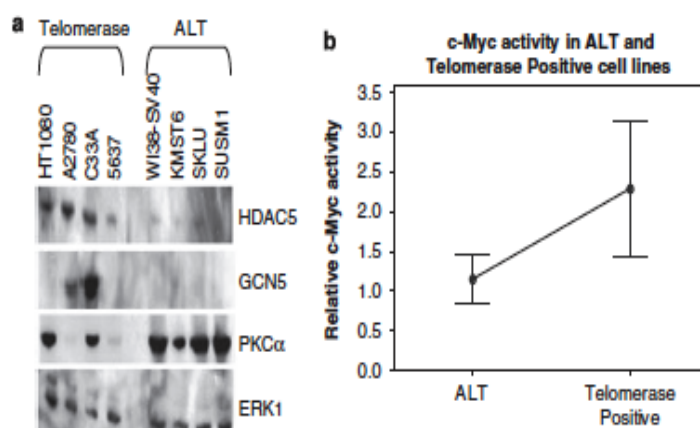


Figure 5 The telomerase reverse transcriptase (TERT) regulatory network is shown at the protein level and predicted c-MYC activity is confirmed as significantly lower in alternative lengthening of telomeres (ALT). (a) Western blotting shows protein level differences in three molecules of the 297 gene network. Fifteen micrograms of cell extracts were run on NuPAGE 4–12% Bis–Tris gels, transferred to Millipore nitrocellulose membrane and probed with appropriate antibodies. Blots were then stripped and reprobed with extracellular signal-regulated kinase 1 loading control. The panels shown are representative panels of two separate blots. (b) Analysis of c-Myc activity using enzyme-linked immunosorbent assay (ELISA) shows significantly lower activity in ALT cells. The interval plot shows the average of six ALT cell lines (WI38-SV40, KMST6, SKLU, SUSM1, SAOS and U2OS) and four telomerase cell lines (A2780, C33A, HT1080 and 5637) on three separate occasions with four replicates of each cell line. Crosshairs show the mean expression for each group and error bars show 95% confidence intervals of the mean. The *t*-test results were *t*-value = 2.51; *P*-value = 0.015; *d.f.* = 51.

More importantly, however, network analysis expands our understanding of TERT regulation beyond previously recognized mechanisms to new pathways upstream of those already known to be involved. Overall, this network highlights a potential mechanism of regulating the ALT phenotype through repression of hTERT and provides a platform for further expansions of regulatory mechanisms present in tissue or tumour-specific situations to enable us to understand the differential regulation of biological processes and how they vary in different tumour types and normal tissues.

Discussion

The molecular mechanisms regulating the decision to activate telomerase or ALT during tumorigenesis are currently poorly understood. We have shown earlier that lack of expression of the telomerase genes human telomerase RNA and hTERT is associated with chromatin remodelling at the promoters, suggesting that forced repression of these genes may cause the cells to utilize the ALT mechanism for immortalization (Atkinson *et al.*, 2005). In this study, we have used gene expression profiling of telomerase and ALT cell lines and liposarcomas to investigate other signalling pathways and networks that may be operating to control the ALT phenotype and the decision to activate telomerase or ALT for immortalization. To our knowledge, this is the first study of global gene regulation of TMM.

We uncovered a gene expression signature with the power to distinguish telomerase positive and ALT through hierarchical clustering methods in tumour cell lines. Further refinement of this signature using gene expression profiles from liposarcoma tissue samples

revealed a 297 gene signature that has significant association with TMM. Although the role of these signatures in the regulation of the ALT phenotype remains to be fully investigated, we have uncovered some of the underlying biology by combining clinical samples with cell line profiles. A network analysis of interactions within the refined signature highlighted a signalling network involved in repression of hTERT in ALT liposarcoma samples and cell lines. Western blot validation of three of the molecules in the network confirmed that this pattern can also be observed at the protein level. Consistent with our earlier work (Atkinson *et al.*, 2005; Cairney *et al.*, 2008), this again points to forced repression of hTERT in ALT and may in part explain the decision to activate telomerase or ALT at the molecular level. Although hTERT expression alone is insufficient to discriminate ALT and telomerase positive in clinical samples, hTERT repression is clearly important for regulation of the ALT phenotype. This network of interactions also highlighted the potential for lower c-Myc activity in cells using the ALT mechanism. Upon direct investigation using c-Myc activity ELISAs, a lower level of c-Myc activity in ALT was confirmed. This is consistent with the fact that c-Myc is a known hTERT transcriptional activator (Hao *et al.*, 2008) and may show a further mechanism by which the decision to activate either ALT or telomerase is influenced.

This candidate network further highlights the importance of a global analysis of gene expression. Where significant expression of one gene may be of importance in certain circumstances, it is more likely, as evidenced by this example, that small changes in a combination of genes in a signalling pathway are responsible for defining a phenotype. By investigating signalling networks on a global scale, we are better advantaged to discover the biology underlying the ALT phenotype and its regulation in mesenchymal malignancies.

In addition to the hTERT regulatory network, a number of stem cell-related genes were also highlighted within the large gene signature. The possibility that the decision to activate either telomerase or ALT is made at the cellular level is an interesting hypothesis to consider. Cancer biology in many ways parallels that of stem cell biology as pathways regulating the self-renewal phenotype and replicative lifespan of stem cells are commonly deregulated in cancer. With the growing interest in stem cells as the cell of origin for certain tumours, investigating the potential origin for ALT immortality may improve our understanding of the regulation of telomere maintenance. The preponderance of ALT in mesenchymal malignancies prompted us to investigate any relationship between hMSCs and ALT or telomerase-positive cell lines and liposarcoma tissues. hMSCs are an adult stem cell population with limited replicative lifespan and no detectable telomerase activity (Zimmermann *et al.*, 2003), which is at least partly due to active repression of the telomerase genes at the chromatin level, similar to the situation in ALT cell lines (Serakinci *et al.*, 2006; Cairney and Keith, 2008). However, hMSCs do not show characteristic molecular markers of ALT (Bernardo *et al.*, 2007; Zhao *et al.*, 2008). It is therefore possible that hMSCs upon transformation could become either ALT or telomerase-positive tumours. There is, however, a need for accurate models of the molecular details of the decision between these two mechanisms, such as ours, before manipulation of the resulting TMM can be achieved.

Hierarchical clustering showed that the expression profile of the signature genes in hMSCs was more closely related to ALT than to telomerase-positive cell lines with the larger signature, and also to ALT liposarcomas when the refined 297 gene signature was utilized, suggesting a mesenchymal stem cell origin for ALT.

Mesenchymal stem cells are known to be potential targets for transformation *in vitro*. Lack of any TMM in these cells may be a tumour suppressor mechanism, as transduction with hTERT has been shown to extend their lifespan and induce neoplastic characteristics after long-term culture *in vitro* and tumour formation *in vivo* (Serakinci *et al.*, 2004). In addition, several studies have shown the ability of MSC to transform spontaneously after long-term culture *in vitro* in murine systems (Miura *et al.*, 2006; Zhou *et al.*, 2006), although the situation in human systems remains unclear, with conflicting reports suggesting that the capacity for spontaneous transformation may be dependant on the tissue of origin (Rubio *et al.*, 2005; Wang *et al.*, 2005; Miura *et al.*, 2006; Bernardo *et al.*, 2007). More recently, several studies have linked hMSCs with mesenchymal malignancies, including Ewing's sarcoma (Tirode *et al.*, 2007; Riggi *et al.*, 2008) and malignant fibrous histiocytoma (Matushansky *et al.*, 2007). Stem-like tumour-initiating cells have also been isolated from various mesenchymal tumours (Gibbs *et al.*, 2005; Wu *et al.*, 2007). Taken together, these data suggest that the stem cell origin for cancer extends to mesenchymal malignancies.

Although the preponderance of ALT in mesenchymal tissues has been documented previously on numerous

occasions, to our knowledge this is the first time the link to a mesenchymal stem cell origin for ALT has been made. Furthermore, this is not simply reflective of the mesenchymal origin of ALT cell lines as both the ALT and telomerase-positive liposarcoma samples are mesenchymally derived and only the ALT liposarcomas cluster with hMSCs. The significance of this association is unknown at present, but certainly warrants further investigation.

In conclusion, we have uncovered a gene expression signature capable of distinguishing telomerase-positive from ALT in cell lines and liposarcoma tissue samples. This signature contains a regulatory signalling network involving hTERT repression in ALT and is indicative of a novel hMSC origin for ALT. The results presented allow us to postulate two potential models for the target cell of origin for ALT and telomerase immortalization: either (1) two separate cells of origin exist for telomerase-positive and ALT-expressing malignancies or (2) telomerase-positive and ALT tumours arise from the same cell of origin. In the latter case, the cell of origin would be the hMSCs, whereby telomerase-positive tumours obtain molecular profiles over time that diversify them from the hMSC origin, whereas ALT tumours maintain the stem cell profile, perhaps in part through mechanisms such as repression of the telomerase genes. The data presented here favour the latter scenario; however, further investigation is required in the other tumour types known to utilize the ALT mechanism, such as glioma (Chen *et al.*, 2006), adrenocortical carcinoma, breast carcinoma, malignant melanoma, lung carcinoma, ovarian carcinoma (Bryan *et al.*, 1997) and renal carcinoma (Mehle *et al.*, 1996). A better understanding of the regulation of TMM in the cell of origin will increase our knowledge of the biology underlying these tumour types and may highlight novel areas for therapeutic intervention.

Materials and methods

Cell lines and RNA extraction

The ALT cell lines used were SKLU (lung adenocarcinoma), SUSM1 (liver fibroblasts), KMST6 (lung fibroblasts), WI38-SV40 (SV40 immortalized lung fibroblasts), SAOS (osteosarcoma) and U2OS (osteosarcoma). Telomerase-positive cells used were C33a (cervical carcinoma), HT1080 (fibrosarcoma), A2780 (ovarian carcinoma) and 5637 (bladder carcinoma). Normal cell strains used were WI38 (normal lung fibroblasts) and IMR90 (normal lung fibroblasts). Bone marrow hMSCs were isolated as described earlier (Serakinci *et al.*, 2006) and cultured using Dulbecco's modified Eagle's medium with low glucose plus Glutamax supplemented with 17% Hyclone fetal bovine serum (Thermo Fisher Scientific, Waltham, MA, USA) at 5% CO₂.

RNA was extracted using the Nucleospin II RNA extraction kit (Macherey-Nagel, Duren, Germany) following the manufacturers' instructions.

Liposarcoma cases and RNA extraction

A subset of 17 liposarcoma samples (9 ALT and 8 telomerase positive) from a larger study population earlier described (Cairney *et al.*, 2008) were used for gene expression analysis.

Frozen tissue was disrupted using a Hybaid Ribolyser (Hybaid, Teddington, UK) at a setting of 5.5 for 5 × 10 s pulses with 30-s pauses in between and RNA was extracted using the RNeasy Lipid kit (Qiagen Inc., Hilden, Germany) as per the manufacturers' instructions.

Gene expression microarray hybridization, normalization and quality control

In total, 4 ALT cell lines (WI38-SV40, KMST6, SKLU and SUSM1) and 4 telomerase-positive cell lines (A2780, C33a, HT1080 and 5637), 2 normal fibroblasts (WI38, IMR90), 4 hMSCs and 17 liposarcoma samples were examined using gene expression microarrays. Two separate RNA samples for each were amplified and labelled using the Agilent Low RNA Input Linear Amplification Kit PLUS, 1-colour and hybridized to Agilent whole human genome 4 × 44 K gene expression arrays as per the manufacturers' instructions. Raw data were extracted from scanned images using Agilent feature extraction software (Agilent Technologies).

All array data was then imported into GeneSpring GX (version 7.3.1, Agilent Technologies) and normalised to the 50th, for cell line arrays, or 70th percentile for hMSC and liposarcoma arrays respectively to ensure equal medians across all samples. Further quality control involved filtering based on flag values where only those genes that had non-absent flag values for at least half of the samples were included in downstream analysis. A box plot of the distribution of the resulting genome (Figure 1a) was plotted using Minitab version 14 (Minitab, Coventry, UK) to assess comparability of groups. Data files submitted to GEO for Public access under accession number GSE14533.

Statistical analysis, signature generation and clustering

All statistical analysis and signature generation were carried out within GeneSpring GX. The 1305 gene signature was generated from cell line expression profiles using Welch's analysis of variance with a false discovery rate of 0.05 and Benjamini and Hochberg multiple testing correction. A similar analysis in liposarcoma samples generated no results and therefore to generate the refined 297 gene signature, Fisher's exact test using a *P*-value of ≤ 0.05 was performed using the liposarcoma expression profiles to test for significant association of gene expression with TMM. From this analysis, 422 genes were also present within the 1305 signature. The genes that had fold-change values in the same direction for both cell line and liposarcoma data (that is, an increased or decreased expression in ALT compared with telomerase positive) were included in the refined signature.

All hierarchical clustering was performed using the Spearman's correlation, average linkage and merging branches with a similarity correlation of ≤ 0.001 .

Q-PCR validation of microarray data

Expression of some genes within the 1305 signature was validated by Q-PCR using the DyNamo Hot Star SYBR Green Kit (Finnzymes, Espoo, Finland) and Opticon 2 DNA Engine from MJ Research (Waltham, MA, USA). Primer sequences for Q-PCR validation were as follows:

MYEOVF: 5'-TGGGAGGACACGCAAGTT, MYEOVR: 5'-CCAGCAGCCAAAGCAAAG, WNT5BF: 5'-AGGAGG GAGGTTGTGTT, WNT5BR: 5'-GAACCGTGGAGGAT GAAG, DSC54F: 5'-ACCTTCTACGAAATGGA, DSC54R: 5'-ACTGTGGCTTATTCCCAT, NSUN5F: 5'-TGAGACC ACATCAGCAG and NSUN5R: 5'-GAGAGGACAGGCA TCTTC.

Expression of each gene was normalized to glyceraldehyde 3-phosphate dehydrogenase as a loading control: GAPDHF: 5'-ACCACAGTCCATGCCATCAC, GAPDHR: 5'-TCCAC CACCCTGTTGCTGTA.

Analysis of public data

Normalized gene expression data for a compendium of 61 samples from various normal cell types were downloaded from the National Center for Biotechnology Information Gene Expression Omnibus (series GSE3239). Comparison with cell line and hMSC data was carried out in Microsoft Excel.

Network analysis in Metacore

Expression data from the 297 gene signature were converted to fold change in ALT over telomerase positive and uploaded into Metacore analytical suite. Network analysis was performed using the analyse network algorithm within the software.

Western blotting validation of network analysis

Fifteen micrograms of protein equivalents were separated on 10% Bis-Tris gels using NuPAGE MES running buffer (Invitrogen, Renfrewshire, UK), and then blotted onto nitrocellulose membrane (Millipore, Watford, UK) and blocked in phosphate buffered saline Tween-20 containing 5% nonfat dried milk. Membranes were probed with the following antibodies: HDAC5 rabbit polyclonal (Active Motif, Rixenstart, Belgium), PKC α rabbit polyclonal and KAT2A/GCN5 rabbit polyclonal (both from Abcam, Cambridge, UK) and secondary anti-rabbit IgG horseradish peroxidase-linked antibody (New England Biolabs UK, Hitchin, UK). After visualization, membranes were stripped of bound primary and secondary antibodies by submerging in 1% SDS and 0.2 M glycine (pH 2.5) and shaken for 1 h at room temperature, and rinsed and reblocked before probing with loading control antibody extracellular signal-regulated kinase 1 rabbit polyclonal (1:3000) (Santa Cruz Biotechnology, Heidelberg, Germany).

c-MYC DNA-binding ELISA

Nuclear extracts of approximately 8×10^4 cells of each of the six ALT cell lines (WI38-SV40, KMST6, SKLU, SUSM1, SAOS and U2OS) and four telomerase-positive cell lines (A2780, C33a, HT1080 and 5637) were extracted in triplicate using an Active motif nuclear extraction kit (Active Motif, Rixenstart, Belgium) as per the manufacturer's instructions. c-MYC DNA-binding ELISAs (Active Motif) were performed on three separate occasions with four technical replicates of each cell line as per the manufacturer's instructions. A standard curve of 5, 2.5, 1.25 and 0.625 ng/well recombinant c-MYC protein (Active Motif) was run on each assay to allow relative quantification. Results of all ALT and telomerase-positive cells were grouped and a *t*-test was carried out using Minitab (version 14).

Conflict of interest

The authors declare no conflict of interest.

Acknowledgements

This work was supported by the Cancer Research UK, European Community Grants LSHC-CT-2004-502943, LSHC-CT-2005-0018806 and Health-F2-2007-200950 Glasgow University and Italian Association for Cancer Research.

References

- Atkinson SP, Hoare SF, Glasspool RM, Keith WN. (2005). Lack of telomerase gene expression in alternative lengthening of telomere cells is associated with chromatin remodeling of the hTR and hTERT gene promoters. *Cancer Res* **65**: 7585–7590.
- Bernardo ME, Zaffaroni N, Novara F, Cometa AM, Avanzini MA, Moretta A et al. (2007). Human bone marrow derived mesenchymal stem cells do not undergo transformation after long-term *in vitro* culture and do not exhibit telomere maintenance mechanisms. *Cancer Res* **67**: 9142–9149.
- Bryan TM, Englezou A, Dalla-Pozza L, Dunham MA, Reddel RR. (1997). Evidence for an alternative mechanism for maintaining telomere length in human tumors and tumor-derived cell lines. *Nat Med* **3**: 1271–1274.
- Cairney CJ, Hoare SF, Daidone MG, Zaffaroni N, Keith WN. (2008). High level of telomerase RNA gene expression is associated with chromatin modification, the ALT phenotype and poor prognosis in liposarcoma. *Br J Cancer* **98**: 1467–1474.
- Cairney CJ, Keith WN. (2008). Telomerase redefined: integrated regulation of hTR and hTERT for telomere maintenance and telomerase activity. *Biochimie* **90**: 13–23.
- Chen YJ, Hakin-Smith V, Teo M, Xinarianos GE, Jellinek DA, Carroll T et al. (2006). Association of mutant TP53 with alternative lengthening of telomeres and favorable prognosis in glioma. *Cancer Res* **66**: 6473–6476.
- Costa A, Daidone MG, Daprai L, Villa R, Cantu S, Plotti S et al. (2006). Telomere maintenance mechanisms in liposarcomas: association with histologic subtypes and disease progression. *Cancer Res* **66**: 8918–8924.
- Gibbs CP, Kukekov VG, Reith JD, Tchigrinova O, Suslov ON, Scott EW et al. (2005). Stem-like cells in bone sarcomas: implications for tumorigenesis. *Neoplasia* **7**: 967–976.
- Hakin-Smith V, Jellinek DA, Levy D, Carroll T, Teo M, Timperley WR et al. (2003). Alternative lengthening of telomeres and survival in patients with glioblastoma multiforme. *Lancet* **361**: 836–838.
- Hao H, Nancay Y, Lei F, Xiong W, Wen S, Guofu H et al. (2008). siRNA directed against c-Myc inhibits proliferation and down-regulates human telomerase reverse transcriptase in human colon cancer Colo 320 cells. *J Exp Clin Cancer Res* **27**: 27.
- Henson JD, Hannay JA, McCarthy SW, Royds JA, Yeager TR, Robinson RA et al. (2005). A robust assay for alternative lengthening of telomeres in tumors shows the significance of alternative lengthening of telomeres in sarcomas and astrocytomas. *Clin Cancer Res* **11**: 217–225.
- Henson JD, Neumann AA, Yeager TR, Reddel RR. (2002). Alternative lengthening of telomeres in mammalian cells. *Oncogene* **21**: 998–610.
- Huang PR, Tsai ST, Hsieh KH, Wang TC. (2008). Heterogeneous nuclear ribonucleoprotein A3 binds single-stranded telomeric DNA and inhibits telomerase extension *in vitro*. *Biochim Biophys Acta* **1783**: 193–202.
- Jiang WQ, Zhong ZH, Henson JD, Reddel RR. (2007). Identification of candidate alternative lengthening of telomeres genes by methionine restriction and RNA interference. *Oncogene* **26**: 4635–4647.
- Johnson JE, Varkonyi RJ, Schwalm J, Cragle R, Klein-Szanto A, Patchefsky A et al. (2005). Multiple mechanisms of telomere maintenance exist in liposarcomas. *Clin Cancer Res* **11**: 5347–5355.
- Matushansky I, Hernandez E, Soci ND, Mills JE, Matos TA, Edgar MA et al. (2007). Derivation of sarcomas from mesenchymal stem cells via inactivation of the Wnt pathway. *J Clin Invest* **117**: 3248–3257.
- Mehle C, Piatyszek MA, Ljungberg B, Shay JW, Roos G. (1996). Telomerase activity in human renal cell carcinoma. *Oncogene* **13**: 161–166.
- Miura M, Miura Y, Padilla-Nash HM, Molinolo AA, Fu B, Patel V et al. (2006). Accumulated chromosomal instability in murine bone marrow mesenchymal stem cells leads to malignant transformation. *Stem Cells* **24**: 1095–1103.
- Riggi N, Suva ML, Suva D, Cironi L, Provero P, Tercier S et al. (2008). EWS-FLI-1 expression triggers a Ewing's sarcoma initiation program in primary human mesenchymal stem cells. *Cancer Res* **68**: 2176–2185.
- Rubio D, Garcia-Castro J, Martin MC, de la Fuente R, Cigudosa JC, Lloyd AC et al. (2005). Spontaneous human adult stem cell transformation. *Cancer Res* **65**: 3035–3039.
- Serakinci N, Guddberg P, Burns JS, Abdallah B, Schrodder H, Jensen T et al. (2004). Adult human mesenchymal stem cell as a target for neoplastic transformation. *Oncogene* **23**: 5095–5098.
- Serakinci N, Hoare SF, Kassem M, Atkinson SP, Keith WN. (2006). Telomerase promoter reprogramming and interaction with general transcription factors in the human mesenchymal stem cell. *Regen Med* **1**: 125–131.
- Tirode F, Laud-Duval K, Priour A, Delorme B, Charbord P, Delattre O. (2007). Mesenchymal stem cell features of Ewing tumors. *Cancer Cell* **11**: 421–429.
- Ulaner GA, Hoffman AR, Otero J, Huang HY, Zhao Z, Mazumdar M et al. (2004). Divergent patterns of telomere maintenance mechanisms among human sarcomas: sharply contrasting prevalence of the alternative lengthening of telomeres mechanism in Ewing's sarcomas and osteosarcomas. *Genes Chromosomes Cancer* **41**: 155–162.
- Ulaner GA, Huang HY, Otero J, Zhao Z, Ben-Porat L, Satagopan JM et al. (2003). Absence of a telomere maintenance mechanism as a favorable prognostic factor in patients with osteosarcoma. *Cancer Res* **63**: 1759–1763.
- Wang Y, Huso DL, Harrington J, Kellner J, Jeong DK, Turney J et al. (2005). Outgrowth of a transformed cell population derived from normal human BM mesenchymal stem cell culture. *Cytotherapy* **7**: 509–519.
- Wu C, Wei Q, Utomo V, Nadesan P, Whetstone H, Kandel R et al. (2007). Side population cells isolated from mesenchymal neoplasms have tumor initiating potential. *Cancer Res* **67**: 8216–8222.
- Yeager TR, Neumann AA, Englezou A, Huschtscha LI, Noble JR, Reddel RR. (1999). Telomerase-negative immortalized human cells contain a novel type of promyelocytic leukemia (PML) body. *Cancer Res* **59**: 4175–4179.
- Zhao YM, Li JY, Lan JP, Lai XY, Luo Y, Sun J et al. (2008). Cell cycle dependent telomere regulation by telomerase in human bone marrow mesenchymal stem cells. *Biochem Biophys Res Commun* **369**: 1114–1119.
- Zhong ZH, Jiang WQ, Cesare AJ, Neumann AA, Wadhwa R, Reddel RR. (2007). Disruption of telomere maintenance by depletion of the MRE11/RAD50/NBS1 complex in cells that use alternative lengthening of telomeres. *J Biol Chem* **282**: 29314–29322.
- Zhou YF, Bosch-Marce M, Okuyama H, Krishnamachary B, Kimura H, Zhang L et al. (2006). Spontaneous transformation of cultured mouse bone marrow-derived stromal cells. *Cancer Res* **66**: 10849–10854.
- Zimmermann S, Voss M, Kaiser S, Kapp U, Waller CF, Martens UM. (2003). Lack of telomerase activity in human mesenchymal stem cells. *Leukemia* **17**: 1146–1149.



Telomerase upregulation is a postcrisis event during senescence bypass and immortalization of two Nijmegen breakage syndrome T cell cultures

Sofie Degerman,¹ Jan Konrad Siwicki,² Pia Osterman,¹ Kyle Lafferty-Whyte,³ W. Nicol Keith³ and Göran Roos¹

¹Department of Medical Biosciences, Pathology, Umeå University, SE-90185 Umeå, Sweden

²Department of Immunology, Maria Skłodowska-Curie Memorial Cancer Centre and Institute of Oncology, PL-02 781 Warsaw, Poland

³Centre for Oncology and Applied Pharmacology, Cancer Research UK Beatson Laboratories, University of Glasgow, Glasgow, Scotland

response and senescence controlling genes, including downregulation of *ATM*, *CDKN1B* (p27), *CDKN2D* (p19) and *ASF1A* and upregulation of *CDK4*, *TWIST1*, *TP73L* (p63) and *SYK*. Telomerase upregulation was thus found to be uncoupled to escape of growth crisis but rather a later event in the immortalization process of NBS T cell cultures.

Key words: hTERT; immortalization; senescence; T-cell; telomerase; telomere.

Summary

Our knowledge on immortalization and telomere biology is mainly based on genetically manipulated cells analyzed before and many population doublings post growth crisis. The general view is that growth crisis is telomere length (TL) dependent and that escape from crisis is coupled to increased expression of the telomerase reverse transcriptase (*hTERT*) gene, telomerase activity upregulation and TL stabilization. Here we have analyzed the process of spontaneous immortalization of human T cells, regarding pathways involved in senescence and telomerase regulation. Two Nijmegen breakage syndrome (NBS) T cell cultures (S3R and S4) showed gradual telomere attrition until a period of growth crisis followed by the outgrowth of immortalized cells. Whole genome expression analysis indicated differences between pre-, early post- and late postcrisis cells. Early postcrisis cells demonstrated a logarithmic growth curve, very short telomeres and, notably, no increase in *hTERT* or telomerase activity despite downregulation of several negative *hTERT* regulators (e.g. *FOS*, *JUN D*, *SMAD3*, *RUNX2*, *TNF- α* and *TGF- β -R2*). Thereafter, *cMYC* mRNA increased in parallel with increased *hTERT* expression, telomerase activity and elongation of short telomeres, indicating a step-wise activation of *hTERT* transcription involving reduction of negative regulators followed by activation of positive regulator(s). Gene expression analysis indicated that cells escaped growth crisis by deregulated DNA damage

Introduction

Cellular immortalization is recognised as a major hallmark of cancer and is a multi-step process that requires numerous cell-type specific changes resulting in telomere length stabilization and abrogation of cell-cycle checkpoints. Whilst these endpoints of the immortalization process are well recognised, the route to immortalization is complex and the effector processes which lead to the establishment and maintenance of cancer cell immortality are only now beginning to be elucidated (Deng *et al.*, 2008; Fridman & Tainsky, 2008; Caino *et al.*, 2009; Kuilman & Peeper, 2009; Lafferty-Whyte *et al.*, 2009a,b).

Telomere maintenance is an important aspect of the biological process of immortalization and bypass of senescence. At every round of replication telomere DNA is lost due to the DNA end replication problem and additional processing of the telomere end. The progressive telomere shortening is believed to be a tumor suppressive mechanism since critically short telomeres can induce DNA damage response resulting in growth arrest. The 'telomere hypothesis' for cell immortalization states that growth crisis is telomere length dependent and that escape from crisis is coupled to increased expression of the telomerase reverse transcriptase (*hTERT*) gene, telomerase activity upregulation and telomere length stabilization. However, this hypothesis is mainly based on data from *in vitro* studies of genetically manipulated cells (primarily fibroblasts and epithelial cells) immortalized either by viral transformation (e.g. SV40 or HPV) or transfection with the *hTERT* and/or *cMYC* genes and analyzed many population doublings post growth crisis (Shay *et al.*, 1991; Wright & Shay, 1992; Harley, 2002; Shay & Wright, 2005; Stewart & Weinberg, 2006; Deng *et al.*, 2008).

These cell systems have proved valuable in establishing the hypothesis but the interpretation of experimental data may be difficult due to unintended alterations introduced by the procedures used. Thus, additional models are required to progress and refine our understanding of how cells can escape from growth crisis and the timing of the critical steps during the

Correspondence

Göran Roos, Department of Medical Biosciences, Pathology, Umeå University, Bldg 6M, 2nd floor, SE-90187 Umeå, Sweden. Tel.: +46 90 785 1801, or +46 70 6308692; fax: +46 90 785 4484; e-mail: goran.roos@medbio.umu.se

Accepted for publication 11 January 2010

process of senescence bypass (Fridman & Tainsky, 2008; Caino *et al.*, 2009; Lafferty-Whyte *et al.*, 2009a,b).

In this study two primary Nijmegen Breakage syndrome (NBS) T cell cultures (S3R and S4), established following mitogen stimulation and subsequent growth in the presence of IL-2 (Siwicki *et al.*, 2003), were used as an *in vitro* model of spontaneously immortalized human T cells to gain further insights into the molecular changes responsible for the escape from growth crisis. We found that T lymphocytes derived from NBS patients homozygous for the *NBS1* 625del5 mutation frequently acquire unlimited growth potential in IL-2 driven cultures (Siwicki *et al.*, 2008). This probably results from an impaired function of the NBS1 protein, which is involved in double strand break repair but also has functions at the telomeres (Ranganathan *et al.*, 2001; Howlett *et al.*, 2006; Zhang *et al.*, 2006). The 5bp deletion (657del5) in the *NBS1* gene results in a truncated NBS1 protein (NBS1 p21) but an additional form (NBS1 p70) is produced in B and T lymphocytes by alternative translation (Maser *et al.*, 2001; Siwicki *et al.*, 2003). NBS1 p70 is able to sustain many of the functions of the full-length protein (Kruger *et al.*, 2007). We have shown that spontaneously immortalized NBS T cells can stabilize their telomeres for long periods of time. Therefore these cell cultures represent an attractive model system to study telomere biology in the immortalization process (Siwicki *et al.*, 2003). Further, the fact that patients with the NBS1 mutation are prone to develop malignancies and especially of lymphoid origin give further support to the notion that our model is relevant for studies of neoplastic transformation.

There are few publications on long term cultured lymphocytes and telomere biology. Counter *et al.* studied EBV-transformed B-cells and found a continuous loss of telomeres until the cells entered proliferative crisis and died or activated telomerase, stabilized their telomeres and became immortalized. Telomerase activation was suggested as a common step in the immortalization process (Counter *et al.*, 1994). Wiesner *et al.* cultured normal B-cells for over 370 population doublings (PD) by continuous stimulation with CD40L and IL-4 and recorded high levels of telomerase at all time points analyzed and stabilization of telomere length, but no growth crisis period was observed (Wiesner *et al.*, 2008).

We have analyzed the S3R and S4 lines at different time points, pre- and postcrisis, with a special focus on gene expression events involved in telomerase activity and telomere length regulation. Our data demonstrate that upregulation of *hTERT* transcription, telomerase activation and telomere length stabilization occurred *after* growth crisis. Escape from crisis was associated with downregulation of DNA damage response genes and altered expression of cell cycle regulators and genes controlling the cellular senescence program.

Results

Both S3R and S4 T cell lines spontaneously immortalized through escape from growth crisis and emerged from a single clone

During IL2-dependent propagation both the S3R and S4 cell cultures entered a growth crisis after 20 and 62 PD, respectively (Fig. 1). The growth crisis was associated with slowdown in cell growth and a high rate of cell death and typical cellular characteristics for cells in crisis, but also with a significant proportion of dividing cells. After crisis, that lasted 14 (S3R) and 7 (S4) weeks, the growth rate of both cell lines increased up to one doubling per day. During establishment of the S3R and S4 lines, a gradual shift occurred from a polyclonal to a monoclonal pattern of T cell receptor (TCR) rearrangements (Table 1). In S4, the single clone that escaped growth crisis (69 PD) dominated even before growth crisis (48 PD) (Table 1 and data not shown). In the S3R cell culture, several clones were present close to entry of growth crisis (17 PD), whereas the early postcrisis culture (27 PD) was dominated by one clone and the established cell line seemed monoclonal after 76 PD (Table 1).

Telomere length measurement techniques highlight consistent precrisis telomere shortening and postcrisis telomere maintenance

Two methods were used to follow telomere length in the S3R and S4 cultures. Telomere length distribution of all chromosomes was evaluated using Southern blotting [Fig. 2A (S3R)

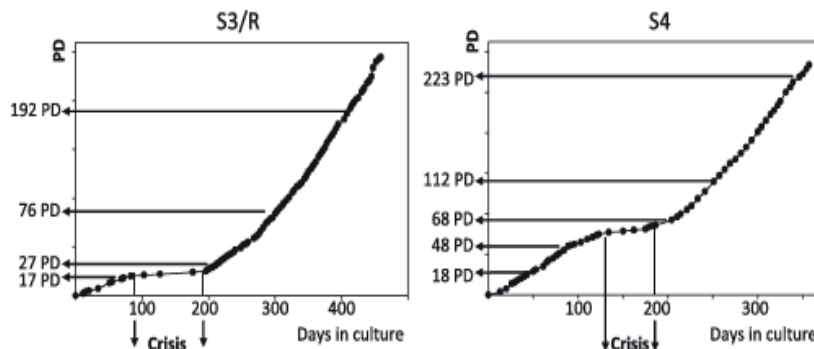


Fig. 1 Growth curves of Nijmegen breakage syndrome T cell line S3R and S4. A growth crisis period lasted for 14 (S3R) and 7 (S4) weeks corresponding to 20–25 PD in line S3R and 62–67 PD in line S4. Cells escaping growth crisis had increased growth rate compared to precrisis cells. PD, population doublings.

Table 1 T cell receptor (TCR) rearrangement clonality analysis. During establishment of the S3R and S4 lines, a gradual shift occurred from a polyclonal to a monoclonal pattern of TCR rearrangements. The numbers given in the table represents the size of the different TCR (Ty1, Ty3, Ty10, Ty11, T81) PCR products

S3R			
TCR	17 PD	27 PD	76 PD/192 PD
Ty1	319 + 324 + 326 + 327 + 522 + 523 + 525 + 526	324	324
Ty3	309 + 311 + 320 + 515	311 + 320	-
T81	489	-	-
S4			
TCR	12 PD	48 PD	69 PD/112 PD/223 PD
Ty1	220 + 226 + 230 + 233 + 240 + 242 + 247	233 + 240 + 242	233
Ty10,11	182 + 189 + 200	189	-

PD, population doublings.

and (Siwicki et al., 2003) (S4)] and single telomere length analysis (STELA) analysis was used to visualize the length of single chromosome telomere ends (Fig. 2B). The two techniques gave correlating results. In S4 gradual telomere attrition was observed until crisis when very short telomeres were present (Siwicki et al., 2003). S3R showed a drastic decrease in telomere length comparing pre- (17 PD) and postcrisis (27 PD) cells by Southern blot (Fig. 2A). In the postcrisis cells there was an elongation of telomere length observed followed by stabilization of the telomeres for over 100 PD [Fig. 2A and (Siwicki et al., 2003)].

The STELA method allowed detailed analysis of the telomere ends of single chromosomes (Xp and Yp) and telomeres were amplified with a subtelomeric primer located 0.4 kbp upstream of the telomere repeats together with a primer at the telomere end giving a minimal theoretical product length of 0.4 kbp. In early postcrisis S3R (27 PD) and S4 (68 PD) cells the telomeres were still critically short with telomere products ranging from 0.4 to 3 kbp. Quantification of the STELA data (Fig. 2C) demonstrated a reduced fraction of the shortest telomeres and a general elongation of the Xp and Yp telomeres in long-term cultured S3R (192 PD) and S4 (112 PD) cells compared to early postcrisis cells (S3R 27 PD and S4 68 PD).

Alterations to the shelterin complex and telomere maintenance mechanisms occur after escape from growth crisis

Telomerase activity was expressed at low levels in precrisis S3R and S4 cells (Fig. 3). Cells analyzed shortly after growth crisis (at 27 PD for S3R and 74 PD for S4) showed unchanged telomerase

activity (S3R and S4) and *hTERT* mRNA levels (S3R) (Fig. 3). *hTERT* RNA and telomerase upregulation were found to be later events in the immortalization process, in S3R analyzed at 76 PD and in S4 at 112 PD (telomerase activity measured at 130 PD). The RNA component of telomerase, *hTR*, has also been shown to be a limiting factor for telomerase activity (Cairney & Keith, 2008) but in the S3R and S4 cultures only slight changes in *hTR* expression were noted (Fig. 3). In S4 the *hTR* level was somewhat lower in immortalized cells compared to precrisis cells and in S3R *hTR* levels increased slightly after growth crisis after which the levels were stable.

The shelterin complex, consisting of six components (TRF1, TRF2, RAP1, TIN2, POT1 and TPP1), is important for telomere stability and for telomerase access to the telomeres (Palm & de Lange, 2008). mRNA levels of the shelterin genes were analyzed at increasing PD by RT-PCR. The general trend was reduced expression of the shelterin genes with increasing PD and more than twofold changes of certain components were observed in the long term cultured cells, S3R 197 PD (*TRF2*, *TIN2* and *RAP1*), and S4 223 PD (*POT1* and *RAP1*) (Fig. 4).

Unsupervised clustering of whole genome gene expression arrays separates pre- and postcrisis cells and indicates common gene expression changes between cell lines

Changes in gene expression profiles during the immortalization process were examined by whole genome gene expression arrays at different stages in the immortalization process. There were 1898 differently expressed ($P < 0.01$) genes comparing precrisis with postcrisis S3R and S4 cells. Unsupervised cluster analysis of the total data set demonstrated that pre- and postcrisis cells clustered separately in both the S3R and S4 cultures (Fig. 5A,B). Also, when all samples from the two lines were included in the cluster analysis pre- and postcrisis cells clustered separately indicating common alterations in gene expression during immortalization (Fig. 5C).

Gene expression analysis of *hTERT* regulatory genes reveals dynamic changes to *hTERT* regulation

The finding that activation of telomerase and *hTERT* transcription were late events in the immortalization process made us focus further analysis on the processes potentially regulating these cellular activities. We examined the expression of potential *hTERT* regulators at different passages before (17 PD), early after (27 PD) and late after (76 PD, 197 PD) the growth crisis period in S3R, and before (12 PD and 48 PD) and after (112 PD and 223 PD) growth crisis in S4. Altered expression of genes known to be able to regulate the *hTERT* promoter accumulated postcrisis, indicating a timed series of gene expression changes leading to the upregulation of telomerase activity (Fig. 6A–C). Some of the genes with altered expression in the array analysis (*cMYC*, *FOS*, *JUN D*, *SMAD3* and *MAD*) were further verified by RT-PCR showing a good correlation with the array data (Table 2).

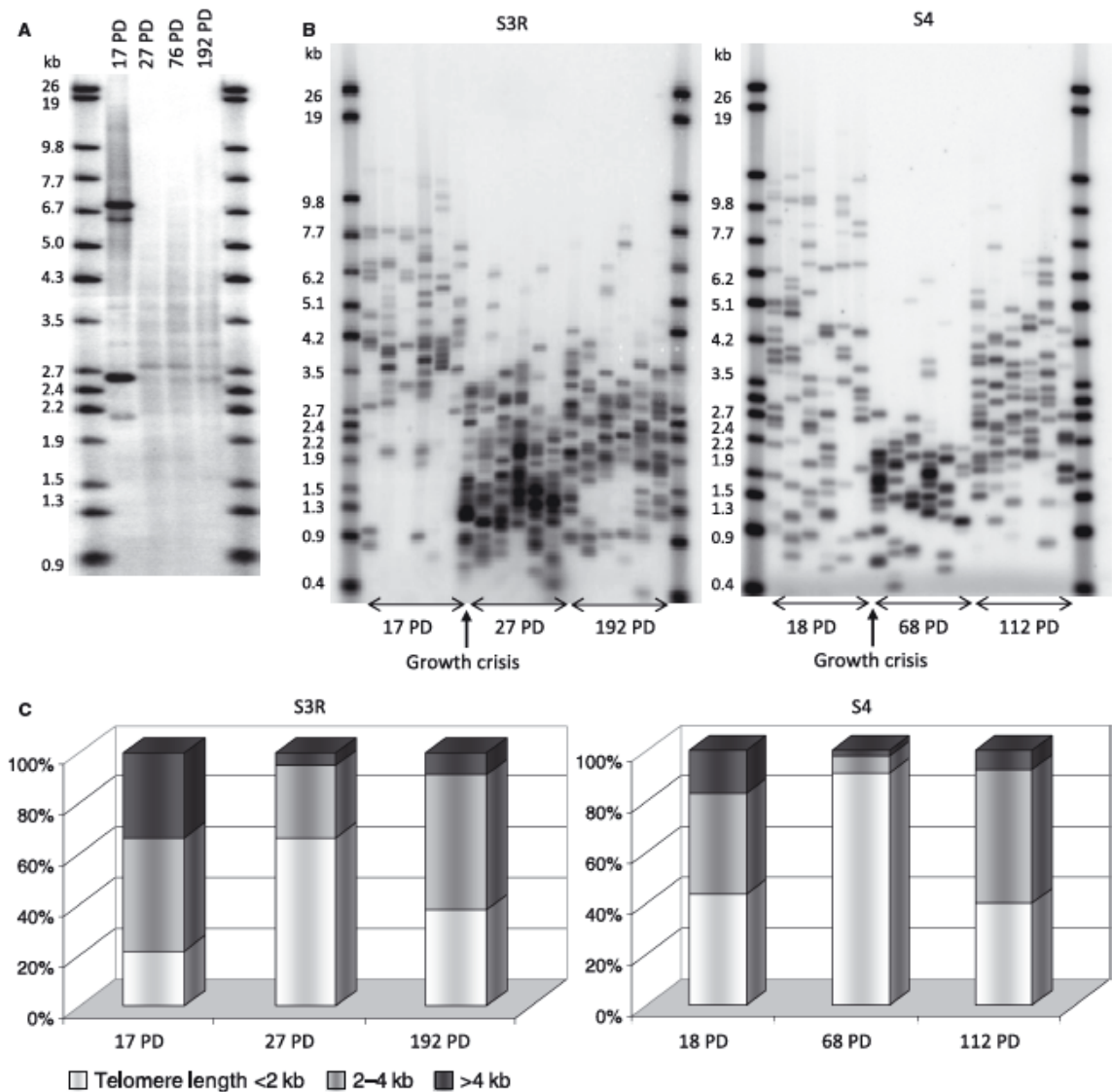


Fig. 2 Telomere length measurement techniques highlight consistent precrisis telomere shortening and postcrisis telomere maintenance. Telomere length measurements by Southern blot and single telomere length analysis (STELA). (A) Southern blot of line S3R. (B) STELA of S3R and S4 cell cultures at increasing population doublings (PD) where 27 PD (S3R) and 68 PD (S4) represent early-postcrisis cells. (C) Quantification of STELA product lengths expressed as the % of total STELA products within 0-2, 2-4 and > 4 kb, respectively.

Several negative regulators of *hTERT* transcription (*SMAD3*, *FOS*, *FOS B*, *JUN D*, *RUNX2*, *MAD*, *TNF- α* , *TGF β -R2* and *TGF β -R3*) were downregulated in early postcrisis S3R cells (27 PD) (Fig. 6A,C) but with no concomitant increase in *hTERT* transcription (Fig. 3). In S4 cells *FOS*, *FOS B*, *RUNX2*, *SMAD3*, *JUN D*, *TNF- α* , *TGF β -R2* and *TGF β -R3* were repressed postcrisis (112 PD and 223 PD). *cMYC*, a positive regulator of *hTERT* transcription, was increased in parallel with increased *hTERT* mRNA expression and telomerase activation in both S3R (76 PD) and S4 (112 PD) (Fig. 6B,C).

Investigation of biological process changes highlights dynamic alterations to senescence, DNA damage responses and cell cycle signaling

Although our study shows that telomerase activation and escape from crisis are separate events these two processes still exist within the larger context of senescence bypass and immortalization. The regulation of cellular senescence involves many genes and pathways controlling processes of significance for cell proliferation, DNA damage response and cell structure integrity

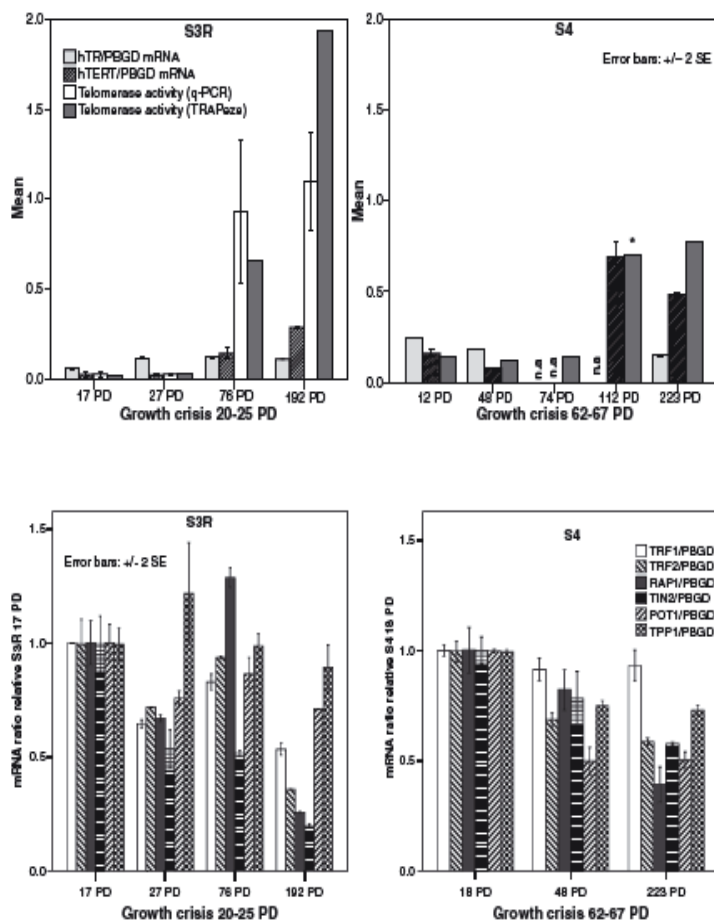


Fig. 3 Increase of hTERT and telomerase activity are late events in senescence bypass and immortalization. *hTERT* and *hTR* mRNA levels (RT-PCR) and telomerase activity [TRA-PeZe assay (S3R and S4 (Siwicki et al., 2003)) and q-PCR (S3R) in S3R and S4. Relative mRNA levels were normalized to the housekeeping gene *PBGD*. To visualize the results in the same figure hTR/*PBGD* mRNA and telomerase activity (TRA-PeZe) were divided by 100. na, not analyzed. *Telomerase activity was measured at 130 PD. PD, population doublings.

Fig. 4 Expression of the shelterin complex genes generally decreases with increasing population doublings (PD) after crisis escape. mRNA expression (RT-PCR) of the shelterin complex genes normalized to *PBGD* expression in lines S3R and S4 at increasing PD. Fold change was calculated using S3R 17 PD or S4 18 PD as a reference.

(Fridman & Tainsky, 2008). We examined changes in expression of larger biological processes through the interrogation of Meta-core pathway maps and comparison of the resulting *P*-value for each map at each passage. The comparison of such *P*-values allows simultaneous statistical assessment of the number of alterations to each individual pathway whilst correcting for pathway and gene list size. This analysis highlighted a number of cellular signaling processes with relevance to the kinetics of telomere maintenance and senescence bypass (Fig. 7A). An increase in the significance of alterations to senescence signaling pathways in general can be seen with increasing passage number in both T cell lines and interestingly a decrease in the significance of the senescence associated secretory elements (Kuilman & Peeper, 2009) is also highlighted by our analysis (Fig. 7A). Although we see a decrease in significance of the secretory senescence pathways due to the reduced number of twofold changes in later passages we see an increase in actual expression levels of individual secretory senescence molecules (e.g. *IL-6*) (Fig. 7A and Supporting Information Table S1). This may be reflective of a general activation of the secretory senescence program, perhaps induced by persistent DNA damage (Rodier et al., 2009), which once established and bypassed requires no further alterations for the continued proliferation of the cells.

Although the establishment of an inflammatory secretory signaling network has previously been seen to be essential for senescence induction (Kuilman et al., 2008), we suggest that the establishment of such network does not pose a significant barrier to senescence bypass.

Examples of individual genes found to be downregulated in early postcrisis S3R cells (27 PD) are *ATM*, *CCND3* (cyclin D3), *CDKN1B* (p27), *CDKN2D* (p19) and *ASF1A*, while examples of upregulated genes are *CDK4*, *TWIST1*, *TP73L* (p63), *CDKN1A* (p21) and *SYK* (Fig. 7B,C and Supporting Information Table S1). In long term cultured S3R (76 and 192 PD) and S4 cells (112 PD and 223 PD), *ATR* and *CDKN2B* (p15) were reduced and *cMYC* was increased (Fig. 7B,C and Supporting Information Table S1). These changes highlight the overlapping nature of senescence and telomerase regulation as many of the genes play roles in both processes.

Furthermore, with the escape from crisis an increase in alterations to cell cycle signaling and DNA damage induced responses can be seen with increasing number of population doublings (Fig. 7A). Alterations to both of these signaling pathways would be required to prevent the onset of senescence and overcome the cell cycle barriers to allow cells to proceed to immortalization.

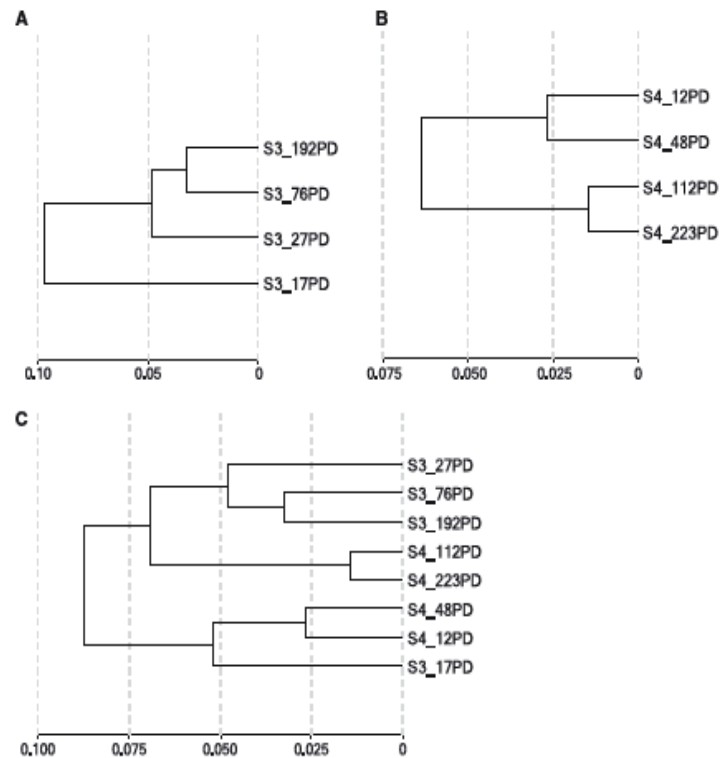


Fig. 5 Unsupervised clustering analysis of gene expression in line S3R (A), S4 (B) and S3R and S4 (C) separates pre- and postcrisis cells.

Immunoblotting confirms mRNA expression data

Selected proteins were analyzed by western blotting at different population doublings in line S3R to confirm that genes with changed gene expression on the mRNA level also showed alterations on the protein level (Fig. 7C). We found good correlations between the gene expression array data and protein expression. Syk, p63 and Twist1 protein levels increased and p27 decreased postcrisis at 27 PD, 76 PD and 192 PD. cMyc increased at 76 PD and 192 PD in line with the mRNA data.

Discussion

Our knowledge of the immortalization process is progressing rapidly. Recent advances have introduced pathways and networks of gene interactions which contribute to the mechanism and process of immortalization (Fridman & Tainsky, 2008; Caino *et al.*, 2009; Lafferty-Whyte *et al.*, 2009a,b). Early studies emanate mainly from studies focused on comparing normal with genetically manipulated cells cultured many passages after they were immortalized. Most of these studies were performed on fibroblasts or epithelial cells and it is not known to what extent the data can be applied to other cell types. In the present study we have used a model where T cells from NBS patients spontaneously become immortalized, due to emergence of genetic aberrations or epigenetic changes. Two cell lines (S3R and S4) were followed during this process to identify critical steps in attaining an immortal phenotype with a focus on factors regulating telomerase activity and telomere length. We found that telomerase

upregulation was uncoupled to escape of growth crisis but instead was a later event in the immortalization process.

The original telomere hypothesis for senescence and immortalization (the M1 and M2 model) states that human cells bypass two stages to become immortalized, i.e. senescence induction (M1) and critically short telomeres (M2, or 'crisis'). The senescence stage is likely caused by p53- and pRB-dependent DNA damage responses initiated by short telomeres, oncogene activation, cellular stress or DNA damage. Senescence might be bypassed by inactivation of tumor suppressor genes, resulting in extended rounds of replication and continuing telomere attrition. This eventually leads to loss of telomere capping activity and finally severe chromosomal instability and crisis (M2) (Shay *et al.*, 1991; Wright & Shay, 1992; Harley, 2002; Shay & Wright, 2005; Stewart & Weinberg, 2006; Deng *et al.*, 2008). The growth curves of the S3R and S4 cell cultures showed a plateau phase with high cell death characteristic of 'crisis' (M2) and cells escaping from this phase had an increased growth rate compared to the precrisis cells. No synchronized senescence (M1) stage was observed during culture, but the initial polyclonal cultures gradually became oligo- to monoclonal indicating that individual clones were lost due to senescence and subsequent cell death.

Escape from growth crisis is a very rare event for human cells and postcrisis cells have a mechanism for ensuring intact telomeres, either by activating telomerase or by the alternative lengthening of telomeres (ALT) mechanism (Stewart & Weinberg, 2006; Lafferty-Whyte *et al.*, 2009b). The ALT mechanism for telomere stabilization involves homologous recombination,

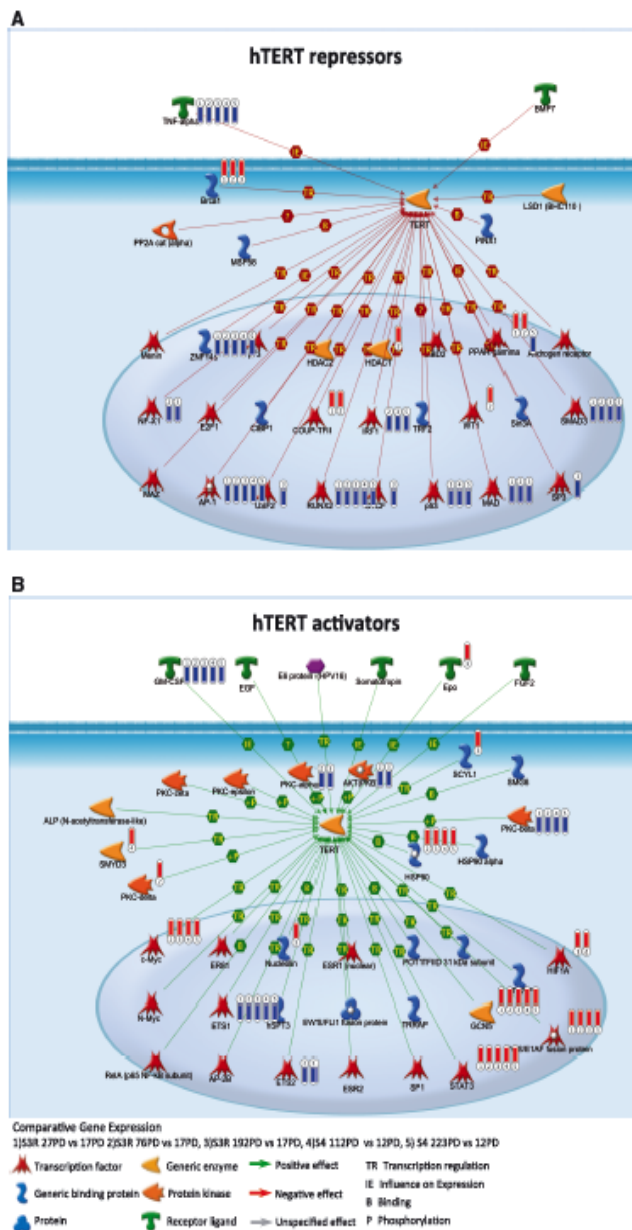


Fig. 6 Gene expression alterations in hTERT regulatory molecules highlight dynamic changes in telomerase regulation. Significant ($P < 0.01$) gene expression changes in cultures S3R and S4 in (A) known hTERT repressors and (B) known hTERT activators. Red thermometers show increase in expression and blue decrease in expression where 1 = S3R 27 PD/17 PD, 2 = S3R 76 PD/17 PD, 3 = S3R 192 PD/17 PD, 4 = S4 112 PD/12 PD, 5 = S4 223 PD/12 PD. (C) Fold change bar plot of gene expression array data of activating and repressing factors for hTERT regulation. Postcrisis S3R cells at 27 PD, 76 PD and 192 PD were compared to precrisis cells at 17 PD. In line S4, precrisis cells at 12 PD were used as reference for precrisis 48 PD and postcrisis 112 PD and 223 PD cells. PD, population doublings.

characterized by telomerase negative cells with very heterogeneous telomere lengths. ALT has not been described to occur in lymphoid cells and we did not find signs of ALT in our T cells. S3R cells analyzed shortly after growth crisis expressed low levels of *hTERT* mRNA and telomerase activity at the same levels as in precrisis cells and had critically short telomeres. The increased telomerase activity together with telomere elongation was recorded first at later time points. These data indicate that maintenance of telomeres *per se* was not the main factor for overcoming the M2 phase in our NBS T cell cultures. In contrast to telomerase negative fibroblasts, proliferating lymphocytes generally express telomerase at low levels, as did the S3R and S4 cells during precrisis culture. This weak telomerase activity was insufficient to maintain telomere length and very short telomeres were documented close to growth crisis.

The STELA technique revealed critically short telomeres in the early postcrisis cells suggesting that growth crisis indeed was telomere length dependent, in accordance with the telomere hypothesis. Cells escaping growth crisis had unchanged levels of telomerase activity compared to precrisis cells and might have gained 'resistance' to growth inhibitory signals induced by short telomeres enabling additional rounds of replication.

Escape from crisis can theoretically be explained by a selection of rare cells with long telomeres 'hidden' in the crisis population (Derre *et al.*, 2007). This possibility was assessed using TCR gene rearrangement analysis. We could show that the initial polyclonal cultures gradually became oligo- and monoclonal indicating a selection process during culture. In parallel with the

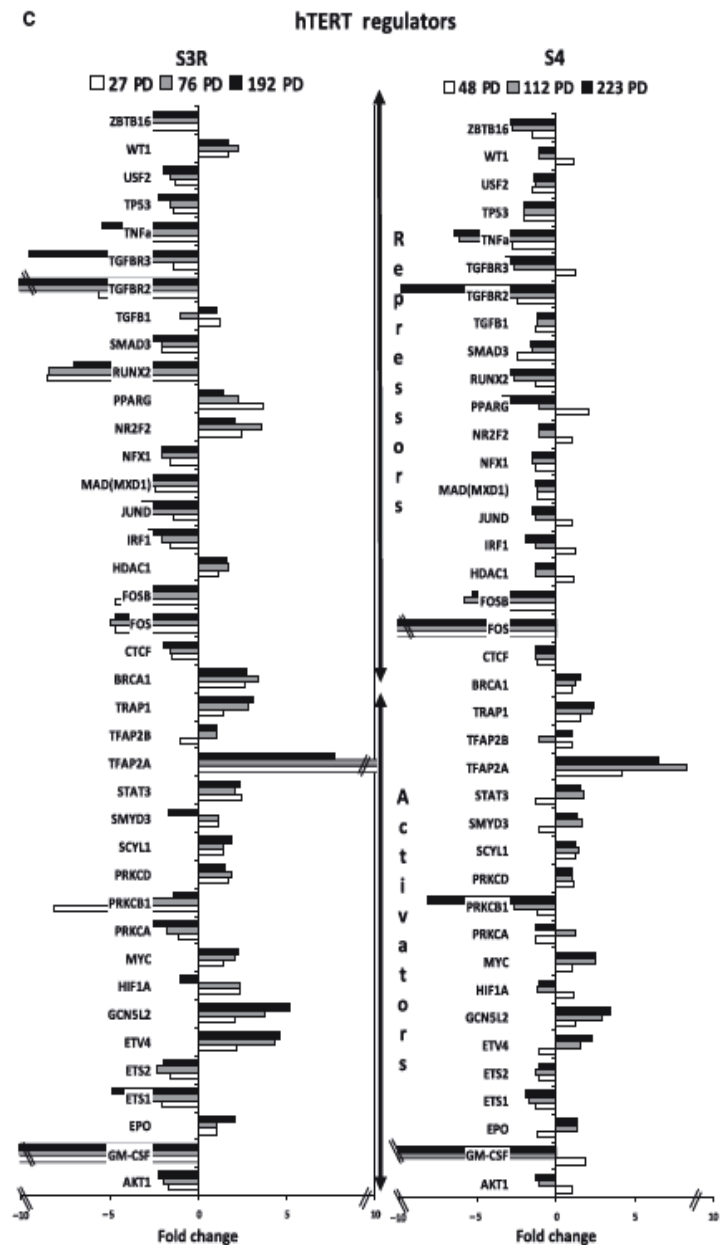


Fig. 6 (continued).

Table 2 Validation of gene expression of hTERT promoter regulating factors confirms telomerase regulation patterns. RT-PCR verification of selected genes from the array in S3R and S4 at increasing population doublings (PD)

mRNA	S3R			S4		
	Fold change vs. 17 PD			Fold change vs. 12 PD		
	27 PD	76 PD	192 PD	48 PD	112 PD	223 PD
<i>cMyc/PBGD</i>	1.1	1.9	2.3	-2.1	1.9	1.8
<i>MAD/PBGD</i>	-5.0	-10.8	-13.8	-1.1	1.0	-1.8
<i>SMAD3/PBGD</i>	-2.5	-2.2	-4.7	-1.9	-1.3	-2.6
<i>FOS/PBGD</i>	-13.2	-8.9	-10.9	-39.4	-76.6	-164.3
<i>JunD/PBGD</i>	-2.5	-5.9	-6.4	-1.6	-2.8	-4.3

clonal development, the telomeres gradually shortened and were critically short at the time when the cultures were monoclonal. Thus, the telomere elongation recorded postcrisis occurred in a monoclonal cell population with very short telomeres, indicating that the cells surviving crisis were not selected due to having long telomeres.

In the immortalized T cell lines the telomeres were stabilized for more than 100 PD. This seemingly regulated balance between telomere shortening and lengthening might be influenced by the shelterin genes (*TRF1*, *TRF2*, *RAP1*, *TIN2*, *POT1* and *TPP1*). The shelterin complex is important for telomere stability and telomere elongation in cell lines but there is no consensus regarding the relevance of shelterin component levels for

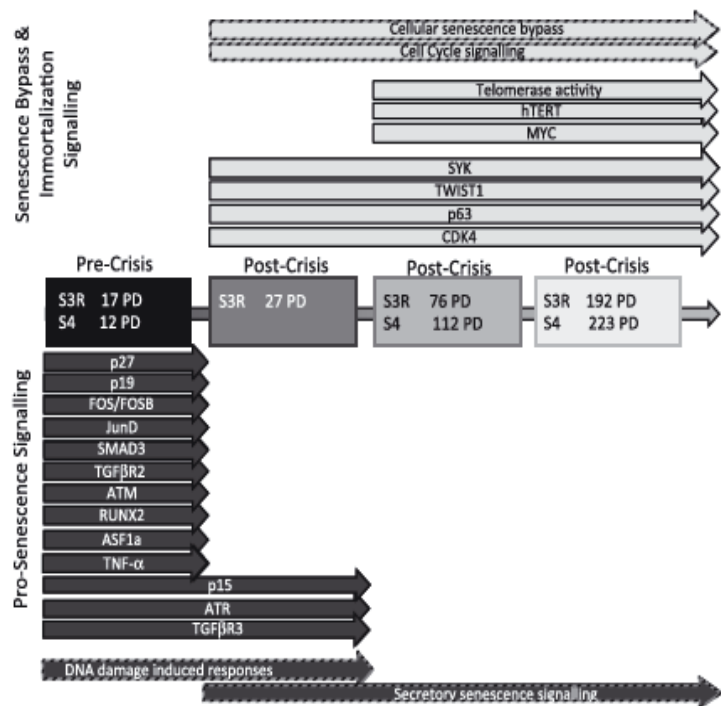


Fig. 8 Senescence bypass and immortalization signalling. Step-wise model of the immortalization process of Nijmegen breakage syndrome T-cells with special focus on telomerase and senescence regulation, showing genes and process alterations that seem to be driving immortalization.

telomere length regulation in tumors (Palm & de Lange, 2008; Cookson & Laughton, 2009). A fairly stable expression of the six shelterin genes was shown during the immortalization process, but we noticed a general decreased expression of the shelterin genes with increasing PD and a twofold reduction of *RAP1*, *TRF2* and *TIN2* in line S3R and of *RAP1* and *POT1* in line S4 in long term cultured cells. Chebel *et al.* (2009) showed that during T lymphocyte long-term culture and repeated re-stimulations, the expression of shelterin genes and most evident *RAP1* decreased (Chebel *et al.*, 2009). We found no obvious relation to entry or exit of crisis and/or telomere elongation and shelterin gene expression, but it cannot be excluded that shelterin factors are of importance for immortalization due to differential binding to the telomere ends. Thus, there is a possibility that in cells with very short telomeres, as in crisis, the shelterin complex might direct telomerase to critically short telomere ends and thereby telomerase could be important for cells to survive crisis. The optimal experiment to test this possibility would be to inhibit telomerase in precrisis cells. In our model system we used primary NBS T cells with no experimental procedures affecting the genetic set up of the cells. Inhibition of hTERT or hTR would need genetic modification of a large number of precrisis cells followed over a long period of time. Since immortalization is a very rare event it is not feasible to test this experimentally in our system. Another problem is that experimental hTERT/hTR inhibition does not give 100% inhibition. Thus, at present even if such studies were an option they would likely be fraught with issues of interpretation. Data from other well defined model systems are needed to further generalize our data in this respect.

Short or unprotected telomeres can induce DNA damage signals via ATM and/or ATR and trigger senescence (d'Adda di

Fagagna *et al.*, 2003; Herbig *et al.*, 2004). Early postcrisis S3R cells had down regulated *ATM* expression which could contribute to a 'resistance' to short telomeres due to reduced damage signaling, allowing cells to continue proliferation despite critically short telomeres and unchanged telomerase activity. *ATM* and *ATR* were downregulated in postcrisis S4 cells and *ATR* was also reduced in S3R at later passages indicating that a reduced DNA damage response makes cells more prone to immortalize (Jones *et al.*, 2004). The reduction of *ATM* and *ATR* in postcrisis cells, in combination with the defective *NBS1* gene, probably contributed to the impaired G1/S checkpoint observed after irradiation of the S4 and S3R cell lines (Siwicki *et al.*, 2003) and data not shown] since the *ATM* and *NBS1* gene products are interacting in the DNA damage response (Difilippantonio & Nussenzweig, 2007). Even if the *NBS1* mutation thereby can promote the establishment of immortalized cells, it is not a necessary event since normal T cells have been immortalized using a similar culture system (Siwicki *et al.*, 2000). However, this does not exclude that the late telomerase activation observed postcrisis might be related to the *NBS1* defect.

Gain of unlimited growth potential is a multistep process involving many cellular pathways. To study these processes in more detail we used a whole genome expression array and unsupervised clustering showed a separation of pre- and postcrisis cells, suggesting common genetic changes during the immortalization process. The observation that increase in telomerase activity and hTERT transcription were postcrisis events lead us to initially focus the array analysis on the expression of putative *hTERT* gene regulators (Bilsland *et al.*, 2009; Lafferty-Whyte *et al.*, 2009b). A large number of factors have been described to control the *hTERT* promoter, including activators (e.g. cMyc,

HIF1a, Sp1, estrogen and Ets) and repressors (e.g. WT1, Smad3, JunD, Fos, Runx2, p53 and menin) (Xiao et al., 2003; Isenmann et al., 2007; Cukusic et al., 2008; Kyo et al., 2008; Xu et al., 2008; Dwyer & Liu, 2010). In line S3R we were able to analyze cells very early after crisis and found that this stage was associated with decreased expression of several inhibitors of *hTERT* promoter activity (*SMAD3*, *TGF β -R2*, *FOS*, *FOS B*, *TNF- α* , *RUNX2*, *JUN D* and *MAD*), but with no concurrent increase in *hTERT* transcription or telomerase activity. In postcrisis S4 (112 PD) we could confirm the downregulation of several of these negative *hTERT* regulators (*TGF β -R2* and *TGF β -R3*, *FOS*, *FOS B*, *RUNX2*, *TNF- α* and *JUN D*).

Smad3, a negative regulator of *hTERT*, is associated with TGF β signaling (Li et al., 2006). Postcrisis cells showed downregulation of SMAD3 but the array data did not show changes in TGF β but instead a strong reduction of TGF β -R2 and TGF β -R3 expression. Recently, the level of TGF β -R2 was suggested to dictate the biological effect of TGF β on its downstream targets (Rojas et al., 2009) and TGF β -R3 has been shown to signal through Smad3 (You et al., 2007). The continuous downregulation of TGF β -R2 and TGF β -R3 in postcrisis S3R and S4 cells might thus have reduced the signaling via Smad3 resulting in reduced repression of the *hTERT* promoter.

TNF- α , a multifunctional cytokine associated with negative *hTERT* transcriptional regulation and senescence induction (Beyne-Rauzy et al., 2004), was strongly downregulated postcrisis which could be of importance for telomerase upregulation and senescence bypass in S3R and S4. GM-CSF (*CSF2*), which was one of the most downregulated genes in our analysis, can modulate *hTERT* transcription both positively and negatively but only in combination with other genes (Mano et al., 2000; Beyne-Rauzy et al., 2004). Additional knowledge is needed regarding GM-CSF and *hTERT* regulation in order to draw conclusions from this finding.

hTERT transcription is also negatively controlled by the AP-1 (transcription factor activator protein 1) complex consisting mainly of Jun (c-Jun, JunB or JunD) and Fos (c-Fos, FosB, Fra1 or Fra2) family members (Takakura et al., 2005). AP-1 activity is regulated by *JUN* and *FOS* gene transcription (Shaulian & Karin, 2002) and we found that c-FOS and FOS B together with *JUN D* were downregulated in postcrisis S3R and S4 cells, suggesting a release of the inhibitory effect of AP-1 on the *hTERT* promoter.

An additional negative *hTERT* regulator is Mad which binds to E-box elements on the *hTERT* promoter as a heterodimer with Max. Mad/Max competes with the activating c-Myc/Max heterodimer for promoter binding and a switch from Mad/Max to cMyc/Max allows transcriptional activation of *hTERT* (Wang et al., 1998; Oh et al., 2000; Xu et al., 2001). In line S3R, *MAD* was downregulated in early postcrisis cells (27 PD) and at 76 PD an increase in cMYC was seen in parallel with increased *hTERT* mRNA expression and telomerase upregulation. This suggests a switch from Mad/Max to cMyc/Max when telomerase was upregulated in S3R. Immortalized S4 cells also showed increased cMYC levels but *MAD* levels were only reduced in long-term cultured cells (223 PD). The increase in cMYC was moderate

(around twofold) in both lines but it is possible that it was sufficient for *hTERT* activation since several inhibitors (see above) were also reduced in early postcrisis cells (S3R). Taken together, the data argue for a combined effect of a number of co-acting genes leading to *hTERT* upregulation.

Our study further emphasizes the fact that telomere maintenance by telomerase exists as a stage in a series of events leading to senescence bypass and eventual immortalization. We were therefore also interested in identifying other processes involved in the series of events leading to immortalization. A number of studies have tried to characterize such processes in different cellular systems. In a recent review, Fridman & Tainsky (2008) compiled data from over 60 studies, the majority of which were performed on fibroblasts and epithelial cells (Fridman & Tainsky, 2008). They identified universal genes regulating senescence/immortalization representing six major pathways: the cell cycle (pRB/p53), cytoskeletal, interferon, insulin growth factor, MAP kinase and oxidative stress. Similarly, in our T cells we found alterations to the cell cycle and DNA damage signaling pathways postcrisis. These molecular events, together with the changes in telomere length observed at each population doubling indicates that growth crisis was provoked by critically short telomeres.

The immortalized cells also showed deregulation of genes involved in senescence. We noted that although alterations to senescence signaling overall increased with increasing population doublings postcrisis, the significance of the proinflammatory secretory senescence signaling (Kuilman et al., 2008; Rodier et al., 2009) decreased with increasing population doubling whilst increased expression of individual secretory molecules (e.g. *IL-6*) was observed. The decreased significance of secretory senescence pathway with increased population doubling showed that although the number of molecular changes occurring in the cell is increasing with population doubling there is no increase in the number of alterations to this pathway. This is suggestive of a situation whereby the secretory senescence network required for senescence induction is successfully established but this does not prevent effective senescence bypass.

As mentioned previously we also noted an increase in alterations to cell cycle signaling with increasing population doublings. The permanent withdrawal from the cell cycle during senescence requires many molecules of the cell cycle machinery (Bringold & Serrano, 2000; Lundberg et al., 2000; Roninson, 2003; Fridman & Tainsky, 2008). The increasing alteration to these signaling pathways would therefore be required for senescence bypass. For example, in both immortalized T cell lines various cell cycle inhibitors were downregulated such as *CDKN1B* (p27), *CDKN2B* (p15) and *CDKN2D* (p19) (Lundberg et al., 2000; Kim & Sharpless, 2006; Abukhdeir & Park, 2008; Majumder et al., 2008). *CDK4*, a positive factor for G1/S progression (Lazarov et al., 2002), was upregulated in postcrisis cells and together these events drive cell cycle progression. In contrast, postcrisis S3R cells and S4 cells at 48 PD, showed upregulation of the CDK inhibitor *CDKN1A* (p21). The increased *CDKN1A* (p21) expression was observed despite a reduction of the *TP53*

(p53) gene that positive regulates *CDKN1A* (p21) expression (Abukhdeir & Park, 2008). It has recently been demonstrated that the expression of *CDKN1A* (p21) was critical in preventing DNA-damage accumulation in leukemic stem cells (Viale et al., 2009) suggesting a survival advantage of *CDKN1A* (p21) up-regulation in line S3R and S4.

Previous analyses have shown a seemingly functional (but perhaps delayed) p53/p21 response after gamma irradiation of the S4 and S3R lines (Siwicki et al., 2003) and data not shown). Therefore, it is hard to draw conclusions about the importance of p53 for the immortalization process in these cells. However, the p53-related *TP73L* (p63) was strongly upregulated in the postcrisis cells apparently due to gain of chromosomal region 3q24-qter (Siwicki et al., 2004) and data not shown). p63 is overexpressed in anaplastic large cell lymphoma cells and in some other malignancies (Gualco et al., 2008), but the functional consequences of this overexpression is not known. It is worth noting that both immortal T cell lines S3R and S4 reveal phenotypic features typical of anaplastic large cell lymphoma (Siwicki et al., 2008). Since the product of the *TP73L* gene, p63, appear in several splice variants with different properties further studies are needed to elucidate the relevance of p63 upregulation for immortalization of T cells (Deyoung & Ellisen, 2007).

Further, the senescence associated gene *TWIST1* was strongly increased in both immortalized cell lines. *TWIST1* has been described to over-ride oncogene induced senescence in fibroblasts and epithelial cells (Ansieau et al., 2008), and our data suggest that *TWIST1* also can be of significance for senescence bypass in T-cells. Moreover, postcrisis cells demonstrated strong upregulation of *SYK*, which promotes cell survival and is overexpressed in peripheral T-cell lymphomas and chronic lymphocytic leukemia (Baudot et al., 2009; Buchner et al., 2009).

Cellular senescence is accompanied by extensive changes in chromatin structure and Senescence Associated Heterochromatin Foci (SAHF) are often demonstrated in senescent cells. These foci contribute to senescence-associated cell cycle arrest by inclusion and condensation of proliferation promoting genes into these structures, thereby silencing their expression. Two chromatin regulators, HIRA and Asf1a, drive the formation of SAHF by interaction with histones (Adams, 2007). Immortalization of our T lines was associated with downregulation of *ASF1a* which might have contributed to bypass of senescence by inhibiting formation of SAHF.

Interestingly, several gene expression changes (e.g. *ATM*, *CDK4*, *CDKN1B*) identified as important for overcoming growth crisis, were present already in S4 cells at 48 PD (Supporting Information Table S1). The oligo-clonal cell population present at that stage was dominated by the clone that later escaped growth crisis, further indicating that the immortalization process is stepwise and made possible due to additional genetic changes.

In conclusion, spontaneously immortalized NBS T cell lines were used to study molecular changes responsible for bypass of senescence and escape of growth crisis with a focus on telomere biology. Our main finding of telomerase and senescence regu-

lating factors are summarized in the form of a model (Fig. 8) showing genes that seems to be driving the immortalization process in T-cells. One major finding was that telomerase upregulation was a late event in the immortalization process. Escape from crisis and immortalization were associated with changed expression of multiple genes involved in the DNA damage response, cell cycle progression and cellular senescence control. The activation of hTERT in postcrisis cells occurred in a step-wise manner with initial down regulation of several transcriptional repressors followed by upregulation of *cMYC*. Thereby *hTERT* transcription and telomerase activity increased and telomere length was stabilized. These data give further, previously unknown, insights into telomere biology and immortalization. Future studies will be directed to analyze the mechanisms responsible for the altered expression of genes of interest. For this we need more fine mapped data on genetic alterations, including expression of micro RNAs and their targets and modifications of the chromatin landscape.

Experimental procedures

Cell cultures

Both S3R and S4 cell line were established from peripheral blood mononuclear cells (PBMC) derived from NBS patients homozygous for the 657del5 mutation of the *NBS1* gene (not diagnosed with any malignancy when the cultures were started) (Siwicki et al., 2003). S4 line: PBMC derived from patient S4 were suspended in a standard medium RPMI 1640, 10–12% FCS (Invitrogen, Stockholm, Sweden), 50 $\mu\text{g mL}^{-1}$ gentamycin (Sigma Aldrich, St Louis, MO, USA), activated for 24 h with 20 $\mu\text{g mL}^{-1}$ of wheat germ agglutinin (WGA, Pharmacia, Uppsala, Sweden) and subsequently cultured in standard medium supplemented with 20 U mL^{-1} of rIL-2 (R&D systems, Minneapolis, MN, USA). S3R line: after the initial 24 h WGA activation, PBMC derived from patient S3R were incubated for 72 h in standard medium without mitogen, and subsequently propagated in the presence of 20% of Lymphocult-T-LF (Biotest Diagnostics, Dreieich, Germany). Starting from the 20th day of culture, these cells were cultured in standard medium supplemented with rIL-2 (20 U mL^{-1}) with re-stimulation of the cells at 7 PD, 14 PD and 20 PD by 3-day incubation in the presence of both WGA (5 $\mu\text{g mL}^{-1}$) and of PHA-P (1 $\mu\text{g mL}^{-1}$) (Wellcome, Beckenham, England) and with no further re-stimulation. Viable cells were assessed every 3–7 days by trypan blue exclusion test and suspended in fresh standard medium supplemented with rIL-2.

TCR rearrangement analysis

Line S3R: Clonality analysis of the TCR V γ 1–4 and TCR V δ 1–3 genes was performed by PCR amplification in 50 μL reactions containing; 1 \times PCR buffer(-Mg) (Invitrogen, Stockholm, Sweden), 1.5 mM MgCl_2 , 0.25 μM of each of the primers (D4-labelled reverse primers), 0.2 mM of each dNTP and 1 U of Platinum Taq DNA Polymerase (Invitrogen) and 500 ng (TCR V γ

1–4 reaction) or 100 ng (TCR V δ 1–3 reaction) DNA template. Cycle conditions were initiated with 10 min at 95 °C, followed by 30 s at 94 °C, 30 s at 60 °C (TCR V γ 1–4) or 62 °C (TCR V δ 1–3) and 45 s at 72 °C for 34 cycles, and terminated with 7 min at 72 °C. One microlitre of the PCR product was mixed with 40 μ L sample loading solution (Beckman Coulter, Bromma, Sweden) and 0.5 μ L of the DNA size standard kit-600 (Beckman Coulter). The PCR products were separated and size analyzed in the CEQ 8000 Genetic Analysis System (Beckman Coulter).

The following primers were used:

TCR V γ 1–4; V1F: CAG GCC GAC TGG GTC ATC TGC, V2F: CAG CCC GCC TGG AAT GTG TGG, V3F: GAC ATA CCT TGC AAG ATA TCG AGC, V4F: CTG AAA TAT CTA TTT CCA GAC CAG C, Reverse primer mix: TCRGJ1-R: TTA CCA GGT GAA GTT ACT ATG AGC+ TCRGJ2-R: AAG AAA ACT TAC CTG TAA TGA TAA GC+ TCRGJ3-R: CCG TAT ATG CAC AAA GCC AAA TC.

TCR V δ 1–3; V δ 1F: ACT CAA GCC CAG TCA TCA GTA TCC, V δ 2F: ACC AAA CAG TGC CTG TGT CAA TAG G, V δ 3F: GAC CAG ACG GTG GCG AGT GGC, J δ 1R: ACC TCT TCC CAG GAG TCC TCC.

Line S4: TCR rearrangements in line S4 have been previously analyzed (Siwicki et al., 2003).

Southern blot

Telomere length distributions of all chromosomes were analyzed by Southern blot using 5 μ g of *Hinf*-1 (Roche Diagnostics GmbH, Mannheim, Germany) digested genomic DNA separated by electrophoresis on a 0.6% agarose gel in 0.1 M TBE buffer. The separated DNA fragments were depurinated (0.25 M HCl for 15 min), denaturated (1.5 M NaCl, 0.5 M NaOH for 1 h), neutralized (1.5 M NaCl, 0.5 M Tris-HCl pH 7.2, 1 mM EDTA for 1 h) and transferred to a nylon membrane (HybondTM-XL; Amersham Biosciences, Buckinghamshire, UK) using 20 \times SSC buffer over night. The membrane was prehybridized in QuikHyb hybridization solution (Agilent Technologies, Stratagene Products Division, La Jolla, CA, USA) and then hybridized with a telomeric ³²P-labeled (TTAGGG)₄ probe with added salmon sperm DNA for 1 h at 45 °C. After washing in 2 \times SSC and 0.1% SDS the membrane was exposed to a phosphor screen and scanned in a Typhoon 9400 scanner (Amersham Biosciences). Quantification of the results was performed with the Quantity One software (Bio-Rad Laboratories AB, Sundbyberg, Sweden).

Single telomere length analysis

To study the telomere length of single chromosomes we used the STELA method (Baird et al., 2003; Xu & Blackburn, 2007). In short, DNA was digested with *Eco*R1 enzyme and a telorette3 linker (5'-TGCTCCGTGCATCTGGCCTAACC-3') was ligated to the end of the telomeres. A set of negative controls were also included, DNA-telorette3 linker, DNA + irrelevant linker, water-telorette3 linker and water + telorette3 linker. In a 10 μ L ligation reaction we used 20 ng DNA, 1 μ M telorette3 linker, 1 U T4 DNA ligase (Roche Diagnostics GmbH)

and 1 \times ligation buffer (Roche Diagnostics). A teltail primer (5'-TGCTCCGTGCATCTGGCATC-3') complementary to the linker was used together with a chromosome specific subtelomeric primer XpYpE2 (5'-GTTGTCTCAGGGTCTAGTG-3') to amplify the telomeres. In the PCR reaction (15 μ L) we used: 300 pg ligated DNA, 1 \times buffer IV without MgCl₂ (ABgene Ltd, Surrey, UK), 1.5 mM MgCl₂, 0.5 μ M teltail primer, 0.5 μ M XpYpE2 primer, 0.3 mM per dNTP and 1.5 U Extensor Hi-Fidelity PCR enzyme mix (ABgene). The PCR was run at 94 °C 2 min, 25 cycles at 94 °C 15 s, 65 °C 30 s and 68 °C 10 min, followed by 68 °C 20 min. Twelve to eighteen PCR reactions were run for each sample and the products were separated in an agarose gel and transferred to a HybondTM-XL membrane (Amersham Biosciences). A subtelomeric probe was PCR amplified from the XpYp subtelomeric region (primers XpYpE2 5'-GTTGTCTCAGGGTCTAGTG-3', XpYpB2 5'-TCTGAAAGTGGACC(A/T)ATCAG-3'), purified, ³²P-labelled and hybridized to the membrane. The membrane was exposed to a phosphor screen and scanned in a Typhoon 9400 scanner (Amersham Biosciences). Quantification of the results was performed with the Quantity One software (Bio-Rad Laboratories).

RT-PCR

Total RNA was isolated from cell cultures using TRIZOL Reagent (Invitrogen), according to the manufacturer's protocol. Concentrations of total RNA were measured by spectrophotometry (NanoDrop; Thermo Scientific, Wilmington, DE, USA) and RNA quality was analyzed with the 2100 Bioanalyzer (Agilent Technologies, Santa Clara, CA, USA). RNA integrity number was > 9 in all samples. cDNA was prepared by reverse transcription with the Superscript II Reverse transcriptase kit (Invitrogen) together with random hexamers (Applied Biosystems, Inc., Foster City, CA, USA) and RNase inhibitor RNasin (Promega Biotech AB, Nacka, Sweden) according to the manufacturer's instruction (Invitrogen).

Gene expression levels of selected genes were analyzed by quantitative PCR as duplicates and a standard curve was included in every assay to monitor PCR efficiency. Amplification and detection was performed in a Light Cycler instrument (Roche Diagnostics GmbH). *hTERT*, *PBGD*, *cMYC*, *TRF1*, *TRF2*, *POT1*, *TIN2* and *RAP1* mRNA levels were quantified using the Light Cycler FastStart DNA Master SYBR Green I kit (Roche Diagnostics) and *hTR* with the Light Cycler TeloTTAGGG hTR quantification kit (Roche Diagnostics). The primer sets used were: hTERT-F: 5'-CGAGCTGCTCAGGCTTTCT-3' hTERT-R: 5'-GCCACCCTTCAAGTGCTGT-3', PBGD-F: 5'-CTAAGATTGGAGAGAAAGC-3', PBGD-R: 5'-CAGGGTTTCTAGGGTCTT-3', cMYC-F: 5'-TACCCTCTCAACGACAGCAGCTCGCCAACTCCT-3', cMYC-R: 5'-TCTTGACATTTCTCTCGGTGTCGAGGACC-3', TRF1-F: 5'-AGGGCTGATTCCAAG-3', TRF1-R: 5'-GCAACAGCGCAGAGG-3', TRF2-F: AAACGAAAGTTCAGC-3', TRF2-R: TCCTCAAGACCAAT-3', POT1-F: 5'-TCCAGATTCCAGCATCAGA-3', POT1-R: 5'-GCATTCCAACCACGGATA-3', TIN2-F: 5'-TGTGGATTGGCCTCG-3', TIN2-R: 5'-GAGAAGAGGTGATA-

GAGACT-3', RAP1-F: 5'-GCCTTGTTGAAAGCGA-3', RAP2-R: 5'-TCTGGAGTCTCTTATTCTGT-3'. To verify products and primer specificity melting curve analyses were performed. The following genes were analyzed by TaqMan assays on demand according to manufacturers protocol with the TaqMan Universal PCR Mastermix in the ABI PRISM 7900HT Instrument (Applied Biosystems, Inc.): c-FOS(Hs00170630_m1), JUN D(Hs00534289_s1), SMAD3(Hs00232222_m1), MAD(Hs002311-37_m1) and TPP1 (Hs00368526_g1).

The relative mRNA levels of the analyzed genes were normalized to a housekeeping gene (PBGD) and fold change were calculated using S3R 17 PD or S4 12/18 PD respectively as a precrisis reference by the $2^{-\Delta\Delta C_t}$ method (Schmittgen & Livak, 2008).

Gene expression analysis

Two hundred nanograms of total RNA of each sample was used for cRNA production by the Illumina TotalPrep RNA amplification kit (Ambion Inc, St. Austin, TX, USA) according to the provided protocol. In brief, reverse transcription with T7 oligo (dT) primer was used for first strand cDNA synthesis. The cDNA then underwent second strand synthesis and RNA degradation, followed by purification. *In vitro* transcription technology, along with biotin-NTP mix, was employed to generate multiple copies of biotinylated cRNA. The labeled cRNA was purified and then quantified by the NanoDrop (Thermo Scientific). The quality of cRNA was evaluated using the RNA 6000 pico kit (Agilent Technologies) in the Agilent 2100 Bioanalyzer (Agilent Technologies).

A total of 750 ng biotinylated cRNA was used for hybridization to a human HT12 Illumina Beadchip gene expression array (Illumina, San Diego, CA, USA) according to the manufacturer's protocol. The arrays were scanned using the Illumina Bead Array Reader (Illumina). For data analysis and normalization the Illumina® BeadStudio 3.2 software was used and cell signaling pathway and network analysis was done with the Metacore software (GeneGo Inc., St. Joseph, MI, USA). Samples were normalized by the cubic spline algorithm, genes with signal below background levels were excluded, and differentially expressed genes were identified by fold change calculations and with the Illumina custom differential expression algorithm (described in the Illumina Gene Expression Module user guide) to identify statistically ($P < 0.01$) differently expressed genes. Unsupervised gene cluster analysis by the absolute correlation metric approach of the array data was visualized in dendrograms.

hTERT activator and inhibitor maps were created using the Map Editor tool in Metacore from GeneGo (Bilsland *et al.*, 2009; Lafferty-Whyte *et al.*, 2009b). Pathway analysis was also performed using Metacore. In brief, twofold changes ($P < 0.01$) between each timepoint and precrisis (S3R 17 PD or S4 12 PD) were uploaded and analyzed using the Functional Ontology Enrichment GeneGo Pathway Maps tool. $-\log(P\text{-values})$ for relevant pathway maps were exported to Excel and visualized using a 3D bar graph.

Telomerase activity

Total protein was extracted using CHAPS lysis buffer (3-[(3-cholamidopropyl) dimethyl-ammonio]-1-propane sulphate) for 30 min on ice, centrifuged at 16 000 g for 30 min at 4 °C, and the supernatants were snap-frozen in liquid nitrogen, and stored at -80 °C until analysis. Total protein concentration was estimated by bicinchoninic acid protein assay (Pierce, Rockford, IL, USA). Telomerase activity was measured in CHAPS protein extracts (supplemented with 1 U μL^{-1} RNasin and 1 mM DTT) by the TRAPEze method (TRAPEze Telomerase Detection kit; Oncor Inc., Gaithersburg, MA, USA) according to the guidelines given by the supplier. The relative telomerase activity level was expressed as units of total product generated (TPG) corresponding to 0.05 μg of protein/assay. Line S4 was previously analyzed for telomerase activity by the same method (Siwicki *et al.*, 2003).

Further, S3R was analyzed with a quantitative telomerase detection kit (q-PCR) method supplied by Allied Biotech (Ijamsville, MD, USA), according to the protocol, using the BIORAD iQ5 real-time PCR detection system (Bio-Rad Laboratories). A supplied standard curve (TSR) with given concentrations were used as reference and each assay was run in duplicates on 0.1 μg CHAPS extract (supplied with 1 U μL^{-1} RNasin and 1 mM DTT) and quantified against the standard curve.

Immunoblotting

Protein expression levels were analyzed by western blotting. Twenty-five microgram of CHAPS extracts were separated by 7.5% or 10% SDS-PAGE electrophoresis and transferred to a PVDF membrane (Millipore, Bedford, MA, USA). Membranes were blocked in TBS containing 5% dried milk and 0.1% Tween-20 and probed with monoclonal mouse antibodies against TWIST1 (1:50, ab50887; Abcam, Cambridge, UK), Syk (1:1000, ab3993; Abcam) cMyc (1:1000, ab11917; Abcam), p27^{KIP1} (K25020; Transduction Laboratories, Lexington, KY, USA), p63 (1:50, 4A4; Dako, Glostrup, Denmark) (kind gift from Karin Nylander, Umea University, Sweden) and β -actin antibodies (1:5000; Chemicon International, Temecula, CA, USA). After a second incubation with horseradish peroxidase-conjugated anti-mouse or anti-rabbit antibodies (1:20 000; Dako), proteins were visualized using an enhanced chemiluminescent detection system (ECL-advance; Amersham Biosciences) and detected with the Bio-Rad ChemiDoc XRS gel documentation system using the Quantity One software (Bio-Rad Laboratories).

Acknowledgments

Supported by grants from the Swedish Cancer Society (GR), the Swedish Research Council (GR), the Medical Faculty, Umeå University (GR), Lion's Cancer Research Foundation, Umeå (SD, GR), and Cancer Research UK (WNK). The research leading to these results has received funding from the European Community's Seventh Framework Programme FP7/2007–2011 under grant agreement no. 200950 (GR, WNK).

Author contributions

GR and SD conceived and designed the experiments; SD, KLW, JKS and PO performed the experiments; SD, KLW, WNK and GR analyzed the data; SD, KLW, JKS, WNK and GR wrote the paper.

References

- Abukhdeir AM, Park BH (2008) P21 and p27: roles in carcinogenesis and drug resistance. *Expert Rev. Mol. Med.* **10**, e19.
- Adams PD (2007) Remodeling of chromatin structure in senescent cells and its potential impact on tumor suppression and aging. *Gene* **397**, 84–93.
- d'Adda di Fagagna F, Reaper PM, Clay-Farrace L, Fiegler H, Carr P, Von Zglinicki T, Saretzki G, Carter NP, Jackson SP (2003) A DNA damage checkpoint response in telomere-initiated senescence. *Nature* **426**, 194–198.
- Ansieau S, Bastid J, Doreau A, Morel AP, Bouchet BP, Thomas C, Fauvet F, Puisieux I, Doglioni C, Piccinin S, Maestro R, Voeltzel T, Selmi A, Valsesia-Wittmann S, Caron de Fromental C, Puisieux A (2008) Induction of EMT by twist proteins as a collateral effect of tumor-promoting inactivation of premature senescence. *Cancer Cell* **14**, 79–89.
- Baird DM, Rowson J, Wynford-Thomas D, Kipling D (2003) Extensive allelic variation and ultrashort telomeres in senescent human cells. *Nat. Genet.* **33**, 203–207.
- Baudot AD, Jeandel PY, Mouska X, Maurer U, Tartare-Deckert S, Raynaud SD, Cassuto JP, Ticchioni M, Deckert M (2009) The tyrosine kinase Syk regulates the survival of chronic lymphocytic leukemia B cells through PKCdelta and proteasome-dependent regulation of Mcl-1 expression. *Oncogene* **28**, 3261–3273.
- Beyne-Rauzy O, Recher C, Dastugue N, Demur C, Pottier G, Laurent G, Sabatier L, Mansat-De Mas V (2004) Tumor necrosis factor alpha induces senescence and chromosomal instability in human leukemic cells. *Oncogene* **23**, 7507–7516.
- Bilsland AE, Hoare S, Stevenson K, Plumb J, Gomez-Roman N, Cairney C, Burns S, Lafferty-Whyte K, Roffey J, Hammonds T, Keith WN (2009) Dynamic telomerase gene suppression via network effects of GSK3 inhibition. *PLoS ONE* **4**, e6459.
- Bringold F, Serrano M (2000) Tumor suppressors and oncogenes in cellular senescence. *Exp. Gerontol.* **35**, 317–329.
- Buchner M, Fuchs S, Prinz G, Pfeifer D, Bartholome K, Burger M, Chevallier N, Vallat L, Timmer J, Gribben JG, Jumaa H, Veelken H, Dierks C, Zirikli K (2009) Spleen tyrosine kinase is overexpressed and represents a potential therapeutic target in chronic lymphocytic leukemia. *Cancer Res.* **69**, 5424–5432.
- Caino MC, Meshki J, Kazanietz MG (2009) Hallmarks for senescence in carcinogenesis: novel signaling players. *Apoptosis* **14**, 392–408.
- Cairney CJ, Keith WN (2008) Telomerase redefined: integrated regulation of hTR and hTERT for telomere maintenance and telomerase activity. *Biochimie* **90**, 13–23.
- Chebel A, Bauwens S, Gerland LM, Belleville A, Urbanowicz I, de Climens AR, Tourmeur Y, Chien WW, Catallo R, Salles G, Gilson E, Ffrench M (2009) Telomere uncapping during in vitro T-lymphocyte senescence. *Aging Cell* **8**, 52–64.
- Cookson JC, Laughton CA (2009) The levels of telomere-binding proteins in human tumours and therapeutic implications. *Eur. J. Cancer* **45**, 536–550.
- Counter CM, Botelho FM, Wang P, Harley CB, Bacchetti S (1994) Stabilization of short telomeres and telomerase activity accompany immortalization of Epstein-Barr virus-transformed human B lymphocytes. *J. Virol.* **68**, 3410–3414.
- Cukusic A, Skrobot Vidacek N, Sopta M, Rubelj I (2008) Telomerase regulation at the crossroads of cell fate. *Cytogenet. Genome Res.* **122**, 263–272.
- Deng Y, Chan SS, Chang S (2008) Telomere dysfunction and tumour suppression: the senescence connection. *Nat. Rev. Cancer* **8**, 450–458.
- Derre L, Bruyninx M, Baumgaertner P, Devevre E, Corthesy P, Touvrey C, Mahnke YD, Pircher H, Voelter V, Romero P, Speiser DE, Rufer N (2007) In vivo persistence of codominant human CD8+ T cell clones is not limited by replicative senescence or functional alteration. *J. Immunol.* **179**, 2368–2379.
- Deyoung MP, Ellisen LW (2007) p63 and p73 in human cancer: defining the network. *Oncogene* **26**, 5169–5183.
- Difilippantonio S, Nussenzweig A (2007) The NBS1-ATM connection revisited. *Cell Cycle* **6**, 2366–2370.
- Dwyer JM, Liu JP (2010) Ets2 Transcription Factor, Telomerase Activity And Breast Cancer. *Clin. Exp. Pharmacol. Physiol.* **37**, 83–87.
- Fridman AL, Tainsky MA (2008) Critical pathways in cellular senescence and immortalization revealed by gene expression profiling. *Oncogene* **27**, 5975–5987.
- Gualco G, Weiss LM, Bacchi CE (2008) Expression of p63 in anaplastic large cell lymphoma but not in classical Hodgkin's lymphoma. *Hum. Pathol.* **39**, 1505–1510.
- Harley CB (2002) Telomerase is not an oncogene. *Oncogene* **21**, 494–502.
- Herbig U, Jobling WA, Chen BP, Chen DJ, Sedivy JM (2004) Telomere shortening triggers senescence of human cells through a pathway involving ATM, p53, and p21(CIP1), but not p16(INK4a). *Mol. Cell* **14**, 501–513.
- Howlett NG, Sciric Z, D'Andrea AD, Schiestl RH (2006) Impaired DNA double strand break repair in cells from Nijmegen breakage syndrome patients. *DNA Repair (Amst.)* **5**, 251–257.
- Ibenmann S, Cakouros D, Zannettino A, Shi S, Gronthos S (2007) hTERT transcription is repressed by Cbfa1 in human mesenchymal stem cell populations. *J. Bone Miner. Res.* **22**, 897–906.
- Jones GG, Reaper PM, Pettitt AR, Sherrington PD (2004) The ATR-p53 pathway is suppressed in noncycling normal and malignant lymphocytes. *Oncogene* **23**, 1911–1921.
- Kim WY, Sharpless NE (2006) The regulation of INK4/ARF in cancer and aging. *Cell* **127**, 265–275.
- Kruger L, Demuth I, Neitzel H, Varon R, Sperling K, Chrzanowska KH, Seemanova E, Digweed M (2007) Cancer incidence in Nijmegen breakage syndrome is modulated by the amount of a variant NBS protein. *Carcinogenesis* **28**, 107–111.
- Kuilman T, Peeper DS (2009) Senescence-messaging secretome: SMS-ing cellular stress. *Nat. Rev. Cancer* **9**, 81–94.
- Kuilman T, Michaloglou C, Vredeveld LC, Douma S, van Doorn R, Desmet CJ, Aarden LA, Mooi WJ, Peeper DS (2008) Oncogene-induced senescence relayed by an interleukin-dependent inflammatory network. *Cell* **133**, 1019–1031.
- Kyo S, Takakura M, Fujiwara T, Inoue M (2008) Understanding and exploiting hTERT promoter regulation for diagnosis and treatment of human cancers. *Cancer Sci.* **99**, 1528–1538.
- Lafferty-Whyte K, Cairney CJ, Jamieson NB, Oien KA, Keith WN (2009a) Pathway analysis of senescence-associated miRNA targets reveals common processes to different senescence induction mechanisms. *Biochim. Biophys. Acta* **1792**, 341–352.
- Lafferty-Whyte K, Cairney CJ, Will MB, Serakinci N, Daidone MG, Zaffaroni N, Bilsland A, Keith WN (2009b) A gene expression signature classifying telomerase and ALT immortalization reveals an hTERT regulatory network and suggests a mesenchymal stem cell origin for ALT. *Oncogene* **28**, 3765–3774.

- Lazarov M, Kubo Y, Cai T, Dajee M, Tarutani M, Lin Q, Fang M, Tao S, Green CL, Khavari PA (2002) CDK4 coexpression with Ras generates malignant human epidermal tumorigenesis. *Nat. Med.* **8**, 1105–1114.
- Li H, Xu D, Toh BH, Liu JP (2006) TGF- β and cancer: is Smad3 a repressor of hTERT gene? *Cell Res.* **16**, 169–173.
- Lundberg AS, Hahn WC, Gupta P, Weinberg RA (2000) Genes involved in senescence and immortalization. *Curr. Opin. Cell Biol.* **12**, 705–709.
- Majumder PK, Grisanzio C, O'Connell F, Barry M, Brito JM, Xu Q, Guney I, Berger R, Herman P, Bikoff R, Fedele G, Baek WK, Wang S, Ellwood-Yen K, Wu H, Sawyers CL, Signoretti S, Hahn WC, Loda M, Sellers WR (2008) A prostatic intraepithelial neoplasia-dependent p27 Kip1 checkpoint induces senescence and inhibits cell proliferation and cancer progression. *Cancer Cell* **14**, 146–155.
- Mano Y, Shimizu T, Tanuma S, Takeda K (2000) Synergistic down-regulation of telomerase activity and hTERT mRNA expression by combination of retinoic acid and GM-CSF in human myeloblastic leukemia ML-1 cells. *Anticancer Res.* **20**, 1649–1652.
- Maser RS, Zinkel R, Petrini JH (2001) An alternative mode of translation permits production of a variant NBS1 protein from the common Nijmegen breakage syndrome allele. *Nat. Genet.* **27**, 417–421.
- Oh S, Song YH, Yim J, Kim TK (2000) Identification of Mad as a repressor of the human telomerase (hTERT) gene. *Oncogene* **19**, 1485–1490.
- Palm W, de Lange T (2008) How shelterin protects mammalian telomeres. *Annu. Rev. Genet.* **42**, 301–334.
- Ranganathan V, Heine WF, Ciccone DN, Rudolph KL, Wu X, Chang S, Hai H, Ahearn IM, Livingston DM, Resnick I, Rosen F, Seemanova E, Jarolim P, DePinto RA, Weaver DT (2001) Rescue of a telomere length defect of Nijmegen breakage syndrome cells requires NBS and telomerase catalytic subunit. *Curr. Biol.* **11**, 962–966.
- Rodier F, Coppe JP, Patil CK, Hoeljmakers WA, Munoz DP, Raza SR, Freund A, Campeau E, Davalos AR, Campisi J (2009) Persistent DNA damage signalling triggers senescence-associated inflammatory cytokine secretion. *Nat. Cell Biol.* **11**, 973–979.
- Rojas A, Padidam M, Cress D, Grady WM (2009) TGF- β receptor levels regulate the specificity of signaling pathway activation and biological effects of TGF- β . *Biochim. Biophys. Acta* **1793**, 1165–1173.
- Roninson IB (2003) Tumor cell senescence in cancer treatment. *Cancer Res.* **63**, 2705–2715.
- Schmittgen TD, Livak KJ (2008) Analyzing real-time PCR data by the comparative C(T) method. *Nat. Protoc.* **3**, 1101–1108.
- Shaulian E, Karin M (2002) AP-1 as a regulator of cell life and death. *Nat. Cell Biol.* **4**, E131–E136.
- Shay JW, Wright WE (2005) Senescence and immortalization: role of telomeres and telomerase. *Carcinogenesis* **26**, 867–874.
- Shay JW, Pereira-Smith OM, Wright WE (1991) A role for both RB and p53 in the regulation of human cellular senescence. *Exp. Cell Res.* **196**, 33–39.
- Siwicki JK, Hedberg Y, Nowak R, Loden M, Zhao J, Landberg G, Roos G (2000) Long-term cultured IL-2-dependent T cell lines demonstrate p16^{INK4a} overexpression, normal pRb/p53, and upregulation of cyclins E or D2. *Exp. Gerontol.* **35**, 375–388.
- Siwicki JK, Degerman S, Chrzanowska KH, Roos G (2003) Telomere maintenance and cell cycle regulation in spontaneously immortalized T-cell lines from Nijmegen breakage syndrome patients. *Exp. Cell Res.* **287**, 178–189.
- Siwicki JK, Berglund M, Rygiel J, Pienkowska-Grela B, Grygalewicz B, Degerman S, Golovleva I, Chrzanowska KH, Lagercrantz S, Blennow E, Roos G, Larsson C (2004) Spontaneously immortalized human T lymphocytes develop gain of chromosomal region 2p13–24 as an early and common genetic event. *Genes Chromosomes Cancer* **41**, 133–144.
- Siwicki JK, Rymkiewicz G, Blachnio K, Rygiel J, Kuzniar P, Ploski R, Janusz A, Skurzak H, Chrzanowska K, Steffen J (2008) Spontaneously immortalized T lymphocytes from Nijmegen Breakage Syndrome patients display phenotypes typical for lymphoma cells. *Leuk. Res.* **32**, 569–577.
- Stewart SA, Weinberg RA (2006) Telomeres: cancer to human aging. *Annu. Rev. Cell Dev. Biol.* **22**, 531–557.
- Takakura M, Kyo S, Inoue M, Wright WE, Shay JW (2005) Function of AP-1 in transcription of the telomerase reverse transcriptase gene (TERT) in human and mouse cells. *Mol. Cell. Biol.* **25**, 8037–8043.
- Viale A, De Franco F, Orleth A, Cambiaghi V, Giuliani V, Bossi D, Ronchini C, Ronzoni S, Muradore I, Monestiroli S, Gobbi A, Alcalay M, Minucci S, Pelicci PG (2009) Cell-cycle restriction limits DNA damage and maintains self-renewal of leukaemia stem cells. *Nature* **457**, 51–56.
- Wang J, Xie LY, Allan S, Beach D, Hannon GJ (1998) Myc activates telomerase. *Genes Dev.* **12**, 1769–1774.
- Wiesner M, Zentz C, Mayr C, Wimmer R, Hammerschmidt W, Zeidler R, Moosmann A (2008) Conditional immortalization of human B cells by CD40 ligation. *PLoS ONE* **3**, e1464.
- Wright WE, Shay JW (1992) The two-stage mechanism controlling cellular senescence and immortalization. *Exp. Gerontol.* **27**, 383–389.
- Xiao X, Athanasiou M, Sidorov IA, Horikawa I, Cremona G, Blair D, Barret JC, Dimitrov DS (2003) Role of Ets/Id proteins for telomerase regulation in human cancer cells. *Exp. Mol. Pathol.* **75**, 238–247.
- Xu L, Blackburn EH (2007) Human cancer cells harbor T-stumps, a distinct class of extremely short telomeres. *Mol. Cell* **28**, 315–327.
- Xu D, Popov N, Hou M, Wang Q, Bjorkholm M, Gruber A, Menkel AR, Henriksson M (2001) Switch from Myc/Max to Mad1/Max binding and decrease in histone acetylation at the telomerase reverse transcriptase promoter during differentiation of HL60 cells. *Proc. Natl. Acad. Sci. U S A* **98**, 3826–3831.
- Xu D, Dwyer J, Li H, Duan W, Liu JP (2008) Ets2 maintains hTERT gene expression and breast cancer cell proliferation by interacting with c-Myc. *J. Biol. Chem.* **283**, 23567–23580.
- You HJ, Bruinsma MW, How T, Ostrander JH, Blobel GC (2007) The type III TGF- β receptor signals through both Smad3 and the p38 MAP kinase pathways to contribute to inhibition of cell proliferation. *Cardiogenesis* **28**, 2491–2500.
- Zhang Y, Zhou J, Lim CU (2006) The role of NBS1 in DNA double strand break repair, telomere stability, and cell cycle checkpoint control. *Cell Res.* **16**, 45–54.

Supporting Information

Additional supporting information may be found in the online version of this article:

Table S1 Fold change table of gene expression array data on cellular senescence associated genes. Postcrisis S3R cells at 27 PD, 76 PD and 192 PD were compared to precrisis cells at 17 PD. In line S4, precrisis cells at 12 PD were used as reference for precrisis 48 PD and postcrisis 112 PD and 223 PD cells.

As a service to our authors and readers, this journal provides supporting information supplied by the authors. Such materials are peer-reviewed and may be re-organized for online delivery, but are not copy-edited or typeset. Technical support issues arising from supporting information (other than missing files) should be addressed to the authors.